

Iron and Nickel-Catalyzed Functionalization of Heteroarenes and Hydrogenation of Ketones

by

Shidheshwar Baliram Ankade

(Registration Number: 10CC18J26001)

**A thesis submitted to the
Academy of Scientific & Innovative Research
for the award of the degree of
DOCTOR OF PHILOSOPHY
in
SCIENCE**

under the supervision of
Dr. Benudhar Punji



**CSIR-NATIONAL CHEMICAL LABORATORY
Pune**



Academy of Scientific and Innovative Research
AcSIR Headquarters, CSIR-HRDC campus
Sector 19, Kamla Nehru Nagar
Ghaziabad, U.P. - 201 002, India

June 2023

Certificate

This is to certify that the work incorporated in this Ph.D. thesis entitled "*Iron and Nickel-Catalyzed Functionalization of Heteroarenes and Hydrogenation of Ketones*", submitted by *Shidheshwar Baliram Ankade* to the Academy of Scientific and Innovative Research (AcSIR), in partial fulfillment of the requirements for the award of the Degree of *Doctor of Philosophy in Science*, embodies original research work carried out by the student. We, further certify that this work has not been submitted to any other University or Institution in part or full for the award of any degree or diploma. Research materials obtained from other sources and used in this research work have been duly acknowledged in the thesis. Images, illustrations, figures, tables *etc.*, used in the thesis from other sources, have also been duly cited and acknowledged.



Mr. Shidheshwar Baliram Ankade

Research Student

Date: 30/06/2023



Dr. Benudhar Punji

Research Supervisor

Date: 30/06/2023

STATEMENTS OF ACADEMIC INTEGRITY

I, **Shidheshwar Baliram Ankade**, a Ph.D. student of the Academy of Scientific and Innovative Research (AcSIR) with Registration No. 10CC18J26001 hereby undertake that, the thesis entitled “**Iron and Nickel-Catalyzed Functionalization of Heteroarenes and Hydrogenation of Ketones**” has been prepared by me and that the document reports original work carried out by me and is free of any plagiarism in compliance with the UGC Regulations on “*Promotion of Academic Integrity and Prevention of Plagiarism in Higher Educational Institutions (2018)*” and the CSIR Guidelines for “*Ethics in Research and in Governance (2020)*”.

Signature of the Student

Date : 30/06/2023

Place : CSIR-NCL, Pune

It is hereby certified that the work done by the student, under my supervision, is plagiarism-free in accordance with the UGC Regulations on “*Promotion of Academic Integrity and Prevention of Plagiarism in Higher Educational Institutions (2018)*” and the CSIR Guidelines for “*Ethics in Research and in Governance (2020)*”.

NA

Signature of the Co-supervisor (if any)

Name :

Date :

Place :

Signature of the Supervisor

Name : Dr. Benudhar Punji

Date : 30/06/2023

Place : CSIR-NCL, Pune



*Dedicated to My Parents and
Teachers*

ACKNOWLEDGEMENTS

I would like to thank all the people who contributed in some way to the work described in this thesis. First of all, I would like to express my enormous gratitude to my research supervisor **Dr. Benudhar Punji** for his valuable guidance and scholarly input. His motivation, inspiration, encouragement, and persistent guidance have helped me to realize my dreams to reality. I am grateful to him for his patience, advices, and continuous support provided during every stage of my research work. I am thankful to him for giving me an opportunity to work under his valuable guidance.

I would also like to thank Dr. E. Balaraman, Dr. Sailaja Krishnamurthy, Dr. Sakya S. Sen, and Dr. Ravindar Kontham for being my doctoral advisory committee (DAC) members and providing me with valuable suggestions during the DAC meetings. I am grateful to Prof. Ashish Lele, Director, CSIR-NCL, and Prof. Ashwini K. Nangia (Former Directors, NCL) for giving me this opportunity and providing all the necessary infrastructure and facilities. I also acknowledge the financial support of CSIR, New Delhi in terms of junior and senior research fellowships.

I also wish to thank all my seniors Drs. Shrikant Khake, Hanuman Prasad Pandiri, Vineeta Soni, Ulhas Patel, Dilip Pandey, Abad Ali, Rahul Jagtap, Dipesh Sharma and juniors Vijaykumar M, Surydev Kumar Verma, Anand Shabade, Sadhna Bansal, Chandini Pradhan, Rameshwar Pawar, Yogesh Ramasane, Rahul K. Singh, Shana, Pragnya, Sandip, Chandrakant, Banmali Sahu, Tamal, and Suvajit for their valuable time and cooperation. I extend my thanks to our collaborators Dr. Sailja Krishnamurthy and Pragnya Samal for the timely help with DFT analysis. I would also like to thank Mrs. B. Santhakumari, for HRMS analysis, Dr. Rajamohanan, Dr. Ajithkumar, Dr. Uday Kiran for NMR facilities, and Dr. Rajesh Gonnade for XRD facilities.

I would like to thank Dr. Samir Chikkali and his group members, Drs. Shahaji Gayakwad, Vijay Kosti, Satej Deshmukh, Nilesh Mote, Swechchha Pandey, and Bhausahab Rajput for their valuable scientific advice and help in lab practices. I greatly acknowledge other lab colleagues Dr. Anirban, Dnyaneshwar, Rohit, Dr. Dipa, Ravi, Rohit, Dr. Shailaja, Dr. Pawal, Amol, Kishor, Rajkumar, Poonam, Nikita, Maula, Rohan, and Uday for keeping the healthy environment in the lab and for their valuable scientific discussions. Further, I extend my special thanks to *Tanuja Tewari* for her generous support and motivation.

Also, I would like to thank research trainees Janhavi, Vaishali, Jagnyesh, Ankita, Tejaswini, Mahesh, Lekshmi, Ishita, Harshada, Vishal, Sachin, Mital, and Darsana for their cooperation. I especially thanks to Drs. Santosh Panchal, Madan Ambhore, and Nilesh Deshpande for their valuable suggestions. My sincere thanks to the people in various parts of

ACKNOWLEDGEMENTS

the institute and the SAC office staff for their cooperation. I would also like to acknowledge all the staff members of NMR, Mass spectroscopy, Microanalysis, Library, Administration, and technical divisions of NCL for their assistance during the course of my work.

A special thank goes to all my friends from CSIR-NCL, IISER Pune, and IIT Mumbai, Dr. Basvaraj kote, Dr. Priyanka Deshmukh-Jagtap, Umatai Hale, Gopal Deshmukh, Ramesh Hiremath, Sandip Kaulage, Pragati Shukla, Vishnu, Nirmala Mohanta, Dashrath (Ravi) Sutar, Dr. Durgaprasad Shinde, Dr. Mahesh Shinde, Dr. Sagar Thorat, Dr. Balasaheb Borade, Dr. Shrikant Nikam, Navnath Kakade, Ganesh Kamble, Pooja Fulare, Indrajeet, Mahendra Wagh, Sairam Veer, Dr Aakash Nidhankar, Sangram Dongre, Pavan, Manish, Avinash Jadhav, Minakshi Pawar, Amit, Nutan, Buddhabhushan, Pooja, Swapnil Halnor, Balaji, Sanjay, Ajay, Pavan, Jayesh, Aakash, Sharad, Jagjivin Sabane, Satish More, Dr. Shubhangi, Dr. Madhukar, Kailas, Priyanka, Samir, Sachin, Pradeep and many others for the cherished friendships and creating a wonderful atmosphere around me outside the lab.. Also, I would like to take this opportunity to thank all my childhood and college friends Shivhar Ambegave, Aakash Zalke, Sandip Mule, Sonu Wankhede, Ram Sadgeer, Ratnadeep Mali Patil, Balasaheb Gade, Rajesh Gade, Uday Suryawanshi, Kailash Malshette, Rameshwar Ankade, and also thanks to Shripat Daithanekar and Pradeep Desale for their help and support.

My family is always a source of inspiration and great moral support for me in perceiving my education, I am thankful to God for having such a supportive family. Words are insufficient to express my gratitude towards my family. I take this opportunity to express gratitude to my mother **Bharatbai** and father **Baliram Ankade** for their tons of love, sacrifice, blessings, unconditional support, and encouragement. I express my deep and paramount gratitude to my sister-in-law **Archana Ankade**, and brother **Namdev Ankade** who stood up behind me throughout my Ph.D. career and became my strong moral support. Without their constant support and encouragement, I could not stand with this dissertation. I love to thank my source of inspiration, my lovely niece **Prerna** and nephew **Shrirang** for their love and affection. I also extend my special thanks to a new member of my family, my beloved wife **Divya** for her unconditional support and motivation in the last stage of my Ph.D. career.

Above all, I owe it all to Almighty God for granting me the wisdom, health, and strength to undertake this research task and enabling me to its completion.


[Shidheshwar Baliram Ankade](#)

Abbreviations

Å	Angstrom
acac	Acetylacetonate
AcOH	Acetic acid
AdCOOH	1-Adamantanecarboxylic acid
aq	Aqueous
bathocuproine	2,9-Dimethyl-4,7-diphenyl-1,10-phenanthroline
bpy	2,2'-Bipyridine
BDMAE	Bis(2-dimethylaminoethyl) ether
BINOL	1,1'-Bi-2-naphthol
br s	Broad singlet
°C	Degree Celsius
Calcd	Calculated
Cat	Catalyst
cm	Centimeter
cod	1,5-cyclo-octadiene
Cy	Cyclohexyl
Cyp	Cyclopentyl
DCE	1,2-dichloroethane
dcype	1,2 Bis(dicyclohexylphosphino)ethane
DFT	Density functional theory
DIPEA	<i>N,N</i> -Diisopropylethylamine
DME	Dimethoxy ethane
DMA	<i>N,N</i> -dimethylacetamide
DMAP	4-Dimethylaminopyridine
DMF	<i>N,N</i> -dimethylformamide
DMSO	Dimethyl sulfoxide
<i>Dt</i> BEDA	<i>N,N'</i> -Di- <i>tert</i> -butyl ethylenediamine
dtbpy	4,4'-Di- <i>tert</i> -butyl bipyridine
dppen	<i>cis</i> -1,2-Bis(diphenylphosphino)ethylene
dppf	1,1'-Bis(diphenylphosphino)ferrocene
dppz	Dipyrido[3,2- <i>a</i> :2',3'- <i>c</i>]phenazine
dppbz	1,2-Bis(diphenylphosphanyl)benzene

equiv	Equivalent
EtOH	Ethanol
EtOAc	Ethylacetate
Galvinoxyl	2,6-Di- <i>tert</i> -butyl- α -(3,5-di- <i>tert</i> -butyl-4-oxo-2,5-cyclohexadien-1-ylidene)- <i>p</i> -tolylxy
HRMS	High resolution mass spectrometry
HFIP	Hexafluoro isopropanol
LiHMDS	Lithium bis(trimethylsilyl)amide
MALDI	Matrix Assisted Laser Desorption/ionization
MeSCOOH	2,4,6-trimethylbenzoic acid
NaHMDS	Sodium bis(trimethylsilyl)amide
Neocuproine	2,9-dimethyl-1,10-phenanthroline
<i>n</i> -Bu ₄ NBr	<i>n</i> -Tetrabutyl ammonium bromide
NMP	1-Methyl-2-pyrrolidone
NMR	Nuclear Magnetic Resonance
OTf	Trifluoromethanesulfonate
Pcyp ₃	Tricyclo pentyl phosphine
phen	1.10-Phenanthroline
PIP	2-Pyridinyl isopropyl
Piv	Pivalate
PMe ₃	Trimethyl phosphine
py	Pyridinyl
P(<i>i</i> Pr) ₃	<i>tri</i> -Isopropyl phosphine
<i>t</i> -AmOH	<i>tert</i> -Amyl alcohol
TBHP	<i>tert</i> -Butylhydroperoxide
TBAF	tetra- <i>n</i> -Butylammonium fluoride
TEMPO	(2,2,6,6-Tetramethylpiperidin-1-yl)oxyl
TMEDA	<i>N,N,N',N'</i> -Tetramethylethylenediamine
TFA	Trifluoroacetic acid
TFE	Trifluoroethanol
TIPS	Triisopropylsilyl
Xantphos	4,5-Bis(diphenylphosphino)-9,9-dimethylxanthene
XPS	X-ray photoelectron spectroscopy

Synopsis Report

	Synopsis of the thesis to be submitted to the Academy of Scientific and Innovative Research for the award of the degree of Doctor of Philosophy in Chemical Science
Name of the Candidate	Mr. Ankade Shidheshwar Baliram
Enrollment No. and Date	Ph. D. in Chemical Sciences (10CC18J26001); 1 st January 2018
Title of the Thesis	Iron and Nickel-Catalyzed Functionalization of Heteroarenes and Hydrogenation of Ketones
Research Supervisor	Dr. Benudhar Punji

1. Introduction

The thesis title is “**Iron and Nickel-Catalyzed Functionalization of Heteroarenes and Hydrogenation of Ketones**”. The thesis is divided into six different chapters. Chapter-1 deals with the detailed literature survey on employing 3d transition metal catalysts in the functionalization of heteroarenes and transfer hydrogenation of ketones. In particular, advances made with the late 3d transition metals such as iron, cobalt, nickel, and copper catalysts in selective C–H bond functionalization of heteroarenes are discussed. In addition, various methods for the functionalization of isatins and the implication of different pincer catalysts based on 3d metals for the transfer hydrogenation of ketones are described. Chapter-2 deals with the Ni(II)-catalyzed intramolecular C–H/C–H oxidative coupling in indoles *via* chelation assistance for the synthesis of biologically relevant indolones. Detailed mechanistic studies have been performed, and a plausible catalytic cycle is proposed. Chapter-3 describes the nickel-catalyzed regioselective C–H alkylation of heteroarenes using alkene as a coupling partner. Chapter-4 presents the iron-catalyzed synthesis of 3-substituted 3-amino oxindoles with the construction of stereogenic quaternary center at the C3 position. A detail mechanistic investigation has performed to elucidate the reaction mechanism. Chapter-5 contains the synthesis of NNN-based pincer nickel complexes for the transfer hydrogenation of ketones using isopropanol as a hydrogen source. Chapter-6 presents overall summary of the thesis work, followed by the future direction related to the field.

2. Statement of the Problem

Heteroarenes are the privileged structural motif in many biologically active compounds and natural products. Therefore, significant advances have been made in the selective functionalization of heteroarenes employing noble metal catalysts i.e. 4d/5d transition metal



Dr. Benudhar Punji (Supervisor)



Shidheshwar B. Ankade (Student)

Synopsis Report

catalysts. These rare metals are high in cost and are naturally limited, affecting their usage in the sustainable synthesis of functionalized heteroarenes. Owing to the sustainability and cost advantage, the 3d transition metal catalyst has been substantially explored for the selective functionalization of heteroarenes. However, the harsh reaction conditions and relatively low stability of involved metal-organic intermediates, make the catalyst system more challenging to control, thus leading to undesired side reactions. Thus, there is an enormous demand to develop efficient protocols for heteroarene functionalization using 3d transition metal catalysts. Furthermore, various phosphine-based chiral ligands along with 3d metals have been employed for enantioselective hydrogenation of ketones to get the chiral alcohols. However, the synthesis of sensitive phosphine ligands needs special inert atmosphere techniques and handling of synthesized phosphine ligands is difficult. Thus, there is a need to develop suitable phosphine-free chiral complexes for the synthesis of chiral alcohols.

3. Objectives

As discussed in the above section, the functionalization of heteroarene is restricted to the use of precious noble metals or limited to harsh reaction conditions and the use of sensitive reagents. Though there are many challenges associated with 3d metals as catalysts, the use of a suitable ligand during the catalysis can control the metal reactivity and selectivity. Thus, our objective is to look into the problem related to these precedented approaches and attempt to resolve those by developing suitable catalytic systems to achieve mild reaction conditions by employing the earth-abundant 3d transition metals.

4. Methodology and Result

Chapter 2. Ni(II)-Catalyzed C–H/C–H Oxidative Coupling: Facile Synthesis of Indeno-Indolone and 3,4-Dihydro-Indolone Derivatives

The indole represents a privileged structural motif in many biologically active compounds and natural products. In particular, polycyclic derivatives of indole, possessing five- and six-membered rings, are of great significance due to their enormous pharmacological activities. Precedented approaches are limited to the use of noble metal catalysts. Thus, in this chapter, nickel(II)-catalyzed intramolecular C(sp²)-H/C(sp³)-H and C(sp²)-H/C(sp²)-H oxidative couplings in indoles are demonstrated *via* chelation assistance (Scheme 1).¹ This reaction provided a direct approach for synthesizing diversely functionalized, pharmaceutically



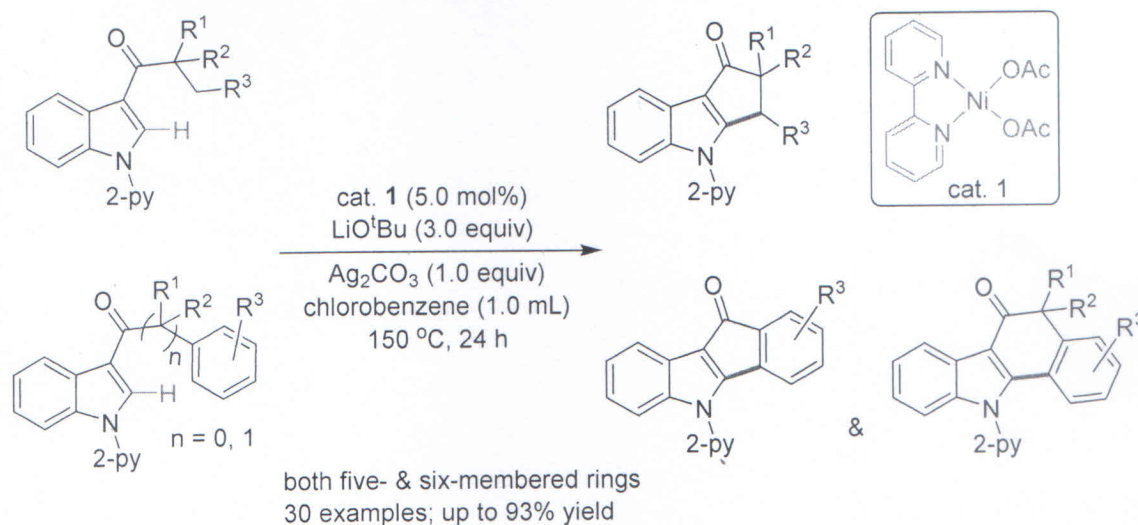
Dr. Benudhar Punji (Supervisor)



Shidheshwar B. Ankade (Student)

Synopsis Report

relevant hydrocyclopentaindolones, hydrocarbazoles, and indenoindolones with the tolerance of sensitive functionalities by employing an air-stable nickel complex, (bpy)Ni(OAc)₂. The oxidative coupling in diverse indoles suggested the intramolecular C(sp²)-H/C(sp³)-H coupling exclusively proceeded through a six-membered nickelacycle providing five-membered ring products, whereas the C(sp²)-H/C(sp²)-H coupling followed a six-membered or a seven-membered nickelacycle affording five- or six-membered cyclized products.



Scheme 1. Nickel-catalyzed intramolecular C(sp²)-H/C(sp³)-H and C(sp²)-H/C(sp²)-H oxidative coupling.

Initial mechanistic studies highlighted the coupling reaction proceeds *via* a single-electron transfer (SET) pathway. An extensive mechanistic investigations including the controlled study, kinetic analysis, deuterium labeling experiments, and DFT calculations supported a Ni(II)/Ni(III) pathway for the oxidative coupling comprising the rate-limiting reductive elimination process. Furthermore, the intramolecular oxidative coupling was demonstrated with a gram-scale reaction, and the 2-pyridinyl directing group was smoothly removed to establish the synthetic utility of the protocol.

Chapter 3. Regioselective C-H Alkylation of Heteroarenes with Alkenes Using Nickel as a Catalyst

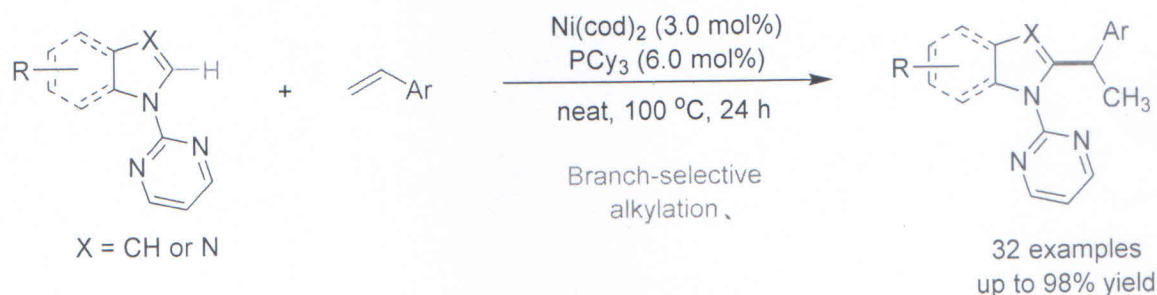
Alkylated heteroarenes are privileged structural motifs with diverse applications in the pharmaceutical and perfumery industries. The alkyl group in biologically relevant heteroarenes

Dr. Benudhar Punji (Supervisor)

Shidheshwar B. Ankade (Student)

Synopsis Report

enhances the lipophilic character of the designed molecules. Various alkylating reagents have been employed for the C–H bond alkylation of heteroarenes.² Particularly, alkylation using alkene as a coupling partner is a straightforward and atom-economical process that proceeds through hydroarylation protocol. Precedented approaches are restricted to the alkylation of highly activated heteroarenes with aromatic arenes using a nickel catalyst. In this chapter, solvent-free regioselective C–H alkylation of heteroarenes with alkenes in the presence of nickel catalyst is discussed (Scheme 2). The coupling of diverse aromatic alkenes with heteroarenes including indole, imidazole, and benzimidazole derivatives provided moderate to excellent yields of alkylated products. This nickel-catalyzed reaction exclusively provided the Markovnikov selective alkylated products.



Scheme 2. Nickel-catalyzed regioselective C–H alkylation of heteroarenes.

Chapter 4. Iron-Catalyzed Synthesis of 3-substituted 3-Amino Oxindoles: An Efficient Route to the Construction of Quaternary Stereocenter

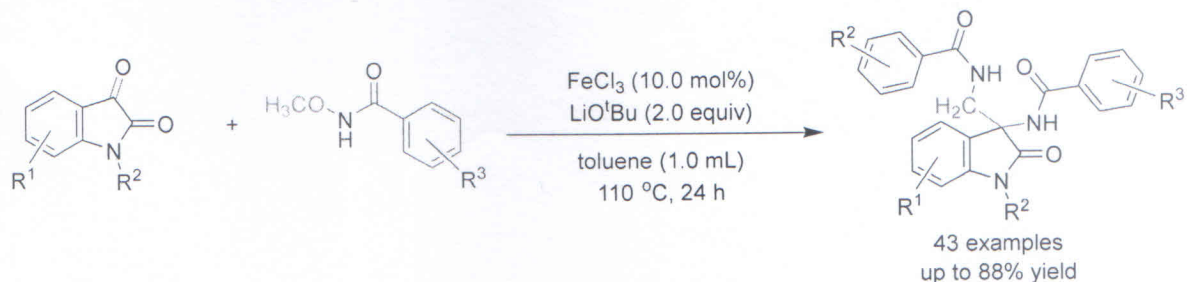
An oxindole skeleton bearing a stereogenic quaternary center at C-3 position, such as 3-substituted-3-amino oxindole, has been considered as privileged scaffold in a variety of biologically active natural products and pharmaceutically important compounds. Thus, the direct synthesis of 3-substituted 3-amino oxindole, particularly oxindoles containing amide functionality at C-3 position is not precedented yet. This chapter describes the straightforward synthesis of 3-substituted-3-amino-2-oxindoles with the generation of a stereogenic quaternary center in the presence of highly abundance and inexpensive iron(III) catalyst (Scheme 3). The coupling of *N*-methoxy benzamides with isatin derivatives provided the various biologically relevant 3-substituted-3-amino oxindoles in the presence of a simple iron(III) salt. This protocol is readily applicable for the construction of tetrasubstituted carbon centers using

Dr. Benudhar Punji (Supervisor)

Shidheshwar B. Ankade (Student)

Synopsis Report

diversely substituted *N*-methoxy benzamides and isatins to afford desired products in moderate to good yields. This reaction tolerates diverse functionalities such as halides, alkenyl, ether, heteroaryls, and gave moderate to good yield of the desired products.



Scheme 3. Iron-catalyzed synthesis of 3-substituted 3-amino oxindoles.

An extensive mechanistic investigation revealed that the reaction proceeds *via* the formation of isatin ketimine and *N*-(hydroxymethyl)benzamide intermediates. Controlled experiments including deuterium labeling studies suggested an *N*-methoxy group of benzamide is a source of methylene group in products. The scalability of this protocol was demonstrated with a gram-scale reaction and further functionalization of 3-substituted 3-amino oxindole was carried out. This reaction proceeds *via* a single-electron transfer (SET) pathway.

Chapter 5. Synthesis of Oxazoline Based Pincer Nickel Complexes: Implication towards Transfer Hydrogenation of Ketones

This chapter describes the synthesis and characterization of a series of NNN-based chiral and achiral pincer nickel complexes and their application toward the transfer hydrogenation of the ketones using isopropanol as a hydrogen source.³ Both the achiral [(^{R'2}-OxNNN^{Et2})-H] and chiral [(*R*)-(^{R'1}-OxNNN^{Et2})-H] ligands were synthesized in good yields. Treatment of these ligands with (DME)NiCl₂ afforded the amido-pincer nickel complexes, (^{R'2}-OxNNN^{Et2})NiCl and [(*R*)-(^{R'1}-OxNNN^{Et2})NiCl] under mild conditions. All the ligand precursors and nickel complexes were thoroughly characterized by the NMR spectroscopy, HRMS, or elemental analysis. The single-crystal X-ray diffraction study elucidated the molecular structure of complexes (OxNNN^{Et2})NiCl, (*R*)-(PhCH₂-OxNNN^{Et2})NiCl and (*R*)-(iPrCH₂-OxNNN^{Et2})NiCl. The synthesized nickel complexes were employed for the transfer hydrogenation of ketones using isopropanol as a hydrogen source (Scheme 4). The range of functional groups such as -F, -Cl, -Br, -OMe were tolerated under the reaction condition and provide respective products in high yield.

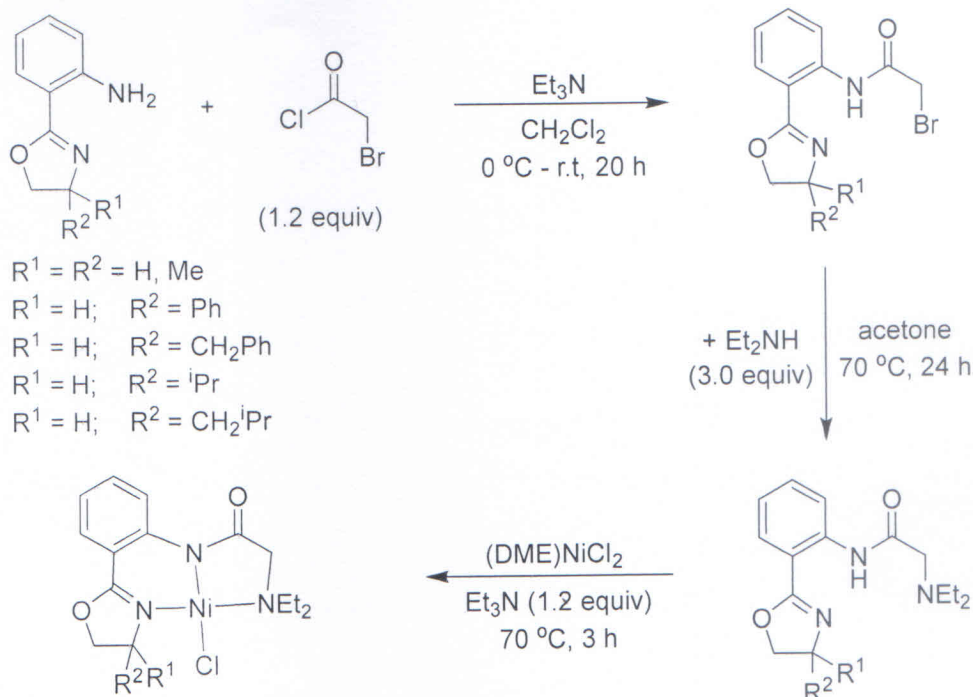
Dr. Benudhar Punji (Supervisor)

Shidheshwar B. Ankade (Student)

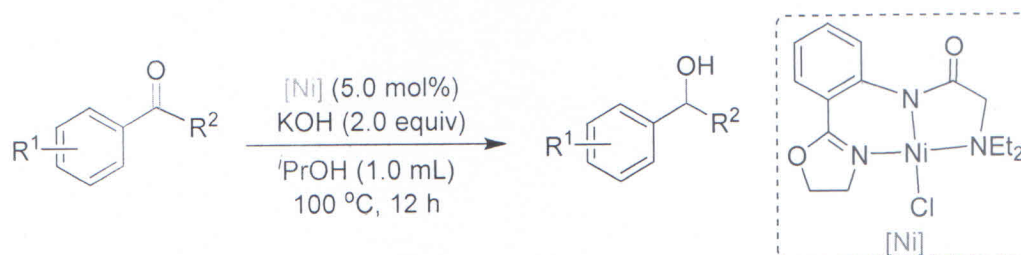
Synopsis Report

Highly bulky ketones, heteroarene-substituted ketones, and aliphatic ketones remained unreactive under the optimized reaction condition. Despite many attempts, we could not achieve enantioselective hydrogenation of ketones, which needs further investigation.

(a) Synthesis of chiral NNN-oxazolonyl ligands and nickel complexes.



(b) Nickel-catalyzed transfer hydrogenation of ketones.



Scheme 4. Oxazoline-based nickel complexes for the transfer hydrogenation of ketones.

5. References

1. Ankade, S. B.; Samal, P. P.; Soni, V.; Gonnade, R. G.; Krishnamurthy, S.; Punji, B., *ACS Catal.* **2021**, *11*, 12384-12393.
2. Ankade, S. B.; A. B. Shabade.; V. Soni.; and B. Punji, *ACS Catal.* **2021**, *11*, 3268-3292.
3. Jagtap, R. A.; Ankade, S. B.; Gonnade, R. G.; and B. Punji, *New J. Chem.* **2021**, *45*, 11927-11936

Dr. Benudhar Punji (Supervisor)

Shidheshwar B. Ankade (Student)

TABLE OF CONTENTS

	Page No.
Chapter 1. Introduction	1
1.1 C–H /C–H Oxidative Coupling of Heteroarenes	3
1.1.1 Iron-Catalyzed Oxidative Coupling	4
1.1.2 Cobalt-Catalyzed Oxidative Coupling	5
1.1.3 Nickel-Catalyzed Oxidative Coupling	7
1.1.4 Copper-Catalyzed Oxidative Coupling	11
1.2 C–H Bond Alkylation of Heteroarenes	19
1.2.1 C–H Bond Alkylation Using Alkyl Halides	20
1.2.1.1 Manganese-Catalyzed Alkylation	21
1.2.1.2 Iron-Catalyzed Alkylation	22
1.2.1.3 Cobalt-Catalyzed Alkylation	24
1.2.1.4 Nickel-Catalyzed Alkylation	25
1.2.2 C–H Bond Alkylation Using Alkenes	28
1.2.2.1 Iron-Catalyzed Alkylation	28
1.2.2.2 Cobalt-Catalyzed Alkylation	29
1.2.2.3 Nickel-Catalyzed Alkylation	31
1.2.2.4 Copper-Catalyzed Alkylation	33
1.3 Synthesis of 3,3-Disubstituted 3-Amino Oxindoles	33
1.3.1 Nickel-Catalyzed Synthesis of 3-Amino Oxindoles	35
1.3.2 Copper-Catalyzed Synthesis of 3-Amino Oxindoles	35
1.4 Hydrogenation of Ketone	36
1.4.1 Iron-Catalyzed Hydrogenation of Ketones	38
1.4.2 Manganese-Catalyzed Hydrogenation of Ketones	38
1.5 References	39
Chapter 2. Ni(II)-Catalyzed C–H/C–H Oxidative Coupling: Facile Synthesis of Indeno-Indolone and 3,4-Dihydro-Indolone Derivatives	
2.1 INTRODUCTION	53
2.2 RESULTS AND DISCUSSION	55

TABLE OF CONTENTS

2.2.1	Optimization of Reaction Condition	55
2.2.2	Effect of <i>N</i> -Substituents on C–H/C–H Oxidative Cyclization	58
2.2.3	Substrate Scope for C–H/C–H Intramolecular Oxidative Cyclization	59
2.2.4	Gram-Scale Synthesis and Synthesis of Free- <i>NH</i> 3,4-Dihydro- Indolone	65
2.2.5	Mechanistic Aspects	65
2.2.5.1	External Additive Experiments and Radical Clock Experiment	65
2.2.5.2	Electronic Effect Study	66
2.2.5.3	H/D Scrambling Experiment	67
2.2.5.4	Kinetic Isotope Effect (KIE) Study	68
2.2.5.5	DFT-Based Calculations	70
2.2.6	Probable Catalytic Cycle	73
2.3	CONCLUSION	74
2.4	EXPERIMENTAL SECTION	75
2.4.1	Procedure for Synthesis of (bpy)Ni(OAc) ₂	75
2.4.2	Synthesis and Characterization of Starting Compounds	76
2.4.3	Synthesis of Deuterated Compounds	99
2.4.4	Procedure for Oxidative Cyclization and Characterization Data	101
2.4.5	2D NMR Spectrum Analysis of 24	119
2.4.6	Procedure for Removal of Directing Group	119
2.4.7	Mechanistic Experiments	121
2.4.7.1	Procedure for External Addition Experiment and Radical Clock Experiment	121
2.4.7.2	Representative Procedure for Electronic Effect Study	121
2.4.7.3	Kinetic Isotope Effect Study	122
2.4.7.4	DFT Energy Calculations	123
2.4.8	X-ray Structure Analysis	125
2.4.9	¹ H and ¹³ C NMR Spectra of Selected Cyclized Compounds	130
2.5	REFERENCES	136

Chapter 3. Regioselective C–H Alkylation of Heteroarenes with Alkenes using Nickel as a Catalyst

TABLE OF CONTENTS

3.1	INTRODUCTION	143
3.2	RESULTS AND DISCUSSION	144
3.2.1	Optimization of Reaction Conditions	144
3.2.2	Effect of Directing Groups on C–H Alkylation	146
3.2.3	Substrate Scope for C–H Alkylation	147
3.2.4	Large-Scale Synthesis of 3aa	151
3.2.5	Removal of Directing Group and Functionalization	151
3.2.6	Mechanistic Aspects	152
3.2.6.1	External Additive Experiments	152
3.2.6.2	Deuterium Labeling Experiments	152
3.3	CONCLUSION	154
3.4	EXPERIMENTAL SECTION	155
3.4.1	Procedure for C–H Alkylation and Characterization Data	156
3.4.2	Procedure for Removal of Directing Group	172
3.4.3	Procedure for Synthesis of compound 9	172
3.4.4	Mechanistic Experiments	173
3.4.4.1	Procedure for External Additive Experiments	173
3.4.4.2	Procedure for Deuterium Labeling Experiments	174
3.4.5	¹ H and ¹³ C NMR Spectra of Alkylated Compounds	176
3.5	REFERENCES	184
Chapter 4. Iron-Catalyzed Synthesis of 3,3-disubstituted 3-Amino Oxindoles: An Efficient Route to the Construction of Quaternary Stereocenter		
4.1	INTRODUCTION	187
4.2	RESULTS AND DISCUSSION	188
4.2.1	Optimization of Reaction Conditions	188
4.2.2	Substrate Scope for Synthesis of 3-Amino-2-Oxindoles	192
4.2.2.1	Substrate Scope with Benzamides	192
4.2.2.2	Substrate Scope with Isatins	192
4.2.3	Gram Scale Synthesis and Derivatization of 3-Amino Oxindoles	195
4.2.4	Mechanistic Aspects	196
4.2.4.1	External Additive Experiments	196

TABLE OF CONTENTS

4.2.4.2	Deuterium Labeling and Controlled Experiments	197
4.2.4.3	DFT-Based Calculations	202
4.2.5	Probable Catalytic Cycle	204
4.3	CONCLUSION	206
4.4	EXPERIMENTAL SECTION	207
4.4.1	Synthesis and Characterization of Starting Compounds	207
4.4.2	Synthesis of 3-Amino Oxindoles and Characterization Data	208
4.4.3	Procedure for Removal of <i>N</i> -Me Group	235
4.4.4	Procedure for Partial Reduction of C-3 Aminated Oxindole	236
4.4.5	Procedure for Synthesis of <i>N</i> -(3-(aminomethyl)-1-methyl-2-oxoindolin-3-yl)benzamide	237
4.4.6	Mechanistic Experiments	238
4.4.6.1	Procedure for External Addition Experiment	238
4.4.6.2	Deuterium Labeling Experiments	239
4.4.6.3	Procedure for Controlled Experiments	239
4.4.6.4	Synthesis and Characterization of Intermediates	240
4.4.6.5	Procedure for Reaction of Intermediates	241
4.4.6.6	DFT Energy Calculations	242
4.4.7	X-ray Structure Analysis	243
4.4.8	MALDI-TOF Spectra of Intermediates	246
4.4.9	¹ H and ¹³ C NMR Spectra of Aminated Compounds	248
4.5	REFERENCES	255
Chapter 5. Oxazoline Based Pincer Nickel Complexes: Implication towards Transfer Hydrogenation of Ketones		
5.1	INTRODUCTION	259
5.2	RESULTS AND DISCUSSION	260
5.2.1	Synthesis and Characterization of (R ¹ -OxNNN ^{Et2})-H Ligands and Nickel Complexes	260
5.2.2	Transfer Hydrogenation of Ketones	266
5.2.3	Substrate Scope for the Transfer Hydrogenation of Ketones	267
5.2.4	Probable Catalytic Cycle	269
5.3	CONCLUSIONS	270

TABLE OF CONTENTS

5.4	EXPERIMENTAL SECTION	270
5.4.1	Procedure for Synthesis of Ligand Precursor	271
5.4.2	Synthesis of (^{R-Ox} NNN ^{Et2})-H ligands	273
5.4.3	Synthesis nickel complexes (^{R'-Ox} NNN ^{Et2})NiCl	276
5.4.4	Representative procedure for transfer hydrogenation of ketones	278
5.4.5	X-ray Structure Analysis	279
5.4.6	¹ H and ¹³ C NMR Spectra of Nickel Complexes	281
5.4.7	¹ H and ¹³ C NMR Spectra of Hydrogenated Compound	286
5.5	REFERENCES	287
Chapter 6. Summary and Outlook		
6.1	Summary	294
6.2	Outlook	295
	Abstract	296
	List of Publication	297
	List of Conference	299
	Publications Copy	300

Chapter-1

Introduction

Heteroarenes are the privileged structural motifs that have been paid significant attention due to their existence in many biologically active compounds and natural products. Among the various class of heteroarenes, indole and isatin represent important core moiety, exists in diverse biologically active molecules and natural products, including functional materials.¹⁻³ Considering the importance of indole and its derivatives, catalytic functionalization of indoles and isatins is crucial for both the academic as well as industrial research. The traditional cross-coupling has found extensive applications in academia and across industries, however, the protocol still needs prefunctionalized organometallic substrates, that involve multi-steps synthesis and lead to the formation of stoichiometric metallic-waste.⁴

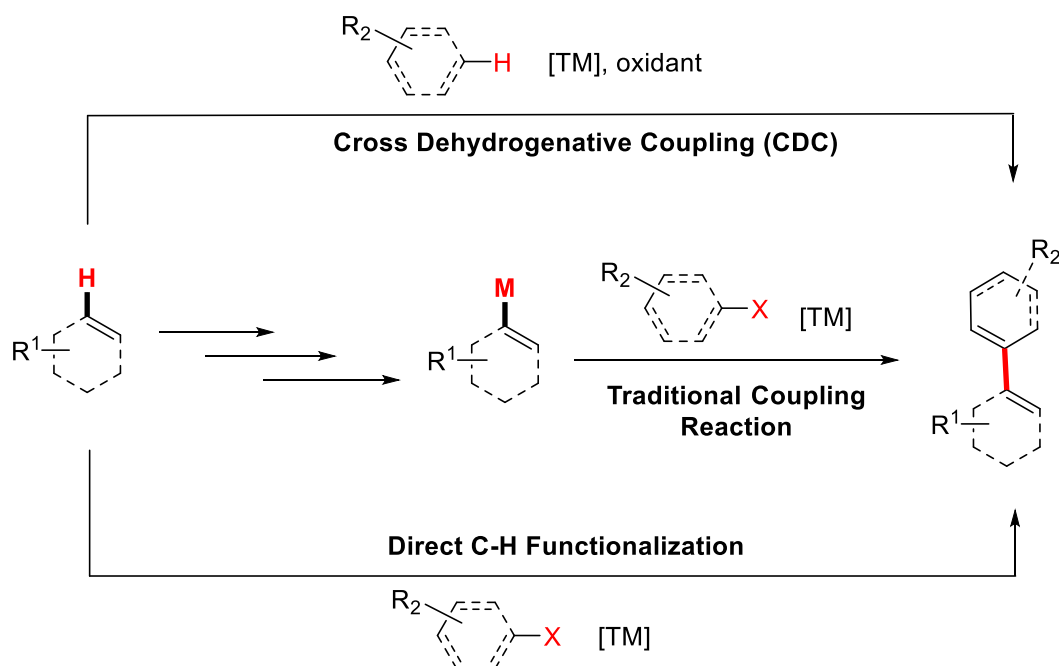
The transition-metal-catalyzed C–H bond functionalization of indoles and related heteroarenes has appeared as a powerful and sustainable surrogate to the traditional coupling reactions because such a process overcomes the prefunctionalization step and avoids the formation of organometallic wastes.⁵⁻⁷ Therefore, various effective protocols were flourished for the synthesis of functionalized heteroarenes employing noble metal catalysts based on Pd, Rh, and Ru catalysts.⁵⁻¹⁰ However, the use of precious metal catalysts for such transformations is restricted because of their high cost and low abundance. Recently, the 3d transition metals have captivated remarkable attention in the functionalization of heteroarenes due to their low toxicity and cost-effective nature. The 3d transition metal catalysts have been less scrutinized as compared to 4d and 5d metal catalysts for such transformations. This is an account of the less reactivity of many first-row transition metal catalysts and the involvement of less stable organometallic intermediates. However, in certain cases, the low stability of metal-carbon intermediate in the case of 3d metal compared to their 4d analog provided exceptional reactivity.¹¹ Notably, the high reactivity of the involved intermediate makes the catalytic system more difficult to control, consequently, it leads to unsolicited side reactions. Thus, the use of suitable ligands along with 3d metal precursors can control the selectivity as well as undesired reactivities.

In addition to the C–H functionalization, the hydrogenation of ketones to alcohols is an important chemical transformation in organic synthesis and pharmaceutical industries.¹² Chiral alcohols are important synthetic intermediates in medicinal chemistry, and fine chemicals.¹³⁻¹⁵ In past few year, noble metal catalysts have been extensively employed for enantioselective hydrogenation of ketones to get the chiral alcohols.¹⁶⁻²⁵ However, the 3d transition metal catalysts were rarely studied for this transformations. In this chapter, the comprehensive literature reports of the 3d transition metal-catalyzed functionalization of heteroarenes and hydrogenation of ketones were summarized. Particularly, the first-row metal-catalyzed

oxidative coupling of heteroarenes alkylation of indoles, functionalization of isatins, and hydrogenation of ketones are discussed.

1.1 C–H/C–H OXIDATIVE COUPLING

The C–H bond activation of heteroarenes catalyzed by transition metal catalysts is a powerful and attractive method. Functionalized heteroarenes are the key motif of organic compounds with diverse applications in medicinal chemistry and material sciences. Traditionally, transition metal catalysts have been employed for C–H functionalization of heteroarenes using pre-functionalized substrates.²⁶⁻²⁹ Alternately, C–H bond functionalization strategy significantly reduces the number of steps and minimizes the formation of organometallic waste as a byproduct, however, this method requires one of the prefunctionalized or preactivated substrate as a coupling partner.^{8,30-37} More recently, transition metal-catalyzed C–H/C–H oxidative coupling has been established as an important tool for building complex molecules from simple precursors,³⁸⁻⁴² as it does not necessitate the preactivation/prefunctionalization of substrates (Scheme 1.1).



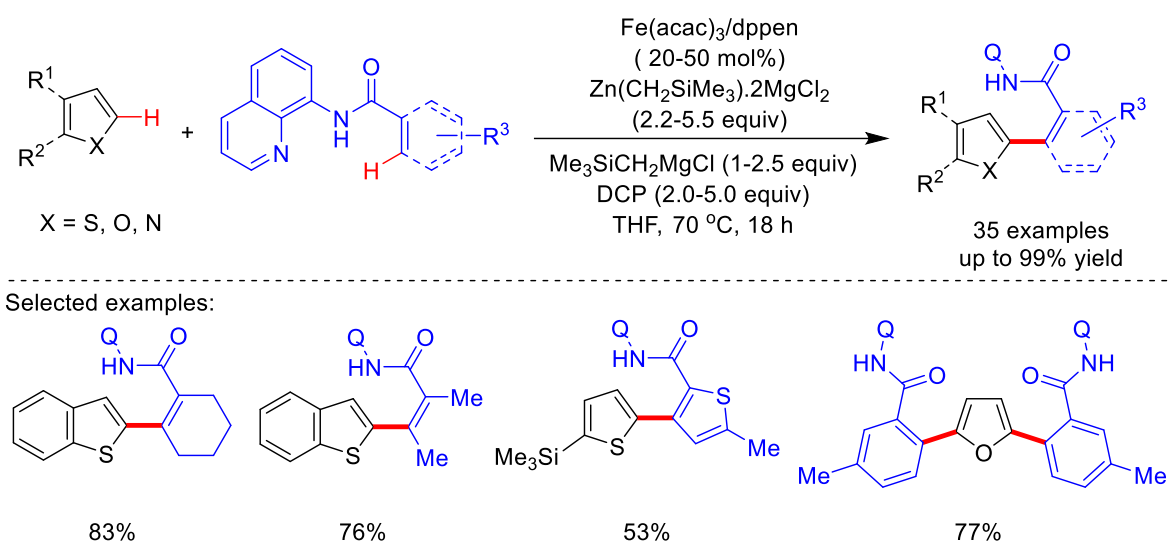
Scheme 1.1. Comparison between traditional coupling, C–H bond functionalization, and CDC reactions.

Remarkable progress have been achieved for the oxidative coupling of heteroarenes employing noble metal catalysts.^{10,43-56} Owing to the sustainability and cost advantage,⁵⁷⁻⁶⁸ the 3d-metal

catalyst for C(sp²)-H/C(sp²)-H coupling has been substantially explored.^{42,69-74} However, the coupling of a more strenuous C(sp³)-H bond continues to remain challenging.^{75,76} This section describes various oxidative coupling reactions employing 3d transition metal catalysts.

1.1.1 Iron-Catalyzed C-H/C-H Oxidative Coupling

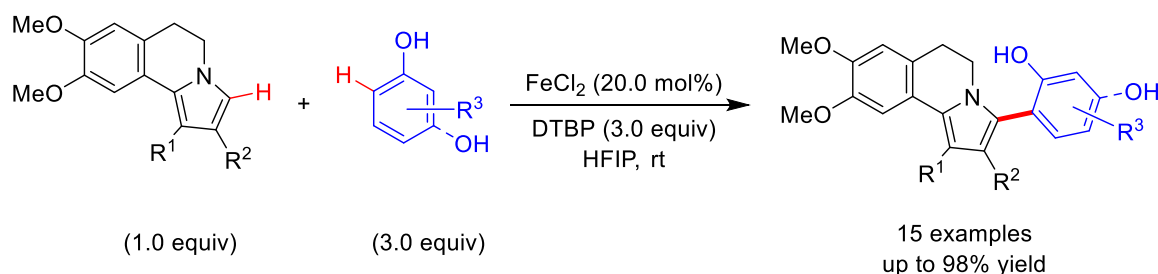
Iron is an inexpensive, highly abundant, and relatively less toxic transition metal that has been used for various chemical transformations.⁷⁷⁻⁷⁹ The notable achievement has been gained in the iron-catalyzed C-H bond functionalization of heteroarenes.⁸⁰⁻⁸³ However, the oxidative coupling using iron as a catalyst is extremely limited. Nakamura described the oxidative coupling of thiophene with benzamide derivatives using bidentate chelation assistance catalyzed by an iron catalyst (Scheme 1.2).⁸⁴ Other heteroarenes, including benzofuran, pyrazole, and furans were smoothly reacted with various benzamide derivatives provided high yields of desired products. Mechanistic studies reveal the reaction follows sequential two-fold C-H activation on the iron(III) species.



Scheme 1.2. Iron-catalyzed coupling of heteroarenes with benzamides.

A dihydropyrrolo[2,1-*a*]isoquinoline is considered as an important structural framework due to its existence in pharmaceutically important compounds and bioactive natural products. Thus, the functionalization of their derivatives is most desirable. Cui has presented an iron-catalyzed protocol for The coupling of dihydropyrrolo[2,1-*a*]isoquinoline with phenols was demonstrated by Cui using an iron catalyst (Scheme 1.3).⁸⁵ A range of functionalized dihydropyrrolo[2,1-*a*]isoquinolines were synthesized using FeCl₂/DTBP catalytic system at

room temperature. The reaction involves the radical cation of heteroarene as the key intermediate. In 2016, Xia group reported the dimerization of indoles employing an iron catalyst and DDQ as an oxidant.⁸⁶ This protocol is also applicable to the synthesis of moschamine-related alkaloids.

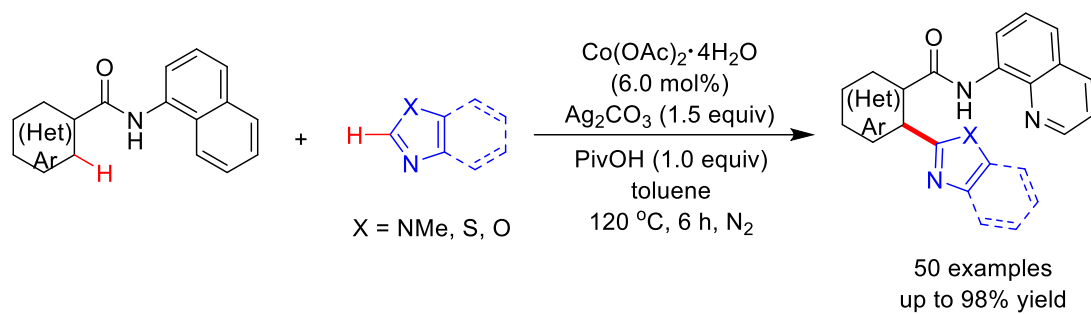


Scheme 1.3. Fe(II)-catalyzed oxidative coupling of heteroarene with phenols.

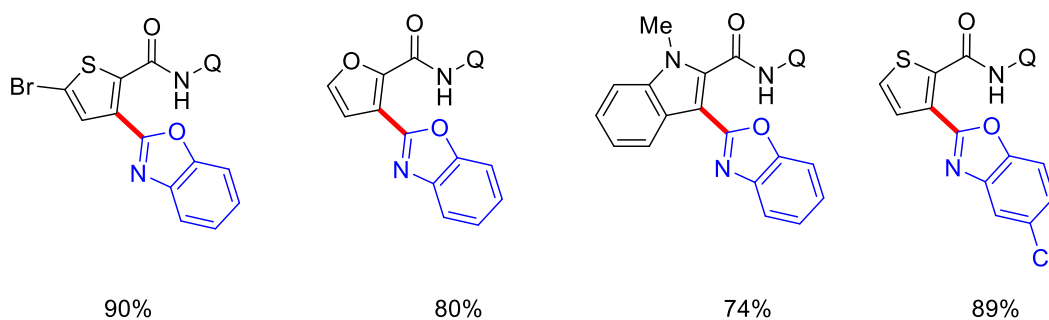
1.1.2 Cobalt-Catalyzed C–H/C–H Oxidative Coupling

Being one of the biologically relevant and less expensive transition metal, cobalt has been substantially explored in C–H functionalization reaction.^{87,88} Cobalt catalysts have been employed for the C–H bond functionalization of hetero(arenes) under relatively mild reaction conditions *via* a chelation assistance strategy.⁸⁹⁻⁹¹ However, the cross-oxidative coupling of heteroarenes remains challenging due to the competitive homocoupling vs heterocoupling reactions. In 2016, You group described the bidentate chelation-assisted coupling of 1,3-azoles with various heteroarenes (Scheme 1.4).⁷¹ The reaction tolerated the various synthetic important functionalities under the reaction conditions using Ag_2CO_3 as a renewable oxidant. Preliminary mechanistic studies reveal the reaction follows the SET pathway.

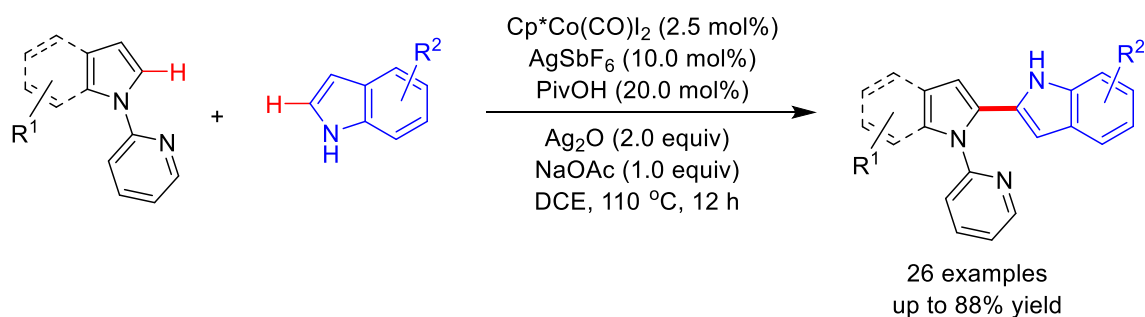
Li group reported the coupling of *N*-(2-pyridyl)indole with free *NH* indoles using cobalt catalyst through monodentate chelation-assistance (Scheme 1.5).⁶⁴ A range of diversely substituted indoles were participated in this cross-coupling to give good yields and excellent selectivities with the tolerance of sensitive functionalities. The use of free *NH* indoles was crucial for this reaction, and *N*-substituted indoles were unreactive under this protocol. A KIE study highlighted the C–H bond cleavage of the C-3 position of free indole plays a crucial role in this reaction and involved in the rate-limiting step. This reaction proceeds through Co(I)/Co(III) pathway and involves the migration of the cobalt-carbon bond from C-3 position to C-2 position of free indoles (Figure 1.1).



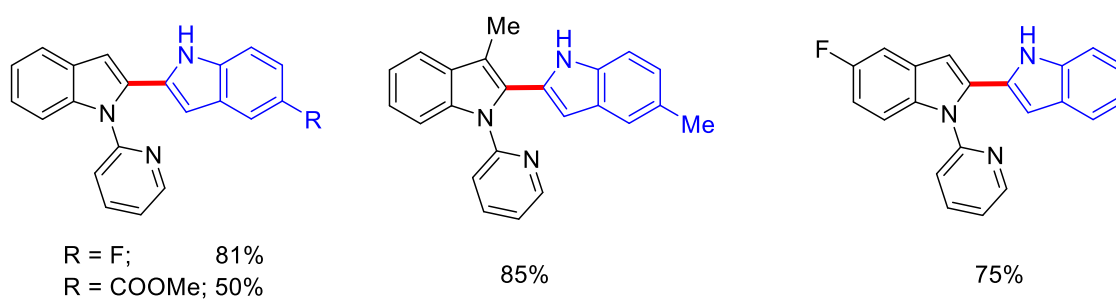
Selected examples:



Scheme 1.4. Co-catalyzed cross-oxidative coupling of heteroarenes.



Selected examples:



Scheme 1.5. Co-catalyzed cross-coupling of distinct indoles.

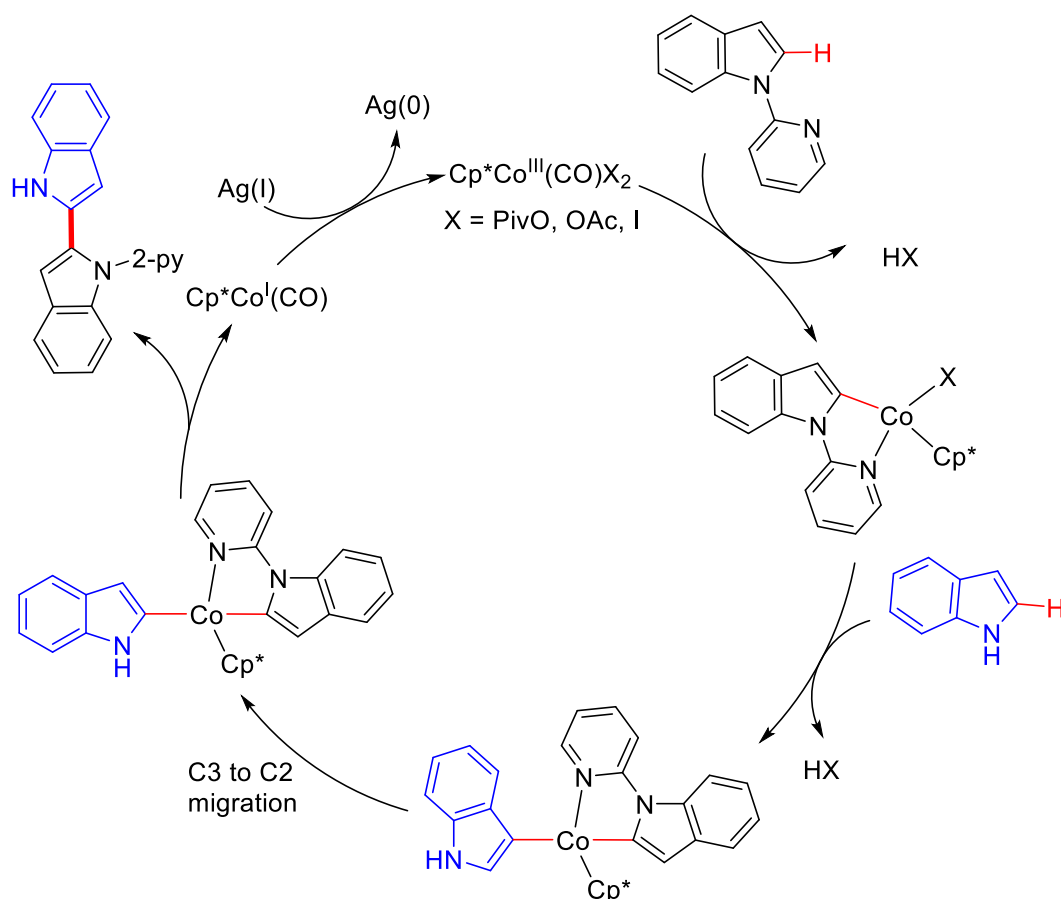
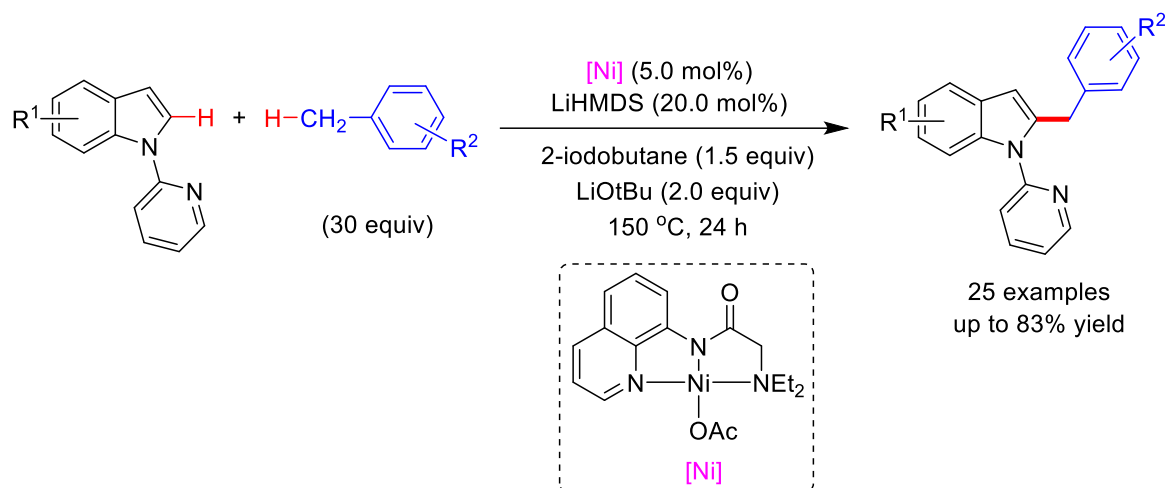


Figure 1.1. Possible catalytic cycle for cross-coupling of indoles.

1.1.3 Nickel-Catalyzed C–H/C–H Oxidative Coupling

Nickel is an earth-abundant metal that has been utilized for the direct C–H functionalization reactions.⁹²⁻⁹⁵ Significant progress has been achieved for the coupling of arenes or heteroarenes with organometallic reagents or (hetero)aryl(pseudo)halides to synthesize (hetero)biaryl compounds.⁹⁶⁻⁹⁹ However, the CDC reaction is attractive as it does not need the preactivated/prefunctionalized substrates. Cai demonstrated nickel-catalyzed C(sp³)–H coupling of 1,4-dioxane with C-2 and C-3-positions of indoles using DTBP as the oxidant.¹⁰⁰ Interestingly, the use of nickel precursor decides the selectivity in this reaction. The reaction using Ni(acac)₂ provided the C-3 coupled product whereas NiF₂ provided the C-2 coupled products. Punji group found that a Ni(II) precatalyst can effectively catalyze the coupling of indoles with C(sp³)–H bond of toluene derivatives (Scheme 1.6).¹⁰¹ A range of indoles could be coupled with diverse toluenes using of 2-iodobutane as a mild oxidant. Notably, an excess of C(sp³)–H containing partner is used in these reactions to favor the intermolecular coupling entropically. Detailed mechanistic studies highlighted the reaction proceeds through the SET process (Figure 1.2).



Scheme 1.6. Ni(II)-catalyzed coupling of indole with diverse toluenes.

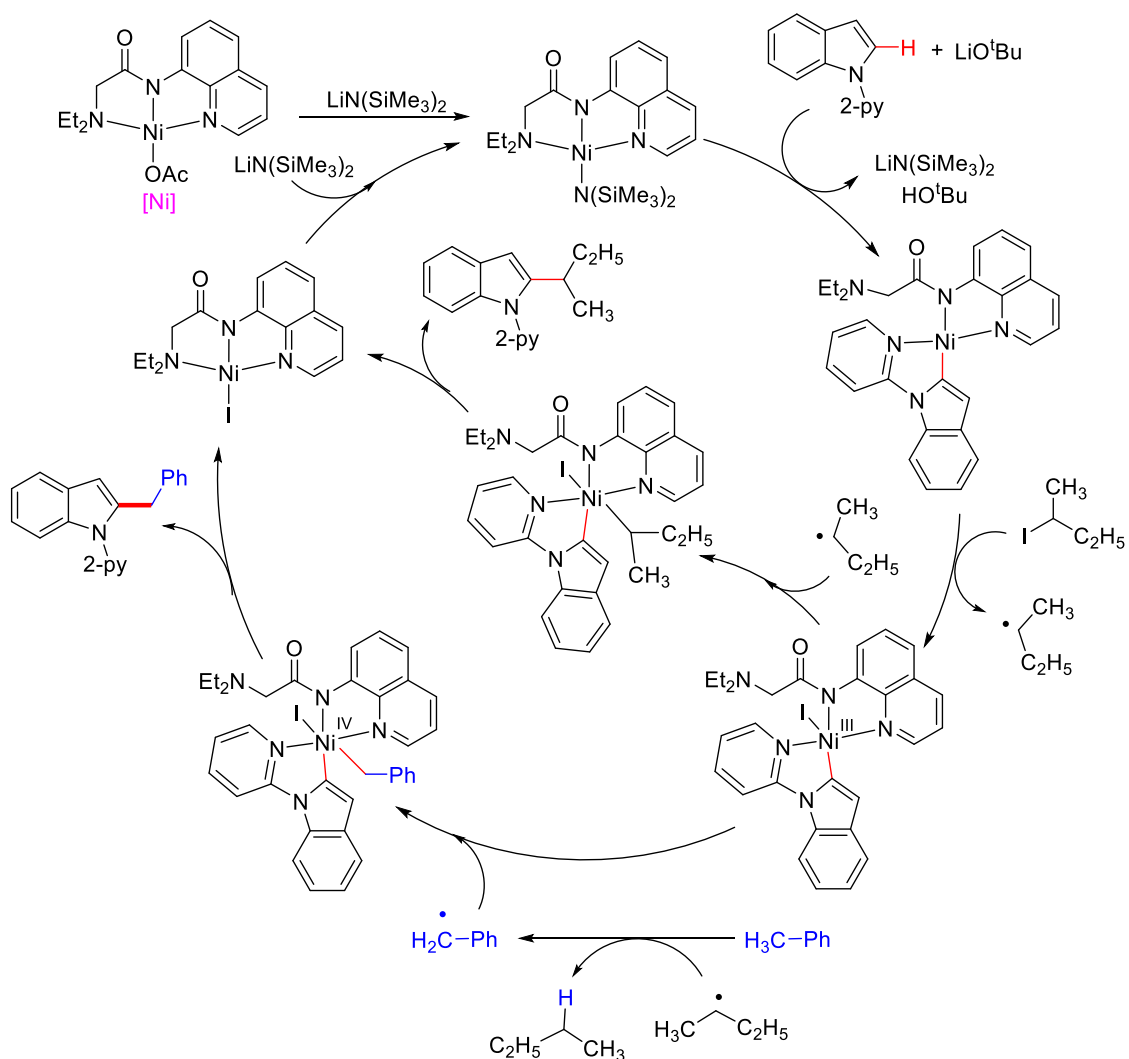
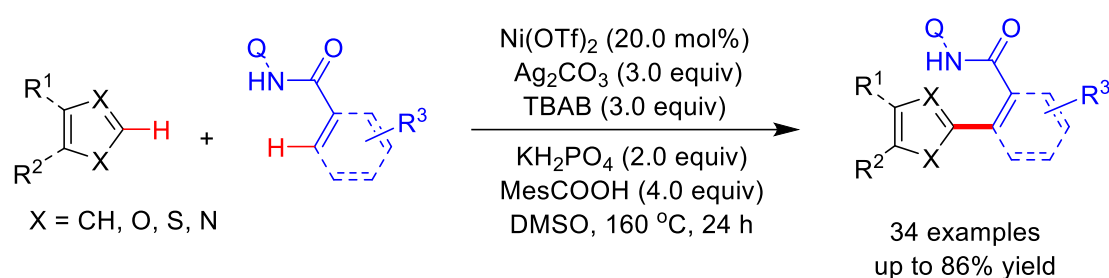
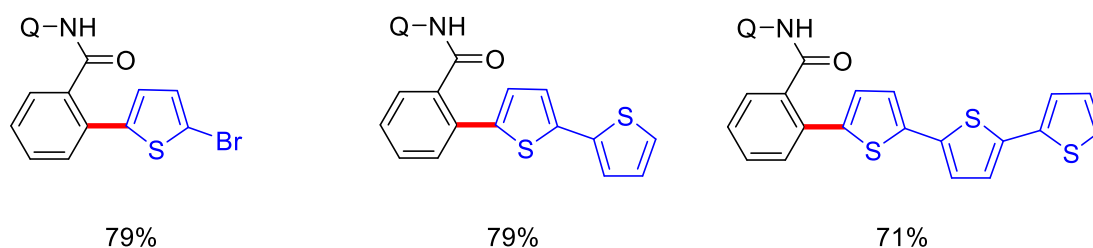


Figure 1.2. Plausible catalytic cycle for Ni-catalyzed oxidative coupling.

Similarly, the nickel-catalyzed oxidative coupling of β -azolyl propanoic acid derivatives with benzothiazoles demonstrated by You and co-workers.¹⁰² The coupling of benzothiazole derivative was occurred with β -azolyl propanoic acid derivatives at 160 °C using Ag_2CO_3 as an oxidant. Further, Wang *et. al* reported both the $\text{C}(\text{sp}^2)\text{-H}/\text{C}(\text{sp}^3)\text{-H}$ and $\text{C}(\text{sp}^2)\text{-H}/\text{C}(\text{sp}^2)\text{-H}$ oxidative coupling of heteroarenes with amide derivatives under nickel catalysis (Scheme 1.7).¹⁰³ Both aliphatic as well as aromatic amides underwent oxidative coupling with a range of heteroarenes in the presence $\text{Ni}(\text{OTf})_2$ and KH_2PO_4 as an additive. DFT study suggested the use of KH_2PO_4 is important in this reaction and the anion exchange occurs between nickel precursor and KH_2PO_4 to generate the active nickel species.



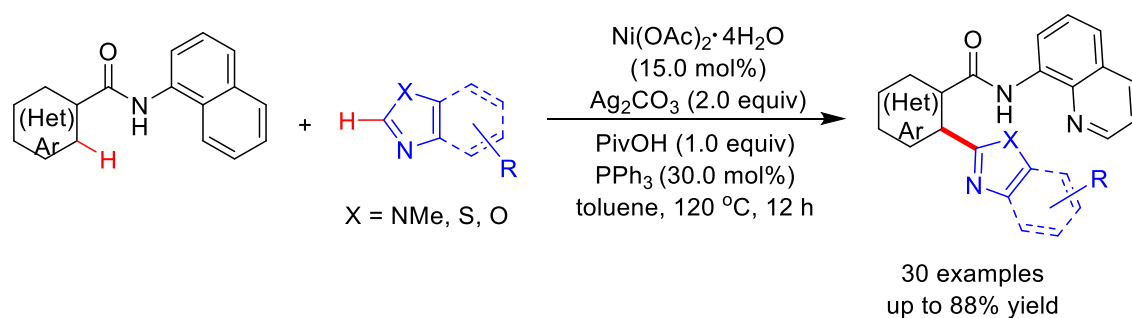
Selected examples: (Q = 8-quinolinyl)



Scheme 1.7. Ni(II)-catalyzed oxidative coupling of benzamides with heteroarenes.

Nickel-catalyzed heteroarylation of heteroarenes with azoles was demonstrated by You using bidentate directing group (Scheme 1.8).⁷² The reaction was compatible with diverse synthetically important functionalities and shows broad substrate scopes. The recycling of silver salt was demonstrated to reduce the cost and minimizes the formation of waste in the reaction. The kinetic experiments suggest the breaking of the C–H bond of (hetero)aromatic carboxamide is the rate-limiting step in this catalysis. A possible reaction mechanism is proposed involving an active Ni(III) species (Figure 1.3). In 2019, Ni(0)-mediated C–H/C–H coupling of bulky phosphino-pyridine derivatives has been presented by Anderson group.¹⁰⁴ The reaction operates *via* transfer of hydrogen to one of the 1,5-COD ligand of $\text{Ni}(\text{COD})_2$

catalyst. The formation of cyclooctene suggested that 1,5-COD acts as an oxidant for the double C–H bond activation in this reaction.



Scheme 1.8. Nickel(II)-catalyzed oxidative coupling of heteroarenes.

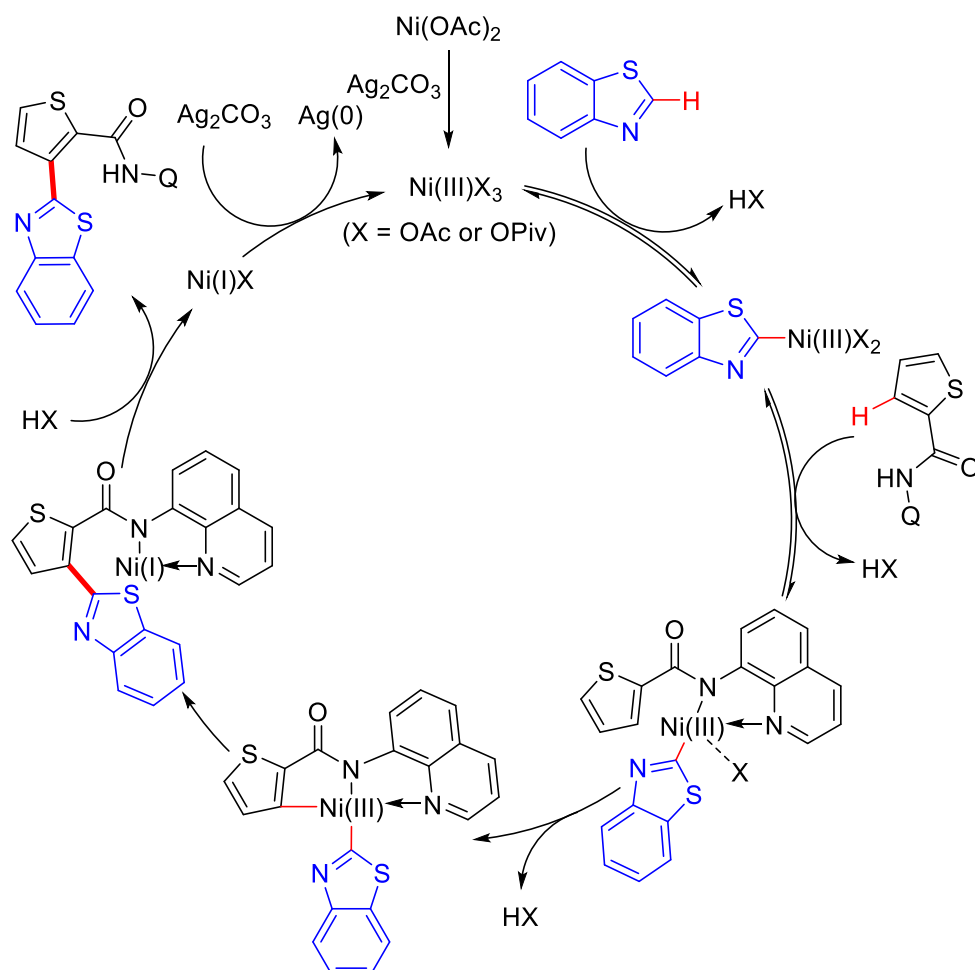
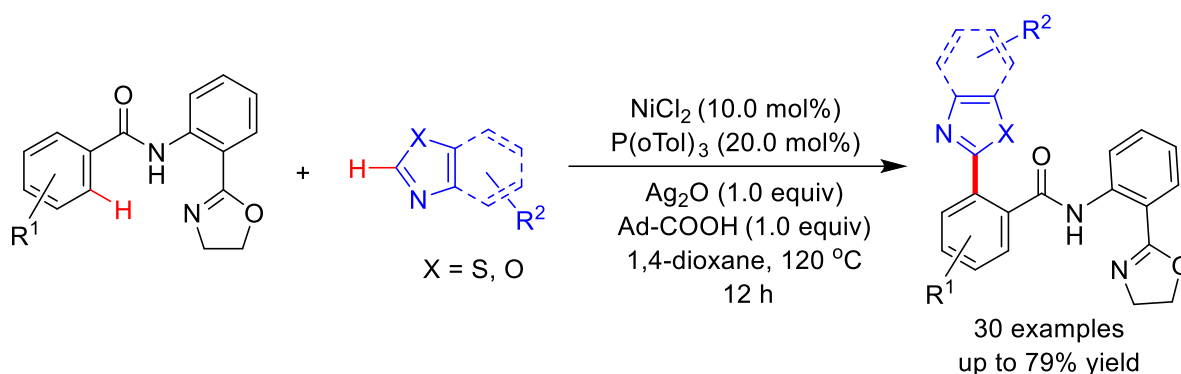


Figure 1.3. Proposed mechanism for oxidative coupling using nickel catalyst.

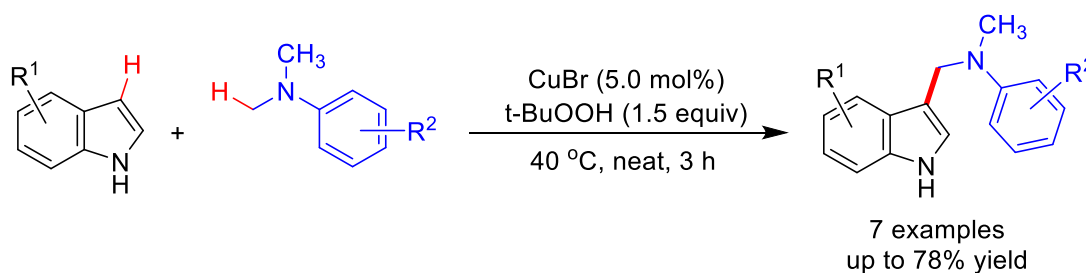
Recently, Punniyamurthy group reported the dehydrogenative coupling of aryl amides with azoles catalyzed by nickel(II) salts (Scheme 1.9).¹⁰⁵ The reaction developed the wide substrate scope with the compatibility of various important functionalities. The reaction is also applicable for the late-stage functionalization of commercially available drug candidates such as caffeine, pentoxifylline and doxofylline.



Scheme 1.9. Oxidative coupling of aryl amides using nickel catalyst.

1.1.4 Copper-Catalyzed C–H/C–H Oxidative Coupling

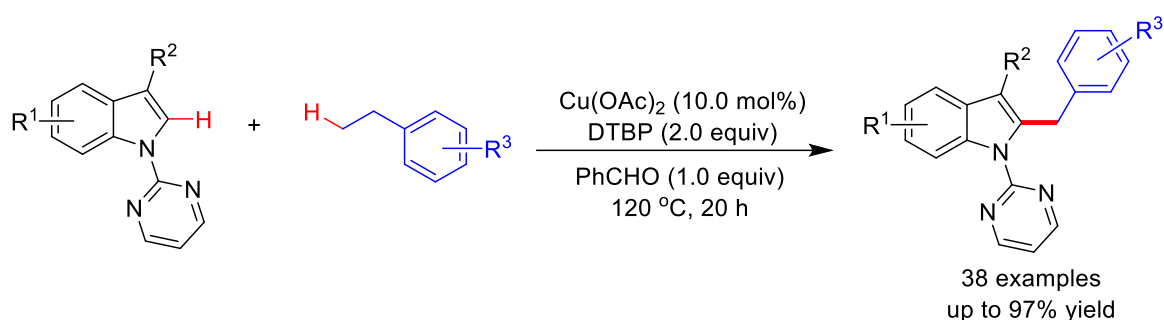
Copper catalyst has been extensively employed for the oxidative coupling of arenes and heteroarenes. Haung described the coupling of *N,N*-dimethylanilines with free *NH* indoles using a copper catalyst to synthesize the various alkylated indoles.⁷⁵ The indoles containing halides, nitro, and ester were well tolerated using 5 mol% of CuBr and 1.5 equiv of TBHP at 40 °C under neat conditions (Scheme 1.10).



Scheme 1.10. Oxidative coupling of anilines with indoles using copper catalyst.

Wen and Zhang demonstrated the dehydrogenative coupling of *N*-pyrimidylindoles with alkylarenes under copper catalysis in presence of DTBP as a mild oxidant (Scheme 1.11).⁷⁶ The substrates bearing synthetically important functionalities including halides, cyano and ester group were well tolerated with this catalytic system. The indole containing substituents

at C-3 position were also reacted smoothly to provide desired products in quantitative yields. The use of benzaldehyde in this protocol significantly enhances the product yields but the role of benzaldehyde was unclear. The kinetic experiments suggested that the benzylic C–H bond cleavage might be participate in the rate-limiting step. Preliminary mechanistic experiments suggested the reaction involves the formation of benzylic radical during the catalytic process (Figure 1.4). In addition, the coupling of the C(sp³)–H bond of propanoic acid derivatives with azoles using a copper catalyst is demonstrated by You group.¹⁰⁶



Scheme 1.11. Cu-catalyzed benzylation of indoles.

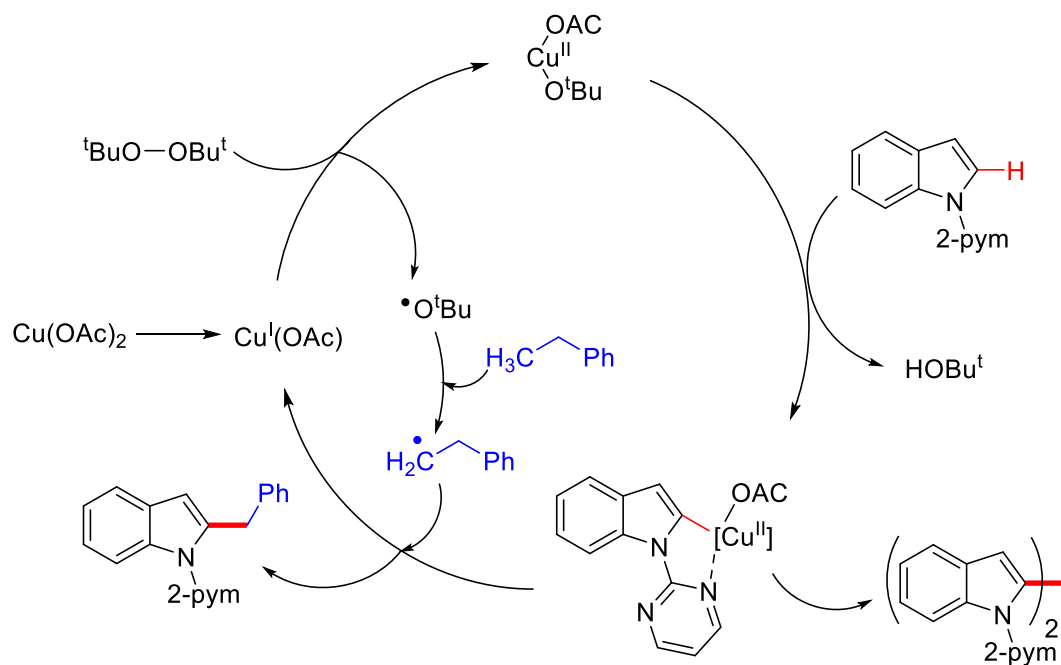
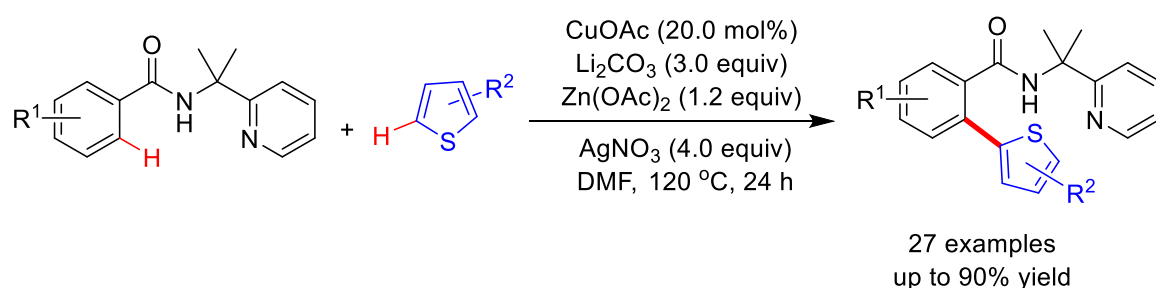
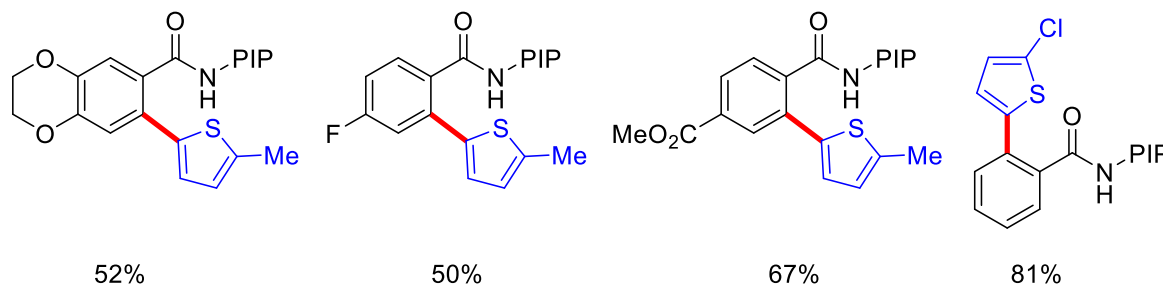


Figure 1.4. Plausible catalytic cycle for Cu-catalyzed benzylation of indoles.

Hetero-biaryl compounds are found in biologically active compounds and medicinal chemistry. Significant advancement was made in copper-catalyzed (hetero)arylation of heteroarenes. However, the main challenge in Cu-catalyzed oxidative coupling is the selectivity in terms of homo-coupling *vs* cross-coupling. Miura and Balm group independently reported the Cu-mediated oxidative coupling of arenes with azoles and 1,3,4-oxadiazoles, respectively.¹⁰⁷⁻¹¹⁰ Shi developed the oxidative coupling of benzamides with thiophenes in the presence Cu(OAc) and silver nitrate at 120 °C (Scheme 1.12).¹¹¹ The excess of thiophenes is required to achieve the hetero-coupled product in quantitative amounts. The scalability of this reaction was shown by demonstrating the gram-scale synthesis of cross-coupled products.. The reaction follows the Cu(II)/Cu(III) pathway to get the desired products (Figure 1.5).



Selected examples:



Scheme 1.12. Oxidative coupling of benzamides with thiophenes using copper catalyst.

In significant development, Daugulis disclosed the cross-dehydrogenative of arenes with heteroarenes under CuI/phenanthroline catalytic system using iodine as an oxidant (Scheme 1.13).¹¹² The reaction does not need the use of directing group and demonstrate the broad scope with tolerability of sensitive functional groups. The substrates including electron-deficient as well as electron-rich arenes, and five- or six-membered heteroarenes successfully participated in this coupling reaction under standard conditions.

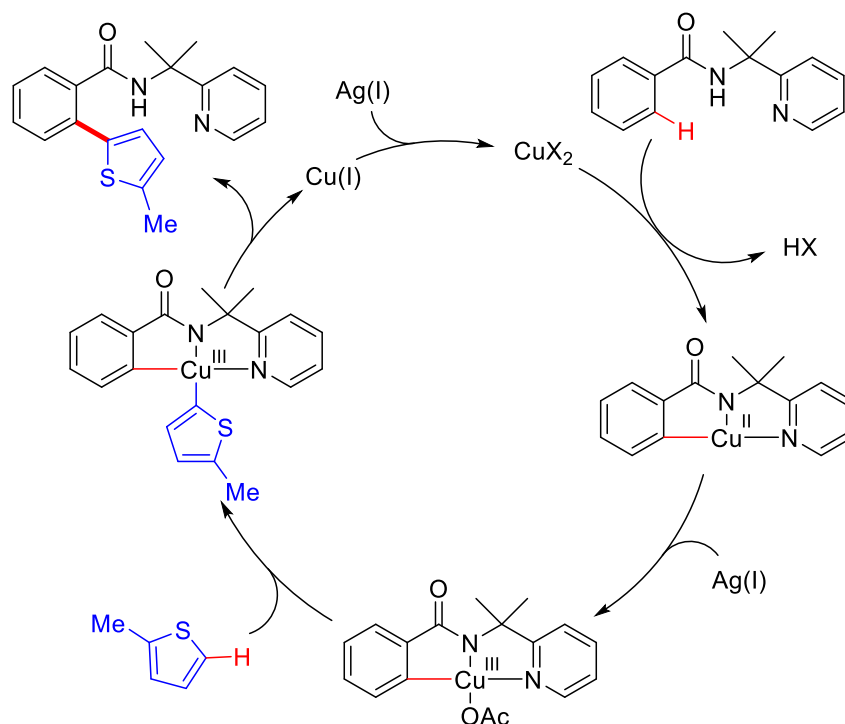
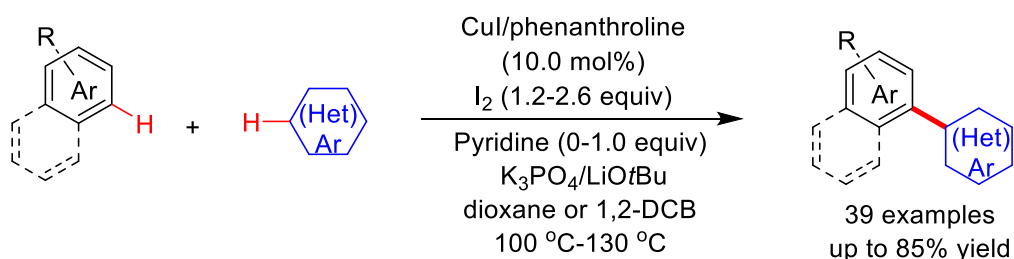


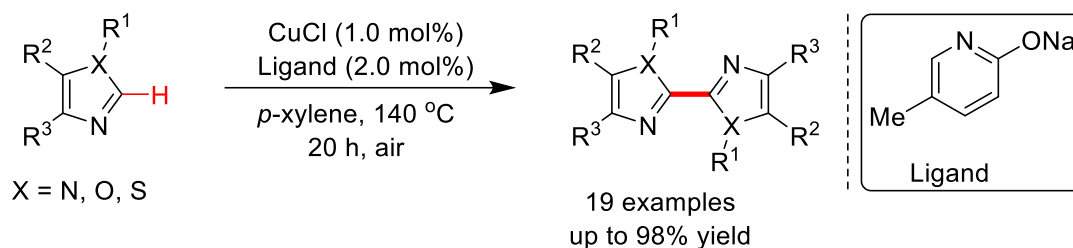
Figure 1.5. Proposed catalytic cycle for cross-oxidative coupling using copper catalyst.



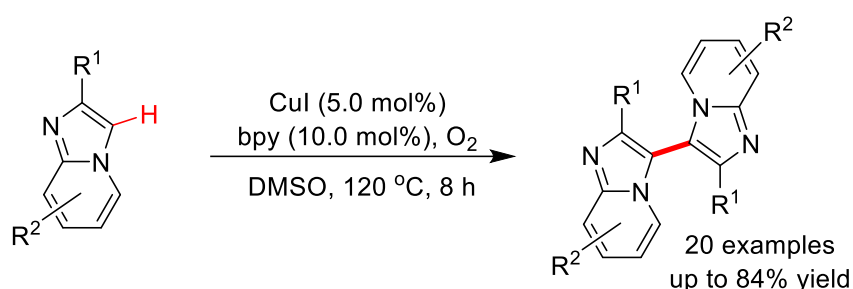
Scheme 1.13. Copper-catalyzed coupling of heteroarenes.

The direct oxidative coupling of two heteroarenes is a difficult task due to the formation of homocoupled and cross-coupled products in the reaction. The formation of homocoupled product is more feasible than cross-coupled product. In that viewpoint, Mori and Bao independently synthesized diverse biazoles using 10-20 mol% of Cu(II)-catalysts using air as an oxidant.^{113,114} Further, Fujita and Yamaguchi disclosed the homocoupling of azoles under CuCl/2-pyridonate catalytic system using air as a green oxidant (Scheme 1.14).¹¹⁵ The reaction provided various biazoles using only 1.0 mol% of Cu(I) catalyst and the use of 2-pyridonate ligand facilitates the homocoupling reactions. Similarly, Cao group described the Cu(I)-catalyzed homocoupling of imidazo[1,2-*a*]pyridines using oxygen as a sole oxidant (Scheme 1.15).¹¹⁶ The reaction proceeded smoothly with diversely substituted imidazo[1,2-*a*]pyridines and provided good yields of homocoupled products with excellent regioselectivity. This

protocol tolerated the halide substituents on the pyridine rings. Next, the copper-catalyzed homocoupling of azine *N*-oxides was demonstrated to get diverse hetero-coupled products.¹¹⁷

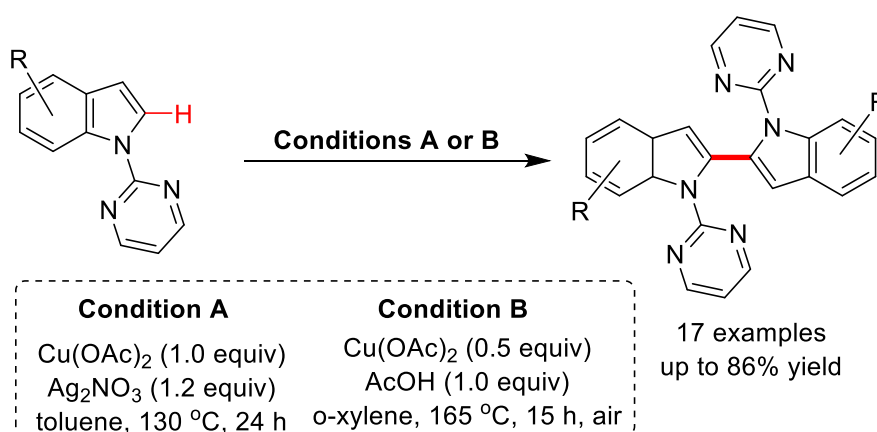


Scheme 1.14. Cu(I)-catalyzed homocoupling of azoles.



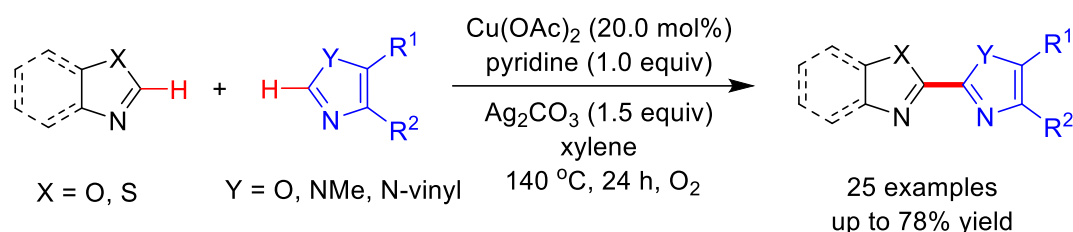
Scheme 1.15. Cu(I)-catalyzed homocoupling of imidazo[1,2-*a*]pyridines.

Biindoles are present in many bioactive compounds and alkaloids. Thus, the homocoupling of indoles was disclosed to synthesize biindole derivatives under copper-mediated catalysis.¹¹⁸ Both the electron-donor and electron-accepter substituents on indoles were efficiently participated in this catalysis using silver nitrate as an oxidant. In 2014, Miura developed an effective protocol for the synthesis of biindoles using 50 mol% of $\text{Cu}(\text{OAc})_2$ catalyst using 2-pyrimidinyl as a directing group (Scheme 1.16).



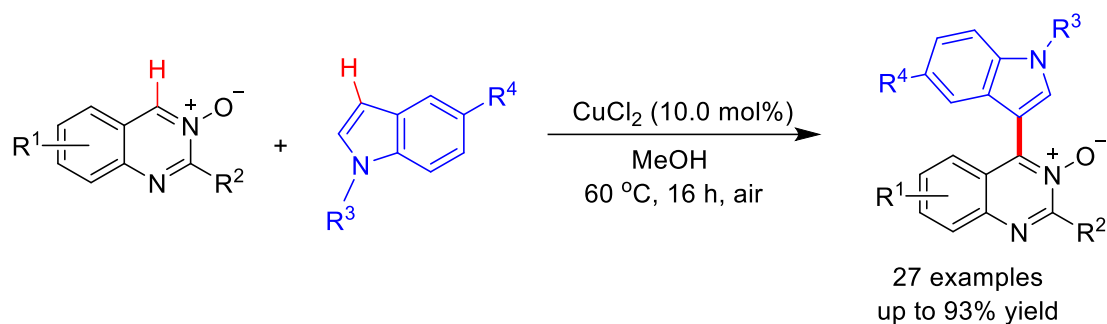
Scheme 1.16. Cu-catalyzed/mediated homocoupling of indoles.

Significant effort has been given to achieve the hetero-coupling of two heteroarenes. The use of electronically distinct heteroarenes, directing group strategy or using one of the coupling partner is in excess providing the solution for the challenging cross-coupling over the homocoupling reactions. In an early reports, Wang group developed the Cu-mediated hetero-coupling of azoles.¹¹⁹ A range of azoles were cross-coupled in the absence of any additive under standard conditions. Further, Lan and You reported the Cu(II)-catalyzed cross-coupling of distinct azoles in the presence of silver salt at 140 °C under air atmosphere (Scheme 1.17).¹²⁰ A series of azoles such as oxazoles, thiazoles, oxadiazoles, and imidazoles were efficiently coupled to afford the coupled products in quantitative yields. The synthetically important functionalities such as halides, aldehyde, ester, vinyl, and nitro were compatible with this catalytic system.



Scheme 1.17. Cross-coupling of two azoles using copper catalyst.

In parallel to the development of cross-coupling of heteroarenes, cross-coupling of various azoles was demonstrated by Li and co-workers under dual catalysis.¹²¹ The coupling of diversely substituted azoles was carried out using of $\text{Co}(\text{NO}_3)_2 \cdot 6\text{H}_2\text{O}$ and $\text{Cu}(\text{OAc})_2 \cdot \text{H}_2\text{O}$ in 1:1 ratio and air as a green oxidant. Further, Miura, Hirano and co-workers extended this coupling protocols by the Cu-mediated cross-coupling of azine *N*-oxides with oxazoles.¹²² In 2019, Ding, Peng group described the coupling of quinazoline-3-oxides with indoles in the presence of copper catalyst under air atmosphere (Scheme 1.18).¹²³ The reaction showed the broad substrate scopes under mild conditions to synthesize the diverse 4-(indole-3-yl)quinazolines in moderate to good yields. Notably, free *NH* indoles were also efficiently coupled with quinazoline-3-oxides affording coupled products in moderate yields. The controlled experiment suggested the key role of oxygen in this reaction, only a trace amount of coupled product was observed under inert conditions. The probable catalytic cycle was also proposed to understand the reaction mechanism (Figure 1.6).



Scheme 1.18. Cross-coupling of quinazoline-3-oxides with indoles using copper catalyst.

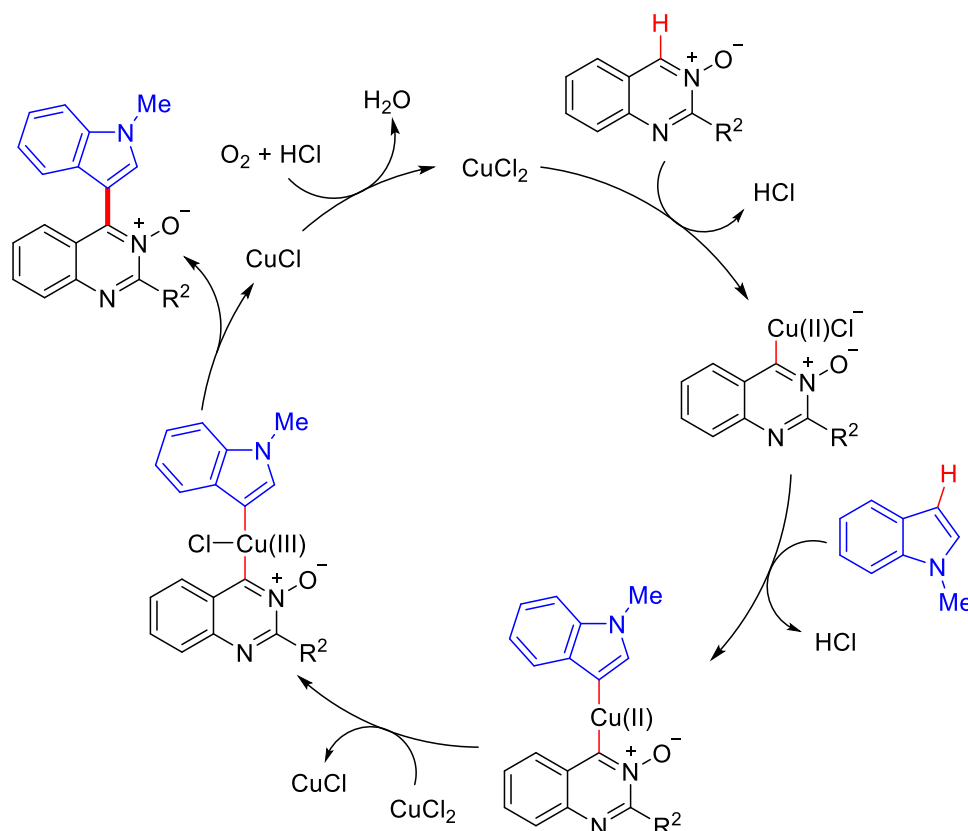
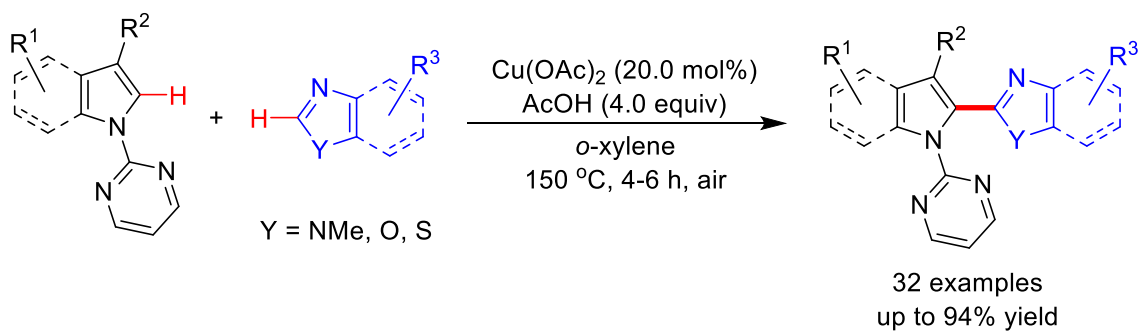


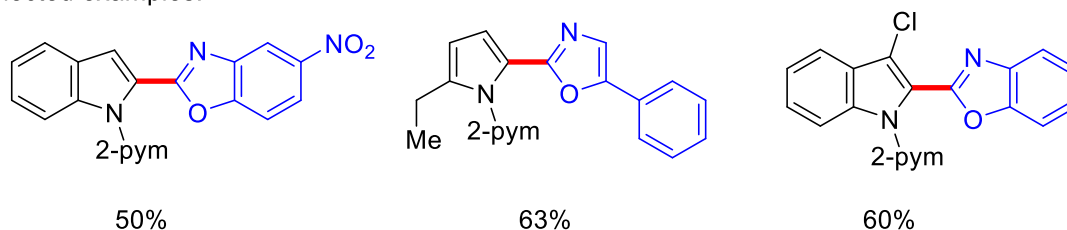
Figure 1.6. Proposed cycle for Cu-catalyzed oxidative coupling.

In addition, Miura and Hirano employed the copper catalyst for the coupling of 2-pyrimidinyl indoles with 1,3-azoles under relatively harsh reaction conditions (Scheme 1.19).⁷⁰ In particular, the reaction was performed using stoichiometric amount of copper catalyst under inert atmosphere whereas the catalytic amount of copper could catalyze this coupling reaction under air atmosphere. This protocol is suitable for both the electron-rich as well as an electron-poor substrate to afford the biheteroaryl compounds in quantitative yields. The reaction mechanism is proposed to proceed through reversible C–H bond activation of both the substrates followed by irreversible reductive elimination promoted by oxygen (Figure 1.7). In

line with these reports, Miura has also disclosed the Cu-mediated coupling of 2-pyridones with various azoles at 150 °C.¹²⁴



Selected examples:



Scheme 1.19. Cross-coupling of indoles with azoles using copper catalyst.

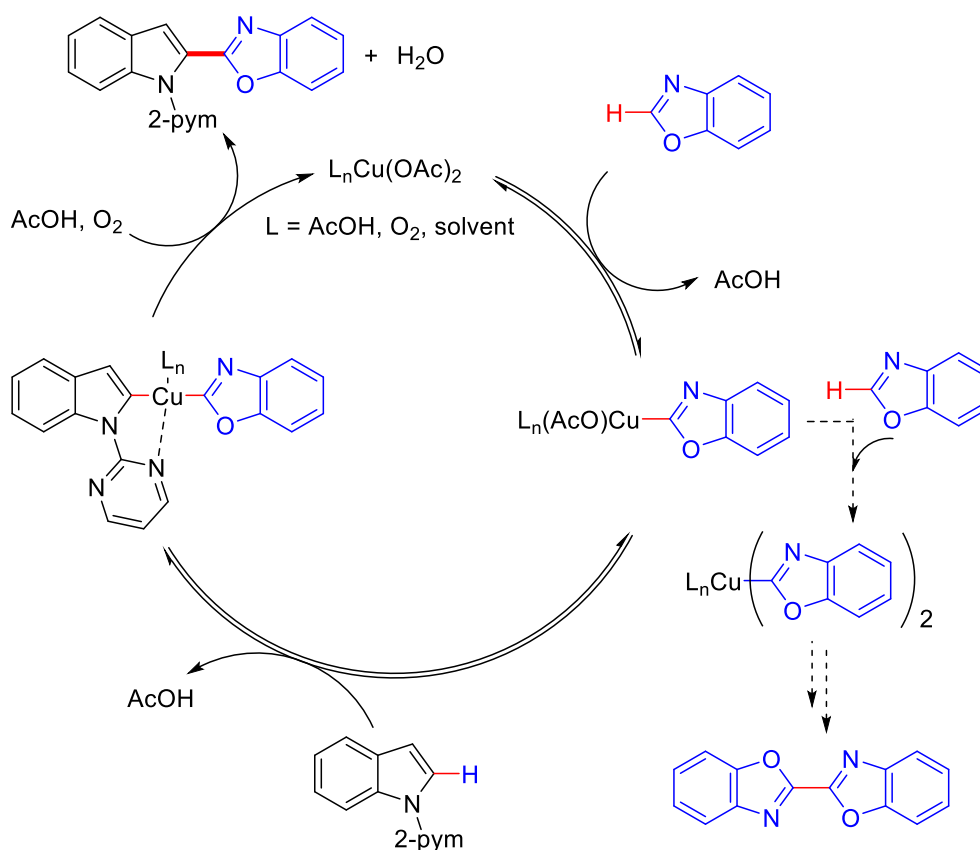


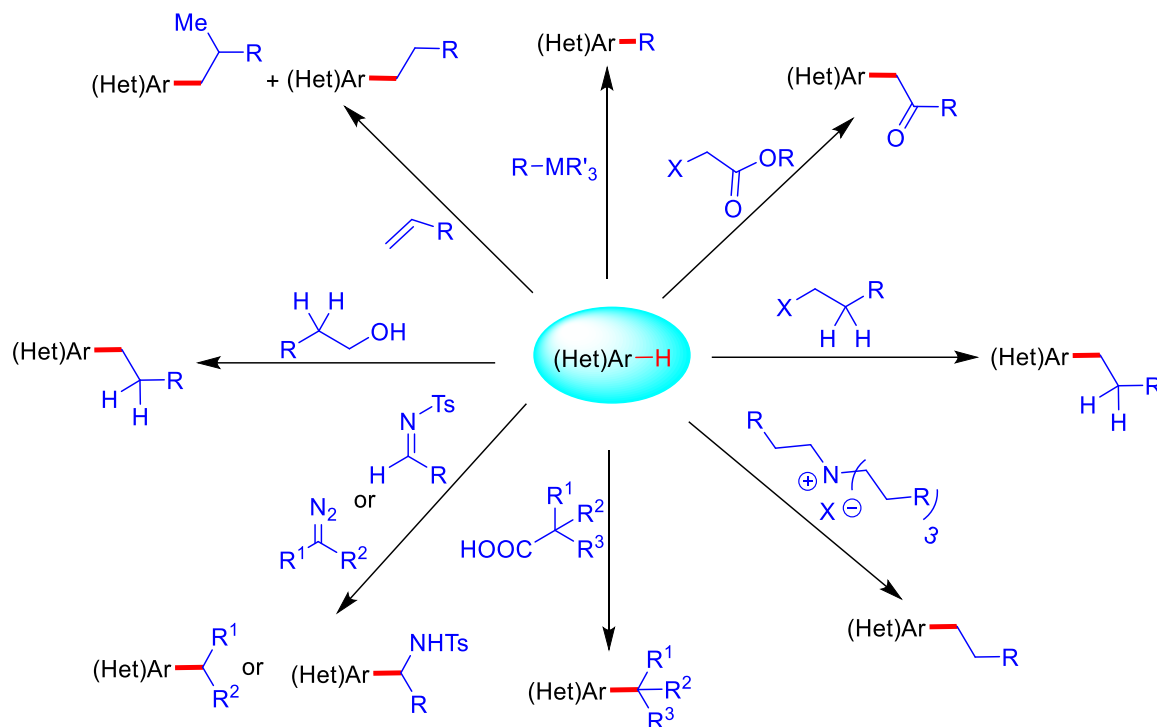
Figure 1.7. Possible mechanism for Cu-catalyzed coupling of indoles with 1,3-azoles.

1.2 C–H BOND ALKYLATION OF HETEROARENES

Alkylated (hetero)arenes are the privileged structural motifs with vast applications in pharmaceutical and perfumery industries as well as in functional materials. They possess intrinsic lipophilic character due to the presence of alkyl chain; thus, provide desired characteristic features for the drugs and agrochemicals. Classical alkylation strategy is mostly based on Friedel-Crafts reaction^{125,126} or radical alkylation,¹²⁷ both of which suffer from several drawbacks, including reaction inefficiency, low selectivity and limited substrate scope. The transition-metal-catalyzed cross-coupling of organometallic substrates with alkyl electrophile has been developed as an important alternative protocol for the alkylation.^{128,129} Various precious metal catalysts as well as inexpensive 3d metal catalysts have been efficiently demonstrated for this process, and could address many limitations associated with earlier approaches. Though, this traditional cross-coupling has found extensive applications in academia and across industries, the protocol still needs prefunctionalized organometallic substrates, thus, involves multi-steps synthesis and lead to formation of stoichiometric metallic-waste. In last few years, transition-metal-catalyzed C–H bond alkylation has turned up as a powerful and sustainable alternative to traditional alkylation.^{33,130-136} Notably, compared to the installation of aryl, alkenyl or alkynyl functionalities, the C–H bond alkylation is more challenging due to the various reasons. However, recent advancement in this area led to the development of a number of environment-friendly and efficient processes for direct introduction of alkyl groups onto the organic scaffolds with the assistance of transition metal catalysts.^{137,138}

A variety of alkylating reagents are used for the C–H alkylation of (hetero)arenes. The alkylating source includes alkyl halides, alkenes, alkyl organometallic reagents, azo-alkyls, carboxylic acid derivatives, alkanes and alcohols (Scheme 1.20).¹³⁹ Particularly, the alkyl halides and alkenes are most commonly employed for alkylation, whereas the azo-alkyls are gaining recent attention. Indoles are crucial structural features in various natural products, drugs and biologically active compounds, which motivate researchers to develop selective and efficient protocols for indole functionalization, particularly through C–H bond activation catalyzed by transition-metal catalysts.¹⁴⁰⁻¹⁴³ While numerous methods were developed for the selective arylation,¹⁴⁴⁻¹⁴⁸ and alkenylation^{149,150} of indoles, the C–H alkylation with alkenes and unactivated alkyl halides having β -hydrogen atom is given particular attention though it is associated with several challenges and difficulties. Particularly, the C-2 and C-3 selective C–H alkylation of indoles is explored both *via* non-directed and directed strategies. A numerous

alkylating reagents have been used for the C–H bond alkylation in doles including alcohols,¹⁵¹ diazo compounds,^{80,152} and Togni's reagent.¹⁵³ In this section, the alkylation of indoles using alkyl halides and alkenes as a coupling partners is discussed.



Scheme 1.20. Different Alkylating Agents Used in C–H bond Alkylation.

1.2.1 C–H Bond Alkylation Using Alkyl Halides

The direct alkylation of C–H bond with alkyl halides provides a straightforward, clean and targeted product. Moreover, alkyl halides are prevalent chemical building blocks that are widely commercially available and easily synthesized from simple and abundant starting compounds. However, the use of unactivated alkyl halides containing β -hydrogens in transition-metal-catalyzed C–C bond-forming reactions posed a significant challenge mainly due to the difficulty in oxidative addition of electron-rich sp^3 -hybridized alkyl halides onto the low-valent transition metals and the tendency of alkyl-metal intermediates to rapid β -hydride elimination rather than the desired C–C reductively eliminated alkylation (Figure 1.8).¹⁵⁴⁻¹⁵⁶ Overcoming these challenges, there has been a substantial progress in the field of selective coupling of alkyl halides with C–H bond of arenes and heteroarenes to achieve alkylation.

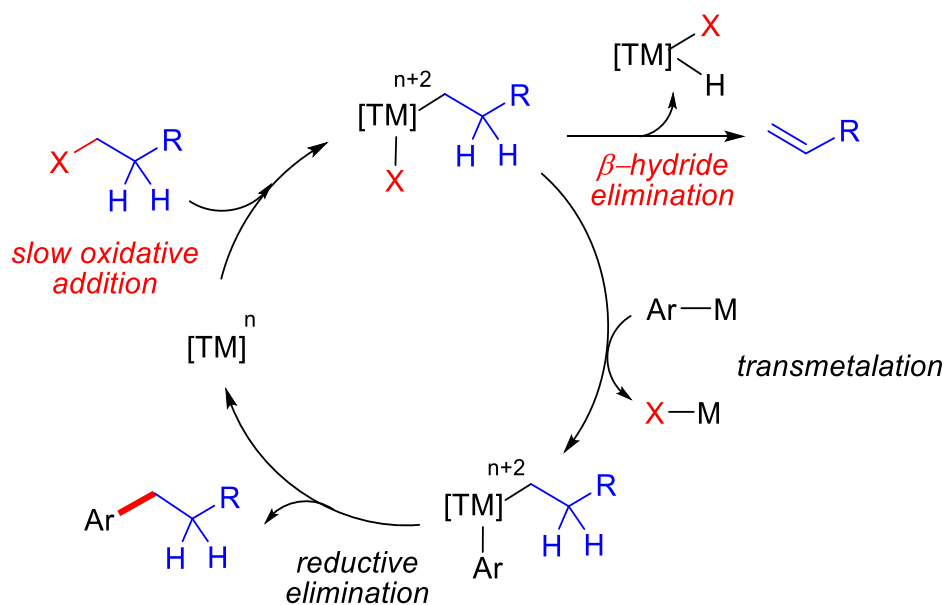
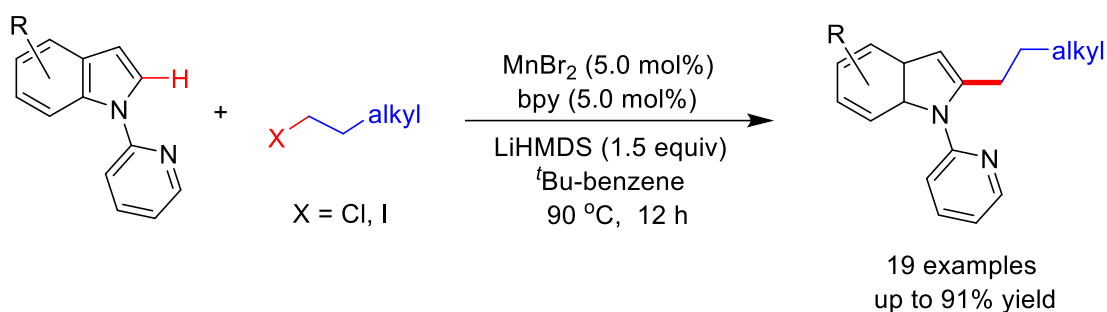


Figure 1.8. General mechanism for TM-catalyzed cross-coupling of unactivated alkyl halides.

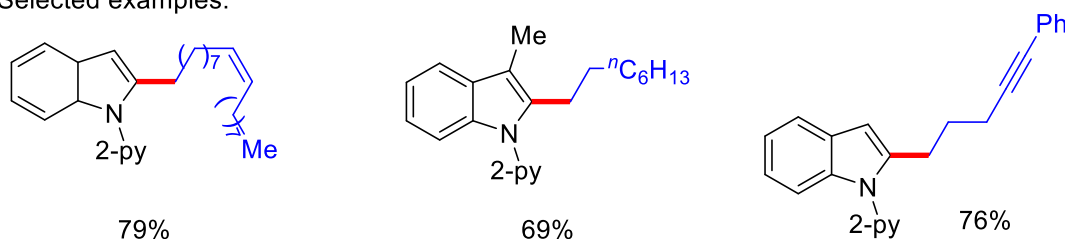
1.2.1.1 Manganese-Catalyzed C–H Alkylation

Manganese is the third most earth abundant transition metal and overall the twelfth most earth-abundant element. Additionally, manganese exhibits the wide range of oxidation state ranging from +III to +VII and it has the ability to form complex with a coordination number up to seven. Manganese catalyst has been extensively employed for the C–H bond functionalization of (hetero)arenes.¹³¹

Punji and co-workers disclosed the regioselective alkylation of indoles with alkyl iodides using a MnBr_2/bpy catalyst system at mild reaction conditions (Scheme 1.21).¹⁵⁷ This protocol established that the use of an inorganic base LiHMDS could facilitate the alkylation, without employing Grignard reagent, a commonly used base in Mn-catalysis. Notably, the installation of 2-pyridinyl substituent at the *N*-atom of indole is essential. Thus, the alkyl iodides having long alkyl chain, alkenyl, alkynyl were efficiently coupled with diverse indole derivatives to give the corresponding alkylated products. The alkylation proceeds *via* reversible C–H metalation pathway following a single-electron transfer (SET) process and involving alkyl radical intermediate (Figure 1.9).



Selected examples:



Scheme 1.21. Mn-catalyzed C–H alkylation of indoles with alkyl halides.

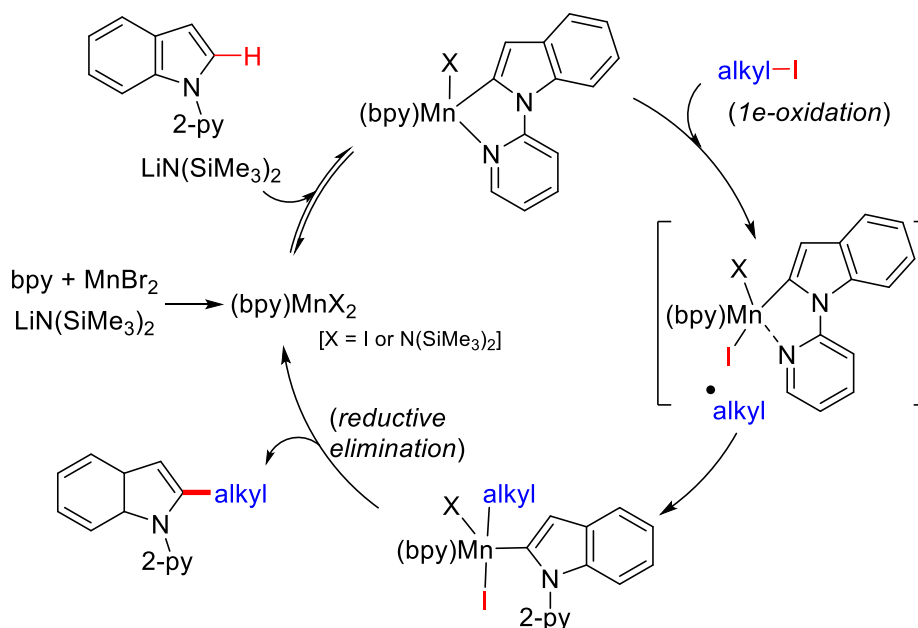
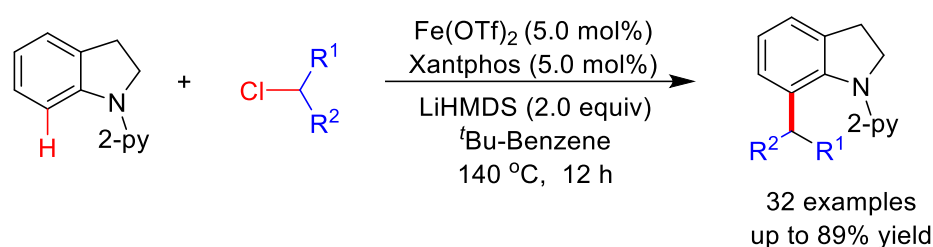


Figure 1.9. Proposed mechanism for Mn-catalyzed C–H alkylation of indoles with alkyl halides.

1.2.1.2 Iron-Catalyzed C–H Alkylation

Iron is an inexpensive, highly abundant and relatively less toxic transition metal. The remarkable progress have been achieved in the iron-catalyzed C–H functionalizations.¹⁵⁸⁻¹⁶¹ Recently, Punji has disclosed a methodology for regioselective C-7 alkylation of indolines with

primary and secondary alkyl chlorides using a cheap iron catalyst (Scheme 1.22).¹⁶² Thus, Fe(OTf)₂/xantphos system efficiently coupled a diverse range of unactivated alkyl chlorides at the C-7 position of 2-pyridinyl indolines in the presence of LiHMDS base. The alkyl chlorides containing different alkyl chain, tert-butyl, phenoxy, thiophenyl, heteroaryl, alkenyl and silyl moieties tolerated well under the optimized reaction conditions and delivered the desired alkylated products in excellent yields. The C-7 alkylated indolines can be easily converted to corresponding C-7 alkylated indoles and the easily removal of directing group obtained synthetically useful free-NH indoles.



Scheme 1.22. Fe-catalyzed C–H alkylation of indoline with alkyl chlorides.

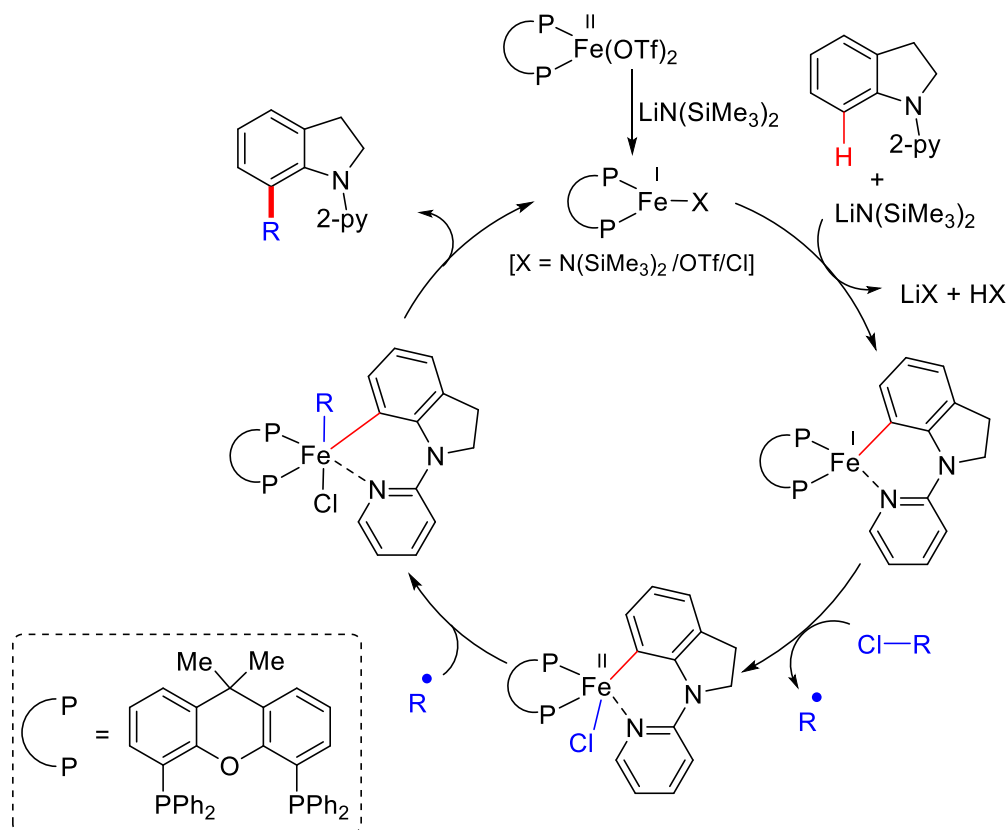
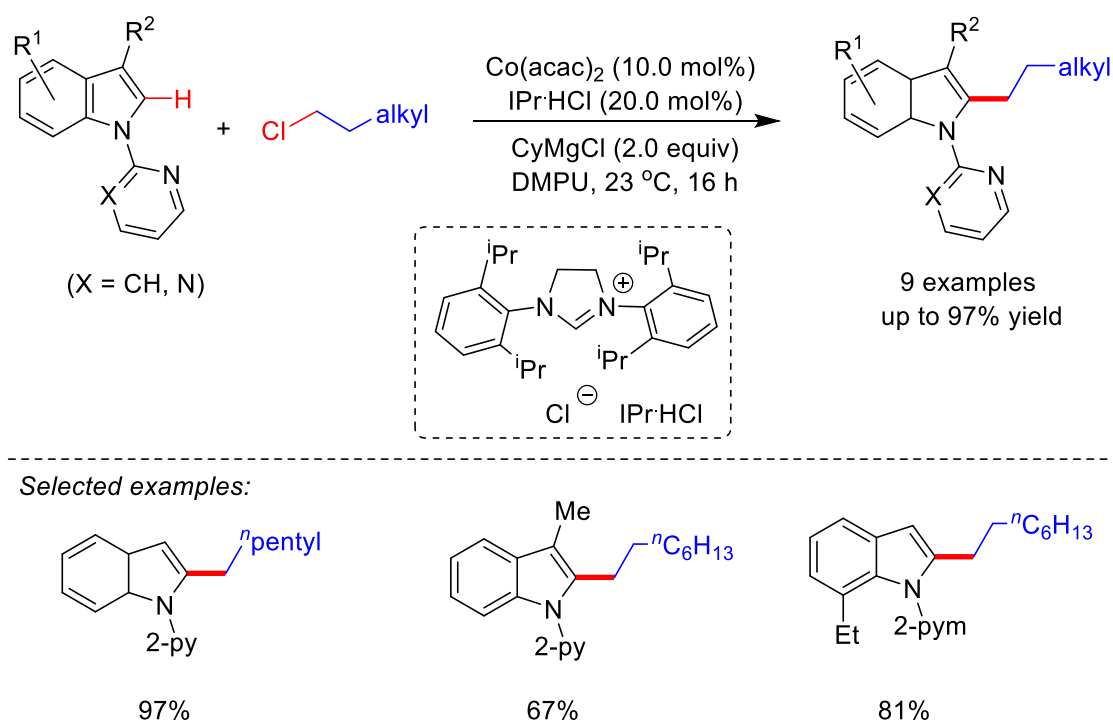


Figure 1.10. Proposed cycle for Fe-catalyzed C–H alkylation of indoline with alkyl chlorides.

Detailed experimental study, kinetic analysis and computational studies supported a SET pathway involving Fe(I)/Fe(III) protocol. The reaction begins with one-electron reduction of (Xantphos)Fe(II) complex to active Fe(I) in the presence of LiHMDS. Then coordination of indoline substrate to Fe(I) followed by the rate-limiting C–H metalation led to the formation of Fe(I) species. Abstraction of a halogen atom from the electrophile alkyl chloride *via* a single-electron process generates alkyl radical and Fe(II) species. Reattachment of alkyl radical followed by reductive elimination gave an alkylated product and regenerates the active catalyst in the presence of LiHMDS (Figure 1.10).

1.2.1.3 Cobalt-Catalyzed C–H Alkylation

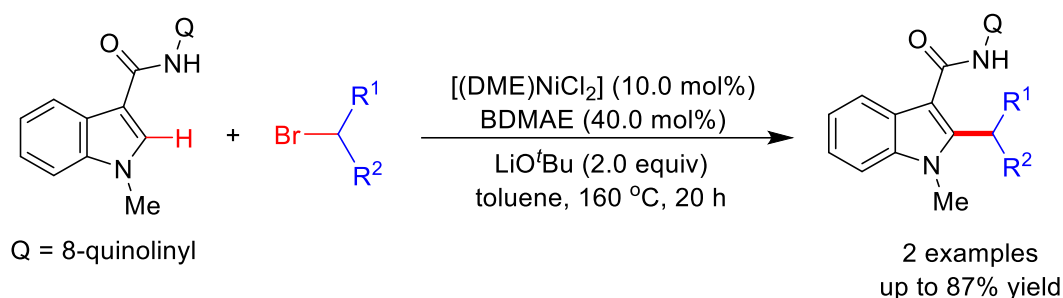
In last few years, cobalt complexes have been extensively used as catalyst in the C–H functionalization of heteroarenes.^{130,163} In an interesting contribution, Ackermann demonstrated the coupling of unactivated and challenging primary alkyl chlorides with indoles using Co(acac)₂/IPrHCl catalyst system (Scheme 1.23).⁹¹ This protocol showed the alkylation of both 2-pyridinyl and 2-pyrimidinyl *N*-substituted indoles selectively at C-2 position in the presence of excess of CyMgCl. Though, it has shown limited scope, the coupling of alkyl chlorides at mild conditions is notable.



Scheme 1.23. C–H alkylation of indoles with alkyl chlorides using cobalt catalyst.

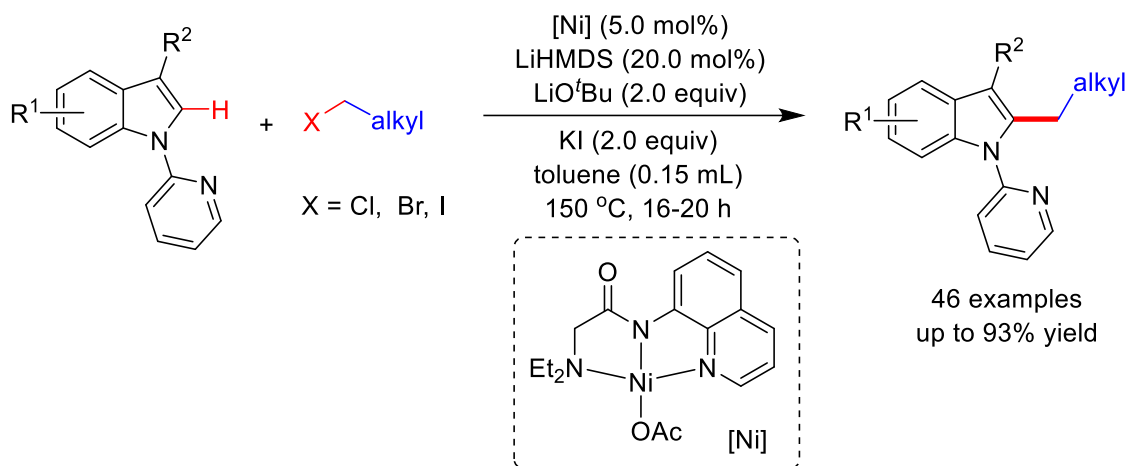
1.2.1.4 Nickel-Catalyzed C–H Alkylation

Nickel is an environmentally benign metal with low cost. In last past decades, nickel complexes have been utilized for the C–H functionalization indoles and other heteroarenes.¹⁶⁴ At early stage, Ackermann has described two examples of regioselective C-2 alkylation of indoles with challenging secondary alkyl bromides using a (DME)NiCl₂/BDMAE system through bidentate chelation assistance (Scheme 1.24).¹⁶⁵ In this protocol, the installation of quinolinyl-carboxamide group at C-3 position of indole is required.



Scheme 1.24. Nickel-catalyzed C–H alkylation of indoles using bidentate chelation-assistance.

In a remarkable development, Punji and co-workers described the alkylation of indole with alkyl halides through monodentate chelation catalyzed by nickel catalyst (Scheme 1.25).¹⁶⁶ The well-defined nickel catalyst could be able to couple diverse alkyl iodides with indoles using catalytic amount of LiHMDS. The catalytic reaction proceeds through the transformation of catalyst to the active amido complex (Figure 1.11). The coordination of indole to Ni followed by C–H nickelation generates nickel(II) intermediate, which triggers the formation of alkyl radical followed by radical rebound to generate Ni(IV) species. At the end, reductive elimination gives the alkylated product and regenerates the active catalyst by the reaction with LiHMDS.



Scheme 1.25. Nickel-catalyzed C–H alkylation of indoles using monodentate chelation-assistance.

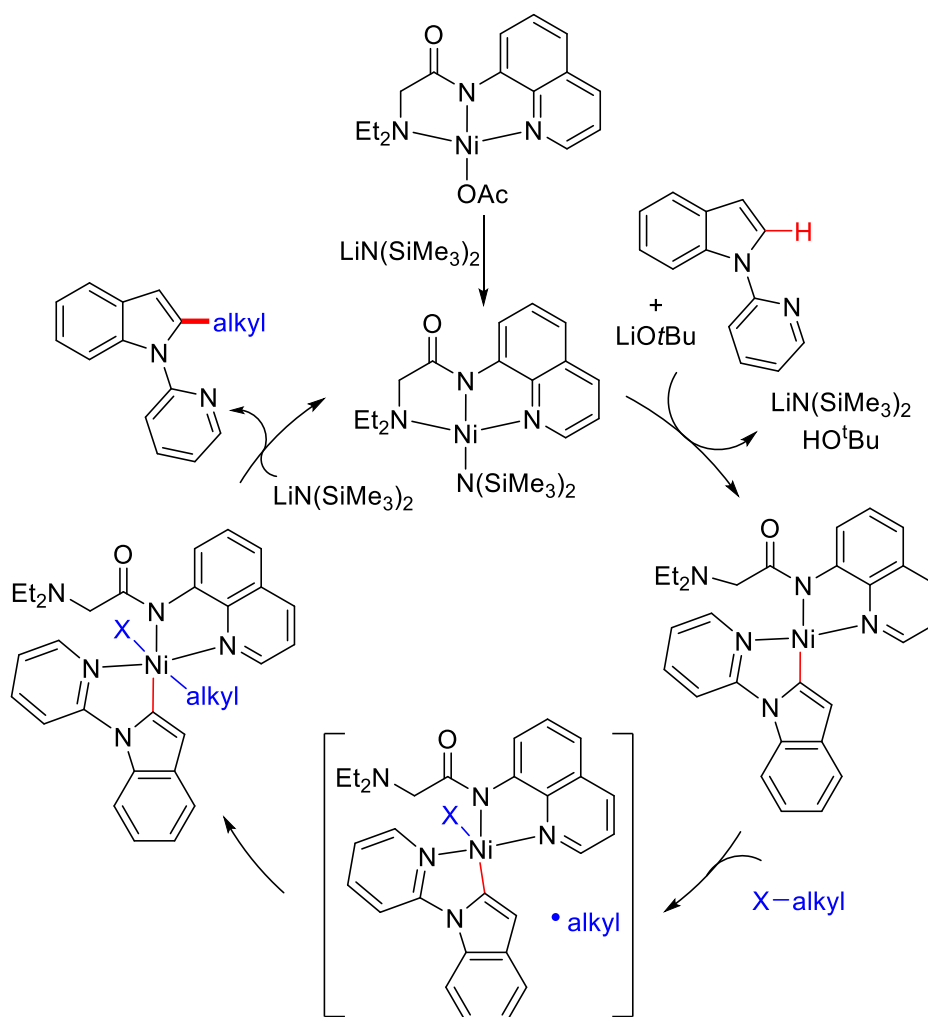
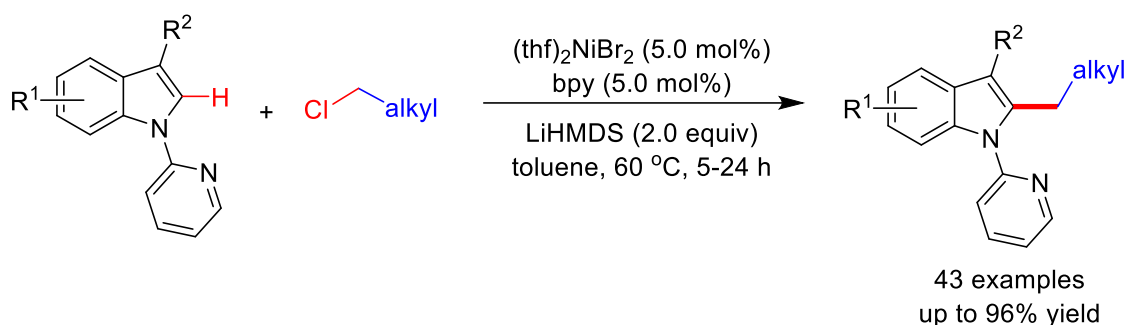


Figure 1.11. Proposed catalytic cycle for Ni-catalyzed C–H alkylation of indole with alkyl halides.

Later, the punji group also demonstrated the coupling of challenging alkyl chlorides with indoles using a simple $(\text{thf})_2\text{NiBr}_2/\text{bpy}$ system (Scheme 1.26).⁶³ Notably, the use of LiHMDS as a base was crucial for the reaction to achieve alkylation with both primary and secondary alkyl chlorides at 60 °C. As expected, due to use of strong base, the tolerability of sensitive functional groups was very poor. Detailed mechanistic study suggested a Ni(I)/Ni(III) pathway for this reaction involving two-step one-electron oxidative addition of alkyl chlorides (Figure 1.12). Also, the formation of paramagnetic species is confirmed by resulted g value (2.2) from EPR analysis.



Scheme 1.26. Nickel-catalyzed C–H alkylation of indoles using alkyl chlorides under mild reaction conditions

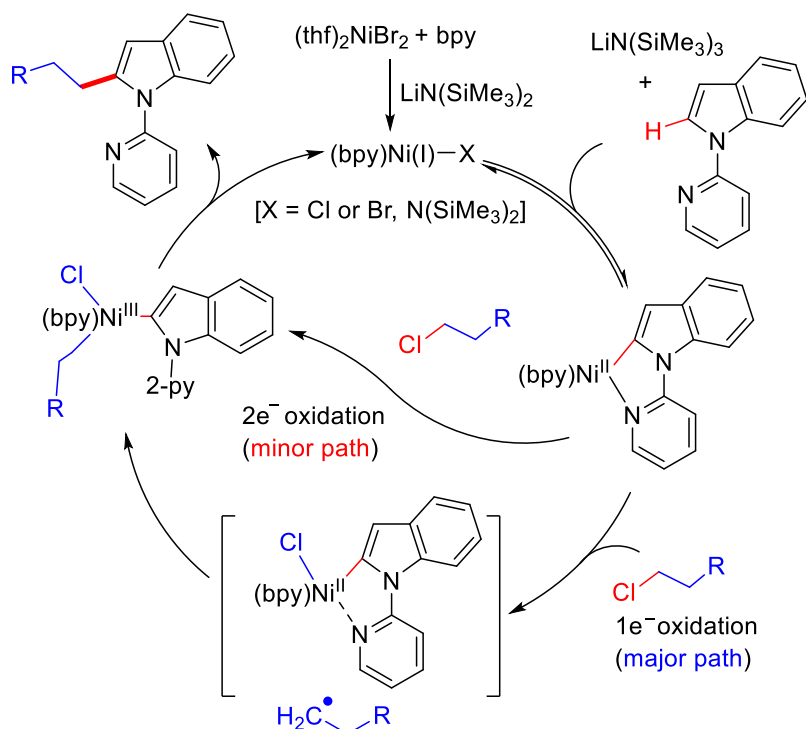


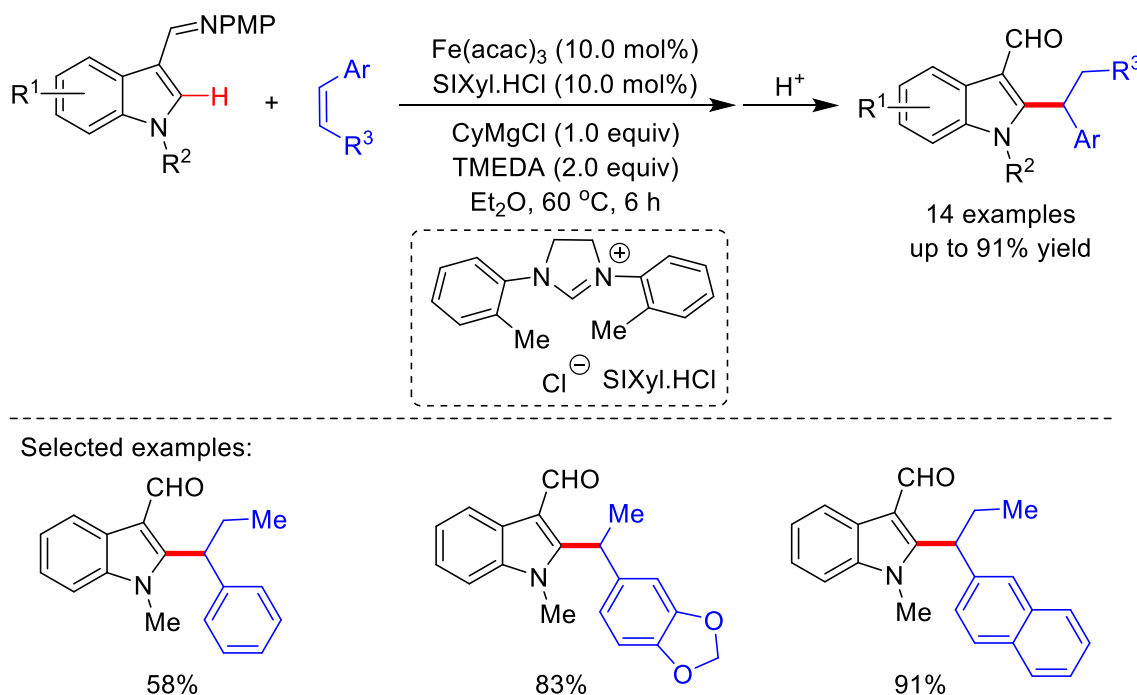
Figure 1.12. Proposed catalytic cycle for Ni-catalyzed C–H alkylation.

1.2.2 C–H Bond Alkylation Using Alkenes

Regioselective alkylation of (hetero)arene through C–H functionalization strategy provided an alternative method for the traditional coupling reaction. The use of alkenes for the alkylation is extensively studied that proceed *via* hydroarylation protocol.¹⁶⁷ Though a range of cheap alkenes can be used as coupling partners for the alkylation *via* hydrofunctionalization, the linear *versus* branched selectivity poses a major hurdle. Transition metal catalysts have been substantially employed for alkylation of heteroarenes with alkenes. In this section, we have summarized the reports for alkylation of heteroarenes with alkenes using 3d transition metal catalysts.

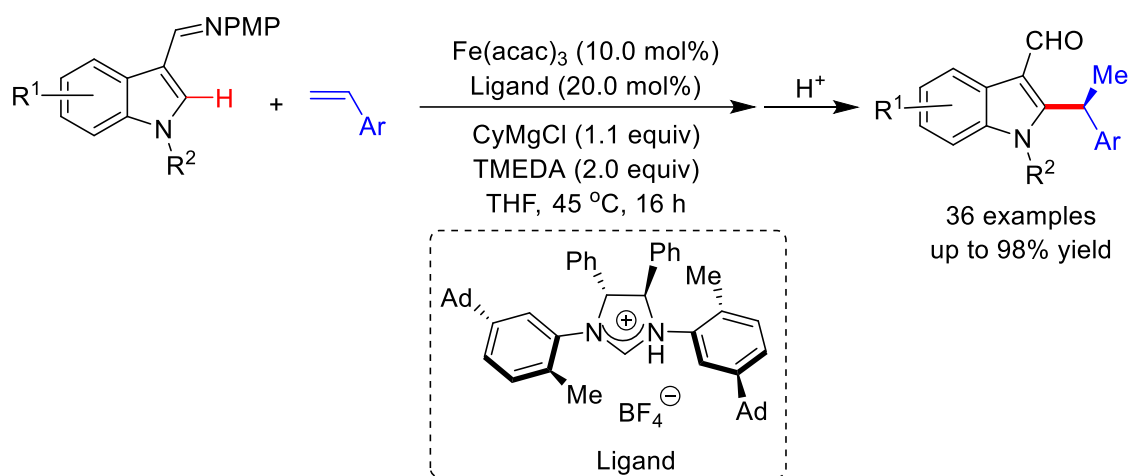
1.2.2.1 Iron-Catalyzed C–H Alkylation

Iron is an earth-abundant metal with low cost and less toxicity. In an early efforts, Yoshikai developed an imine-directed alkylation of indoles with vinylarenes with iron/NHC catalytic system (Scheme 1.27).¹⁶⁸ The installation of the directing group imine at C-3 position of indole is required to achieve the regioselective C–H Alkylation. The use of Grignard reagent is essential to reduce Fe(III) salt to a low valent iron species, which could be an active catalyst in this catalytic process. This protocol synthesized various C-3 formyl 1,1-diarylethane using diverse styrene derivatives as coupling partners under iron catalysis.



Scheme 1.27. Iron-catalyzed C–H alkylation of indoles with alkenes.

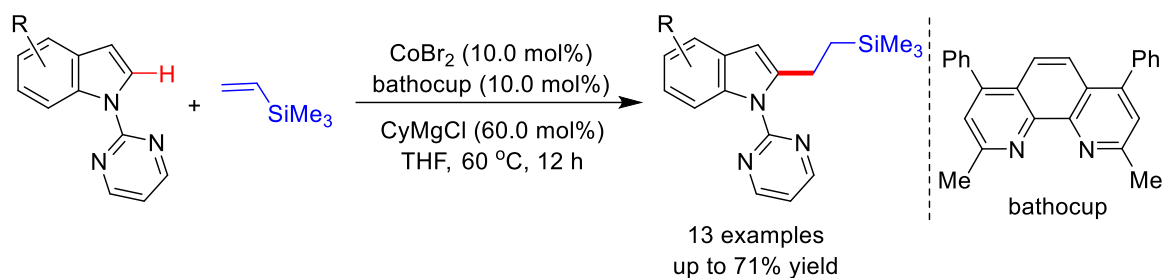
Notably, the use of allyl benzene as an alkylating partner provided 1,1-diarylpropane *via* olefin isomerization-hydroarylation pathway. In 2017, Ackermann group demonstrated the enantioselective alkylation of indoles with styrene derivatives employing iron catalyst (Scheme 1.28).¹⁶⁹ A range of styrenes were smoothly reacted with C3 imine directed indoles under iron catalysis with high enantioselectivity. The substituents on NHC ligand play a key role in controlling the enantioselectivity in this catalysis. The use of TMEDA and CyMgCl is essential for this transformation without which significantly decreased product yield or reaction was not occurred.



Scheme 1.28. The enantioselective alkylation of indoles with styrenes using iron catalyst.

1.2.2.2 Cobalt-Catalyzed C–H Alkylation

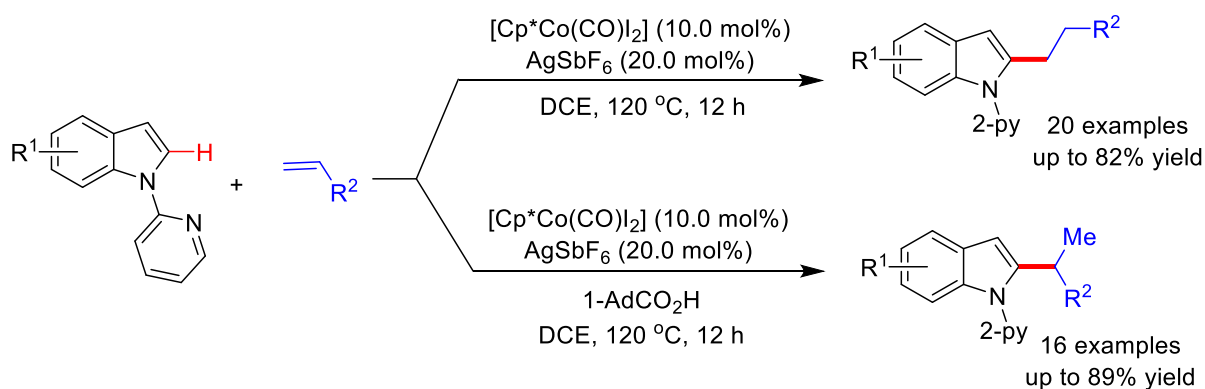
Cobalt catalysts have been extensively employed for the alkylation of heteroarenes.^{170,171} Generally, low-valent cobalt species is an active catalyst in C–H alkylation reactions. In an initial contribution, Yoshikai disclosed the regioselective alkylation of *N*-pyrimidinyl indoles with vinylsilanes using cobalt/bathocuproine catalytic system (Scheme 1.29).¹⁷² A series of indoles were coupled with vinylsilanes under mild conditions. This protocol was not suitable for other alkenes such as norbornene and 1-octene, those afforded alkylated product in very low yields under the standard conditions. The reaction is limited to the use of vinylsilanes as a coupling partners and provided selectively linear alkylated products.



Scheme 1.29. Cobalt-catalyzed alkylation of indoles with vinylsilanes.

The regioselective alkylation of indoles with malemides was described by Prabhu group.¹⁷³ This protocol used easily removalable pyrimidinyl as a directing group and furnishes various 3-arylated succinimide derivatives in good to excellent yields. Further, Li has developed the indole C–H hydroarylation of various conjugated alkenes in the presence $[\text{Cp}^*\text{Co}(\text{CO})\text{I}_2]$ as a catalyst and AgSbF_6 as an additive.¹⁷⁴ The hydroarylation of acrolein, glyoxylates and enones afforded desired products in moderate to good yields under mild conditions.

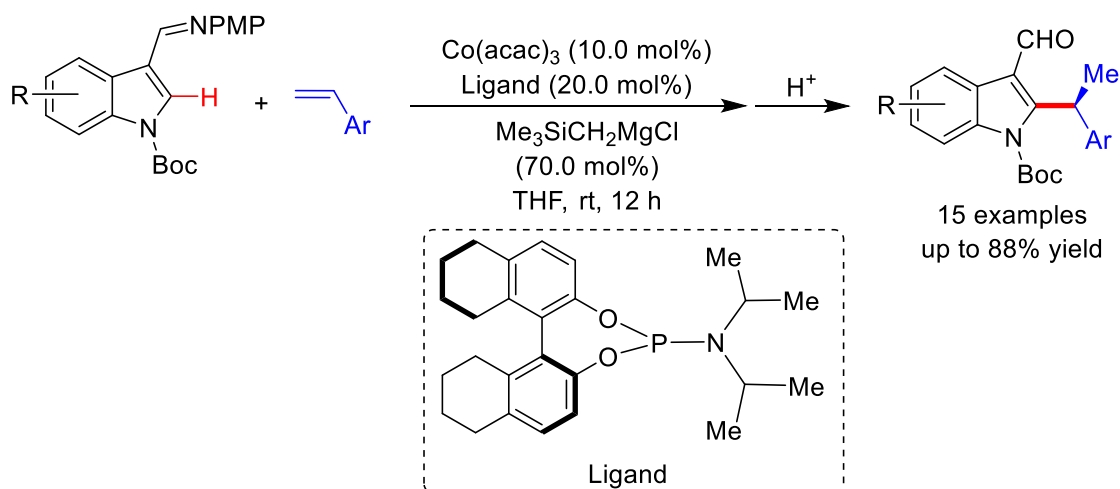
Furthermore, Ackermann was developed an elegant protocol for regioselective alkylation of indoles in the presence of Co(III) catalyst through monodentate chelation (Scheme 1.30).¹⁷⁵ In this approach, the selectivity for the hydroarylation was controlled by the use of additive. The use of sterically crowded 1-AdCO₂H in this reaction resulted in branch-selective alkylated product, whereas the linear-selective alkylation was achieved in the absence of 1-AdCO₂H.



Scheme 1.30. Linear and branch-selective alkylation of indoles with alkenes.

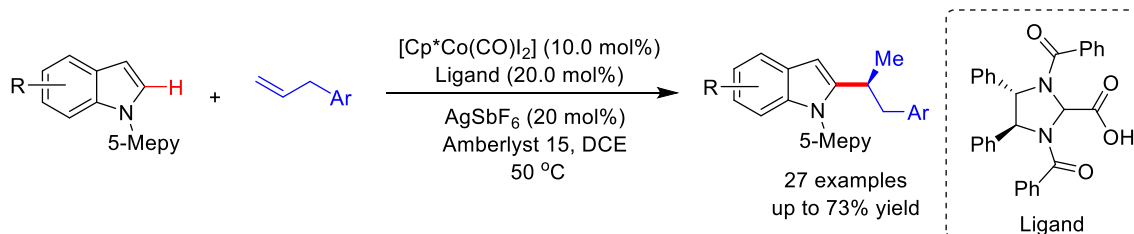
Enantioselective alkylation of indoles with styrenes in the presence of cobalt catalyst and chiral phosphoramidite was demonstrated by Yoshikai.¹⁷⁶ A series of indoles and styrene derivatives provided desired 1,1-diarylethanes in moderate to good yields and good enantioselectivities

(Scheme 1.31). Deuterium labelling experiments suggested that the enantioselectivity was controlled by the insertion of styrene and reductive elimination steps.



Scheme 1.31. Enantioselective alkylation of indoles with alkenes using cobalt catalyst.

Later, Ackermann extended the cobalt-catalyzed enantioselective alkylation in the presence of chiral carboxylic acid (Scheme 1.32).¹⁷⁷ The reaction does not need the use of Grignard reagent and proceeds with mild conditions. This protocol tolerated the various sensitive functional groups such as chloro, bromo, iodo, hydroxyl and ester substituents. A range of allyl benzenes were smoothly reacted with diverse indoles under optimized conditions. In addition, A chiral carboxylic acid chiral carboxylic acid enantioselective alkylation of indoles with maleimide was demonstrated using cobalt catalyst.¹⁷⁸ In 2021, Hong and Shi disclosed the enantioselective alkylation of indoles and pyrroles with unactivated terminal alkenes in the presence of cobalt catalyst.

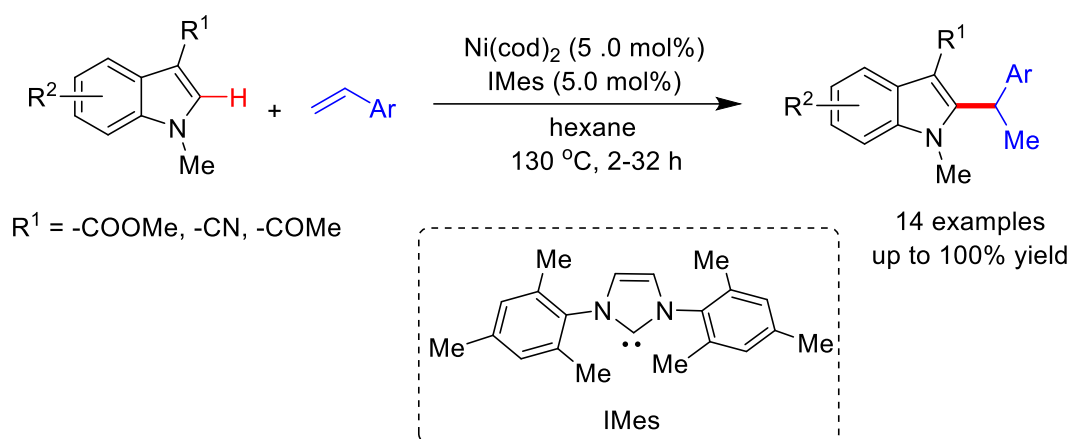


Scheme 1.32. Enantioselective alkylation of indoles with allyl benzenes using cobalt catalyst.

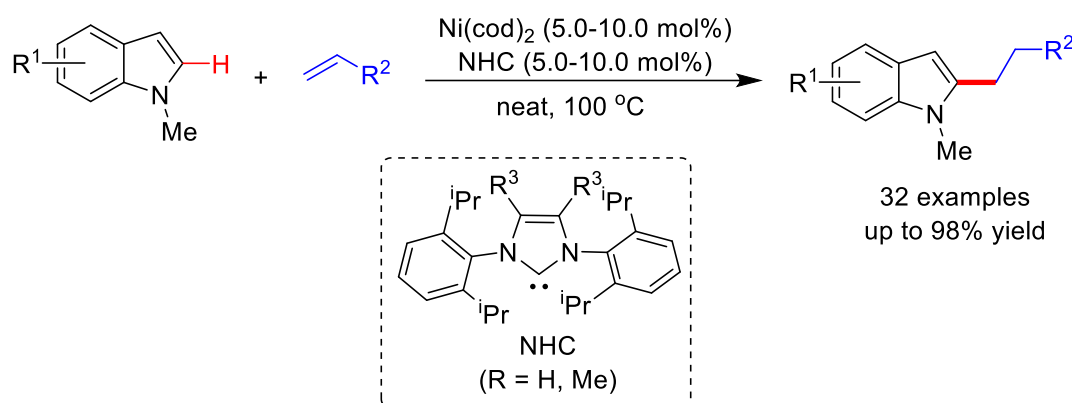
1.2.2.3 Nickel-Catalyzed C–H Alkylation

In 2010, nickel-catalyzed regioselective C–H alkylation of heteroarenes with vinylarenes was demonstrated by Nakao and Hiyama *via* hydroheteroarylation strategy

(Scheme 1.33)¹⁷⁹ Various alkenes such as styrenes, allylbenzene, cyclic alkene and internal alkenes were participated in this reaction and provided selectively branch-alkylated products. The reaction of unactivated aliphatic alkenes dominantly afforded the linear-alkylated products. The electron-poor substituents such as acetyl, ester or cyano group at C-3 position is essential to achieve the C–H alkylation. Thus, this protocol is limited to the highly deficient indoles. In addition to indoles, the oxazole, benzoxazole, imidazole, benzthioazole, and benzofuran were reacted nicely with styrene to produce desired 1,1-diarylethane in moderate to good yields.



Scheme 1.33. Ni-catalyzed alkylation of indoles with alkenes.



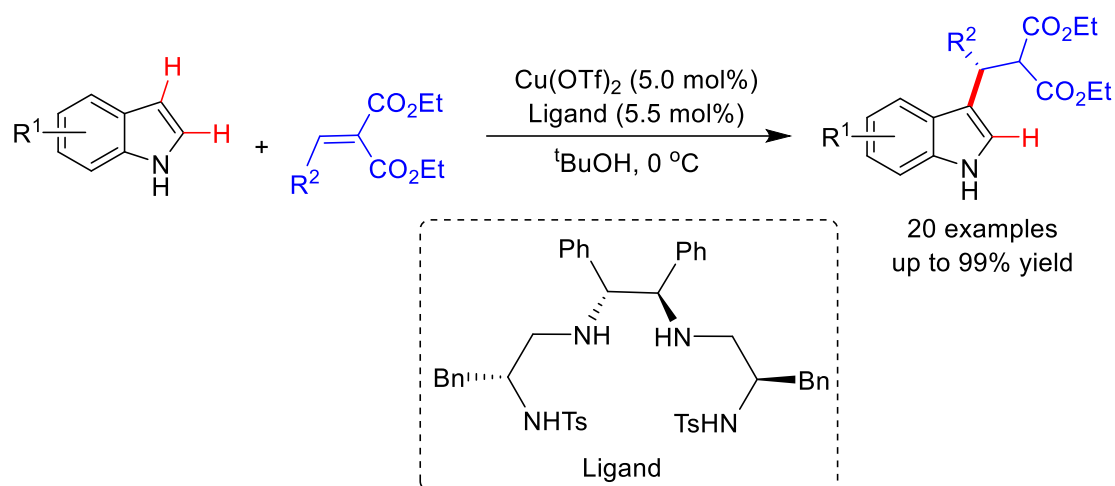
Scheme 1.34. Ni-catalyzed linear-selective alkylation of indoles with unactivated alkenes.

Following this report, Nakao and Hartwig disclosed the regioselective alkylation of indoles and other heteroarenes with unactivated alkenes under nickel/NHC system (Scheme 1.34).¹⁸⁰ The reaction exclusively provided the linear alkylated products with unactivated alkenes. This protocol is compatible with various important functional groups such as carbonyl, amides,

sulfonamides, silyl ethers, esters, boronate esters, acetals, and free amines. The alkenes such as styrenes, stilbenes and vinyl siloxanes were unreactive under this catalytic system.

1.2.2.4 Copper-Catalyzed C–H Alkylation

Wan group reported the enantioselective alkylation of free *NH* indoles with arylidene malonates using a copper catalyst (Scheme 1.35).¹⁸¹ Various arylidene malonates and indoles were participated under this reaction conditions affording alkylated products in good yields with high enantiomeric excess. Notably, the reaction of *N*-methyl indole provided only 64% ee under the optimized conditions, indicating the crucial role of free *NH* of indoles in enantioselectivity.



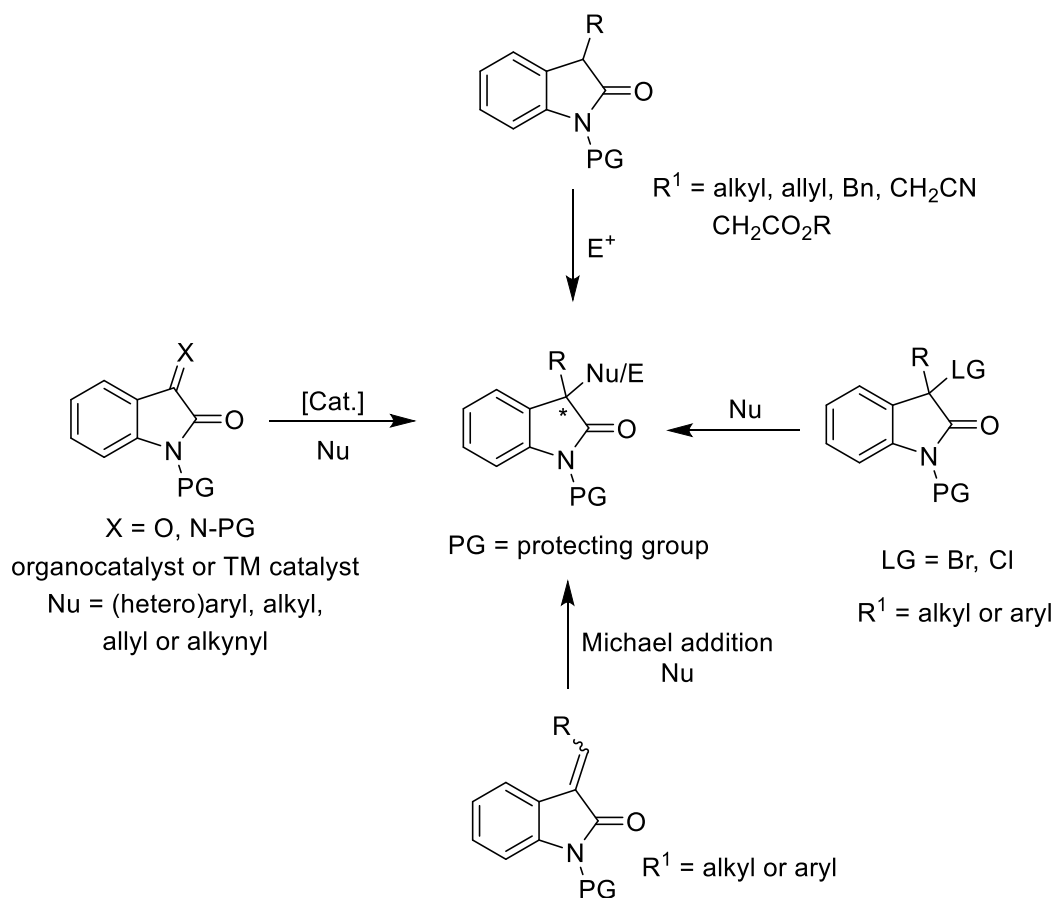
Scheme 1.35. Copper-catalyzed Friedel-Craft enantioselective alkylation of indoles.

1.3 SYNTHESIS OF STEROGENIC 3,3-DISUBSTITUTED 3-AMINO OXINDOLE

Isatin and its derivatives are an important heterocyclic compounds exhibiting wide range of pharmaceutical applications. Thus, the significant attention has been given for their functionalizations. The high reactivity of the C-3 carbonyl group provided the easy transformation of isatin into various C-3 substituted 2-oxindoles. An oxindole-bearing tetrasubstituted stereogenic quaternary center present in various biologically active compounds and naturally occurring alkaloids.¹⁸²⁻¹⁸⁷ Several protocols have been established for the synthesis of diverse 3,3-substituted oxindoles (Scheme 1.36).¹⁸⁸ The nucleophilic addition or spiro cyclization at the C-3 carbonyl of isatins allow the straightforward synthesis of diverse 3,3-disubstituted oxindoles generating quaternary stereocenters. In particular, stereogenic 3,3-disubstituted-3-amino-2-oxindoles have been considered as a privileged

structural motif in a variety of biologically active compounds such as cholecystinin-B receptor antagonists AG-041R,¹⁸⁹ anti-malarial agent NITD609,¹⁹⁰ or spirohydantoin DP2 receptor antagonist¹⁹¹. Indeed, due to the presence of two nitrogen atoms in spirohydantoin which increased the stability of the CRTH2 (DP2) receptor in human plasma and showed good potency and high bioavailability of DP2 receptor antagonists.¹⁹¹ Thus, the development of their synthetic methods is highly desirable.

Considering the importance of chiral 3-amino oxindoles in pharmaceuticals, significant attention has been devoted for their synthesis using organocatalysts or chiral transition metal catalysts.¹⁹²⁻¹⁹⁶ Generally, for the synthesis of stereogenic 3-amino oxindoles, the nucleophilic addition of different nucleophiles to the isatins or isatin derived ketimines is the most efficient and straightforward synthetic approach.¹⁹⁷⁻²¹⁸ These nucleophilic addition reaction includes, Mannich reaction, Morita-Baylis-Hillman reaction, Henry reaction, *aza*-Friedel-Craft reaction and Strecker reaction. On the other hand, direct functionalization of oxindoles or 3-substituted oxindoles also provides access for the synthesis of stereogenic 3-substituted 3-amino oxindoles.²¹⁹⁻²²³

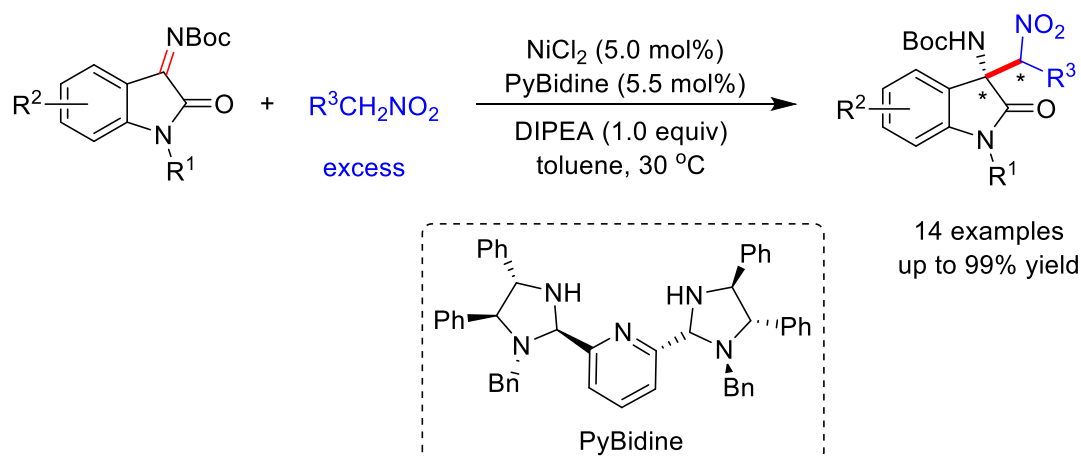


Scheme 1.36. Synthetic strategies for the synthesis of 3,3'-disubstituted oxindoles.

In last few year's, organocatalyst has been extensively employed for the synthesis of chiral 3-substituted oxindoles constructing quaternary stereocenters. Recent development was focus on the use of transition metal catalyst for their synthesis. In this background, 3d metal catalyst based on nickel and copper metal along with suitable chiral ligands were studied for the synthesis of various C-3 amino oxindoles.

1.3.1 Nickel-Catalyzed Synthesis of 3-Substituted Amino Oxindoles

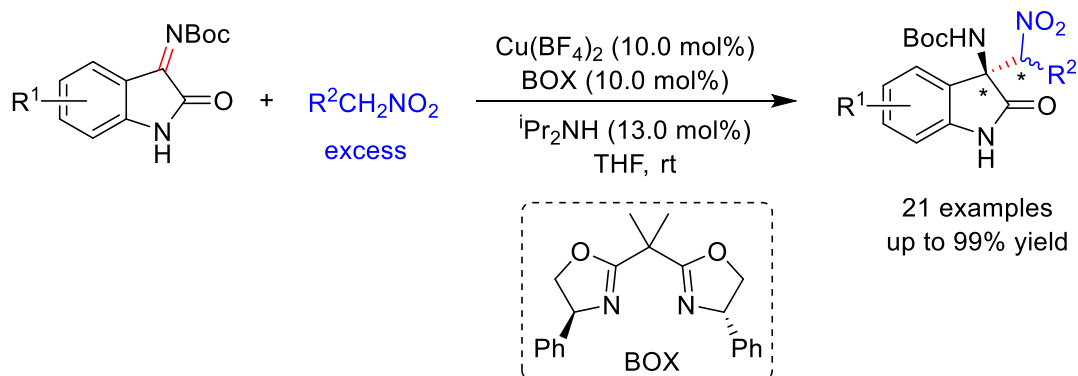
Arai group described the synthesis of chiral 3-amino oxindoles catalyzed by nickel catalyst (Scheme 1.37).²²⁴ The addition of nitromethane to the isatin-derived ketimines provided the 3-amino oxindoles with the generation of stereogenic quaternary center at C-3 position. The sensitive functionalities such as -F, -Cl, -Br, acetyl and allyl groups were tolerated under this catalytic system and produced desired oxindoles with high yields and high enantioselectivities.



Scheme 1.37. Nickel-catalyzed synthesis of C-3 aminated oxindoles.

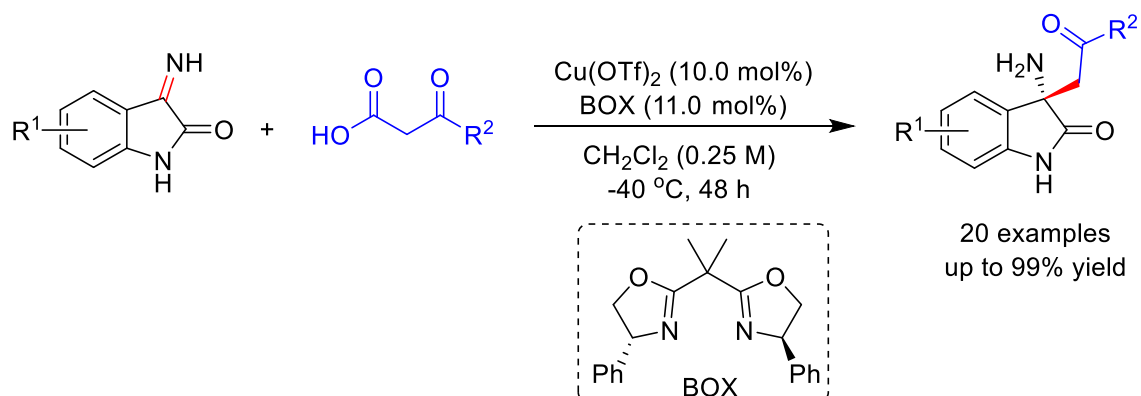
1.3.2 Copper-Catalyzed Synthesis of 3-Substituted Amino Oxindoles

An enantioselective aza-Henry reaction with isatin-derived ketimines was demonstrated by Blay and Pedro using Cu(II)-Box catalyst system (Scheme 1.38).²⁰⁰ The reaction does not require the protection of *NH* group of isatin generating stereogenic quaternary centers with high yields and enantiomeric excess. The substrates containing methoxy, nitro, and halides were participated in this reaction providing excellent enantioselectivities. Similarly, Kureshy extended aza-Henry reaction using chiral Cu(II) macrocyclic salen complex to synthesize C-3 amino oxindoles at room temperatures.²²⁵



Scheme 1.38. Copper-catalyzed synthesis of chiral 3,3'-disubstituted oxindoles.

The enantioselective decarboxylative Mannich-type addition of β -keto acids to the isatin-derived ketimines was presented by Morimoto and Ohshima.²²⁶ The reaction of various β -keto acids with diverse free *NH* isatin ketimines was occurred in the presence of $\text{Cu}(\text{OTf})_2$ and bis(oxazoline) ligand at $-40\text{ }^\circ\text{C}$ (Scheme 1.39). This protocol was applicable for the synthesis of (+)-AG-041R, a gastrin/CCK-B receptor antagonist. The reaction of acetophenone or its trimethylsilyl enol ether with isatin ketimines was not occurred indicating the importance of acid moiety in this reaction.



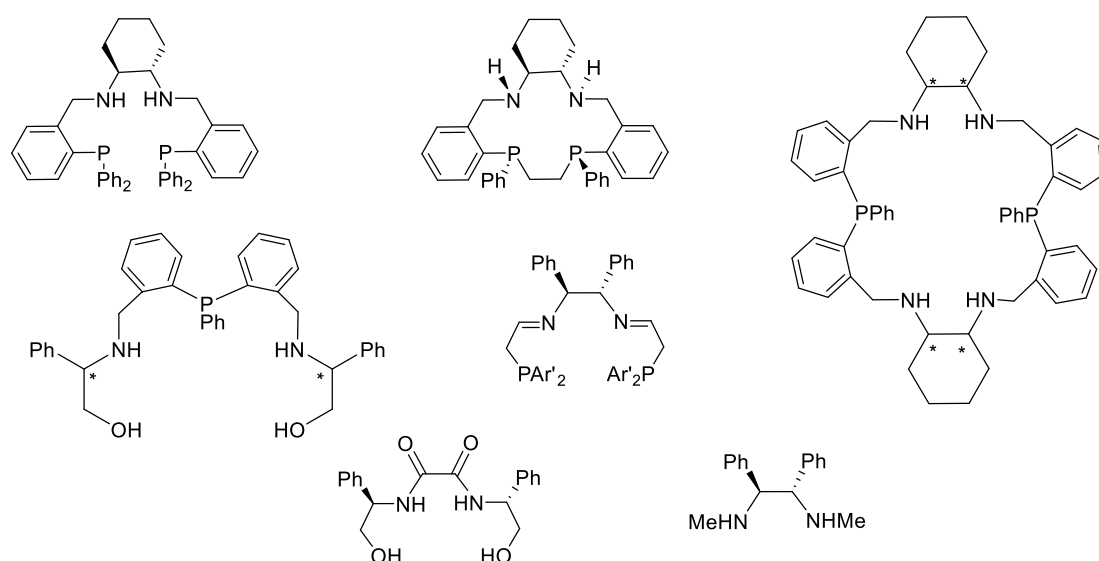
Scheme 1.39. Copper-catalyzed synthesis of C-3 aminated oxindoles.

1.4 HYDROGENATION OF KETONES

The hydrogenation of ketones is an important chemical transformation in organic synthesis, and applied in chemical industry for producing fragrance, flavors and fine chemical intermediates. The traditional approach for the reduction of ketones uses stoichiometric amounts of metal hydride reagents. However, these approaches generate stoichiometric amount of harmful waste products.²²⁷ Compared to a traditional approach, catalytic hydrogenation protocol represents an environmental friendly and atom economic alternative. In early stage,

many heterogeneous catalysts have been employed for the hydrogenation of ketones to corresponding alcohols. Unfortunately, these catalysts require harsh reaction conditions that led to the formation of undesired side products. Thus, significant progress has been achieved in development of homogeneous catalysts for hydrogenation of ketones that can perform the reaction at mild conditions. In general, hydrogenation reactions are of two types (i) hydrogenation using molecular hydrogen and (ii) transfer hydrogenation. The hydrogen using molecular hydrogen is required a requisite experimental setup and flammable pressurized hydrogen gas. Hence, transfer hydrogenation is emerged as convenient and effective alternative approach as it need simply hydrogen source such as alcohols, avoiding pressurized hydrogen.^{228,229} A remarkable progress has been achieved in transfer hydrogenation ketones employing precious metal catalysts such as ruthenium,^{16-19,230} rhodium,²⁰⁻²² osmium,²³ and iridium.^{20,24,25}

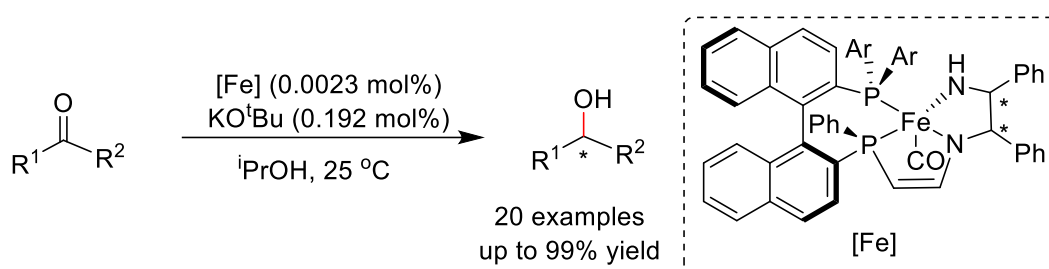
Recently, significant attention has been given to the hydrogenation of ketones to achieve chiral alcohols, particularly employing the earth-abundant 3d transition metal catalysts.²³¹ Among 3d metals, manganese, iron and cobalt complexes are substantially explored in the hydrogenation of ketones.²³² However, nickel complexes for such reactions are elusive. Various chiral ligands were developed for the enantioselective transfer hydrogenation of ketones to get chiral alcohols (Figure 1.13). These chiral ligands were employed in transfer hydrogenation of ketones along with manganese, iron, cobalt and nickel metal precursors. However, the development of phosphine free catalytic system for the synthesis of chiral alcohols is highly desirable.



Scheme 1.13. Representative chiral ligands for transfer hydrogenation of ketones.

1.4.1 Iron-Catalyzed Hydrogenation of Ketones

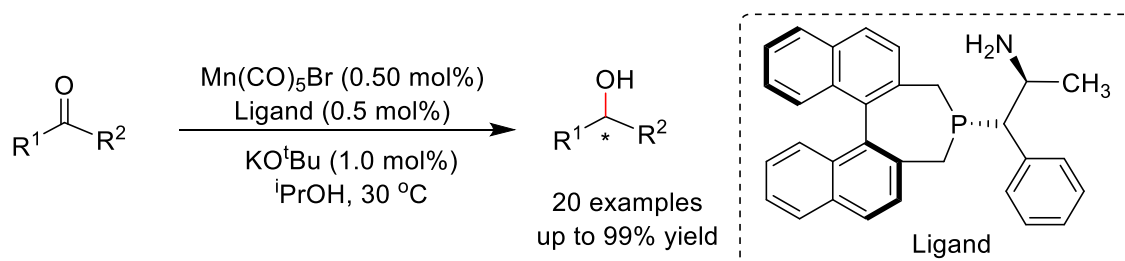
Zuo and co-workers developed a chiral iron catalyst for the enantioselective transfer hydrogenation of ketones to synthesize the chiral alcohols using isopropanol as a hydrogen source (Scheme 1.40).²³³ The substrates bearing synthetically important functional groups such as chloro, bromo, cyano, and $-\text{CF}_3$ were tolerated under this catalytic system. A range of ketones were efficiently hydrogenated to provide desired chiral alcohols with good enantioselectivities.



Scheme 1.40. Iron-catalyzed enantioselective transfer hydrogenation of ketones.

1.4.2 Manganese-Catalyzed Hydrogenation of Ketones

The enantioselective transfer hydrogenation of ketones to get chiral alcohols was demonstrated by Sortais and Bastin under manganese catalysis (Scheme 1.41).²³⁴ The combination of $\text{Mn}(\text{CO})_5\text{Br}$ with bidentate chiral amino-phosphine ligand provided diverse chiral alcohols using isopropanol as a hydrogen source. Various aromatic ketones were efficiently reduced under the reaction conditions and the enantioselectivities for the alcohol product was obtained up to 99%. This protocol was also compatible with heteroaryl ketone and dialkyl ketone providing desired alcohols in good yields but with low enantioselectivities.



Scheme 1.41. Manganese-catalyzed asymmetric transfer hydrogenation of ketones.

1.5 REFERENCES

- (1) Kraft, A.; Grimdsdale, A. C.; Holmes, A. B. *Angew. Chem. Int. Ed.* **1998**, *37*, 402-428.
- (2) Nicolaou, K. C.; Bulger, P. G.; Sarlah, D. *Angew. Chem. Int. Ed.* **2005**, *44*, 4442-4489.
- (3) Carey, J. S.; Laffan, D.; Thomson, C.; Williams, M. T. *Org. Biomol. Chem.* **2006**, *4*, 2337-2347.
- (4) Alberico, D.; Scott, M. E.; Lautens, M. *Chem. Rev.* **2007**, *107*, 174-238.
- (5) Lyons, T. W.; Sanford, M. S. *Chem. Rev.* **2010**, *110*, 1147-1169.
- (6) Ackermann, L. *Chem. Rev.* **2011**, *111*, 1315-1345.
- (7) Arockiam, P. B.; Bruneau, C.; Dixneuf, P. H. *Chem. Rev.* **2012**, *112*, 5879-5918.
- (8) Yamaguchi, J.; Yamaguchi, A. D.; Itami, K. *Angew. Chem. Int. Ed.* **2012**, *51*, 8960-9009.
- (9) Zhang, M.; Zhang, Y.; Jie, X.; Zhao, H.; Li, G.; Su, W. *Org. Chem. Front.*, *1*, 843-895.
- (10) Yang, Y.; Lan, J.; You, J. *Chem. Rev.* **2017**, *117*, 8787-8863.
- (11) Ananikov, V. P. *ACS Catal.* **2015**, *5*, 1964-1971.
- (12) Noyori, R.; Ohkuma, T. *Angew. Chem. Int. Ed.* **2001**, *40*, 40-73.
- (13) Magano, J.; Dunetz, J. R. *Org. Process Res. Dev.* **2012**, *16*, 1156-1184.
- (14) Knowles, W. S. *Angew. Chem. Int. Ed.* **2002**, *41*, 1998-2007.
- (15) Xie, J.-H.; Zhou, Q.-L. *Acc. Chem. Res.* **2008**, *41*, 581-593.
- (16) Noyori, R.; Hashiguchi, S. *Acc. Chem. Res.* **1997**, *30*, 97-102.
- (17) Ito, J.-i.; Sugino, K.; Matsushima, S.; Sakaguchi, H.; Iwata, H.; Ishihara, T.; Nishiyama, H. *Organometallics* **2016**, *35*, 1885-1894.
- (18) Liu, T.; Chai, H.; Wang, L.; Yu, Z. *Organometallics* **2017**, *36*, 2914-2921.
- (19) Chai, H.; Liu, T.; Zheng, D.; Yu, Z. *Organometallics* **2017**, *36*, 4268-4277.
- (20) Murata, K.; Ikariya, T.; Noyori, R. *J. Org. Chem.* **1999**, *64*, 2186-2187.
- (21) Yang, L.; Krüger, A.; Neels, A.; Albrecht, M. *Organometallics* **2008**, *27*, 3161-3171.
- (22) Farrell, K.; Müller-Bunz, H.; Albrecht, M. *Organometallics* **2015**, *34*, 5723-5733.
- (23) Chelucci, G.; Baldino, S.; Baratta, W. *Acc. Chem. Res.* **2015**, *48*, 363-379.
- (24) Mestroni, G.; Zassinovich, G.; Camus, A.; Martinelli, F. *J. Organometallic Chem.* **1980**, *198*, 87-96.

-
- (25) Bartoszewicz, A.; Ahlsten, N.; Martín-Matute, B. *Chem. Eur. J.* **2013**, *19*, 7274-7302.
- (26) Suzuki, A. *Angew. Chem. Int. Ed.* **2011**, *50*, 6722-6737.
- (27) Negishi, E. *Angew. Chem. Int. Ed.* **2011**, *50*, 6738-6764.
- (28) Johansson Seechurn, C. C. C.; Kitching, M. O.; Colacot, T. J.; Snieckus, V. *Angew. Chem. Int. Ed.* **2012**, *51*, 5062-5085.
- (29) Biffis, A.; Centomo, P.; Del Zotto, A.; Zecca, M. *Chem. Rev.* **2018**, *118*, 2249-2295.
- (30) Giri, R.; Shi, B.-F.; Engle, K. M.; Mangel, N.; Yu, J.-Q. *Chem. Soc. Rev.* **2009**, *38*, 3242-3272.
- (31) Lyons, T. W.; Sanford, M. S. *Chem. Rev.* **2010**, *110*, 1147-1169.
- (32) Colby, D. A.; Bergman, R. G.; Ellman, J. A. *Chem. Rev.* **2010**, *110*, 624-655.
- (33) Gensch, T.; Hopkinson, M. N.; Glorius, F.; Wencel-Delord, J. *Chem. Soc. Rev.* **2016**, *45*, 2900-2936.
- (34) Wei, Y.; Hu, P.; Zhang, M.; Su, W. *Chem. Rev.* **2017**, *117*, 8864-8907.
- (35) Ma, W.; Gandeepan, P.; Li, J.; Ackermann, L. *Org. Chem. Front.* **2017**, *4*, 1435-1467.
- (36) Dong, Z.; Ren, Z.; Thompson, S. J.; Xu, Y.; Dong, G. *Chem. Rev.* **2017**, *117*, 9333-9403.
- (37) Zhang, Y.-F.; Shi, Z.-J. *Acc. Chem. Res.* **2019**, *52*, 161-169.
- (38) Yeung, C. S.; Dong, V. M. *Chem. Rev.* **2011**, *111*, 1215-1292.
- (39) Li, B.-J.; Shi, Z.-J. *Chem. Soc. Rev.* **2012**, *41*, 5588-5598.
- (40) Girard, S. A.; Knauber, T.; Li, C.-J. *Angew. Chem. Int. Ed.* **2014**, *53*, 74-100.
- (41) Liu, C.; Yuan, J.; Gao, M.; Tang, S.; Li, W.; Shi, R.; Lei, A. *Chem. Rev.* **2015**, *115*, 12138-12204.
- (42) Bansal, S.; Shabade, A. B.; Punji, B. *Advanced Synthesis & Catalysis* **2021**, *363*, 1998-2022.
- (43) Stuart, D. R.; Fagnou, K. *Science* **2007**, *316*, 1172-1175.
- (44) Stuart, D. R.; Villemure, E.; Fagnou, K. *J. Am. Chem. Soc.* **2007**, *129*, 12072-12073.
- (45) Dwight, T. A.; Rue, N. R.; Charyk, D.; Josselyn, R.; DeBoef, B. *Org. Lett.* **2007**, *9*, 3137-3139.
- (46) Potavathri, S.; Pereira, K. C.; Gorelsky, S. I.; Pike, A.; LeBris, A. P.; DeBoef, B. *J. Am. Chem. Soc.* **2010**, *132*, 14676-14681.
-

-
- (47) Xi, P.; Yang, F.; Qin, S.; Zhao, D.; Lan, J.; Gao, G.; Hu, C.; You, J. *J. Am. Chem. Soc.* **2010**, *132*, 1822-1824.
- (48) Yeung, C. S.; Dong, V. M. *Chem. Rev.* **2011**, *111*, 1215-1292.
- (49) Zhao, D.; You, J.; Hu, C. *Chem. Eur. J.* **2011**, *17*, 5466-5492.
- (50) Campbell, A. N.; Meyer, E. B.; Stahl, S. S. *Chem. Commun.* **2011**, *47*, 10257-10259.
- (51) Wang, Z.; Li, K.; Zhao, D.; Lan, J.; You, J. *Angew. Chem. Int. Ed.* **2011**, *50*, 5365-5369.
- (52) Pintori, D. G.; Greaney, M. F. *J. Am. Chem. Soc.* **2011**, *133*, 1209-1211.
- (53) Wang, F.; Song, G.; Du, Z.; Li, X. *J. Org. Chem.* **2011**, *76*, 2926-2932.
- (54) Qin, X.; Liu, H.; Qin, D.; Wu, Q.; You, J.; Zhao, D.; Guo, Q.; Huang, X.; Lan, J. *Chem. Sci.* **2013**, *4*, 1964-1969.
- (55) Cambeiro, X. C.; Ahlsten, N.; Larrosa, I. *J. Am. Chem. Soc.* **2015**, *137*, 15636-15639.
- (56) Yan, S.-Y.; Zhang, Z.-Z.; Shi, B.-F. *Chem. Commun.* **2017**, *53*, 10287-10290.
- (57) Gandeepan, P.; Koeller, J.; Ackermann, L. *ACS Catalysis* **2017**, *7*, 1030-1034.
- (58) Khake, S. M.; Soni, V.; Gonnade, R. G.; Punji, B. *Chem. Eur. J.* **2017**, *23*, 2907-2914.
- (59) Cabrero-Antonino, J. R.; Adam, R.; Junge, K.; Beller, M. *Chem. Sci.* **2017**, *8*, 6439-6450.
- (60) Wang, C.; Rueping, M. *ChemCatChem* **2018**, *10*, 2681-2685.
- (61) Soni, V.; Sharma, D. M.; Punji, B. *Chem. Asian J.* **2018**, *13*, 2516-2521.
- (62) Kalepu, J.; Gandeepan, P.; Ackermann, L.; Pilarski, L. T. *Chem. Sci.* **2018**, *9*, 4203-4216.
- (63) Pandey, D. K.; Ankade, S. B.; Ali, A.; Vinod, C. P.; Punji, B. *Chem. Sci.* **2019**, *10*, 9493-9500.
- (64) Li, T.; Yang, Y.; Li, B.; Yang, P. *Chem. Commun.* **2019**, *55*, 353-356.
- (65) Banjare, S. K.; Nanda, T.; Ravikumar, P. C. *Org. Lett.* **2019**, *21*, 8138-8143.
- (66) Jagtap, R. A.; Vinod, C. P.; Punji, B. *ACS Catal.* **2019**, *9*, 431-441.
- (67) Shah, T. A.; De, P. B.; Pradhan, S.; Punniyamurthy, T. *Chem. Commun.* **2019**, *55*, 572-587.
- (68) Gandeepan, P.; M \ddot{a} lller, T.; Zell, D.; Cera, G.; Warratz, S.; Ackermann, L. *Chem. Rev.* **2019**, *119*, 2192-2452.
- (69) Zhang, C.; Tang, C.; Jiao, N. *Chem. Soc. Rev.* **2012**, *41*, 3464-3484.
-

- (70) Nishino, M.; Hirano, K.; Satoh, T.; Miura, M. *Angew. Chem. Int. Ed.* **2012**, *51*, 6993-6997.
- (71) Tan, G.; He, S.; Huang, X.; Liao, X.; Cheng, Y.; You, J. *Angew. Chem. Int. Ed.* **2016**, *55*, 10414-10418.
- (72) Cheng, Y.; Wu, Y.; Tan, G.; You, J. *Angew. Chem. Int. Ed.* **2016**, *55*, 12275-12279.
- (73) Miao, J.; Ge, H. *Eur. J. Org. Chem.* **2015**, *2015*, 7859-7868.
- (74) Arun, V.; Mahanty, K.; De Sarkar, S. *ChemCatChem* **2019**, *11*, 2243-2259.
- (75) Yang, F.; Li, J.; Xie, J.; Huang, Z.-Z. *Org. Lett.* **2010**, *12*, 5214-5217.
- (76) Zhang, H.-J.; Su, F.; Wen, T.-B. *J. Org. Chem.* **2015**, *80*, 11322-11329.
- (77) Norinder, J.; Matsumoto, A.; Yoshikai, N.; Nakamura, E. *J. Am. Chem. Soc.* **2008**, *130*, 5858-5859.
- (78) Bera, A.; Kabadwal, L. M.; Bera, S.; Banerjee, D. *Chem. Commun.* **2022**, *58*, 10-28.
- (79) Banjare, S. K.; Pati, B. V.; Ravikumar, P. C. In *Handbook of CH-Functionalization 2023*, p 1-32.
- (80) Cai, Y.; Zhu, S.-F.; Wang, G.-P.; Zhou, Q.-L. *Adv. Synth. Catal.* **2011**, *353*, 2939-2944.
- (81) Chakraborty, S.; Ahmed, J.; Shaw, B. K.; Jose, A.; Mandal, S. K. *Chem. Eur. J.* **2018**, *24*, 17651-17655.
- (82) Cera, G.; Haven, T.; Ackermann, L. *Angew. Chem. Int. Ed.* **2016**, *55*, 1484-1488.
- (83) Kabadwal, L. M.; Bera, S.; Banerjee, D. *Chem. Commun.* **2020**, *56*, 4777-4780.
- (84) Doba, T.; Matsubara, T.; Ilies, L.; Shang, R.; Nakamura, E. *Nat. Catal.* **2019**, *2*, 400-406.
- (85) Cui, H.-L. *Org. Biomole. Chem.* **2020**, *18*, 4085-4089.
- (86) Liang, K.; Yang, J.; Tong, X.; Shang, W.; Pan, Z.; Xia, C. *Org. Lett.* **2016**, *18*, 1474-1477.
- (87) Mishra, A.; Dwivedi, A. D.; Shee, S.; Kundu, S. *Chem. Commun.* **2020**, *56*, 249-252.
- (88) Nanda, T.; Banjare, S. K.; Kong, W.-Y.; Guo, W.; Biswal, P.; Gupta, L.; Linda, A.; Pati, B. V.; Mohanty, S. R.; Tantillo, D. J.; Ravikumar, P. C. *ACS Catal.* **2022**, *12*, 11651-11659.
- (89) Li, B.; Wu, Z.-H.; Gu, Y.-F.; Sun, C.-L.; Wang, B.-Q.; Shi, Z.-J. *Angew. Chem. Int. Ed.* **2011**, *50*, 1109-1113.

-
- (90) Song, W.; Ackermann, L. *Angew. Chem. Int. Ed.* **2012**, *51*, 8251-8254.
- (91) Punji, B.; Song, W.; Shevchenko, G. A.; Ackermann, L. *Chem. Eur. J.* **2013**, *19*, 10605-10610.
- (92) Luis, C. M. C.; Naoto, C. *Chem. Lett.* **2015**, *44*, 410-421.
- (93) Harry, N. A.; Saranya, S.; Ujwaldev, S. M.; Anilkumar, G. *Catal. Sci. Tech.* **2019**, *9*, 1726-1743.
- (94) Khake, S. M.; Chatani, N. *Trends in Chemistry* **2019**, *1*, 524-539.
- (95) Khake, S. M.; Chatani, N. *Chem* **2020**, *6*, 1056-1081.
- (96) Tobisu, M.; Hyodo, I.; Chatani, N. *J. Am. Chem. Soc.* **2009**, *131*, 12070-12071.
- (97) Canivet, J.; Yamaguchi, J.; Ban, I.; Itami, K. *Org. Lett.* **2009**, *11*, 1733-1736.
- (98) Hachiya, H.; Hirano, K.; Satoh, T.; Miura, M. *Angew. Chem. Int. Ed.* **2010**, *49*, 2202-2205.
- (99) Qu, G.-R.; Xin, P.-Y.; Niu, H.-Y.; Wang, D.-C.; Ding, R.-F.; Guo, H.-M. *Chem. Commun.* **2011**, *47*, 11140-11142.
- (100) Jin, L.-K.; Wan, L.; Feng, J.; Cai, C. *Org. Lett.* **2015**, *17*, 4726-4729.
- (101) Soni, V.; Khake, S. M.; Punji, B. *ACS Catal.* **2017**, *7*, 4202-4208.
- (102) Tan, G.; Zhang, L.; Liao, X.; Shi, Y.; Wu, Y.; Yang, Y.; You, J. *Org. Lett.* **2017**, *19*, 4830-4833.
- (103) Wang, X.; Xie, P.; Qiu, R.; Zhu, L.; Liu, T.; Li, Y.; Iwasaki, T.; Au, C.-T.; Xu, X.; Xia, Y.; Yin, S.-F.; Kambe, N. *Chem. Commun.* **2017**, *53*, 8316-8319.
- (104) Mannava, V.; Jesse, K. A.; Anderson, J. S. *Organometallics* **2019**, *38*, 4554-4559.
- (105) Sarkar, T.; Maharana, P. K.; Roy, S.; Punniyamurthy, T. *Chem. Commun.* **2022**, *58*, 5980-5983.
- (106) Tan, G.; Zhang, L.; Liao, X.; Shi, Y.; Wu, Y.; Yang, Y.; You, J. *Org. Lett.* **2017**, 4830-4833.
- (107) Kitahara, M.; Umeda, N.; Hirano, K.; Satoh, T.; Miura, M. *J. Am. Chem. Soc.* **2011**, *133*, 2160-2162.
- (108) Nishino, M.; Hirano, K.; Satoh, T.; Miura, M. *Angew. Chem. Int. Ed.* **2013**, *52*, 4457-4461.
- (109) Odani, R.; Hirano, K.; Satoh, T.; Miura, M. *J. Org. Chem.* **2013**, *78*, 11045-11052.
- (110) Zou, L.-H.; Mottweiler, J.; Priebbenow, D. L.; Wang, J.; Stubenrauch, J. A.; Bolm, C. *Chem. Eur. J.* **2013**, *19*, 3302-3305.
-

- (111) Zhao, S.; Yuan, J.; Li, Y.-C.; Shi, B.-F. *Chem. Commun.* **2015**, *51*, 12823-12826.
- (112) Do, H.-Q.; Daugulis, O. *J. Am. Chem. Soc.* **2011**, *133*, 13577-13586.
- (113) Monguchi, D.; Yamamura, A.; Fujiwara, T.; Somete, T.; Mori, A. *Tetrahedron Lett.* **2010**, *51*, 850-852.
- (114) Li, Y.; Jin, J.; Qian, W.; Bao, W. *Org. Biomole. Chem.* **2010**, *8*, 326-330.
- (115) Zhu, M.; Fujita, K.-i.; Yamaguchi, R. *Chem. Commun.* **2011**, *47*, 12876-12878.
- (116) Lei, S.; Cao, H.; Chen, L.; Liu, J.; Cai, H.; Tan, J. *Adv. Synth. Catal.* **2015**, *357*, 3109-3114.
- (117) Jha, A. K.; Jain, N. *Eur. J. Org. Chem.* **2017**, *2017*, 4765-4772.
- (118) Le, J.; Gao, Y.; Ding, Y.; Jiang, C. *Tetrahedron Lett.* **2016**, *57*, 1728-1731.
- (119) Mao, Z.; Wang, Z.; Xu, Z.; Huang, F.; Yu, Z.; Wang, R. *Org. Lett.* **2012**, *14*, 3854-3857.
- (120) Qin, X.; Feng, B.; Dong, J.; Li, X.; Xue, Y.; Lan, J.; You, J. *J. Org. Chem.* **2012**, *7677-7683*.
- (121) Li, Y.; Qian, F.; Ge, X.; Liu, T.; Jalani, H. B.; Lu, H.; Li, G. *Green Chem.* **2019**, *21*, 5797-5802.
- (122) Odani, R.; Hirano, K.; Satoh, T.; Miura, M. *J. Org. Chem.* **2015**, *80*, 2384-2391.
- (123) Yang, Q.; Yin, Z.; Zheng, L.; Yuan, J.; Wei, S.; Ding, Q.; Peng, Y. *RSC Adv.* **2019**, *9*, 5870-5877.
- (124) Odani, R.; Hirano, K.; Satoh, T.; Miura, M. *Angew. Chem. Int. Ed.* **2014**, *53*, 10784-10788.
- (125) Roberts, R. M.; Khalaf, A. A. *Friedel-Crafts alkylation chemistry : a century of discovery*; Marcel Dekker: New York, 1984; Vol. 10.
- (126) Bandini, M.; Tragni, M. *Org. Biomole. Chem.* **2009**, *7*, 1501-1507.
- (127) Minisci Francesco, E. V., and Francesca Fontana *Heterocycles* **1989**, *28*, 489-519.
- (128) Netherton, M. R.; Fu, G. C. *Adv. Synth. Catal.* **2004**, *346*, 1525-1532.
- (129) Hu, X. *CHIMIA* **2012**, *66*, 154.
- (130) Moselage, M.; Li, J.; Ackermann, L. *ACS Catal.* **2016**, *6*, 498-525.
- (131) Liu, W.; Ackermann, L. *ACS Catal.* **2016**, *6*, 3743-3752.
- (132) Cera, G.; Ackermann, L. *Top. Curr. Chem.* **2016**, *374*, 57.
- (133) Nareddy, P.; Jordan, F.; Szostak, M. *ACS Catal.* **2017**, *7*, 5721-5745.
- (134) Wedi, P.; van Gemmeren, M. *Angew. Chem. Int. Ed.* **2018**, *57*, 13016-13027.

- (135) Gandeepan, P.; Müller, T.; Zell, D.; Cera, G.; Warratz, S.; Ackermann, L. *Chem. Rev.* **2019**, *119*, 2192-2452.
- (136) Singh, K. S. *Catalysts* **2019**, *9*, 173.
- (137) Ackermann, L. *J. Org. Chem.* **2014**, *79*, 8948-8954.
- (138) Messaoudi, S.; Brion, J.-D.; Alami, M. d. *Eur. J. Org. Chem.* **2010**, *2010*, 6495-6516.
- (139) Pan, S.; Shibata, T. *ACS Catal.* **2013**, *3*, 704-712.
- (140) Leitch, J. A.; Bhonoah, Y.; Frost, C. G. *ACS Catal.* **2017**, *7*, 5618-5627.
- (141) Jagtap, R. A.; Punji, B. *Asian J. Org. Chem.* **2020**, *9*, 326-342.
- (142) Rej, S.; Ano, Y.; Chatani, N. *Chem. Rev.* **2020**, *120*, 1788-1887.
- (143) Kumar, P.; Nagtilak, P. J.; Kapur, M. *New J. Chem.* **2021**, *45*, 13692-13746.
- (144) Lu, M.-Z.; Lu, P.; Xu, Y.-H.; Loh, T.-P. *Org. Lett.* **2014**, *16*, 2614-2617.
- (145) Sollert, C.; Devaraj, K.; Orthaber, A.; Gates, P. J.; Pilarski, L. T. *Chem. Eur. J.* **2015**, *21*, 5380-5386.
- (146) Jagtap, R. A.; Soni, V.; Punji, B. *ChemSusChem* **2017**, *10*, 2242-2248.
- (147) Pandey, D. K.; Vijaykumar, M.; Punji, B. *J. Org. Chem.* **2020**, *84*, 12800-12808.
- (148) Pandey, D. K.; Shabade, A. B.; Punji, B. *Adv. Synth. Catal.* **2020**, *362*, 2534-2540.
- (149) Moselage, M.; Sauermann, N.; Richter, S. C.; Ackermann, L. *Angew. Chem. Int. Ed.* **2015**, *54*, 6352-6355.
- (150) Zell, D.; Dhawa, U.; Müller, V.; Bursch, M.; Grimme, S.; Ackermann, L. *ACS Catal.* **2017**, *7*, 4209-4213.
- (151) Jana, U.; Maiti, S.; Biswas, S. *Tetrahedron Lett.* **2007**, *48*, 7160-7163.
- (152) Liu, X.-G.; Zhang, S.-S.; Wu, J.-Q.; Li, Q.; Wang, H. *Tetrahedron Lett.* **2015**, *56*, 4093-4095.
- (153) Shimizu, R.; Egami, H.; Nagi, T.; Chae, J.; Hamashima, Y.; Sodeoka, M. *Tetrahedron Lett.* **2010**, *51*, 5947-5949.
- (154) Ackermann, L. *Chem. Commun.* **2010**, *46*, 4866-4877.
- (155) Hu, X. *Chem. Sci.* **2011**, *2*, 1867-1886.
- (156) Ankade, S. B.; Shabade, A. B.; Soni, V.; Punji, B. *ACS Catal.* **2021**, *11*, 3268-3292.
- (157) Jagtap, R. A.; Verma, S. K.; Punji, B. *Org. Lett.* **2020**, *22*, 4643-4647.

- (158) Dombay, T.; Werncke, C. G.; Jiang, S.; Grellier, M.; Vendier, L.; Bontemps, S. b.; Sortais, J.-B.; Sabo-Etienne, S.; Darcel, C. *J. Am. Chem. Soc.* **2015**, *137*, 4062-4065.
- (159) Shang, R.; Ilies, L.; Nakamura, E. *Chem. Rev.* **2017**, *117*, 9086-9139.
- (160) Das, J.; Vellakkaran, M.; Sk, M.; Banerjee, D. *Org. Lett.* **2019**, *21*, 7514-7518.
- (161) Empel, C.; Jana, S.; Koenigs, R. M. *Molecules* **2020**, *25*, 880.
- (162) Jagtap, R. A.; Samal, P. P.; Vinod, C. P.; Krishnamurty, S.; Punji, B. *ACS Catal.* **2020**, *10*, 7312-7321.
- (163) Chandra, D.; Manisha; Sharma, U. *Chem. Rec.* **2022**, *22*, e202100271.
- (164) Das, J.; Vellakkaran, M.; Banerjee, D. *Chem. Commun.* **2019**, *55*, 7530-7533.
- (165) Song, W.; Lackner, S.; Ackermann, L. *Angew. Chem. Int. Ed.* **2014**, *53*, 2477-2480.
- (166) Soni, V.; Jagtap, R. A.; Gonnade, R. G.; Punji, B. *ACS Catal.* **2016**, *6*, 5666-5672.
- (167) Evano, G.; Theunissen, C. *Angew. Chem. Int. Ed.* **2019**, *58*, 7202-7236.
- (168) Wong, M. Y.; Yamakawa, T.; Yoshikai, N. *Org. Lett.* **2015**, *17*, 442-445.
- (169) Loup, J.; Zell, D.; Oliveira, J. o. C. A.; Keil, H.; Stalke, D.; Ackermann, L. *Angew. Chem. Int. Ed.* **2017**, *56*, 14197-14201.
- (170) Patel, M.; Ajay, U.; Padala, K.; Naveen, T. *Asian J. Org. Chem.* **2022**, *11*, e202200201.
- (171) Santhoshkumar, R.; Cheng, C.-H. *Beilstein J. Org. Chem.* **2018**, *14*, 2266-2288.
- (172) Ding, Z.; Yoshikai, N. *Beilstein J. Org. Chem.* **2012**, *8*, 1536-1542.
- (173) Muniraj, N.; Prabhu, K. R. *ACS Omega* **2017**, *2*, 4470-4479.
- (174) Li, J.; Zhang, Z.; Ma, W.; Tang, M.; Wang, D.; Zou, L.-H. *Adv. Synth. Catal.* **2017**, *359*, 1717-1724.
- (175) Zell, D.; Bursch, M.; Müller, V.; Grimme, S.; Ackermann, L. *Angew. Chem. Int. Ed.* **2017**, *56*, 10378-10382.
- (176) Lee, P.-S.; Yoshikai, N. *Org. Lett.* **2015**, *17*, 22-25.
- (177) Pesciaioli, F.; Dhawa, U.; Oliveira, J. C. A.; Yin, R.; John, M.; Ackermann, L. *Angew. Chem. Int. Ed.* **2018**, *57*, 15425-15429.
- (178) Kurihara, T.; Kojima, M.; Yoshino, T.; Matsunaga, S. *Asian J. Org. Chem.* **2020**, *9*, 368-371.
- (179) Nakao, Y.; Kashihara, N.; Kanyiva, K. S.; Hiyama, T. *Angew. Chem. Int. Ed.* **2010**, *49*, 4451-4454.

- (180) Schramm, Y.; Takeuchi, M.; Semba, K.; Nakao, Y.; Hartwig, J. F. *J. Am. Chem. Soc.* **2015**, *137*, 12215-12218.
- (181) Wu, J.; Wang, D.; Wu, F.; Wan, B. *J. Org. Chem.* **2013**, *78*, 5611-5617.
- (182) Galliford, C. V.; Prof Scheidt, K. A. *Angew. Chem. Int. Ed.* **2007**, *46*, 8748-8758.
- (183) Klein, J. E. M. N.; Taylor, R. J. K. *Eur. J. Org. Chem.* **2011**, *2011*, 6821-6841.
- (184) Liu, Y.-L.; Wang, B.-L.; Cao, J.-J.; Chen, L.; Zhang, Y.-X.; Wang, C.; Zhou, J. *J. Am. Chem. Soc.* **2010**, *132*, 15176-15178.
- (185) Paniagua-Vega, D.; Cerda-Garcia-Rojas, C. M.; Ponce-Noyola, T.; Ramos-Valdivia, A. C. *Nat. prod. commun.* **2012**, *7*, 1441-1444.
- (186) Kaur, J.; Chimni, S. S.; Mahajan, S.; Kumar, A. *RSC Adv.* **2015**, *5*, 52481-52496.
- (187) Aslam, N. A.; Babu, S. A.; Rani, S.; Mahajan, S.; Solanki, J.; Yasuda, M.; Baba, A. *Eur. J. Org. Chem.* **2015**, *2015*, 4168-4189.
- (188) Zhou, F.; Liu, Y.-L.; Zhou, J. *Adv. Synth. Catal.* **2010**, *352*, 1381-1407.
- (189) Ochi, M.; Kawasaki, K.; Kataoka, H.; Uchio, Y.; Nishi, H. *Biochem. Biophys. Res. Commun.* **2001**, *283*, 1118-1123.
- (190) Rottmann, M.; McNamara, C.; Yeung, B. K. S.; Lee, M. C. S.; Zou, B.; Russell, B.; Seitz, P.; Plouffe, D. M.; Dharia, N. V.; Tan, J.; Cohen, S. B.; Spencer, K. R.; González-Pérez, G. E.; Lakshminarayana, S. B.; Goh, A.; Suwanarusk, R.; Jegla, T.; Schmitt, E. K.; Beck, H.-P.; Brun, R.; Nosten, F.; Renia, L.; Dartois, V.; Keller, T. H.; Fidock, D. A.; Winzeler, E. A.; Diagana, T. T. *Science* **2010**, *329*, 1175-1180.
- (191) Crosignani, S.; Jorand-Lebrun, C.; Page, P.; Campbell, G.; Colovray, V. r.; Missotten, M.; Humbert, Y.; Cleva, C.; Arrighi, J.-F. o.; Gaudet, M. n.; Johnson, Z.; Ferro, P.; Chollet, A. *ACS Med. Chem. Lett.* **2011**, *2*, 644-649.
- (192) Zhou, F.; Liu, Y.-L.; Zhou, J. *Adv. Synth. Catal.* **2010**, *352*, 1381-1407.
- (193) Shen, K.; Liu, X.; Lin, L.; Feng, X. *Chem. Sci.* **2012**, *3*, 327-334.
- (194) Dalpozzo, R.; Bartoli, G.; Bencivenni, G. *Chem. Soc. Rev.* **2012**, *41*, 7247-7290.
- (195) Kaur, J.; Chimni, S. S. *Org. Biomol. Chem.* **2018**, *16*, 3328-3347.
- (196) Kaur, J.; Kaur, B. P.; Chimni, S. S. *Org. Biomol. Chem.* **2020**, *18*, 4692-4708.
- (197) Wang, D.; Liang, J.; Feng, J.; Wang, K.; Sun, Q.; Zhao, L.; Li, D.; Yan, W.; Wang, R. *Adv. Synth. Catal.* **2012**, *355*, 548-558.
- (198) Zhao, J.; Fang, B.; Luo, W.; Hao, X.; Liu, X.; Lin, L.; Feng, X. *Angew. Chem. Int. Ed.* **2014**, *54*, 241-244.

- (199) Kumar, A.; Kaur, J.; Chimni, S. S.; Jassal, A. K. *RSC Adv.* **2014**, *4*, 24816-24819.
- (200) Holmquist, M.; Blay, G.; Pedro, J. R. *Chem. Commun.* **2014**, *50*, 9309-9312.
- (201) Lesma, G.; Meneghetti, F.; Sacchetti, A.; Stucchi, M.; Silvani, A. *Beilstein J. Org. Chem.* **2014**, *10*, 1383-1389.
- (202) Engl, O. D.; Fritz, S. P.; Wennemers, H. *Angew. Chem. Int. Ed.* **2015**, *54*, 8193-8197.
- (203) Fang, B.; Liu, X.; Zhao, J.; Tang, Y.; Lin, L.; Feng, X. *J. Org. Chem.* **2015**, *80*, 3332-3338.
- (204) He, Q.; Wu, L.; Kou, X.; Butt, N.; Yang, G.; Zhang, W. *Org. Lett.* **2016**, *18*, 288-291.
- (205) Menapara, T.; Choudhary, M. K.; Tak, R.; Kureshy, R. I.; Khan, N.-u. H.; Abdi, S. H. R. *J. Mole. Catal. A: Chemical* **2016**, *421*, 161-166.
- (206) Dai, J.; Xiong, D.; Yuan, T.; Liu, J.; Chen, T.; Shao, Z. *Angew. Chem. Int. Ed.* **2017**, *56*, 12697-12701.
- (207) Hajra, S.; Bhosale, S. S.; Hazra, A. *Org. Biomol. Chem.* **2017**, *15*, 9217-9225.
- (208) Cheng, C.; Lu, X.; Ge, L.; Chen, J.; Cao, W.; Wu, X.; Zhao, G. *Org. Chem. Front.* **2017**, *4*, 101-114.
- (209) Chen, Q.; Xie, L.; Li, Z.; Tang, Y.; Zhao, P.; Lin, L.; Feng, X.; Liu, X. *Chem. Commun.* **2018**, *54*, 678-681.
- (210) Sawa, M.; Miyazaki, S.; Yonesaki, R.; Morimoto, H.; Ohshima, T. *Org. Lett.* **2018**, *20*, 5393-5397.
- (211) Huang, Q.; Cheng, Y.; Yuan, H.; Chang, X.; Li, P.; Li, W. *Org. Chem. Front.* **2018**, *5*, 3226-3230.
- (212) Wang, J.-Y.; Li, M.-W.; Li, M.-F.; Hao, W.-J.; Li, G.; Tu, S.-J.; Jiang, B. *Org. Lett.* **2018**, *20*, 6616-6621.
- (213) Kang, T.; Cao, W.; Hou, L.; Tang, Q.; Zou, S.; Liu, X.; Feng, X. *Angew. Chem. Int. Ed.* **2019**, *58*, 2464-2468.
- (214) Arai, T.; Araseki, K.; Kakino, J. *Org. Lett.* **2019**, *21*, 8572-8576.
- (215) Hajra, S.; Laskar, S.; Jana, B. *Chem. Eur. J.* **2019**, *25*, 14688-14693.
- (216) Li, G.; Liu, M.; Zou, S.; Feng, X.; Lin, L. *Org. Lett.* **2020**, *22*, 8708-8713.
- (217) Yonesaki, R.; Kusagawa, I.; Morimoto, H.; Hayashi, T.; Ohshima, T. *Chem. Asian. J.* **2020**, *15*, 499-502.

- (218) Yang, W.; Dong, P.; Xu, J.; Yang, J.; Liu, X.; Feng, X. *Chem. Eur. J.* **2021**, *27*, 9272-9275.
- (219) Bui, T.; Borregan, M.; Barbas, C. F., III *J. Org. Chem.* **2009**, *74*, 8935-8938.
- (220) Qian, Z.-Q.; Zhou, F.; Du, T.-P.; Wang, B.-L.; Ding, M.; Zhao, X.-L.; Zhou, J. *Chem. Commun.* **2009**, 6753-6755.
- (221) Cheng, L.; Liu, L.; Wang, D.; Chen, Y.-J. *Org. Lett.* **2009**, *11*, 3874-3877.
- (222) Mouri, S.; Chen, Z.; Mitsunuma, H.; Furutachi, M.; Matsunaga, S.; Shibasaki, M. *J. Am. Chem. Soc.* **2010**, *132*, 1255-1257.
- (223) Lai, Y.-H.; Wu, R.-S.; Huang, J.; Huang, J.-Y.; Xu, D.-Z. *Org. Lett.* **2020**, *22*, 3825-3829.
- (224) Arai, T.; Matsumura, E.; Masu, H. *Org. Lett.* **2014**, *16*, 2768-2771.
- (225) Menapara, T.; Choudhary, M. K.; Tak, R.; Kureshy, R. I.; Khan, N.-u. H.; Abdi, S. H. R. *Journal of Molecular Catalysis A: Chemical* **2016**, *421*, 161-166.
- (226) Sawa, M.; Miyazaki, S.; Yonesaki, R.; Morimoto, H.; Ohshima, T. *Org. Lett.* **2018**, 5393-5397.
- (227) Hoye, R. C. *J. Chem. Educ.* **1999**, *76*, 33.
- (228) Wang, D.; Astruc, D. *Chem. Rev.* **2015**, *115*, 6621-6686.
- (229) Gladiali, S.; Alberico, E. *Chem. Soc. Rev.* **2006**, *35*, 226-236.
- (230) Shee, S.; Paul, B.; Kundu, S. *ChemistrySelect* **2017**, *2*, 1705-1710.
- (231) Li, Y.-Y.; Yu, S.-L.; Shen, W.-Y.; Gao, J.-X. *Acc. Chem. Res.* **2015**, *48*, 2587-2598.
- (232) Ganguli, K.; Shee, S.; Panja, D.; Kundu, S. *Dalton Trans.* **2019**, *48*, 7358-7366.
- (233) Huo, S.; Wang, Q.; Zuo, W. *Dalton Trans* **2020**, *49*, 7959-7967.
- (234) Azouzi, K.; Bruneau-Voisine, A.; Vendier, L.; Sortais, J.-B.; Bastin, S. p. *Catal. Commun.* **2020**, *142*, 106040.

Objectives of the Present Study

In last few years, significant efforts were devoted for the C–H bond functionalization of heteroarenes as well as hydrogenation of ketones using base metal catalysts. Particularly, 3d transition metal catalysts have been employed for the oxidative coupling, C–H alkylation, functionalization of isatins, and hydrogenation reactions. However, the harsh reaction conditions, use of activated substrates, use of bidentate directing groups, or use of strong oxidant, is required in most of the presented methods. Hence, the objective of the present work was to develop an environmentally benign and efficient protocols for the C–H functionalization of unactivated heteroarenes *via* monodentate chelation using base metals like iron and nickel. In particular, C–H functionalization of indole and related heteroarenes are significant as they are considered as privileged structural motif in many biologically active compounds and natural products. Additionally, the design of a novel chiral nickel complexes for the synthesis of chiral alcohols *via* hydrogenation reactions, was another objective of the present work.

The results obtained from the present study is discussed in Chapters 2-5. In Chapter 2, nickel(II)-catalyzed intramolecular C(sp²)–H/C(sp³)–H and C(sp²)–H/C(sp²)–H oxidative couplings in indoles *via* chelation assistance is described. This study represents the first example of intramolecular C(sp²)–H/C(sp³)–H oxidative coupling using base metal catalyst. This reaction provided a direct approach for synthesizing diversely functionalized, pharmaceutically relevant hydrocyclopentaindolones, hydrocarbazoles, and indenoindolones with the tolerance of sensitive functionalities by employing an air-stable nickel complex, (bpy)Ni(OAc)₂. Further, an extensive mechanistic investigation was carried out including the controlled study, kinetic analysis, deuterium labeling experiments, and DFT calculations supported a Ni(II)/Ni(III) pathway for the oxidative coupling comprising the rate-limiting reductive elimination process. Furthermore, the intramolecular oxidative coupling was demonstrated with a gram-scale reaction, and the 2-pyridinyl directing group was smoothly removed to establish the synthetic utility of the protocol.

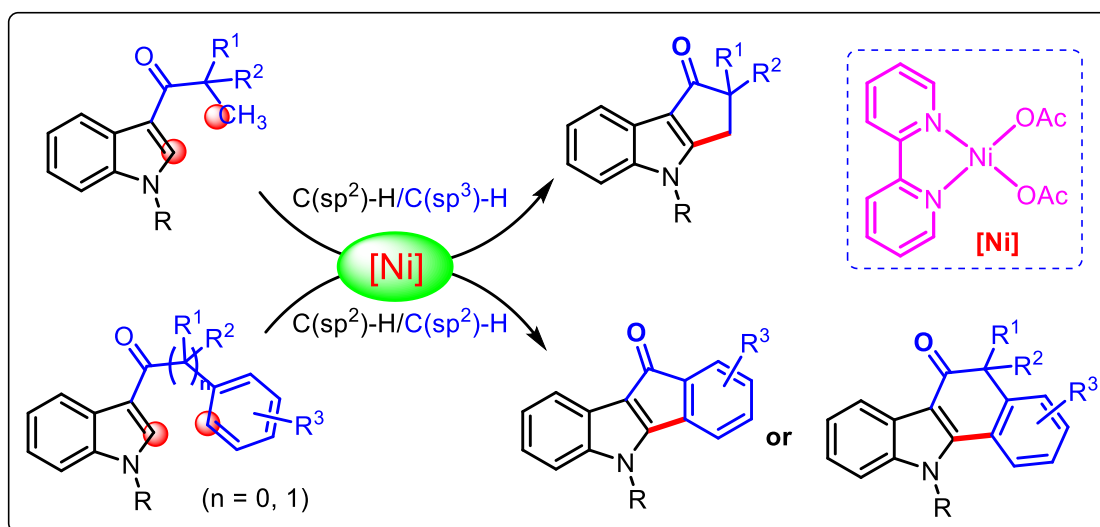
The solvent-free nickel-catalyzed protocol for the regioselective alkylation of indoles and related heteroarenes with alkenes *via* hydroarylation strategy is described in Chapter 3. The coupling of diverse aromatic alkenes with heteroarenes including indole, imidazole, and benzimidazole derivatives provided moderate to excellent yields of alkylated products. This nickel-catalyzed reaction exclusively provided the Markovnikov selective alkylated products. This method is applicable to the alkylation of both electron-rich as well as electron-poor indoles to get the branch-selective alkylated products. Preliminary mechanistic studies suggested the alkylation reaction proceeds through single-electron transfer (SET) pathway.

Further, the functionalization of isatin employing highly abundant and inexpensive iron catalyst is discussed in Chapter 4. We serendipitously discovered a new reaction *via* a novel strategy for the synthesis of 3,3-disubstituted 3-amino oxindoles which generate stereogenic quaternary centers. The coupling of various *N*-methoxy benzamide with isatin derivatives provided the diverse biologically relevant 3-substituted-3-amino oxindoles with the tolerance of synthetically important functional groups. The advantages of this method are (i) the use of accessible *N*-methoxy benzamides and isatins (ii) the generation of stereogenic quaternary centers (iii) the cleavage of N–O bond and the incorporation of the methylene group (iv) the use of an earth-abundant iron catalyst, (v) excellent scope with the tolerance of sensitive and synthetic useful functionalities. In addition, a detailed mechanistic investigations revealed that the reaction proceeds *via* the formation of isatin ketimine and *N*-(hydroxymethyl)benzamide intermediates. Controlled experiments including deuterium labeling studies suggested an *N*-methoxy group of benzamide is a source of methylene group in products. The scalability of this protocol was demonstrated with a gram-scale reaction and further functionalization of 3-substituted 3-amino oxindole was carried out. This reaction proceeds *via* a single-electron transfer (SET) pathway.

Chapter 5 describes the synthesis and characterization of a series of novel NNN-based chiral and achiral pincer nickel complexes and their application toward the transfer hydrogenation of the ketones using isopropanol as a hydrogen source. All the ligand precursors and nickel complexes were thoroughly characterized by the NMR spectroscopy, HRMS, or elemental analysis. A range of ketones were hydrogenated providing desired alcohols employing synthesized nickel complexes. Despite many attempts, we could not achieve our major objective which was enantioselective hydrogenation of ketones to get the chiral alcohols.

Chapter-2

Ni(II)-Catalyzed C–H/C–H Oxidative Coupling: Facile Synthesis of Indeno-Indolone and 3,4- Dihydro-Indolone Derivatives



This chapter has been adapted from the publication “Ni(II)-Catalyzed Intramolecular C–H/C–H Oxidative Coupling: An Efficient Route to Functionalized Cycloindolones and Indenoindolones” **Ankade, S. B.**; Samal, P. P.; Soni, V.; Gonnade, R. G.; Krishnamurty, S.; and Punji, B. *ACS Catal.* **2021**, *11*, 12384–12393.

2.1 INTRODUCTION

The indole represents a privileged structural motif, embedded in diverse biologically active molecules and natural products, including functional materials.¹⁻⁶ Particularly, polycyclic derivatives of indole, possessing five- and six-membered rings, are of great significance due to their enormous pharmacological activities like anticancer,⁷⁻¹⁰ anti-Alzheimer's disease,¹¹ antihypertensive,¹² anti-inflammatory¹³ and anti-migraine,^{14,15} inhibitors of protein kinase CK2,¹⁶ and their direct use in the development of potential therapeutic agents (Figure 2.1).¹⁷⁻²² Therefore, significant effort has been devoted in developing efficient protocols for the site-selective functionalization of indoles.²³⁻²⁵ Most synthetic methods leading to polycyclic indoles rely on sequential multi-step processes,²⁶⁻³⁰ limiting the creation of substitution diversity in the final product and/or needed harsh conditions. Recent progress in C–H functionalization led to the synthesis of various chiral and achiral five- and six-membered-ring products *via* hydrofunctionalization³¹⁻⁴¹ or direct intramolecular couplings.⁴²⁻⁴⁵ Notably, many of these protocols utilize high loading of expensive noble metal catalysts like palladium, rhodium, iridium and/or acidic reaction conditions.

More recently, oxidative coupling has been established as a powerful tool for building complex molecules from simple precursors,⁴⁶⁻⁵¹ as it does not necessitate the prefunctionalization of substrates. Owing to the sustainability and cost advantage,⁵²⁻⁶⁶ the 3d-metal catalyst for C(sp²)–H/C(sp²)–H oxidative coupling has been substantially explored.^{51,67-73} However, activating and coupling a more strenuous C(sp³)–H bond remains challenging.^{74,75} In relevant to this work, nickel catalysts have been successfully applied to the C(sp²)–H/C(sp³)–H oxidative couplings in amides.^{76,77} In fact, Chatani reported an oxidative coupling involving C(sp³)–H bond in toluene derivatives with benzamides in the Ni(II)-catalyzed reaction.⁷⁸ Similarly, Cai demonstrated the C(sp³)–H coupling of 1,4-dioxane with C-2 and C-3-positions of indoles (Scheme 2.1.a).⁷⁹ Our group found that a Ni(II) precatalyst can effectively catalyze the C(sp²)–H/C(sp³)–H oxidative coupling of indoles with toluene using 2-iodobutane as a mild oxidant (Scheme 2.1.b).⁸⁰ Notably, an excess of C(sp³)–H containing partner is used in these reactions to favor the intermolecular coupling entropically; a privilege cannot be exercised in the intramolecular couplings. Therefore, the C(sp²)–H/C(sp³)–H intramolecular coupling to achieve biologically significant polycyclic indoles remains an open challenge. Despite substantial development in the synthesis of diverse polycyclic indole skeleton,³¹⁻⁴¹ a method for constructing 5- and 6-membered-ring products, cyclopentaindolones and hydrocarbazolones, is not precedented. In this Chapter, we discuss and introduce a unified approach to synthesize biologically relevant polycyclic indoles through

the intramolecular C(sp²)-H/C(sp³)-H and C(sp²)-H/C(sp²)-H oxidative couplings, under a sustainable and environmentally benign Ni(II)-catalysis.

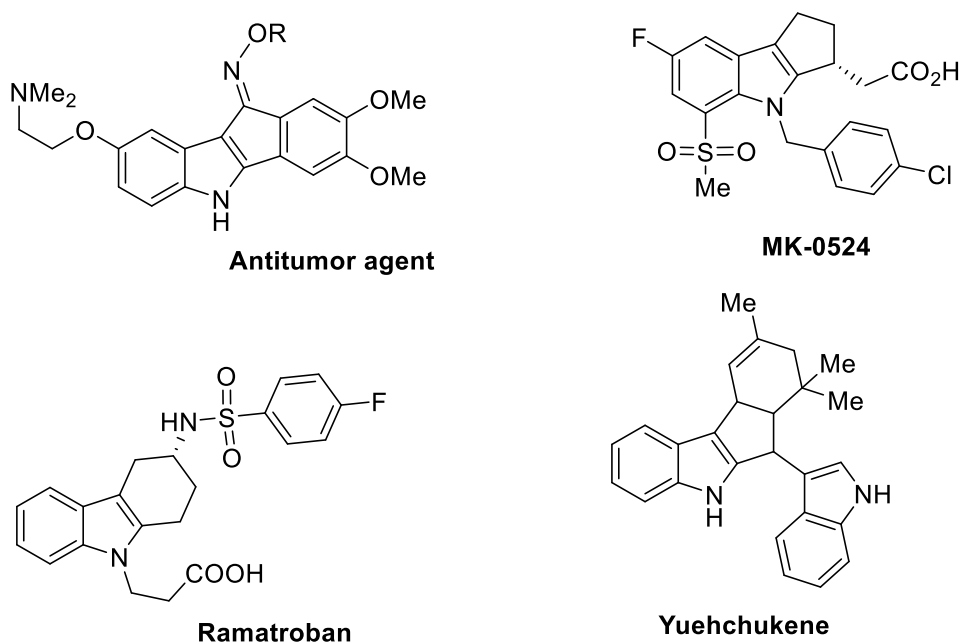
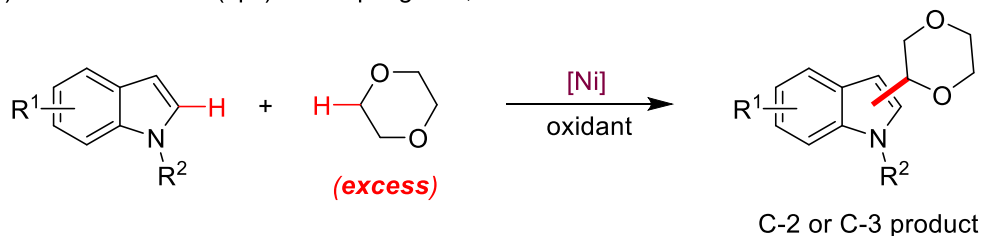
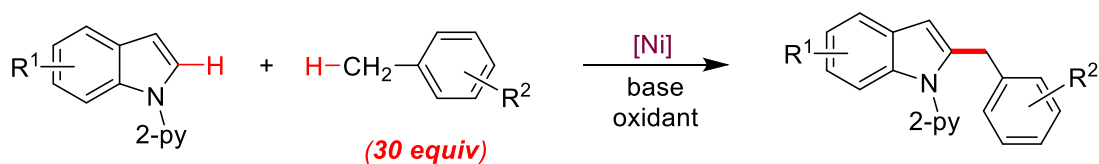


Figure 2.1. Selected bioactive polycyclic indoles.

a) Intermolecular C(sp³)-H coupling of 1,4-dioxane



b) Intermolecular C(sp³)-H coupling of toluene derivatives

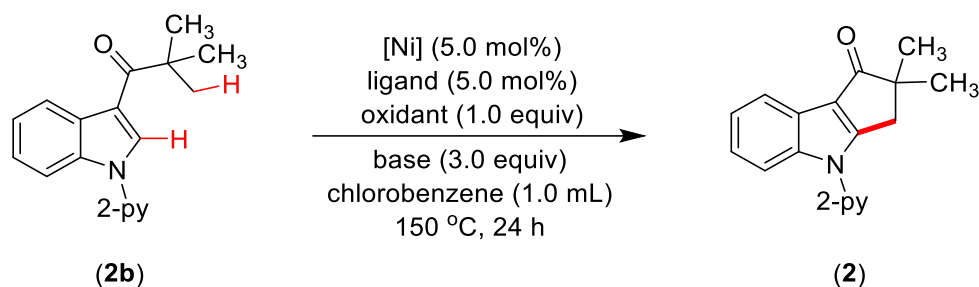


Scheme 2.1. Ni(II)-Catalyzed Oxidative C(sp²)-H/C(sp³)-H Couplings.

2.2 RESULTS AND DISCUSSION

2.2.1 Optimization of Reaction Conditions for C(sp²)-H/C(sp³)-H Oxidative Coupling

We commenced the investigation of the reaction parameters for the synthesis of 3,4-dihydrocyclopenta[*b*]indolone derivative *via* intramolecular C(sp²)-H/C(sp³)-H oxidative coupling in 2,2-dimethyl-1-(1-(pyridin-2-yl)-*1H*-indol-3-yl)propan-1-one (**2b**) using nickel catalyst (Table 2.1). Initial attempts were made to screen various nickel precursors as catalysts in the presence of LiO^tBu and oxidant Ag₂CO₃ in chlorobenzene (entries 1-4). Among various Ni(II) catalysts, the Ni(OAc)₂ was more efficient, affording cyclized product **2** in 59% yield. Notably, the Ni(0) precursor, Ni(cod)₂ as a catalyst, provided 41% of the desired cyclized compound. The ancillary phosphine-based ligands, such as PPh₃, dppf or xantphos, were less effective, whereas the presence of nitrogen-based ligands enhanced the product yield (entries 5-9) and afforded **2** in 85% with Ni(OAc)₂/bpy system. The use of sterically congested ligand neocuproine in this nickel catalysis system led to a diminishing yield of **2** (entry 10). The silver oxidants, such as AgOAc or Ag₂O were less productive, whereas Ag(OTf) was incompetent in the reaction (entries 11-13). Moreover, the employment of other metal oxidants MnO₂, Cu(OAc)₂, Cu₂O or organic oxidants ^tBuOOH, ^tBuOO^tBu, and benzoyl peroxide were less effective or not suitable for the reaction (entries 14-19). Thus, Ag₂CO₃ was chosen as a suitable oxidant for the intramolecular coupling reaction. Notably, the use a catalytic amount of Ag₂CO₃ (10 mol%) in the reaction afforded only 15% of product **2**. The use of inorganic bases like Cs₂CO₃, KO^tBu, and NaO^tBu was ineffective for the coupling, while the presence of LiHMDS {LiN(SiMe₃)₂} afforded a moderate yield of **2** (entries 20-23). Moreover, the employment of 3.0 equiv of the base, *i.e.* LiO^tBu, was essential to achieve quantitative yield. The screening of various solvents indicated the smooth progress of the reaction in chlorobenzene. Intriguingly, the reaction requires an elevated temperature of 150 °C for 24 h to achieve quantitative conversion, and performing a reaction at a lower temperature resulted in a low product yield. As the in-situ generated catalyst system of Ni(OAc)₂ and bpy provided good conversion, we have synthesized and characterized the nickel complex (bpy)Ni(OAc)₂ (**1**).

Table 2.1 Optimization of reaction conditions.

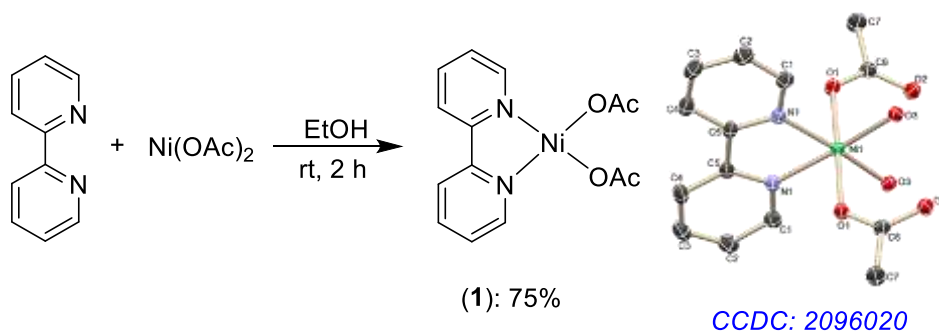
Entry	[Ni]	Ligand	Base	Oxidant	2 (%) ^a
1	(DME)NiCl ₂	-	LiO ^t Bu	Ag ₂ CO ₃	20
2	Ni(OAc) ₂	-	LiO ^t Bu	Ag ₂ CO ₃	62 (59)
3	Ni(OTf) ₂	-	LiO ^t Bu	Ag ₂ CO ₃	24
4	Ni(cod) ₂	-	LiO ^t Bu	Ag ₂ CO ₃	46 (41)
5	Ni(OAc) ₂	PPh ₃	LiO ^t Bu	Ag ₂ CO ₃	11
6	Ni(OAc) ₂	dppf	LiO ^t Bu	Ag ₂ CO ₃	37
7	Ni(OAc) ₂	xantphos	LiO ^t Bu	Ag ₂ CO ₃	35
8	Ni(OAc) ₂	phen	LiO ^t Bu	Ag ₂ CO ₃	53 (50)
9	Ni(OAc) ₂	bpy	LiO ^t Bu	Ag ₂ CO ₃	87 (85)
10	Ni(OAc) ₂	neocuproine	LiO ^t Bu	Ag ₂ CO ₃	5
11	Ni(OAc) ₂	bpy	LiO ^t Bu	AgOAc	65 (64)
12	Ni(OAc) ₂	bpy	LiO ^t Bu	Ag ₂ O	28
13	Ni(OAc) ₂	bpy	LiO ^t Bu	Ag(OTf)	NR
14	Ni(OAc) ₂	bpy	LiO ^t Bu	MnO ₂	NR
15	Ni(OAc) ₂	bpy	LiO ^t Bu	Cu(OAc) ₂	55
16	Ni(OAc) ₂	bpy	LiO ^t Bu	Cu ₂ O	10
17	Ni(OAc) ₂	bpy	LiO ^t Bu	^t BuOOH	NR
18	Ni(OAc) ₂	bpy	LiO ^t Bu	^t BuOO ^t Bu	NR
19	Ni(OAc) ₂	bpy	LiO ^t Bu	(PhCOO) ₂	NR
20	Ni(OAc) ₂	bpy	LiHMDS	Ag ₂ CO ₃	73

21	Ni(OAc) ₂	bpy	NaO ^t Bu	Ag ₂ CO ₃	NR
22	Ni(OAc) ₂	bpy	KO ^t Bu	Ag ₂ CO ₃	NR
23	Ni(OAc) ₂	bpy	Cs ₂ CO ₃	Ag ₂ CO ₃	NR
24	cat. 1	--	LiO^tBu	Ag₂CO₃	91 (89)
25	--	bpy	LiO ^t Bu	Ag ₂ CO ₃	NR
26	cat. 1	--	--	Ag ₂ CO ₃	NR
27	cat. 1	--	LiO ^t Bu	--	NR

Reaction conditions: **2b** (0.056 g, 0.20 mmol), [Ni] (5.0 mol%), ligand (5.0 mol%; 10 mol% for PPh₃), LiO^tBu (0.048 g, 0.60 mmol), oxidant (0.20 mmol, 1.0 equiv), solvent (1.0 mL). Cat **1** = (bpy)Ni(OAc)₂ used in 5.0 mol %. ^aGC yield, isolated yield is in parenthesis. 2-py = 2-Pyridinyl, dppf = 1,1'-Bis(diphenylphosphino)ferrocene, xantphos = (9,9-Dimethyl-9H-xanthene-4,5-diyl)bis(diphenylphosphane), phen = 1,10-Phenanthroline, bpy = 2,2'-Bipyridine. NR = No Reaction.

Thus, the reaction of Ni(OAc)₂ with 1.0 equiv of bpy in EtOH at room temperature produced (bpy)Ni(OAc)₂ (**1**) in 75% yield as a light green solid (Scheme 2.2).⁸¹ The complex **1** is NMR inactive and hence, was characterized by elemental analysis. An X-ray diffraction study established the molecular structure of the complex. Notably, the crystal structure of **1** shows two coordinated H₂O molecules in an octahedral fashion. We assume that the ubiquitous H₂O molecule might have been incorporated into the structure during the crystallization process.

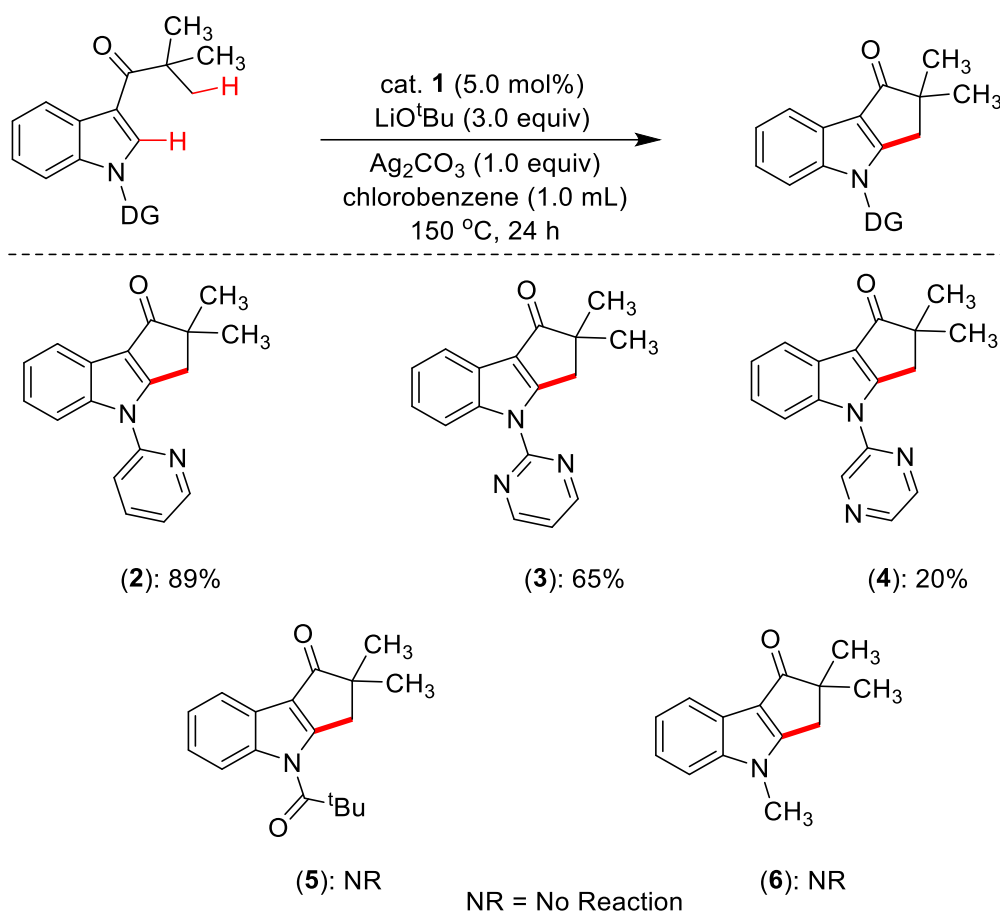
Notably, the use of well-defined complex, (bpy)Ni(OAc)₂ (**1**), as a catalyst provided an improved yield of **2** (89%) under the optimized conditions in chlorobenzene (Table 2.1, entry 24). Lowering the catalyst loading led to a decrease in the yield of **2**. A nickel catalyst, a base and an oxidant are essential for the reaction, without which no cyclized product was observed (entries 25-27). After an exhaustive screening of all the reaction components and parameters, the intramolecular oxidative cyclization was found to occur efficiently using (bpy)Ni(OAc)₂ (**1**; 5 mol %) in the presence of LiO^tBu and Ag₂CO₃ in chlorobenzene at 150 °C.



Scheme 2.2. Synthesis of (bpy)Ni(OAc)₂ (**1**) and X-ray structure of **1**·(H₂O)₂.

2.2.2. Effect of *N*-Substituents on C–H/C–H Oxidative Cyclization

The effect of the nitrogen substituents of 3-pivaloyl-indole on the oxidative coupling was investigated employing various *N*-protected 3-pivaloyl-indole (Scheme 2.3). The intramolecular coupling in *N*-2-pyridinyl-3-pivaloyl-indole (**2b**) afforded product **2** in 89% yield. Similarly, the substrate *N*-2-pyrimidinyl-3-pivaloyl-indole (**3b**) and *N*-2-pyrazinyl-3-pivaloyl-indole (**4b**) reacted efficiently to produce desired products **3** and **4** in 65% and 20% yields, respectively. Intriguingly, a –CO^tBu group as *N*-substituent as a directing group did not afford the cyclized product, highlighting that strong σ -donor nitrogen coordination is essential for this intramolecular oxidative coupling. As expected, the *N*-methyl-3-pivaloyl-indole did not produce the oxidative cyclized product. All these observations indicate that a sigma *N*-donor substituent at the *N*-atom of 3-pivaloyl-indole is essential.



Scheme 2.3. Role of directing groups on C–H/C–H oxidative cyclization.

2.2.3. Substrate Scope for C–H/C–H Intramolecular Oxidative Cyclization

The scope and limitation of the present protocol were investigated for the synthesis of diversely substituted 3,4-dihydro-indolones. Both the electron-donating and electron-withdrawing substituents were well tolerated to deliver the desired products **7–12** (Scheme 2.4). Indoles with synthetically useful functionalities like -Cl, -Br, -CN provided moderate to good yields. The tolerability of such moieties provides scope for further derivatization to complex organic compounds. The low yield in compound **12** is attributed to the partial decomposition of starting compound or the product under the reaction condition. Unfortunately, the 3-pivaloyl-indole bearing a -NO₂ group at the C-6 position did not afford the desired cyclized product under the reaction conditions.

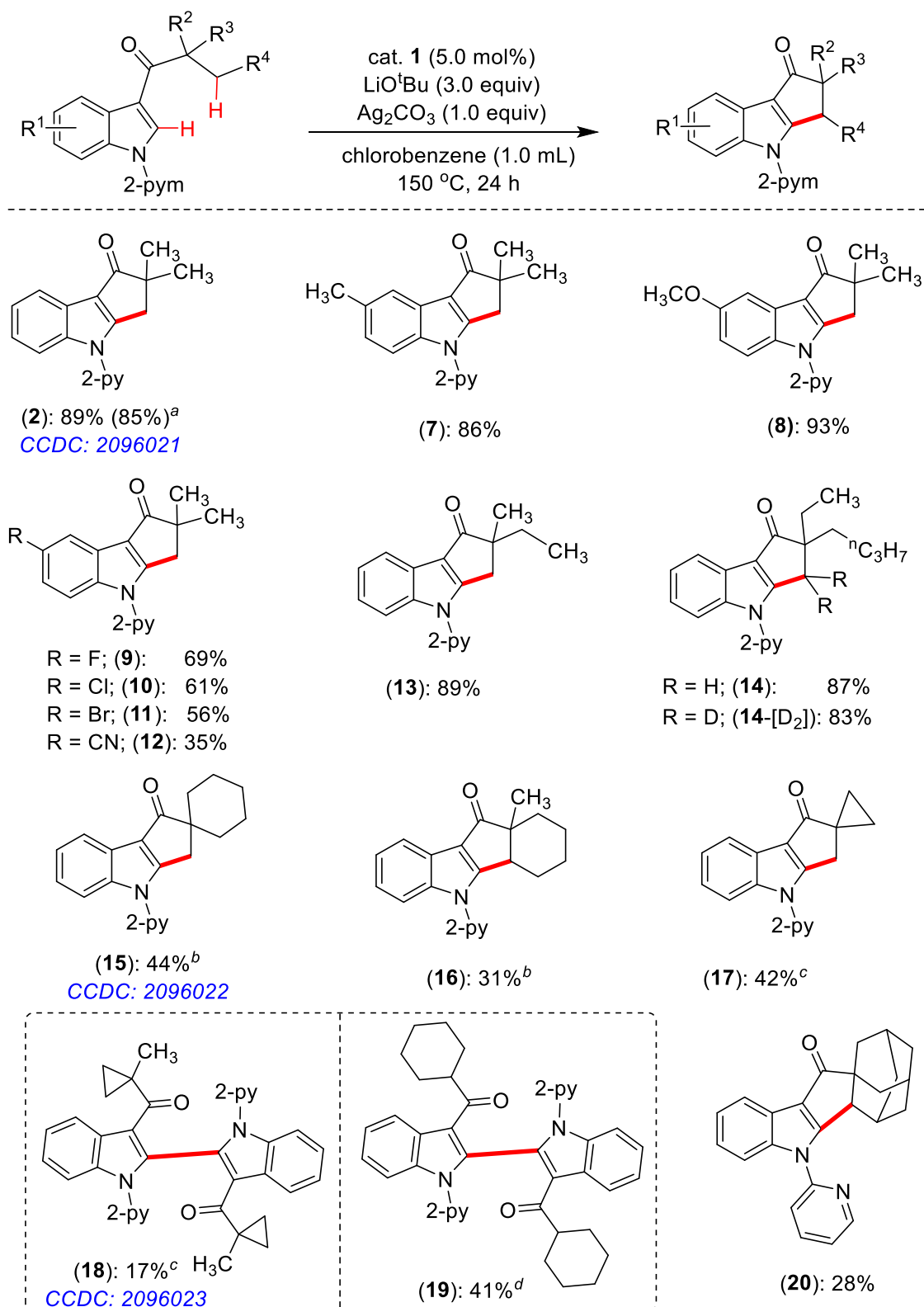
Next, the focus was devoted to the C(sp³)–H activation of substituents at C-3 acyl in indoles. The cyclization was highly selective towards the primary C(sp³)–H activation than the secondary C(sp³)–H bond in the acyclic alkyl-substituted acyl-moiety in indoles providing dihydro-indolones **13** and **14** in 89% and 87% yields, respectively. Interestingly, a deuterated substrate afforded the desired product **14**-[D₂] in 83% yield. The cyclohexyl-methyl-substituted

acyl-indole provided two possible products **15** and **16** upon primary C(sp³)–H and secondary C(sp³)–H bonds activation. We assume that the suitable conformation of the cyclohexyl ring provided access to both the primary and secondary C(sp³)–H bonds for nickelation. Notably, the cyclopropyl-methyl-substituted substrate afforded the cyclized product **17** by C(sp²)–H/C(sp³)–H oxidative coupling, and a substantial amount of self-coupled compound **18** was obtained. Surprisingly, the cyclohexyl-acyl-indole led to only intermolecular C(sp²)–H/C(sp²)–H self-coupling and provided compound **19** in 41% yield. The sterically demanding substrate adamantan-1-yl(1-(pyridin-2-yl)-*IH*-indol-3-yl)methanone is low reactive under the optimized reaction condition and produced **20** in 28% yield. The compounds **2**, **15** and **18** were characterized by an X-ray diffraction study to gain additional structural information. Interestingly, all the C(sp²)–H/C(sp³)–H intramolecular coupling led to the formation of only a five-membered ring, even though a C(sp³)–H bond for the possible formation of a six-membered ring was available. This indicates the importance of tertiary substitution which originates from the “Thorpe-Ingold effect”.^{82,83} Therefore, the employment of substrate containing –CO^tPr or –COEt moieties in place of –CO^tBu did not participate in the cyclization. Similarly, the indole derivative with –CH^tBu substituent at the C-3 position was not reactive highlighting the necessity of carbonyl motif in the linkage. Moreover, indole with –COCH^tBu substituent at the C-3 was unreactive probably due to the unfavorable formation of a seven-membered nickelacycle *via* C(sp²)–H/C(sp³)–H activation. These findings suggest that the oxidative coupling is solely dependent on the tertiary substitution and the C(sp²)–H/C(sp³)–H coupling is highly selective for the formation of five-membered ring products.

The intramolecular coupling was extended to the C(sp²)–H/C(sp²)–H oxidative cyclization to synthesize indenoindolone derivatives (Scheme 2.5). Thus, the C-3 benzoylated indole efficiently participated in the reaction to achieve 2-pyridinyl-indenoindolone **21** in an 86% yield. Similarly, a C-3, 2-methyl-benzoylated indole afforded compound **22** in 91% yield by C(sp²)–H/C(sp²)–H oxidative cyclization. Notably, a probable six-membered cyclic product, *via* C(sp³)–H (CH₃) activation, was not observed in this reaction. Interestingly, the 2,6-dimethylbenzoylated indole did not afford the intramolecular cyclization product; instead, an intermolecular self-coupled product **23** was observed in 37% yield. This finding suggests that an intramolecular C(sp²)–H/C(sp³)–H coupling to generate a six-membered cycle *via* a seven-membered nickelacycle is not feasible. The intramolecular oxidative coupling in *meta*-substituted aroylindoles proceeded with excellent site selectivity at the less sterically hindered position to deliver compounds **24–26** in good yields. The methyl and methoxy substituents at the *para* position of 3-aryloindole afforded the desired products **27** and **28** in 81% and 86%

yields, respectively. Notably, the substrate 3-naphthoyl-(*N*-2-pyridinyl)-indole underwent intramolecular oxidative coupling selectively at sterically less hindered position and delivered product **29** in 30% yield. Unfortunately, a heteroarene-derived substrate, 3-furanyl-(*N*-2-pyridinyl)-indole as well as 3-thiotolyl-(*N*-2-pyridinyl)-indole could not undergo cyclization.

To understand the selectivity in the formation of five/six-membered cyclic core *versus* the activation of C(sp²)-H or C(sp³)-H bond, we have employed 2-methyl-2-phenyl-1-(1-(pyridin-2-yl)-1*H*-indol-3-yl)propan-1-one for the reaction. Notably, this substrate produced a mixture of five-membered cyclic product, **30** and six-membered cyclic compound **31** by the C(sp²)-H/C(sp³)-H and C(sp²)-H/C(sp²)-H bonds activation, respectively. Similarly, the 2-methyl-2-phenyl-substituted substrate **32b** delivered both the possible products, **32** and **33** in 64% yield. As expected, the compound 2,2-diphenyl-1-(1-(pyridin-2-yl)-1*H*-indol-3-yl)propan-1-one (**34b**) under the reaction conditions undergo intramolecular cyclization to afford **34** and **35** in 16% and 15% yields, respectively. All these reactions outcome established that the C(sp²)-H/C(sp³)-H intramolecular oxidative cyclization exclusively proceed *via* a six-membered nickelacycle to afford a five-membered cyclized product, whereas the C(sp²)-H/C(sp²)-H intramolecular oxidative cyclization can occur both *via* the six-membered and seven-membered nickelacycle to deliver five-membered and six-membered cyclized products, respectively. In general, the intermediacy of a favorable six-membered nickelacycle is well-known in the coupling reactions, whereas a seven-membered nickelacycle is exceedingly rare.

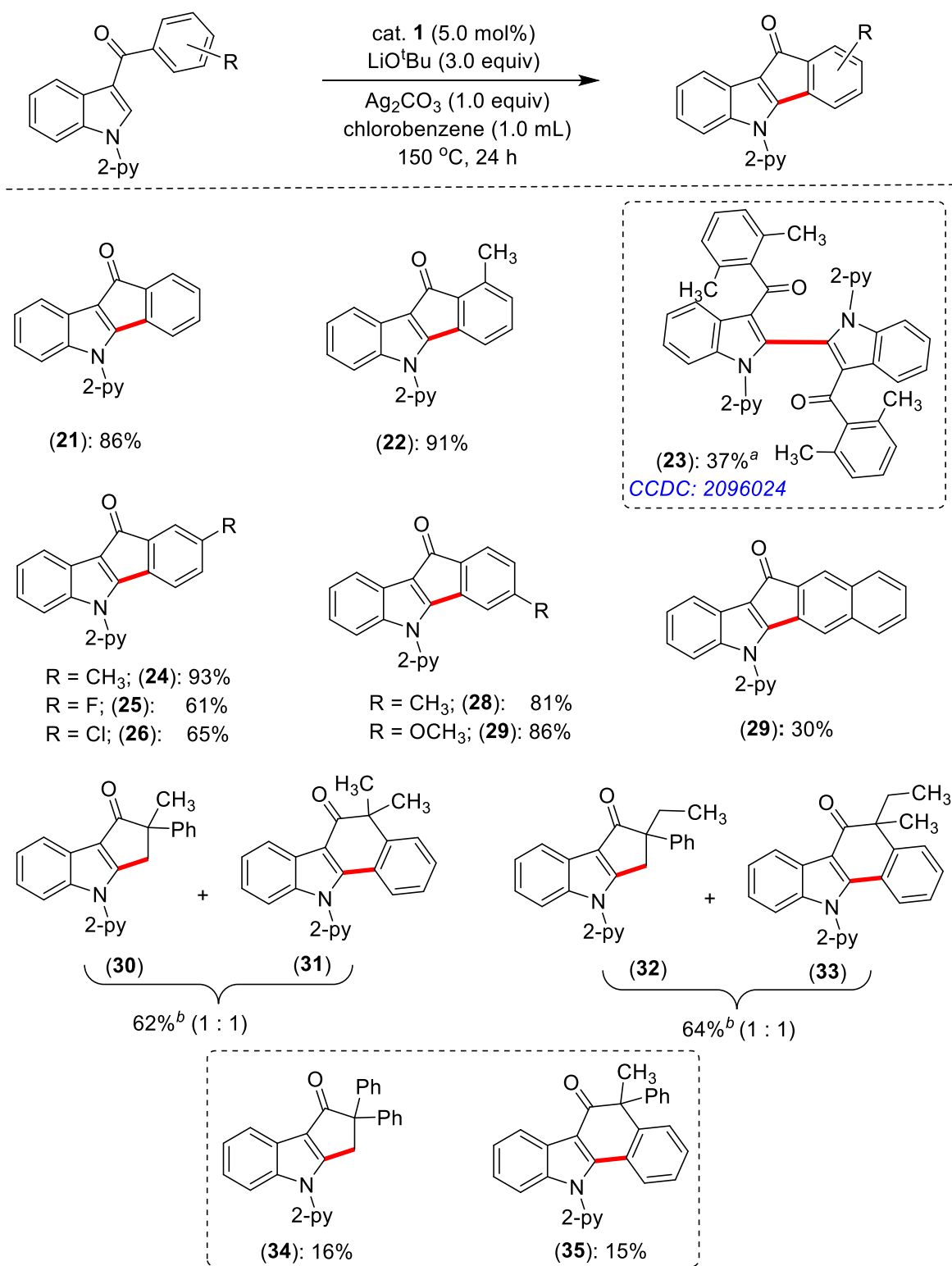


Scheme 2.4. Scope for intramolecular C(sp²)-H/C(sp³)-H oxidative cyclization.

(Reactions were conducted on a 0.2 mmol scale. ^aYield from 1.0 g scale reaction. ^bProducts **15** and **16** were obtained from the same starting compound *via* C(sp²)-H/-CH₃(sp³)-H and C(sp²)-H/-CH₂(sp³)-H oxidative coupling, respectively. ^cProducts **17** and **18** were obtained from the same starting compound *via* C(sp²)-H/-CH₃(sp³)-H and homocoupling. ^dSubstrate **19b** provided only self-coupled product **19**.)

Notably, a probable six-membered cyclic product, *via* C(sp³)–H (CH₃) activation, was not observed in this reaction. Interestingly, the 2,6-dimethylbenzoylated indole did not afford the intramolecular cyclization product; instead, an intermolecular self-coupled product **23** was observed in 37% yield. This finding suggests that an intramolecular C(sp²)–H/C(sp³)–H coupling to generate a six-membered cycle *via* a seven-membered nickelacycle is not feasible. The intramolecular oxidative coupling in *meta*-substituted arylindoles proceeded with excellent site selectivity at the less sterically hindered position to deliver compounds **24–26** in good yields. The methyl and methoxy substituents at the *para* position of 3-arylindole afforded the desired products **27** and **28** in 81% and 86% yields, respectively. Notably, the substrate 3-naphthoyl-(*N*-2-pyridinyl)-indole underwent intramolecular oxidative coupling selectively at sterically less hindered position and delivered product **29** in 30% yield. Unfortunately, a heteroarene-derived substrate, 3-furanyl-(*N*-2-pyridinyl)-indole as well as 3-thiophenyl-(*N*-2-pyridinyl)-indole could not undergo cyclization.

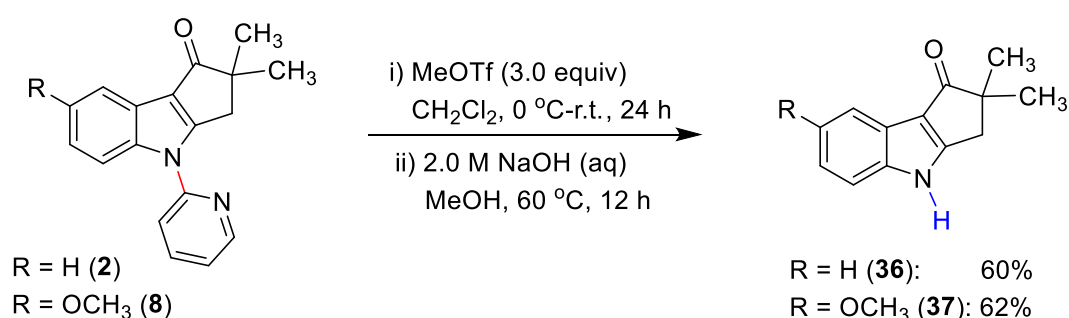
To understand the selectivity in the formation of five/six-membered cyclic core *versus* the activation of C(sp²)–H or C(sp³)–H bond, we have employed 2-methyl-2-phenyl-1-(1-(pyridin-2-yl)-1*H*-indol-3-yl)propan-1-one for the reaction. Notably, this substrate produced a mixture of five-membered cyclic product, **30** and six-membered cyclic compound **31** by the C(sp²)–H/C(sp³)–H and C(sp²)–H/C(sp²)–H bonds activation, respectively. Similarly, the 2-methyl-2-phenyl-substituted substrate **32b** delivered both the possible products, **32** and **33** in 64% yield. As expected, the compound 2,2-diphenyl-1-(1-(pyridin-2-yl)-1*H*-indol-3-yl)propan-1-one (**34b**) under the reaction conditions undergo intramolecular cyclization to afford **34** and **35** in 16% and 15% yields, respectively. All these reactions outcome established that the C(sp²)–H/C(sp³)–H intramolecular oxidative cyclization exclusively proceed *via* a six-membered nickelacycle to afford a five-membered cyclized product, whereas the C(sp²)–H/C(sp²)–H intramolecular oxidative cyclization can occur both *via* the six-membered and seven-membered nickelacycle to deliver five-membered and six-membered cyclized products, respectively. In general, the intermediacy of a favorable six-membered nickelacycle is well-known in the coupling reactions, whereas a seven-membered nickelacycle is exceedingly rare.



Scheme 2.5. Scope for intramolecular C(sp²)-H/C(sp²)-H oxidative cyclization (Reactions were conducted on a 0.2 mmol scale. ^aSubstrate **23b** gave only oxidative self-coupled product **23**. ^bProducts **30** and **31** as well as **32** and **33** were obtained as a mixture *via* C(sp²)-H/C(sp³)-H and C(sp²)-H/C(sp²)-H oxidative couplings, and verified by ¹H NMR analysis upon isolation. ^c Employing 10.0 mol% of cat. **1**.)

2.2.4 Gram-Scale Synthesis and Synthesis of Free-NH 3,4-Dihydro-Indolones

Given the importance of cyclopent[*b*]indol-1-one derivatives in pharmaceutically important compounds. A gram-scale reaction of compound **2b** (1.0 g, 3.6 mmol) was performed and provided cyclized product **2** in 85% yield under standard conditions, suggesting the possible advantage of the scalability of this protocol. Furthermore, considering the synthetic importance of functionalized free *NH* cyclopent[*b*]indol-1-one, we have demonstrated removing the 2-pyridinyl group from the cyclized compound. Thus, the cyclized indoles **2** and **8** were treated with MeOTf followed by NaOH (2.0 M) reaction, leading to the formation of cyclized free *NH* indoles **36** and **37**, respectively (Scheme 2.6).

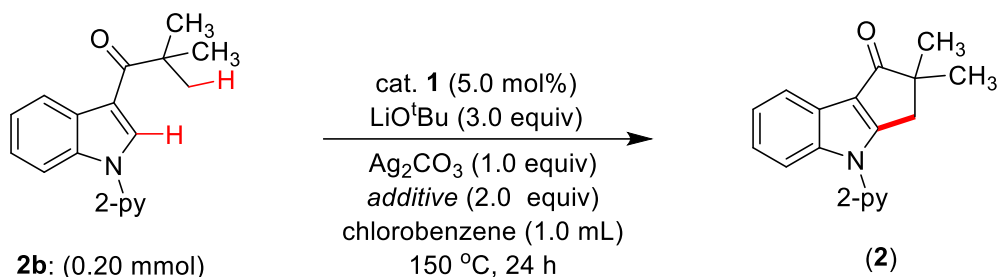


Scheme 2.6. Removal of directing group.

2.2.5 Mechanistic Aspects

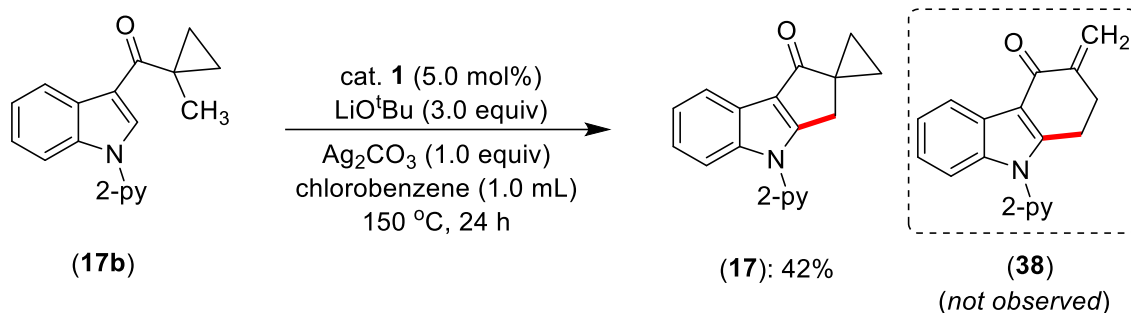
2.2.5.1 External Additive Experiments and Radical Clock Experiment

The controlled intramolecular cyclization reactions have been performed to understand the participation of an active catalyst and the reaction pathway. The presence of radical marker TEMPO or galvinoxyl substantially suppressed the standard catalytic reaction (Scheme 2.7). However, the reaction was completely quenched in the presence of radical inhibitor BHT (butylated hydroxytoluene). These findings tentatively suggest the involvement of an odd-electron species, either a carbon-centric radical or an odd-electron nickel species. Notably, a radical clock experiment using (1-methylcyclopropyl)(1-(pyridin-2-yl)-1*H*-indol-3-yl)methanone (**17b**) exclusively produced specific cyclized product **17** in 42%, and the probable $-\text{CH}_2^\bullet$ radical-mediated ring-opening-cyclized compound **38** was not observed (Scheme 2.8). This finding ruled out the participation of a carbon-centric radical species. However, as the radical capture experiments suppressed the catalytic reaction, we assumed the involvement of an odd-electron nickel species.



additive	2 (%)
No additive	89
TEMPO	25
Glavinoxyl	13
BHT	--

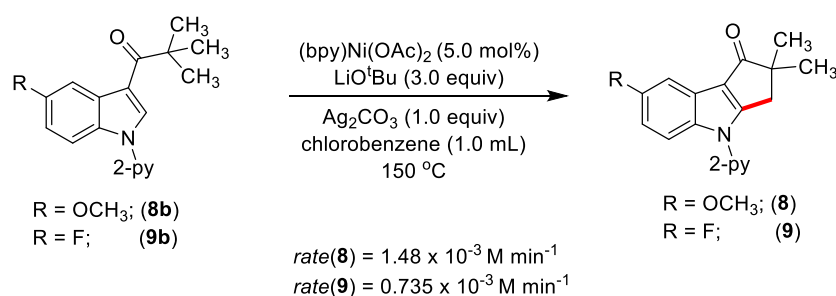
Scheme 2.7. External additive experiments.



Scheme 2.8. Radical-clock experiment.

2.2.5.2 Electronic Effect Study

To demonstrate the electronic effect of substrates on the cyclization reaction, the kinetic analysis of electronically distinct substrates (**8b** and **9b**) was performed. Thus, the data indicate that intramolecular cyclization is faster for an electronically-rich substrate than an electronically-deficient substrate (Figure 2.2). This data tentatively supports an electrophilic type of C(2)–H nickelation.⁸⁴



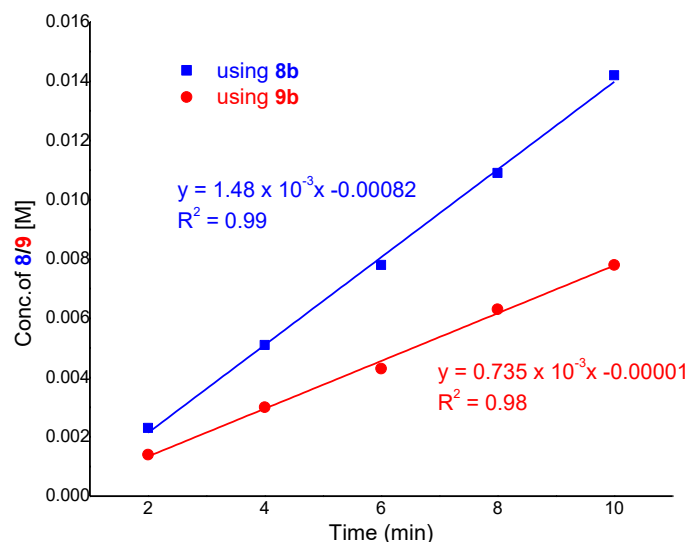
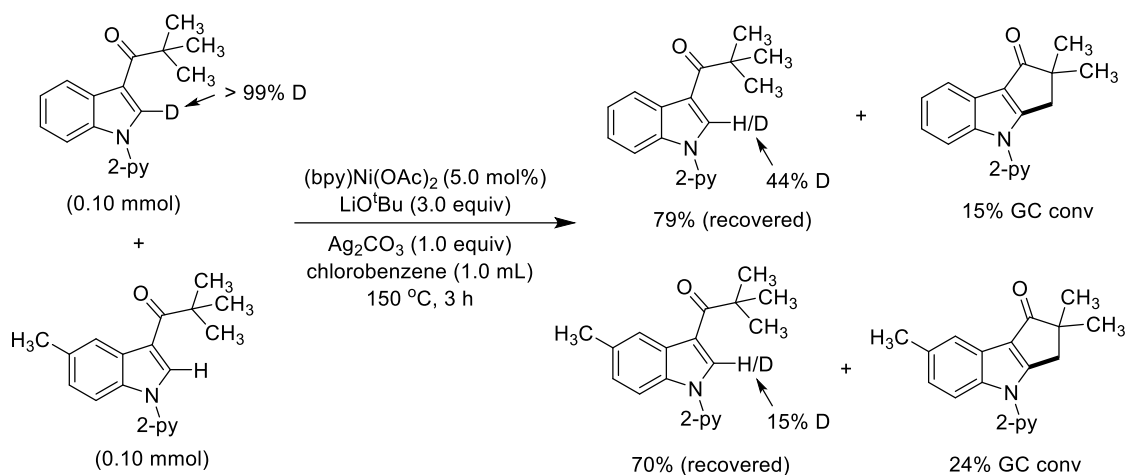


Figure 2.2. Time-dependent formation of **8** and **9**.

2.2.5.3 H/D Scrambling Experiment

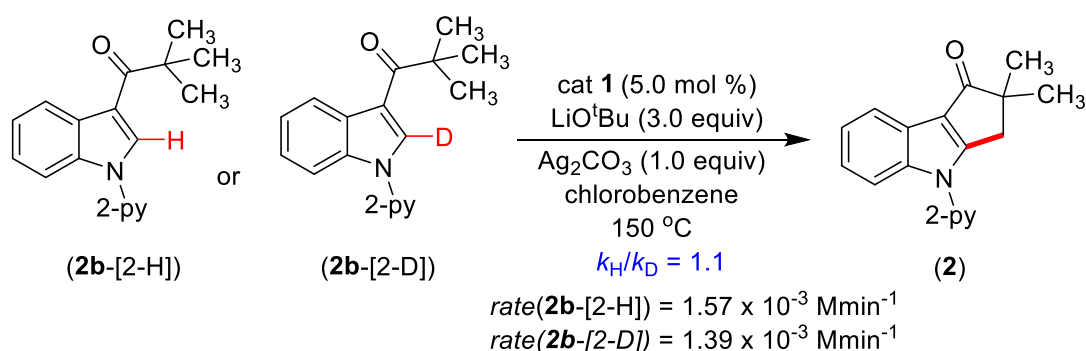
The deuterium scrambling experiment was carried out to understand the nature of cleavage of C(2)–H in indoles. Therefore, the reaction of 2,2-dimethyl-1-(1-(pyridin-2-yl)-*1H*-indol-3-yl-2-d)propan-1-one (**2b**-[2-D]; 0.028 g, 0.10 mmol), 2,2-dimethyl-1-(5-methyl-1-(pyridin-2-yl)-*1H*-indol-3-yl)propan-1-one (**7b**; 0.029 g, 0.10 mmol), (bpy)Ni(OAc)₂ (0.0034 g, 0.01 mmol, 5.0 mol %), Ag₂CO₃ (0.056 g, 0.20 mmol, 1.0 equiv) and LiO^tBu (0.048 g, 0.60 mmol, 3 equiv) was performed at 150 °C for 3 h. At ambient temperature, the reaction mixture was quenched with distilled H₂O (10.0 mL) and the crude product was extracted with EtOAc (15 mL x 3). The combined organic extract was dried over Na₂SO₄ and the volatiles were evaporated *in vacuo*. The remaining residue was purified by column chromatography on silica gel to recover **2b**-[2-D] (0.022 g, 79%), **7b** (0.021 g, 70%), and products **2** (15%), **7** (24%) were observed by Gas Chromatograph analysis. The ¹H NMR analysis of the recovered **2b**-[2-D] shows a significant D/H exchange at C(2)–D position and **7b** shows 15% incorporation of deuterium at the C(2)–H position (Scheme 2.9).



Scheme 2.9. Deuterium scrambling experiment.

2.2.5.4 Kinetic Isotope Effect (KIE) Study

The kinetic isotope effect (KIE) study was performed to know whether the involvement of the C(sp²)-H or C(sp³)-H bond cleavage is in the rate-determining step. Thus, the kinetic analysis of the substrate **2b**-[2-H] and **2b**-[2-D] showed a KIE value of 1.2 (Figure 2.3). This low KIE value indicates the C(sp²)-H bond breaking might not be in the rate-determining step. Interestingly, the independent reaction rate determination of the substrates **14b**-[H₃] and **14b**-[D₃] provided a KIE value of 1.9 (Figure 2.4). As this value is not high enough, we assume that the methyl C(sp³)-H activation/nickelation might not be involved in the rate-limiting step.⁸⁵ Notably, the methyl C(sp³)-H nickelation is ~ 5 times slower than the C(2)(sp²)-H nickelation highlighting the importance of [CH₃]-C(sp³)-H bond activation.



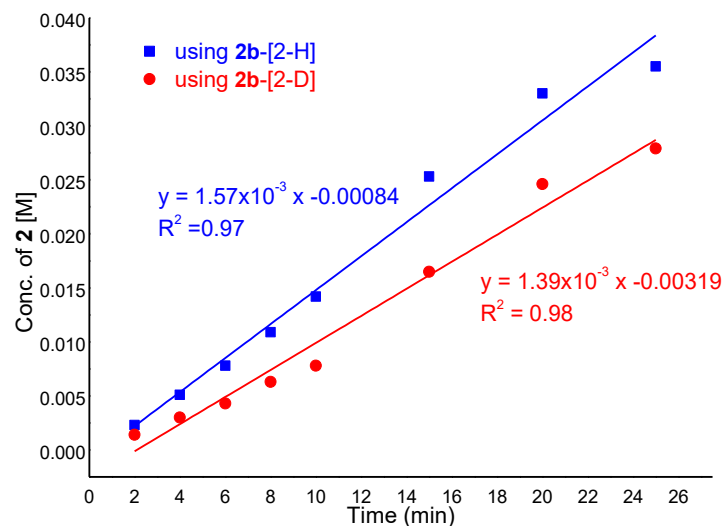


Figure 2.3. Time-dependent formation of **2** using substrates **2b**-[2-H] and **2b**-[2-D].

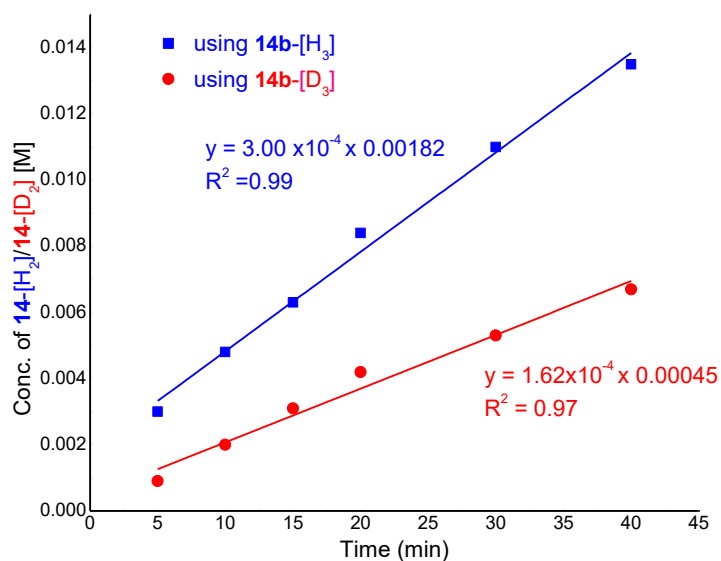
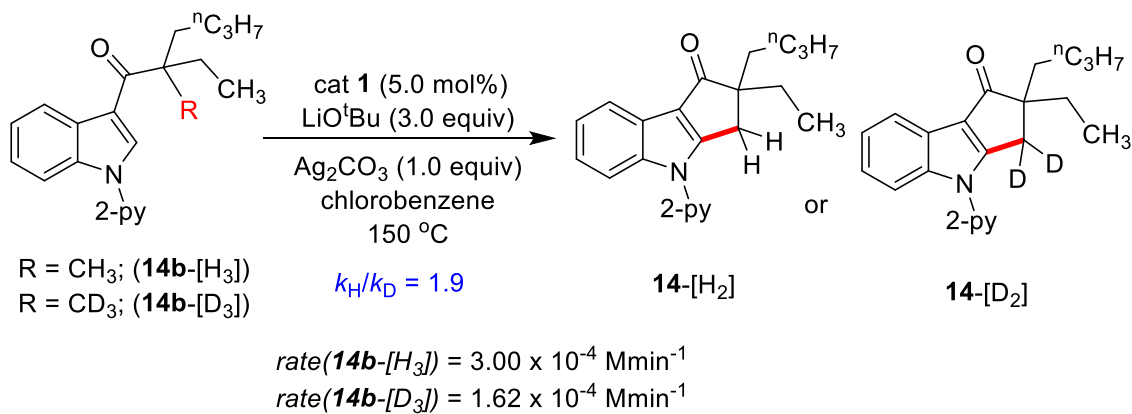


Figure 2.4. Time-dependent formation of **14**-[H₂] or **14**-[D₂].

2.2.5.5 DFT Based Calculations

Density Functional Theory-based studies were carried out using PBE functional to obtain additional mechanistic insights into the Ni-catalyzed intramolecular C(sp²)-H/C(sp³)-H oxidative coupling. Initially, we aim to understand the nickel catalyst's electronic state involved in the process. For all the species, studies have been performed for the low spin state *i.e.* Ni(II) (singlet) and Ni(I) (doublet). Notably, the C(2)-H activation of indole substrate **2b** with the Ni(II) species is more favorable ($\Delta G = -25.3$ kcal/mol) than with the Ni(I) complex ($\Delta G = -10.47$ kcal/mol) (Figure 2.5). Moreover, an examination of the formation of Ni(I) species from various Ni complexes shows that the process is less feasible (Figure 2.6). Further, the employed oxidative catalytic conditions would support an oxidative pathway,⁶⁹ rather than a reductive approach involving a low-valent active Ni-species in the presence of an oxidant. Therefore, we considered Ni(II) species as the active catalyst for further calculations and determined the spontaneity of the reaction pathway.

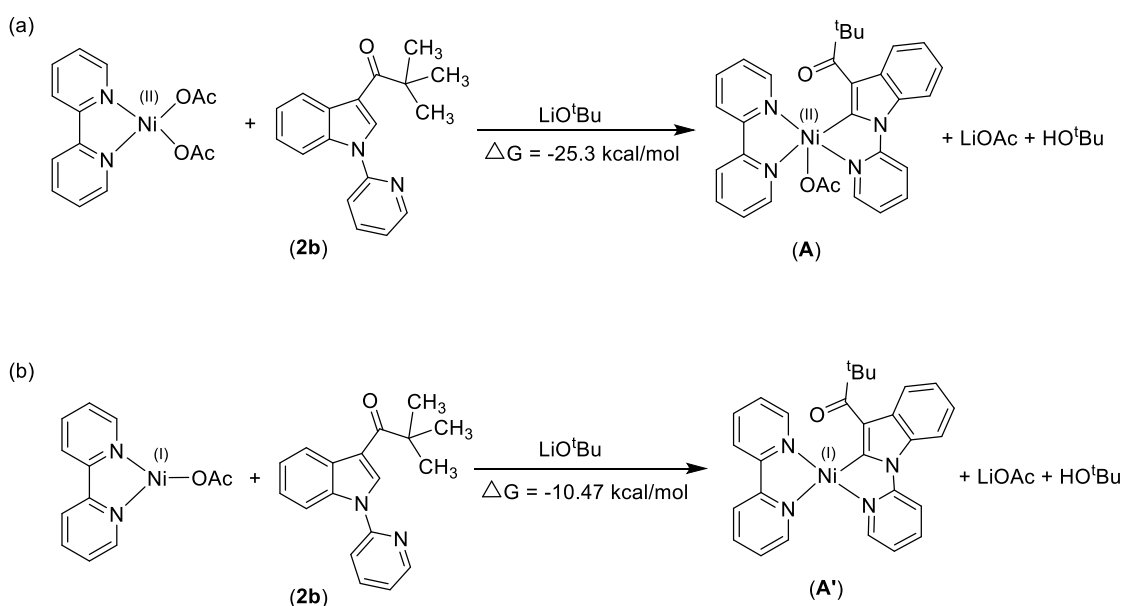


Figure 2.5. Gibbs free energies for the C–H activation at Ni(II) and Ni(I) species.

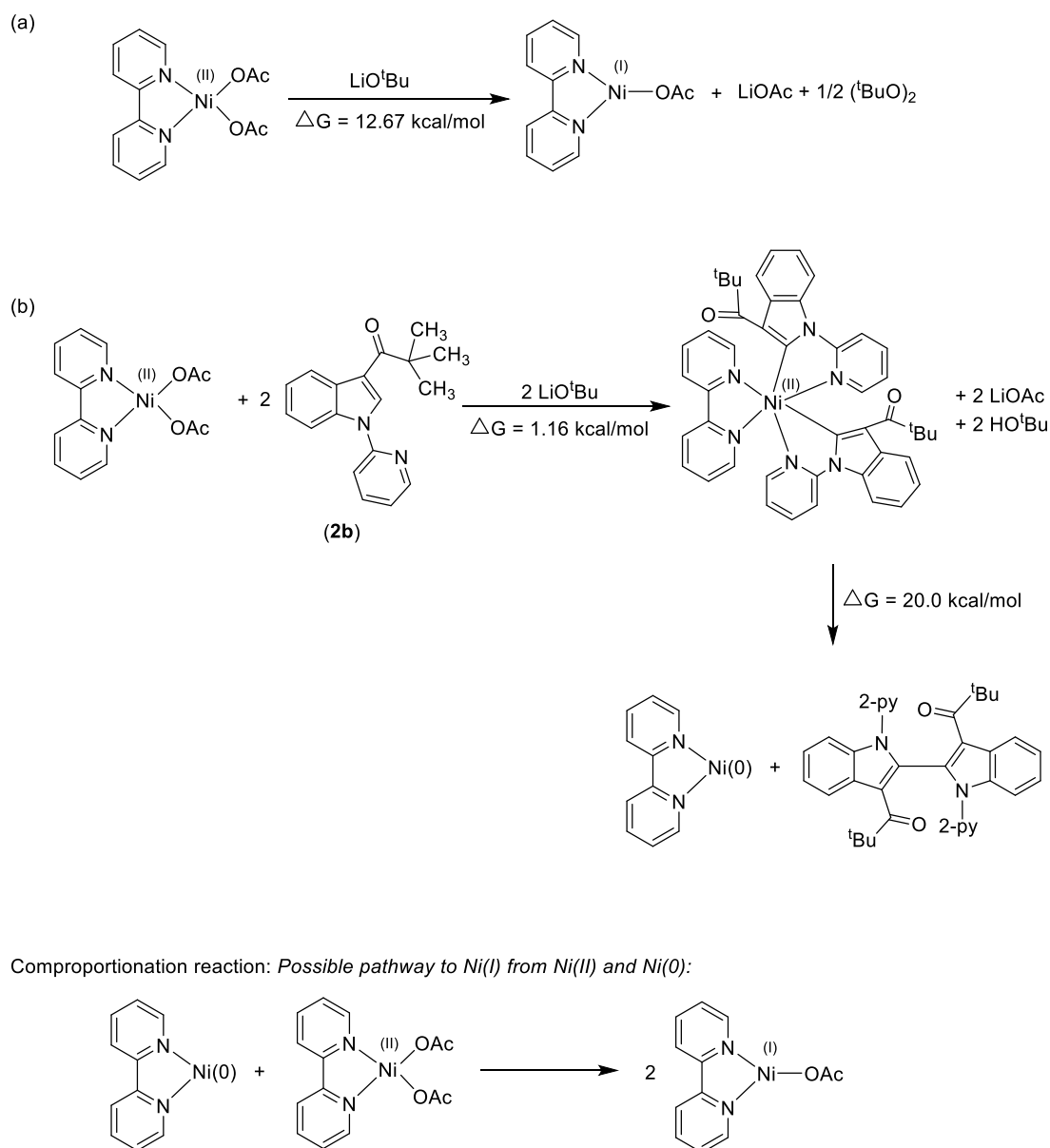


Figure 2.6. Gibbs free energies for the formation of various Ni(I) species from Ni(II) and Ni(0) species.

The possible reaction pathways for the C(sp²)-H/C(sp³)-H oxidative coupling beginning with Ni(II) species are shown in Figure 2.7. The reaction first initiates through C(sp²)-H bond activation of **2b** with Ni(II) catalyst to form the nickel intermediate **A** via the transition state **TS-1**. A reasonable energy barrier (18.8 kcal/mol) for this process is consistent with the experimental observation that supports a facile C(2)-H activation. Thereafter, the oxidation of intermediate **A** with Ag₂CO₃ leads to the formation of **B** [*i.e.* Ni(II) to Ni(III)], which is endergonic by 0.2 kcal/mol. Beginning with intermediate **B**, two possibilities for the C(sp³)-H bond activation is hypothesized: (a) single-electron transfer (SET) process triggered

by Ni(III) to generate methylene radical or (b) base-assisted nickelation of C(sp³)–H bond. The single-electron transfer process through **TS-2** in the presence of Ag₂CO₃ results in the formation of radical intermediate **C**, for which the energy barrier is 35.51 kcal/mol. This species could proceed through radical recombination resulting in Ni(IV) intermediate **D**, which is exergonic by 4.24 kcal/mol. The reductive elimination *via* **TS-3** leads to product **2** and the regeneration of the catalyst following an energy barrier of 12.74 kcal/mol. The high overall energy barrier (35.71 kcal/mol) observed for this SET pathway is aligned with the experimental findings, wherein a carbon-based radical process was ruled out.

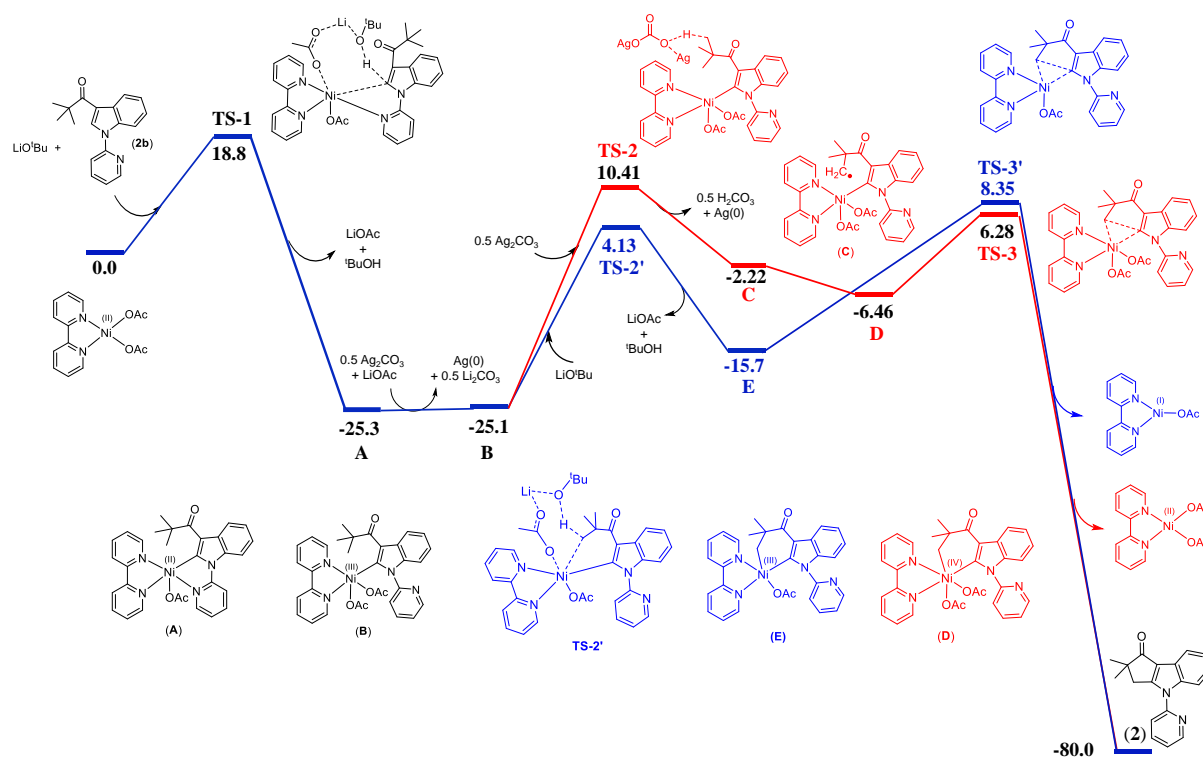


Figure 2.7. Free energy profile for the Ni-catalyzed oxidative coupling. The free energy values are given in kcal/mol.

The second possibility of C(sp³)–H bond activation *via* base assistance would result in Ni(III) species **E** *via* **TS-2'** having an energy barrier of 29.23 kcal/mol. The C(sp³)–H bond activation by this process is found to be more favorable than the SET pathway. The reductive elimination *via* **TS-3'** would lead to product **2**, following an energy barrier of 24.05 kcal/mol. The Ni(I) species further undergo oxidation to form the active catalyst *i.e.* Ni(II) species. The free energy accompanying this oxidation is -5.0 kcal/mol. Notably, the investigation of probable oxidation of Ni(III) intermediate **E** to Ni(IV) **D** revealed that the process is not favorable ($\Delta G = 35.77$ kcal/mol). Thus, the reductive elimination is proposed to proceed *via*

TS-3' resulting in product **2**. All the above studies indicate that the reaction coordinates inculcating the singlet spin state of Ni(II) is facile and prefers a base-assisted C(sp³)-H activation pathway involving a Ni(III) species rather than a radical path *i.e.* [Ni(II) to Ni(IV)]. The overall energy barrier observed for the reductive elimination step (33.65 kcal/mol) is higher than that of the C(sp³)-H bond nickelation (29.43 kcal/mol), which tentatively supports a probable rate-limiting reductive elimination process. Considering the observed kinetic isotope effect (KIE = 1.9) for the C(sp³)-H bond nickelation, we assume that the C(sp³)-H activation could be one of the rate-influencing steps.

2.2.6 Probable Catalytic Cycle

Based on the experimental results, DFT calculations and literature precedents,^{69,78,80,86-88} we have proposed a tentative catalytic pathway for the C(sp²)-H/C(sp³)-H oxidative coupling (Figure 2.8). The indole **2b** would coordinate to catalyst (bpy)Ni(OAc)₂ (**1**), followed by a reversible C(2)-H nickelation leading to the electron-rich species **A**. Deuterium scrambling study supports this proposal. Intermediate **A** would undergo 1e oxidation to afford the unsaturated Ni(III) species **B**.⁶⁹ The intermediate **B** would trigger the base-assisted C(sp³)-H bond activation to generate a nickelacycle **E**. Considering the outcome of the radical-clock study, we have ruled out the formation of a radical intermediate from -CH₃.⁸⁰ The reductive elimination of cyclized product **2** from intermediate **E**, a probable rate-limiting step, would generate a Ni(I) complex that undergoes one-electron oxidation or comproportionation reaction with **B** to regenerate the active catalyst.

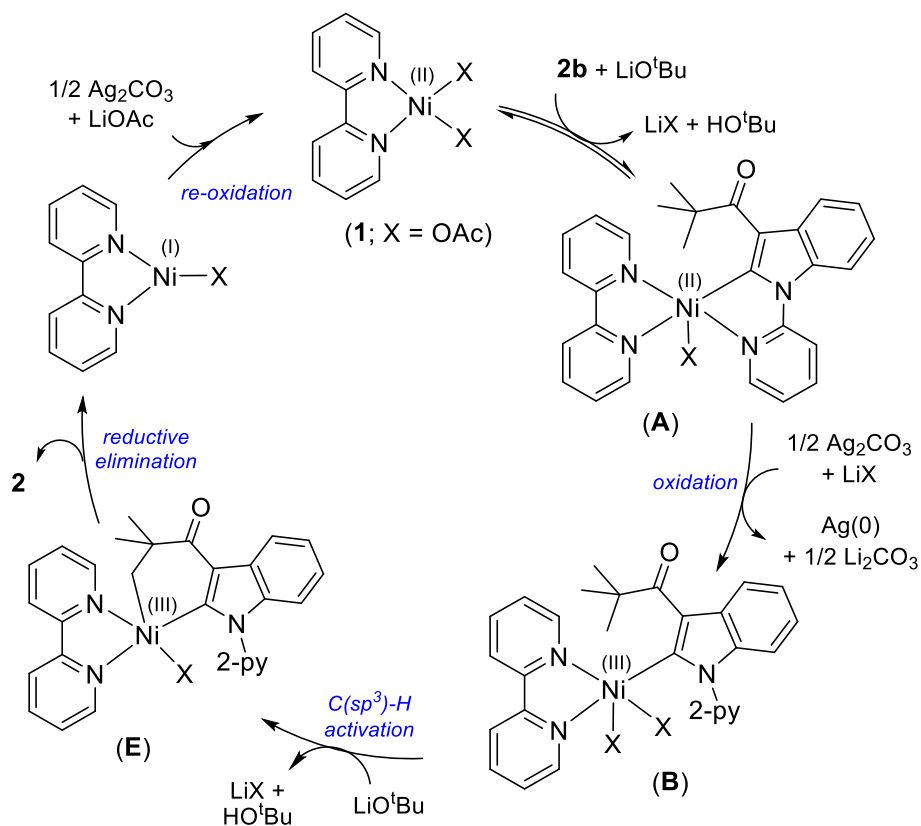


Figure 2.8. Plausible catalytic cycle.

2.3 CONCLUSION

In summary, we have developed an efficient protocol for the intramolecular chemoselective $\text{C}(\text{sp}^2)\text{-H}/\text{C}(\text{sp}^3)\text{-H}$ and $\text{C}(\text{sp}^2)\text{-H}/\text{C}(\text{sp}^2)\text{-H}$ oxidative couplings in indoles catalyzed by an air-stable and structurally characterized nickel complex, $(\text{bpy})\text{Ni}(\text{OAc})_2$. This reaction provided a direct and cost-effective approach for synthesizing diversely functionalized, pharmaceutically relevant hydrocyclopentaindolones, hydrocarbazolones and indenoindolones with the tolerance of sensitive functionalities. The intramolecular $\text{C}(\text{sp}^2)\text{-H}/\text{C}(\text{sp}^3)\text{-H}$ coupling exclusively proceeded through a six-membered nickelacycle providing five-membered ring products, whereas the $\text{C}(\text{sp}^2)\text{-H}/\text{C}(\text{sp}^2)\text{-H}$ coupling followed a six-membered or a seven-membered nickelacycle affording five- or six-membered cyclized products. An extensive mechanistic investigation by the controlled study, kinetic analysis, deuterium labeling experiments, and DFT calculations supported a Ni(II)/Ni(III) pathway for the oxidative coupling comprising the rate-limiting reductive elimination process. Furthermore, the intramolecular oxidative coupling was demonstrated with a gram-scale reaction, and the 2-pyridinyl directing group was smoothly removed to establish the synthetic utility of the protocol.

2.4 EXPERIMENTAL SECTION

All the manipulations were conducted under an argon atmosphere either in a glove box or using standard Schlenk techniques in pre-dried glasswares. The catalytic reactions were performed in flame-dried reaction vessels with a Teflon screw cap. Solvents were dried over Na/benzophenone or CaH₂ and distilled prior to use. Liquid reagents were flushed with argon prior to use. The starting compounds **2a**,⁸⁹ **7a-11a**,⁹⁰ **21a**,⁸⁹ **22a**,⁹¹ **27a**,⁹¹ **28a**,⁹¹ **26a**,⁹² **29a**,⁹² were synthesized according to the previously described procedures. The nickel complex (bpy)Ni(OAc)₂ (**1**) was synthesized by a modified literature procedure.⁹³ All other chemicals were obtained from commercial sources and were used without further purification. High-resolution mass spectrometry (HRMS) mass spectra were recorded on a Thermo Scientific Q-Exactive, Accela 1250 pump. NMR: (¹H and ¹³C) spectra were recorded at 400 or 500 MHz (¹H), 100 or 125 MHz {¹³C, DEPT (distortionless enhancement by polarization transfer)}, 377 MHz (¹⁹F), respectively in CDCl₃ solutions, if not otherwise specified; chemical shifts (δ) are given in ppm. The ¹H and ¹³C NMR spectra are referenced to residual solvent signals (CDCl₃: δ H = 7.26 ppm, δ C = 77.2 ppm).

GC Method. Gas Chromatography analyses were performed using a Shimadzu GC-2010 gas chromatograph equipped with a Shimadzu AOC-20s auto sampler and a Restek RTX-5 capillary column (30 m x 0.25 mm x 0.25 μ m). The instrument was set to an injection volume of 1 μ L, an inlet split ratio of 10:1, and inlet and detector temperatures of 250 and 320 °C, respectively. UHP-grade argon was used as carrier gas with a flow rate of 30 mL/min. The temperature program used for all the analyses is as follows: 80 °C, 1 min; 30 °C/min to 200 °C, 2 min; 30 °C/min to 260 °C, 3 min; 30 °C/min to 300 °C, 15 min. Response factors for all the necessary compounds with respect to standard *n*-hexadecane were calculated from the average of three independent GC runs.

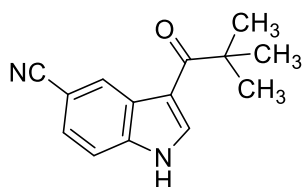
2.4.1 Procedure for Synthesis of (bpy)Ni(OAc)₂ (**1**)

The complex **1** was synthesized by a modified literature procedure.⁹³ In an oven-dried Schlenk flask, a solution of bpy (0.50 g, 3.2 mmol) in EtOH (5 mL) was added to a solution of Ni(OAc)₂ (0.56 g, 3.2 mmol) in EtOH (5 mL) at room temperature. During the addition, the colour changed from light-green to grey in colour. The reaction mixture was stirred at room temperature for 2 h during which the solution became dark green. The reaction mixture was filtered to remove trace insoluble material, and the filtrate was evaporated in *vacuo*. The obtained residue was washed with THF and the solid was dried under *vacuo* to obtain an

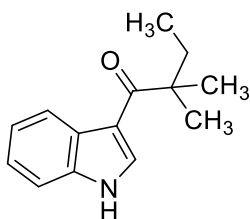
analytical pure compound of (bpy)Ni(OAc)₂ (**1**). Yield: 0.794 g, 75%. Anal. Calcd for C₁₄H₁₄N₂NiO₄·(H₂O): C, 47.91; H, 4.60; N, 7.98. Found: C, 47.29; H, 4.27; N, 8.69.

2.4.2 Synthesis and Characterization of Starting Compounds

Representative Procedure A (Synthesis of 3-Acylindoles). *Synthesis of 3-Pivaloyl-1H-indole-5-carbonitrile (12a):* To the solution of 1H-indole-5-carbonitrile (1.76 g, 12.38 mmol) in HFIP (5.0 mL) in a round bottom flask, the pivaloyl chloride (0.50 g, 4.15 mmol) was added. The resultant mixture was stirred at room temperature for 5 h. The volatiles were evaporated under reduced pressure and the crude product was purified by column chromatography on silica gel (petroleum ether/EtOAc: 1/1) to yield **12a** (0.40 g, 43%) as a brown solid.

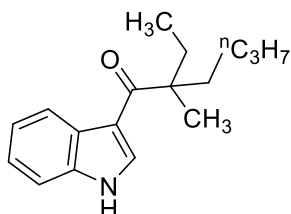


3-Pivaloyl-1H-indole-5-carbonitrile (12a): ¹H-NMR (400 MHz, CDCl₃): δ = 9.02 (br s, 1H, NH), 8.49-8.46 (m, 1H, Ar-H), 7.36-7.34 (m, 1H, Ar-H), 7.25-7.21 (m, 2H, Ar-H), 1.38 (s, 9H, CH₃). ¹³C{¹H}-NMR (100 MHz, CDCl₃): δ = 203.3 (CO), 135.6 (C_q, CN), 135.6 (C_q), 127.5 (2C, C_q), 123.7 (CH), 123.1 (CH), 122.7 (CH), 114.1 (C_q), 111.3 (CH), 44.3 (C_q), 29.1 (3C, CH₃). HRMS (ESI): *m/z* Calcd for C₁₄H₁₄N₂O + H⁺ [M + H]⁺ 227.1179; Found 227.1174.

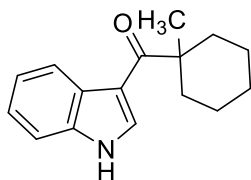


1-(1H-Indol-3-yl)-2,2-dimethylbutan-1-one (13a): The representative procedure **A** was followed using 1H-indole (1.30 g, 11.10 mmol), 2,2-dimethylbutanoyl chloride (0.50 g, 3.71 mmol). Purified by column chromatography on silica gel (petroleum ether/EtOAc: 3/1) yielded **13a** (0.50 g, 63%) as a light-brown solid. ¹H-NMR (500 MHz, CDCl₃): δ = 9.69 (br s, 1H, NH), 8.42-8.40 (m, 1H, Ar-H), 7.74 (d, *J* = 3.1 Hz, 1H, Ar-H), 7.28-7.26 (m, 1H, Ar-H), 7.16-7.13 (m, 2H, Ar-H), 1.74 (q, *J* = 7.5 Hz, 2H, CH₂), 1.24 (s, 6H, CH₃), 0.72 (t, *J* = 7.3 Hz, 3H, CH₃).

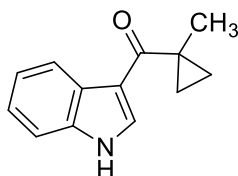
$^{13}\text{C}\{^1\text{H}\}$ -NMR (125 MHz, CDCl_3): δ = 203.9 (CO), 135.8 (C_q), 131.0 (CH), 127.4 (C_q), 123.6 (CH), 122.8 (CH), 122.6 (CH), 114.6 (C_q), 111.7 (CH), 48.2 (C_q), 35.2 (CH_2), 26.6 (2C, CH_3), 9.4 (CH_3). HRMS (ESI): m/z Calcd for $\text{C}_{14}\text{H}_{17}\text{NO} + \text{H}^+$ $[\text{M} + \text{H}]^+$ 216.1383; Found 216.1380.



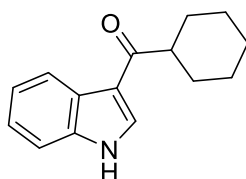
2-Ethyl-1-(1H-indol-3-yl)-2-methylhexan-1-one (14a): The representative procedure A was followed using 1H-indole (1.07 g, 9.13 mmol), 2-ethyl-2-methylhexanoyl chloride (0.54 g, 3.06 mmol). Purified by column chromatography on silica gel (petroleum ether/EtOAc: 3/1) yielded **14a** (0.48 g, 61%) as a light-brown solid. ^1H -NMR (500 MHz, CDCl_3): δ = 8.99 (br s, 1H, *NH*), 8.53-8.51 (m, 1H, Ar-H), 7.92 (d, J = 3.0 Hz, 1H, Ar-H), 7.41-7.38 (m, 1H, Ar-H), 7.29-7.24 (m, 2H, Ar-H), 2.05-1.89 (m, 2H, CH_2), 1.74-1.61 (m, 2H, CH_2), 1.30 (s, 3H, CH_3), 1.28-1.10 (m, 4H, CH_2), 0.84-0.78 (m, 6H, CH_3). $^{13}\text{C}\{^1\text{H}\}$ -NMR (125 MHz, CDCl_3): δ = 203.0 (CO), 135.5 (C_q), 129.6 (CH), 127.6 (C_q), 123.6 (CH), 123.2 (CH), 122.6 (CH), 115.6 (C_q), 111.3 (CH), 52.0 (C_q), 41.1 (CH_2), 34.0 (CH_2), 26.7 (CH_2), 23.6 (CH_2), 22.3 (CH_3), 14.0 (CH_3), 9.0 (CH_3). HRMS (ESI): m/z Calcd for $\text{C}_{17}\text{H}_{23}\text{NO} + \text{H}^+$ $[\text{M} + \text{H}]^+$ 258.1852; Found 258.1852.



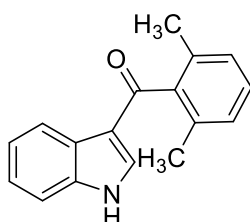
(1H-Indol-3-yl)(1-methylcyclohexyl)methanone (15a): The representative procedure A was followed using 1H-indole (2.19 g, 18.69 mmol), 1-methylcyclohexane-1-carbonyl chloride (1.00 g, 6.23 mmol). Purified by column chromatography on silica gel (petroleum ether/EtOAc: 1/1) yielded **15a** (0.90 g, 60%) as a white solid. ^1H -NMR (400 MHz, CDCl_3): δ = 8.93 (br s, 1H, *NH*), 8.48-8.46 (m, 1H, Ar-H), 7.85 (d, J = 2.5 Hz, 1H, Ar-H), 7.36-7.33 (m, 1H, Ar-H), 7.24-7.21 (m, 2H, Ar-H), 2.55-2.22 (m, 2H, CH_2), 1.55-1.43 (m, 8H, CH_2), 1.36 (s, 3H, CH_3). $^{13}\text{C}\{^1\text{H}\}$ -NMR (100 MHz, CDCl_3): δ = 203.5 (CO), 135.5 (C_q), 129.9 (CH), 127.6 (C_q), 123.6 (CH), 123.1 (CH), 122.6 (CH), 114.7 (C_q), 111.3 (CH), 48.4 (C_q), 37.3 (2C, CH_2), 27.1 (CH_3), 26.3 (CH_2), 23.2 (2C, CH_2). HRMS (ESI): m/z Calcd for $\text{C}_{16}\text{H}_{19}\text{NO} + \text{H}^+$ $[\text{M} + \text{H}]^+$ 242.1539; Found 242.1535.



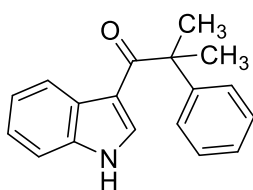
(1*H*-Indol-3-yl)(1-methylcyclopropyl)methanone (17a): The representative procedure **A** was followed using 1*H*-indole (2.19 g, 18.69 mmol), 1-methylcyclopropane-1-carbonyl chloride (0.80 g, 6.75 mmol). Purified by column chromatography on silica gel (petroleum ether/EtOAc: 1/1) yielded **17a** (0.86 g, 64%) as a white solid. ¹H-NMR (400 MHz, CDCl₃): δ = 9.15 (br s, 1H, *NH*), 8.34-8.32 (m, 1H, Ar-H), 7.90 (d, *J* = 3.0 Hz, 1H, Ar-H), 7.37-7.35 (m, 1H, Ar-H), 7.25-7.22 (m, 2H, Ar-H), 1.53 (s, 3H, CH₃), 1.24 (vq, *J* = 4.2 Hz, 2H, CH₂), 0.71 (vq, *J* = 4.0 Hz, 2H, CH₂). ¹³C{¹H}-NMR (100 MHz, CDCl₃): δ = 198.5 (CO), 136.1 (C_q), 131.7 (CH), 126.4 (C_q), 123.7 (CH), 122.6 (CH), 122.5 (CH), 116.1 (C_q), 111.6 (CH), 26.6 (C_q), 23.3 (CH₃), 15.0 (2C, CH₂). HRMS (ESI): *m/z* Calcd for C₁₃H₁₃NO + H⁺ [M + H]⁺ 200.1075; Found 200.1075.



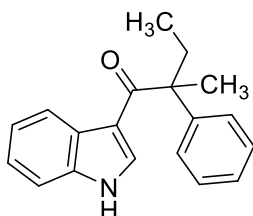
Cyclohexyl(1*H*-indol-3-yl)methanone (19a): The representative procedure **A** was followed using 1*H*-indole (2.40 g, 20.49 mmol), cyclohexanecarbonyl chloride (1.00 g, 6.82 mmol). Purified by column chromatography on silica gel (petroleum ether/EtOAc: 3/1) yielded **19a** (1.10 g, 71%) as a white solid. ¹H-NMR (400 MHz, CDCl₃): δ = 9.17 (br s, 1H, *NH*), 8.38-8.36 (m, 1H, Ar-H), 7.84 (d, *J* = 3.0 Hz, 1H, Ar-H), 7.38-7.34 (m, 1H, Ar-H), 7.25-7.21 (m, 2H, Ar-H), 3.02 (tt, *J* = 8.3 Hz, 3.0 Hz, 1H, CH), 1.89-1.80 (m, 4H, CH₂), 1.71-1.68 (m, 1H, CH₂), 1.63-1.53 (m, 2H, CH₂), 1.39-1.17 (m, 3H, CH₂). ¹³C{¹H}-NMR (100 MHz, CDCl₃): δ = 200.8 (CO), 136.7 (C_q), 131.4 (CH), 125.9 (C_q), 123.8 (CH), 122.8 (CH), 122.6 (CH), 117.0 (C_q), 111.7 (CH), 48.0 (CH), 30.1 (2C, CH₂), 26.2 (3C, CH₂). HRMS (ESI): *m/z* Calcd for C₁₅H₁₇NO + H⁺ [M + H]⁺ 228.1388; Found 228.1396.



(1*H*-Indol-3-yl)(1-methylcyclohexyl)methanone (23a): The representative procedure **A** was followed using 1*H*-indole (1.25 g, 10.67 mmol) and 2,6-dimethylbenzoyl chloride (0.60 g, 3.56 mmol). Purified by column chromatography on silica gel (petroleum ether/EtOAc: 1/1) yielded **23a** (0.50 g, 56%) as a white solid. ¹H-NMR (400 MHz, CDCl₃): δ = 8.51-8.49 (m, 1H, Ar-H), 7.99-7.96 (m, 1H, Ar-H), 7.82-7.77 (m, 1H, Ar-H), 7.44 (d, *J* = 8.2 Hz, 1H, Ar-H), 7.33 (br s, 1H), 7.23-7.14 (m, 2H, Ar-H), 7.02 (d, *J* = 7.5 Hz, 2H, Ar-H), 2.19 (s, 6H, CH₃). ¹³C{¹H}-NMR (100 MHz, CDCl₃): δ = 195.4 (C_q, CO), 151.3 (C_q), 149.6 (CH), 139.0 (CH), 136.3 (C_q), 134.3 (C_q), 128.6 (CH), 127.8 (CH), 124.8 (C_q), 124.0 (CH), 122.2 (CH), 120.1 (2C, C_q), 116.2 (CH), 112.8 (CH), 19.6 (2C, CH₃). HRMS (ESI): *m/z* Calcd for C₁₇H₁₅NO + H⁺ [M + H]⁺ 250.1226; Found 250.1224.

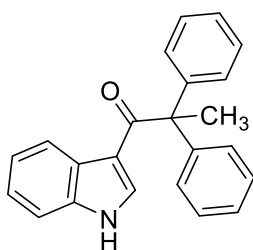


1-(1*H*-Indol-3-yl)-2-methyl-2-phenylpropan-1-one (30a): The representative procedure **A** was followed using 1*H*-indole (0.96 g, 8.19 mmol) and 2-methyl-2-phenylpropanoyl chloride (0.50 g, 2.74 mmol). Purified by column chromatography on silica gel (petroleum ether/EtOAc: 1/1) yielded **30a** (0.40 g, 55%) as a white solid. ¹H-NMR (500 MHz, CDCl₃): δ = 8.52 (d, *J* = 7.6 Hz, 1H, Ar-H), 8.32 (br s, 1H, *NH*), 7.39-7.24 (m, 8H, Ar-H), 6.80 (d, *J* = 3.1 Hz, 1H, Ar-H), 1.66 (s, 6H, CH₃). ¹³C{¹H}-NMR (125 MHz, CDCl₃): δ = 200.3 (CO), 147.4 (C_q), 135.2 (C_q), 132.3 (CH), 128.8 (2C, CH), 127.2 (C_q), 126.7 (CH), 126.6 (CH), 125.9 (CH), 124.7 (C_q), 123.7 (CH), 123.0 (CH), 122.7 (CH), 111.1 (CH), 52.1 (C_q), 28.5 (2C, CH₃). HRMS (ESI): *m/z* Calcd for C₁₈H₁₇NO + H⁺ [M + H]⁺ 264.1383; Found 264.1386.



1-(1*H*-Indol-3-yl)-2-methyl-2-phenylbutan-1-one (32a): The representative procedure **A** was followed using 1*H*-indole (0.89 g, 7.60 mmol), 2-methyl-2-phenylbutanoyl chloride (0.50 g, 2.54 mmol). Purified by column chromatography on silica gel (petroleum ether/EtOAc:

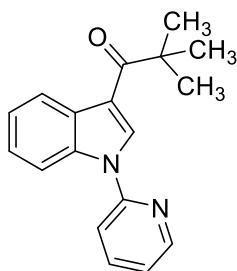
1/1) yielded **32a** (0.45 g, 64%) as a white solid. $^1\text{H-NMR}$ (500 MHz, CDCl_3): δ = 8.69 (br s, 1H, *NH*), 8.53 (d, J = 8.0 Hz, 1H, Ar-H), 7.37-7.25 (m, 8H, Ar-H), 6.83 (s, 1H, Ar-H), 2.29-2.20 (m, 1H, CH_2), 2.18-2.11 (m, 1H, CH_2), 1.62 (s, 3H, CH_3), 0.81 (t, J = 7.2 Hz, 3H, CH_3). $^{13}\text{C}\{^1\text{H}\}$ -NMR (125 MHz, CDCl_3): δ = 200.6 (CO), 146.5 (C_q), 135.3 (C_q), 132.2 (CH), 128.7 (2C, CH), 127.1 (2C, CH), 126.7 (CH), 126.4 (C_q), 123.5 (CH), 122.8 (CH), 122.6 (CH), 115.0 (C_q), 111.3 (CH), 55.6 (C_q), 32.5 (CH_2), 24.8 (CH_3), 8.8 (CH_3). HRMS (ESI): m/z Calcd for $\text{C}_{19}\text{H}_{19}\text{NO} + \text{H}^+$ $[\text{M} + \text{H}]^+$ 278.1539; Found 278.1544.



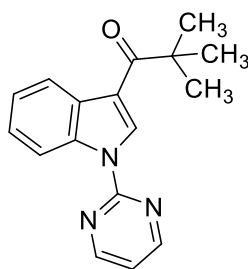
1-(1H-Indol-3-yl)-2,2-diphenylpropan-1-one (34a): The representative procedure **A** was followed using 1H-indole (1.00 g, 8.54 mmol) and 2,2-diphenylpropanoyl chloride (0.70 g, 2.86 mmol). Purified by column chromatography on silica gel (petroleum ether/EtOAc: 1/1) yielded **34a** (0.60 g, 64%) as a white solid. $^1\text{H-NMR}$ (400 MHz, CDCl_3): δ = 8.68 (br s, 1H, *NH*), 8.49 (d, J = 7.1 Hz, 1H, Ar-H), 7.30-7.19 (m, 13H, Ar-H), 6.68 (d, J = 3.2 Hz, 1H, Ar-H), 2.11 (s, 3H, CH_3). $^{13}\text{C}\{^1\text{H}\}$ -NMR (100 MHz, CDCl_3): δ = 198.4 (CO), 145.3 (C_q), 144.8 (C_q), 135.2 (C_q), 132.9 (CH), 129.0 (2C, CH), 128.6 (C_q), 128.4 (C_q), 128.3 (CH), 127.8 (CH), 127.4 (CH), 126.8 (CH), 123.7 (CH), 123.1 (CH), 122.8 (CH), 122.2 (CH), 119.2 (CH), 114.4 (CH), 111.2 (CH), 102.9 (CH), 61.2 (C_q), 29.5 (CH_3). HRMS (ESI): m/z Calcd for $\text{C}_{23}\text{H}_{19}\text{NO} + \text{H}^+$ $[\text{M} + \text{H}]^+$ 326.1545; Found 326.1548.

Representative Procedure B: Synthesis of (1-(Pyridin-2-yl)-3-acylindoles

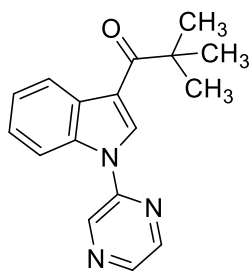
Synthesis of 2,2-Dimethyl-1-(1-(pyridin-2-yl)-1H-indol-3-yl)propan-1-one (2b). To the mixture of 1-(1H-indol-3-yl)-2,2-dimethylpropan-1-one (**2a**; 1.0 g, 4.97 mmol) and KOH (0.69 g, 12.3 mmol) in DMSO (20 mL), the 2-bromopyridine (1.17 g, 7.41 mmol) was added. The resultant reaction mixture was stirred at 135 °C for 30 h. The reaction mixture was cooled to ambient temperature, quenched with cold water (15 mL), and extracted with ethyl acetate (20 mL x 3). The combined organic extract was dried over Na_2SO_4 and the volatiles were evaporated under *vacuo*. The remaining residue was purified by column chromatography on silica gel (petroleum ether/EtOAc: 5/1) yielded **2b** (0.95 g, 69%) as a light-yellow solid.



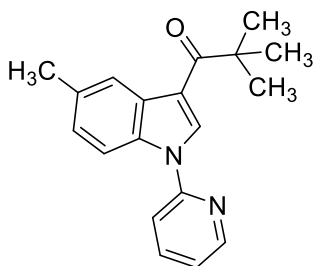
2,2-Dimethyl-1-(1-(pyridin-2-yl)-1H-indol-3-yl)propan-1-one (2b): $^1\text{H-NMR}$ (500 MHz, CDCl_3): δ = 8.62 (d, J = 4.2 Hz, 1H, Ar-H), 8.59-8.57 (m, 1H, Ar-H), 8.49 (s, 1H, Ar-H), 7.94-7.92 (m, 1H, Ar-H), 7.90-7.87 (m, 1H, Ar-H), 7.60 (d, J = 8.3 Hz, 1H, Ar-H), 7.37-7.33 (m, 2H, Ar-H), 7.30-7.28 (m, 1H, Ar-H), 1.48 (s, 9H, CH_3). $^{13}\text{C}\{^1\text{H}\}$ -NMR (125 MHz, CDCl_3): δ = 202.9 (CO), 151.2 (C_q), 149.6 (CH), 138.9 (CH), 134.8 (C_q), 131.8 (CH), 129.6 (C_q), 124.3 (CH), 123.7 (CH), 123.5 (CH), 121.9 (CH), 116.2 (CH), 115.4 (C_q), 111.8 (CH), 44.5 (C_q), 28.9 (3C, CH_3). HRMS (ESI): m/z Calcd for $\text{C}_{18}\text{H}_{18}\text{N}_2\text{O} + \text{H}^+$ [M + H] $^+$ 279.1492; Found 279.1498.



2,2-Dimethyl-1-(1-(pyrimidin-2-yl)-1H-indol-3-yl)propan-1-one (3b): The 1-(1H-indol-3-yl)-2,2-dimethylpropan-1-one (**2a**; 0.80 g, 3.97 mmol) was added to a solution of NaH (0.10 g, 4.17 mmol) in DMF at 0 °C and was stirred for 0.5 h. 2-Chloropyrimidine (0.54 g, 4.71 mmol) was added to the mixture at 0 °C and the resulting reaction mixture was stirred at 135 °C for 24 h. The reaction mixture was cooled to ambient temperature, quenched with cold water (15 mL) and extracted with ethyl acetate (20 mL x 3). The combined organic extract was dried over Na_2SO_4 and the volatiles were evaporated in *vacuo*. Purification by column chromatography on silica gel (petroleum ether/EtOAc: 5/1) yielded **3b** (0.66 g, 59%) as a brown solid. $^1\text{H-NMR}$ (500 MHz, CDCl_3): δ = 9.04 (s, 1H, Ar-H), 8.83-8.80 (m, 1H, Ar-H), 8.75 (d, J = 5.3 Hz, 2H, Ar-H), 8.52-8.49 (m, 1H, Ar-H), 7.42-7.35 (m, 2H, Ar-H), 7.18-7.15 (m, 1H, Ar-H), 1.49 (s, 9H, CH_3). $^{13}\text{C}\{^1\text{H}\}$ -NMR (125 MHz, CDCl_3): δ = 203.3 (CO), 158.4 (2C, CH), 157.5 (C_q), 135.2 (C_q), 131.1 (CH), 130.3 (C_q), 124.9 (CH), 124.1 (CH), 123.2 (CH), 117.6 (CH), 116.3 (C_q), 116.0 (CH), 44.7 (C_q), 28.9 (3C, CH_3). HRMS (ESI): m/z Calcd for $\text{C}_{17}\text{H}_{17}\text{N}_3\text{O} + \text{H}^+$ [M + H] $^+$ 280.1444; Found 280.1443.

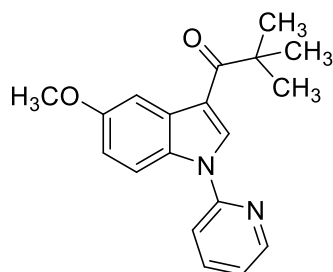


2,2-Dimethyl-1-(1-(pyrazin-2-yl)-1H-indol-3-yl)propan-1-one (4b): The 1-(1H-indol-3-yl)-2,2-dimethylpropan-1-one (**2a**; 0.50 g, 2.48 mmol) was added to a solution of NaH (0.065 g, 2.71 mmol) in DMF at 0 °C and was stirred for 0.5 h. To the resultant solution, 2-iodopyrazine (0.61 g, 2.96 mmol) was added at 0 °C and was stirred at 135 °C for 24 h. The reaction mixture was cooled to ambient temperature, quenched with cold water (15 mL) and extracted with ethyl acetate (20 mL x 3). The combined organic extract was dried over Na₂SO₄ and the volatiles were evaporated in *vacuo*. Purification by column chromatography on silica gel (petroleum ether/EtOAc: 5/1) yielded **4b** (0.39 g, 56%) as a brown solid. ¹H-NMR (400 MHz, CDCl₃): δ = 9.02 (s, 1H, Ar-H), 8.56-8.52 (m, 3H, Ar-H), 8.45 (s, 1H, Ar-H), 8.01-7.99 (m, 1H, Ar-H), 7.39-7.34 (m, 2H, Ar-H), 1.47 (s, 9H, CH₃). ¹³C{¹H}-NMR (100 MHz, CDCl₃): δ = 202.7 (CO), 148.1 (C_q), 143.4 (CH), 142.0 (CH), 137.6 (CH), 134.6 (C_q), 130.5 (CH), 129.7 (C_q), 124.9 (CH), 124.0 (CH), 123.9 (CH), 116.7 (C_q), 111.9 (CH), 44.7 (C_q), 28.8 (3C, CH₃). HRMS (ESI): *m/z* Calcd for C₁₇H₁₇ON₃ + H⁺ [M + H]⁺ 280.1444; Found 280.1443.

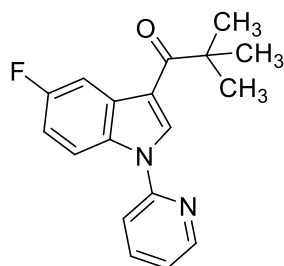


2,2-Dimethyl-1-(5-methyl-1-(pyridin-2-yl)-1H-indol-3-yl)propan-1-one (7b): The representative procedure **B** was followed using 2,2-dimethyl-1-(5-methyl-1H-indol-3-yl)propan-1-one (**7a**; 1.0 g, 4.64 mmol), 2-bromopyridine (1.10 g, 6.96 mmol) and KOH (0.65 g, 11.58 mmol). Purification by column chromatography on silica gel (petroleum ether/EtOAc: 5/1) yielded **7b** (0.80 g, 59%) as a light-yellow solid. ¹H-NMR (500 MHz, CDCl₃): δ = 8.62-8.61 (m, 1H, Ar-H), 8.46 (s, 1H, Ar-H), 8.39 (s, 1H, Ar-H), 7.91-7.87 (m, 1H, Ar-H), 7.81 (d, *J* = 8.3 Hz, 1H, Ar-H), 7.60 (d, *J* = 8.3 Hz, 1H, Ar-H), 7.30-7.26 (m, 1H, Ar-H), 7.17 (dd, *J* = 8.5, 1.5 Hz, 1H, Ar-H), 2.50 (s, 3H, CH₃), 1.47 (s, 9H, CH₃). ¹³C{¹H}-NMR (125 MHz, CDCl₃): δ = 203.1 (CO), 151.4 (C_q), 149.7 (CH), 138.8 (CH), 133.2 (C_q), 133.1 (C_q), 131.8

(CH), 130.0 (C_q), 125.8 (CH), 123.5 (CH), 121.7 (CH), 116.0 (CH), 115.1 (C_q), 111.5 (CH), 44.6 (C_q), 29.0 (3C, CH₃), 21.7 (CH₃). HRMS (ESI): *m/z* Calcd for C₁₉H₂₀N₂O + H⁺ [M + H]⁺ 293.1648; Found 293.1649.

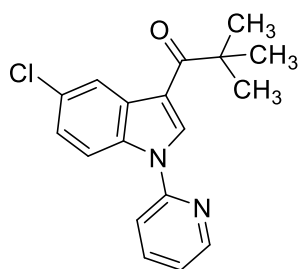


1-(5-Methoxy-1-(pyridin-2-yl)-1H-indol-3-yl)-2,2-dimethylpropan-1-one (8b): The representative procedure **B** was followed using 1-(5-methoxy-1H-indol-3-yl)-2,2-dimethylpropan-1-one (**8a**; 1.0 g, 4.32 mmol), 2-bromopyridine (1.02 g, 6.46 mmol) and KOH (0.60 g, 10.69 mmol). Purification by column chromatography on silica gel (petroleum ether/EtOAc: 3/1) yielded **8b** (1.0 g, 75%) as a yellow solid. ¹H-NMR (500 MHz, CDCl₃): δ = 8.60 (d, *J* = 3.0 Hz, 1H, Ar-H), 8.46 (s, 1H, Ar-H), 8.12 (d, *J* = 2.2 Hz, 1H, Ar-H), 7.90-7.85 (m, 2H, Ar-H), 7.57 (d, *J* = 8.3 Hz, 1H, Ar-H), 7.29-7.26 (m, 1H, Ar-H), 6.98 (dd, *J* = 9.1, 2.2 Hz, 1H, Ar-H), 3.93 (s, 3H, OCH₃), 1.49 (s, 9H, CH₃). ¹³C{¹H}-NMR (125 MHz, CDCl₃): δ = 203.1 (CO), 156.8 (C_q), 151.3 (C_q), 149.6 (CH), 138.8 (CH), 132.0 (CH), 130.6 (C_q), 129.7 (C_q), 121.7 (CH), 115.7 (CH), 115.0 (C_q), 114.7 (CH), 112.9 (CH), 104.6 (CH), 55.8 (OCH₃), 44.5 (C_q), 29.0 (3C, CH₃). HRMS (ESI): *m/z* Calcd for C₁₉H₂₀N₂O₂ + H⁺ [M + H]⁺ 309.1598; Found 309.1595.

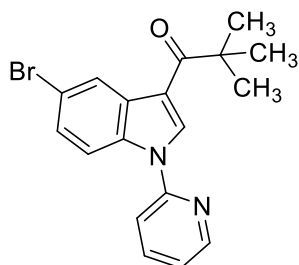


1-(5-Fluoro-1-(pyridin-2-yl)-1H-indol-3-yl)-2,2-dimethylpropan-1-one (9b): The representative procedure **B** was followed using 1-(5-fluoro-1H-indol-3-yl)-2,2-dimethylpropan-1-one (**9a**; 0.50 g, 2.28 mmol), 2-bromopyridine (0.54 g, 3.42 mmol) and KOH (0.32 g, 5.70 mmol). Purification by column chromatography on silica gel (petroleum ether/EtOAc: 5/1) yielded **9b** (0.45 g, 67%) as a yellow solid. ¹H-NMR (400 MHz, CDCl₃): δ = 8.63-8.61 (m, 1H, Ar-H), 8.46 (s, 1H, Ar-H), 8.25 (dd, *J* = 9.9, 3.0 Hz, 1H, Ar-H), 7.94-

7.89 (m, 2H, Ar-H), 7.56 (d, $J = 8.3$ Hz, 1H, Ar-H), 7.34-7.31 (m, 1H, Ar-H), 7.10-7.04 (m, 1H, Ar-H), 1.46 (s, 9H, CH₃). ¹³C{¹H}-NMR (100 MHz, CDCl₃): $\delta = 202.6$ (CO), 160.0 (d, ¹ $J_{C-F} = 238.6$ Hz, C_q), 151.2 (C_q), 149.7 (CH), 139.1 (CH), 132.8 (CH), 131.4 (C_q), 130.6 (d, ³ $J_{C-F} = 10.5$ Hz, C_q), 122.1 (CH), 115.9 (CH), 115.3 (d, ⁴ $J_{C-F} = 4.7$ Hz, C_q), 113.0 (d, ³ $J_{C-F} = 9.5$ Hz, CH), 112.6 (d, ² $J_{C-F} = 25.8$ Hz, CH), 109.1 (d, ² $J_{C-F} = 24.9$ Hz, CH), 44.5 (C_q), 28.9 (3C, CH₃). ¹⁹F-NMR (376 MHz, CDCl₃): $\delta = -119.8$ (s). HRMS (ESI): m/z Calcd for C₁₈H₁₇FN₂O + H⁺ [M + H]⁺ 297.1398; Found 297.1406.

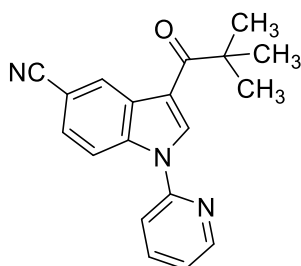


1-(5-Chloro-1-(pyridin-2-yl)-1H-indol-3-yl)-2,2-dimethylpropan-1-one (10b): The representative procedure **B** was followed using 1-(5-chloro-1H-indol-3-yl)-2,2-dimethylpropan-1-one (**10a**; 0.40 g, 1.70 mmol), 2-bromopyridine (0.40 g, 2.53 mmol) and KOH (0.24 g, 4.28 mmol). Purification by column chromatography on silica gel (petroleum ether/EtOAc: 5/1) yielded **10b** (0.39 g, 74%) as a white solid. ¹H-NMR (400 MHz, CDCl₃): $\delta = 8.56$ -8.55 (m, 1H, Ar-H), 8.52 (s, 1H, Ar-H), 8.38 (s, 1H, Ar-H), 7.87-7.81 (m, 2H, Ar-H), 7.48 (d, $J = 8.1$ Hz, 1H, Ar-H), 7.27-7.19 (m, 2H, Ar-H), 1.40 (s, 9H, CH₃). ¹³C{¹H}-NMR (100 MHz, CDCl₃): $\delta = 202.5$ (CO), 151.0 (C_q), 149.6 (CH), 139.1 (CH), 133.2 (C_q), 132.4 (CH), 130.7 (C_q), 129.3 (C_q), 124.6 (CH), 123.2 (CH), 122.2 (CH), 115.9 (CH), 114.9 (C_q), 113.2 (CH), 44.5 (C_q), 28.8 (3C, CH₃). HRMS (ESI): m/z Calcd for C₁₈H₁₇ON₂Cl + H⁺ [M + H]⁺ 313.1102; Found 313.1103.

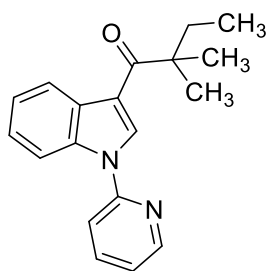


1-(5-Bromo-1-(pyridin-2-yl)-1H-indol-3-yl)-2,2-dimethylpropan-1-one (11b): The representative procedure **B** was followed using 1-(5-bromo-1H-indol-3-yl)-2,2-dimethylpropan-1-one (**11a**; 0.50 g, 1.78 mmol), 2-bromopyridine (0.42 g, 2.66 mmol) and

KOH (0.25 g, 4.46 mmol). Purification by column chromatography on silica gel (petroleum ether/EtOAc: 5/1) yielded **11b** (0.40 g, 63%) as a white solid. $^1\text{H-NMR}$ (400 MHz, CDCl_3): δ = 8.94 (m, 1H, Ar-H), 8.67-8.65 (m, 1H, Ar-H), 8.49 (s, 1H, Ar-H), 8.07-8.05 (m, 1H, Ar-H), 7.99-7.95 (m, 1H, Ar-H), 7.59-7.56 (m, 2H, Ar-H), 7.41-7.38 (m, 1H, Ar-H), 1.47 (s, 9H, CH_3). $^{13}\text{C}\{^1\text{H}\}$ -NMR (100 MHz, CDCl_3): δ = 202.4 (CO), 150.7 (C_q), 149.9 (CH), 139.3 (CH), 136.5 (C_q), 133.1 (CH), 129.2 (CH), 127.4 (CH), 122.8 (CH), 120.0 (C_q), 116.3 (CH), 115.5 (C_q), 113.2 (CH), 107.0 (C_q), 44.7 (C_q), 28.7 (3C, CH_3). HRMS (ESI): m/z Calcd for $\text{C}_{18}\text{H}_{17}\text{BrN}_2\text{O} + \text{H}^+$ $[\text{M} + \text{H}]^+$ 357.0597, 359.0852; Found 357.0605, 359.0859.

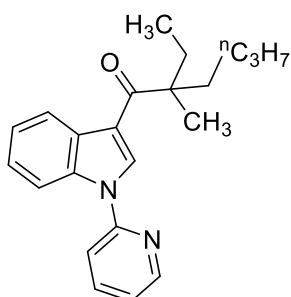


3-Pivaloyl-1-(pyridin-2-yl)-1H-indole-5-carbonitrile (12b): The representative procedure **B** was followed using 3-pivaloyl-1H-indole-5-carbonitrile (**12a**; 0.20 g, 0.88 mmol), 2-bromopyridine (0.20 g, 1.27 mmol) and KOH (0.12 g, 2.14 mmol). Purification by column chromatography on silica gel (petroleum ether/EtOAc: 3/1) yielded **12b** (0.13 g, 49%) as a white solid. $^1\text{H-NMR}$ (400 MHz, CDCl_3): δ = 8.94-8.93 (m, 1H, Ar-H), 8.69-8.68 (m, 1H, Ar-H), 8.65-8.62 (m, 2H, Ar-H), 8.20 (dd, J = 8.9, 1.9 Hz, 1H, Ar-H), 8.00 (td, J = 7.9, 1.8 Hz, 1H, Ar-H), 7.61 (d, J = 8.0 Hz, 1H, Ar-H), 7.42-7.39 (m, 1H, Ar-H), 1.47 (s, 9H, CH_3). $^{13}\text{C}\{^1\text{H}\}$ -NMR (100 MHz, CDCl_3): δ = 202.2 (CO), 150.5 (C_q), 150.0 (CH), 145.0 (2C, C_q), 139.5 (CH), 135.3 (CH), 134.4 (C_q), 133.8 (C_q), 123.9 (CH), 122.9 (CH), 118.6 (CH), 116.1 (CH), 115.6 (C_q), 109.1 (CH), 44.7 (C_q), 28.7 (3C, CH_3). HRMS (ESI): m/z Calcd for $\text{C}_{19}\text{H}_{17}\text{N}_3\text{O} + \text{H}^+$ $[\text{M} + \text{H}]^+$ 304.1444; Found 304.1441.

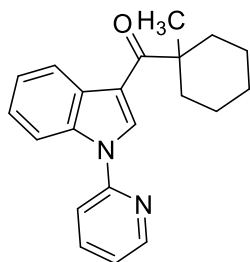


2,2-Dimethyl-1-(1-(pyridin-2-yl)-1H-indol-3-yl)butan-1-one (13b): The representative procedure **B** was followed using 1-(1H-indol-3-yl)-2,2-dimethylbutan-1-one

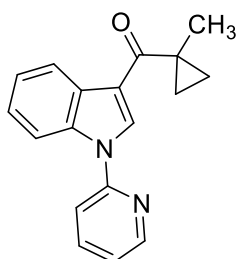
(**13a**; 0.40 g, 1.86 mmol), 2-bromopyridine (0.43 g, 2.72 mmol) and KOH (0.26 g, 4.63 mmol). Purification by column chromatography on silica gel (petroleum ether/EtOAc: 5/1) yielded **13b** (0.41 g, 75%) as a white solid. $^1\text{H-NMR}$ (500 MHz, CDCl_3): δ = 8.61 (d, J = 4.5 Hz, 1H, Ar-H), 8.59- 8.57 (m, 1H, Ar-H), 8.48 (s, 1H, Ar-H), 7.96-7.87 (m, 2H, Ar-H), 7.61 (d, J = 8.3 Hz, 1H, Ar-H), 7.37-7.33 (m, 2H, Ar-H), 7.31-7.28 (m, 1H, Ar-H), 1.96 (q, J = 7.6 Hz, 2H, CH_2), 1.42 (s, 6H, CH_3), 0.88 (t, J = 8.3 Hz, 3H, CH_3). $^{13}\text{C}\{^1\text{H}\}$ -NMR (125 MHz, CDCl_3): δ = 202.8 (CO), 151.3 (C_q), 149.6 (CH), 138.9 (CH), 134.8 (C_q), 131.3 (CH), 129.7 (C_q), 124.3 (CH), 123.7 (CH), 123.5 (CH), 121.8 (CH), 116.2 (CH), 116.0 (C_q), 111.8 (CH), 48.5 (C_q), 35.0 (CH_2), 26.4 (2C, CH_3) 9.5 (CH_3). HRMS (ESI): m/z Calcd for $\text{C}_{19}\text{H}_{20}\text{N}_2\text{O} + \text{H}^+$ [$\text{M} + \text{H}$] $^+$ 293.1648; Found 293.1645.



2-Ethyl-2-methyl-1-(1-(pyridin-2-yl)-1H-indol-3-yl)hexan-1-one (14b): The representative procedure **B** was followed using 2-ethyl-1-(1H-indol-3-yl)-2-methylhexan-1-one (**14a**; 0.40 g, 1.55 mmol), 2-bromopyridine (0.36 g, 2.28 mmol) and KOH (0.21 g, 3.74 mmol). Purification by column chromatography on silica gel (petroleum ether/EtOAc: 5/1) yielded **14b** (0.45 g, 87%) as a white solid. $^1\text{H-NMR}$ (400 MHz, CDCl_3): δ = 8.65-8.63 (m, 1H, Ar-H), 8.58-8.55 (m, 1H, Ar-H), 8.48 (s, 1H, Ar-H), 7.97-7.93 (m, 1H, Ar-H), 7.92-7.89 (m, 1H, Ar-H), 7.63-7.60 (m, 1H, Ar-H), 7.36-7.34 (m, 2H, Ar-H), 7.33-7.29 (m, 1H, Ar-H), 2.12-1.98 (m, 2H, CH_2), 1.80-1.65 (m, 2H, CH_2), 1.35 (s, 3H, CH_3), 1.32-1.15 (m, 4H, CH_2), 0.88-0.81 (m, 6H, CH_3). $^{13}\text{C}\{^1\text{H}\}$ -NMR (100 MHz, CDCl_3): δ = 202.7 (CO), 151.5 (C_q), 149.7 (CH), 138.9 (CH), 134.8 (C_q), 130.8 (CH), 129.8 (C_q), 124.4 (CH), 123.8 (CH), 123.5 (CH), 121.8 (CH), 116.7 (C_q), 116.2 (CH), 111.9 (CH), 52.3 (C_q), 40.8 (CH_2), 33.9 (CH_2), 26.8 (CH_2), 23.6 (CH_2), 22.2 (CH_3), 14.1 (CH_3), 9.1 (CH_3). HRMS (ESI): m/z Calcd for $\text{C}_{22}\text{H}_{26}\text{N}_2\text{O} + \text{H}^+$ [$\text{M} + \text{H}$] $^+$ 335.2123; Found 335.2132.

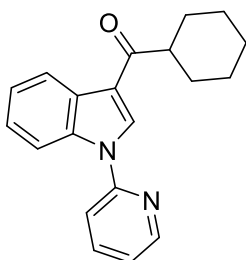


(1-Methylcyclohexyl)(1-(pyridin-2-yl)-1H-indol-3-yl)methanone (15b): The representative procedure **B** was followed using (1H-indol-3-yl)(1-methylcyclohexyl)methanone (**15a**; 0.50 g, 2.07 mmol), 2-bromopyridine (0.49 g, 3.10 mmol) and KOH (0.29 g, 5.17 mmol). Purification by column chromatography on silica gel (petroleum ether/EtOAc: 5/1) yielded **15b** (0.43 g, 65%) as a white solid. $^1\text{H-NMR}$ (500 MHz, CDCl_3): δ = 8.64-8.62 (m, 1H, Ar-H), 8.56-8.54 (m, 1H, Ar-H), 8.46 (s, 1H, Ar-H), 7.95-7.88 (m, 2H, Ar-H), 7.62 (d, J = 7.6 Hz, 1H, Ar-H), 7.36-7.33 (m, 2H, Ar-H), 7.31-7.28 (m, 1H, Ar-H), 2.34-2.30 (m, 2H, CH_2), 1.62-1.39 (m, 11H, 4 CH_2 and CH_3). $^{13}\text{C}\{^1\text{H}\}$ -NMR (125 MHz, CDCl_3): δ = 203.1 (CO), 151.4 (C_q), 149.6 (CH), 138.9 (CH), 134.8 (C_q), 131.1 (CH), 129.9 (C_q), 124.3 (CH), 123.7 (CH), 123.5 (CH), 121.8 (CH), 116.2 (CH), 115.9 (C_q), 111.8 (CH), 48.6 (C_q), 37.2 (2C, CH_2), 27.0 (CH_3), 26.3 (CH_2), 23.2 (2C, CH_2). HRMS (ESI): m/z Calcd for $\text{C}_{21}\text{H}_{22}\text{N}_2\text{O} + \text{H}^+$ [$\text{M} + \text{H}$] $^+$ 319.1805; Found 319.1806.

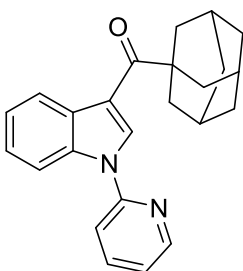


(1-Methylcyclopropyl)(1-(pyridin-2-yl)-1H-indol-3-yl)methanone (17b): The representative procedure **B** was followed using (1H-indol-3-yl)(1-methylcyclopropyl)methanone (**17a**; 0.80 g, 4.02 mmol), 2-bromopyridine (0.94 g, 5.95 mmol) and KOH (0.56 g, 9.98 mmol). Purification by column chromatography on silica gel (petroleum ether/EtOAc: 5/1) yielded **17b** (0.78 g, 70%) as a white solid. $^1\text{H-NMR}$ (500 MHz, CDCl_3): δ = 8.62 (d, J = 4.9 Hz, 1H, Ar-H), 8.47 (s, 1H, Ar-H), 8.43-8.41 (m, 1H, Ar-H), 7.99-7.97 (m, 1H, Ar-H), 7.92-7.89 (m, 1H, Ar-H), 7.60 (d, J = 8.0 Hz, 1H, Ar-H), 7.36-7.34 (m, 2H, Ar-H), 7.32-7.29 (m, 1H, Ar-H), 1.64 (s, 3H, CH_3), 1.33 d, J = 4.2 Hz, 2H, CH_2), 0.79 (d, J = 4.2 Hz, 2H, CH_2). $^{13}\text{C}\{^1\text{H}\}$ -NMR (125 MHz, CDCl_3): δ = 198.1 (CO), 151.4 (C_q), 149.6 (CH), 138.9 (CH), 135.4 (C_q), 132.6 (CH), 128.6 (C_q), 124.4 (CH), 123.5 (CH), 123.1 (CH), 121.9

(CH), 117.3 (C_q), 116.1 (CH), 112.2 (CH), 26.7 (C_q), 23.2 (CH₃), 15.2 (2C, CH₂). HRMS (ESI): *m/z* Calcd for C₁₈H₁₆N₂O + H⁺ [M + H]⁺ 277.1341; Found 277.1346.

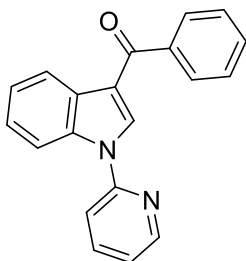


Cyclohexyl(1-(pyridin-2-yl)-1H-indol-3-yl)methanone (19b): The representative procedure **B** was followed using cyclohexyl(1H-indol-3-yl)methanone (**19a**; 1.0 g, 4.40 mmol), 2-bromopyridine (1.04 g, 6.58 mmol) and KOH (0.61 g, 10.87 mmol). Purification by column chromatography on silica gel (petroleum ether/EtOAc: 5/1) yielded **19b** (1.12 g, 84%) as a white solid. ¹H-NMR (400 MHz, CDCl₃): δ = 8.64-8.62 (m, 1H, Ar-H), 8.54-8.50 (m, 1H, Ar-H), 8.42 (s, 1H, Ar-H), 7.96-7.88 (m, 2H, Ar-H), 7.63 (d, *J* = 8.2 Hz, 1H, Ar-H), 7.38-7.29 (m, 3H, Ar-H), 3.19-2.11 (m, 1H, CH), 1.97-1.85 (m, 4H, CH₂), 1.77-1.59 (m, 3H, CH₂), 1.46-1.24 (m, 3H, CH₂). ¹³C{¹H}-NMR (100 MHz, CDCl₃): δ = 200.4 (CO), 151.2 (C_q), 149.6 (CH), 139.0 (CH), 135.9 (C_q), 132.5 (CH), 128.1 (C_q), 124.5 (CH), 123.6 (CH), 123.3 (CH), 121.9 (CH), 118.1 (C_q), 116.2 (CH), 112.1 (CH), 48.0 (CH), 30.0 (2C, CH₂), 26.1 (3C, CH₂). HRMS (ESI): *m/z* Calcd for C₂₀H₂₀N₂O + H⁺ [M + H]⁺ 305.1648; Found 305.1648.

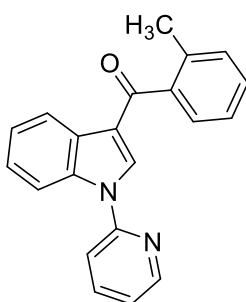


Adamantan-1-yl(1-(pyridin-2-yl)-1H-indol-3-yl)methanone (20b): The representative procedure **B** was followed using adamantan-1-yl(1H-indol-3-yl)methanone (**20a**; 0.50 g, 1.79 mmol), 2-bromopyridine (0.42 g, 2.66 mmol) and KOH (0.25g, 4.46 mmol). Purification by column chromatography on silica gel (petroleum ether/EtOAc: 5/1) yielded **20b** (0.41 g, 64%) as a white solid. ¹H-NMR (500 MHz, CDCl₃): δ = 8.65-8.63 (m, 1H, Ar-H), 8.57 (s, 1H, Ar-H), 8.56-8.53 (m, 1H, Ar-H), 7.93-7.89 (m, 2H, Ar-H), 7.62 (d, *J* = 7.6 Hz, 1H, Ar-H), 7.36-7.29 (m, 3H, Ar-H), 2.19-2.14 (m, 6H, CH₂, 3H, CH), 1.83-1.82 (m, 6H, CH₂). ¹³C{¹H}-NMR (125 MHz, CDCl₃): δ = 202.9 (CO), 151.4 (C_q), 149.7 (CH), 138.9 (CH), 134.7 (C_q), 131.4

(CH), 129.9 (C_q), 124.3 (CH), 123.8 (CH), 123.5 (CH), 121.9 (CH), 116.4 (CH), 115.6 (C_q), 111.7 (CH), 47.4 (C_q), 40.5 (3C, CH₂), 37.0 (3C, CH₂), 28.6 (3C, CH). HRMS (ESI): *m/z* Calcd for C₂₄H₂₄N₂O + H⁺ [M + H]⁺ 357.1961; Found 357.1971.

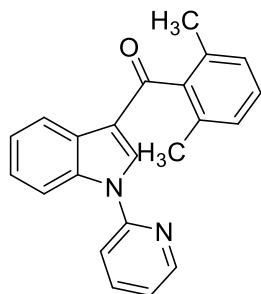


Phenyl(1-(pyridin-2-yl)-1H-indol-3-yl)methanone (21b): The representative procedure **B** was followed using (1H-indol-3-yl)(phenyl)methanone (**21a**; 0.40 g, 1.81 mmol), 2-bromopyridine (0.43 g, 2.72 mmol) and KOH (0.25 g, 4.46 mmol). Purification by column chromatography on silica gel (petroleum ether/EtOAc: 5/1) yielded **21b** (0.30 g, 56%) as a light-yellow solid. ¹H-NMR (400 MHz, CDCl₃): δ = 8.60-8.59 (m, 1H, Ar-H), 8.52-8.50 (m, 1H, Ar-H), 8.18 (s, 1H, Ar-H), 8.05-8.03 (m, 1H, Ar-H), 7.91-7.86 (m, 3H, Ar-H), 7.59-7.56 (m, 2H, Ar-H), 7.53-7.49 (m, 2H, Ar-H), 7.43-7.38 (m, 2H, Ar-H), 7.31-7.28 (m, 1H, Ar-H). ¹³C{¹H}-NMR (100 MHz, CDCl₃): δ = 191.6 (CO), 151.3 (C_q), 149.6 (CH), 140.5 (2C, C_q), 139.0 (CH), 135.9 (C_q), 135.2 (CH), 131.7 (CH), 129.0 (2C, CH), 128.6 (2C, CH), 124.8 (CH), 123.8 (CH), 123.1 (CH), 122.1 (CH), 118.3 (C_q), 116.1 (CH), 112.5 (CH). HRMS (ESI): *m/z* Calcd for C₂₀H₁₄N₂O + H⁺ [M + H]⁺ 299.1179; Found 299.1184.

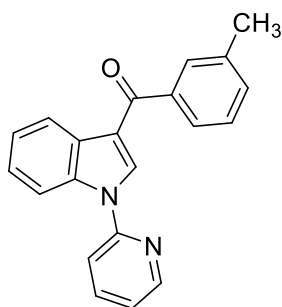


1-(2-(o-tolyl)-1H-indol-3-yl)pyridin-2-ylmethanone (22b): The representative procedure **B** was followed using (1H-indol-3-yl)(2-tolyl)methanone (**22a**; 1.0 g, 4.25 mmol), 2-bromopyridine (1.00 g, 6.33 mmol) and KOH (0.59 g, 10.51 mmol). Purification by column chromatography on silica gel (petroleum ether/EtOAc: 5/1) yielded **22b** (1.10 g, 83%) as a light-yellow solid. ¹H-NMR (400 MHz, CDCl₃): δ = 8.56-8.52 (m, 2H, Ar-H), 8.04-8.02 (m, 1H, Ar-H), 7.94 (s, 1H, Ar-H), 7.86-7.82 (m, 1H, Ar-H), 7.52-7.48 (m, 2H, Ar-H), 7.41-7.35 (m, 3H, Ar-H), 7.30-7.25 (m, 3H, Ar-H), 2.44 (s, 3H, CH₃). ¹³C{¹H}-NMR (100 MHz,

CDCl_3): $\delta = 193.6$ (CO), 151.1 (C_q), 149.5 (CH), 140.6 (C_q), 138.9 (CH), 136.2 (C_q), 136.1 (C_q), 136.0 (CH), 131.0 (CH), 129.7 (CH), 127.9 (C_q), 127.8 (CH), 125.3 (CH), 124.8 (CH), 123.8 (CH), 123.0 (CH), 122.1 (CH), 119.7 (C_q), 116.1 (CH), 112.6 (CH), 19.8 (CH_3). HRMS (ESI): m/z Calcd for $\text{C}_{21}\text{H}_{16}\text{N}_2\text{O} + \text{H}^+$ $[\text{M} + \text{H}]^+$ 313.1335; Found 313.1331.

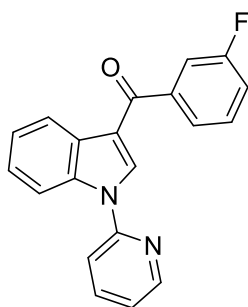


(2,6-Dimethylphenyl)(1-(pyridin-2-yl)-1H-indol-3-yl)methanone (23b): The representative procedure **B** was followed using (2,6-dimethylphenyl)(1H-indol-3-yl)methanone (**23a**; 0.40 g, 1.60 mmol), 2-bromopyridine (0.38 g, 2.41 mmol) and KOH (0.22 g, 3.92 mmol). Purification by column chromatography on silica gel (petroleum ether/EtOAc: 5/1) yielded **23b** (0.35 g, 67%) as a white solid. $^1\text{H-NMR}$ (400 MHz, CDCl_3): $\delta = 8.56$ (d, $J = 5.0$ Hz, 1H, Ar-H), 8.05-8.03 (m, 1H, Ar-H), 7.88-7.84 (m, 2H, Ar-H), 7.51 (d, $J = 8.2$ Hz, 1H, Ar-H), 7.40 (s, 2H, Ar-H) 7.29-7.21 (m, 3H, Ar-H), 7.08 (d, $J = 7.7$ Hz, 2H, Ar-H), 2.26 (s, 6H, CH_3). $^{13}\text{C}\{^1\text{H}\}$ -NMR (100 MHz, CDCl_3): $\delta = 195.4$ (CO), 151.2 (C_q), 149.6 (CH), 141.4 (C_q), 139.0 (2C, CH), 136.3 (C_q), 134.3 (2C, C_q), 128.6 (CH), 127.7 (2C, CH), 127.4 (C_q), 124.8 (CH), 124.0 (CH), 122.2 (CH), 120.1 (C_q), 116.2 (2C, CH), 112.8 (CH), 19.6 (2C, CH_3). HRMS (ESI): m/z Calcd for $\text{C}_{22}\text{H}_{18}\text{N}_2\text{O} + \text{H}^+$ $[\text{M} + \text{H}]^+$ 327.1492; Found 327.1487.

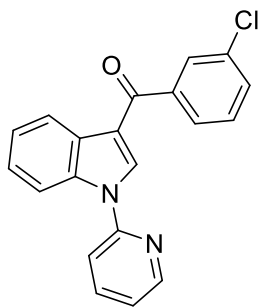


(1-(Pyridin-2-yl)-1H-indol-3-yl)(m-tolyl)methanone (24b): The representative procedure **B** was followed using (1H-indol-3-yl)(m-tolyl)methanone (**24a**; 0.26 g, 1.11 mmol), 2-bromopyridine (0.27 g, 1.71 mmol) and KOH (0.16 g, 2.85 mmol). Purification by column chromatography on silica gel (petroleum ether/EtOAc: 5/1) yielded **24b** (0.22 g, 63%) as a light-brown solid. $^1\text{H-NMR}$ (400 MHz, CDCl_3): $\delta = 8.61$ -8.60 (m, 1H, Ar-H), 8.51-8.49 (m,

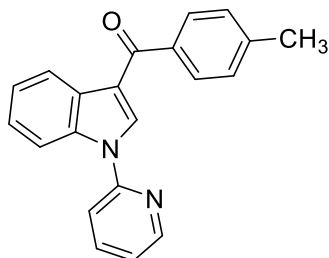
1H, Ar-H), 8.17 (s, 1H, Ar-H), 8.07-8.03 (m, 1H, Ar-H), 7.91-7.86 (m, 1H, Ar-H), 7.71-7.68 (m, 2H, Ar-H), 7.57 (d, $J = 8.3$ Hz, 1H, Ar-H), 7.41-7.38 (m, 4H, Ar-H), 7.31-7.28 (m, 1H, Ar-H), 2.45 (s, 3H, CH₃). ¹³C{¹H}-NMR (100 MHz, CDCl₃): $\delta = 191.8$ (CO), 151.4 (C_q), 149.6 (CH), 140.6 (C_q), 139.0 (CH), 138.4 (C_q), 135.9 (C_q), 135.1 (CH), 132.4 (CH), 129.5 (CH), 128.5 (C_q), 128.3 (CH), 126.2 (CH), 124.8 (CH), 123.8 (CH), 123.0 (CH), 122.0 (CH), 118.4 (C_q), 116.1 (CH), 112.5 (CH), 21.6 (CH₃). HRMS (ESI): m/z Calcd for C₂₁H₁₆N₂O + H⁺ [M + H]⁺ 313.1335; Found 313.1334.



(3-Fluorophenyl)(1-(pyridin-2-yl)-1H-indol-3-yl)methanone (25b): The representative procedure **B** was followed using (3-fluorophenyl)(1H-indol-3-yl)methanone (**25a**; 1.0 g, 4.18 mmol), 2-bromopyridine (0.99 g, 6.27 mmol) and KOH (0.58 g, 10.34 mmol). Purification by column chromatography on silica gel (petroleum ether/EtOAc: 5/1) yielded **25b** (0.90 g, 68%) as a brown solid. ¹H-NMR (400 MHz, CDCl₃): $\delta = 8.62$ -8.60 (m, 1H, Ar-H), 8.52-8.47 (m, 1H, Ar-H), 8.18 (s, 1H, Ar-H), 8.04-8.01 (m, 1H, Ar-H), 7.93-7.89 (m, 1H, Ar-H), 7.70-7.67 (m, 1H, Ar-H), 7.61-7.57 (m, 2H, Ar-H), 7.51-7.46 (m, 1H, Ar-H), 7.44-7.40 (m, 2H, Ar-H), 7.34-7.24 (m, 2H, Ar-H). ¹³C{¹H}-NMR (100 MHz, CDCl₃): $\delta = 189.9$ (d, ⁴ $J_{C-F} = 2.1$ Hz, CO), 162.8 (d, ¹ $J_{C-F} = 247.7$ Hz, C_q), 151.2 (C_q), 149.7 (CH), 142.6 (d, ³ $J_{C-F} = 6.5$ Hz, C_q), 139.0 (CH), 136.0 (C_q), 135.3 (CH), 130.2 (d, ³ $J_{C-F} = 7.2$ Hz, CH), 128.4 (C_q), 125.0 (CH), 124.7 (d, ⁴ $J_{C-F} = 2.9$ Hz, CH), 124.0 (CH), 123.0 (CH), 122.2 (CH), 118.6 (d, ² $J_{C-F} = 21.8$ Hz, CH), 118.0 (C_q), 116.2 (CH), 115.8 (d, ² $J_{C-F} = 22.5$ Hz, CH), 112.5 (CH). ¹⁹F-NMR (376 MHz, CDCl₃): $\delta = -112.0$ (s). HRMS (ESI): m/z Calcd for C₂₀H₁₃N₂FO + H⁺ [M + H]⁺ 317.1085; Found 317.1081.

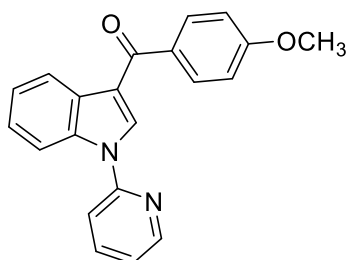


(3-Chlorophenyl)(1-(pyridin-2-yl)-1H-indol-3-yl)methanone (26b): The representative procedure **B** was followed using (3-chlorophenyl)(1H-indol-3-yl)methanone (**26a**; 0.60 g, 2.35 mmol), 2-bromopyridine (0.55 g, 3.48 mmol) and KOH (0.33 g, 5.88 mmol). Purification by column chromatography on silica gel (petroleum ether/EtOAc: 5/1) yielded **26b** (0.51 g, 65%) as a light brown solid. ¹H-NMR (400 MHz, CDCl₃): δ = 8.63-8.61 (m, 1H, Ar-H), 8.51-8.49 (m, 1H, Ar-H), 8.19 (s, 1H, Ar-H), 8.04-8.02 (m, 1H, Ar-H), 7.94-7.90 (m, 1H, Ar-H), 7.69 (d, *J* = 7.6 Hz, 1H, Ar-H), 7.62-7.57 (m, 2H, Ar-H), 7.52-7.46 (m, 1H, Ar-H), 7.44-7.40 (m, 2H, Ar-H), 7.34-7.30 (m, 2H, Ar-H). ¹³C{¹H}-NMR (100 MHz, CDCl₃): δ = 189.9 (CO), 160.2 (C_q), 149.7 (CH), 142.7 (C_q), 138.0 (CH), 136.0 (C_q), 135.3 (CH), 130.2 (CH), 125.0 (2C, CH), 124.7 (2C, C_q), 124.0 (2C, CH), 123.1 (2C, CH), 122.2 (CH), 116.2 (CH), 116.0 (C_q), 112.5 (CH). HRMS (ESI): *m/z* Calcd for C₂₀H₁₃ClN₂O + H⁺ [M + H]⁺ 333.0789; Found 333.0786.

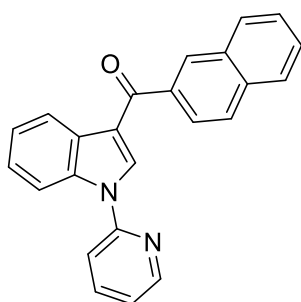


(1-(Pyridin-2-yl)-1H-indol-3-yl)(p-tolyl)methanone (27b): The representative procedure **B** was followed using (1H-indol-3-yl)(p-tolyl)methanone (**27a**; 0.70 g, 2.98 mmol), 2-bromopyridine (0.70 g, 4.43 mmol) and KOH (0.41 g, 7.31 mmol). Purification by column chromatography on silica gel (petroleum ether/EtOAc: 5/1) yielded **27b** (0.65 g, 70%) as a light-brown solid. ¹H-NMR (400 MHz, CDCl₃): δ = 8.56-8.55 (m, 1H, Ar-H), 8.47-8.42 (m, 1H, Ar-H), 8.14 (s, 1H, Ar-H), 8.03-7.99 (m, 1H, Ar-H), 7.86-7.81 (m, 1H, Ar-H), 7.78 (d, *J* = 7.9 Hz, 2H, Ar-H), 7.53 (d, *J* = 8.1 Hz, 1H, Ar-H), 7.38-7.33 (m, 2H, Ar-H), 7.28-7.22 (m, 3H, Ar-H), 2.41 (s, 3H, CH₃). ¹³C{¹H}-NMR (100 MHz, CDCl₃): δ = 191.3 (CO), 151.4 (C_q), 149.6 (CH), 142.2 (C_q), 138.9 (CH), 137.8 (C_q), 135.9 (C_q), 134.9 (CH), 129.2 (4C, CH), 128.6

(C_q), 124.8 (CH), 123.7 (CH), 123.0 (CH), 121.9 (CH), 118.5 (C_q), 116.0 (CH), 112.5 (CH), 21.7 (CH₃). HRMS (ESI): m/z Calcd for C₂₁H₁₆N₂O + H⁺ [M + H]⁺ 313.1335; Found 313.1335.

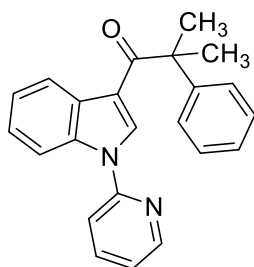


(4-Methoxyphenyl)(1-(pyridin-2-yl)-1H-indol-3-yl)methanone (28b): The representative procedure **B** was followed using (1H-indol-3-yl)(4-methoxyphenyl)methanone (**28a**; 0.20 g, 0.796 mmol), 2-bromopyridine (0.19 g, 1.20 mmol) and KOH (0.11 g, 1.96 mmol). Purification by column chromatography on silica gel (petroleum ether/EtOAc: 5/1) yielded **28b** (0.15 g, 57%) as a light-yellow solid. ¹H-NMR (400 MHz, CDCl₃): δ = 8.58-8.57 (m, 1H, Ar-H), 8.46-8.42 (m, 1H, Ar-H), 8.18 (s, 1H, Ar-H), 8.06-8.02 (m, 1H, Ar-H), 7.92 (d, J = 8.3 Hz, 2H, Ar-H), 7.88-7.83 (m, 1H, Ar-H), 7.55 (d, J = 8.3 Hz, 1H, Ar-H), 7.40-7.36 (m, 2H, Ar-H), 7.28-7.25 (m, 1H, Ar-H), 6.99 (d, J = 8.3 Hz, 2H, Ar-H), 3.87 (s, 3H, OCH₃). ¹³C{¹H}-NMR (100 MHz, CDCl₃): δ = 190.3 (CO), 162.6 (C_q), 151.3 (C_q), 149.5 (CH), 138.9 (CH), 135.8 (C_q), 134.3 (CH), 133.0 (C_q), 131.2 (2C, CH), 128.7 (C_q), 124.6 (CH), 123.5 (CH), 122.9 (CH), 121.9 (CH), 118.4 (C_q), 115.9 (CH), 113.8 (2C, CH), 112.5 (CH), 55.5 (OCH₃). HRMS (ESI): m/z Calcd for C₂₁H₁₆N₂O₂ + H⁺ [M + H]⁺ 329.1290; Found 329.1288.

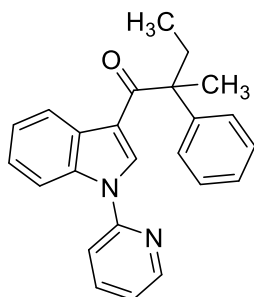


Naphthalen-2-yl(1-(pyridin-2-yl)-1H-indol-3-yl)methanone (29b): The representative procedure **B** was followed using (1H-indol-3-yl)(naphthalen-2-yl)methanone (**29a**; 0.88 g, 3.24 mmol), 2-bromopyridine (0.77 g, 4.87 mmol) and KOH (0.45 g, 8.02 mmol). Purification by column chromatography on silica gel (petroleum ether/EtOAc: 5/1) yielded **29b** (0.70 g, 62%) as a brown solid. ¹H-NMR (500 MHz, CDCl₃): δ = 8.60 (m, 1H, Ar-H), 8.53-8.51 (m, 1H, Ar-H), 8.41 (s, 1H, Ar-H), 8.24 (s, 1H, Ar-H), 8.10-8.07 (m, 1H, Ar-H), 8.02-7.97 (m, 3H, Ar-H), 7.94-7.87 (m, 2H, Ar-H), 7.62-7.55 (m, 3H, Ar-H), 7.45-67.41 (m, 2H, Ar-H), 7.32-7.28

(m, 1H, Ar-H). $^{13}\text{C}\{^1\text{H}\}$ -NMR (125 MHz, CDCl_3): δ = 191.6 (CO), 151.4 (C_q), 149.6 (CH), 139.0 (CH), 137.9 (C_q), 136.0 (C_q), 135.2 (CH), 135.0 (C_q), 132.7 (C_q), 129.8 (CH), 129.4 (CH), 128.6 (C_q), 128.5 (CH), 128.0 (CH), 127.9 (CH), 126.8 (CH), 125.7 (CH), 124.9 (CH), 123.9 (CH), 123.1 (CH), 122.1 (CH), 118.6 (C_q), 116.1 (CH), 112.6 (CH). HRMS (ESI): m/z Calcd for $\text{C}_{24}\text{H}_{16}\text{N}_2\text{O} + \text{H}^+$ $[\text{M} + \text{H}]^+$ 349.1335; Found 349.1337.

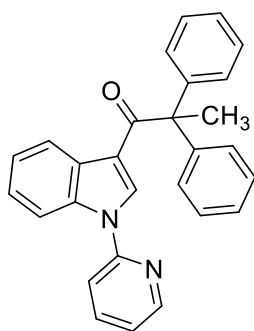


2-Methyl-2-phenyl-1-(1-(pyridin-2-yl)-1H-indol-3-yl)propan-1-one (30b): The representative procedure **B** was followed using 1-(1H-indol-3-yl)-2-methyl-2-phenylpropan-1-one (**30a**; 0.25 g, 0.95 mmol), 2-bromopyridine (0.22 g, 1.39 mmol) and KOH (0.13 g, 2.32 mmol). Purification by column chromatography on silica gel (petroleum ether/EtOAc: 5/1) yielded **30b** (0.20 g, 62%) as a colourless sticky liquid. ^1H -NMR (500 MHz, CDCl_3): δ = 8.61 (d, J = 8.0 Hz, 1H, Ar-H), 8.51 (s, 1H, Ar-H), 8.06 (d, J = 8.0 Hz, 1H, Ar-H), 7.75-7.72 (m, 1H, Ar-H), 7.46 (d, J = 7.6 Hz, 2H, Ar-H), 7.40-7.28 (m, 6H, Ar-H), 7.18 (t, J = 5.7 Hz, 1H, Ar-H), 7.01 (d, J = 8.0 Hz, 1H, Ar-H), 1.74 (s, 6H, CH_3). $^{13}\text{C}\{^1\text{H}\}$ -NMR (125 MHz, CDCl_3): δ = 200.2 (CO), 151.4 (C_q), 149.1 (CH), 146.9 (C_q), 138.7 (CH), 134.9 (C_q), 133.4 (CH), 129.2 (C_q), 128.8 (2C, CH), 126.8 (CH), 126.5 (2C, CH), 124.3 (CH), 123.5 (CH), 123.1 (CH), 121.5 (CH), 115.7 (C_q), 115.4 (CH), 112.7 (CH), 52.2 (C_q), 28.2 (2C, CH_3). HRMS (ESI): m/z Calcd for $\text{C}_{23}\text{H}_{20}\text{N}_2\text{O} + \text{H}^+$ $[\text{M} + \text{H}]^+$ 341.1654; Found 341.1656.

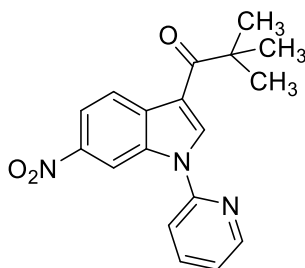


2-Methyl-2-phenyl-1-(1-(pyridin-2-yl)-1H-indol-3-yl)butan-1-one (32b): The representative procedure **B** was followed using 1-(1H-indol-3-yl)-2-methyl-2-phenylbutan-1-one (**32a**; 0.30 g, 1.08 mmol), 2-bromopyridine (0.25 g, 1.58 mmol) and KOH (0.15 g, 2.67

mmol). Purification by column chromatography on silica gel (petroleum ether/EtOAc: 5/1) yielded **32b** (0.25 g, 65%) as a colourless liquid. $^1\text{H-NMR}$ (400 MHz, CDCl_3): δ = 8.60-8.58 (m, 1H, Ar-H), 8.51-8.50 (m, 1H, Ar-H), 8.05 (d, J = 7.6 Hz, 1H, Ar-H), 7.76-7.72 (m, 1H, Ar-H), 7.44-7.28 (m, 7H, Ar-H), 7.20-7.16 (m, 2H, Ar-H), 7.01 (d, J = 8.3 Hz, 1H, Ar-H), 2.37-2.28 (m, 1H, CH_2), 2.22-2.13 (m, 1H, CH_2), 1.66 (s, 3H, CH_3), 0.84 (t, J = 7.6 Hz, 3H, CH_3). $^{13}\text{C}\{^1\text{H}\}$ -NMR (100 MHz, CDCl_3): δ = 200.2 (CO), 151.5 (C_q), 149.2 (CH), 146.1 (C_q), 138.7 (CH), 134.9 (C_q), 133.0 (CH), 129.2 (C_q), 128.7 (2C, CH), 127.1 (2C, CH), 126.8 (CH), 124.3 (CH), 123.5 (CH), 123.0 (CH), 121.5 (CH), 116.2 (C_q), 115.4 (CH), 112.7 (CH), 52.8 (C_q), 32.3 (CH_2), 24.5 (CH_3), 8.80 (CH_3). HRMS (ESI): m/z Calcd for $\text{C}_{24}\text{H}_{22}\text{N}_2\text{O} + \text{H}^+$ [$\text{M} + \text{H}$] $^+$ 355.1810; Found 355.1813.



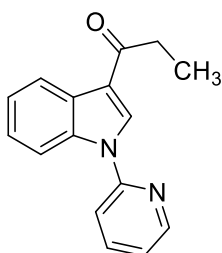
2,2-Diphenyl-1-(1-(pyridin-2-yl)-1H-indol-3-yl)propan-1-one (34b): The representative procedure **B** was followed using 1-(1H-indol-3-yl)-2,2-diphenylpropan-1-one (**34a**; 0.50 g, 1.54 mmol), 2-bromopyridine (0.36 g, 2.28 mmol) and KOH (0.21 g, 3.74 mmol). Purification by column chromatography on silica gel (petroleum ether/EtOAc: 5/1) yielded **34b** (0.40 g, 65%) as a brown solid. $^1\text{H-NMR}$ (500 MHz, CDCl_3): δ = 8.64-8.62 (m, 1H, Ar-H), 8.53-8.52 (m, 1H, Ar-H), 8.11-8.09 (m, 1H, Ar-H), 7.77-7.73 (m, 1H, Ar-H), 7.42-7.28 (m, 12H, Ar-H), 7.22-7.19 (m, 1H, Ar-H), 7.13 (s, 1H, Ar-H), 6.98 (d, J = 8.3 Hz, 1H, Ar-H), 2.20 (s, 3H, CH_3). $^{13}\text{C}\{^1\text{H}\}$ -NMR (125 MHz, CDCl_3): δ = 198.5 (CO), 151.6 (C_q), 149.2 (CH), 145.1 (2C, C_q), 138.7 (CH), 134.9 (C_q), 133.9 (CH), 129.3 (C_q), 129.0 (4C, CH), 128.4 (4C, CH), 126.9 (2C, CH), 124.5 (CH), 123.8 (CH), 123.3 (CH), 121.6 (CH), 117.3 (C_q), 115.5 (CH), 112.9 (CH), 61.4 (C_q), 29.4 (CH_3).



2,2-Dimethyl-1-(6-nitro-1-(pyridin-2-yl)-1H-indol-3-yl)propan-1-one:

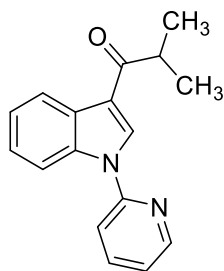
The

representative procedure **B** was followed using 2,2-dimethyl-1-(6-nitro-1H-indol-3-yl)propan-1-one (0.22 g, 0.89 mmol), 2-bromopyridine (0.21 g, 1.33 mmol) and KOH (0.12 g, 2.22 mmol). Purification by column chromatography on silica gel (petroleum ether/EtOAc: 3/1) yielded 2,2-dimethyl-1-(6-nitro-1-(pyridin-2-yl)-1H-indol-3-yl)propan-1-one (0.15 g, 52%) as a yellow solid. $^1\text{H-NMR}$ (400 MHz, CDCl_3): δ = 8.93-8.92 (m, 1H, Ar-H), 8.69-8.67 (m, 1H, Ar-H), 8.65 (s, 1H, Ar-H), 8.62 (s, 1H, Ar-H), 8.19 (dd, J = 8.8, 2.1 Hz, 1H, Ar-H), 8.00 (td, J = 7.9, 1.8 Hz, 1H, Ar-H), 7.61 (d, J = 8.2 Hz, 1H, Ar-H), 7.42-7.39 (m, 1H, Ar-H), 1.47 (s, 9H, CH_3). $^{13}\text{C}\{^1\text{H}\}$ -NMR (100 MHz, CDCl_3): δ = 202.2 (CO), 150.5 (C_q), 150.0 (CH), 145.0 (C_q), 139.5 (CH), 135.3 (CH), 134.4 (C_q), 133.8 (C_q), 123.9 (CH), 122.9 (CH), 118.6 (CH), 116.1 (CH), 115.6 (C_q), 109.1 (CH), 44.7 (C_q), 28.7 (3C, CH_3).

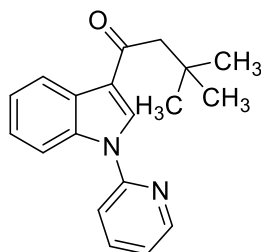


1-(1-(Pyridin-2-yl)-1H-indol-3-yl)propan-1-one:

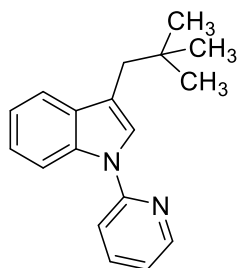
The representative procedure **B** was followed using 1-(1H-indol-3-yl)propan-1-one (0.30 g, 1.73 mmol), 2-bromopyridine (0.40 g, 2.59 mmol) and KOH (0.24 g, 4.32 mmol). Purification by column chromatography on silica gel (petroleum ether/EtOAc: 5/1) yielded 1-(1-(pyridin-2-yl)-1H-indol-3-yl)propan-1-one (0.31 g, 72%) as a light yellow solid. $^1\text{H-NMR}$ (400 MHz, CDCl_3): δ = 8.54- 8.53 (m, 1H, Ar-H), 8.48-8.45 (m, 1H, Ar-H), 8.33 (s, 1H, Ar-H), 7.94-7.92 (m, 1H, Ar-H), 7.82-7.78 (m, 1H, Ar-H), 7.52-7.49 (m, 1H, Ar-H), 7.32-7.27 (m, 2H, Ar-H), 7.24-7.20 (m, 1H, Ar-H), 2.93 (q, J = 7.6 Hz, 2H, CH_2), 1.24 (t, J = 7.6 Hz, 3H, CH_3). $^{13}\text{C}\{^1\text{H}\}$ -NMR (100 MHz, CDCl_3): δ = 197.1 (CO), 151.0 (C_q), 149.3 (CH), 138.8 (CH), 135.6 (C_q), 132.5 (CH), 127.6 (C_q), 124.3 (CH), 123.4 (CH), 122.8 (CH), 121.8 (CH), 118.7 (C_q), 115.8 (CH), 112.3 (CH), 32.9 (CH_2), 8.8 (CH_3).



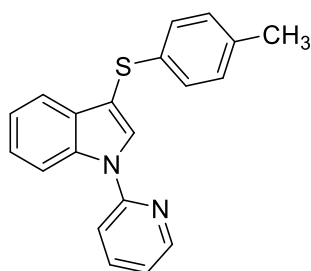
2-Methyl-1-(1-(pyridin-2-yl)-1H-indol-3-yl)propan-1-one: The representative procedure **B** was followed using 1-(1H-indol-3-yl)-2-methylpropan-1-one (0.25 g, 1.33 mmol), 2-bromopyridine (0.31 g, 1.99 mmol) and KOH (0.19 g, 3.32 mmol). Purification by column chromatography on silica gel (petroleum ether/EtOAc: 5/1) yielded 2-methyl-1-(1-(pyridin-2-yl)-1H-indol-3-yl)propan-1-one (0.23 g, 65%) as a white solid. $^1\text{H-NMR}$ (400 MHz, CDCl_3): δ = 8.62-8.61 (m, 1H, Ar-H), 8.54-8.51 (m, 1H, Ar-H), 8.43 (s, 1H, Ar-H), 7.98-7.96 (m, 1H, Ar-H), 7.91-7.86 (m, 1H, Ar-H), 7.61 (d, J = 7.6 Hz, 1H, Ar-H), 7.38-7.33 (m, 2H, Ar-H), 7.31-7.28 (m, 1H, Ar-H), 3.45 (sept, J = 6.8 Hz, 1H, CH), 1.29 (d, J = 6.8 Hz, 6H, CH_3). $^{13}\text{C}\{^1\text{H}\}$ -NMR (100 MHz, CDCl_3): δ = 201.0 (CO), 151.2 (C_q), 149.6 (CH), 138.9 (CH), 135.9 (C_q), 132.6 (CH), 128.1 (C_q), 124.5 (CH), 123.6 (CH), 123.2 (CH), 121.9 (CH), 117.9 (C_q), 116.0 (CH), 112.2 (CH), 37.4 (CH), 19.9 (2C, CH_3).



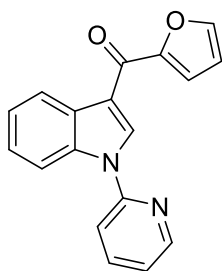
3,3-Dimethyl-1-(1-(pyridin-2-yl)-1H-indol-3-yl)butan-1-one: The representative procedure **B** was followed using 1-(1H-indol-3-yl)-3,3-dimethylbutan-1-one (0.40 g, 1.86 mmol), 2-bromopyridine (0.44 g, 2.79 mmol) and KOH (0.26 g, 4.65 mmol). Purification by column chromatography on silica gel (petroleum ether/EtOAc: 5/1) yielded 3,3-dimethyl-1-(1-(pyridin-2-yl)-1H-indol-3-yl)butan-1-one (0.38 g, 70%) as a white solid. $^1\text{H-NMR}$ (400 MHz, CDCl_3): δ = 8.63-8.62 (m, 1H, Ar-H), 8.57-8.54 (m, 1H, Ar-H), 8.35 (s, 1H, Ar-H), 7.98-7.94 (m, 1H, Ar-H), 7.92-7.88 (m, 1H, Ar-H), 7.61 (d, J = 8.1 Hz, 1H, Ar-H), 7.38-7.33 (m, 2H, Ar-H), 7.32-7.29 (m, 1H, Ar-H), 2.80 (s, 2H, CH_2), 1.13 (s, 9H, CH_3). $^{13}\text{C}\{^1\text{H}\}$ -NMR (100 MHz, CDCl_3): δ = 196.5 (CO), 151.3 (C_q), 149.6 (CH), 139.0 (CH), 135.8 (C_q), 133.2 (CH), 127.9 (C_q), 124.5 (CH), 123.6 (CH), 123.4 (CH), 121.9 (CH), 120.9 (C_q), 116.1 (CH), 112.2 (CH), 52.4 (CH_2), 31.7 (C_q), 30.5 (3C, CH_3).



3-Neopentyl-1-(pyridin-2-yl)-1H-indole: The representative procedure **B** was followed using 3-neopentyl-1H-indole (0.24 g, 1.28 mmol), 2-bromopyridine (0.30 g, 1.92 mmol) and KOH (0.18 g, 3.20 mmol). Purification by column chromatography on silica gel (petroleum ether/EtOAc: 10/1) yielded 3-neopentyl-1-(pyridin-2-yl)-1H-indole (0.19 g, 56%) as a light brown solid. $^1\text{H-NMR}$ (400 MHz, CDCl_3): δ = 8.56-8.55 (m, 1H, Ar-H), 8.20 (d, J = 8.2 Hz, 1H, Ar-H), 7.83-7.78 (m, 1H, Ar-H), 7.61 (d, J = 7.7 Hz, 1H, Ar-H), 7.50-7.48 (m, 2H, Ar-H), 7.29-7.27 (m, 1H, Ar-H), 7.22-7.18 (m, 1H, Ar-H), 7.17-7.12 (m, 1H, Ar-H), 2.68 (s, 2H, CH_2), 1.01 (s, 9H, CH_3). $^{13}\text{C}\{^1\text{H}\}$ -NMR (100 MHz, CDCl_3): δ = 152.8 (C_q), 149.1 (CH), 138.4 (CH), 135.2 (C_q), 131.9 (C_q), 124.9 (CH), 123.0 (CH), 120.9 (CH), 120.1 (CH), 119.7 (CH), 117.2 (C_q), 114.5 (CH), 113.0 (CH), 39.0 (CH_2), 32.3 (C_q), 29.9 (3C, CH_3).



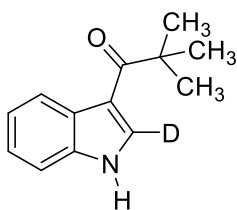
1-(Pyridin-2-yl)-3-(p-tolylthio)-1H-indole: The representative procedure **B** was followed using 3-(p-tolylthio)-1H-indole (0.15 g, 0.62 mmol), 2-bromopyridine (0.15 g, 0.93 mmol) and KOH (0.09 g, 1.55 mmol). Purification by column chromatography on silica gel (petroleum ether/EtOAc: 3/1) yielded 1-(pyridin-2-yl)-3-(p-tolylthio)-1H-indole (0.13 g, 66%) as a white solid. $^1\text{H-NMR}$ (400 MHz, CDCl_3): δ = 8.61-8.59 (m, 1H, Ar-H), 8.23 (d, J = 8.3 Hz, 1H, Ar-H), 7.99 (s, 1H, Ar-H), 7.88-7.84 (m, 1H, Ar-H), 7.62 (d, J = 7.8 Hz, 1H, Ar-H), 7.53 (d, J = 8.2 Hz, 1H, Ar-H), 7.37-7.32 (m, 1H, Ar-H), 7.24-7.20 (m, 2H, Ar-H), 7.12 (d, J = 8.1 Hz, 2H, Ar-H), 7.00 (d, J = 8.0 Hz, 2H, Ar-H), 2.26 (s, 3H, CH_3). $^{13}\text{C}\{^1\text{H}\}$ -NMR (100 MHz, CDCl_3): δ = 152.0 (C_q), 149.3 (CH), 138.8 (CH), 136.0 (C_q), 135.2 (C_q), 134.6 (C_q), 131.7 (CH), 131.2 (C_q), 129.7 (2C, CH), 127.1 (2C, CH), 124.2 (CH), 122.2 (CH), 120.9 (CH), 120.2 (CH), 114.9 (CH), 113.5 (CH), 107.4 (C_q), 21.1 (CH_3).



Furan-2-yl(1-(pyridin-2-yl)-1H-indol-3-yl)methanone: The representative procedure **B** was followed using furan-2-yl(1H-indol-3-yl)methanone (0.20 g, 0.94 mmol), 2-bromopyridine (0.22 g, 1.41 mmol) and KOH (0.13 g, 2.35 mmol). Purification by column chromatography on silica gel (petroleum ether/EtOAc: 5/1) yielded furan-2-yl(1-(pyridin-2-yl)-1H-indol-3-yl)methanone (0.16 g, 59%) as a brown solid. $^1\text{H-NMR}$ (500 MHz, CDCl_3): δ = 8.75 (s, 1H, Ar-H), 8.59-8.57 (m, 1H, Ar-H), 8.52-8.50 (m, 1H, Ar-H), 7.97-7.95 (m, 1H, Ar-H), 7.76-7.72 (m, 1H, Ar-H), 7.57 (s, 1H, Ar-H), 7.47 (d, J = 7.6 Hz, 1H, Ar-H), 7.35-7.28 (m, 3H, Ar-H), 7.19-7.15 (m, 1H, Ar-H), 6.51-6.50 (m, 1H, Ar-H). $^{13}\text{C}\{^1\text{H}\}$ -NMR (125 MHz, CDCl_3): δ = 176.5 (CO), 154.0 (C_q), 150.9 (C_q), 149.2 (CH), 145.3 (CH), 138.7 (CH), 135.2 (C_q), 134.2 (CH), 128.5 (C_q), 124.5 (CH), 123.5 (CH), 122.8 (CH), 121.8 (CH), 116.9 (CH), 116.5 (C_q), 115.9 (CH), 112.4 (CH), 112.1 (CH).

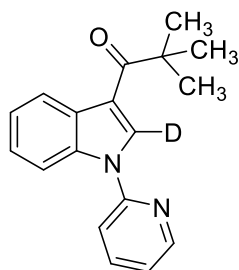
2.4.3 Synthesis of Deuterated Compounds

Synthesis of 1-(1H-indol-3-yl-2-d)-2,2-dimethylpropan-1-one (2a-[2-D])



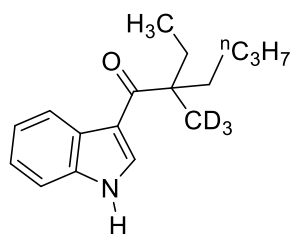
Procedure: To a solution of 1H-indole-2-d (1.17 g, 9.90 mmol) in HFIP (5 mL), pivaloyl chloride (0.40 g, 3.32 mmol) was added and the reaction mixture was stirred at room temperature for 5 h. The volatiles were evaporated *in vacuo* and purified by column chromatography on silica gel (petroleum ether/EtOAc: 3/1) to yield 1-(1H-indol-3-yl-2-d)-2,2-dimethylpropan-1-one (**2a**-[2-D]; 0.51 g, 76%) as a white solid. $^1\text{H-NMR}$ (400 MHz, CDCl_3): δ = 9.02 (s, 1H, NH), 8.49-8.46 (m, 1H, Ar-H), 7.36-7.33 (m, 1H, Ar-H), 7.25-7.21 (m, 2H, Ar-H), 1.38 (s, 9H, CH_3). $^{13}\text{C}\{^1\text{H}\}$ -NMR (100 MHz, CDCl_3): δ = 203.3 (CO), 135.5 (C_q), 127.5 (C_q), 123.7 (CH), 123.1 (CH), 122.7 (CH), 114.1 (C_q), 111.4 (CH), 44.3 (C_q), 29.1 (3C, CH_3). HRMS (ESI): m/z Calcd for $\text{C}_{13}\text{H}_{14}\text{DNO} + \text{H}^+$ [$\text{M} + \text{H}$] $^+$ 203.1289; Found 203.1286.

Synthesis of 2,2-dimethyl-1-(1-(pyridin-2-yl)-1H-indol-3-yl-2-d)propan-1-one-2-D (2b-[2-D])



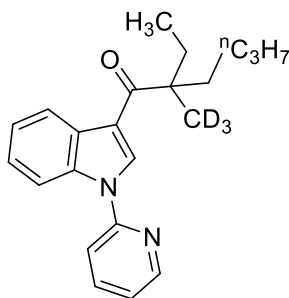
A mixture of 1-(1H-indol-3-yl-2-d)-2,2-dimethylpropan-1-one (**2a**-[2-D]; 0.50 g, 2.47 mmol), 2-bromopyridine (0.58 g, 3.67 mmol), CuI (0.047 g, 0.247 mmol, 10.0 mol %), *N,N'*-dimethyl-ethylenediamine (0.043 g, 0.49 mmol, 20.0 mol %) and K₃PO₄ (1.41 g, 6.64 mmol) in toluene (15 mL) was stirred vigorously at 120 °C under an argon atmosphere for 30 h. At ambient temperature, the reaction mixture was quenched with distilled H₂O (10.0 mL) and the crude product was extracted with EtOAc (15 mL x 3). The combined organic extract was dried over Na₂SO₄ and the volatiles were evaporated *in vacuo*. The remaining residue was purified by column chromatography on silica gel (petroleum ether/EtOAc: 5/1) to yield 2,2-dimethyl-1-(1-(pyridin-2-yl)-1H-indol-3-yl-2-d)propan-1-one (**2b**-[2-D]; 0.45 g, 65%; > 99% D incorporation) as a light yellow solid. ¹H-NMR (500 MHz, CDCl₃): δ = 8.64-8.62 (m, 1H, Ar-H), 8.59-8.56 (m, 1H, Ar-H), 7.95-7.89 (m, 2H, Ar-H), 7.62 (d, *J* = 8.3 Hz, 1H, Ar-H), 7.37-7.29 (m, 3H, Ar-H), 1.48 (s, 9H, CH₃). ¹³C{¹H}-NMR (125 MHz, CDCl₃): δ = 202.9 (CO), 151.3 (C_q), 149.7 (CH), 138.9 (CH), 134.8 (C_q), 129.7 (C_q), 124.4 (CH), 123.7 (CH), 123.6 (CH), 121.9 (CH), 116.2 (CH), 115.3 (C_q), 111.8 (CH), 44.6 (C_q), 29.0 (3C, CH₃). HRMS (ESI): *m/z* Calcd for C₁₈H₁₇DN₂O + H⁺ [M + H]⁺ 280.1560; Found 280.1567.

Synthesis of 2-Ethyl-1-(1H-indol-3-yl)-2-(methyl-d₃)hexan-1-one (14a-[D₃]):



The representative procedure **A** was followed, using 1H-indole (0.78 g, 6.66 mmol) and 2-ethyl-2-(methyl-d₃)hexanoyl chloride (0.40 g, 2.23 mmol). Purification by column chromatography on silica gel (petroleum ether/EtOAc: 1/1) yielded **14a**-[D₃] (0.33 g, 57%) as a white solid. ¹H-NMR (400 MHz, CDCl₃): δ = 9.83 (s, 1H, *NH*), 8.55-8.52 (m, 1H, Ar-H),

7.92-7.91 (m, 1H, Ar-H), 7.42-7.39 (m, 1H, Ar-H), 7.28-7.22 (m, 2H, Ar-H), 2.02-1.88 (m, 2H, CH₂), 1.72-1.59 (m, 2H, CH₂), 1.31-1.07 (m, 4H, CH₂), 0.83-0.75 (m, 6H, CH₃). ¹³C{¹H}-NMR (100 MHz, CDCl₃): δ = 203.8 (CO), 135.7 (C_q), 130.4 (CH), 127.4 (C_q), 123.5 (CH), 122.8 (CH), 122.5 (CH), 115.2 (C_q), 111.7 (CH), 51.8 (C_q), 41.1 (CH₂), 34.0 (CH₂), 26.7 (CH₂), 23.5 (CH₂), 14.0 (CH₃), 9.0 (CH₃). HRMS (ESI): *m/z* Calcd for C₁₇H₂₀D₃NO + H⁺ [M + H]⁺ 261.2046; Found 261.2059.

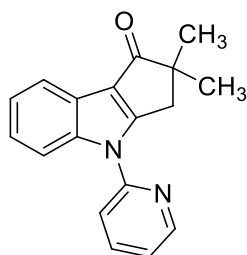


2-Ethyl-2-(methyl-d₃)-1-(1-(pyridin-2-yl)-1H-indol-3-yl)hexan-1-one ((14b-[D₃])). The representative procedure **B** was followed using 2-ethyl-1-(1H-indol-3-yl)-2-(methyl-d₃)hexan-1-one (**14a**-[D₃]; 0.3 g, 1.15 mmol), 2-bromopyridine (0.27 g, 1.71 mmol) and KOH (0.16 g, 2.85 mmol). Purification by column chromatography on silica gel (petroleum ether/EtOAc: 5/1) yielded **14b**-[D₃] (0.28 g, 72%) as a white solid. ¹H-NMR (400 MHz, CDCl₃): δ = 8.65-8.63 (m, 1H, Ar-H), 8.59-8.55 (m, 1H, Ar-H), 8.48 (s, 1H, Ar-H), 7.97-7.89 (m, 2H, Ar-H), 7.61 (d, *J* = 8.3 Hz, 1H, Ar-H), 7.36-7.34 (m, 2H, Ar-H), 7.32-7.29 (m, 1H, Ar-H), 2.13-1.98 (m, 2H, CH₂), 1.80-1.65 (m, 2H, CH₂), 1.35-1.13 (m, 4H, CH₂), 0.88-0.81 (m, 6H, CH₃). ¹³C{¹H}-NMR (100 MHz, CDCl₃): δ = 202.8 (CO), 151.4 (C_q), 149.7 (CH), 138.9 (CH), 134.8 (C_q), 130.8 (C_q), 129.7 (CH), 124.4 (CH), 123.8 (CH), 123.5 (CH), 121.8 (CH), 116.7 (C_q), 116.2 (CH), 111.8 (CH), 52.1 (C_q), 40.8 (CH₂), 33.8 (CH₂), 26.8 (CH₂), 23.6 (CH₂), 14.1 (CH₃), 9.1 (CH₃). HRMS (ESI): *m/z* Calcd for C₂₂H₂₃D₃N₂O + H⁺ [M + H]⁺ 338.2312; Found 338.2324.

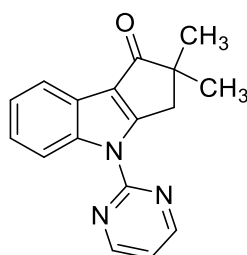
2.4.4 Procedure for Oxidative Cyclization and Characterization Data

Representative Procedure C. Synthesis of 2,2-dimethyl-4-(pyridin-2-yl)-3,4-dihydrocyclopenta[*b*]indol-1(2H)-one (2): To a flame-dried screw-cap tube equipped with magnetic stir bar were introduced 2,2-dimethyl-1-(1-(pyridin-2-yl)-1H-indol-3-yl)propan-1-one (**2b**; 0.056 g, 0.20 mmol), (bpy)Ni(OAc)₂ (**1**; 0.0034 g, 0.01 mmol, 5.0 mol %), Ag₂CO₃ (0.056 g, 0.20 mmol, 1.0 equiv) and LiO^tBu (0.048 g, 0.60 mmol, 3 equiv) inside the glove box. To the above mixture in the tube was added chlorobenzene (1.0 mL). The resultant

reaction mixture in the tube was immersed in a preheated oil bath at 150 °C and stirred for 24 h. At ambient temperature, the reaction mixture was quenched with distilled H₂O (10.0 mL) and the crude product was extracted with EtOAc (15 mL x 3). The combined organic extract was dried over Na₂SO₄ and the volatiles were evaporated *in vacuo*. The remaining residue was purified by column chromatography on silica gel (petroleum ether/EtOAc: 1/1) to yield **2** (0.049 g, 89%) as a brown solid.

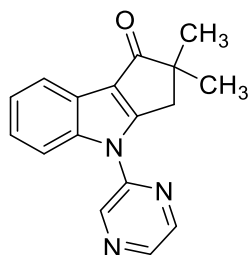


Characterization Data of 2. ¹H-NMR (500 MHz, CDCl₃): δ = 8.65-8.63 (m, 1H, Ar-H), 8.00-7.98 (m, 1H, Ar-H), 7.93 (td, *J* = 7.6, 1.5 Hz, 1H, Ar-H), 7.79-7.77 (m, 1H, Ar-H), 7.57 (d, *J* = 8.3 Hz, 1H, Ar-H), 7.36-7.30 (m, 3H, Ar-H), 3.18 (s, 2H, CH₂), 1.34 (s, 6H, CH₃). ¹³C{¹H}-NMR (125 MHz, CDCl₃): δ = 201.7 (CO), 164.4 (C_q), 150.6 (C_q), 149.8 (CH), 141.8 (C_q), 138.9 (CH), 124.3 (CH), 123.4 (CH), 122.7 (C_q), 122.3 (CH), 121.4 (CH), 120.1 (C_q), 117.5 (CH), 112.4 (CH), 51.4 (C_q), 39.7 (CH₂), 25.8 (2C, CH₃). HRMS (ESI): *m/z* Calcd for C₁₈H₁₆N₂O + H⁺ [M + H]⁺ 277.1335; Found 277.1344.

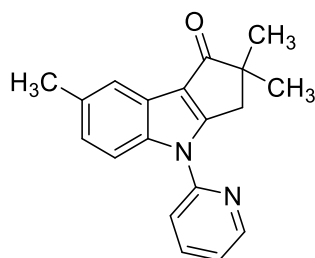


2,2-Dimethyl-4-(pyrimidin-2-yl)-3,4-dihydrocyclopenta[b]indol-1(2H)-one (3): The representative procedure **C** was followed, using 2,2-dimethyl-1-(1-(pyrimidin-2-yl)-1H-indol-3-yl)propan-1-one (**3b**; 0.056 g, 0.20 mmol). Purification by column chromatography on silica gel (petroleum ether/EtOAc: 1/1) yielded **3** (0.036 g, 65%) as a brown solid. ¹H-NMR (400 MHz, CDCl₃): δ = 8.77-8.76 (m, 3H, Ar-H), 7.97-7.95 (m, 1H, Ar-H), 7.39-7.32 (m, 2H, Ar-H), 7.19-7.17 (m, 1H, Ar-H), 3.48 (s, 2H, CH₂), 1.35 (s, 6H, CH₃). ¹³C{¹H}-NMR (100 MHz, CDCl₃): δ = 202.6 (CO), 165.3 (C_q), 158.4 (2C, CH), 158.0 (C_q), 141.7 (C_q), 124.8 (CH), 124.0

(CH), 123.3 (C_q), 122.0 (C_q), 120.8 (CH), 117.7 (CH), 117.0 (CH), 50.9 (C_q), 43.3 (CH₂), 25.7 (2C, CH₃). HRMS (ESI): m/z Calcd for C₁₇H₁₅N₃O + H⁺ [M + H]⁺ 278.1288; Found 278.1285.

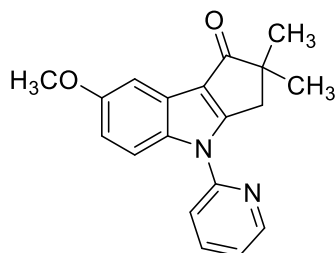


2,2-Dimethyl-4-(pyrazin-2-yl)-3,4-dihydrocyclopenta[b]indol-1(2H)-one (4): The representative procedure **C** was followed, using 2,2-dimethyl-1-(1-(pyrazin-2-yl)-1H-indol-3-yl)propan-1-one (**4b**; 0.056 g, 0.20 mmol). Purification by column chromatography on silica gel (petroleum ether/EtOAc: 1/1) yielded **4** (0.011 g, 20%) as a brown solid. ¹H-NMR (400 MHz, CDCl₃): δ = 9.00 (s, 1H, Ar-H), 8.62 (s, 2H, Ar-H), 8.02-8.00 (m, 1H, Ar-H), 7.87-7.85 (m, 1H, Ar-H), 7.37-7.35 (m, 2H, Ar-H), 3.22 (s, 2H, CH₂), 1.36 (s, 6H, CH₃). ¹³C{¹H}-NMR (100 MHz, CDCl₃): δ = 201.6 (CO), 163.9 (C_q), 147.7 (C_q), 143.6 (CH), 142.5 (CH), 141.5 (C_q), 138.9 (CH), 124.9 (CH), 124.1 (CH), 123.0 (C_q), 121.7 (CH), 121.6 (C_q), 112.5 (CH), 51.6 (C_q), 40.0 (CH₂), 25.8 (2C, CH₃). HRMS (ESI): m/z Calcd for C₁₇H₁₅N₃O + H⁺ [M + H]⁺ 278.1288; Found 278.1285.



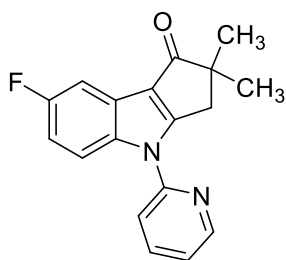
2,2,7-Trimethyl-4-(pyridin-2-yl)-3,4-dihydrocyclopenta[b]indol-1(2H)-one (7): The representative procedure **C** was followed, using 2,2-dimethyl-1-(5-methyl-1-(pyridin-2-yl)-1H-indol-3-yl)propan-1-one (**7b**; 0.059 g, 0.201 mmol). Purification by column chromatography on silica gel (petroleum ether/EtOAc: 1/1) yielded **7** (0.050 g, 86%) as a light-yellow solid. ¹H-NMR (400 MHz, CDCl₃): δ = 8.62-8.61 (m, 1H, Ar-H), 7.91 (td, J = 7.6, 1.5 Hz, 1H, Ar-H), 7.79 (s, 1H, Ar-H), 7.66 (d, J = 8.3 Hz, 1H, Ar-H), 7.55 (d, J = 7.6 Hz, 1H, Ar-H), 7.33-7.30 (m, 1H, Ar-H), 7.12 (d, J = 8.3 Hz, 1H, Ar-H), 3.17 (s, 2H, CH₂), 2.46 (s, 3H, CH₃), 1.33 (s, 6H, CH₃). ¹³C{¹H}-NMR (100 MHz, CDCl₃): δ = 201.7 (CO), 164.4 (C_q), 150.7 (C_q), 149.7 (CH), 140.0 (C_q), 138.8 (CH), 133.1 (C_q), 125.5 (CH), 122.9 (C_q), 122.1

(CH), 121.3 (CH), 119.8 (C_q), 117.2 (CH), 112.1 (CH), 51.3 (C_q), 39.8 (CH₂), 25.8 (2C, CH₃), 21.4 (CH₃). HRMS (ESI): m/z Calcd for C₁₉H₁₈N₂O + H⁺ [M + H]⁺ 291.1492; Found 291.1489.



7-Methoxy-2,2-dimethyl-4-(pyridin-2-yl)-3,4-dihydrocyclopenta[b]indol-1(2H)-one

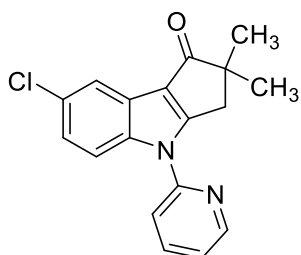
(8): The representative procedure was followed, using 1-(5-methoxy-1-(pyridin-2-yl)-1H-indol-3-yl)-2,2-dimethylpropan-1-one (**8b**; 0.062 g, 0.201 mmol). Purification by column chromatography on silica gel (petroleum ether/EtOAc: 1/1) yielded **8** (0.057 g, 93%) as a yellow solid. ¹H-NMR (400 MHz, CDCl₃): δ = 8.63-8.58 (m, 1H, Ar-H), 7.90 (t, J = 7.6 Hz, 1H, Ar-H), 7.70 (d, J = 9.1 Hz, 1H, Ar-H), 7.52 (d, J = 8.3 Hz, 1H, Ar-H), 7.46-7.42 (m, 1H, Ar-H), 7.32-7.29 (m, 1H, Ar-H), 6.90 (dd, J = 9.2, 3.1 Hz, 1H, Ar-H), 3.86 (s, 3H, OCH₃), 3.17 (s, 2H, CH₂), 1.33 (s, 6H, CH₃). ¹³C{¹H}-NMR (100 MHz, CDCl₃): δ = 201.7 (CO), 164.2 (C_q), 156.6 (C_q), 150.7 (C_q), 149.7 (CH), 138.9 (CH), 136.3 (C_q), 123.6 (C_q), 122.1 (CH), 120.0 (C_q), 117.0 (CH), 113.7 (CH), 113.5 (CH), 103.3 (CH), 55.9 (OCH₃), 51.3 (C_q), 39.9 (CH₂), 25.8 (2C, CH₃). HRMS (ESI): m/z Calcd for C₁₉H₁₈N₂O₂ + H⁺ [M + H]⁺ 307.1441; Found 307.1439.



7-Fluoro-2,2-dimethyl-4-(pyridin-2-yl)-3,4-dihydrocyclopenta[b]indol-1(2H)-one

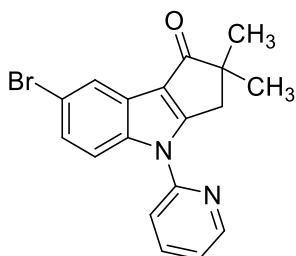
(9): The representative procedure **C** was followed, using 1-(5-fluoro-1-(pyridin-2-yl)-1H-indol-3-yl)-2,2-dimethylpropan-1-one (**9b**; 0.060 g, 0.202 mmol). Purification by column chromatography on silica gel (petroleum ether/EtOAc: 1/1) yielded **9** (0.041 g, 69%) as a brown solid. ¹H-NMR (500 MHz, CDCl₃): δ = 8.63 (m, 1H, Ar-H), 7.96-7.92 (m, 1H, Ar-H), 7.75 (dd, J = 9.1, 4.5 Hz, 1H, Ar-H), 7.63 (dd, J = 9.1, 3.0 Hz, 1H, Ar-H), 7.52 (d, J = 8.3 Hz, 1H, Ar-H), 7.37-7.34 (m, 1H, Ar-H), 7.01 (td, J = 9.1, 2.2 Hz, 1H, Ar-H), 3.17 (s, 2H, CH₂),

1.33 (s, 6H, CH₃). ¹³C{¹H}-NMR (125 MHz, CDCl₃): δ = 201.3 (CO), 165.1 (C_q), 159.7 (d, ¹J_{C-F} = 240.5 Hz, C_q), 150.4 (C_q), 149.8 (CH), 139.1 (CH), 138.1 (C_q), 123.4 (d, ³J_{C-F} = 10.5 Hz, C_q), 122.5 (CH), 119.8 (d, ⁴J_{C-F} = 3.8 Hz, C_q), 117.1 (CH), 113.7 (d, ³J_{C-F} = 9.5 Hz, CH), 112.0 (d, ²J_{C-F} = 25.8 Hz, CH), 107.1 (d, ²J_{C-F} = 23.9 Hz, CH), 51.4 (C_q), 39.8 (CH₂), 25.8 (2C, CH₃). ¹⁹F-NMR (376 MHz, CDCl₃): δ = -119.5 (s). HRMS (ESI): *m/z* Calcd for C₁₈H₁₅ON₂F + H⁺ [M + H]⁺ 295.1241; Found 295.1238.



7-Chloro-2,2-dimethyl-4-(pyridin-2-yl)-3,4-dihydrocyclopenta[b]indol-1(2H)-one

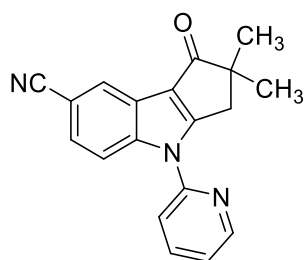
(**10**): The representative procedure **C** was followed, using 1-(5-chloro-1-(pyridin-2-yl)-1H-indol-3-yl)-2,2-dimethylpropan-1-one (**10b**; 0.063 g, 0.201 mmol). Purification by column chromatography on silica gel (petroleum ether/EtOAc: 1/1) yielded **10** (0.038 g, 61%) as a brown solid. ¹H-NMR (400 MHz, CDCl₃): δ = 8.59-8.57 (m, 1H, Ar-H), 7.91-7.87 (m, 2H, Ar-H), 7.68 (d, *J* = 8.8 Hz, 1H, Ar-H), 7.75 (d, *J* = 7.7 Hz, 1H, Ar-H), 7.32-7.29 (m, 1H, Ar-H), 7.20 (dd, *J* = 8.8, 2.1 Hz, 1H, Ar-H), 3.12 (s, 2H, CH₂), 1.28 (s, 6H, CH₃). ¹³C{¹H}-NMR (100 MHz, CDCl₃): δ = 201.2 (CO), 164.9 (C_q), 150.3 (C_q), 149.9 (CH), 140.2 (C_q), 139.1 (CH), 129.2 (C_q), 124.5 (CH), 123.7 (C_q), 122.6 (CH), 121.0 (CH), 119.6 (C_q), 117.3 (CH), 113.8 (CH), 51.5 (C_q), 39.8 (CH₂), 25.8 (2C, CH₃). HRMS (ESI): *m/z* Calcd for C₁₈H₁₅N₂ClO + H⁺ [M + H]⁺ 311.0946; Found 311.0943.



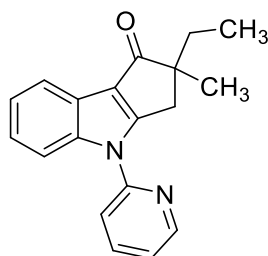
7-Bromo-2,2-dimethyl-4-(pyridin-2-yl)-3,4-dihydrocyclopenta[b]indol-1(2H)-one

(**11**): The representative procedure **C** was followed, using 1-(5-bromo-1-(pyridin-2-yl)-1H-indol-3-yl)-2,2-dimethylpropan-1-one (**11b**; 0.072 g, 0.202 mmol). Purification by column chromatography on silica gel (petroleum ether/EtOAc: 1/1) yielded **11** (0.040 g, 56%) as a

light-brown solid. $^1\text{H-NMR}$ (400 MHz, CDCl_3): δ = 8.66-8.64 (m, 1H, Ar-H), 8.00-7.92 (m, 2H, Ar-H), 7.80-7.68 (m, 1H, Ar-H), 7.59-7.52 (m, 1H, Ar-H), 7.39-7.30 (m, 1H, Ar-H), 7.28-7.25 (m, 1H, Ar-H), 3.18 (s, 2H, CH_2), 1.34 (s, 3H, CH_3). $^{13}\text{C}\{^1\text{H}\}$ -NMR (100 MHz, CDCl_3): δ = 201.2 (CO), 164.8 (C_q), 150.3 (C_q), 149.9 (CH), 140.6 (C_q), 139.1 (CH), 129.3 (C_q), 127.2 (CH), 124.1 (C_q), 122.6 (CH), 119.5 (C_q), 117.3 (CH), 114.1 (CH), 112.5 (CH), 51.5 (C_q), 39.8 (CH_2), 25.8 (2C, CH_3). HRMS (ESI): m/z Calcd for $\text{C}_{18}\text{H}_{15}\text{ON}_2\text{Br} + \text{H}^+$ [$\text{M} + \text{H}$] $^+$ 355.0441, 357.0426; Found 355.0431, 357.0416.

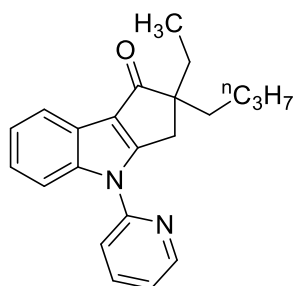


2,2-Dimethyl-1-oxo-4-(pyridin-2-yl)-1,2,3,4-tetrahydrocyclopenta[b]indole-7-carbonitrile (12): The representative procedure **C** was followed, using 3-pivaloyl-1-(pyridin-2-yl)-1*H*-indole-5-carbonitrile (**12b**; 0.061 g, 0.201 mmol). Purification by column chromatography on silica gel (petroleum ether/EtOAc: 1/2) yielded **12** (0.021 g, 35%) as a brown solid. $^1\text{H-NMR}$ (400 MHz, CDCl_3): δ = 8.67 (m, 1H, Ar-H), 8.28 (s, 1H, Ar-H), 8.02 - 7.97 (m, 1H, Ar-H), 7.90 (d, J = 8.5 Hz, 1H, Ar-H), 7.54 (d, J = 8.5 Hz, 2H, Ar-H), 7.44-7.41 (m, 1H, Ar-H), 3.19 (s, 2H, CH_2), 1.35 (s, 6H, CH_3). $^{13}\text{C}\{^1\text{H}\}$ -NMR (100 MHz, CDCl_3): δ = 201.0 (CO), 165.9 (C_q), 150.1 (CH), 149.8 (C_q), 143.6 (C_q), 139.3 (CH), 127.6 (CH), 125.9 (CH), 123.2 (CH), 122.5 (C_q), 120.1 (C_q), 119.6 (C_q), 117.6 (CH), 113.8 (CH), 106.8 (C_q), 51.8 (C_q), 39.7 (CH_2), 25.7 (2C, CH_3). HRMS (ESI): m/z Calcd for $\text{C}_{19}\text{H}_{15}\text{ON}_3 + \text{H}^+$ [$\text{M} + \text{H}$] $^+$ 302.1288; Found 302.1284.

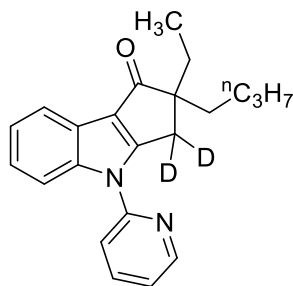


2-Ethyl-2-methyl-4-(pyridin-2-yl)-3,4-dihydrocyclopenta[b]indol-1(2H)-one (13): The representative procedure **C** was followed, using 2,2-dimethyl-1-(1-(pyridin-2-yl)-1*H*-indol-3-yl)butan-1-one (**13b**; 0.059 g, 0.202 mmol). Purification by column chromatography

on silica gel (petroleum ether/EtOAc: 1/1) yielded **13** (0.052 g, 89%) as a light brown solid. $^1\text{H-NMR}$ (500 MHz, CDCl_3): δ = 8.64 (dd, J = 4.5, 1.5 Hz, 1H, Ar-H), 8.00-8.97 (m, 1H, Ar-H), 7.95-7.91 (m, 1H, Ar-H), 7.80-7.75 (m, 1H, Ar-H), 7.57 (d, J = 8.3 Hz, 1H, Ar-H), 7.36-7.28 (m, 3H, Ar-H), 3.25 (d, J = 17.5 Hz, 1H, CH_2), 3.01 (d, J = 17.5 Hz, 1H, CH_2), 1.83-1.74 (m, 1H, CH_2), 1.69-1.60 (m, 1H, CH_2), 1.31 (s, 3H, CH_3), 0.87 (t, J = 7.6 Hz, 3H, CH_3). $^{13}\text{C}\{^1\text{H}\}$ -NMR (125 MHz, CDCl_3): δ = 201.6 (CO), 165.0 (C_q), 150.5 (C_q), 149.8 (CH), 141.7 (C_q), 138.9 (CH), 124.3 (CH), 123.3 (CH), 122.5 (2C, C_q), 122.3 (CH), 121.3 (CH), 117.4 (CH), 112.4 (CH), 55.4 (C_q), 36.3 (CH_2), 31.1 (CH_2), 24.3 (CH_3), 9.2 (CH_3). HRMS (ESI): m/z Calcd for $\text{C}_{19}\text{H}_{18}\text{N}_2\text{O} + \text{H}^+$ $[\text{M}+\text{H}]^+$ 291.1492; Found 291.1489.

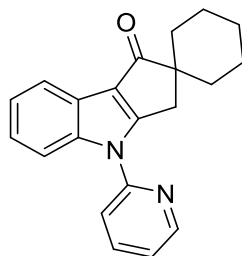


2-Butyl-2-ethyl-4-(pyridin-2-yl)-3,4-dihydrocyclopenta[b]indol-1(2H)-one (14): The representative procedure **C** was followed, using 2-ethyl-2-methyl-1-(1-(pyridin-2-yl)-1H-indol-3-yl)hexan-1-one (**14b**; 0.067 g, 0.20 mmol). Purification by column chromatography on silica gel (petroleum ether/EtOAc: 1/1) yielded **14** (0.058 g, 87%) as a colorless liquid. $^1\text{H-NMR}$ (500 MHz, CDCl_3): δ = 8.67-8.66 (m, 1H, Ar-H), 8.01-7.99 (m, 1H, Ar-H), 7.96-7.93 (m, 1H, Ar-H), 7.81-7.79 (m, 1H, Ar-H), 7.60 (d, J = 8.0 Hz, 1H, Ar-H), 7.36-7.30 (m, 3H, Ar-H), 3.13 (s, 2H, CH_2), 1.83-1.58 (m, 4H, CH_2), 1.32-1.18 (m, 4H, CH_2), 0.84 (q, J = 7.2 Hz, 6H, CH_3). $^{13}\text{C}\{^1\text{H}\}$ -NMR (125 MHz, CDCl_3): δ = 201.4 (CO), 165.4 (C_q), 150.7 (C_q), 149.8 (CH), 141.7 (C_q), 138.9 (CH), 124.3 (CH), 123.4 (CH), 122.9 (C_q), 122.4 (C_q), 122.3 (CH), 121.4 (CH), 117.4 (CH), 112.5 (CH), 59.1 (C_q), 37.5 (CH_2), 33.6 (CH_2), 30.6 (CH_2), 26.7 (CH_2), 23.5 (CH_2), 14.1 (CH_3), 9.0 (CH_3). HRMS (ESI): m/z Calcd for $\text{C}_{22}\text{H}_{24}\text{N}_2\text{O} + \text{H}^+$ $[\text{M} + \text{H}]^+$ 333.1961; Found 333.1968.



2-Butyl-2-ethyl-4-(pyridin-2-yl)-3,4-dihydrocyclopenta[b]indol-1(2H)-one-3,3-d₂

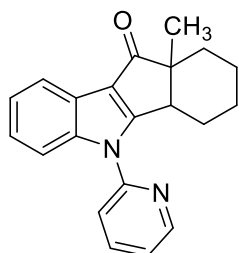
(14-[D₂]): The representative procedure **C** was followed, using 2-ethyl-2-(methyl-d₃)-1-(1-(pyridin-2-yl)-1H-indol-3-yl)hexan-1-one (**14b**-[D₃]; 0.068 g, 0.201 mmol). Purification by column chromatography on silica gel (petroleum ether/EtOAc: 1/1) yielded **14**-[D₂] (0.056 g, 83%) as a colorless liquid. ¹H-NMR (400 MHz, CDCl₃): δ = 8.67-8.65 (m, 1H, Ar-H), 8.01-7.92 (m, 2H, Ar-H), 7.81-7.79 (m, 1H, Ar-H), 7.60 (d, *J* = 8.1 Hz, 1H, Ar-H), 7.37-7.30 (m, 3H, Ar-H), 1.84-1.58 (m, 4H, CH₂), 1.31-1.18 (m, 4H, CH₂), 0.87-0.82 (m, 6H, CH₃). ¹³C{¹H}-NMR (100 MHz, CDCl₃): δ = 201.4 (CO), 165.4 (C_q), 150.7 (C_q), 149.9 (CH), 141.8 (C_q), 138.9 (CH), 124.3 (CH), 123.4 (CH), 123.0 (C_q), 122.4 (C_q), 122.3 (CH), 121.5 (CH), 117.4 (CH), 112.5 (CH), 60.0 (C_q), 37.5 (CH₂), 30.6 (CH₂), 26.7 (CH₂), 23.5 (CH₂), 14.1 (CH₃), 9.0 (CH₃). HRMS (ESI): *m/z* Calcd for C₂₂H₂₂D₂N₂O + H⁺ [M + H]⁺ 335.2087; Found 335.2086.



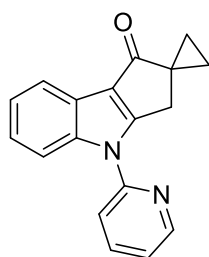
4'-(Pyridin-2-yl)-3',4'-dihydro-1'H-spiro[cyclohexane-1,2'-cyclopenta[b]indol]-1'-

one (15): The representative procedure **C** was followed, using (1-methylcyclohexyl)(1-(pyridin-2-yl)-1H-indol-3-yl)methanone (**15b**; 0.064 g, 0.201 mmol). Purification by column chromatography on silica gel (petroleum ether/EtOAc: 1/1) yielded **15** (0.028 g, 44%) and **16** (0.020 g, 31%) as white solids. ¹H-NMR (500 MHz, CDCl₃): δ = 8.67-8.66 (m, 1H, Ar-H), 8.00-7.93 (m, 2H, Ar-H), 7.79-7.74 (m, 1H, Ar-H), 7.60 (d, *J* = 7.6 Hz, 1H, Ar-H), 7.38-7.35 (m, 1H, Ar-H), 7.33-7.29 (m, 2H, Ar-H), 3.16 (s, 2H, CH₂), 1.88-1.72 (m, 6H, CH₂), 1.54 (d, *J* = 12.9 Hz, 2H, CH₂), 1.43-1.37 (m, 2H, CH₂). ¹³C{¹H}-NMR (125 MHz, CDCl₃): δ = 201.6 (CO), 165.4 (C_q), 150.6 (C_q), 149.9 (CH), 141.8 (C_q), 138.9 (CH), 124.3 (CH), 123.4 (CH), 122.7 (C_q), 122.4 (CH), 121.5 (CH), 120.7 (C_q), 117.6 (CH), 112.4 (CH), 56.6 (C_q), 35.8 (CH₂),

33.7 (2C, CH₂), 25.4 (CH₂), 23.5 (2C, CH₂). HRMS (ESI): m/z Calcd for C₂₁H₂₀N₂O + H⁺ [M + H]⁺ 317.1648; Found 317.1643.

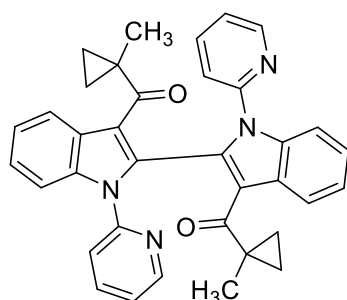


10a-Methyl-5-(pyridin-2-yl)-1,3,4,4a,5,10a-hexahydroindeno[1,2-b]indol-10(2H)-one (16): ¹H-NMR (400 MHz, CDCl₃): δ = 8.68-8.66 (m, 1H, Ar-H), 8.02-7.94 (m, 2H, Ar-H), 7.65-7.62 (m, 1H, Ar-H), 7.58 (d, J = 8.0 Hz, 1H, Ar-H), 7.40-7.37 (m, 1H, Ar-H), 7.34-7.28 (m, 2H, Ar-H), 3.50 (t, J = 6.0 Hz, 1H, CH), 1.97-1.93 (m, 1H, CH₂), 1.71-1.64 (m, 2H, CH₂), 1.56-1.49 (m, 2H, CH₂), 1.36-1.29 (m, 5H, CH₂, CH₃), 1.26-1.23 (m, 1H, CH₂). ¹³C{¹H}-NMR (100 MHz, CDCl₃): δ = 201.9 (CO), 168.3 (C_q), 150.5 (C_q), 150.0 (CH), 142.2 (C_q), 139.0 (CH), 138.0 (C_q), 124.3 (CH), 123.4 (CH), 122.8 (CH), 122.4 (C_q), 121.6 (CH), 118.6 (CH), 111.8 (CH), 54.9 (C_q), 43.6 (CH), 30.4 (CH₂), 25.7 (CH₃), 24.4 (CH₂), 18.7 (CH₂), 18.4 (CH₂). HRMS (ESI): m/z Calcd for C₂₁H₂₀N₂O + H⁺ [M + H]⁺ 317.1648; Found 317.1646.

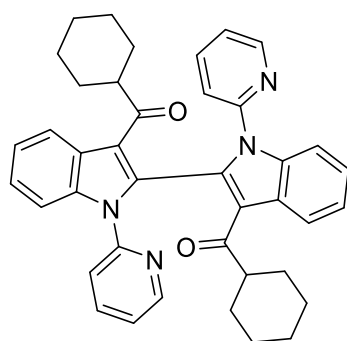


4-(Pyridin-2-yl)-3,4-dihydro-1H-spiro[cyclopenta[b]indole-2,1'-cyclopropan]-1-one (17): The representative procedure C was followed, using (1-methylcyclopropyl)(1-(pyridin-2-yl)-1H-indol-3-yl)methanone (**17b**; 0.055 g, 0.20 mmol). Purification by column chromatography on silica gel (petroleum ether/EtOAc: 1/1) yielded **17** (0.023 g, 42%) as a light-brown solid and **18** (0.010 g, 17%) as a brown solid. ¹H-NMR (400 MHz, CDCl₃): δ = 8.64-8.62 (m, 1H, Ar-H), 8.03-8.00 (m, 1H, Ar-H), 7.95-7.91 (m, 1H, Ar-H), 7.81-7.79 (m, 1H, Ar-H), 7.62-7.59 (m, 1H, Ar-H), 7.35-7.31 (m, 3H, Ar-H), 3.42 (s, 2H, CH₂), 1.42-1.40 (m, 2H, CH₂), 1.06-1.03 (m, 2H, CH₂). ¹³C{¹H}-NMR (100 MHz, CDCl₃): δ = 197.0 (CO), 164.3 (C_q), 150.7 (C_q), 149.8 (CH), 141.1 (C_q), 138.9 (CH), 124.3 (CH), 123.6 (C_q), 123.4

(CH), 122.4 (C_q), 122.3 (CH), 121.3 (CH), 117.3 (CH), 112.3 (CH), 33.6 (CH₂), 33.0 (C_q), 14.9 (2C, CH₂). HRMS (ESI): *m/z* Calcd for C₁₈H₁₄N₂O + H⁺ [M + H]⁺ 275.1179; Found 275.1189.

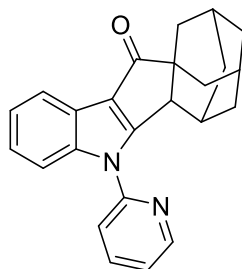


1-(3'-(1-Methylcyclopropane-1-carbonyl)-1,1'-di(pyridin-2-yl)-1H,1'H-[2,2'-biindol]-3-yl)-2-(1-methylcyclopropyl)ethane-1,2-dione (18): ¹H-NMR (400 MHz, CDCl₃): δ = 8.29-8.28 (m, 2H, Ar-H), 7.92-7.90 (m, 2H, Ar-H), 7.61-7.59 (m, 2H, Ar-H), 7.50-7.45 (m, 2H, Ar-H), 7.32-7.21 (m, 6H, Ar-H), 7.12-7.09 (m, 2H, Ar-H), 1.69-1.62 (m, 2H, CH₂), 1.44 (s, 6H, CH₃), 1.33-1.28 (m, 2H, CH₂), 0.94-0.90 (m, 2H, CH₂), 0.74-0.69 (m, 2H, CH₂). ¹³C{¹H}-NMR (100 MHz, CDCl₃): δ = 200.8 (2C, CO), 150.3 (2C, C_q), 148.4 (2C, CH), 138.5 (2C, CH), 136.5 (2C, C_q), 131.1 (2C, C_q), 125.5 (2C, C_q), 124.1 (2C, CH), 122.5 (2C, CH), 122.4 (2C, CH), 121.2 (2C, C_q), 121.1 (2C, CH), 120.8 (2C, CH), 112.8 (2C, CH), 27.6 (2C, C_q), 20.5 (2C, CH₃), 18.7 (2C, CH₂), 15.1 (2C, CH₂). HRMS (ESI): *m/z* Calcd for C₃₆H₃₀N₄O₂ + H⁺ [M + H]⁺ 551.2447; Found 551.2440.



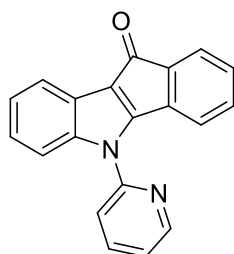
(1,1'-Di(pyridin-2-yl)-1H,1'H-[2,2'-biindole]-3,3'-diyl)bis(cyclohexylmethanone) (19): The representative procedure **C** was followed, using cyclohexyl(1-(pyridin-2-yl)-1H-indol-3-yl)methanone (**19b**; 0.061 g, 0.20 mmol). Purification by column chromatography on silica gel (petroleum ether/EtOAc: 1/1) yielded **19** (0.025 g, 41%) as a light-yellow solid. ¹H-NMR (500 MHz, CDCl₃): δ = 8.37-8.35 (m, 2H, Ar-H), 8.07-8.05 (m, 2H, Ar-H), 7.73-7.71 (m, 2H, Ar-H), 7.67-7.62 (m, 2H, Ar-H), 7.57-7.54 (m, 2H, Ar-H), 7.33-7.30 (m, 4H, Ar-H), 7.19-7.15 (m, 2H, Ar-H), 2.59-2.54 (m, 2H, CH), 1.72-1.51 (m, 11H, CH₂), 1.40-1.31 (m, 2H,

CH₂), 1.09-0.88 (m, 7H, CH₂). ¹³C{¹H}-NMR (125 MHz, CDCl₃): δ = 200.0 (2C, CO), 150.5 (2C, C_q), 148.9 (2C, CH), 138.2 (2C, CH), 137.2 (2C, C_q), 134.8 (2C, C_q), 126.2 (2C, C_q), 124.2 (2C, CH), 123.2 (CH), 123.1 (CH), 123.9 (2C, CH), 122.1 (2C, CH), 121.8 (2C, CH), 117.8 (2C, C_q), 112.1 (2C, CH), 49.1 (2C, CH), 29.9 (2C, CH₂), 28.0 (2C, CH₂), 26.3 (2C, CH₂), 26.1 (2C, CH₂), 25.9 (2C, CH₂). HRMS (ESI): *m/z* Calcd for C₄₀H₃₈N₄O₂ + H⁺ [M + H]⁺ 607.3073; Found 607.3076.



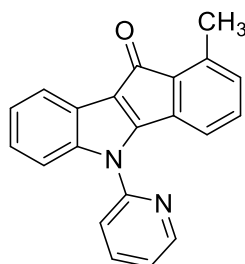
5-(Pyridin-2-yl)-5,5b,6,7,8,9,10,11-octahydro-12H-6,10:8,11a-

dimethanocycloocta[4,5]cyclopenta[1,2-b]indol-12-one (20): The representative procedure C was followed, using adamantan-1-yl(1-(pyridin-2-yl)-1*H*-indol-3-yl)methanone (**20b**; 0.072 g, 0.202 mmol). Purification by column chromatography on silica gel (petroleum ether/EtOAc: 1/1) yielded **20** (0.020 g, 28%) as a white solid. ¹H-NMR (400 MHz, CDCl₃): δ = 8.41 (s, 1H, Ar-H), 7.67-7.62 (m, 2H, Ar-H), 7.56-7.52 (m, 1H, Ar-H), 7.36-7.33 (m, 1H, Ar-H), 7.28-7.21 (m, 3H, Ar-H), 2.62 (s, 1H, CH), 2.04 (s, 1H, CH), 1.88-1.86 (m, 7H, CH₂, CH), 1.60 (s, 5H, CH₂, CH). ¹³C{¹H}-NMR (100 MHz, CDCl₃): δ = 207.2 (CO), 150.0 (C_q), 148.7 (CH), 139.0 (CH), 136.2 (C_q), 128.9 (C_q), 126.9 (2C, C_q), 124.4 (CH), 122.4 (CH), 122.3 (CH), 121.8 (CH), 120.8 (CH), 111.7 (CH), 47.7 (C_q), 40.9 (CH), 37.5 (2C, CH₂), 36.6 (3C, CH₂), 28.1 (3C, CH). HRMS (ESI): *m/z* Calcd for C₂₄H₂₂N₂O + H⁺ [M + H]⁺ 355.1805; Found 355.1799.

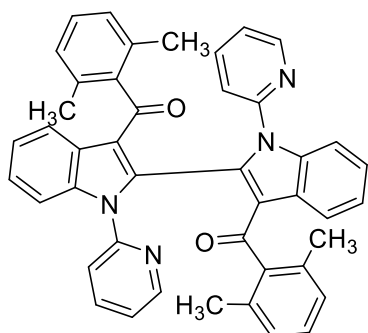


5-(Pyridin-2-yl)indeno[1,2-b]indol-10(5H)-one (21): The representative procedure C was followed, using phenyl(1-(pyridin-2-yl)-1*H*-indol-3-yl)methanone (**21b**; 0.060 g, 0.201 mmol). Purification by column chromatography on silica gel (petroleum ether/EtOAc: 1/1) yielded **21** (0.051 g, 86%) as a light-brown solid. ¹H-NMR (400 MHz, CDCl₃): δ = 8.35-8.34

(m, 1H, Ar-H), 7.62 (d, $J = 6.8$ Hz, 2H, Ar-H), 7.57-7.53 (m, 1H, Ar-H), 7.51-7.48 (m, 2H, Ar-H), 7.35-7.29 (m, 2H, Ar-H), 7.22-7.08 (m, 4H, Ar-H). $^{13}\text{C}\{^1\text{H}\}$ -NMR (100 MHz, CDCl_3): $\delta = 191.9$ (CO), 150.3 (C_q), 149.0 (CH), 139.0 (C_q), 138.3 (CH), 136.7 (C_q), 133.4 (C_q), 132.1 (CH), 129.8 (2C, CH), 127.8 (CH), 127.0 (2C, C_q), 124.2 (CH), 122.7 (CH), 122.6 (CH), 121.6 (CH), 121.5 (CH), 119.7 (C_q), 111.9 (CH). HRMS (ESI): m/z Calcd for $\text{C}_{20}\text{H}_{12}\text{ON}_2 + \text{H}^+$ [$\text{M} + \text{H}$] $^+$ 297.1022; Found 297.1017.

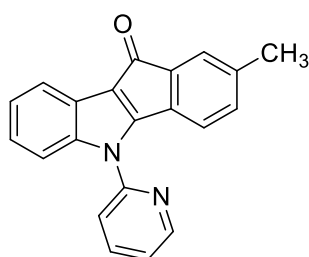


1-Methyl-5-(Pyridin-2-yl)indeno[1,2-b]indol-10(5H)-one (22): The representative procedure **C** was followed, using (1-(pyridin-2-yl)-1*H*-indol-3-yl)(*o*-tolyl)methanone (**22b**; 0.063 g, 0.202 mmol). Purification by column chromatography on silica gel (petroleum ether/EtOAc: 1/1) yielded **22** (0.057 g, 91%) as a white solid. ^1H -NMR (500 MHz, CDCl_3): $\delta = 8.44$ -8.42 (m, 1H, Ar-H), 7.75 (d, $J = 8.3$ Hz, 1H, Ar-H), 7.65 (td, $J = 7.6$ Hz, 1.5 Hz, 1H, Ar-H), 7.59 (d, $J = 8.3$ Hz, 1H, Ar-H), 7.23-7.15 (m, 4H, Ar-H), 7.07-7.03 (m, 2H, Ar-H), 6.96-6.92 (m, 1H, Ar-H), 2.13 (s, 3H, CH_3). $^{13}\text{C}\{^1\text{H}\}$ -NMR (125 MHz, CDCl_3): $\delta = 193.0$ (CO), 150.5 (C_q), 148.9 (CH), 140.2 (C_q), 138.4 (CH), 137.1 (C_q), 136.5 (C_q), 134.8 (C_q), 130.8 (CH), 130.0 (CH), 128.8 (CH), 126.8 (2C, C_q), 125.1 (CH), 124.1 (CH), 122.8 (CH), 121.6 (CH), 121.2 (CH), 119.3 (C_q), 112.1 (CH), 19.9 (CH_3). HRMS (ESI): m/z Calcd for $\text{C}_{21}\text{H}_{14}\text{N}_2\text{O} + \text{H}^+$ [$\text{M} + \text{H}$] $^+$ 311.1179; Found 311.1176.

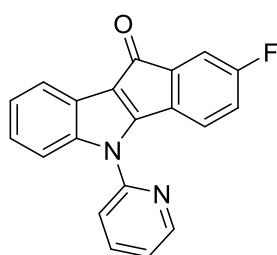


(1,1'-Di(pyridin-2-yl)-1*H*,1'*H*-[2,2'-biindole]-3,3'-diyl)bis((2,6-dimethylphenyl)methanone) (23): The representative procedure **C** was followed, using (2,6-dimethylphenyl)(1-(pyridin-2-yl)-1*H*-indol-3-yl)methanone (**23b**; 0.066 g, 0.202 mmol).

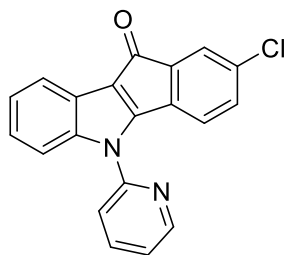
Purification by column chromatography on silica gel (petroleum ether/EtOAc: 1/1) yielded **23** (0.024 g, 37%) as a brown solid. $^1\text{H-NMR}$ (400 MHz, CDCl_3): δ = 8.38-8.37 (m, 2H, Ar-H), 7.87 (d, J = 8.0 Hz, 2H, Ar-H), 7.62-7.56 (m, 4H, Ar-H), 7.16-7.10 (m, 6H, Ar-H), 6.93 (t, J = 7.6 Hz, 4H, Ar-H), 6.88 (t, J = 7.6 Hz, 2H, Ar-H), 6.12 (d, J = 8.3 Hz, 2H, Ar-H), 1.95 (s, 6H, CH_3), 1.58 (s, 6H, CH_3). $^{13}\text{C}\{^1\text{H}\}$ -NMR (100 MHz, CDCl_3): δ = 193.4 (2C, CO), 150.7 (2C, C_q), 149.0 (2C, CH), 142.5 (2C, C_q), 138.1 (2C, CH), 137.6 (2C, C_q), 136.8 (2C, C_q), 134.1 (2C, C_q), 133.2 (2C, C_q), 128.5 (2C, CH), 128.0 (2C, CH), 127.5 (2C, CH), 126.2 (2C, C_q), 124.0 (2C, CH), 123.1 (2C, CH), 122.9 (2C, CH), 121.4 (2C, CH), 119.9 (2C, CH), 117.4 (2C, C_q), 112.5 (2C, CH), 18.9 (2C, CH_3), 18.7 (2C, CH_3). HRMS (ESI): m/z Calcd for $\text{C}_{44}\text{H}_{34}\text{N}_4\text{O}_2 + \text{H}^+$ [M + H] $^+$ 651.2760; Found 651.2756.



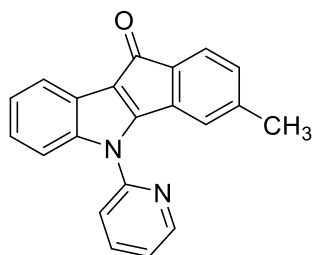
2-Methyl-5-(pyridin-2-yl)indeno[1,2-*b*]indol-10(5H)-one (24): The representative procedure **C** was followed, using (1-(pyridin-2-yl)-1*H*-indol-3-yl)(*m*-tolyl)methanone (**24b**; 0.063 g, 0.202 mmol). Purification by column chromatography on silica gel (petroleum ether/EtOAc: 1/1) yielded **24** (0.058 g, 93%) as a light brown solid. $^1\text{H-NMR}$ (400 MHz, CDCl_3): δ = 8.35-8.34 (m, 1H, Ar-H), 7.58-7.53 (m, 1H, Ar-H), 7.51-7.46 (m, 3H, Ar-H), 7.41 (d, J = 7.8 Hz, 1H, Ar-H), 7.36-7.34 (m, 1H, Ar-H), 7.22-7.18 (m, 1H, Ar-H), 7.15-7.08 (m, 3H, Ar-H), 2.14 (s, 3H, CH_3). $^{13}\text{C}\{^1\text{H}\}$ -NMR (100 MHz, CDCl_3): δ = 192.0 (CO), 150.3 (C_q), 149.0 (CH), 139.0 (C_q), 138.2 (CH), 137.3 (2C, C_q), 136.7 (C_q), 133.6 (C_q), 132.7 (CH), 130.3 (CH), 127.6 (CH), 127.1 (C_q), 126.7 (CH), 124.2 (CH), 122.6 (CH), 121.6 (CH), 121.5 (CH), 119.6 (C_q), 111.7 (CH), 21.1 (CH_3). HRMS (ESI): m/z Calcd for $\text{C}_{21}\text{H}_{14}\text{N}_2\text{O} + \text{H}^+$ [M + H] $^+$ 311.1179; Found 311.1171.



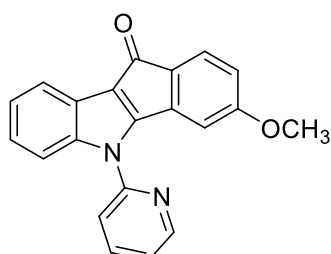
2-Fluoro-5-(pyridin-2-yl)indeno[1,2-*b*]indol-10(5*H*)-one (25): The representative procedure **C** was followed, using (3-fluorophenyl)(1-(pyridin-2-yl)-1*H*-indol-3-yl)methanone (**25b**; 0.064 g, 0.202 mmol). Purification by column chromatography on silica gel (petroleum ether/EtOAc: 1/1) yielded **25** (0.039 g, 61%) as a brown solid. ¹H-NMR (400 MHz, CDCl₃): δ = 8.29-8.28 (m, 1H, Ar-H), 7.52-7.48 (m, 1H, Ar-H), 7.43-7.32 (m, 3H, Ar-H), 7.24 (d, *J* = 9.1 Hz, 1H, Ar-H), 7.18-7.14 (m, 1H, Ar-H), 7.10-7.04 (m, 3H, Ar-H), 6.92-6.87 (m, 1H, Ar-H). ¹³C{¹H}-NMR (100 MHz, CDCl₃): δ = 190.5 (CO), 162.1 (d, ¹*J*_{C-F} = 246.3 Hz, C_q), 150.1 (C_q), 149.1 (CH), 141.1 (d, ³*J*_{C-F} = 6.7 Hz, C_q), 138.4 (CH), 136.7 (C_q), 133.7 (C_q), 129.4 (CH), 126.8 (2C, C_q), 125.3 (CH), 124.6 (CH), 123.0 (CH), 122.8 (CH), 121.5 (d, ³*J*_{C-F} = 6.7 Hz, CH), 119.3 (C_q), 118.9 (d, ²*J*_{C-F} = 21.1 Hz, CH), 116.2 (d, ²*J*_{C-F} = 22.0 Hz, CH), 111.8 (CH). ¹⁹F-NMR (376 MHz, CDCl₃): δ = -113.2 (s). HRMS (ESI): *m/z* Calcd for C₂₀H₁₁N₂OF + H⁺ [M + H]⁺ 315.0928; Found 315.0928.



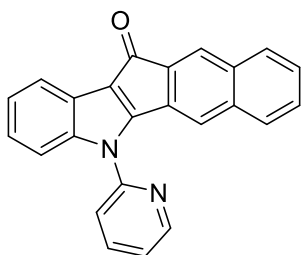
2-Chloro-5-(pyridin-2-yl)indeno[1,2-*b*]indol-10(5*H*)-one (26): The representative procedure **C** was followed, using (3-chlorophenyl)(1-(pyridin-2-yl)-1*H*-indol-3-yl)methanone (**26b**; 0.067 g, 0.201 mmol). Purification by column chromatography on silica gel (petroleum ether/EtOAc: 1/1) yielded **26** (0.043 g, 65%) as a light-yellow liquid. ¹H-NMR (500 MHz, CDCl₃): δ = 8.38-8.37 (m, 1H, Ar-H), 7.59-7.56 (m, 2H, Ar-H), 7.49-7.45 (m, 3H, Ar-H), 7.25-7.11 (m, 5H, Ar-H). ¹³C{¹H}-NMR (125 MHz, CDCl₃): δ = 190.4 (CO), 150.1 (C_q), 149.2 (CH), 140.7 (C_q), 138.3 (CH), 136.7 (C_q), 133.9 (C_q), 133.7 (2C, C_q), 131.7 (CH), 129.5 (CH), 129.1 (CH), 127.5 (CH), 126.9 (C_q), 124.6 (CH), 123.0 (CH), 122.8 (CH), 121.5 (CH), 119.1 (C_q), 111.7 (CH). HRMS (ESI): *m/z* Calcd for C₂₀H₁₁N₂OCl + H⁺ [M + H]⁺ 331.0633; Found 331.0623.



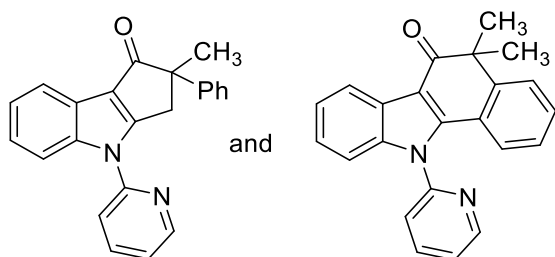
3-Methyl-5-(pyridin-2-yl)indeno[1,2-*b*]indol-10(5H)-one (27): The representative procedure **C** was followed, using (1-(pyridin-2-yl)-1*H*-indol-3-yl)(p-tolyl)methanone (**27b**; 0.063 g, 0.202 mmol). Purification by column chromatography on silica gel (petroleum ether/EtOAc: 1/1) yielded **27** (0.051 g, 81%) as a light-yellow solid. $^1\text{H-NMR}$ (500 MHz, CDCl_3): δ = 8.34-8.33 (m, 1H, Ar-H), 7.56-7.49 (m, 4H, Ar-H), 7.34 (d, J = 8.3 Hz, 1H, Ar-H), 7.19 (t, J = 7.6 Hz, 1H, Ar-H), 7.14-7.07 (m, 2H, Ar-H), 6.98 (d, J = 7.6 Hz, 2H, Ar-H), 2.25 (s, 3H, CH_3). $^{13}\text{C}\{^1\text{H}\}$ -NMR (125 MHz, CDCl_3): δ = 191.7 (CO), 150.4 (C_q), 148.9 (CH), 142.8 (2C, C_q), 138.3 (CH), 136.7 (C_q), 136.3 (C_q), 133.1 (C_q), 130.0 (CH), 128.5 (2C, CH), 127.0 (C_q), 124.1 (CH), 122.6 (CH), 122.4 (CH), 121.5 (CH), 121.4 (CH), 120.1 (C_q), 111.9 (CH), 21.7 (CH_3). HRMS (ESI): m/z Calcd for $\text{C}_{21}\text{H}_{14}\text{N}_2\text{O} + \text{H}^+$ [M + H] $^+$ 311.1179; Found 311.1171.



3-Methoxy-5-(pyridin-2-yl)indeno[1,2-*b*]indol-10(5H)-one (28): The representative procedure **C** was followed, using (4-methoxyphenyl)(1-(pyridin-2-yl)-1*H*-indol-3-yl)methanone (**28b**; 0.066 g, 0.201 mmol). Purification by column chromatography on silica gel (petroleum ether/EtOAc: 1/1) yielded **28** (0.056 g, 86%) as a light-brown solid. $^1\text{H-NMR}$ (400 MHz, CDCl_3): δ = 8.33-8.32 (m, 1H, Ar-H), 7.67-7.63 (m, 2H, Ar-H), 7.55-7.46 (m, 2H, Ar-H), 7.40 (d, J = 7.6 Hz, 1H, Ar-H), 7.22-7.18 (m, 1H, Ar-H), 7.13-7.09 (m, 2H, Ar-H), 6.65 (d, J = 9.1 Hz, 2H, Ar-H), 3.72 (s, 3H, OCH_3). $^{13}\text{C}\{^1\text{H}\}$ -NMR (100 MHz, CDCl_3): δ = 190.6 (CO), 163.0 (2C, C_q), 150.3 (C_q), 148.8 (CH), 138.3 (CH), 136.5 (C_q), 132.6 (C_q), 132.3 (2C, CH), 131.5 (C_q), 129.8 (C_q), 124.1 (CH), 122.5 (CH), 122.3 (CH), 121.5 (CH), 121.3 (CH), 120.3 (C_q), 113.0 (CH), 111.9 (CH), 55.4 (OCH_3). HRMS (ESI): m/z Calcd for $\text{C}_{21}\text{H}_{14}\text{N}_2\text{O}_2 + \text{H}^+$ [M + H] $^+$ 327.1128; Found 327.1126.

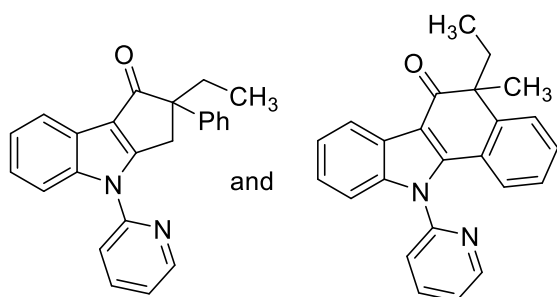


5-(pyridin-2-yl)benzo[5,6]indeno[1,2-b]indol-12(5H)-one (29): The representative procedure **C** was followed, using naphthalen-2-yl(1-(pyridin-2-yl)-1*H*-indol-3-yl)methanone (**29b**; 0.070 g, 0.201 mmol). Purification by column chromatography on silica gel (petroleum ether/EtOAc: 1/1) yielded **29** (0.021 g, 30%) as a dark-brown solid. ¹H-NMR (500 MHz, CDCl₃): δ = 8.37-8.35 (m, 1H, Ar-H), 8.15 (s, 1H, Ar-H), 7.73-7.66 (m, 2H, Ar-H), 7.62 (d, J = 8.3 Hz, 2H, Ar-H), 7.54-7.53 (m, 1H, Ar-H), 7.49-7.41 (m, 2H, Ar-H), 7.38-7.34 (m, 2H, Ar-H), 7.16-7.08 (m, 2H, Ar-H), 7.02-6.98 (m, 1H, Ar-H). ¹³C{¹H}-NMR (125 MHz, CDCl₃): δ = 191.9 (CO), 150.4 (C_q), 149.0 (CH), 138.4 (CH), 136.7 (C_q), 136.0 (C_q), 135.2 (C_q), 133.4 (C_q), 132.1 (C_q), 132.1 (CH), 129.5 (CH), 127.9 (C_q), 127.7 (2C, CH), 127.0 (C_q), 126.2 (CH), 125.2 (CH), 124.2 (CH), 122.7 (CH), 122.6 (CH), 121.7 (CH), 121.3 (CH), 119.9 (C_q), 111.8 (CH). HRMS (ESI): m/z Calcd for C₂₄H₁₄N₂O + H⁺ [M + H]⁺ 347.1179; Found 349.1174.

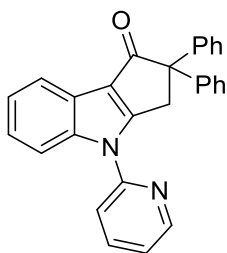


2-Methyl-2-phenyl-4-(pyridin-2-yl)-3,4-dihydrocyclopenta[b]indol-1(2H)-one and 5,5-dimethyl-11-(pyridin-2-yl)-5,11-dihydro-6H-benzo[a]carbazol-6-one (30 and 31): The representative procedure **C** was followed, using 2-methyl-2-phenyl-1-(1-(pyridin-2-yl)-1*H*-indol-3-yl)propan-1-one (**30b**; 0.068 g, 0.20 mmol). Purification by column chromatography on silica gel (petroleum ether/EtOAc: 1/1) yielded mixture of **30** and **31** (0.042 g, 62%) as colorless liquid. ¹H-NMR (500 MHz, CDCl₃): δ = 8.83-8.81 (m, 1H, Ar-H), 8.64-8.62 (m, 1H, Ar-H), 8.46 (d, J = 7.6 Hz, 1H, Ar-H), 8.06-8.02 (m, 2H, Ar-H), 7.95-7.91 (m, 1H, Ar-H), 7.82-7.80 (m, 1H, Ar-H), 7.61-7.57 (m, 3H, Ar-H), 7.52 (d, J = 8.3 Hz, 1H, Ar-H), 7.42-7.27 (m, 10 H, Ar-H), 7.21 (t, J = 7.6 Hz, 1H, Ar-H), 7.10 (d, J = 7.6 Hz, 1H, Ar-H), 6.97 (t, J = 7.6 Hz, 1H, Ar-H), 6.62 (d, J = 6.8 Hz, 1H, Ar-H), 3.68 (d, J = 18.3 Hz, 1H, CH₂), 3.50 (d, J = 18.3 Hz, 1H, CH₂), 1.79 (s, 3H, CH₃), 1.63 (s, 6H, CH₃). ¹³C{¹H}-NMR (125 MHz, CDCl₃):

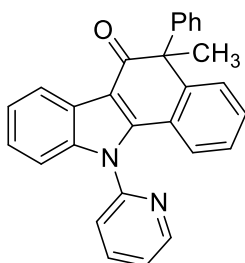
$\delta = 199.1$ (CO), 198.6 (CO), 165.0 (C_q), 151.7 (C_q), 150.8 (CH), 150.5 (C_q), 149.9 (CH), 149.1 (C_q), 144.5 (C_q), 144.0 (C_q), 141.9 (C_q), 140.5 (C_q), 139.5 (CH), 139.0 (CH), 129.1 (CH), 128.7 (2C, CH), 127.7 (CH), 126.7 (CH), 126.2 (2C, CH), 126.0 (CH), 125.0 (C_q), 125.0 (CH), 124.7 (CH), 124.6 (CH), 124.3 (CH), 123.9 (CH), 123.6 (C_q), 123.6 (CH), 123.5 (CH), 122.7 (C_q), 122.4 (CH), 122.3 (CH), 121.6 (CH), 121.0 (C_q), 117.3 (CH), 112.5 (CH), 112.3 (C_q), 110.7 (CH), 58.7 (C_q), 48.4 (C_q), 42.3 (CH₂), 28.6 (2C, CH₃), 24.4 (CH₃). HRMS (ESI): m/z Calcd for C₂₃H₁₈N₂O + H⁺ [M + H]⁺ 339.1492; Found 339.1498.



2-Methyl-2-phenyl-4-(pyridin-2-yl)-3,4-dihydrocyclopenta[b]indol-1(2H)-one and 5,5-dimethyl-11-(pyridin-2-yl)-5,11-dihydro-6H-benzo[a]carbazol-6-one (32 and 33): The representative procedure C was followed, using 2-methyl-2-phenyl-1-(1-(pyridin-2-yl)-1H-indol-3-yl)propan-1-one (**32b**; 0.071 g, 0.20 mmol). Purification by column chromatography on silica gel (petroleum ether/EtOAc: 1/1) yielded mixture of **32** and **33** (0.045 g, 64%) as a colorless liquid. ¹H-NMR (400 MHz, CDCl₃): $\delta = 8.84$ -8.82 (m, 1H, Ar-H), 8.66-8.65 (m, 1H, Ar-H), 8.48 (d, $J = 8.3$ Hz, 1H, Ar-H), 8.06-8.01 (m, 2H, Ar-H), 7.97-7.92 (m, 1H, Ar-H), 7.81-7.79 (m, 1H, Ar-H), 7.62-7.59 (m, 2H, Ar-H), 7.53-50 (m, 2H, Ar-H), 7.48-7.46 (m, 2H, Ar-H), 7.38-7.25 (m, 8H, Ar-H), 7.22-7.18 (m, 1H, Ar-H), 7.08 (d, $J = 8.3$ Hz, 1H, Ar-H), 7.00-6.95 (m, 1H, Ar-H), 6.63 (d, $J = 9.1$ Hz, 1H, Ar-H), 3.65 (d, $J = 18.3$ Hz, 1H, CH₂), 3.56 (d, $J = 18.3$ Hz, 1H, CH₂), 2.51-2.42 (m, 1H, CH₂), 2.25 (q, $J = 7.6$ Hz, 2H, CH₂), 1.99-1.91 (m, 1H, CH₂), 1.59 (s, 3H, CH₃), 1.26 (t, $J = 7.6$ Hz, 3H, CH₃), 0.94 (t, $J = 7.6$ Hz, 3H, CH₃). ¹³C{¹H}-NMR (100 MHz, CDCl₃): $\delta = 198.4$ (2C, CO), 165.3 (2C, C_q), 151.8 (C_q), 150.8 (CH), 150.5 (C_q), 149.9 (CH), 147.6 (C_q), 144.4 (C_q), 143.7 (C_q), 141.8 (C_q), 140.5 (C_q), 139.5 (CH), 138.9 (CH), 129.1 (CH), 128.6 (2C, CH), 127.7 (CH), 126.6 (CH), 126.6 (2C, CH), 125.9 (CH), 125.1 (C_q), 124.9 (CH), 124.7 (CH), 124.5 (CH), 124.2 (CH), 123.9 (CH), 123.6 (CH), 123.5 (CH), 122.6 (C_q), 122.4 (2C, CH), 122.2 (C_q), 121.5 (CH), 117.4 (CH), 113.7 (C_q), 112.4 (CH), 110.7 (CH), 63.1 (C_q), 53.1 (C_q), 38.0 (CH₂), 36.0 (CH₂), 30.5 (CH₂), 28.5 (CH₃), 9.7 (CH₃), 9.5 (CH₃). HRMS (ESI): m/z Calcd for C₂₄H₂₀N₂O + H⁺ [M + H]⁺ 353.1648; Found 353.1656.



2,2-Diphenyl-4-(pyridin-2-yl)-3,4-dihydrocyclopenta[b]indol-1(2H)-one (34): The representative procedure **C** was followed, using 2,2-diphenyl-1-(1-(pyridin-2-yl)-1H-indol-3-yl)propan-1-one (**34b**; 0.081 g, 0.201 mmol). Purification by column chromatography on silica gel (petroleum ether/EtOAc: 1/1) yielded **34** (0.013 g, 16%) and **35** (0.012 g, 15%) as brown solid. For **34**: $^1\text{H-NMR}$ (400 MHz, CDCl_3): δ = 8.66-8.65 (m, 1H, Ar-H), 8.03-8.01 (m, 1H, Ar-H), 7.95 (td, J = 7.6, 1.5 Hz, 1H, Ar-H), 7.81-7.79 (m, 1H, Ar-H), 7.63 (d, J = 7.6 Hz, 1H, Ar-H), 7.38-7.28 (m, 11H, Ar-H), 7.26-7.21 (m, 2H, Ar-H), 4.11 (s, 2H, CH_2). $^{13}\text{C}\{^1\text{H}\}$ -NMR (100 MHz, CDCl_3): δ = 195.7 (CO), 164.6 (C_q), 150.4 (C_q), 150.0 (CH), 144.1 (C_q), 141.9 (2C, C_q), 139.0 (CH), 128.5 (4C, CH), 128.3 (4C, CH), 126.9 (2C, CH), 124.7 (CH), 123.7 (CH), 122.9 (C_q), 122.5 (CH), 121.6 (CH), 121.1 (C_q), 117.4 (CH), 112.4 (CH), 68.2 (C_q), 42.3 (CH_2). HRMS (ESI): m/z Calcd for $\text{C}_{28}\text{H}_{20}\text{N}_2\text{O} + \text{H}^+$ $[\text{M} + \text{H}]^+$ 401.1648; Found 401.1645.



5-Methyl-5-phenyl-11-(pyridin-2-yl)-5,11-dihydro-6H-benzo[a]carbazol-6-one (35): $^1\text{H-NMR}$ (500 MHz, CDCl_3): δ = 8.87-8.86 (m, 1H, Ar-H), 8.37 (d, J = 6.8 Hz, 1H, Ar-H), 8.10-8.05 (m, 1H, Ar-H), 7.65-7.61 (m, 1H, Ar-H), 7.57 (d, J = 7.6 Hz, 1H, Ar-H), 7.35-7.19 (m, 8H, Ar-H), 7.16-7.09 (m, 2H, Ar-H), 6.98 (t, J = 7.6 Hz, 1H, Ar-H), 6.67 (d, J = 9.1 Hz, 1H, Ar-H), 2.03 (s, 3H, CH_3). $^{13}\text{C}\{^1\text{H}\}$ -NMR (125 MHz, CDCl_3): δ = 196.3 (CO), 151.7 (C_q), 150.9 (CH), 149.4 (C_q), 144.6 (C_q), 144.2 (C_q), 140.7 (C_q), 139.6 (2C, CH), 130.6 (CH), 129.0 (CH), 128.6 (2C, CH), 127.8 (2C, CH), 126.9 (CH), 126.2 (CH), 125.0 (CH), 125.0 (C_q), 124.8 (CH), 124.3 (C_q), 124.0 (CH), 123.6 (CH), 122.5 (CH), 112.3 (C_q), 110.7 (CH), 57.0 (C_q), 27.3 (CH_3). HRMS (ESI): m/z Calcd for $\text{C}_{28}\text{H}_{20}\text{N}_2\text{O} + \text{H}^+$ $[\text{M} + \text{H}]^+$ 401.1648; Found 401.1645.

2.4.5 2D NMR Spectrum Analysis of **24**

In order to confirm the cyclization at less hindered carbon, we have performed 2D long-range C, H correlation (HMBC) NMR analysis of representative compound **24**. All the protons and carbons were assigned by 1D and 2D NMR spectroscopy. The HMBC spectrum shows the strong cross peak of CH₃ protons (2.14 ppm) with carbons **a** [139.0 ppm (C_q)], **b** [130.3 ppm (CH)] and **c** [132.7 ppm (CH)] (Figure 2.8). The correlation of CH₃ protons with two CH carbon (130.3 ppm; **b** and 132.7 ppm; **c**) strongly supports the cyclization at less hindered carbon of (1-(pyridin-2-yl)-1H-indol-3-yl)(m-tolyl)methanone **24b** (C–H activation *para*-position to CH₃, instead of *ortho* C–H). This 2D analysis confirms the regioselective cyclization occurs at less hindered carbon.

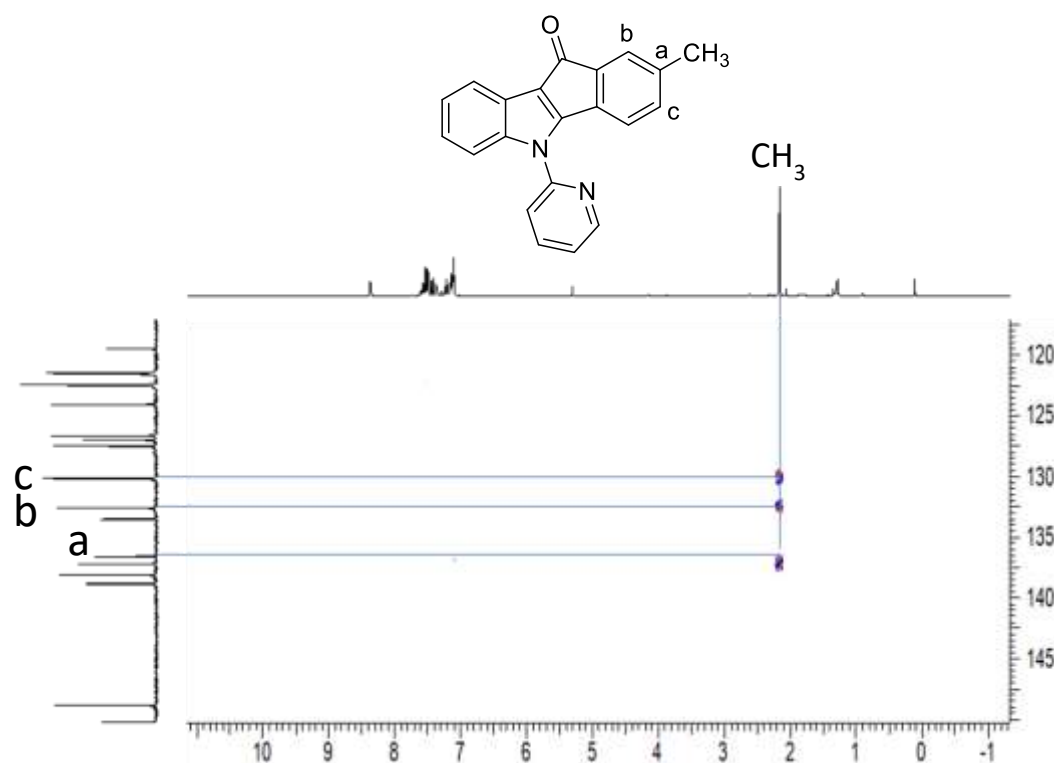
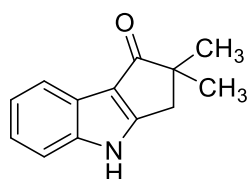


Figure 2.8. HMBC spectrum of **24** showing CH correlation.

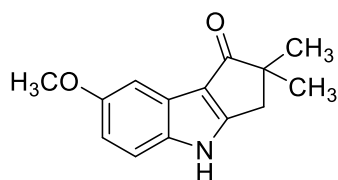
2.4.6 Procedure for Removal of Directing Group

Synthesis of 36:



In an oven dried round bottom flask, 2,2-dimethyl-4-(pyridin-2-yl)-3,4-dihydrocyclopenta[b]indol-1(2H)-one (**2**; 0.10 g, 0.362 mmol) was introduced and CH₂Cl₂ (20 mL) was added into it. Methyl trifluoromethanesulfonate, MeOTf (0.17 g, 1.04 mmol) was added drop wise *via* a syringe to the reaction mixture at 0 °C and the resultant reaction mixture was stirred at room temperature for 12 h. The volatiles were evaporated under vacuum and the residue was redissolved in MeOH (15 mL). To the resultant mixture, NaOH (2 M aq, 5 mL) solution was added and the reaction mixture was stirred at 60 °C for 12 h. At ambient temperature, the volatiles were evaporated under reduced pressure, and the resulting residue was extracted with EtOAc (30 mL x 2). The combined organic extract was washed with brine, dried over Na₂SO₄ and the volatiles were evaporated under vacuo. The remaining residue was purified by column chromatography on silica gel (petroleum ether/EtOAc: 1/1) to yield **36** (0.043 g, 60%) as white solid. ¹H-NMR (400 MHz, CDCl₃): δ = 10.14 (br s, 1H, NH), 7.94 (d, *J* = 7.6 Hz, 1H, Ar-H), 7.52 (d, *J* = 7.6 Hz, 1H, Ar-H), 7.35-7.28 (m, 2H, Ar-H), 3.05 (s, 2H, CH₂), 1.42 (s, 6H, CH₃). ¹³C-NMR (100 MHz, CDCl₃): δ = 203.0 (CO), 164.6 (C_q), 142.7 (C_q), 123.8 (CH), 122.5 (CH), 122.0 (C_q) 120.9 (CH), 118.3 (C_q), 112.5 (CH), 52.0 (C_q), 38.0 (CH₂), 26.0 (2C, CH₃). HRMS (ESI): *m/z* Calcd for C₁₃H₁₃NO + H⁺ [M + H]⁺ 200.1070; Found 200.1071.

Synthesis of 37:



Procedure: The procedure similar to the synthesis of **36** was followed, using 7-methoxy-2,2-dimethyl-4-(pyridin-2-yl)-3,4-dihydrocyclopenta[b]indol-1(2H)-one (**8**; 0.08 g, 0.261 mmol), methyl trifluoromethanesulfonate (MeOTf; 0.128 g, 0.78 mmol). Purification by column chromatography on silica gel (petroleum ether/EtOAc: 1/1) yielded **37** (0.037 g, 62%) as colorless solid. ¹H-NMR (400 MHz, CDCl₃): δ = 10.32 (br s, 1H, NH), 7.34-7.30 (m, 2H, Ar-H), 8.85 (dd, *J* = 8.8, 2.6 Hz, 1H, Ar-H), 3.67 (s, 3H, OCH₃), 2.94 (s, 2H, CH₂), 1.33 (s, 6H, CH₃). ¹³C-NMR (100 MHz, CDCl₃): δ = 202.0 (CO), 164.8 (C_q), 156.0 (C_q), 137.3 (C_q), 122.6 (C_q), 118.0 (C_q), 113.4 (CH), 113.2 (CH), 103.2 (CH), 55.8 (C_q), 51.9 (OCH₃), 38.0 (CH₂), 26.0 (2C, CH₃). HRMS (ESI): *m/z* Calcd for C₁₄H₁₅NO₂ + H⁺ [M + H]⁺ 230.1176; Found 230.1178.

2.4.7 Mechanistic Experiments

2.4.7.1 External Addition Experiment and Radical Clock Experiment

Procedure for external addition experiments: To a flame-dried screw-cap tube equipped with magnetic stir bar were introduced 2,2-dimethyl-1-(1-(pyridin-2-yl)-1*H*-indol-3-yl)propan-1-one (**2b**; 0.056 g, 0.201 mmol), (bpy)Ni(OAc)₂ (0.0034 g, 0.01 mmol, 5.0 mol %), Ag₂CO₃ (0.056 g, 0.20 mmol, 1 equiv) and LiO^tBu (0.048 g, 0.60 mmol, 3 equiv) and TEMPO (0.063 g, 0.40 mmol) [or galvinoxyl (0.169 g, 0.40 mmol) or BHT (0.089 g, 0.40 mmol)] inside the glove box. To the reaction mixture chlorobenzene (1.0 mL) was added and stirred at 150 °C in a pre-heated oil bath for 24 h. At ambient temperature, the reaction mixture was quenched with distilled H₂O (10.0 mL) and the crude product was extracted with EtOAc (15 mL x 3). The combined organic extract was dried over Na₂SO₄ and the volatiles were evaporated *in vacuo*. The remaining residue was purified by column chromatography on silica gel (petroleum ether/EtOAc: 1/1) yielded **2** in 13% and 25%, respectively, in the presence of galvinoxyl and TEMPO. The formation of coupled product **2** was not observed in the presence of BHT.

Procedure for radical clock experiments: To a flame-dried screw-cap tube equipped with magnetic stir bar were introduced (1-methylcyclopropyl)(1-(pyridin-2-yl)-1*H*-indol-3-yl)methanone (**17b**; 0.055 g, 0.20 mmol), (bpy)Ni(OAc)₂ (0.0033 g, 0.01 mmol, 5.0 mol %), Ag₂CO₃ (0.055 g, 0.20 mmol, 1 equiv) and LiO^tBu (0.048 g, 0.60 mmol, 3 equiv) inside the glove box. To the above mixture in the tube was added chlorobenzene (1.0 mL). The resultant reaction mixture in the tube was immersed in a preheated oil bath at 150 °C and stirred for 24 h. At ambient temperature, the reaction mixture was quenched with distilled H₂O (10.0 mL) and the crude product was extracted with EtOAc (15 mL x 3). The combined organic extract was dried over Na₂SO₄ and the volatiles were evaporated *in vacuo*. The remaining residue was purified by column chromatography on silica gel (petroleum ether/EtOAc: 1/1) to yield **17** (0.023 g, 42%) as a light-brown solid and **18** (0.010 g, 17%) as a brown solid.

2.4.7.2 Representative Procedure for Electronic Effect Study

To a flame-dried screw-capped tube equipped with magnetic stir bar were charged 1-(5-methoxy-1-(pyridin-2-yl)-1*H*-indol-3-yl)-2,2-dimethylpropan-1-one (**8b**; 0.062 g, 0.201 mmol, 0.2 M) or 1-(5-fluoro-1-(pyridin-2-yl)-1*H*-indol-3-yl)-2,2-dimethylpropan-1-one (**9b**; 0.060 g, 0.202 mmol, 0.2 M), (bpy)Ni(OAc)₂ (0.0034 g, 0.01 mmol), Ag₂CO₃ (0.056 g, 0.20 mmol), LiO^tBu (0.048 g, 0.60 mmol) and *n*-hexadecane (0.020 mL, 0.070 mmol, internal standard), and chlorobenzene (1.0 mL). The reaction mixture was then stirred at 150 °C in a pre-heated oil bath. At regular intervals (2, 4, 6, 8, 10 min), the reaction vessel was cooled to

ambient temperature and an aliquot of sample was withdrawn to the GC vial. The sample was diluted with ethyl acetate and subjected to GC analysis. The concentration of the product **8** (or **9**) obtained in each sample was determined with respect to the internal standard *n*-hexadecane. The final data was obtained by averaging the results of three independent experiments. The initial rate obtained for the intramolecular coupling of 1-(5-methoxy-1-(pyridin-2-yl)-1*H*-indol-3-yl)-2,2-dimethylpropan-1-one (**8b**) is $1.48 \times 10^{-3} \text{ Mmin}^{-1}$, whereas the rate for the intramolecular coupling of 1-(5-fluoro-1-(pyridin-2-yl)-1*H*-indol-3-yl)-2,2-dimethylpropan-1-one (**9b**) is $0.735 \times 10^{-3} \text{ Mmin}^{-1}$.

2.4.7.3 Kinetic Isotope Effect Study

Representative Procedure for Kinetic Isotope Effect (KIE) Study (For 2b-[2-H] and 2b-[2-D]): To a Teflon-screw capped tube equipped with magnetic stir bar was introduced 2,2-dimethyl-1-(1-(pyridin-2-yl)-1*H*-indol-3-yl)propan-1-one (**2b**-[2-H]; 0.056 g, 0.201 mmol, 0.20 M) {or 2,2-dimethyl-1-(1-(pyridin-2-yl)-1*H*-indol-3-yl-2-d)propan-1-one (**2b**-[2-D]; 0.056 g, 0.20 mmol, 0.20 M)}, (bpy)Ni(OAc)₂ (0.0034 g, 0.01 mmol, 0.01 M), Ag₂CO₃ (0.056 g, 0.20 mmol, 0.20 M), LiO^tBu (0.048 g, 0.60 mmol, 0.60 M) and *n*-hexadecane (0.020 mL, 0.070 mmol, 0.070 M, internal standard), and chlorobenzene (1.0 mL) was added inside the glove box. The reaction mixture was then stirred at 150 °C in a pre-heated oil bath. At regular intervals (2, 4, 6, 8, 10, 15, 20, 25 min, etc.), the reaction vessel was cooled to ambient temperature and an aliquot of sample was withdrawn to the GC vial. The sample was diluted with ethyl acetate and subjected to GC analysis. The concentration of the product **2c** obtained in each sample was determined with respect to the internal standard *n*-hexadecane. The final data was obtained by averaging the results of three independent experiments. The initial rate obtained for the intramolecular coupling of 2,2-dimethyl-1-(1-(pyridin-2-yl)-1*H*-indol-3-yl)propan-1-one (**2b**-[2-H]) is $1.57 \times 10^{-3} \text{ Mmin}^{-1}$, whereas the rate for the intramolecular coupling of 2,2-dimethyl-1-(1-(pyridin-2-yl)-1*H*-indol-3-yl-2-d)propan-1-one (**2b**-[D]) is $1.39 \times 10^{-3} \text{ Mmin}^{-1}$. Therefore, the $k_H/k_D = 1.57 \times 10^{-3} / 1.39 \times 10^{-3} = 1.1$.

KIE Study for 14b and 14b-[D₃]): Representative procedure of KIE study was followed using 2-ethyl-2-methyl-1-(1-(pyridin-2-yl)-1*H*-indol-3-yl)hexan-1-one (**14b**; 0.067 g, 0.20 mmol, 0.02 M) or 2-ethyl-2-(methyl-d₃)-1-(1-(pyridin-2-yl)-1*H*-indol-3-yl)hexan-1-one (**14b**-[D₃]; 0.068 g, 0.20 mmol, 0.020 M). At regular intervals (5, 10, 15, 20, 30, 40, 60, 80 min, etc.), the reaction vessel was cooled to ambient temperature and an aliquot of sample was withdrawn to the GC vial. The sample was diluted with ethyl acetate and subjected to GC analysis. The concentration of the product **14** or **14**-[D₂] obtained in each sample was

determined with respect to the internal standard *n*-hexadecane. The final data was obtained by averaging the results of three independent experiments. The initial rate obtained for the intramolecular coupling of 2-ethyl-2-methyl-1-(1-(pyridin-2-yl)-1*H*-indol-3-yl)hexan-1-one (**14b**) is $3.0 \times 10^{-4} \text{ Mmin}^{-1}$, whereas the rate for the intramolecular coupling of 2-ethyl-2-(methyl- d_3)-1-(1-(pyridin-2-yl)-1*H*-indol-3-yl)hexan-1-one (**14b**-[D_3]) is $1.62 \times 10^{-4} \text{ Mmin}^{-1}$. Therefore, the $k_H/k_D = 3.0 \times 10^{-4}/1.62 \times 10^{-4} = 1.9$.

2.4.7.4 DFT Energy Calculations

All calculations were performed using Density Functional Theory (DFT) based methodology as implemented in the Gaussian 09 package.⁹⁴ All calculations are carried out explicitly in the presence of ligand. The structures are optimized using PBE functional⁹⁵ with TZVP basis set for C, H, O and N atoms and LANL2DZ for Ni, Ag and Li. Vibrational frequency calculations were performed to confirm that each optimized structure corresponds to minima. Solvent effects were included in the calculations as implemented in IEFPCM model⁹⁶ for chlorobenzene. The transition state was characterized by the presence of a single imaginary frequency. The energies reported in the free energy profile are ΔG values incorporated with zero-point energy corrections for the optimized minima at 298.15 K.

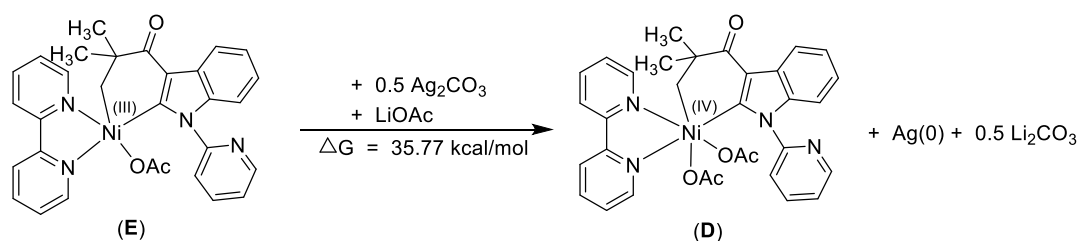


Figure 2.10. Gibbs free energy for the formation of intermediate **D** from the intermediate **E**.

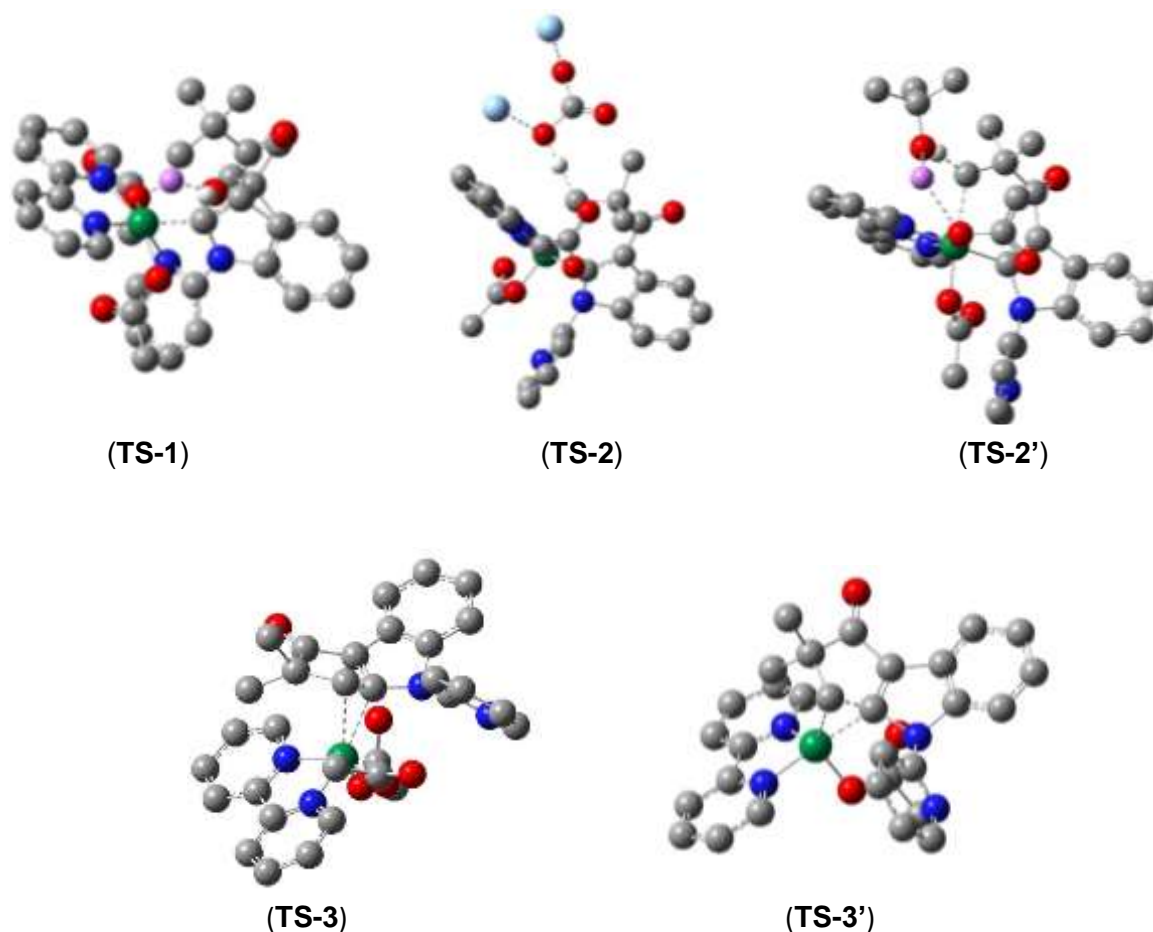


Figure 2.11. Transition States in the Ball and Stick Model. Hydrogen atoms are omitted for the greater clarity except for C–H activation transition states. The color Scheme is as follows: nickel, green; lithium, light purple; silver, sky blue; nitrogen, blue; oxygen, red; carbon, grey; hydrogen, white.

Table 2.2. Absolute Gibbs free energies including zero-point energy correction in Hatrees of all the species involved in the reaction.

Structures	Total Gibbs free Energies (Hartrees)
(bpy)Ni(II)(OAc) ₂ (1)	-1120.714890
Compound 2b	-880.407023
LiO ^t Bu	-240.323495

LiOAc	-235.896605
H ^t OBu	-233.340001
½ (^t BuO) ₂	-232.796140
Ag(0)	-145.733908
½ Ag ₂ CO ₃	-277.570000
½ Li ₂ CO ₃	-139.351220
½ H ₂ CO ₃	-132.410001
(bpy)Ni(0)	-664.113221
2b -dimer	-1759.555780
(bpy)Ni(2b) ₂	-2423.700870
(bpy)Ni(I)(OAc)	-892.3254451
Compound A'	-1543.836051
Intermediate A	-1772.249131
Intermediate B	-2000.630281
Intermediate C	-2000.019911
Intermediate D	-2000.026671
Intermediate E	-1771.702191
2	-879.428970
TS-1	-2241.415422
TS-2	-2278.143690
TS-2'	-2240.907200
TS-3	-2000.006370
TS-3'	-1771.663860

2.4.8 X-ray Structure Analysis

X-ray intensity data measurements of compounds **1**, **2**, **15**, **18** and **23** (Figures 2.12-2.16) was carried out on a Bruker D8 VENTURE Kappa Duo PHOTON II CPAD diffractometer equipped with Incoatech multilayer mirrors optics. The intensity measurements were carried out with Mo and Cu micro-focus sealed tube diffraction sources (MoK_α= 0.71073 Å, Cu K_α= 1.54178 Å). The X-ray generator was operated at 50 kV and 1.4 mA and 50 kV and 1.1 mA for Mo and Cu radiations, respectively. A preliminary set of cell constants and an orientation matrix were calculated from three matrix sets of 36 frames and 40 frames for Mo and Cu radiations, respectively. Data were collected with ω scan width of 0.5° at different settings of

φ and 2θ with a frame time of 10-20 sec depending on the diffraction power of the crystals keeping the sample-to-detector distance fixed at 5.00 cm. The X-ray data collection was monitored by APEX3 program (Bruker, 2016).⁹⁷ All the data were corrected for Lorentzian, polarization and absorption effects using SAINT and SADABS programs (Bruker, 2016). Using the APEX3 (Bruker) program suite, the structure was solved with the ShelXS-97 (Sheldrick, 2008)⁹⁸ structure solution program, using direct methods. The model was refined with a version of ShelXL-2018/3 (Sheldrick, 2015)⁹⁹ using Least Squares minimization. All the hydrogen atoms were placed in a geometrically idealized position and constrained to ride on its parent atoms. An *ORTEP* III¹⁰⁰ view of the compounds was drawn with 50% probability displacement ellipsoids, and H atoms are shown as small spheres of arbitrary radii. Crystal data for all the compounds is given in Table 2.3.

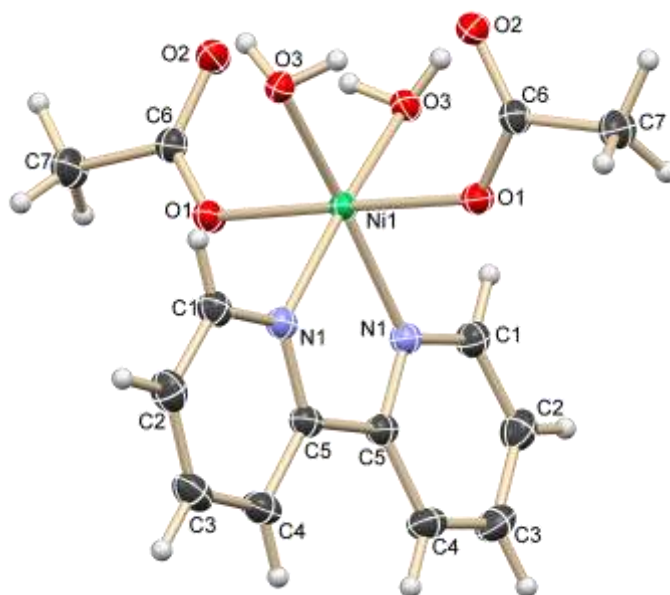


Figure 2.12. ORTEP of compound **1** showing the atom-numbering scheme. The displacement ellipsoids are drawn at the 50% probability level and H atoms are shown as small spheres with arbitrary radii.

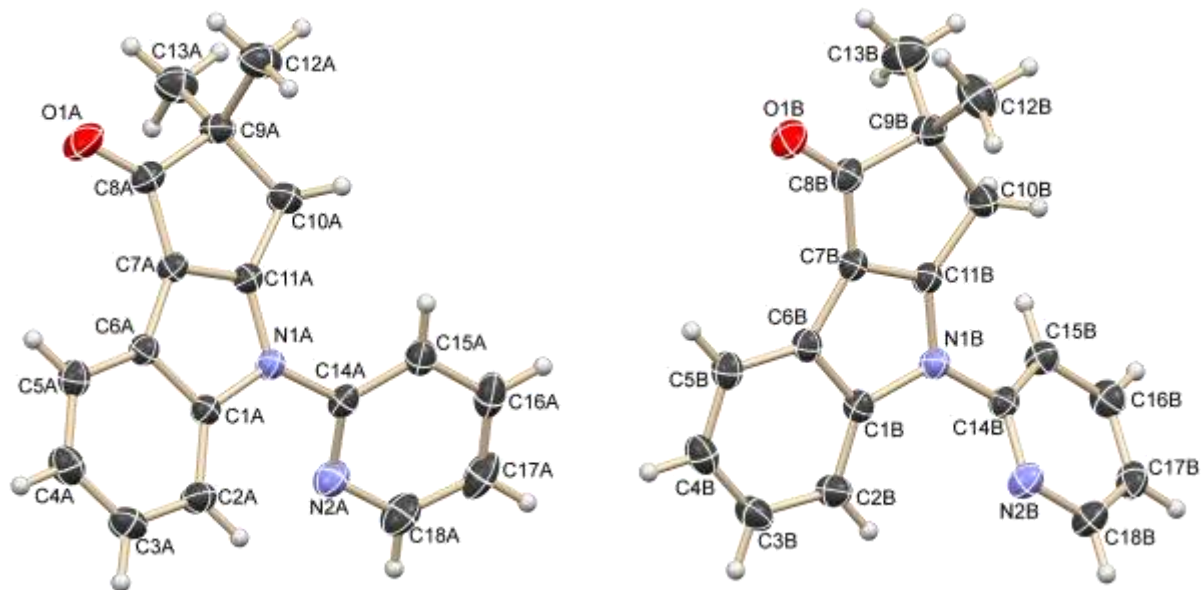


Figure 2.13. ORTEP of compound **2** showing the atom-numbering scheme for both conformers present in the asymmetric unit. The displacement ellipsoids are drawn at the 30% probability level and H atoms are shown as small spheres with arbitrary radii.

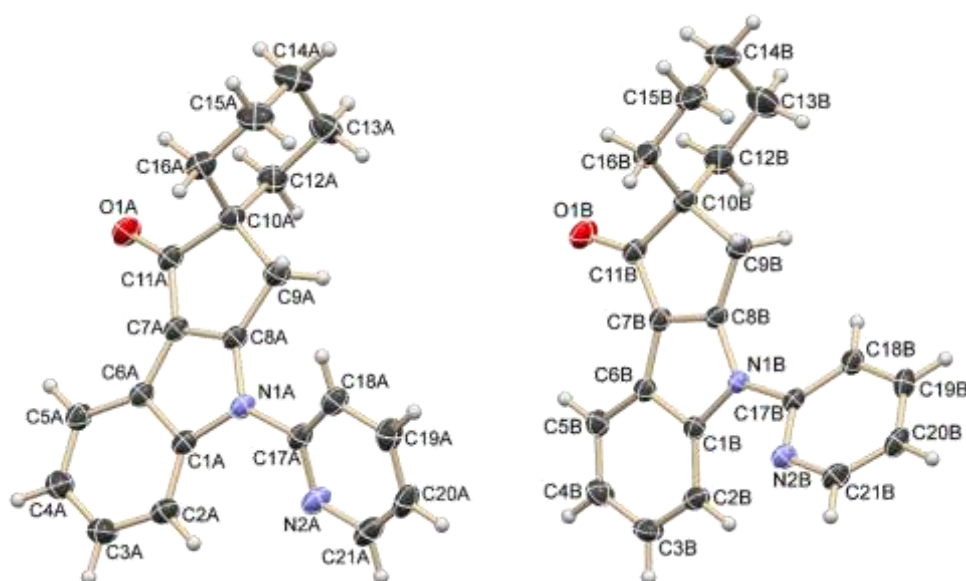


Figure 2.14. ORTEP of compound **15** showing the atom-numbering scheme for both conformers present in the asymmetric unit. The displacement ellipsoids are drawn at the 50% probability level and H atoms are shown as small spheres with arbitrary radii.

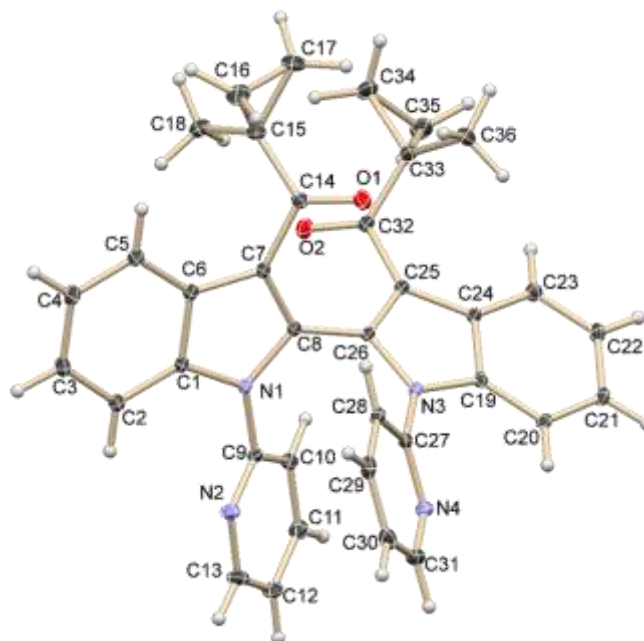


Figure 2.15. ORTEP of compound **18** showing the atom-numbering scheme. The displacement ellipsoids are drawn at the 50% probability level and H atoms are shown as small spheres with arbitrary radii.

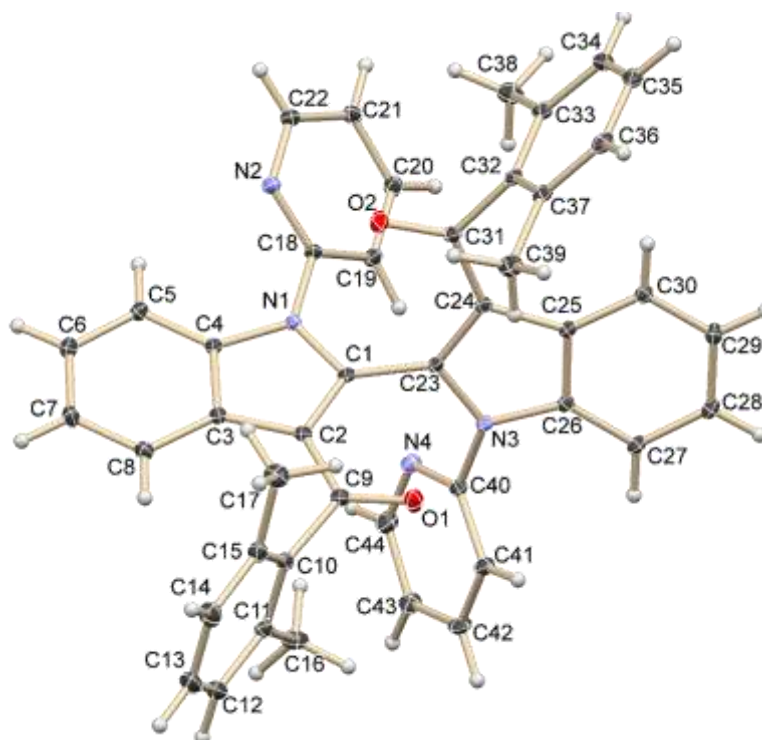
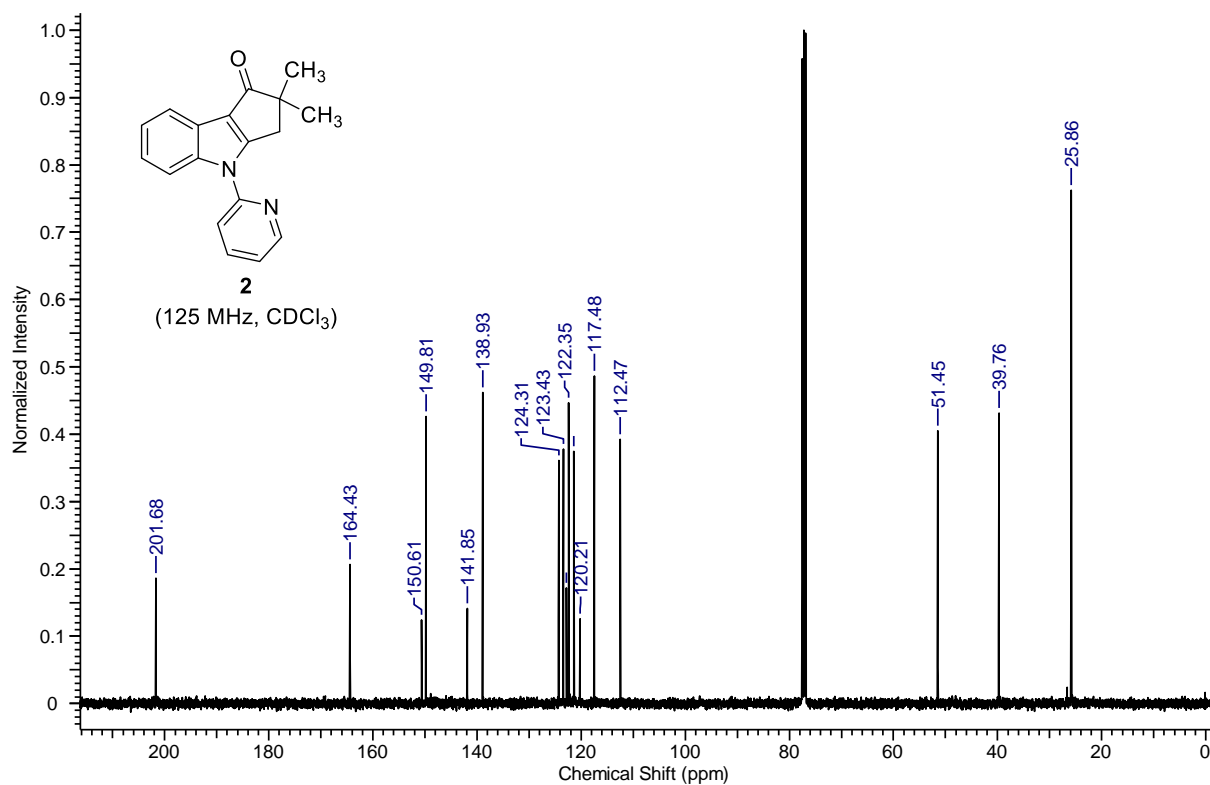
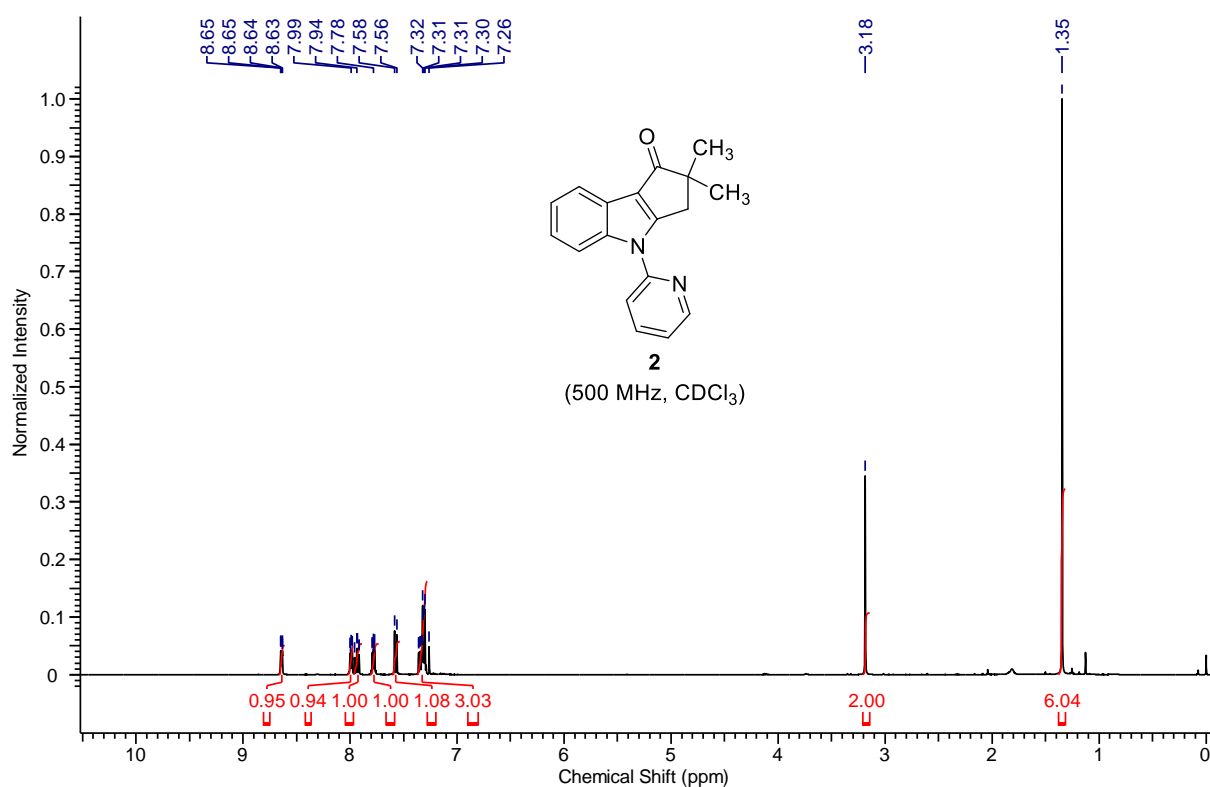
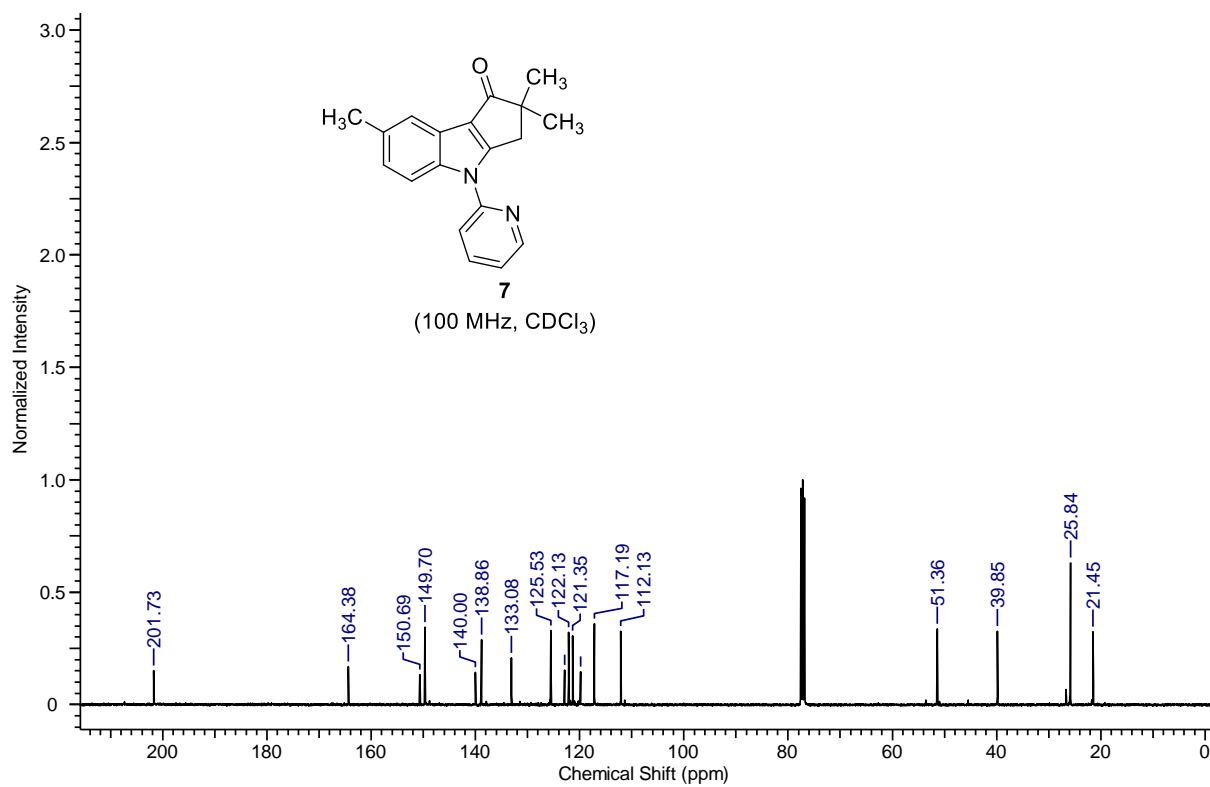
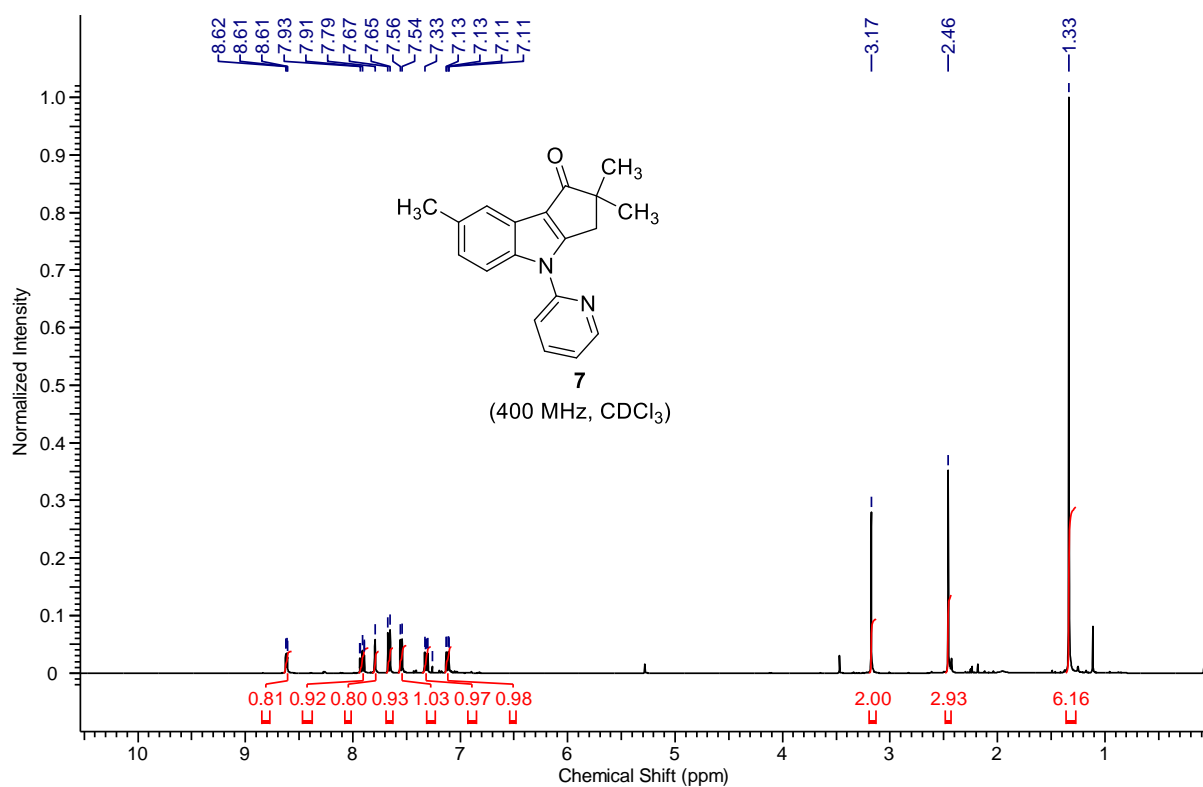


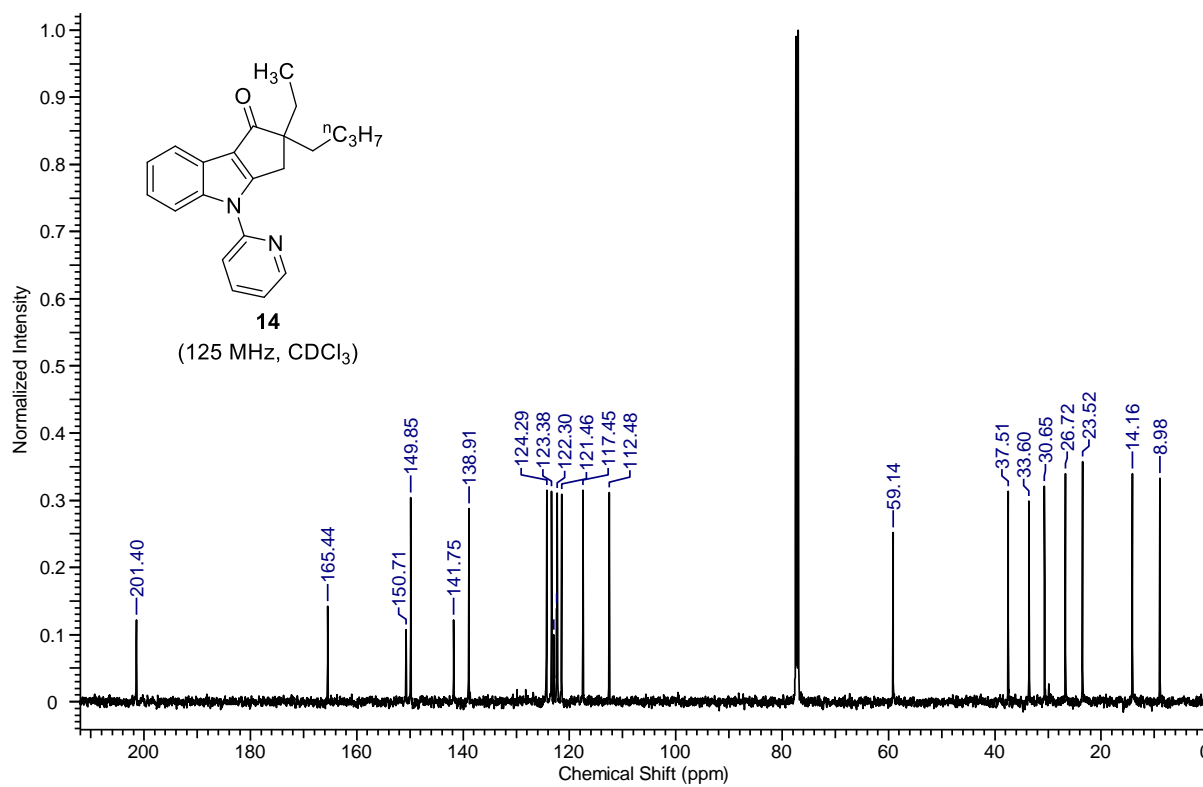
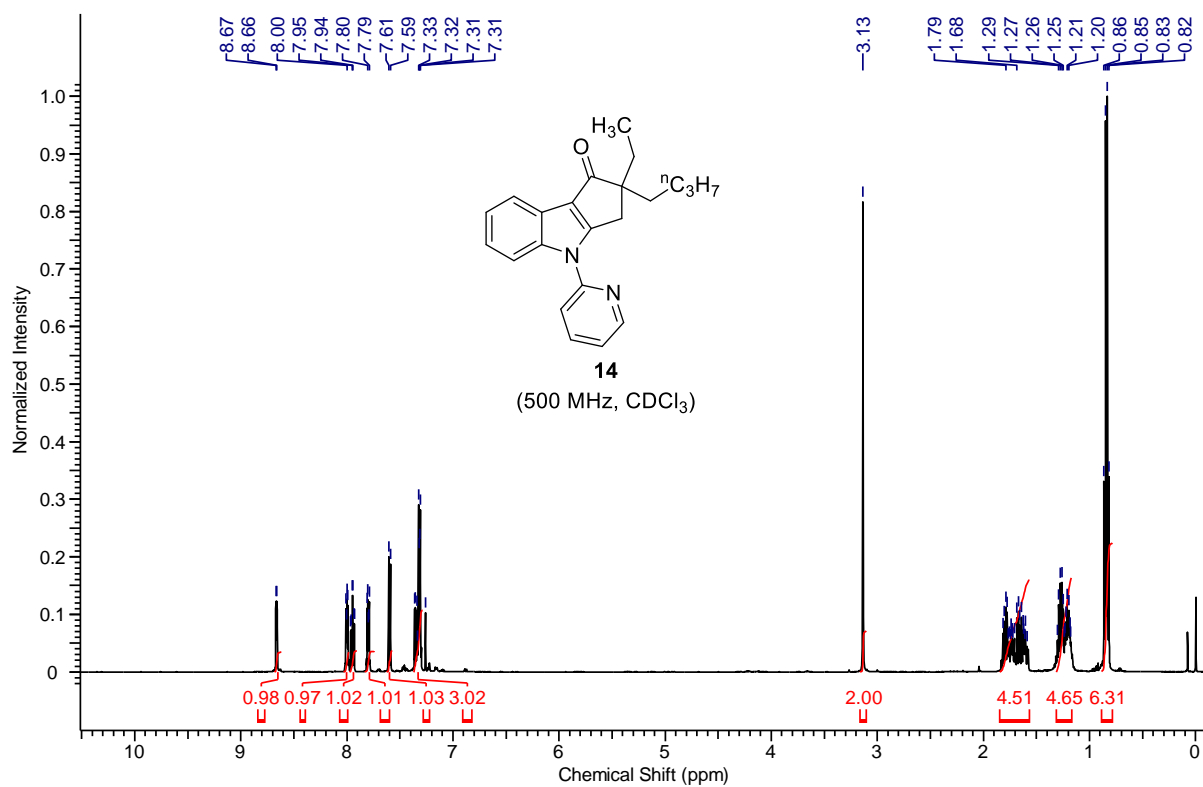
Figure 2.16. ORTEP of compound **23** showing the atom-numbering scheme. The displacement ellipsoids are drawn at the 50% probability level and H atoms are shown as small spheres with arbitrary radii.

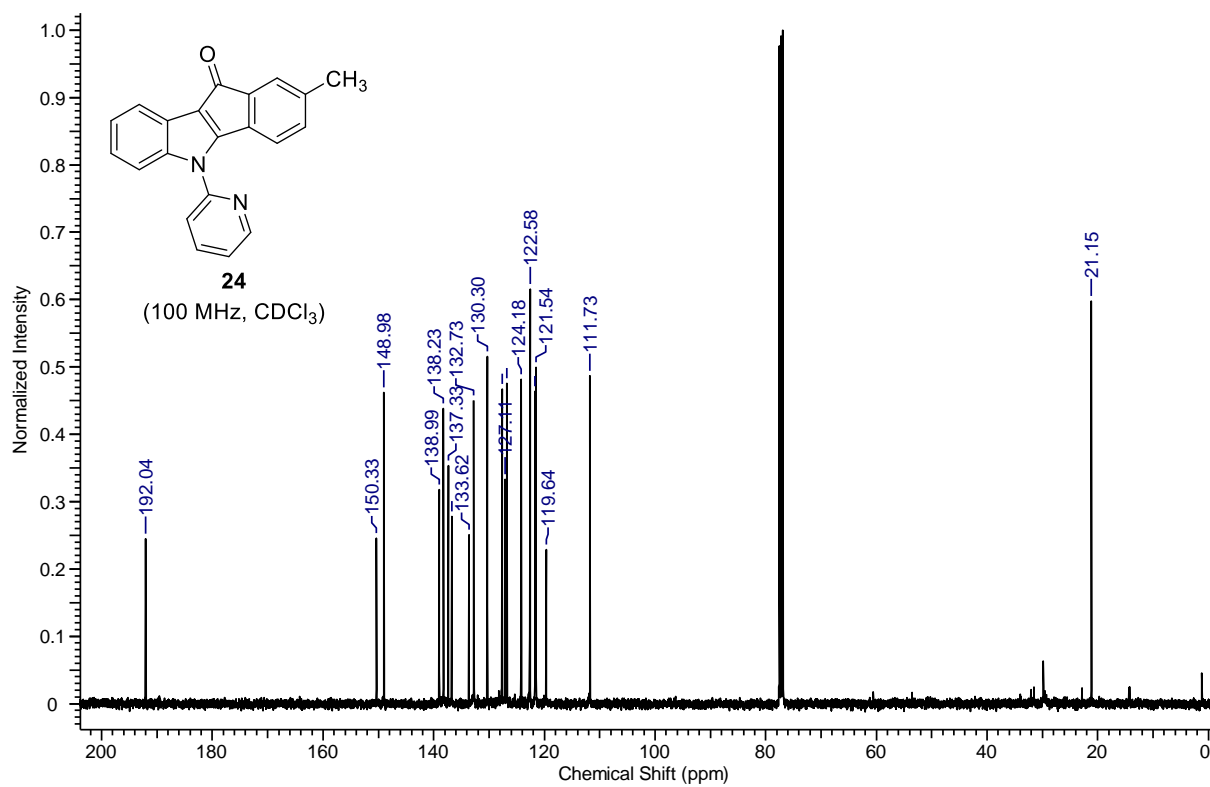
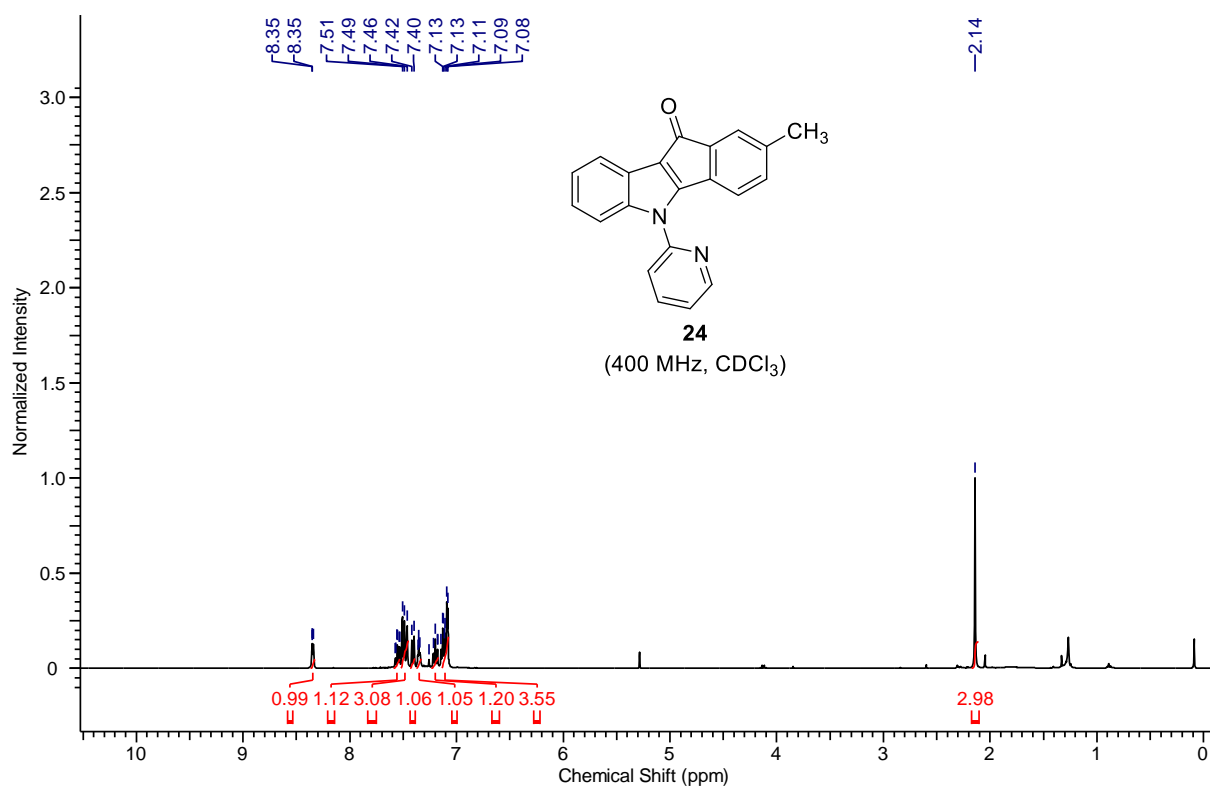
Table 2.3. Crystal data of **1**, **2**, **15**, **18** and **23**.

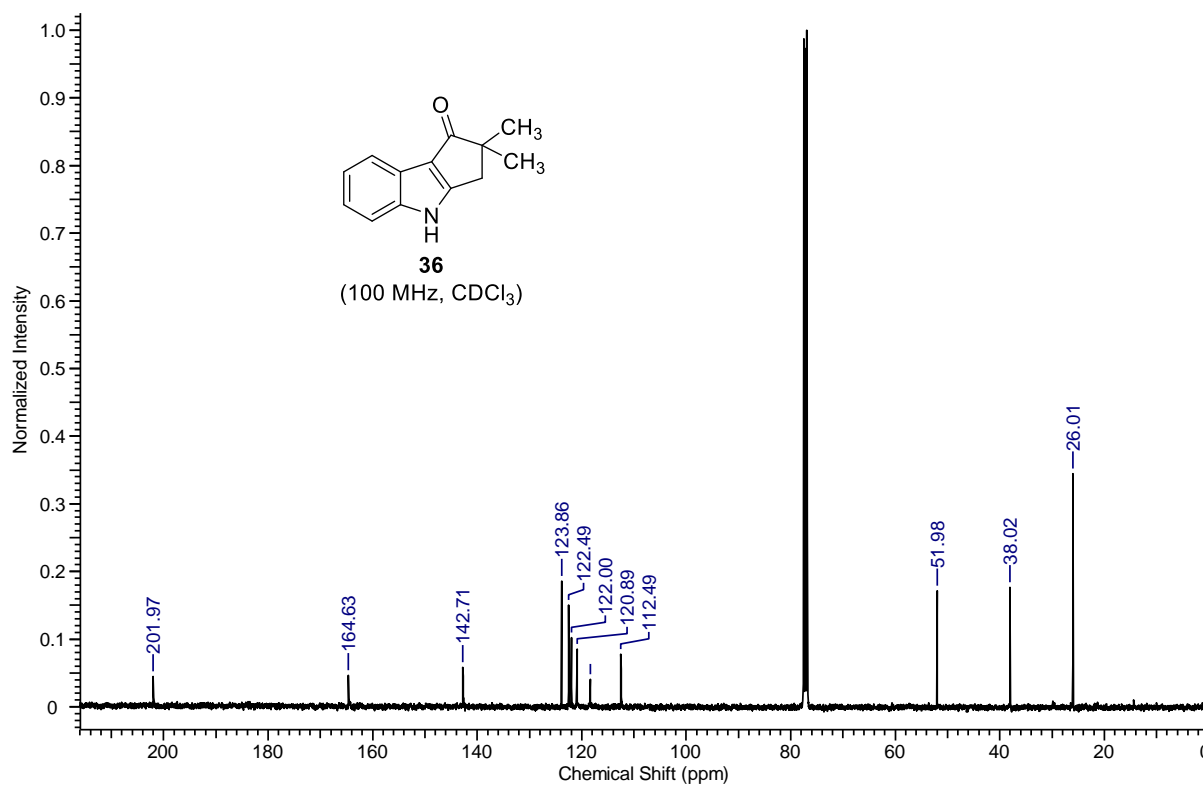
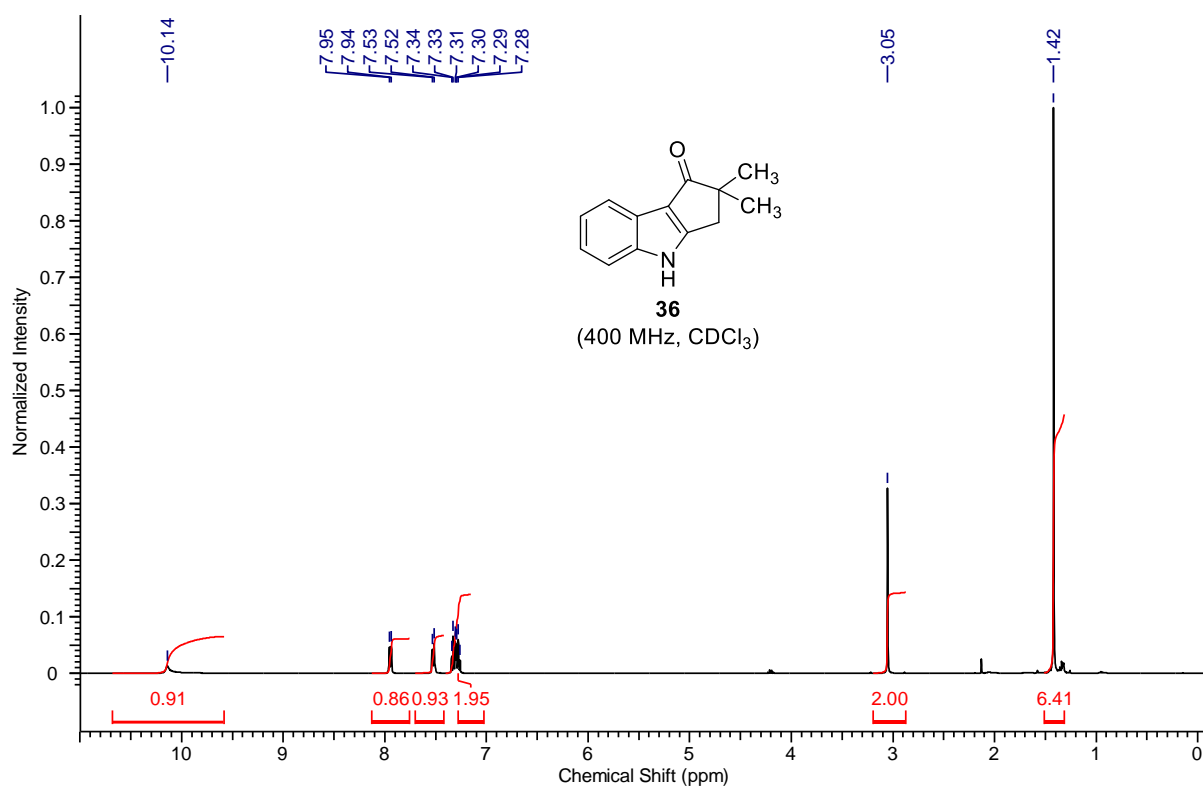
Crystal Data	1	2	15	18	23
Formula	C ₁₄ H ₁₈ N ₂ NiO ₆	C ₁₈ H ₁₆ N ₂ O	C ₂₁ H ₂₀ N ₂ O	C ₃₆ H ₃₀ N ₄ O ₂	C ₄₄ H ₃₄ N ₄ O ₂
Molecular weight	369.01	276.33	316.39	550.64	650.75
Crystal Size, mm	0.33 × 0.22 × 0.17	0.26 × 0.23 × 0.10	0.15 × 0.12 × 0.11	0.32 × 0.27 × 0.25	0.32 × 0.21 × 0.17
Temp. (K)	100(2)	301(2)	298(2)	100(2)	100(2)
Wavelength (Å)	1.54178	0.71073	0.71073	0.71073	0.71073
Crystal Syst.	monoclinic	triclinic	monoclinic	monoclinic	monoclinic
Space Group	<i>C2/c</i>	<i>P-1</i>	<i>P2₁/c</i>	<i>P2₁/c</i>	<i>P2₁/c</i>
<i>a</i> (Å)	15.2287(7)	10.1004(14)	10.5707(12)	16.7476(11)	15.6752(9)
<i>b</i> (Å)	12.7164(5)	10.7210(13)	14.0848(15)	9.0897(5)	13.0378(8)
<i>c</i> (Å)	8.0895(3)	13.770(2)	22.353(2)	18.6802(12)	17.6651(12)
α (°)	90	89.487(4)	90	90	90
β (°)	92.8820(10)	78.138(5)	94.915(4)	96.740(2)	110.456(2)
γ (°)	90	80.183(4)	90	90	90
<i>V</i> /Å ³	1564.58(11)	1437.4(3)	3315.8(6)	2824.0(3)	3382.6(4)
<i>Z</i>	4	4	8	4	4
<i>D</i> _{calc} /g cm ⁻³	1.567	1.277	1.268	1.295	1.278
μ /mm ⁻¹	2.097	0.080	0.079	0.082	0.079
<i>F</i> (000)	768	584	1344	1160	1368
<i>Ab. Correct.</i>	multi-scan	multi-scan	multi-scan	multi-scan	multi-scan
<i>T</i> _{min} / <i>T</i> _{max}	0.545/0.717	0.979/0.992	0.988/0.991	0.974/0.980	0.975/0.987
2 θ _{max}	150.0	56.0	56.0	60.0	60.0
Total reflns.	20123	83501	54791	87933	102423
Unique reflns.	1597	6934	7978	8236	9868
Obs. reflns.	1551	4194	5089	6352	7421
<i>h</i> , <i>k</i> , <i>l</i> (min, max)	(-18, 18), (-15, 15), (-10, 10)	(-13, 13), (-14, 14), (-18, 18)	(-13, 13), (-18, 18), (-29, 29)	(-23, 23), (-12, 12), (-26, 26)	(-22, 22), (-18, 18), (-24, 24)
<i>R</i> _{int} / <i>R</i> _{sig}	0.0592/0.0216	0.0944/0.0457	0.0726/0.0441	0.0757/0.0369	0.0826/0.0410
No. of para.	114	384	433	381	455
<i>RI</i> [<i>I</i> > 2 σ (<i>I</i>)]	0.0317	0.0654	0.0558	0.0452	0.0458
<i>wR2</i> [<i>I</i> > 2 σ (<i>I</i>)]	0.0838	0.1461	0.1221	0.1068	0.1024
<i>RI</i> [all data]	0.0323	0.1164	0.0938	0.0652	0.0687
<i>wR2</i> [all data]	0.0843	0.1759	0.1452	0.1212	0.1179
goodness-of-fit	1.089	1.039	1.069	1.031	1.018
$\Delta\rho$ _{max} , $\Delta\rho$ _{min} (eÅ ⁻³)	+0.431, -0.452	+0.242, -0.189	+0.221, -0.189	+0.413, -0.264	+0.350, -0.248
CCDC No.	2096020	2096021	2096022	2096023	2096024

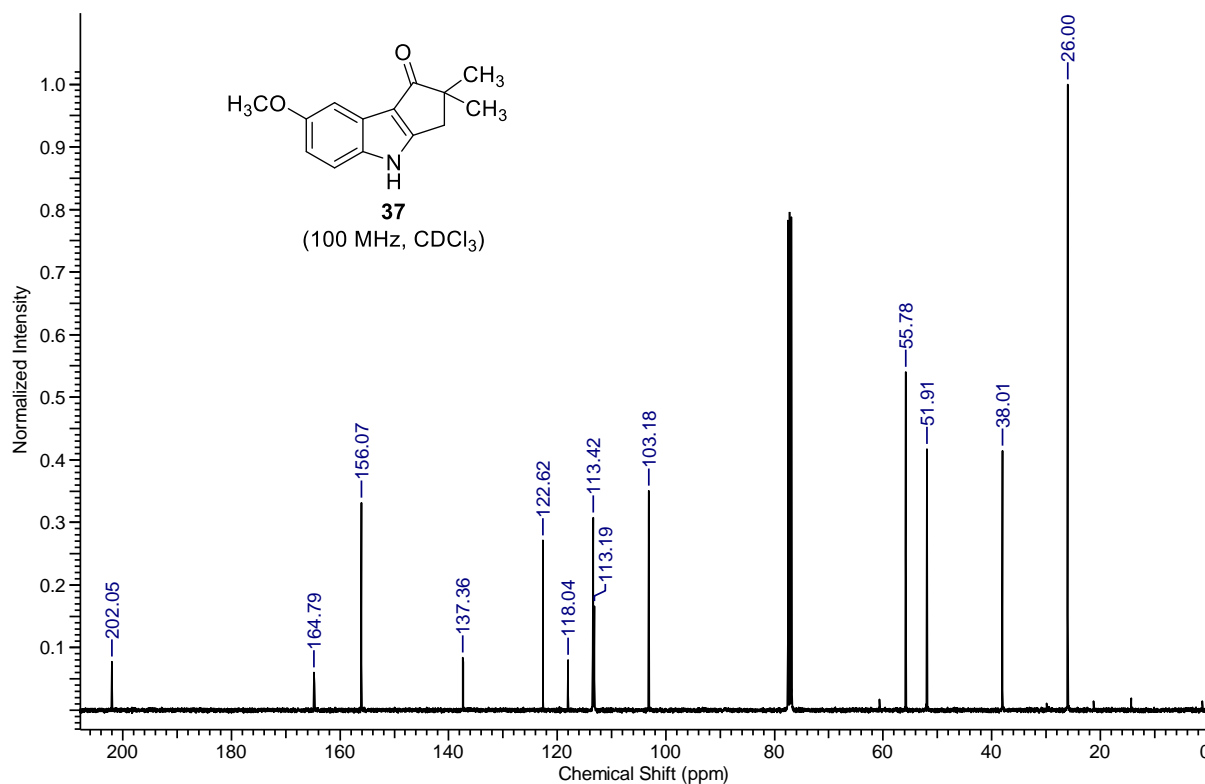
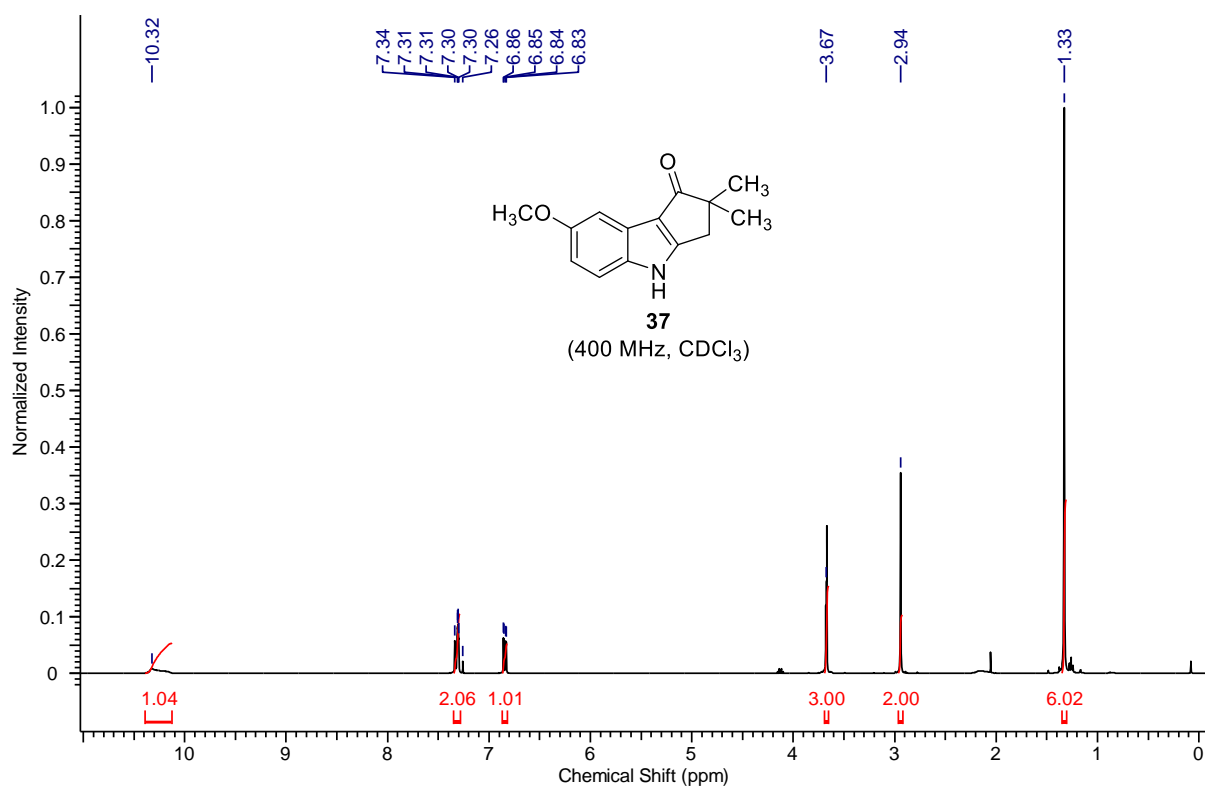
2.4.9 ^1H and ^{13}C NMR Spectra of Selected Cyclized Compounds











2.5 REFERENCES

- (1) Sundberg, R. J., *Indoles; Academic Press: San Diego* **1996**.
- (2) Horton, D. A.; Bourne, G. T.; Smythe, M. L., *Chem. Rev.* **2003**, *103*, 893-930.
- (3) Kochanowska-Karamyan, A. J.; Hamann, M. T., *Chem. Rev.* **2010**, *110*, 4489-4497.
- (4) Sharma, V.; Kumar, P.; Pathak, D., *J. Heterocyclic Chem.* **2010**, *47*, 491-502.
- (5) Melander, R. J.; Minvielle, M. J.; Melander, C., *Tetrahedron* **2014**, *70*, 6363-6372.
- (6) Li, A., *Tetrahedron* **2015**, *71*, 3535-3762.
- (7) Bal, C.; Baldeyrou, B.; Moz, F.; Lansiaux, A.; Colson, P.; Kraus-Berthier, L.; Leonce, S.; Pierre, A.; Boussard, M.-F.; Rousseau, A.; Wierzbicki, M.; Bailly, C., *Biochem. Pharmacol.* **2004**, *68*, 1911-1922.
- (8) Boussard, M. F.; Truche, S.; Rousseau-Rojas, A.; Briss, S.; Descamps, S.; Droual, M.; Wierzbicki, M.; Ferry, G.; Audinot, V.; Delagrangue, P.; Boutin, J. A., *Eur. J. Med. Chem.* **2006**, *41*, 306-320.
- (9) Kashyap, M.; Das, D.; Preet, R.; Mohapatra, P.; Satapathy, S. R.; Siddharth, S.; Kundu, C. N.; Guchhait, S. K., *Bioorg. Med. Chem. Lett.* **2012**, *22*, 2474-2479.
- (10) Kashyap, M.; Kandekar, S.; Baviskar, A. T.; Das, D.; Preet, R.; Mohapatra, P.; Satapathy, S. R.; Siddharth, S.; Guchhait, S. K.; Kundu, C. N.; Banerjee, U. C., *Bioorg. Med. Chem. Lett.* **2013**, *23*, 934-938.
- (11) Dunlop, J.; Marquis, K. L.; Lim, H. K.; Leung, L.; Kao, J.; Cheesman, C.; Rosenzweig-Lipson, S., *CNS Drugs Rev.* **2006**, *12*, 167-177.
- (12) Chen, F. E.; Huang, J., *Chem. Rev.* **2005**, *105*, 4671-4706.
- (13) Chen, J. J.; Budelsky, A. L.; Lawton, G.; Witty, D. R., *In Progress in Medicinal Chemistry*, Elsevier: **2011**, *50*, 49-107.
- (14) Balbisi, E. A., *Int. J. Clin. Pract.* **2004**, *58*, 695-705.
- (15) Sanford, M., *CNS Drugs* **2012**, *26*, 791-811.
- (16) Bit, R. A.; Davis, P. D.; Elliott, L. H.; Harris, W.; Hill, C. H.; Keech, E.; Kumar, H.; Lawton, G.; Maw, A.; Nixon, J. S.; Vesey, D. R.; Wadsworth, J.; Wilkinson, S. E., *J. Med. Chem.* **1993**, *36*, 21-29.
- (17) Ishikura, M.; Imaizumi, K.; Katagiri, N., *Heterocycles* **2000**, *53*, 553-556.
- (18) Gallant, M.; Beaulieu, C.; Berthelette, C.; Colucci, J.; Crackower, M. A.; Dalton, C.; Denis, D.; Ducharme, Y.; Friesen, R. W.; Guay, D.; Gervais, F. o. G.; Hamel, M.; Houle, R.; Krawczyk, C. M.; Kosjek, B.; Lau, S.; Leblanc, Y;

- Lee, E. E.; Levesque, J. F. o.; Mellon, C.; Molinaro, C.; Mullet, W.; O'Neill, G. P.; O'Shea, P.; Sawyer, N.; Sillaots, S.; Simard, D.; Slipetz, D.; Stocco, R.; Sørensen, D.; Truong, V. L.; Wong, E.; Wu, J.; Zaghdane, H.; Wang, Z., *Bioorg. Med. Chem. Lett.* **2011**, *21*, 288-293.
- (19) Levesque, J. F. o.; Day, S. H.; Chauret, N.; Seto, C.; Trimble, L.; Bateman, K. P.; Silva, J. M.; Berthelette, C.; Lachance, N.; Boyd, M.; Li, L.; Sturino, C. F.; Wang, Z.; Zamboni, R.; Young, R. N.; Nicoll-Griffith, D. A., *Bioorg. Med. Chem. Lett.* **2007**, *17*, 3038-3043.
- (20) Nicoll-Griffith, D. A.; Seto, C.; Aubin, Y.; Levesque, J. F. o.; Chauret, N.; Day, S.; Silva, J. M.; Trimble, L. A.; Truchon, J. F. o.; Berthelette, C.; Lachance, N.; Wang, Z.; Sturino, C.; Braun, M.; Zamboni, R.; Young, R. N., *Bioorg. Med. Chem. Lett.* **2007**, *17*, 301-304.
- (21) Ratni, H.; Blum-Kaelin, D.; Dehmlow, H.; Hartman, P.; Jablonski, P.; Masciadri, R.; Maugeais, C.; Patiny-Adam, A.; Panday, N.; Wright, M., *Bioorg. Med. Chem. Lett.* **2009**, *19*, 1654-1657.
- (22) Talaz, O.; Gülçin, I.; Göksu, S.; Saracoglu, N., *Bioorg. Med. Chem.* **2009**, *17*, 6583-6589.
- (23) Sandtorv, A. H., *Adv. Synth. Catal.* **2015**, *357*, 2403-2435.
- (24) Leitch, J. A.; Bhonoah, Y.; Frost, C. G., *ACS Catal.* **2017**, *7*, 5618-5627.
- (25) Jagtap, R. A.; Punji, B., *Asian J. Org. Chem.* **2020**, *9*, 326-342.
- (26) Li, G.; Wang, E.; Chen, H.; Li, H.; Liu, Y.; Wang, P. G., *Tetrahedron* **2008**, *64*, 9033-9043.
- (27) Haag, B. A.; Zhang, Z. G.; Li, J. S.; Knochel, P., *Angew. Chem. Int. Ed.* **2010**, *49*, 9513-9516.
- (28) Yokosaka, T.; Nakayama, H.; Nemoto, T.; Hamada, Y., *Org. Lett.* **2013**, *15*, 2978-2981.
- (29) Liu, J.; Chen, M.; Zhang, L.; Liu, Y., *Chem. Eur. J.* **2015**, *21*, 1009-1013.
- (30) Reddy, A. G. K.; Satyanarayana, G., *Synthesis* **2015**, *47*, 1269-1279.
- (31) Thalji, R. K.; Ellman, J. A.; Bergman, R. G., *J. Am. Chem. Soc.* **2004**, *126*, 7192-7193.
- (32) Harada, H.; Thalji, R. K.; Bergman, R. G.; Ellman, J. A., *J. Org. Chem.* **2008**, *73*, 6772-6779.
- (33) Bandini, M.; Eichholzer, A., *Angew. Chem. Int. Ed.* **2009**, *48*, 9533-9537.

-
- (34) Cera, G.; Crispino, P.; Monari, M.; Bandini, M., *Chem. Commun.* **2011**, *47*, 7803-7805.
- (35) Wu, Q. F.; Zheng, C.; You, S. L., *Angew. Chem. Int. Ed.* **2012**, *51*, 1680-1683.
- (36) Ding, Z.; Yoshikai, N., *Angew. Chem., Int. Ed.* **2013**, *52*, 8574-8578.
- (37) Shibata, T.; Ryu, N.; Takano, H., *Adv. Synth. Catal.* **2015**, *357*, 1131-1135.
- (38) Zhao, F.; Li, N.; Zhu, Y. F.; Han, Z. Y., *Org. Lett.* **2016**, *18*, 1506-1509.
- (39) Yang, X.; Li, Y.; Kong, L.; Li, X., *Org. Lett.* **2018**, *20*, 1957-1960.
- (40) Grugel, C. P.; Breit, B., *Org. Lett.* **2019**, *21*, 5798-5802.
- (41) Diesel, J.; Grosheva, D.; Kodama, S.; Cramer, N., *Angew. Chem. Int. Ed.* **2019**, *58*, 11044-11048.
- (42) Chernyak, N.; Tilly, D.; Li, Z.; Gevorgyan, V., *Chem. Comm.* **2010**, *46*, 150-152.
- (43) Guchhait, S. K.; Kashyap, M., *Synthesis* **2012**, *44*, 619-627.
- (44) Guchhait, S. K.; Kashyap, M.; Kandekar, S., *Tetrahedron Lett.* **2012**, *53*, 3919-3922.
- (45) Tang, T.; Jiang, X.; Wang, J. M.; Sun, Y. X.; Zhu, Y. M., *Tetrahedron* **2014**, *70*, 2999-3004.
- (46) Yeung, C. S.; Dong, V. M., *Chem. Rev.* **2011**, *111*, 1215-1292.
- (47) Li, B. J.; Shi, Z.-J., *Chem. Soc. Rev.* **2012**, *41*, 5588-5598.
- (48) Girard, S. A.; Knauber, T.; Li, C. J., *Angew. Chem. Int. Ed.* **2014**, *53*, 74-100.
- (49) Liu, C.; Yuan, J.; Gao, M.; Tang, S.; Li, W.; Shi, R.; Lei, A., *Chem. Rev.* **2015**, *115*, 12138-12204.
- (50) Zhang, Y. F.; Shi, Z. J., *Acc. Chem. Res.* **2019**, *52*, 161-169.
- (51) Bansal, S.; Shabade, A. B.; Punji, B., *Adv. Synth. Catal.* **2021**, *363*, 1998-2022.
- (52) Yan, S. Y.; Zhang, Z. Z.; Shi, B. F., *Chem. Commun.* **2017**, *53*, 10287-10290.
- (53) Gandeepan, P.; Koeller, J.; Ackermann, L., *ACS Catal.* **2017**, *7*, 1030-1034.
- (54) Khake, S. M.; Soni, V.; Gonnade, R. G.; Punji, B., *Chem. Eur. J.* **2017**, *23*, 2907-2914.
- (55) Cabrero-Antonino, J. R.; Adam, R.; Junge, K.; Beller, M., *Chem. Sci.* **2017**, *8*, 6439-6450.
- (56) Wang, C.; Rueping, M., *ChemCatChem* **2018**, *10*, 2681-2685.
- (57) Soni, V.; Sharma, D. M.; Punji, B., *Chem. Asian J.* **2018**, *13*, 2516-2521.
- (58) Pandey, D. K.; Ankade, S. B.; Ali, A.; Vinod, C. P.; Punji, B., *Chem. Sci.* **2019**, *10*, 9493-9500.
-

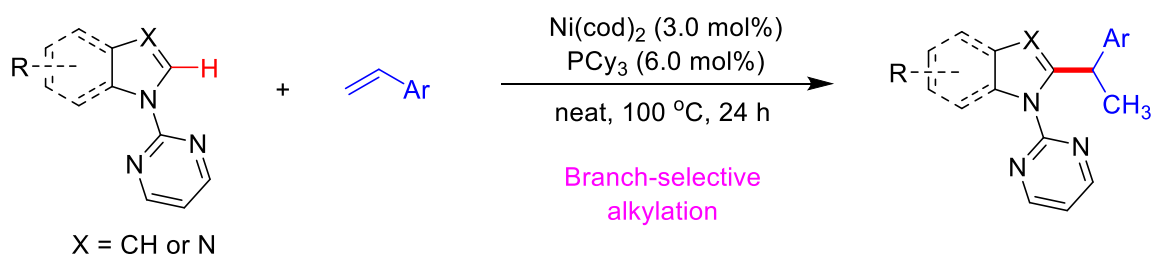
-
- (59) Li, T.; Yang, Y.; Li, B.; Yang, P., *Chem. Commun.* **2019**, *55*, 353-356.
- (60) Banjare, S. K.; Nanda, T.; Ravikumar, P. C., *Org. Lett.* **2019**, *21*, 8138-8143.
- (61) Jagtap, R. A.; Vinod, C. P.; Punji, B., *ACS Catal.* **2019**, *9*, 431-441.
- (62) Jagtap, R. A.; Verma, S. K.; Punji, B., *Org. Lett.* **2020**, *22*, 4643-4647.
- (63) Jagtap, R. A.; Samal, P. P.; Vinod, C. P.; Krishnamurty, S.; Punji, B., *ACS Catal.* **2020**, *10*, 7312-7321.
- (64) Kalepu, J.; Gandeepan, P.; Ackermann, L.; Pilarski, L. T., *Chem. Sci.* **2018**, *9*, 4203-4216.
- (65) Shah, T. A.; De, P. B.; Pradhan, S.; Punniyamurthy, T., *Chem. Commun.* **2019**, *55*, 572-587.
- (66) Gandeepan, P.; Müller, T.; Zell, D.; Cera, G.; Warratz, S.; Ackermann, L., *Chem. Rev.* **2019**, *119*, 2192-2452.
- (67) Nishino, M.; Hirano, K.; Satoh, T.; Miura, M., *Angew. Chem. Int. Ed.* **2012**, *51*, 6993-6997.
- (68) Tan, G.; He, S.; Huang, X.; Liao, X.; Cheng, Y.; You, J., *Angew. Chem. Int. Ed.* **2016**, *55*, 10414-10418.
- (69) Cheng, Y.; Wu, Y.; Tan, G.; You, J., *Angew. Chem. Int. Ed.* **2016**, *55*, 12275-12279.
- (70) Zhang, C.; Tang, C.; Jiao, N., *Chem. Soc. Rev.* **2012**, *41*, 3464-3484.
- (71) Miao, J.; Ge, H., *Eur. J. Org. Chem.* **2015**, *2015*, 7859-7868.
- (72) Maheswari, C. U.; Gadde, S. K.; Kallu, R. R., *Curr. Org. Chem.* **2016**, *20*, 512-579.
- (73) Arun, V.; Mahanty, K.; Sarkar, S. D., *ChemCatChem* **2019**, *11*, 2243-2259.
- (74) Yang, F.; Li, J.; Xie, J.; Huang, Z. Z., *Org. Lett.* **2010**, *12*, 5214-5217.
- (75) Zhang, H. J.; Su, F.; Wen, T. B., *J. Org. Chem.* **2015**, *80*, 11322-11329.
- (76) Tan, G.; Zhang, L.; Liao, X.; Shi, Y.; Wu, Y.; Yang, Y.; You, J., *Org. Lett.* **2017**, *19*, 4830-4833.
- (77) Wang, X.; Xie, P.; Qiu, R.; Zhu, L.; Liu, T.; Li, Y.; Iwasaki, T.; Au, C. T.; Xu, X.; Xia, Y.; Yin, S. F.; Kambe, N., *Chem. Commun.* **2017**, *53*, 8316-8319.
- (78) Aihara, Y.; Tobisu, M.; Fukumoto, Y.; Chatani, N., *J. Am. Chem. Soc.* **2014**, *136*, 15509-15512.
- (79) Jin, L. K.; Wan, L.; Feng, J.; Cai, C., *Org. Lett.* **2015**, *17*, 4726-4729.
- (80) Soni, V.; Khake, S. M.; Punji, B., *ACS Catal.* **2017**, *7*, 4202-4208.

- (81) Bai, F. Y.; Li, X. T.; Zhao, H. Y.; Han, J.; Xing, Y., *J. Coord. Chem.* **2009**, *62*, 3391-3400.
- (82) Beesley, R. M.; Ingold, C. K.; Thorpe, J. F., *J. Chem. Soc., Trans.* **1915**, *107*, 1080-1106.
- (83) Shaw, B. L., *J. Am. Chem. Soc.* **1975**, *97*, 3856-3857.
- (84) Davies, D. L.; Al-Duaij, O.; Fawcett, J.; Giardiello, M.; Hilton, S. T.; Russell, D. R., *Dalton Trans.* **2003**, 4132-4138.
- (85) Simmons, E. M.; Hartwig, J. F., *Angew. Chem. Int. Ed.* **2012**, *51*, 3066-3072.
- (86) Wu, X.-L.; Zhao, Y.; Ge, H., *J. Am. Chem. Soc.* **2014**, *136*, 1789-1792.
- (87) Xu, Z.-Y.; Jiang, Y. Y.; Yu, H. Z.; Fu, Y., *Chem. Asian J.* **2015**, *10*, 2479-2483.
- (88) Luo, F. X.; Cao, Z. C.; Zhao, H. W.; Wang, D.; Zhang, Y. F.; Xu, X.; Shi, Z. J., *Organometallics* **2017**, *36*, 18-21.
- (89) Zhang, L., Yi, F., Zou, J., Qu, S., *Asian. J. chem.* **2013**, *25*, 6117-6120.
- (90) Tran, P. H.; Tran, H. N.; Hansen, P. E.; Do, M. H. N.; Le, T. N., *Molecules* **2015**, *20*, 19605-19619.
- (91) Yu, J.; Zhang, C.; Yang, X.; Su, W., *Org. Biomol. Chem.* **2019**, *17*, 4446-4451.
- (92) Zhang, Z.-W.; Xue, H.; Li, H.; Kang, H.; Feng, J.; Lin, A.; Liu, S., *Org. Lett.* **2016**, *18*, 3918-3921.
- (93) Bai, F. Y.; Li, X. T.; Zhao, H. Y.; Han, J.; Xing, Y., *J. Coord. Chem.* **2009**, *62*, 3391-3400.
- (94) Frisch, M. J.; Trucks, G. W.; Schlegel, H. B.; Scuseria, G. E.; Robb, M. A.; Cheeseman, J. R.; Scalmani, G.; Barone, V.; Mennucci, B.; Petersson, G. A.; Nakatsuji, H.; Caricato, M.; Li, X.; Hratchian, H. P.; Izmaylov, A. F.; Bloino, J.; Zheng, G.; Sonnenberg, J. L.; Hada, M.; Ehara, M.; Toyota, K.; Fukuda, R.; Hasegawa, J.; Ishida, M.; Nakajima, T.; Honda, Y.; Kitao, O.; Nakai, H.; Vreven, T.; Montgomery, J. J. A.; Peralta, J. E.; Ogliaro, F.; Bearpark, M.; Heyd, J. J.; Brothers, E.; Kudin, K. N.; Staroverov, V. N.; Kobayashi, R.; Normand, J.; Raghavachari, K.; Rendell, A.; Burant, J. C.; Iyengar, S. S.; Tomasi, J.; Cossi, M.; Rega, N.; Millam, N. J.; Klene, M.; Knox, J. E.; Cross, J. B.; Bakken, V.; Adamo, C.; Jaramillo, J.; Gomperts, R.; Stratmann, R. E.; Yazyev, O.; Austin, A. J.; Cammi, R.; Pomelli, C.; Ochterski, J. W.; Martin, R. L.; Morokuma, K.; Zakrzewski, V. G.; Voth, G. A.; Salvador, P.; Dannenberg, J. J.; Dapprich, S.; Daniels, A. D.; Farkas, Ö.; Foresman, J. B.; Ortiz, J. V.;

- Cioslowski, J.; Fox, D. J., *Gaussian 09, Revision D.01.Gaussian, Inc.:* Wallingford CT **2009**.
- (95) Perdew, J. P.; Burke, K.; Ernzerhof, M., *Phy. Rev. Lett.* **1996**, *77*, 3865-3868.
- (96) Tomasi, J.; Mennucci, B.; Cammi, R., *Chem. Rev.* **2005**, *105*, 2999-3094.
- (97) Bruker, *APEX3, SAINT and SADABS. Bruker AXS Inc.*, Madison, Wisconsin, USA. **2016**.
- (98) Sheldrick, G. M., *Acta Crystallogr.* **2008**, *A64*, 112-122.
- (99) Sheldrick, G. M., *Acta Crystallogr.* **2015**, *C71*, 3-8.
- (100) Farrugia, L. J., *J. Appl. Cryst.* **2012**, *45*, 849-854.

Chapter-3

Regioselective C–H Alkylation of Heteroarenes with Alkenes using Nickel as a Catalyst



Manuscript Communicated

3.1 INTRODUCTION

The indole is an important heterocyclic compound, which exists in various pharmaceutically important molecules and bioactive natural products, including functional materials.¹⁻⁷ Particularly, alkylated indoles are the privileged structural motifs with diverse applications in medicinal chemistry and perfumery industries as well as in functional materials.⁸⁻¹¹ The alkyl group in biologically relevant indole derivatives enhances the lipophilicity of the designed molecule that provides desired characteristic features for the drugs and agrochemicals. Classical methods for the installation of alkyl groups to the indoles and other heteroarenes are mostly based on Friedel-Crafts reaction^{12,13} or radical alkylation.¹⁴ Notably, these protocols suffer from several drawbacks, such as low selectivity, less efficiency, and limited substrate scope. The transition-metal-catalyzed cross-coupling of organometallic substrates with alkyl electrophile has been developed as an important alternative method for alkylation.^{15,16} Regioselective alkylation of indoles and related heteroarenes *via* C–H bond activation has turned up as an alternative protocol for the traditional cross-coupling reaction as this strategy avoids the use of sensitive organometallic alkyl reagents and minimizes the generation of metallic waste.¹⁷⁻¹⁹

Various alkylating reagents have been used for the alkylation of heteroarenes, including alkyl halides, alkenes, alkyl organometallic reagents, azo-alkyls, carboxylic acid derivatives, alkanes and alcohols.²⁰⁻²⁶ However, the alkylation with alkene is a straightforward and atom-economical process, which proceeds *via* hydroarylation strategy. Though a range of cheap alkenes can be used as coupling partners for the alkylation *via* hydro-functionalization, the linear *versus* branched selectivity poses a major hurdle. Significant progress was acquired by employing precious metal catalysts for the regioselective alkylation of indoles with alkenes, including iridium,²⁷ ruthenium,²⁸ and rhodium²⁹ metal catalysts. Considering the sustainability and cost advantage, the 3d metal catalysts have been extensively utilized for the alkylation of indoles with alkenes. The groups of Yoshikai,^{16,30} Prabhu,³¹ Li,³² and Ackermann³³ developed efficient protocols for the regioselective alkylation of indoles using iron and cobalt catalysts.

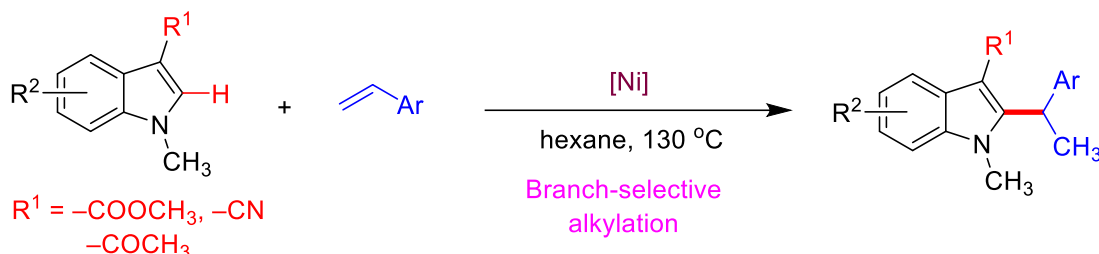
Given the advantages of Ni-catalysis in alkylation reaction, Nakao, Hartwig and co-workers demonstrated the regioselective alkylation of indoles and other heteroarenes with unactivated alkenes under nickel/*N*-heterocyclic carbene system (Scheme 3.1a).³⁴ This protocol is highly selective for the linear-selective alkylation with unactivated alkenes. Unfortunately, the aryl-substituted alkenes were unreactive under this catalytic system. The branch-selective alkylation of indoles was achieved by Nakao and Hiyama, wherein an electron-withdrawing substituent such as acetyl, ester, or cyano group at the C-3 position of

indoles is essential. (Scheme 3.1b).³⁵ Thus, this protocol is limited to the highly deficient indoles and showed limited substrate scopes. We hypothesized that a directing group-assisted strategy at the *N*-center of indoles might address these limitations and can make the process more general for the synthesis of branch-selective C-2 alkylated indoles. By this strategy, the blocking/protection of more reactive C(3)-H would not be necessary and the process can be expanded to both electron-deficient and electron-rich indole compounds. With these objectives, herein, we have developed an efficient protocol for the regioselective alkylation of indoles with alkenes providing exclusively branch alkylated products under neat conditions. The use of an easily removable directing group at the nitrogen of indoles in this reaction overcomes the limitations associated with the presented nickel-catalyzed protocol for C–H alkylation of indoles with alkenes

a) C–H alkylation with unactivated alkenes



b) C–H alkylation with aromatic alkenes



Scheme 3.1. Ni(II)-catalyzed C–H alkylation of indoles.

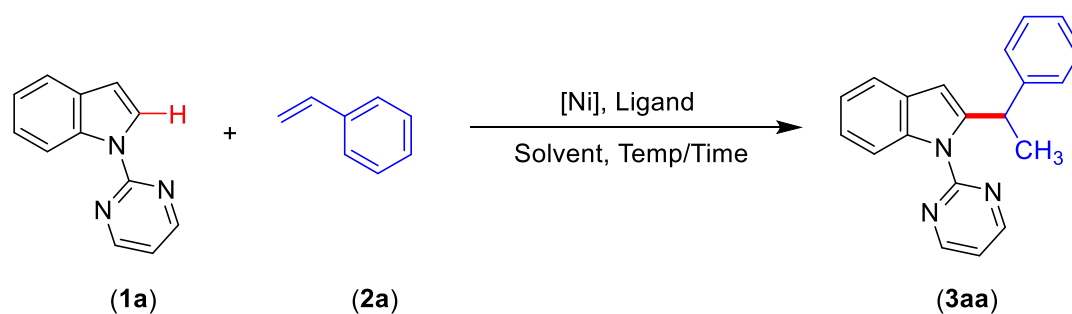
3.2 RESULTS AND DISCUSSION

3.2.1 Optimization of Reaction Conditions for C–H Alkylation

We began our investigations for the C–H alkylation of indole by using 1-(pyrimidin-2-yl)-*1H*-indole and styrene as model substrates. Initially, we screened various nickel(II) precursors such as NiCl₂, NiBr₂, Ni(OAc)₂, and Ni(OTf)₂ in hexane at 100 °C for 24 h (Table 3.1, entries 1–4). The reaction did not produce the alkylated product, however, the use of 5 mol% of Ni(cod)₂ afforded 5% of the coupled product (entry 5). Several monodentate and bidentate phosphine ligands were examined in the presence of 5 mol% of Ni(cod)₂, among

these only tri-cyclohexyl phosphine (PCy₃) provided 2-(1-phenylethyl)-1-(pyrimidin-2-yl)-1*H*-indole (**3aa**) in 95% yield (entry 8). The use of nitrogen-based ligand with Ni(cod)₂ was found as less effective in producing alkylated product with low yield. Thus, Ni(cod)₂ and PCy₃ were chosen as a suitable catalytic combination for the alkylation reaction. The screening of different solvents such as toluene, *tert*-butylbenzene, mesitylene, 1,4-dioxane, THF, and 2-MeTHF indicated the alkylation reaction smoothly occurred in toluene and hexane as a solvent. Notably, the reaction provided a quantitative yield (96%) even at 3 mol% of catalyst loading (entry 22). The reaction at a lower temperature resulted in a low yield of **3aa**, indicating the reaction requires 100 °C temperature to achieve an alkylated product in quantitative yield. Interestingly, the alkylation also proceeded efficiently under neat conditions affording desired product in 97% yield (entry 23). The nickel precursor and PCy₃ ligand are essential for this hydroarylation reaction, without which an alkylated product was not observed. This nickel-catalyzed alkylation reaction is exclusively provided the Markovnikov selective alkylated products. After, an extensive optimization, the alkylation reaction was found to occur efficiently in the presence of 3 mol% of Ni(cod)₂, and 6 mol% of PCy₃ at 100 °C under neat conditions.

Table 3.1 Optimization of reaction conditions.



Entry	[Ni] (5.0 mol%)	Ligand (10.0 mol%)	Solvent (1.0 mL)	Temp./Time (°C/h)	3aa (%) ^a
1	NiCl ₂	-	hexane	100/24	NR
2	NiBr ₂	-	hexane	100/24	NR
3	Ni(OAc) ₂	-	hexane	100/24	NR
4	Ni(OTf) ₂	-	hexane	100/24	NR
5	Ni(cod) ₂	-	hexane	100/24	5
6	Ni(cod) ₂	PMe ₃	hexane	100/24	trace

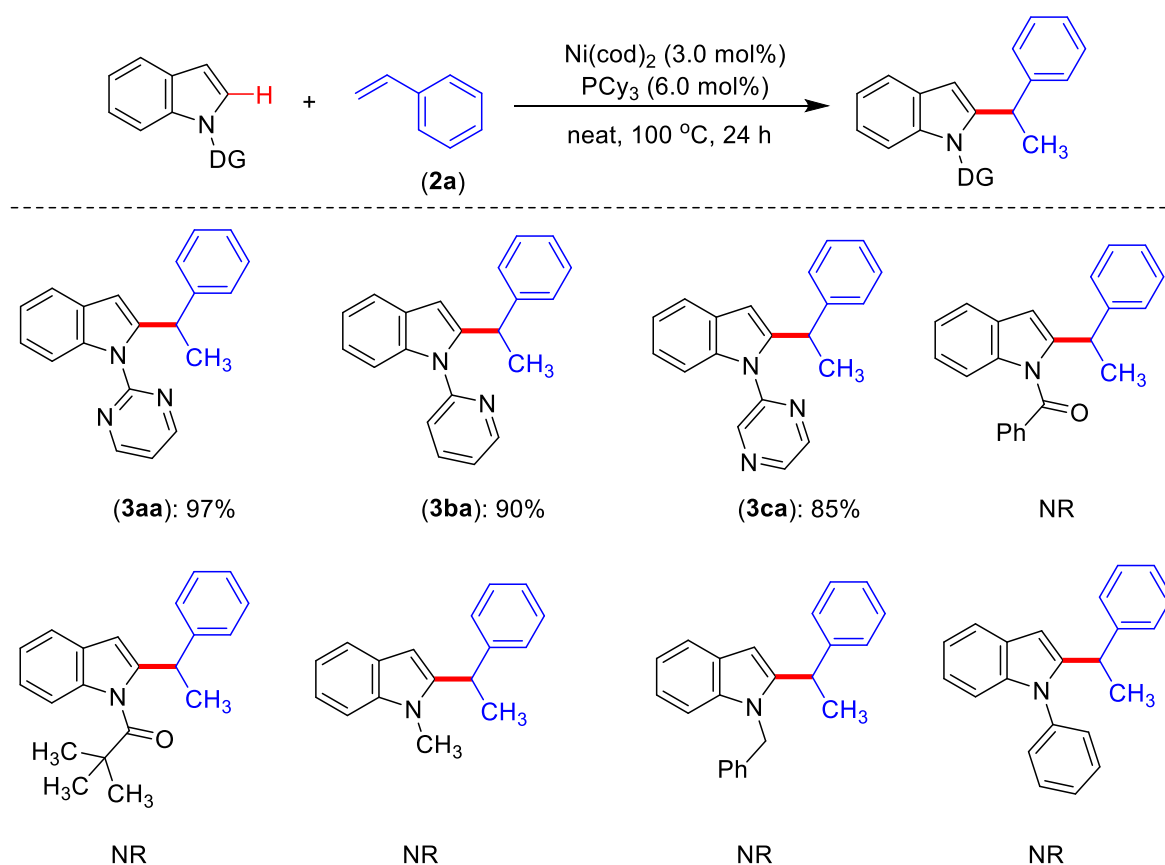
7	Ni(cod) ₂	PPh ₃	hexane	100/24	NR
8	Ni(cod) ₂	PCy ₃	hexane	100/24	97(95)
9	Ni(cod) ₂	dppf (5)	hexane	100/24	NR
10	Ni(cod) ₂	dcype (5)	hexane	100/24	trace
11	Ni(cod) ₂	xantphos (5)	hexane	100/24	NR
12	Ni(cod) ₂	dppen (5)	hexane	100/24	NR
13	Ni(cod) ₂	bpy (5)	hexane	100/24	20
14	Ni(cod) ₂	^t Bu-bpy (5)	hexane	100/24	17
15	Ni(cod) ₂	PCy ₃	toluene	100/24	96
16	Ni(cod) ₂	PCy ₃	^t BuBz	100/24	90
17	Ni(cod) ₂	PCy ₃	mesitylene	100/24	90
18	Ni(cod) ₂	PCy ₃	THF	100/24	65
19	Ni(cod) ₂	PCy ₃	2-MeTHF	100/24	60
20	Ni(cod) ₂	PCy ₃	dioxane	100/24	86
21	Ni(cod) ₂	PCy ₃	hexane	80/24	55
22 ^b	Ni(cod) ₂	PCy ₃	hexane	100/24	98 (96)
23^b	Ni(cod)₂	PCy₃	--	100/24	98 (97)
24	--	PCy ₃	--	100/16	NR

Reaction Conditions: Indole pyrimidine (**1a**, 0.058 g, 0.30 mmol), styrene (**2a**, 0.062 g, 0.60 mmol), solvent (1.0 mL). ^aIsolated yield, ^bEmploying Ni(cod)₂ (3.0 mol%), PCy₃ (6.0 mol%). NR. = No Reaction.

3.2.2. Effect of Directing Groups on C–H Alkylation

We have examined the effect of substituents at the *N*-center of indole on regioselective C–H alkylation reactions employing different *N*-substituted indoles (Scheme 3.2). The regioselective C–H alkylation of 1-(pyrimidin-2-yl)-*1H*-indole (**1a**) with styrene (**2a**) in presence of 3 mol% of Ni(cod)₂ and 6 mol% of PCy₃ provided alkylated product **3aa** in 97% yield. Similarly, the substrates 1-(pyridin-2-yl)-*1H*-indole (**1b**) and 1-(pyrazin-2-yl)-*1H*-indole (**1c**) reacted efficiently to afford alkylated products **3ba** and **3ca** in 90% and 85% yields, respectively. Unfortunately, the indole bearing –CO^tBu and –COPh group as *N*-substituent did

not provide the alkylated products, highlighting that strong σ -donor nitrogen coordination is required for this hydroarylation reaction. As expected, the 1-phenyl-*1H*-indole, 1-benzyl-*1H*-indole, and 1-methyl-*1H*-indole did not afford the desired alkylated products. All these observations indicate that the indole bearing a nitrogen donor substituent at the *N*-atom is essential for the nickel-catalyzed C–H alkylation reaction.

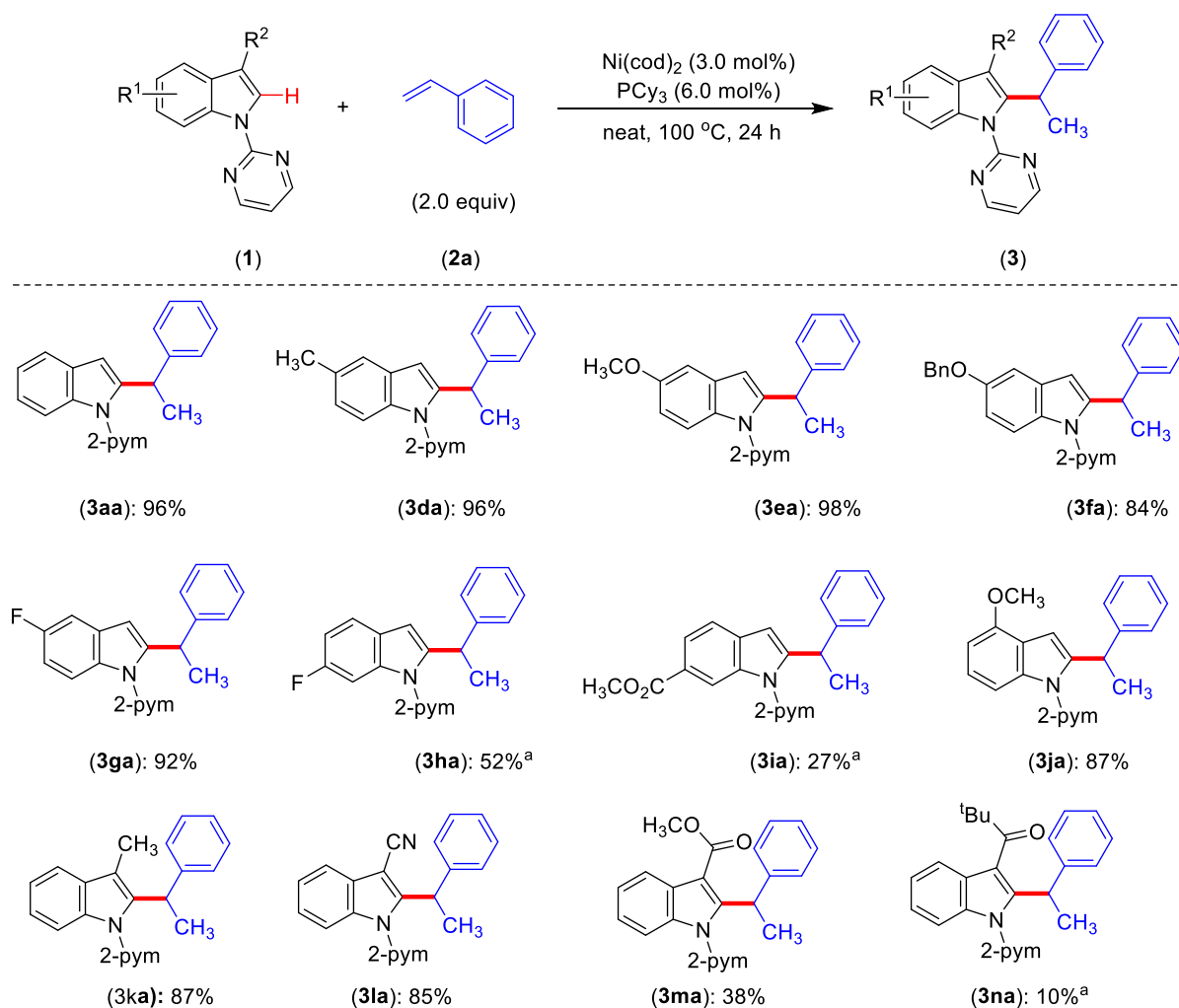


Scheme 3.2. Role of directing group on C–H alkylation reactions.

3.2.3. Substrate Scope for C–H Alkylation

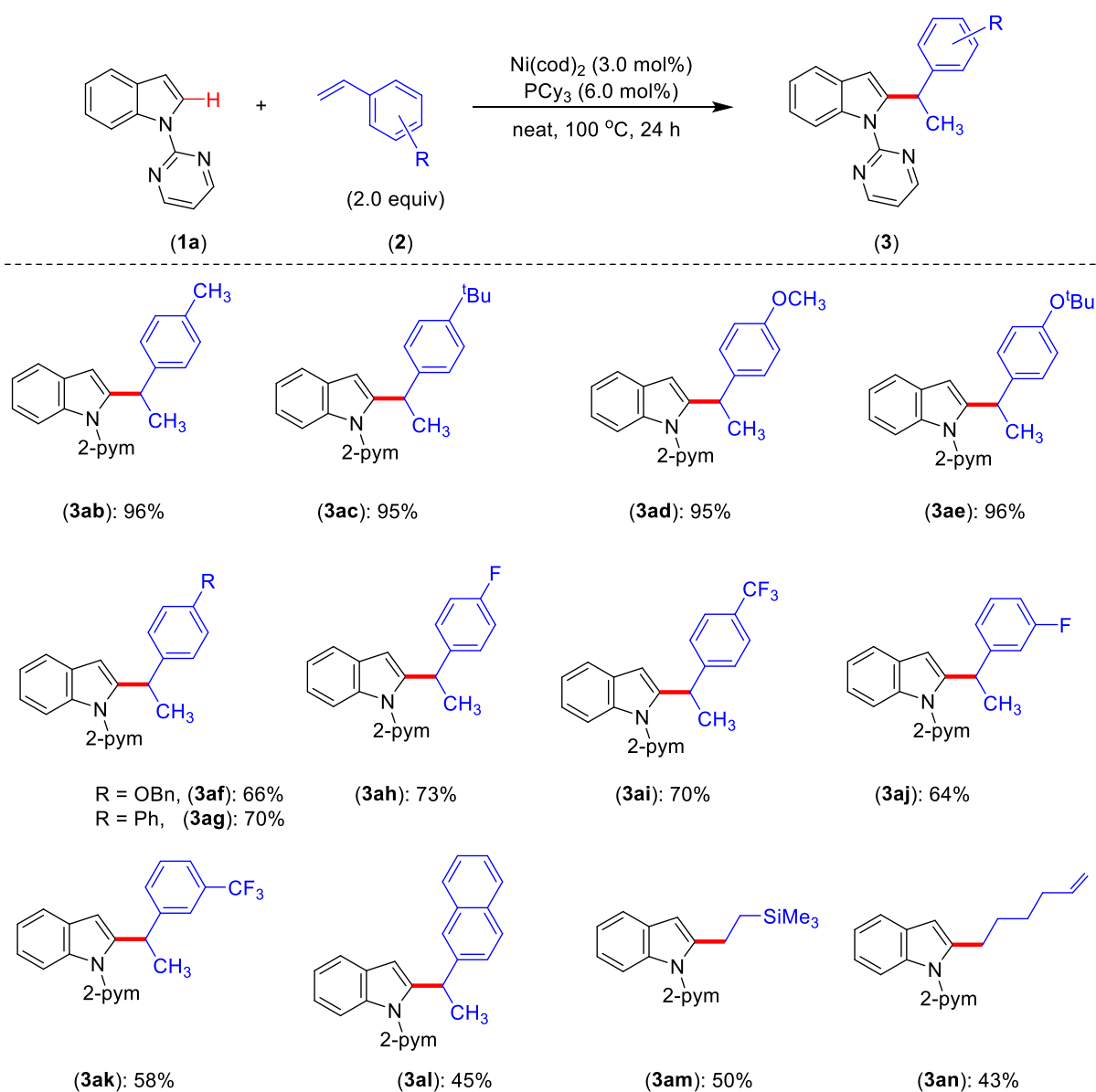
With the optimized reaction condition for the Markovnikov selective alkylation using earth-abundant nickel catalyst, the scope and limitations of alkylation reaction with various indoles were investigated (Scheme 3.3). Indoles bearing electron-donating as well as electron-withdrawing substituents at the C-5 position were well tolerated to afford the alkylated products **3da-3ga** in good to excellent yields. The C–O bond cleavage was not observed in substrates **1e** and **1f**, although Ni(0) catalysts are known to cleave aryl alkyl ethers.^{36,37} Indoles bearing halide substituents such as –Cl, and –Br did not produce the desired products, presumably due to the oxidative addition of C–X bond to Ni(0), thus, deactivating the active catalyst. The indole containing –F and –CO₂Me substituents at the C-6 position were tolerated under the reaction

condition providing **3ha** and **3ia** in moderate yields. The substrate 4-methoxy-1-(pyrimidin-2-yl)-*1H*-indole also provided the alkylated product **3ja** in 66% yield. The C-3 substituted indoles efficiently participated in the reaction providing desired products **3ka-3ma** in moderate to low yields with exclusively Markovnikov selectivity. The possible coordinating groups, such as –CN and –CO₂Me at the C-3 position of indole were also tolerated under the optimized reaction conditions. The substrate 2,2-dimethyl-1-(1-(pyrimidin-2-yl)-*1H*-indol-3-yl)propan-1-one provided the desired product **3na** in a very low yield as analyzed by GCMS. The low yield in compound **3na** is attributed to the steric hindrance of starting compound or the coordinating ability of the carbonyl group under the reaction condition. Unfortunately, the employment of indole containing –CHO group at the C-3 position did not participated in the reaction.



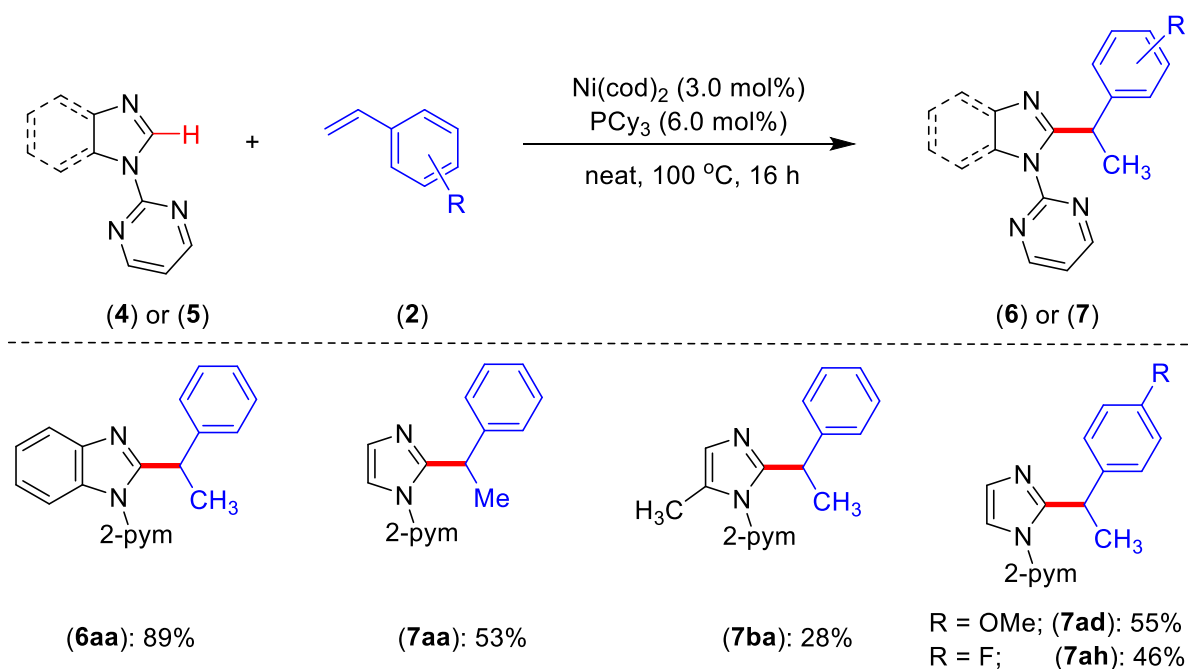
Scheme 3.3. Nickel-catalyzed branch-selective C–H alkylation of indoles. (^aYield was determined by Gas Chromatography).

Next, the scope of alkenes that proceeds *via* the hydroarylation pathway was investigated with 1-(pyrimidin-2-yl)-*1H*-indole (**1a**) under standard conditions (Scheme 3.4). Both the electron-rich and electron-poor vinylarenes have successfully participated in the alkylation reactions. Aromatic terminal alkenes containing alkyl, alkoxy and phenyl substituents at *para*-position provided alkylated products **3ab-3ag** in moderate to excellent yields. The reaction of vinylarenes bearing chloro and bromo substituents was unsuccessful because of the competitive oxidative addition of C–halide bond. Aromatic alkenes bearing pharmaceutically important groups such as –F and –CF₃ were efficiently reacted with 1-(pyrimidin-2-yl)-*1H*-indole afforded desired products **3ah-3ak** in moderate yields.



Scheme 3.4. Nickel-catalyzed hydroheteroarylation of alkenes.

The *meta*-substituted styrenes were also efficiently participated in this reaction to deliver alkylated products in quantitative yields. Particularly, an Ar–F bond was compatible with this catalytic system, even though Ni(0) catalyst is known for the aromatic C–F bond activation.³⁸⁻⁴² The employment of the substrate 2-vinylnaphthalene in this reaction provided a desired product **3al** in low yield. In addition to aromatic arenes, trimethyl(vinyl)silane was employed in this protocol to produce the linear-selective alkylated product **3am** in 91% yield. Similarly, 1,4-hexadiene was also efficiently reacted with **1a** to deliver linear alkylated product **3an** in moderate yield. The reaction exclusively occurred at one terminal alkene, another terminal alkene of 1,4-hexadiene was unreactive under the reaction conditions. Here, we assume that the regioselectivity in the nickel catalyzed hydroarylation with aryl and aliphatic alkenes were controlled by the charge transfer and Pauli repulsion, respectively.⁴³



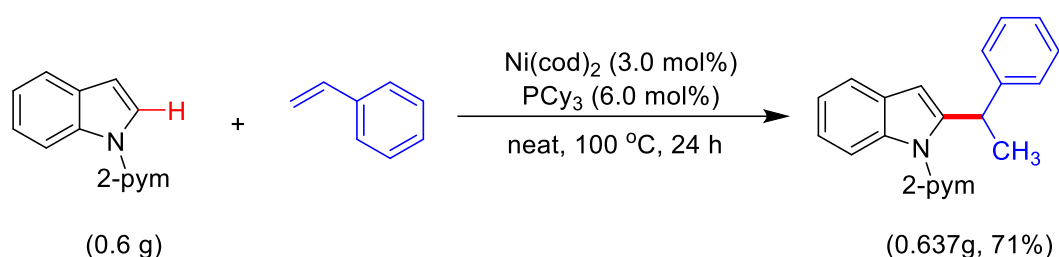
Scheme 3.5. Branch-selective C–H alkylation of azoles with vinylarenes.

The hydroarylation protocol was extended to the alkylation of azole derivatives with vinylarenes for the synthesis of diverse 1,1-(hetero)aryl ethane (Scheme 3.5). The coupling of 1-(pyrimidin-2-yl)-*1H*-benzo[d]imidazole with styrene occurred in the presence of nickel catalyst at 100 °C for 16 h under neat conditions, producing desired product **6aa** in 89% yield. Similarly, the reaction of 2-(*1H*-imidazol-1-yl)pyrimidine, and 2-(5-methyl-*1H*-imidazol-1-yl)pyrimidine provided the alkylated products **7aa** and **7ba** in 53% and 28% yield, respectively. Additionally, the coupling of vinylarenes with 2-(*1H*-imidazol-1-yl)pyrimidine was demonstrated under this catalytic system. Vinylarenes containing both the electro-donating and

electron-withdrawing groups were well tolerated under this hydroarylation protocol. Aromatic arenes, 1-methoxy-4-vinylbenzene and 1-fluoro-4-vinylbenzene were efficiently coupled with 2-(*1H*-imidazol-1-yl)pyrimidine afforded the desired products **7ad** and **7ah** in moderate yields.

3.2.4 Large Scale Synthesis of **3aa**

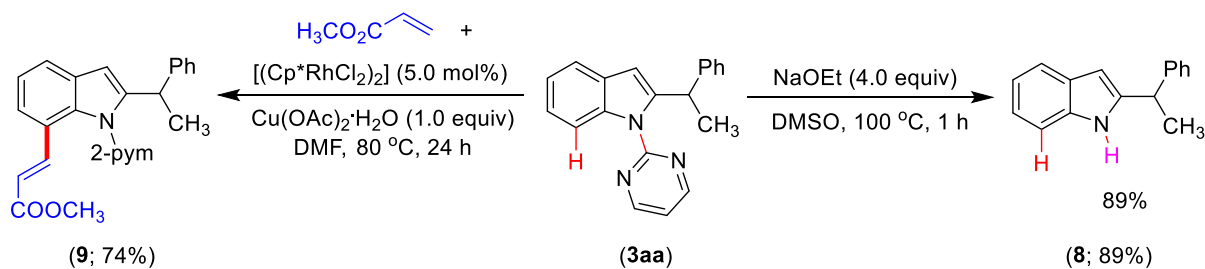
In view of excellent regioselectivity and significant importance of C-2 branch-selective alkylated indoles, we have shown the practical applicability of alkylation reaction by a 3.0 mmol scale alkylation of indole **1a** (0.6 g) with styrene afforded 0.637 g (71%) of product **3aa** under the optimal conditions suggesting the usefulness of scale-up process (Scheme 3.6).



Scheme 3.6. Large scale synthesis of **3aa**.

3.2.5 Removal of Directing Group and Functionalization

Considering the importance of functionalized free *NH* 1,1-heteroaryl-aryl ethane derivatives in pharmaceutically important compounds, we have demonstrated the removal of the 2-pyrimidinyl group from the alkylated compound. Thus, the alkylated product 2-(1-phenylethyl)-1-(pyrimidin-2-yl)-*1H*-indole (**3aa**) was treated with NaOEt at 100 °C for 1 h to afford 2-(1-phenylethyl)-*1H*-indole in 89% yield (Scheme 3.6). Further, the compound **3aa** could be functionalized at C-7 position using rhodium catalyst to deliver methyl (*E*)-3-(2-(1-phenylethyl)-1-(pyrimidin-2-yl)-*1H*-indol-7-yl)acrylate in 74% yield (Scheme 3.7).

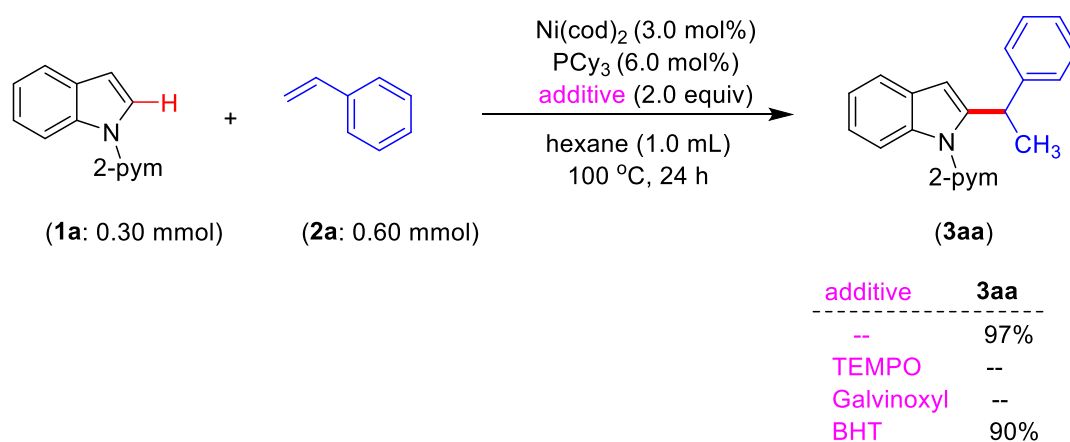


Scheme 3.7. Derivatization of compound **3aa**.

3.2.6 Mechanistic Aspects

3.2.6.1 External Additive Experiments

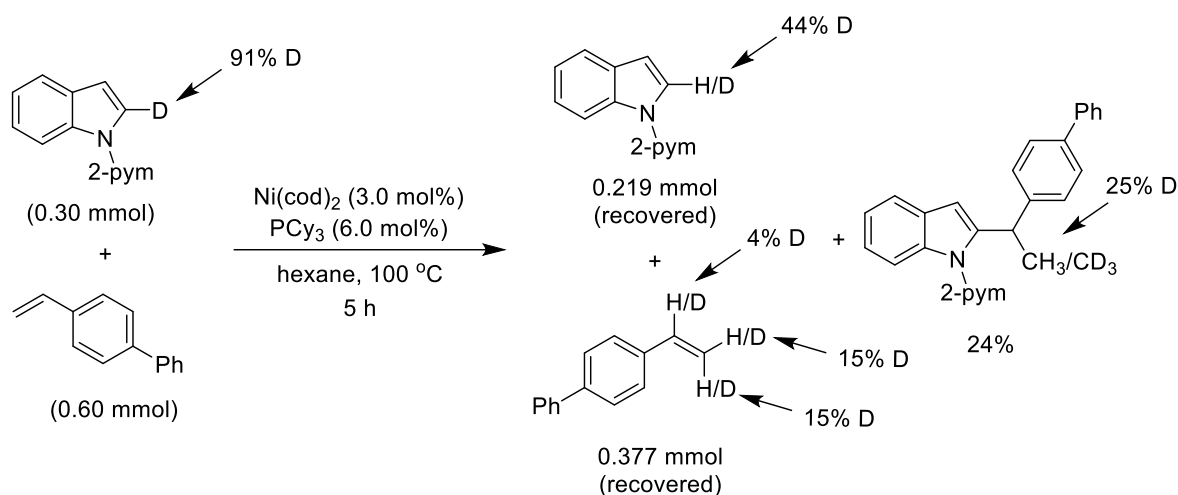
The controlled alkylation reaction with alkene has been performed to understand the reaction pathway and the participation of an active catalyst. The standard alkylation reaction proceeded smoothly in the presence of radical inhibitor BHT (butylated hydroxytoluene), whereas the reaction was completely quenched in the presence of radical scavengers such as TEMPO or galvinoxyl (Scheme 3.8). These findings indicated the involvement of radical species in this catalysis process.



Scheme 3.8. External additive experiments.

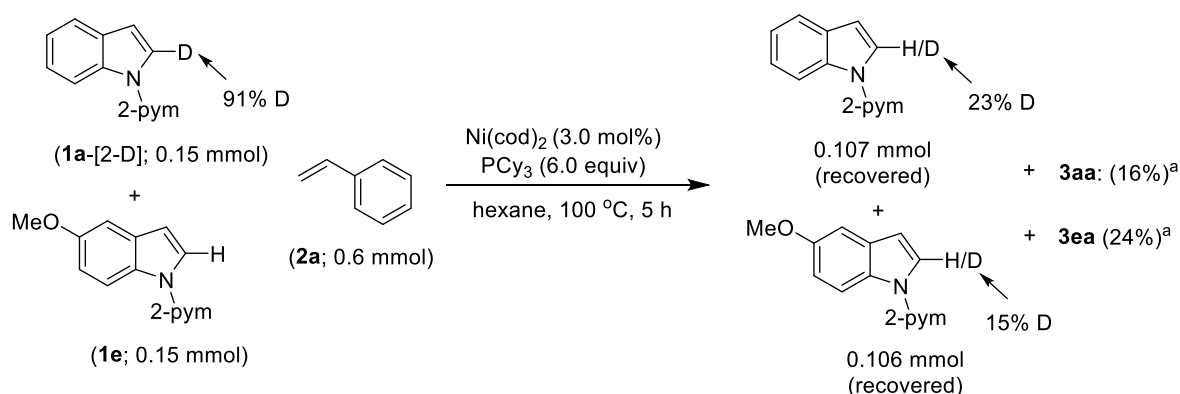
3.2.6.2 Deuterium Labeling Experiments

Controlled Experiment (Reaction of 1a-[2-D] with 2g): The controlled experiment was carried out to understand the reaction mechanism. The reaction of 1-(pyrimidin-2-yl)-1H-indole-2-d (**1a**-[2-D]) with 4-vinyl-1,1'-biphenyl (**2g**) was performed under the standard reaction conditions for 5 h (Scheme 3.9). The ¹H NMR analysis of the recovered starting compounds and alkylated product reveals that the significant H/D scrambling occurs between compound **1a**-[2D] and **2g** prior to the formation of product **3ag**. Thus, the decrease of deuterium content at C-2 position of indole (**1a**-[2-D]) was observed. Moreover, a remarkable deuterium incorporation was observed at α- and β-position of 4-vinyl-1,1'-biphenyl (**2g**). Notably, ¹H NMR analysis of product **3ag**-[H/D] shows the deuterium incorporation occurs at α-position. These results suggest that the C–H bond activation and alkene insertion step is reversible and it follows only one alkene insertion pathway during the catalytic process.



Scheme 3.9. Controlled experiment.

Further, the compounds 1-(pyrimidin-2-yl)-*1H*-indole-2-d (**1a**-[2-D]; 0.15 mmol) and 5-methoxy-1-(pyrimidin-2-yl)-*1H*-indole (**1e**; 0.15 mmol) were treated with styrene (**2a**; 0.6 mmol) under standard reaction condition at 100 °C for 5 h (Scheme 3.10). The ^1H NMR analysis of the recovered starting compound **1e** shows 15% deuterium incorporation at C-2 position, whereas compound **1a**-[2-D] shows 68% loss of deuterium content at C-2 position. This experiment highlights that the C–H bond metalation is reversible and the presence of Ni–H/Ni–D crossover in the catalytic process. Thus, we consider the hydroarylation reaction proceeds through insertion of styrene into the Ni–H bond.



Scheme 3.10. H/D scrambling experiments. (^aGC yield)

Kinetic Isotope Effect (KIE) Study: To understand whether the indole C–H bond cleavage is involved in the rate determining step, the kinetic isotope effect (KIE) study was carried out using 1-(pyrimidin-2-yl)-*1H*-indole (**1a**; 0.059 g, 0.30 mmol, 0.3 M) and [or 1-(pyrimidin-2-yl)-*1H*-indole-2-d (**1a**-[2-D]; 0.059 g, 0.30 mmol, 0.3 M)]. The initial rate

obtained for the alkylation of 1-(pyrimidin-2-yl)-*1H*-indole (**1a**) with styrene was $1.919 \times 10^{-2} \text{ Mmin}^{-1}$, whereas the rate for the alkylation of 1-(pyrimidin-2-yl)-*1H*-indole-2-d (**1a**-[D]) with styrene was $1.733 \times 10^{-2} \text{ Mmin}^{-1}$ (Figure 3.1). Therefore, the $k_H/k_D = 1.919 \times 10^{-2} / 1.733 \times 10^{-2} = 1.1$. This indicates that the C–H bond nickelation is less likely involved in the rate-determining step. These deuterium labeling experiments highlight that the C–H bond cleavage and alkene insertion steps are reversible. Thus, these result tentatively suggests the reductive elimination would be the rate-limiting step.

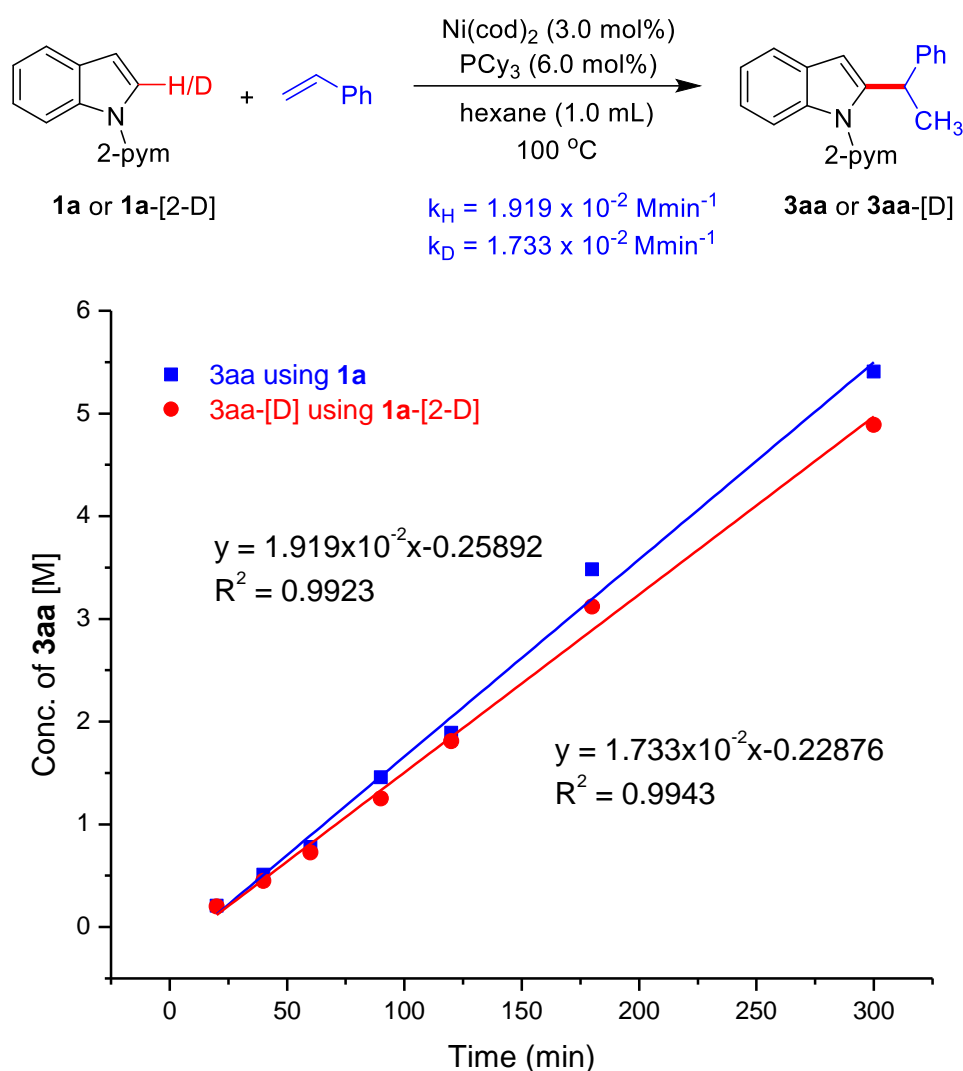


Figure 3.1. Time-dependent formation of **3aa** [or **3aa**-[D]] using **1a** and **1a**-[2-D].

3.3 CONCLUSION

In summary, we have developed an efficient protocol for the C–H alkylation of indoles with alkenes using a nickel catalyst which proceeds *via* a hydroarylation strategy and provided

exclusive branch-selective product. This protocol is applicable for both the electron-rich as well as electron-poor indoles providing desired alkylated products in moderate to excellent yields. The substrates bearing alkyl, alkoxy, fluoro, cyano, ester, and carbonyl groups were well tolerated under the reaction conditions. In addition to indoles, other heteroarenes such as imidazoles and benzimidazoles also successfully participated in this alkylation reaction. This reaction provided a direct and efficient approach for synthesizing various functionalized 1,1-diaryl ethanes under neat conditions. Furthermore, the removal of 2-pyrimidinyl directing was demonstrated to show the synthetic utility of the protocol. Preliminary mechanistic studies suggested that the alkylation reaction proceeds through a single-electron transfer (SET) pathway. The deuterium labelling experiments tentatively supports the rate limiting reductive elimination process.

3.4 EXPERIMENTAL SECTION

All the manipulations were conducted under an argon atmosphere either in a glove box or using standard Schlenk techniques in pre-dried glasswares. The catalytic reactions were performed in flame-dried reaction vessels with a Teflon screw cap. Solvents were dried over Na/benzophenone or CaH₂ and distilled prior to use. Liquid reagents were flushed with argon prior to use. All other chemicals were obtained from commercial sources and were used without further purification. High resolution mass spectrometry (HRMS) mass spectra were recorded on a Thermo Scientific Q-Exactive, Accela 1250 pump. NMR: (¹H and ¹³C) spectra were recorded at 400 or 500 MHz (¹H), 100 or 125 MHz (¹³C, DEPT (distortionless enhancement by polarization transfer)), 377 MHz (¹⁹F), respectively in CDCl₃ solutions, if not otherwise specified; chemical shifts (δ) are given in ppm. The ¹H and ¹³C NMR spectra are referenced to residual solvent signals (CDCl₃: δ H = 7.26 ppm, δ C = 77.2 ppm).

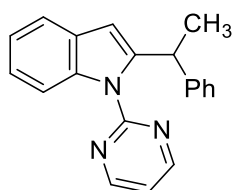
GC Method. Gas Chromatography analyses were performed using a Shimadzu GC-2010 gas chromatograph equipped with a Shimadzu AOC-20s auto sampler and a Restek RTX-5 capillary column (30 m x 0.25 mm x 0.25 μ m). The instrument was set to an injection volume of 1 μ L, an inlet split ratio of 10:1, and inlet and detector temperatures of 250 and 320 °C, respectively. UHP-grade argon was used as carrier gas with a flow rate of 30 mL/min. The temperature program used for all the analyses is as follows: 80 °C, 1 min; 30 °C/min to 200 °C, 2 min; 30 °C/min to 260 °C, 3 min; 30 °C/min to 300 °C, 15 min. Response factors for all the necessary compounds with respect to standard *n*-hexadecane were calculated from the average of three independent GC runs.

3.4.1 Representative Procedure for C–H Alkylation and Characterization Data

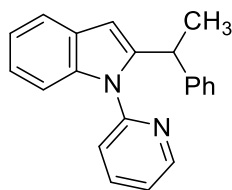
Procedure for the Synthesis of 2-(1-phenylethyl)-1-(pyrimidin-2-yl)-1H-indole (3aa):

To a flame-dried screw-cap tube equipped with magnetic stir bar were introduced 1-(pyrimidin-2-yl)-1H-indole (**1a**; 0.059 g, 0.302 mmol), styrene (**2a**; 0.063 g, 0.605 mmol), Ni(cod)₂ (0.0025 g, 0.009 mmol, 3.0 mol%), and PCy₃ (0.0050 g, 0.018 mmol, 6.0 mol%) inside the glove box. The resultant reaction mixture in the tube was immersed in a preheated oil bath at 100 °C and stirred for 24 h under neat conditions. At ambient temperature, the reaction mixture was diluted with ethyl acetate (5.0 mL). The volatiles were evaporated *in vacuo* and the remaining residue was purified by column chromatography on silica gel (petroleum ether/EtOAc: 50/1) to yield **3aa** (0.088 g, 97%) as a colorless solid.

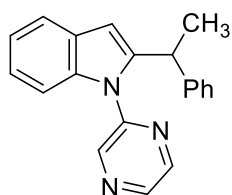
Procedure for a 3.0 mmol scale synthesis of 3aa: To a flame-dried screw-cap tube equipped with magnetic stir bar were introduced 1-(pyrimidin-2-yl)-1H-indole (**1a**; 0.60 g, 3.07 mmol), styrene (**2a**; 0.64 g, 6.14 mmol), Ni(cod)₂ (0.025 g, 0.092 mmol, 3.0 mol%), and PCy₃ (0.050 g, 0.184 mmol, 6.0 mol%) inside the glove box. The resultant reaction mixture in the tube was immersed in a preheated oil bath at 100 °C and stirred for 24 h under neat conditions. At ambient temperature, the reaction mixture was diluted with ethyl acetate (5.0 mL). The volatiles were evaporated *in vacuo* and the remaining residue was purified by column chromatography on silica gel (petroleum ether/EtOAc: 50/1) to yield **3aa** (0.637 g, 71%) as a colorless solid.



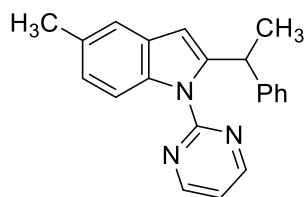
Characterization Data of 3aa. ¹H-NMR (500 MHz, CDCl₃): δ = 8.61 (d, *J* = 4.7 Hz, 2H, Ar–H), 8.03–8.00 (m, 1H, Ar–H), 7.61–7.58 (m, 1H, Ar–H), 7.23–7.16 (m, 2H, Ar–H), 7.08–7.05 (m, 2H, Ar–H), 7.01–6.95 (m, 4H, Ar–H), 6.68 (s, 1H, Ar–H), 5.26 (q, *J* = 7.1 Hz, 1H, CH), 1.66 (d, *J* = 7.2 Hz, 3H, CH₃). ¹³C{¹H}-NMR (125 MHz, CDCl₃): δ = 158.1 (1C, C_q; 2C, CH), 145.7 (C_q) 145.0 (C_q), 137.6 (C_q) 128.9 (C_q), 128.2 (2C, CH), 127.6 (2C, CH), 125.9 (CH), 123.0 (CH), 121.8 (CH), 120.2 (CH), 117.3 (CH), 113.2 (CH), 105.6 (CH), 38.6 (CH), 22.6 (CH₃). HRMS (ESI): *m/z* Calcd for C₂₀H₁₇N₃ + H⁺ [M + H]⁺ 300.1495; Found 300.1499.



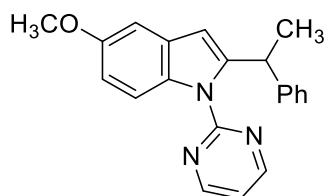
2-(1-Phenylethyl)-1-(pyridin-2-yl)-1H-indole (3ba): The representative procedure was followed, using 1-(pyridin-2-yl)-1H-indole (**1b**; 0.059 g, 0.303 mmol) and styrene (**2a**; 0.063 g, 0.605 mmol). Purification by column chromatography on silica gel (petroleum ether/EtOAc: 50/1) yielded **3ba** (0.082 g, 90%) as a light yellow liquid. $^1\text{H-NMR}$ (400 MHz, CDCl_3): δ = 8.61 (d, J = 4.7 Hz, 1H, Ar-H), 7.70 (d, J = 7.6 Hz, 1H, Ar-H), 7.60 (td, J = 7.7, 1.9 Hz, 1H, Ar-H), 7.23-7.14 (m, 4H, Ar-H), 7.10-7.04 (m, 3H, Ar-H), 6.98 (d, J = 8.0 Hz, 1H, Ar-H), 6.89-6.87 (m, 2H, Ar-H), 6.74 (s, 1H, Ar-H), 4.69 (q, J = 7.0 Hz, 1H, CH), 1.71 (d, J = 7.2 Hz, 3H, CH_3). $^{13}\text{C}\{^1\text{H}\}$ -NMR (100 MHz, CDCl_3): δ = 151.4 (C_q), 149.4 (CH), 145.1 (2C, C_q), 138.1 (CH), 137.9 (C_q), 128.3 (C_q), 128.1 (2C, CH), 127.4 (2C, CH), 126.0 (CH), 122.2 (CH), 122.1 (CH), 122.0 (CH), 120.6 (CH), 120.4 (CH), 109.9 (CH), 101.9 (CH), 37.8 (CH), 22.0 (CH_3). HRMS (ESI): m/z Calcd for $\text{C}_{21}\text{H}_{18}\text{N}_2 + \text{H}^+$ [M + H] $^+$ 299.1546; Found 299.1543.



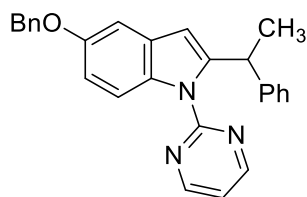
2-(1-Phenylethyl)-1-(pyrazin-2-yl)-1H-indole (3ca): The representative procedure was followed, using 1-(pyrazin-2-yl)-1H-indole (**1c**; 0.059 g, 0.302 mmol) and styrene (**2a**; 0.063 g, 0.605 mmol). Purification by column chromatography on silica gel (petroleum ether/EtOAc: 50/1) yielded **3ca** (0.076 g, 85%) as a colorless solid. $^1\text{H-NMR}$ (500 MHz, CDCl_3): δ = 8.48-8.47 (m, 1H, Ar-H), 8.39 (d, J = 2.5 Hz, 1H, Ar-H), 8.30 (d, J = 1.4 Hz, 1H, Ar-H), 7.67-7.64 (m, 1H, Ar-H), 7.22 (s, 1H, Ar-H), 7.18-7.14 (m, 2H, Ar-H), 7.05-6.99 (m, 3H, Ar-H), 6.80-6.78 (m, 2H, Ar-H), 6.75 (s, 1H, Ar-H), 4.56 (q, J = 7.0 Hz, 1H, CH), 1.66 (d, J = 7.1 Hz, 3H, CH_3). $^{13}\text{C}\{^1\text{H}\}$ -NMR (125 MHz, CDCl_3): δ = 148.3 (C_q), 144.9 (C_q), 144.7 (C_q), 143.5 (2C, CH), 142.4 (CH), 137.9 (C_q), 128.5 (C_q), 128.4 (2C, CH), 127.2 (2C, CH), 126.4 (CH), 122.7 (CH), 121.3 (CH), 120.7 (CH), 109.6 (CH), 103.4 (CH), 37.9 (CH), 22.0 (CH_3). HRMS (ESI): m/z Calcd for $\text{C}_{17}\text{H}_{20}\text{N}_2 + \text{H}^+$ [M+H] $^+$ 300.1495; Found 300.1499.



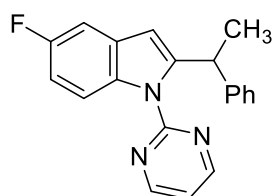
5-Methyl-2-(1-phenylethyl)-1-(pyrimidin-2-yl)-1H-indole (3da): The representative procedure was followed, using 5-methyl-1-(pyrimidin-2-yl)-1H-indole (**1d**; 0.063 g, 0.301 mmol) and styrene (**2a**; 0.063 g, 0.602 mmol). Purification by column chromatography on silica gel (petroleum ether/EtOAc: 50/1) yielded **3da** (0.090 g, 96%) as a colorless liquid. $^1\text{H-NMR}$ (400 MHz, CDCl_3): δ = 8.62 (d, J = 4.9 Hz, 2H, Ar-H), 8.01 (d, J = 8.5 Hz, 1H, Ar-H), 7.44 (s, 1H, Ar-H), 7.14-7.02 (m, 6H, Ar-H), 6.95 (t, J = 4.8 Hz, 1H, Ar-H), 6.67 (s, 1H, Ar-H), 5.33 (q, J = 7.1 Hz, 1H, CH), 2.50 (s, 3H, CH_3), 1.71 (d, J = 7.1 Hz, 3H, CH_3). $^{13}\text{C}\{^1\text{H}\}$ -NMR (100 MHz, CDCl_3): δ = 158.2 (C_q), 157.9 (2C, CH) 145.8 (C_q), 145.0 (C_q), 135.9 (C_q), 131.1 (C_q), 129.2 (C_q), 128.2 (2C, CH), 127.6 (2C, CH), 125.9 (CH), 124.4 (CH), 120.1 (CH), 116.9 (CH), 113.2 (CH), 105.5 (CH), 38.7 (CH), 22.7 (CH_3), 21.5 (CH_3). HRMS (ESI): m/z Calcd for $\text{C}_{21}\text{H}_{19}\text{N}_3+\text{H}^+$ $[\text{M}+\text{H}]^+$ 314.1652; Found 314.1654.



5-Methoxy-2-(1-phenylethyl)-1-(pyrimidin-2-yl)-1H-indole (3ea): The representative procedure was followed, using 5-methoxy-1-(pyrimidin-2-yl)-1H-indole (**1e**; 0.068 g, 0.302 mmol) and styrene (**2a**; 0.063 g, 0.605 mmol). Purification by column chromatography on silica gel (petroleum ether/EtOAc: 30/1) yielded **3ea** (0.097 g, 98%) as a brown solid. $^1\text{H-NMR}$ (500 MHz, CDCl_3): δ = 8.60 (d, J = 4.9 Hz, 2H, Ar-H), 8.05 (d, J = 9.0 Hz, 1H, Ar-H), 7.14-7.10 (m, 3H, Ar-H), 7.05-7.03 (m, 3H, Ar-H), 6.94 (t, J = 4.7 Hz, 1H, Ar-H), 6.91-6.88 (m, 1H, Ar-H), 6.65 (s, 1H, Ar-H), 5.34 (q, J = 7.1 Hz, 1H, CH), 3.89 (s, 3H, OCH_3), 1.69 (d, J = 7.1 Hz, 3H, CH_3). $^{13}\text{C}\{^1\text{H}\}$ -NMR (125 MHz, CDCl_3): δ = 158.1 (C_q), 157.9 (2C, CH) 155.5 (C_q), 145.8 (C_q), 145.7 (C_q), 132.5 (C_q), 129.7 (C_q), 128.2 (2C, CH), 127.6 (2C, CH), 125.9 (CH), 116.9 (CH), 114.5 (CH), 112.0 (CH), 105.7 (CH), 102.6 (CH), 55.9 (OCH_3), 38.8 (CH), 22.7 (CH_3). HRMS (ESI): m/z Calcd for $\text{C}_{21}\text{H}_{19}\text{N}_3\text{O}+\text{H}^+$ $[\text{M}+\text{H}]^+$ 330.1601; Found 330.1605.

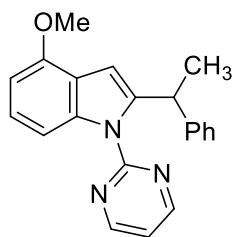


5-(Benzyloxy)-2-(1-phenylethyl)-1-(pyrimidin-2-yl)-1H-indole (3fa): The representative procedure was followed, using 5-(benzyloxy)-1-(pyrimidin-2-yl)-1H-indole (**1f**; 0.091 g, 0.302 mmol) and styrene (**2a**; 0.063 g, 0.604 mmol). Purification by column chromatography on silica gel (petroleum ether/EtOAc: 20/1) yielded **3fa** (0.102 g, 84%) as a light brown solid. $^1\text{H-NMR}$ (400 MHz, CDCl_3): δ = 8.61 (d, J = 4.9 Hz, 2H, Ar-H), 8.04 (d, J = 9.0 Hz, 1H, Ar-H), 7.50 (d, J = 7.1 Hz, 2H, Ar-H), 7.43-7.39 (m, 2H, Ar-H), 7.36-7.32 (m, 1H, Ar-H), 7.17-7.16 (m, 1H, Ar-H), 7.13-7.09 (m, 2H, Ar-H), 7.05-7.02 (m, 3H, Ar-H), 6.97-6.94 (m, 2H, Ar-H), 6.62 (s, 1H, Ar-H), 5.33 (q, J = 7.1 Hz, 1H, CH), 5.16 (s, 2H, CH_2), 1.67 (d, J = 7.1 Hz, 3H, CH_3), 1.20 (s, 9H, CH_3). $^{13}\text{C}\{^1\text{H}\}$ -NMR (100 MHz, CDCl_3): δ = 158.1 (C_q), 158.0 (2C, CH), 154.7 (C_q), 145.8 (2C, C_q) 137.8 (C_q), 132.7 (C_q), 129.7 (C_q), 128.7 (2C, CH), 128.2 (2C, CH), 127.9 (CH), 127.7 (2C, CH), 127.6 (2C, CH), 125.9 (CH), 116.9 (CH), 114.5 (CH), 112.8 (CH), 105.8 (CH), 104.2 (CH), 70.9 (CH_2), 38.8 (CH), 22.7 (CH_3). HRMS (ESI): m/z Calcd for $\text{C}_{27}\text{H}_{23}\text{N}_3\text{O} + \text{H}^+$ $[\text{M}+\text{H}]^+$ 406.1919; Found 406.1923.

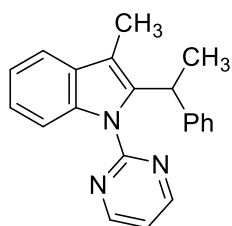


5-Fluoro-2-(1-phenylethyl)-1-(pyrimidin-2-yl)-1H-indole (3ga): The representative procedure was followed, using 5-fluoro-1-(pyrimidin-2-yl)-1H-indole (**1g**; 0.064 g, 0.300 mmol) and styrene (**2a**; 0.062 g, 0.600 mmol). Purification by column chromatography on silica gel (petroleum ether/EtOAc: 50/1) yielded **3ga** (0.088 g, 82%) as a colorless liquid. $^1\text{H-NMR}$ (400 MHz, CDCl_3): δ = 8.62 (d, J = 4.9 Hz, 2H, Ar-H), 8.07-8.04 (m, 1H, Ar-H), 7.32-7.29 (m, 1H, Ar-H), 7.16-7.12 (m, 2H, Ar-H), 7.08-7.02 (m, 3H, Ar-H), 7.00-6.96 (m, 2H, Ar-H), 6.69 (s, 1H, Ar-H), 5.34 (q, J = 7.1 Hz, 1H, CH), 1.71 (d, J = 7.1 Hz, 3H, CH_3). $^{13}\text{C}\{^1\text{H}\}$ -NMR (100 MHz, CDCl_3): δ = 158.9 (d, $^1J_{\text{C-F}}$ = 236.5 Hz, C_q), 158.1 (2C, CH), 157.9 (C_q), 146.8 (C_q), 145.4 (C_q), 133.9 (C_q), 129.6 (d, $^3J_{\text{C-F}}$ = 10.7 Hz, C_q), 128.2 (2C, CH), 127.5 (2C, CH), 126.0 (CH), 117.4 (CH), 114.3 (d, $^3J_{\text{C-F}}$ = 9.1 Hz, CH), 110.6 (d, $^2J_{\text{C-F}}$ = 24.4 Hz, CH), 105.4 (d,

$^4J_{C-F} = 2.3$ Hz, CH), 105.3 (d, $^2J_{C-F} = 17.5$ Hz, CH), 38.7 (CH), 22.5 (CH₃), 21.5 (CH₃). HRMS (ESI): m/z Calcd for C₂₀H₁₆FN₃+H⁺ [M+H]⁺ 318.1401; Found 318.1406.

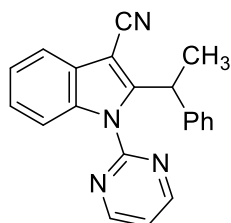


4-Methoxy-2-(1-phenylethyl)-1-(pyrimidin-2-yl)-1H-indole (3ja): The representative procedure was followed, using 4-methoxy-1-(pyrimidin-2-yl)-1H-indole (**1j**; 0.068 g, 0.302 mmol) and styrene (**2a**; 0.063 g, 0.605 mmol). Purification by column chromatography on silica gel (petroleum ether/EtOAc: 30/1) yielded **3ja** (0.066 g, 66%) as a brown solid. ¹H-NMR (400 MHz, CDCl₃): $\delta = 8.65$ (d, $J = 4.9$ Hz, 2H, Ar-H), 8.05 (d, $J = 8.6$ Hz, 1H, Ar-H), 7.64-7.62 (m, 1H, Ar-H), 7.25-7.21 (m, 2H, Ar-H), 6.99 (t, $J = 4.7$ Hz, 1H, Ar-H), 6.92 (d, $J = 8.6$ Hz, 2H, Ar-H), 6.69 (s, 1H, Ar-H), 6.65 (d, $J = 8.6$ Hz, 2H, Ar-H), 5.25 (q, $J = 7.1$ Hz, 1H, CH), 3.69 (s, 3H, OCH₃), 1.67 (d, $J = 7.1$ Hz, 3H, CH₃). ¹³C{¹H}-NMR (100 MHz, CDCl₃): $\delta = 158.1$ (2C, CH), 158.0 (C_q), 157.7 (C_q), 145.4 (C_q), 137.8 (C_q), 137.6 (C_q), 128.9 (C_q), 128.5 (2C, CH), 122.9 (CH), 121.7 (CH), 120.2 (CH), 117.3 (CH), 113.6 (2C, CH), 113.1 (CH), 105.3 (CH), 55.2 (OCH₃), 37.7 (CH), 22.7 (CH₃). HRMS (ESI): m/z Calcd for C₂₁H₁₉N₃O+H⁺ [M+H]⁺ 330.1601; Found 330.1590.

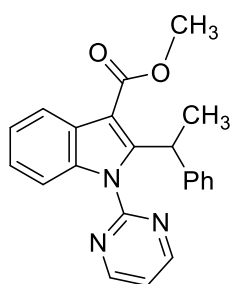


3-Methyl-2-(1-phenylethyl)-1-(pyrimidin-2-yl)-1H-indole (3ka): The representative procedure was followed, using 3-methyl-1-(pyrimidin-2-yl)-1H-indole (**1k**; 0.063 g, 0.301 mmol) and styrene (**2a**; 0.063 g, 0.602 mmol). Purification by column chromatography on silica gel (petroleum ether/EtOAc: 50/1) yielded **3ka** (0.082 g, 87%) as a light brown solid. ¹H-NMR (500 MHz, CDCl₃): $\delta = 8.72$ (d, $J = 4.5$ Hz, 2H, Ar-H), 8.01-8.00 (m, 1H, Ar-H), 7.50-7.49 (d, $J = 7.3$ Hz, 1H, Ar-H), 7.27-7.24 (m, 2H, Ar-H), 7.22-7.18 (m, 4H, Ar-H), 7.12-7.10 (m, 1H, Ar-H), 7.08 (t, $J = 4.9$ Hz, 1H, Ar-H), 5.16 (q, $J = 7.3$ Hz, 1H, CH), 2.06 (s, 3H, CH₃), 1.82 (d, $J = 7.3$ Hz, 3H, CH₃). ¹³C{¹H}-NMR (125 MHz, CDCl₃): $\delta = 158.4$ (1C, C_q; 2C, CH),

144.6 (C_q) 140.3 (C_q), 136.2 (C_q) 130.9 (C_q), 128.1 (2C, CH), 127.4 (2C, CH), 125.7 (CH), 123.0 (CH), 121.5 (CH), 118.0 (CH), 117.3 (CH), 113.2 (C_q), 112.9 (CH), 35.9 (CH), 19.0 (CH₃), 9.5 (CH₃). HRMS (ESI): *m/z* Calcd for C₂₁H₁₉N₃ + H⁺ [M+H]⁺ 314.1652; Found 314.1621.

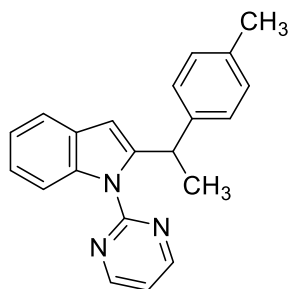


2-(1-Phenylethyl)-1-(pyrimidin-2-yl)-1H-indole-3-carbonitrile (3la): The representative procedure was followed, using methyl 1-(pyrimidin-2-yl)-1H-indole-3-carbonitrile (**1l**; 0.067 g, 0.304 mmol) and styrene (**2a**; 0.063 g, 0.605 mmol). Purification by column chromatography on silica gel (petroleum ether/EtOAc: 30/1) yielded **3la** (0.092 g, 94%) as a brown solid. ¹H-NMR (400 MHz, CDCl₃): δ = 8.77 (d, *J* = 4.9 Hz, 2H, Ar-H), 7.76-7.71 (m, 2H, Ar-H), 7.33-7.23 (m, 3H, Ar-H), 7.16-7.13 (m, 2H, Ar-H), 7.10-7.05 (m, 3H, Ar-H), 5.24 (q, *J* = 7.3 Hz, 1H, CH), 1.99 (d, *J* = 7.3 Hz, 3H, CH₃). ¹³C{¹H}-NMR (100 MHz, CDCl₃): δ = 158.9 (2C, CH), 156.9 (C_q), 152.1 (C_q, CN), 142.8 (C_q), 135.9 (C_q) 128.5 (2C, CH), 128.1 (C_q), 127.5 (2C, CH), 126.7 (CH), 124.9 (CH), 123.5 (CH), 119.5 (CH), 119.1 (CH), 116.0 (C_q), 113.1 (CH), 89.4 (C_q), 38.2 (CH), 20.7 (CH₃). HRMS (ESI): *m/z* Calcd for C₂₁H₁₆N₄ + H⁺ [M+H]⁺ 325.1448; Found 325.1452.

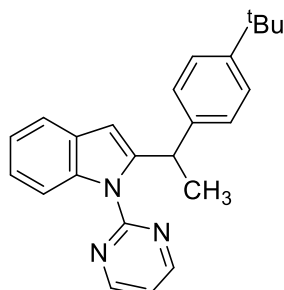


Methyl 2-(1-phenylethyl)-1-(pyrimidin-2-yl)-1H-indole-3-carboxylate (3ma): The representative procedure was followed, using methyl 1-(pyrimidin-2-yl)-1H-indole-3-carboxylate (**1m**; 0.076 g, 0.300 mmol) and styrene (**2a**; 0.062 g, 0.600 mmol). Purification by column chromatography on silica gel (petroleum ether/EtOAc: 30/1) yielded **3ma** (0.041 g, 38%) as a colorless sticky solid. ¹H-NMR (400 MHz, CDCl₃): δ = 8.51 (d, *J* = 4.9 Hz, 2H, Ar-H), 8.12 (d, *J* = 8.0 Hz, 1H, Ar-H), 7.23-7.16 (m, 2H, Ar-H), 7.14-7.09 (m, 1H, Ar-H), 7.00

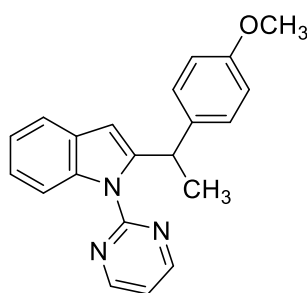
(t, $J = 4.8$ Hz, 1H, Ar-H), 6.96-6.91 (m, 4H, Ar-H), 6.89-6.86 (m, 1H, Ar-H), 5.60 (q, $J = 7.1$ Hz, 1H, CH), 3.85 (s, 3H, OCH₃), 1.91 (d, $J = 7.2$ Hz, 3H, CH₃). ¹³C{¹H}-NMR (100 MHz, CDCl₃): $\delta = 166.2$ (CO), 158.6 (2C, CH), 157.5 (C_q), 152.2 (C_q), 142.2 (C_q), 136.8 (C_q), 127.8 (2C, CH), 127.4 (2C, CH), 126.7 (C_q), 125.6 (CH), 123.6 (CH), 122.9 (CH), 121.8 (CH), 119.5 (CH), 111.4 (CH), 107.6 (C_q), 51.2 (OCH₃), 36.1 (CH), 17.9 (CH₃). HRMS (ESI): m/z Calcd for C₂₂H₁₉N₃O₂ + H⁺ [M+H]⁺ 358.1556; Found 358.1559.



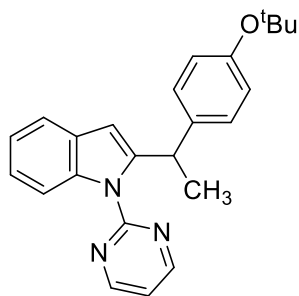
1-(Pyrimidin-2-yl)-2-(1-(p-tolylethyl)-1H-indole (3ab): The representative procedure was followed, using methyl 1-(pyrimidin-2-yl)-1H-indole (**1a**; 0.059 g, 0.302 mmol) and 1-methyl-4-vinylbenzene (**2b**; 0.071 g, 0.601 mmol). Purification by column chromatography on silica gel (petroleum ether/EtOAc: 30/1) yielded **3ab** (0.090 g, 96%) as a colorless liquid. ¹H-NMR (400 MHz, CDCl₃): $\delta = 8.53$ (d, $J = 4.7$ Hz, 2H, Ar-H), 7.92-7.88 (m, 1H, Ar-H), 7.51-7.47 (m, 1H, Ar-H), 7.12-7.07 (m, 2H, Ar-H), 7.02 (d, $J = 8.4$ Hz, 2H, Ar-H), 6.84 (t, $J = 4.9$ Hz, 1H, Ar-H), 6.80 (d, $J = 8.0$ Hz, 2H, Ar-H), 6.54 (s, 1H, Ar-H), 5.13 (q, $J = 7.1$ Hz, 1H, CH), 2.11 (s, 3H, CH₃), 1.56 (d, $J = 7.1$ Hz, 3H, CH₃). ¹³C{¹H}-NMR (100 MHz, CDCl₃): $\delta = 158.2$ (C_q), 158.2 (2C, CH), 148.5 (C_q), 145.6 (C_q), 142.2 (C_q), 137.7 (C_q), 128.9 (C_q), 127.4 (2C, CH), 125.1 (2C, CH), 122.9 (CH), 121.6 (CH), 120.2 (CH), 117.2 (CH), 113.1 (CH), 105.6 (CH), 37.8 (CH), 25.2 (CH₃), 22.4 (CH₃). HRMS (ESI): m/z Calcd for C₂₁H₁₉N₃ + H⁺ [M+H]⁺ 314.1652; Found 314.1655.



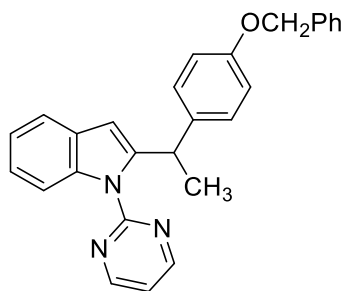
2-(1-(4-(Tert-butyl)phenyl)ethyl)-1-(pyrimidin-2-yl)-1H-indole (3ac): The representative procedure was followed, using methyl 1-(pyrimidin-2-yl)-1H-indole (**1a**; 0.059 g, 0.302 mmol) and 1-(tert-butyl)-4-vinylbenzene (**2c**; 0.097 g, 0.605 mmol). Purification by column chromatography on silica gel (petroleum ether/EtOAc: 70/1) yielded **3ac** (0.102 g, 95%) as a colorless liquid. $^1\text{H-NMR}$ (400 MHz, CDCl_3): δ = 8.51 (d, J = 4.7 Hz, 2H, Ar-H), 7.90-7.87 (m, 1H, Ar-H), 7.51-7.49 (m, 1H, Ar-H), 7.13-7.07 (m, 2H, Ar-H), 7.00 (d, J = 8.2 Hz, 2H, Ar-H), 6.85 (t, J = 4.8 Hz, 1H, Ar-H), 6.81 (d, J = 8.2 Hz, 2H, Ar-H), 6.56 (s, 1H, Ar-H), 5.11 (q, J = 7.1 Hz, 1H, CH), 1.57 (d, J = 7.1 Hz, 3H, CH_3), 1.11 (s, 9H, CH_3). $^{13}\text{C}\{^1\text{H}\}$ -NMR (100 MHz, CDCl_3): δ = 158.2 (C_q), 158.1 (2C, CH), 148.6 (C_q), 145.6 (C_q), 142.4 (C_q), 137.5 (C_q), 128.9 (C_q), 127.3 (2C, CH), 125.0 (2C, CH), 122.9 (CH), 121.7 (CH), 120.2 (CH), 117.2 (CH), 112.9 (CH), 105.3 (CH), 37.9 (CH), 34.3 (C_q), 31.4 (3C, CH_3), 22.4 (CH_3). HRMS (ESI): m/z Calcd for $\text{C}_{24}\text{H}_{25}\text{N}_3 + \text{H}^+$ $[\text{M}+\text{H}]^+$ 356.2127; Found 356.2129.



2-(1-(4-Methoxyphenyl)ethyl)-1-(pyrimidin-2-yl)-1H-indole (3ad): The representative procedure was followed, using methyl 1-(pyrimidin-2-yl)-1H-indole (**1a**; 0.059 g, 0.302 mmol) and 1-methoxy-4-vinylbenzene (**2d**; 0.072 g, 0.609 mmol). Purification by column chromatography on silica gel (petroleum ether/EtOAc: 20/1) yielded **3ad** (0.094 g, 95%) as a brown solid. $^1\text{H-NMR}$ (500 MHz, CDCl_3): δ = 8.57 (d, J = 4.7 Hz, 2H, Ar-H), 8.00 (d, J = 8.3 Hz, 1H, Ar-H), 7.59-7.57 (m, 1H, Ar-H), 7.21-7.15 (m, 2H, Ar-H), 6.92-6.86 (m, 3H, Ar-H), 6.64 (s, 1H, Ar-H), 6.60 (d, J = 8.5 Hz, 2H, Ar-H), 5.21 (q, J = 7.1 Hz, 1H, CH), 3.63 (s, 3H, OCH_3), 1.62 (d, J = 7.1 Hz, 3H, CH_3). $^{13}\text{C}\{^1\text{H}\}$ -NMR (125 MHz, CDCl_3): δ = 158.1 (2C, CH), 157.7 (C_q), 145.4 (C_q), 137.7 (2C, C_q), 137.6 (C_q), 128.9 (C_q), 128.5 (2C, CH), 122.9 (CH), 121.7 (CH), 120.2 (CH), 117.3 (CH), 113.4 (2C, CH), 113.1 (CH), 105.3 (CH), 55.2 (OCH_3), 37.6 (CH), 22.7 (CH_3). HRMS (ESI): m/z Calcd for $\text{C}_{21}\text{H}_{19}\text{N}_3\text{O} + \text{H}^+$ $[\text{M}+\text{H}]^+$ 330.1601; Found 330.1604.

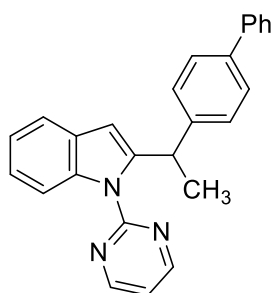


2-(1-(4-(Tert-butoxy)phenyl)ethyl)-1-(pyrimidin-2-yl)-1H-indole (3ae): The representative procedure was followed, using methyl 1-(pyrimidin-2-yl)-1H-indole (**1a**; 0.059 g, 0.302 mmol) and 1-(tert-butoxy)-4-vinylbenzene (**2e**; 0.107 g, 0.607 mmol). Purification by column chromatography on silica gel (petroleum ether/EtOAc: 30/1) yielded **3ae** (0.110 g, 98%) as a colorless sticky solid. $^1\text{H-NMR}$ (400 MHz, CDCl_3): δ = 8.56 (d, J = 4.7 Hz, 2H, Ar-H), 7.95 (d, J = 7.0 Hz, 1H, Ar-H), 7.60-7.58 (m, 1H, Ar-H), 7.21-7.17 (m, 2H, Ar-H), 6.91 (vt, J = 4.7 Hz, 1H, Ar-H), 6.81 (d, J = 8.3 Hz, 2H, Ar-H), 6.67-6.65 (m, 3H, Ar-H), 5.18 (q, J = 7.1 Hz, 1H, CH), 1.65 (d, J = 7.1 Hz, 3H, CH_3), 1.20 (s, 9H, CH_3). $^{13}\text{C}\{^1\text{H}\}$ -NMR (100 MHz, CDCl_3): δ = 158.1 (C_q), 158.0 (2C, CH), 153.2 (C_q), 145.2 (C_q), 140.6 (C_q), 137.5 (C_q), 128.9 (C_q), 127.9 (2C, CH), 123.9 (2C, CH), 122.9 (CH), 121.7 (CH), 120.2 (CH), 117.2 (CH), 112.9 (CH), 105.2 (CH), 78.2 (C_q), 37.9 (CH), 28.9 (3C, CH_3), 22.6 (CH_3). HRMS (ESI): m/z Calcd for $\text{C}_{24}\text{H}_{25}\text{N}_3\text{O} + \text{H}^+$ $[\text{M}+\text{H}]^+$ 372.2070; Found 372.2034.

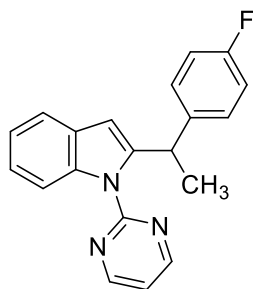


2-(1-(4-(Benzyloxy)phenyl)ethyl)-1-(pyrimidin-2-yl)-1H-indole (3af): The representative procedure was followed, using methyl 1-(pyrimidin-2-yl)-1H-indole (**1a**; 0.059 g, 0.302 mmol) and 1-(benzyloxy)-4-vinylbenzene (**2f**; 0.127 g, 0.604 mmol). Purification by column chromatography on silica gel (petroleum ether/EtOAc: 30/1) yielded **3af** (0.080 g, 66%) as a colorless liquid. $^1\text{H-NMR}$ (400 MHz, CDCl_3): δ = 8.56 (d, J = 4.7 Hz, 2H, Ar-H), 8.01-7.99 (m, 1H, Ar-H), 7.59-7.57 (m, 1H, Ar-H), 7.32-7.31 (m, 3H, Ar-H), 7.30-7.24 (m, 2H, Ar-H), 7.21-7.15 (m, 2H, Ar-H), 6.91-6.85 (m, 3H, Ar-H), 6.69-6.64 (m, 3H, Ar-H), 5.20 (q, J = 7.1 Hz, 1H, CH), 4.88 (s, 2H, CH_2), 1.62 (d, J = 7.1 Hz, 3H, CH_3). $^{13}\text{C}\{^1\text{H}\}$ -NMR (100

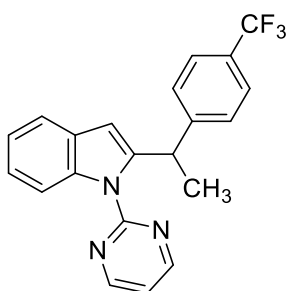
MHz, CDCl₃): δ = 158.1 (1C, C_q; 2C, CH), 156.9 (C_q), 145.3 (C_q) 138.1 (2C, C_q), 137.3 (C_q), 128.9 (C_q), 128.6 (2C, CH), 128.5 (2C, CH), 127.9 (CH), 127.6 (2C, CH), 122.9 (CH), 121.7 (CH), 120.2 (CH), 117.3 (CH), 114.6 (2C, CH), 113.1 (CH), 105.3 (CH), 69.9 (CH₂), 37.7 (CH), 22.7 (CH₃). HRMS (ESI): m/z . Calcd for C₂₇H₂₃N₃O + H⁺ [M+H]⁺ 406.1919; Found 406.1923.



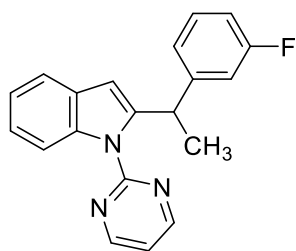
2-(1-([1,1'-Biphenyl]-4-yl)ethyl)-1-(pyrimidin-2-yl)-1H-indole (3ag): The representative procedure was followed, using methyl 1-(pyrimidin-2-yl)-1H-indole (**1a**; 0.059 g, 0.302 mmol) and 4-vinyl-1,1'-biphenyl (**2g**; 0.109 g, 0.604 mmol). Purification by column chromatography on silica gel (petroleum ether/EtOAc: 30/1) yielded **3ag** (0.080 g, 70%) as a light yellow solid. ¹H-NMR (400 MHz, CDCl₃): δ = 8.51 (d, J = 4.9 Hz, 2H, Ar-H), 8.03-8.00 (m, 1H, Ar-H), 7.60-7.57 (m, 1H, Ar-H), 7.22-7.15 (m, 3H, Ar-H), 7.06-7.03 (m, 4H, Ar-H), 6.99-6.95 (m, 4H, Ar-H), 6.84 (t, J = 4.9 Hz, 1H, Ar-H), 6.67 (s, 1H, Ar-H), 5.25 (q, J = 7.1 Hz, 1H, CH), 1.65 (d, J = 7.1 Hz, 3H, CH₃). ¹³C{¹H}-NMR (100 MHz, CDCl₃): δ = 158.0 (1C, C_q; 2C, CH), 145.6 (C_q), 144.9 (2C, C_q), 137.5 (C_q), 128.9 (2C, C_q), 128.1 (4C, CH), 127.5 (3C, CH), 125.9 (CH), 122.9 (CH), 122.9 (CH), 121.7 (CH), 120.2 (CH), 117.2 (CH), 113.2 (CH), 105.5 (CH), 38.5 (CH), 22.6 (CH₃).



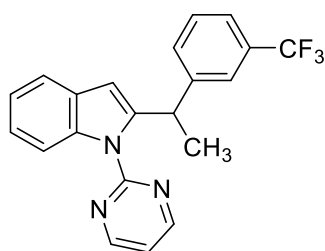
2-(1-(4-Fluorophenyl)ethyl)-1-(pyrimidin-2-yl)-1H-indole (3ah): The representative procedure was followed, using methyl 1-(pyrimidin-2-yl)-1H-indole (**1a**; 0.059 g, 0.302 mmol) and 1-fluoro-4-vinylbenzene (**2h**; 0.074 g, 0.605 mmol). Purification by column chromatography on silica gel (petroleum ether/EtOAc: 50/1) yielded **3ah** (0.070 g, 73%) as a colorless liquid. $^1\text{H-NMR}$ (400 MHz, CDCl_3): δ = 8.52 (d, J = 4.7 Hz, 2H, Ar-H), 7.94 (d, J = 8.0 Hz, 1H, Ar-H), 7.52-7.50 (m, 1H, Ar-H), 7.15-7.09 (m, 2H, Ar-H), 6.88 (t, J = 4.7 Hz, 1H, Ar-H), 6.85-6.82 (m, 2H, Ar-H), 6.66 (vt, J = 8.6 Hz, 2H, Ar-H), 6.59 (s, 1H, Ar-H), 5.17 (q, J = 7.1 Hz, 1H, CH), 1.55 (d, J = 7.1 Hz, 3H, CH_3). $^{13}\text{C}\{^1\text{H}\}$ -NMR (100 MHz, CDCl_3): δ = 161.1 (d, $^1J_{\text{C-F}}$ = 247.9 Hz, C_q), 158.1 (2C, CH), 158.0 (C_q), 144.7 (C_q), 141.1 (d, $^4J_{\text{C-F}}$ = 3.0 Hz, C_q), 137.6 (C_q), 128.9 (d, $^3J_{\text{C-F}}$ = 7.6 Hz, 2C, CH), 128.8 (C_q), 123.1 (CH), 121.8 (CH), 120.3 (CH), 117.3 (CH), 114.9 (d, $^2J_{\text{C-F}}$ = 21.3 Hz, 2C, CH), 113.3 (CH), 105.6 (CH), 37.9 (CH), 22.7 (CH_3). HRMS (ESI): m/z Calcd for $\text{C}_{20}\text{H}_{16}\text{FN}_3 + \text{H}^+$ $[\text{M}+\text{H}]^+$ 318.1401; Found 318.1407.



1-(Pyrimidin-2-yl)-2-(1-(4-(trifluoromethyl)phenyl)ethyl)-1H-indole (3ai): The representative procedure was followed, using methyl 1-(pyrimidin-2-yl)-1H-indole (**1a**; 0.059 g, 0.302 mmol) and 1-(trifluoromethyl)-4-vinylbenzene (**2i**; 0.104 g, 0.604 mmol). Purification by column chromatography on silica gel (petroleum ether/EtOAc: 50/1) yielded **3ai** (0.078 g, 70%) as a colorless liquid. $^1\text{H-NMR}$ (400 MHz, CDCl_3): δ = 8.50 (d, J = 4.7 Hz, 2H, Ar-H), 8.00 (d, J = 7.3 Hz, 1H, Ar-H), 7.53-7.51 (m, 1H, Ar-H), 7.24 (d, J = 8.1 Hz, 2H, Ar-H), 7.17-7.10 (m, 2H, Ar-H), 7.00 (d, J = 8.1 Hz, 2H, Ar-H), 6.87 (t, J = 4.7 Hz, 1H, Ar-H), 6.63 (s, 1H, Ar-H), 5.25 (q, J = 7.1 Hz, 1H, CH), 1.57 (d, J = 7.1 Hz, 3H, CH_3). $^{13}\text{C}\{^1\text{H}\}$ -NMR (100 MHz, CDCl_3): δ = 158.1 (2C, CH), 158.0 (C_q), 150.0 (C_q), 143.8 (C_q), 137.6 (C_q), 128.9 (C_q), 128.2 (q, $^2J_{\text{C-F}}$ = 32.8 Hz, C_q), 127.9 (2C, CH), 127.0 (q, $^1J_{\text{C-F}}$ = 272.3 Hz, C_q), 125.2 (q, $^3J_{\text{C-F}}$ = 3.8 Hz, 2C, CH), 123.3 (CH), 122.0 (CH), 120.3 (CH), 117.3 (CH), 113.6 (CH), 106.1 (CH), 38.7 (CH), 22.5 (CH_3).

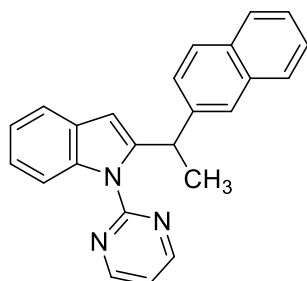


2-(1-(3-Fluorophenyl)ethyl)-1-(pyrimidin-2-yl)-1H-indole (3aj): The representative procedure was followed, using methyl 1-(pyrimidin-2-yl)-1H-indole (**1a**; 0.059 g, 0.302 mmol) and 1-fluoro-3-vinylbenzene (**2j**; 0.074 g, 0.605 mmol). Purification by column chromatography on silica gel (petroleum ether/EtOAc: 50/1) yielded **3aj** (0.061 g, 64%) as a colorless liquid. $^1\text{H-NMR}$ (400 MHz, CDCl_3): δ = 8.50 (d, J = 4.9 Hz, 2H, Ar-H), 7.98 (d, J = 8.0 Hz, 1H, Ar-H), 7.52-7.50 (m, 1H, Ar-H), 7.15-7.08 (m, 2H, Ar-H), 6.95-6.90 (m, 1H, Ar-H), 6.85 (t, J = 4.8 Hz, 1H, Ar-H), 6.67-6.57 (m, 4H, Ar-H), 5.19 (q, J = 7.1 Hz, 1H, CH), 1.56 (d, J = 7.1 Hz, 3H, CH_3). $^{13}\text{C}\{^1\text{H}\}$ -NMR (100 MHz, CDCl_3): δ = 162.8 (d, $^1J_{\text{C-F}}$ = 245.7 Hz, C_q), 158.1 (2C, CH), 158.0 (C_q), 148.5 (d, $^3J_{\text{C-F}}$ = 6.8 Hz, C_q), 144.2 (C_q), 137.6 (C_q), 129.6 (d, $^3J_{\text{C-F}}$ = 8.4 Hz, CH), 128.9 (C_q), 123.1 (CH), 123.0 (d, $^4J_{\text{C-F}}$ = 2.3 Hz, CH), 121.9 (CH), 120.3 (CH), 117.3 (CH), 114.5 (d, $^2J_{\text{C-F}}$ = 21.4 Hz, CH), 113.4 (CH), 112.9 (d, $^2J_{\text{C-F}}$ = 20.6 Hz, CH), 105.8 (CH), 38.5 (d, $^4J_{\text{C-F}}$ = 1.5 Hz, CH), 22.7 (CH_3). HRMS (ESI): m/z Calcd for $\text{C}_{20}\text{H}_{16}\text{FN}_3 + \text{H}^+$ $[\text{M}+\text{H}]^+$ 318.1401; Found 318.1407.

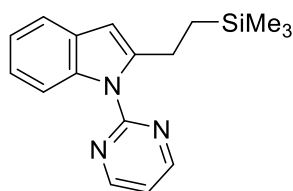


1-(Pyrimidin-2-yl)-2-(1-(3-(trifluoromethyl)phenyl)ethyl)-1H-indole (3ak): The representative procedure was followed, using methyl 1-(pyrimidin-2-yl)-1H-indole (**1a**; 0.059 g, 0.302 mmol) and 1-(trifluoromethyl)-3-vinylbenzene (**2k**; 0.104 g, 0.604 mmol). Purification by column chromatography on silica gel (petroleum ether/EtOAc: 50/1) yielded **3ak** (0.064 g, 58%) as a colorless liquid. $^1\text{H-NMR}$ (400 MHz, CDCl_3): δ = 8.51 (d, J = 4.9 Hz, 2H, Ar-H), 7.97 (d, J = 8.1 Hz, 1H, Ar-H), 7.53-7.51 (m, 1H, Ar-H), 7.22-7.04 (m, 6H, Ar-H), 6.88 (t, J = 4.9 Hz, 1H, Ar-H), 6.63 (s, 1H, Ar-H), 5.23 (q, J = 7.1 Hz, 1H, CH), 1.60 (d, J = 7.1 Hz, 3H, CH_3). $^{13}\text{C}\{^1\text{H}\}$ -NMR (100 MHz, CDCl_3): δ = 158.1 (2C, CH), 158.0 (C_q), 146.8 (C_q), 143.9 (C_q), 137.6 (C_q), 130.7 (CH), 130.2 (q, $^2J_{\text{C-F}}$ = 32.0 Hz, C_q), 128.8 (CH),

128.9 (C_q), 127.0 (q, ¹J_{C-F} = 272.4 Hz, C_q), 124.9 (q, ³J_{C-F} = 3.8 Hz, CH), 123.3 (CH), 122.9 (q, ³J_{C-F} = 3.8 Hz, CH), 121.9 (CH), 120.4 (CH), 117.4 (CH), 113.5 (CH), 105.9 (CH), 38.7 (CH), 22.5 (CH₃).

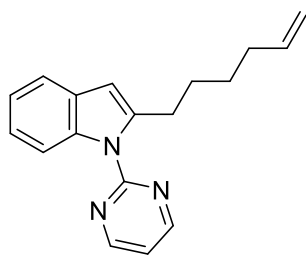


2-(1-(Naphthalen-2-yl)ethyl)-1-(pyrimidin-2-yl)-1H-indole (3al): The representative procedure was followed, using methyl 1-(pyrimidin-2-yl)-1H-indole (**1a**; 0.059 g, 0.302 mmol) and 2-vinylnaphthalene (**2l**; 0.0.093 g, 0.603 mmol). Purification by column chromatography on silica gel (petroleum ether/EtOAc: 50/1) yielded **3al** (0.047 g, 45%) as a colorless liquid. ¹H-NMR (400 MHz, CDCl₃): δ = 8.49 (d, *J* = 4.4 Hz, 2H, Ar-H), 7.98 (d, *J* = 7.2 Hz, 1H, Ar-H), 7.61-7.51 (m, 4H, Ar-H), 7.30 (s, 1H, Ar-H), 7.27-7.25 (m, 2H, Ar-H), 7.15-7.13 (m, 3H, Ar-H), 6.83-6.81 (m, 1H, Ar-H), 6.65 (s, 1H, Ar-H), 5.37 (q, *J* = 6.6 Hz, 1H, CH), 1.64 (d, *J* = 6.6 Hz, 3H, CH₃). ¹³C{¹H}-NMR (100 MHz, CDCl₃): δ = 158.2 (C_q), 158.0 (2C, CH), 144.9 (C_q) 143.3 (C_q), 137.7 (C_q) 133.5 (C_q), 132.1 (C_q), 129.1 (C_q), 127.9 (CH), 127.8 (CH), 127.6 (CH), 126.6 (CH), 125.8 (CH), 125.6 (CH), 125.3 (CH), 123.1 (CH), 121.9 (CH), 120.3 (CH), 117.2 (CH), 113.5 (CH), 105.9 (CH), 38.8 (CH), 22.6 (CH₃). HRMS (ESI): *m/z* Calcd for C₂₄H₁₉N₃ + H⁺ [M+H]⁺ 350.1657; Found 350.1659.

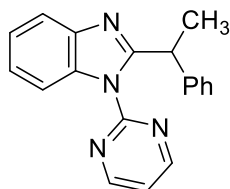


1-(Pyrimidin-2-yl)-2-(2-(trimethylsilyl)ethyl)-1H-indole (3am): The representative procedure was followed, using methyl 1-(pyrimidin-2-yl)-1H-indole (**1a**; 0.059 g, 0.302 mmol) and trimethyl(vinyl)silane (**2m**; 0.061 g, 0.608 mmol). Purification by column chromatography on silica gel (petroleum ether/EtOAc: 70/1) yielded **3am** (0.045 g, 45%) as a colorless liquid. ¹H-NMR (400 MHz, CDCl₃): δ 8.82 (d, *J* = 4.9 Hz, 2H, Ar-H), 8.25 (d, *J* = 7.8 Hz, 1H, Ar-H),

7.56-7.52 (m, 1H, Ar-H), 7.23-7.10 (m, 3H, Ar-H), 6.52 (s, 1H, Ar-H), 3.22-3.18 (m, 2H, CH₂), 0.87-0.82 (m, 2H, CH₂), 0.02 (s, 9H, CH₃). ¹³C{¹H}-NMR (100 MHz, CDCl₃): δ 158.3 (C_q), 158.1 (2C, CH), 145.0 (C_q), 137.1 (C_q), 129.4 (C_q), 122.3 (CH), 121.7 (CH), 119.6 (CH), 117.0 (CH), 113.7 (CH), 105.1 (CH), 23.8 (CH₂), 16.5 (CH₂), -1.9 (3C, CH₃). HRMS (ESI): *m/z*. Calcd for C₂₁H₁₈N₂+H⁺ [M+H]⁺ 296.1583; Found 296.1585.

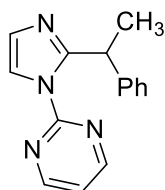


2-(Hex-5-en-1-yl)-1-(pyrimidin-2-yl)-1H-indole: The representative procedure was followed, using methyl 1-(pyrimidin-2-yl)-1H-indole (**1a**; 0.059 g, 0.302 mmol) and hexa-1,5-diene (**2n**; 0.050 g, 0.608 mmol). Purification by column chromatography on silica gel (petroleum ether/EtOAc: 70/1) yielded **3am** (0.036g, 43%) as a colorless liquid. ¹H-NMR (400 MHz, CDCl₃): δ 8.80-8.77 (m, 2H, Ar-H), 8.02-7.98 (m, 1H, Ar-H), 7.57-7.53 (m, 1H, Ar-H), 7.24-7.12 (m, 3H, Ar-H), 6.52 (s, 1H, Ar-H), 5.43-5.32 (m, 1H, CH₂), 5.27-5.13 (m, 1H, CH₂), 4.60-4.26 (m, 1H, CH), 1.95-1.73 (m, 2H, CH₂), 1.68-1.46 (m, 2H, CH₂), 1.41-1.25 (m, 2H, CH₂), 1.02-0.70 (m, 2H, CH₂).

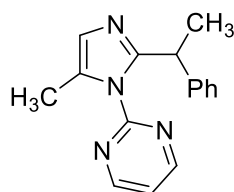


2-(1-Phenylethyl)-1-(pyrimidin-2-yl)-1H-benzo[d]imidazole (6aa): The representative procedure was followed, using 1-(pyrimidin-2-yl)-1H-benzo[d]imidazole (**4a**; 0.059 g, 0.300 mmol) and styrene (**2a**; 0.062 g, 0.600 mmol). Purification by column chromatography on silica gel (petroleum ether/EtOAc: 30/1) yielded **6aa** (0.080 g, 89%) as a brown solid. ¹H-NMR (400

MHz, CDCl₃): δ = 8.64 (d, J = 4.9 Hz, 2H, Ar-H), 8.03-8.01 (m, 1H, Ar-H), 7.89-7.87 (m, 1H, Ar-H), 7.35-7.27 (m, 2H, Ar-H), 7.10-7.00 (m, 6H, Ar-H), 5.41 (q, J = 7.1 Hz, 1H, CH), 1.87 (d, J = 7.1 Hz, 3H, CH₃). ¹³C{¹H}-NMR (100 MHz, CDCl₃): δ = 158.3 (2C, CH), 157.8 (C_q), 156.7 (C_q), 143.9 (C_q), 142.6 (C_q), 134.5 (C_q), 128.3 (2C, CH), 127.6 (2C, CH), 126.3 (CH), 123.8 (CH), 123.4 (CH), 119.7 (CH), 118.4 (CH), 113.7 (CH), 39.9 (CH), 22.2 (CH₃). HRMS (ESI): m/z Calcd for C₁₉H₁₆N₄ + H⁺ [M+H]⁺ 301.1448; Found 301.1416.

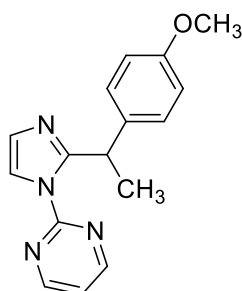


2-(2-(1-Phenylethyl)-1H-imidazol-1-yl)pyrimidine (7aa): The representative procedure was followed, using 2-(1H-imidazol-1-yl)pyrimidine (**5a**; 0.044 g, 0.301 mmol) and styrene (**2a**; 0.062 g, 0.602 mmol). Purification by column chromatography on silica gel (petroleum ether/EtOAc: 20/1) yielded **7aa** (0.040 g, 53%) as a colorless sticky solid. ¹H-NMR (500 MHz, CDCl₃): δ = 8.57 (d, J = 4.9 Hz, 2H, Ar-H), 7.85 (s, 1H, Ar-H), 7.20-7.15 (m, 4H, Ar-H), 7.10 (s, 1H, Ar-H), 7.09-7.03 (m, 2H, Ar-H), 5.37 (q, J = 7.1 Hz, 1H, CH), 1.75 (d, J = 7.1 Hz, 3H, CH₃). ¹³C{¹H}-NMR (125 MHz, CDCl₃): δ = 158.3 (2C, CH), 156.0 (C_q), 152.2 (C_q), 144.9 (C_q), 128.2 (2C, CH), 127.8 (2C, CH), 127.7 (CH), 126.1 (CH), 119.2 (CH), 118.2 (CH), 39.7 (CH), 22.3 (CH₃). HRMS (ESI): m/z Calcd for C₁₅H₁₄N₄ + H⁺ [M+H]⁺ 251.1297; Found 251.1295.

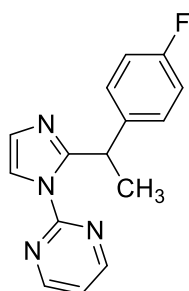


2-(5-Methyl-2-(1-phenylethyl)-1H-imidazol-1-yl)pyrimidine (7ba): The representative procedure was followed, using 2-(5-methyl-1H-imidazol-1-yl)pyrimidine (**5b**; 0.049 g, 0.305 mmol) and styrene (**2a**; 0.062 g, 0.602 mmol). Purification by column chromatography on silica gel (petroleum ether/EtOAc: 20/1) yielded **7ba** (0.022 g, 28%) as a colorless liquid. ¹H-NMR (500 MHz, CDCl₃): δ = 8.56 (d, J = 4.7 Hz, 2H, Ar-H), 7.55 (s, 1H, Ar-H), 7.21-7.15 (m, 4H, Ar-H), 7.09-7.05 (m, 1H, Ar-H), 7.02 (t, J = 4.7 Hz, 1H, Ar-H), 5.35 (q, J = 7.2 Hz, 1H, CH), 2.31 (s, 3H, CH₃), 1.74 (d, J = 7.2 Hz, 3H, CH₃). ¹³C{¹H}-NMR (125 MHz, CDCl₃): δ = 158.2 (2C, CH), 155.9 (C_q), 151.6 (C_q), 145.2 (C_q), 136.8 (C_q), 128.2 (2C, CH), 127.8 (2C, CH),

126.0 (CH), 118.0 (CH), 115.4 (CH), 39.7 (CH), 22.5 (CH₃), 13.9 (CH₃). HRMS (ESI): m/z Calcd for C₁₆H₁₆N₄ + H⁺ [M+H]⁺ 265.1448; Found 265.1449



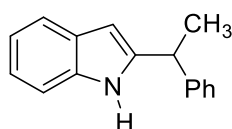
2-(2-(1-(4-Methoxyphenyl)ethyl)-1H-imidazol-1-yl)pyrimidine (7ad): The representative procedure was followed, using 2-(1H-imidazol-1-yl)pyrimidine (**5a**; 0.044 g, 0.301 mmol) and 1-methoxy-4-vinylbenzene (**2d**; 0.081 g, 0.603 mmol). Purification by column chromatography on silica gel (petroleum ether/EtOAc: 20/1) yielded **7ad** (0.047 g, 55%) as a light brown liquid. ¹H-NMR (500 MHz, CDCl₃): δ = 8.61 (d, J = 4.9 Hz, 2H, Ar-H), 7.84 (s, 1H, Ar-H), 7.13-7.07 (m, 4H, Ar-H), 6.72 (d, J = 8.6 Hz, 2H, Ar-H), 5.33 (q, J = 7.2 Hz, 1H, CH), 3.70 (OCH₃), 1.72 (d, J = 7.2 Hz, 3H, CH₃). ¹³C{¹H}-NMR (125 MHz, CDCl₃): δ = 158.3 (2C, CH), 157.9 (C_q), 156.1 (C_q), 152.6 (C_q), 137.1 (C_q), 128.8 (2C, CH), 127.8 (CH), 119.2 (CH), 118.4 (CH), 113.7 (2C, CH), 55.3 (OCH₃), 38.9 (CH), 22.5 (CH₃). HRMS (ESI): m/z Calcd for C₁₆H₁₆N₄ + H⁺ [M+H]⁺ 281.1397; Found 281.1409.



2-(2-(1-(4-Fluorophenyl)ethyl)-1H-imidazol-1-yl)pyrimidine (7ah): The representative procedure was followed, using 2-(1H-imidazol-1-yl)pyrimidine (**5a**; 0.044 g, 0.301 mmol) and 1-fluoro-4-vinylbenzene (**2h**; 0.074 g, 0.605 mmol). Purification by column chromatography on silica gel (petroleum ether/EtOAc: 20/1) yielded **7ah** (0.037 g, 46%) as a colorless liquid. ¹H-NMR (400 MHz, CDCl₃): δ = 8.50 (d, J = 4.0 Hz, 2H, Ar-H), 7.77 (s, 1H, Ar-H), 7.09-7.06 (m, 2H, Ar-H), 7.01-6.97 (m, 2H, Ar-H), 6.77 (vt, J = 7.9 Hz, 2H, Ar-H), 5.27 (q, J = 7.0 Hz, 1H, CH), 1.64 (d, J = 7.0 Hz, 3H, CH₃). ¹³C{¹H}-NMR (100 MHz, CDCl₃): δ = 161.2 (d, ¹J_{C-F} = 244.1 Hz, C_q), 158.3 (2C, CH), 155.9 (C_q), 151.9 (C_q), 140.6 (d, ⁴J_{C-F} = 3.8 Hz, C_q),

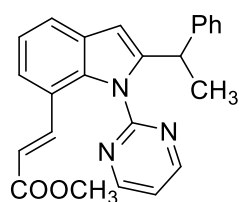
129.2 (d, $^3J_{C-F} = 7.6$ Hz, 2C, CH), 127.7 (CH), 119.2 (CH), 118.4 (CH), 114.9 (d, $^2J_{C-F} = 20.6$ Hz, 2C, CH), 38.9 (CH), 22.4 (CH₃). ^{19}F -NMR (376 MHz, CDCl₃): $\delta = -112.6$ (s). HRMS (ESI): m/z Calcd for C₁₅H₁₄FN₄ + H⁺ [M+H]⁺ 269.1197; Found 269.1189.

3.4.2 Procedure for Removal of Directing Group



Removal of DG from Indole. Synthesis of 2-(1-phenylethyl)-1H-indole (8): In an oven dried round bottom flask, 2-(1-phenylethyl)-1-(pyrimidin-2-yl)-1H-indole (**3aa**; 0.100 g, 0.334 mmol) and NaOEt (0.091 g, 1.337 mmol) was introduced and DMSO (5.0 mL) was added under argon atmosphere. The resultant mixture was stirred at 110 °C for 1 h. At ambient temperature, the reaction was quenched with H₂O (10 mL), and the crude product was extracted with EtOAc (10 mL x 3). The combined organic extract was washed with brine, dried over Na₂SO₄ and the volatiles were evaporated in *vacuo*. The remaining residue was purified by column chromatography on silica gel (petroleum ether/EtOAc: 10/1) to yield 2-(1-phenylethyl)-1H-indole (**8**; 0.067 g, 89%) as a light brown liquid. 1H -NMR (500 MHz, CDCl₃): $\delta = 7.46$ (br s, 1H, NH), 7.19-7.18 (m, 3H, Ar-H), 7.14-7.11 (m, 3H, Ar-H), 7.02-6.97 (m, 3H, Ar-H), 6.30 (s, 1H, Ar-H), 4.06 (q, $J = 7.0$ Hz, 1H, CH), 1.58 (d, $J = 7.0$ Hz, 3H, CH₃). ^{13}C -NMR (125 MHz, CDCl₃): $\delta = 144.8$ (C_q), 143.2 (C_q), 136.3 (C_q), 128.9 (2C, CH), 128.6 (C_q), 127.7 (2C, CH), 126.9 (CH), 121.5 (CH), 120.2 (CH), 119.8 (CH), 110.6 (CH), 99.7 (CH), 39.3 (CH), 21.4 (CH₃). HRMS (ESI): m/z Calcd for C₁₆H₁₅N + H⁺ [M+H]⁺ 222.1283; Found 222.1286.

3.4.3 Procedure for Synthesis of methyl (E)-3-(2-(1-phenylethyl)-1-(pyrimidin-2-yl)-1H-indol-7-yl)acrylate (9)



Representative Procedure for Synthesis of 9. To an oven-dried Schlenk tube equipped with magnetic stir bar were introduced 2-(1-phenylethyl)-1-(pyrimidin-2-yl)-*1H*-indole (**3aa**; 0.060 g, 0.20 mmol), methyl acrylate (0.026 g, 0.30 mmol), [(Cp**RhCl*₂)₂] (0.0092 g, 0.015 mmol, 5.0 mol%), Cu(OAc)₂·H₂O (0.040 g, 0.30 mmol) and dissolved in DMF (1.0 mL). The resultant reaction mixture was stirred at 80 °C for 24 h. At ambient temperature, the reaction mixture was diluted with H₂O (5.0 mL). and the crude product was extracted with EtOAc (10 mL x 3). The combined organic extract was washed with brine, dried over Na₂SO₄ and the volatiles were evaporated in *vacuo*. The remaining residue was purified by column chromatography on silica gel (petroleum ether/EtOAc: 20/1) to yield **9** (0.057 g, 74%) as a light orange liquid. ¹H-NMR (400 MHz, CDCl₃): δ = 8.59 (d, *J* = 4.7 Hz, 2H, Ar-H), 7.69 (d, *J* = 7.7 Hz, 1H, Ar-H), 7.35 (d, *J* = 7.4 Hz, 1H, Ar-H), 7.18 (vt, *J* = 7.7 Hz, 1H, Ar-H), 7.12 (t, *J* = 4.9 Hz, 1H, Ar-H), 7.04–6.96 (m, 4H, Ar-H), 6.83–6.81 (m, 2H, Ar-H), 6.73 (d, *J* = 1.0 Hz, 1H, Ar-H), 6.15 (d, *J* = 15.6 Hz, 1H, CH), 4.66 (q, *J* = 7.1 Hz, 1H, CH), 3.63 (s, 3H, OCH₃), 1.67 (d, *J* = 7.1 Hz, 3H, CH₃). ¹³C{¹H}-NMR (100 MHz, CDCl₃): δ = 167.3 (CO), 158.7 (C_q), 158.6 (2C, CH), 145.8 (C_q) 144.3 (C_q), 142.6 (C_q), 135.7 (C_q) 129.8 (C_q), 128.2 (2C, CH), 127.3 (2C, CH), 126.0 (CH), 122.6 (CH), 122.4 (CH), 121.3 (CH), 119.7 (CH), 119.3 (CH), 117.1 (CH), 103.1 (CH), 51.4 (OCH₃), 37.9 (CH), 22.3 (CH₃).

3.4.4 Mechanistic Experiments

3.4.4.1 External Additive Experiments

Procedure for TEMPO/galvinoxyl/BHT added experiment: To a flame dried screw-capped tube equipped with magnetic stir bar was introduced 1-(pyrimidin-2-yl)-*1H*-indole (**1a**; 0.059 g, 0.302 mmol), styrene (**2a**; 0.063 g, 0.605 mmol), Ni(cod)₂ (0.0025 g, 0.009 mmol), PCy₃ (0.0050 g, 0.018 mmol) and TEMPO (0.094 g, 0.601 mmol) [or galvinoxyl (0.253 g, 0.60 mmol) or BHT (0.132 g, 0.6 mmol)]. To the reaction mixture hexane (1.0 mL) was added and stirred at 100 °C in a pre-heated oil bath for 24 h. At ambient temperature, the reaction mixture was quenched with distilled H₂O (10 mL) and *n*-hexadecane (0.025 mL, 0.088 mmol; internal standard) was added. An aliquot of the sample was subjected to the GC analysis. The formation of coupled product (**3aa**) was not observed in the presence of TEMPO or galvinoxyl, whereas 90% of coupled product **3aa** was formed in the presence of BHT.

3.4.4.2 Deuterium Labeling Experiments

Representative Procedure for Reaction of 1a-[2-D] and 2g. To a flame-dried screw-cap tube equipped with magnetic stir bar were introduced 1-(pyrimidin-2-yl)-*1H*-indole-2-d (**1a**-[2-d]; 0.059 g, 0.30 mmol), 4-vinyl-1,1'-biphenyl (**2g**; 0.108 g, 0.60 mmol), Ni(cod)₂ (0.0025 g, 0.009 mmol, 3.0 mol%), PCy₃ (0.0050 g, 0.018 mmol, 6.0 mol%) and hexane (1.0 mL) was added inside the glove box. The resultant reaction mixture in the tube was immersed in a preheated oil bath at 100 °C and stirred for 5 h. At ambient temperature, the reaction mixture was diluted with ethyl acetate (5.0 mL). The volatiles were evaporated *in vacuo* and the remaining crude product mixture was purified by column chromatography on silica gel (petroleum ether/EtOAc: 50/1 – 20/1). ¹H NMR analysis of recovered starting compounds and alkylated product shows significant H/D scrambling.

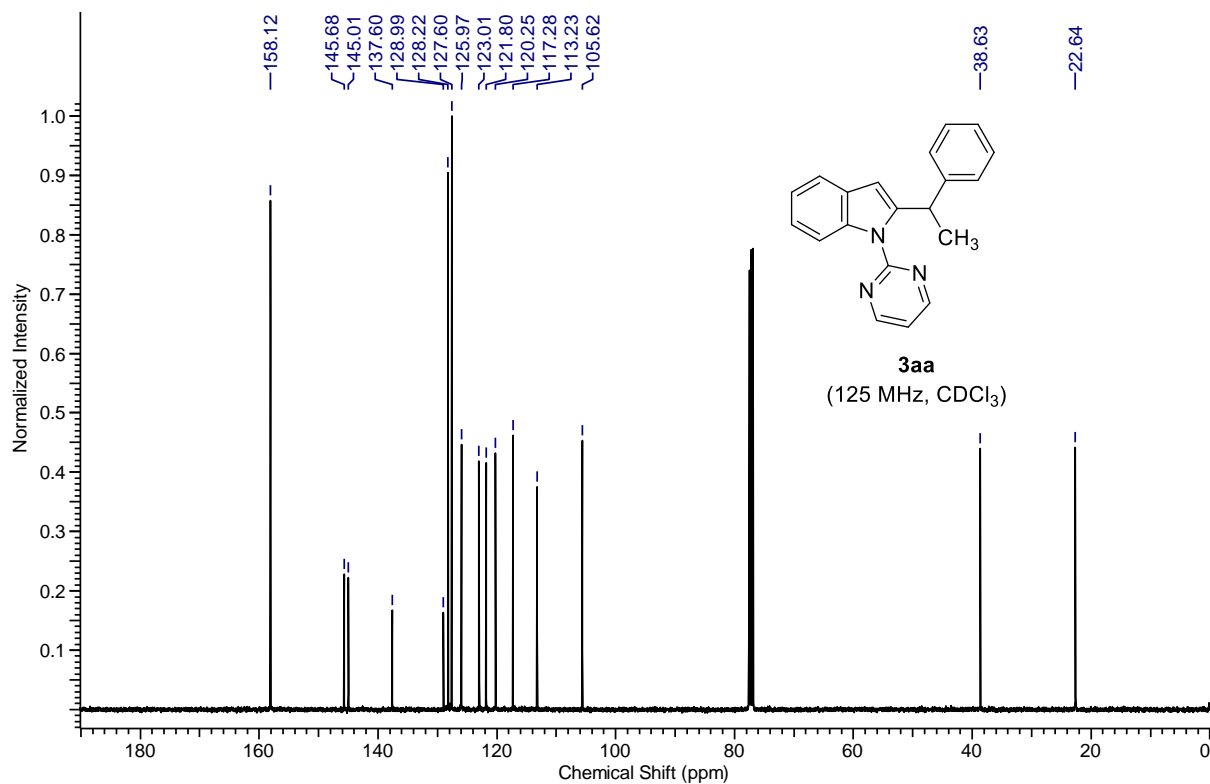
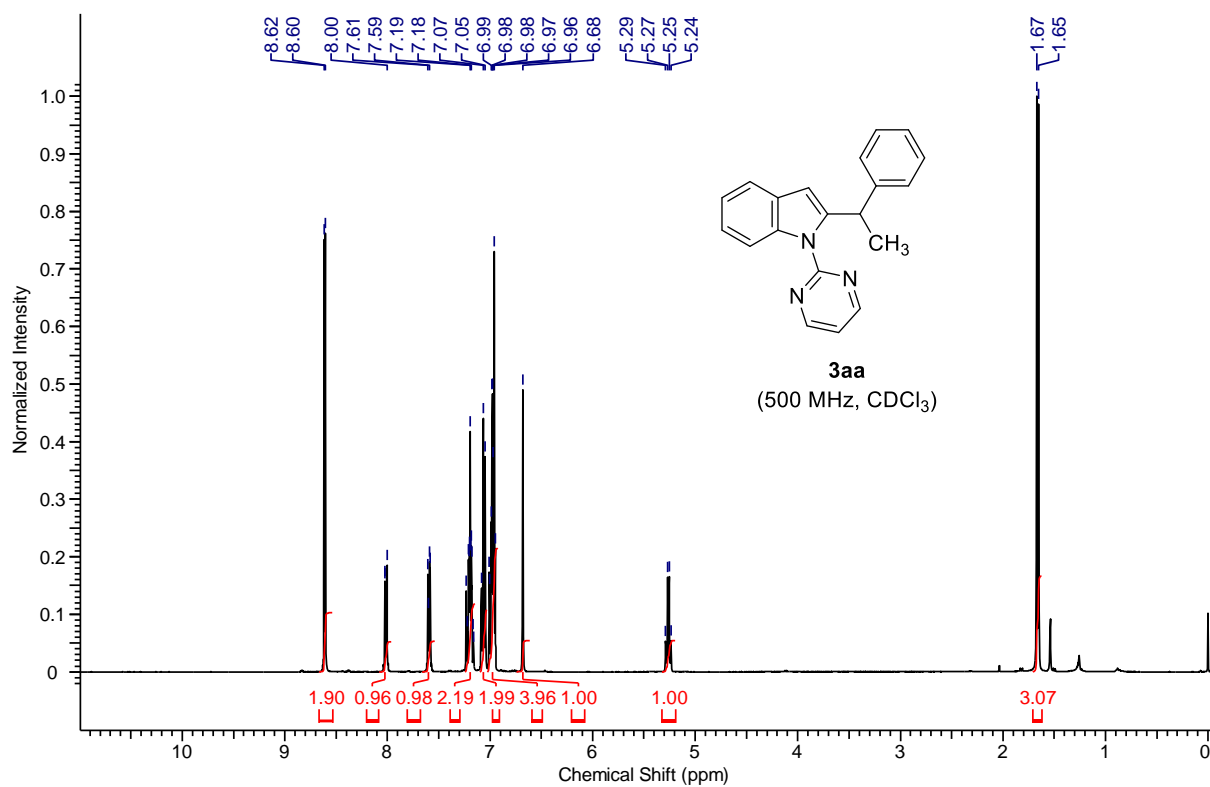
Procedure for H/D Scrambling Experiment (one pot reaction of 1a-[2-D] and 1e). To a flame dried screw-capped tube equipped with magnetic stir bar was introduced 1-(pyrimidin-2-yl)-*1H*-indole-2-d (**1a**-[2-D]; 0.030 g, 0.15 mmol), 5-methoxy-1-(pyrimidin-2-yl)-*1H*-indole (**1e**; 0.034 g, 0.15 mmol), styrene (**2a**; 0.063 g, 0.605 mmol), Ni(cod)₂ (0.0025 g, 0.009 mmol), PCy₃ (0.0050 g, 0.018 mmol). To the reaction mixture hexane (1.0 mL) was added and stirred at 100 °C in a pre-heated oil bath for 5 h. At ambient temperature, the reaction mixture was quenched with distilled H₂O (10 mL) and *n*-hexadecane (0.025 mL, 0.088 mmol; internal standard) was added. The GC analysis of crude reaction mixture shows the coupled products **3aa** and **3ae** was formed in 16% and 24% yield, respectively. ¹H NMR analysis of recovered starting compounds shows extensive H/D scrambling between compound **1a**-[2-D] and **1e**.

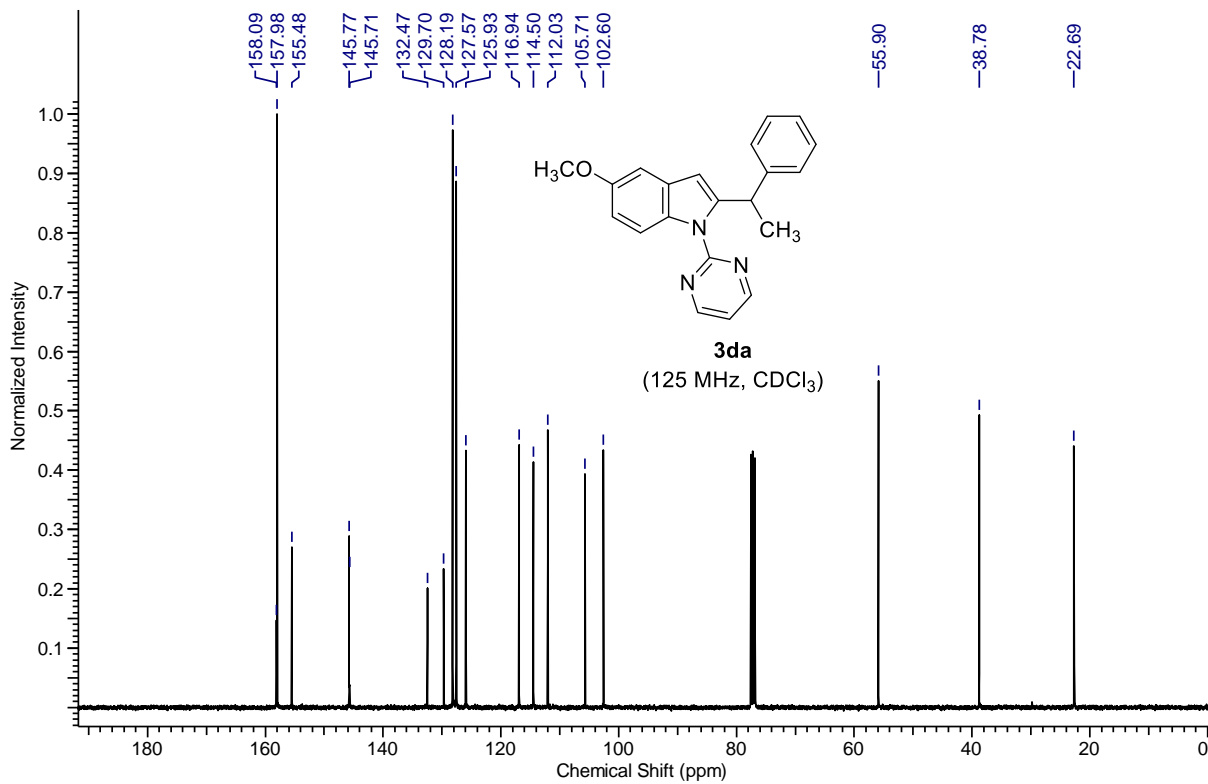
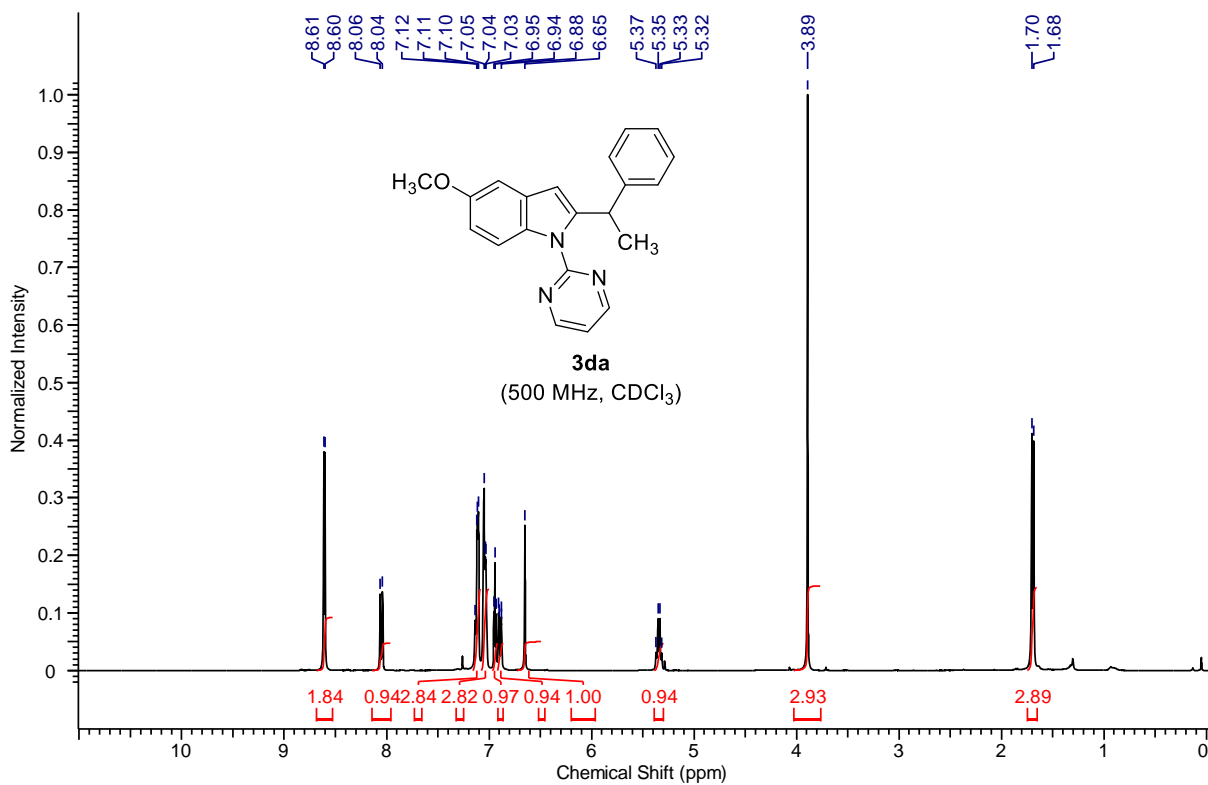
Representative Procedure for Kinetic Isotope Effect (KIE) Study. To a seven different teflon-screw capped tube equipped with magnetic stir bar were introduced 1-(pyrimidin-2-yl)-*1H*-indole (**1a**; 0.059 g, 0.30 mmol, 0.3 M) {or 1-(pyrimidin-2-yl)-*1H*-indole-2-d (**1a**-[2-D]; 0.059 g, 0.30 mmol, 0.3 M)}, styrene (**2a**; 0.063 g, 0.60 mmol, 0.6 M), Ni(cod)₂ (0.0025 g, 0.009 mmol, 0.009 M), PCy₃ (0.0050 g, 0.018 mmol, 0.018 M) and *n*-hexadecane (0.020 mL, 0.070 mmol, 0.070 M, internal standard), and hexane was added inside the glove box. The reaction mixture was then stirred at 100 °C in a pre-heated oil bath. At regular intervals (20, 40, 60, 90, 120, 180, 300 min, etc.), the reaction vessel was cooled to ambient temperature and an aliquot of sample was withdrawn to the GC vial. The sample was diluted with ethyl acetate and subjected to GC analysis. The concentration of the product **3aa** obtained in each sample was determined with respect to the internal standard *n*-hexadecane. The final data was obtained

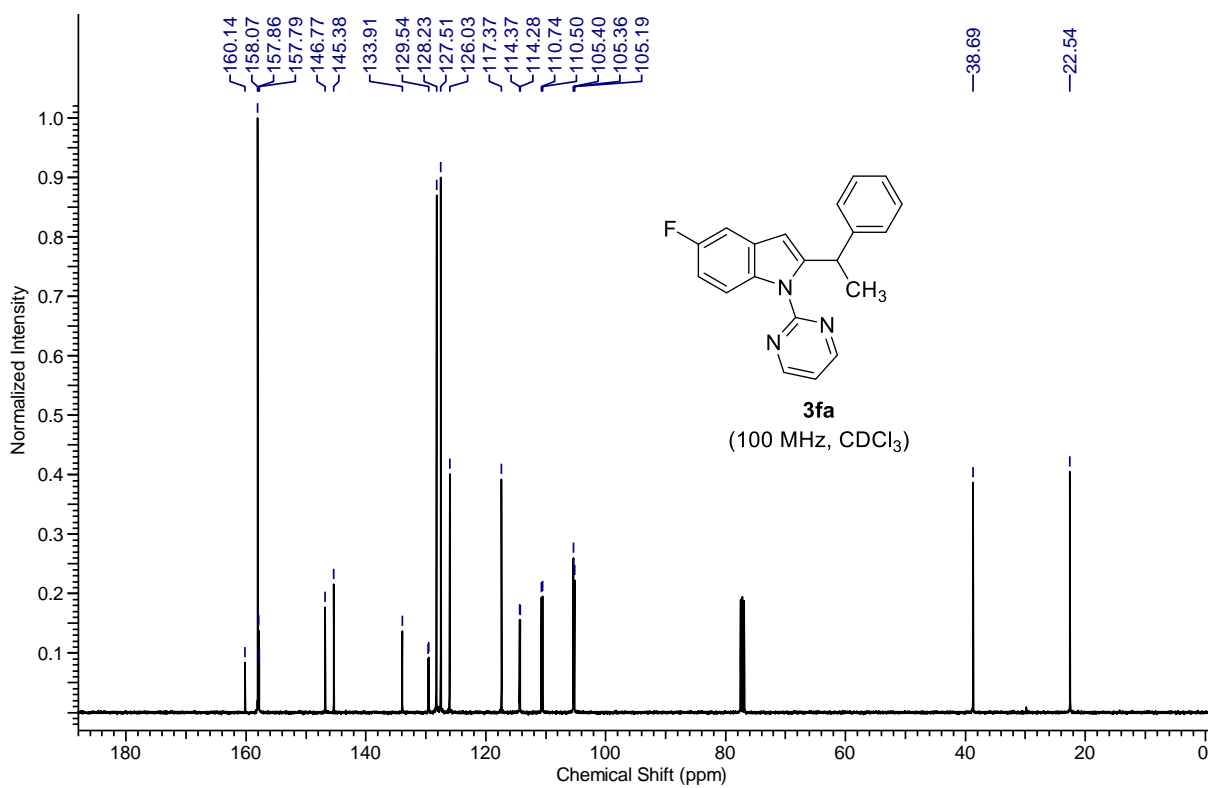
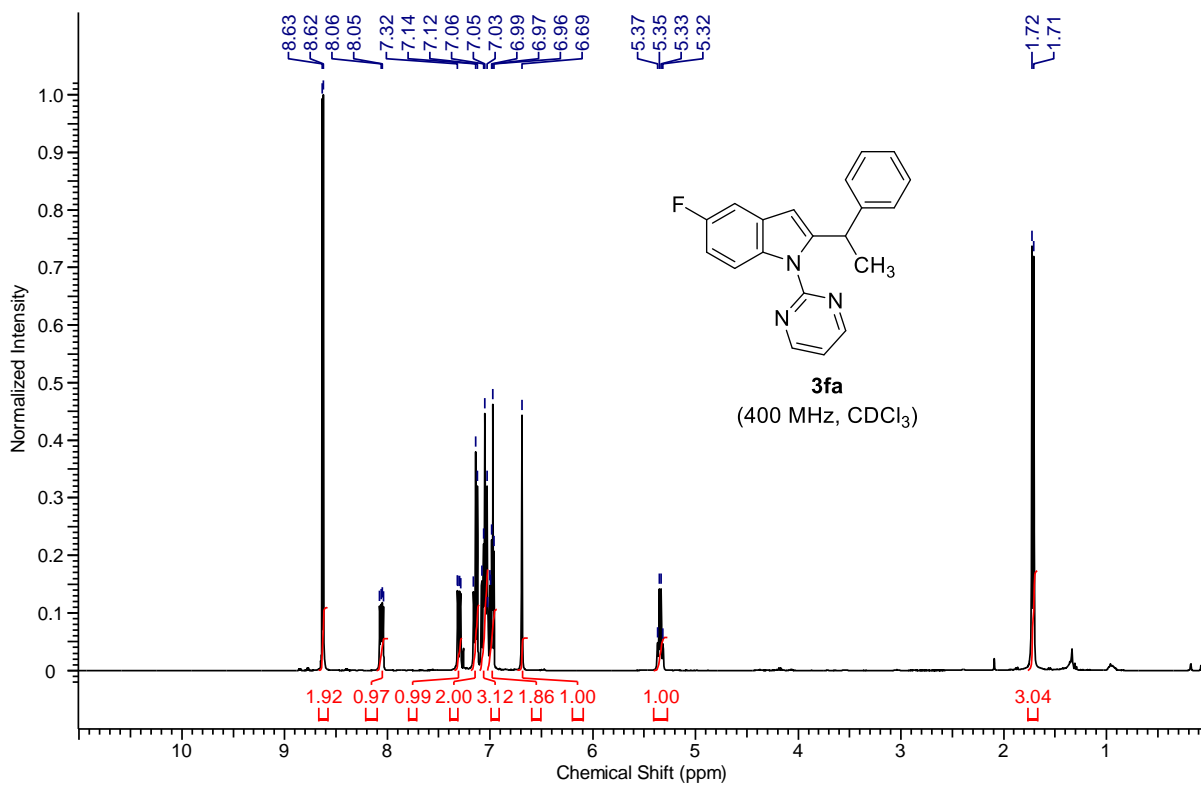
by averaging the results of three independent experiments (Table 3.2). The data of the concentration of the product vs time (min) plot for the early reaction time was drawn (Figure 3.1). The initial rate obtained for the alkylation of 1-(pyrimidin-2-yl)-*1H*-indole (**1a**) was $1.919 \times 10^{-2} \text{ Mmin}^{-1}$, whereas the rate for the alkylation of 1-(pyrimidin-2-yl)-*1H*-indole-2-d (**1a**-[D]) was $1.733 \times 10^{-2} \text{ Mmin}^{-1}$. Therefore, the $k_{\text{H}}/k_{\text{D}} = 1.919 \times 10^{-2}/1.733 \times 10^{-2} = 1.1$.

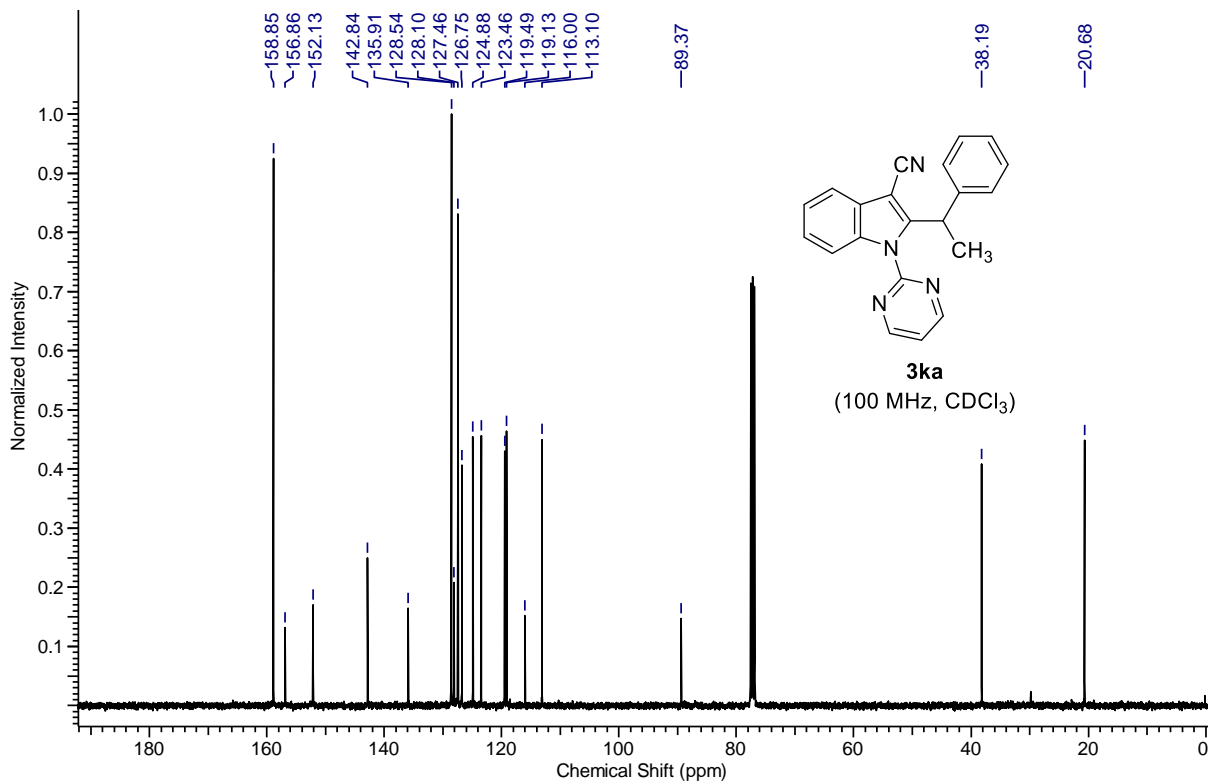
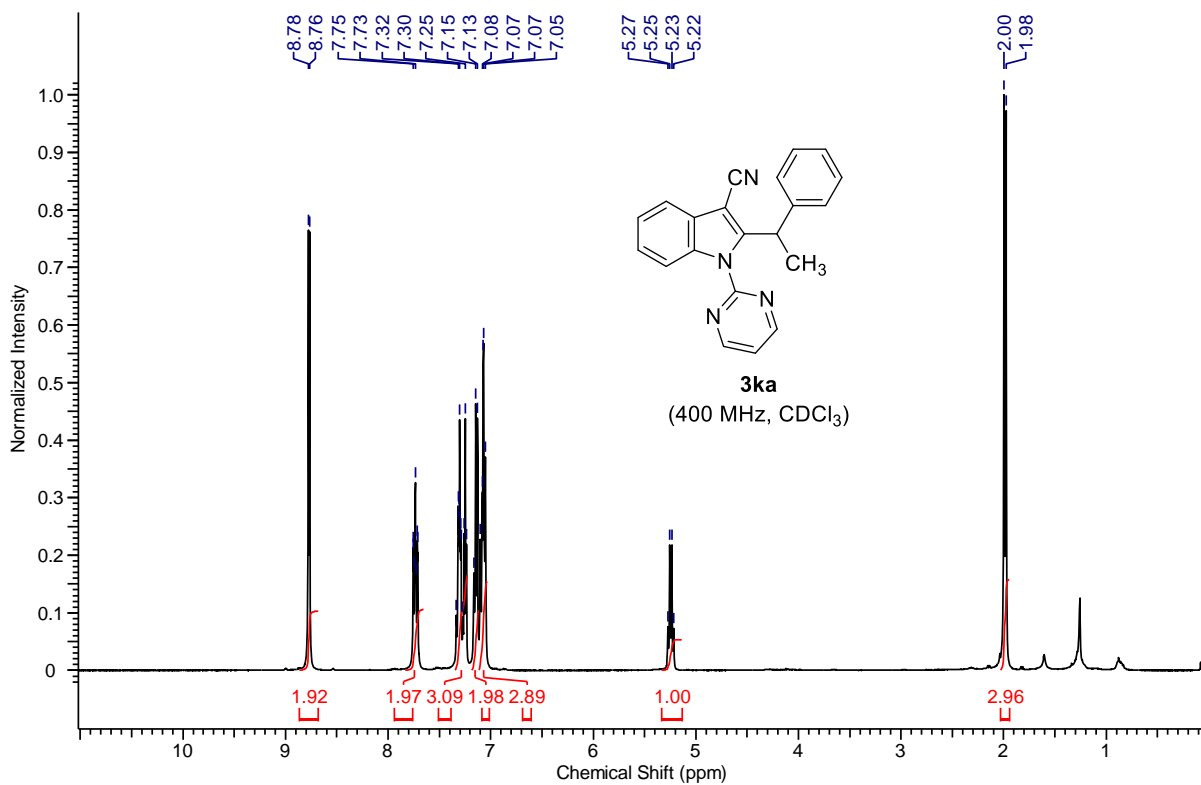
Table 3.2. Concentration of Product 3aa using 1a and 1a-[2-D].

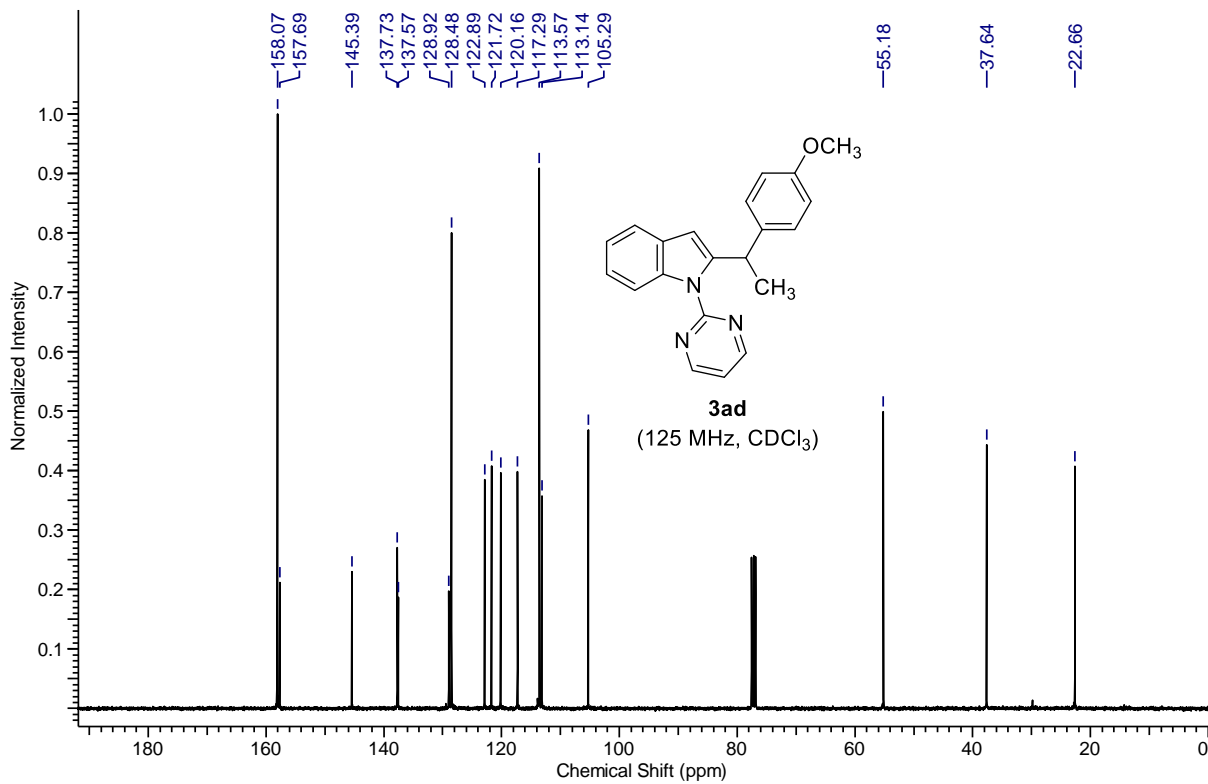
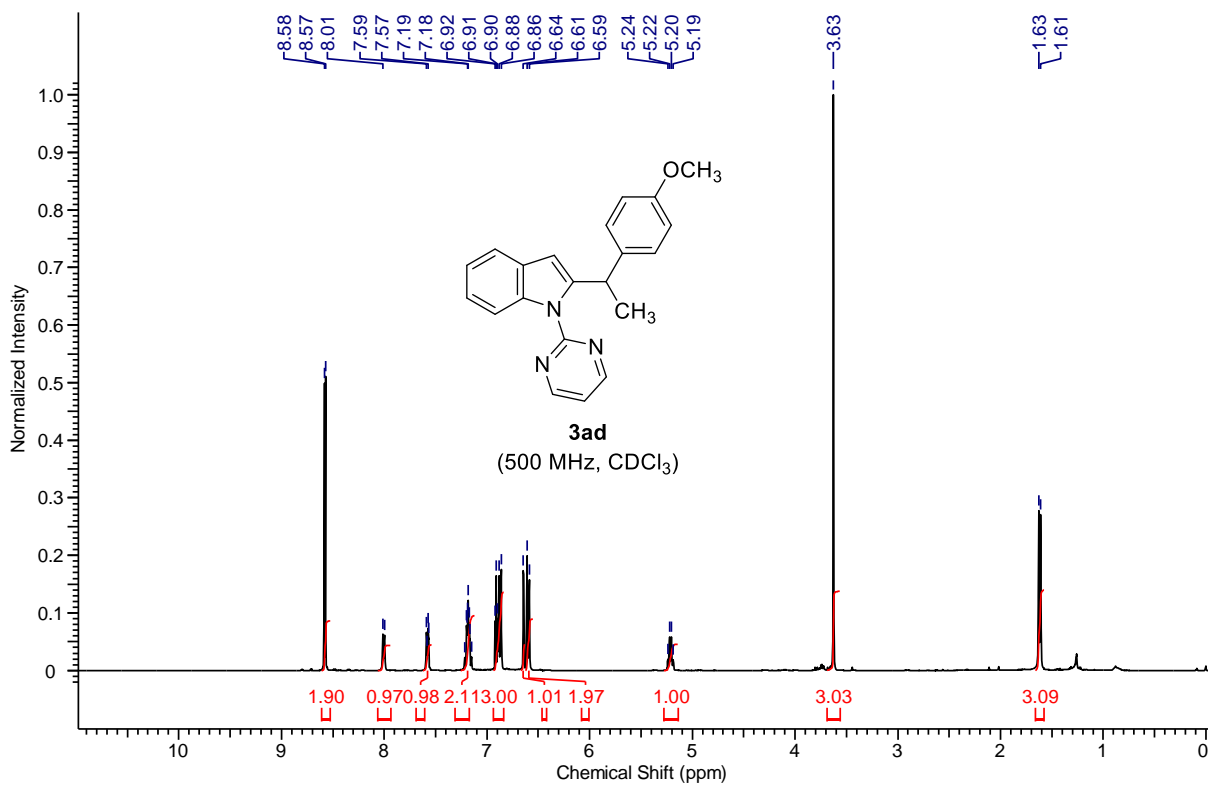
Time (min)	Conc. of 3aa using 1a [M]	Conc. of 3aa using 1a -[2-D] [M]
20	0.207	0.199
40	0.508	0.447
60	0.779	0.724
90	1.457	1.252
120	1.890	1.807
180	3.483	3.118
300	5.408	4.890

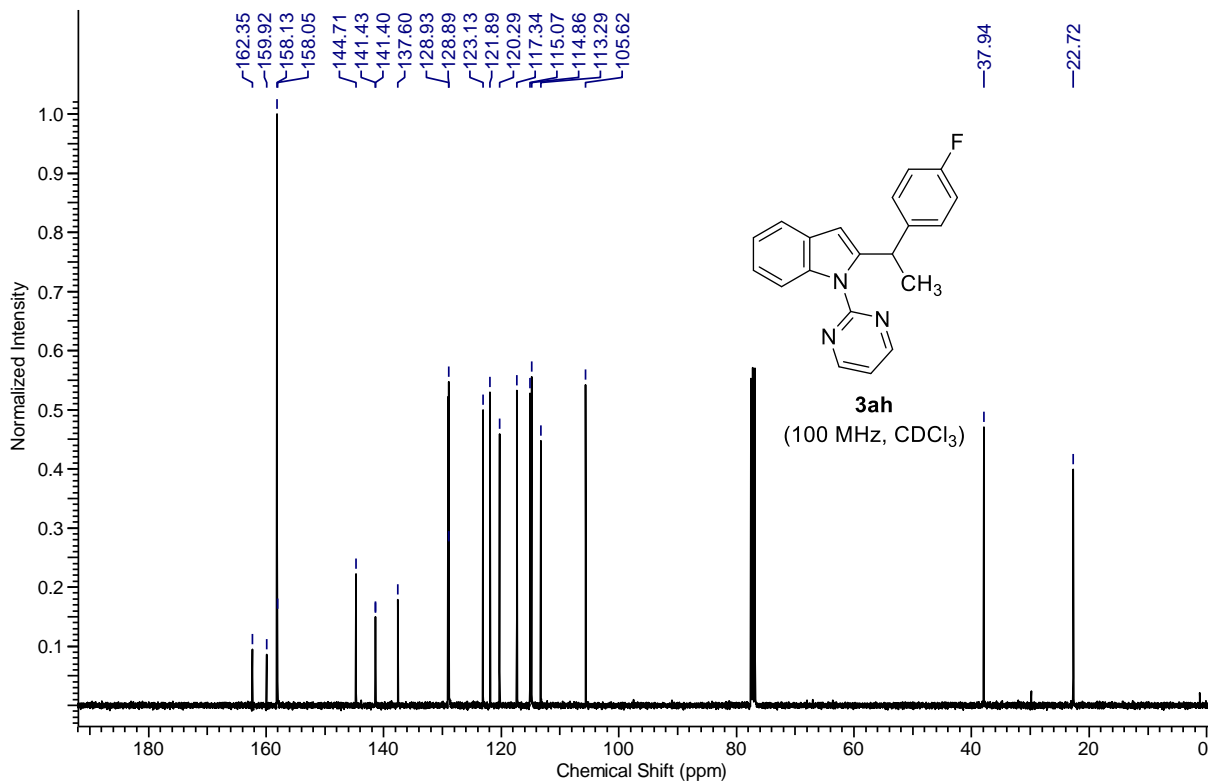
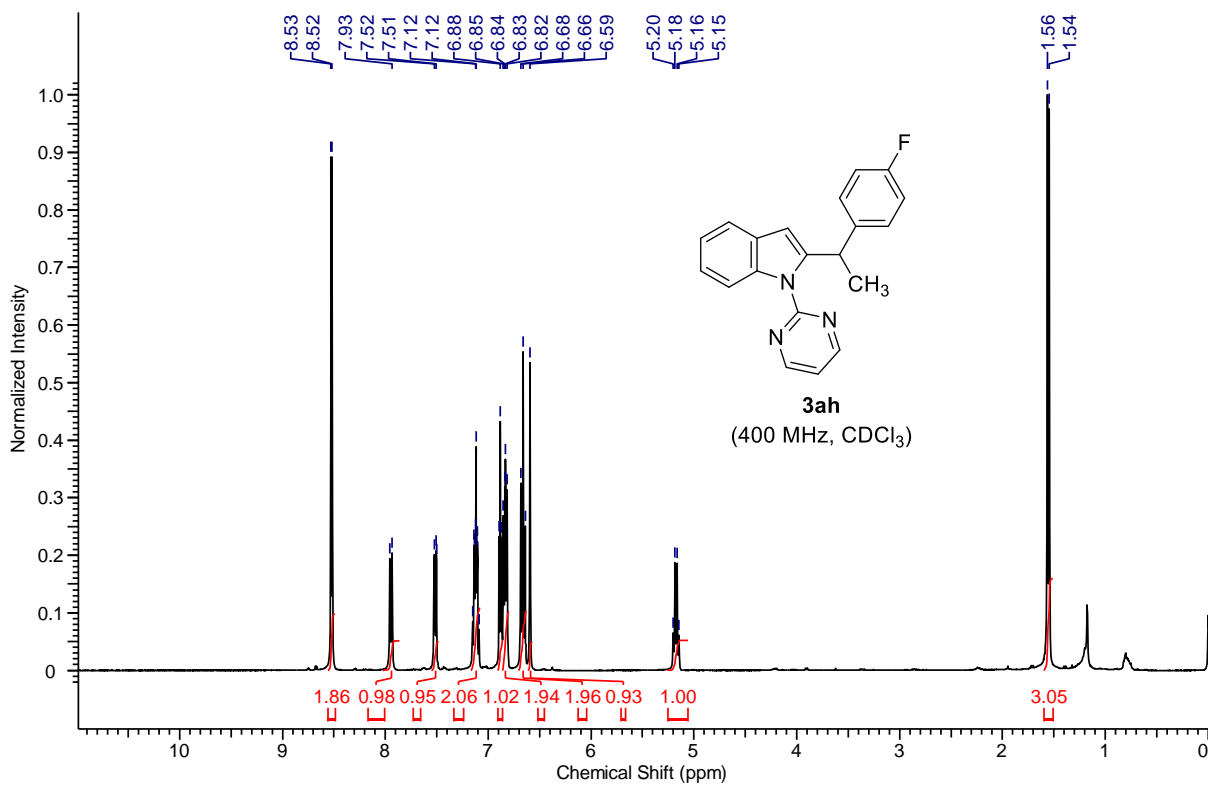
3.4.5 ^1H and ^{13}C NMR Spectra of Alkylated Compounds

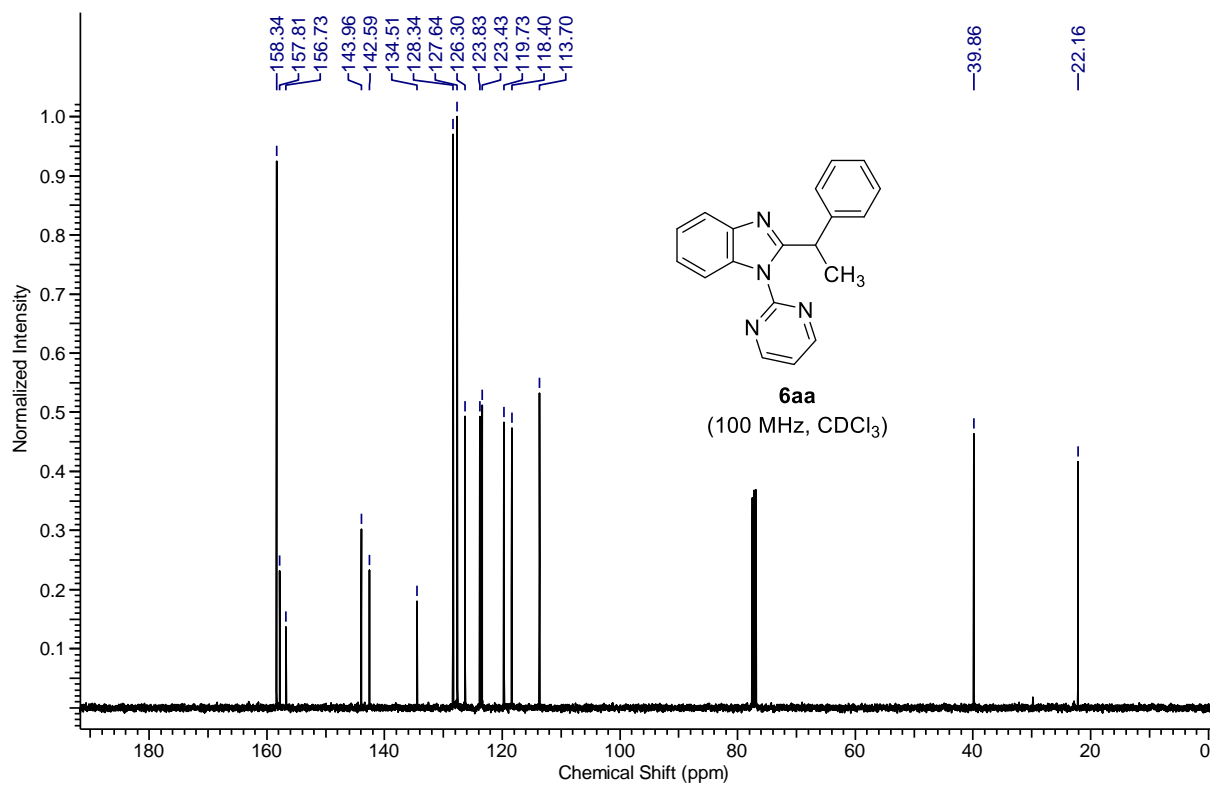
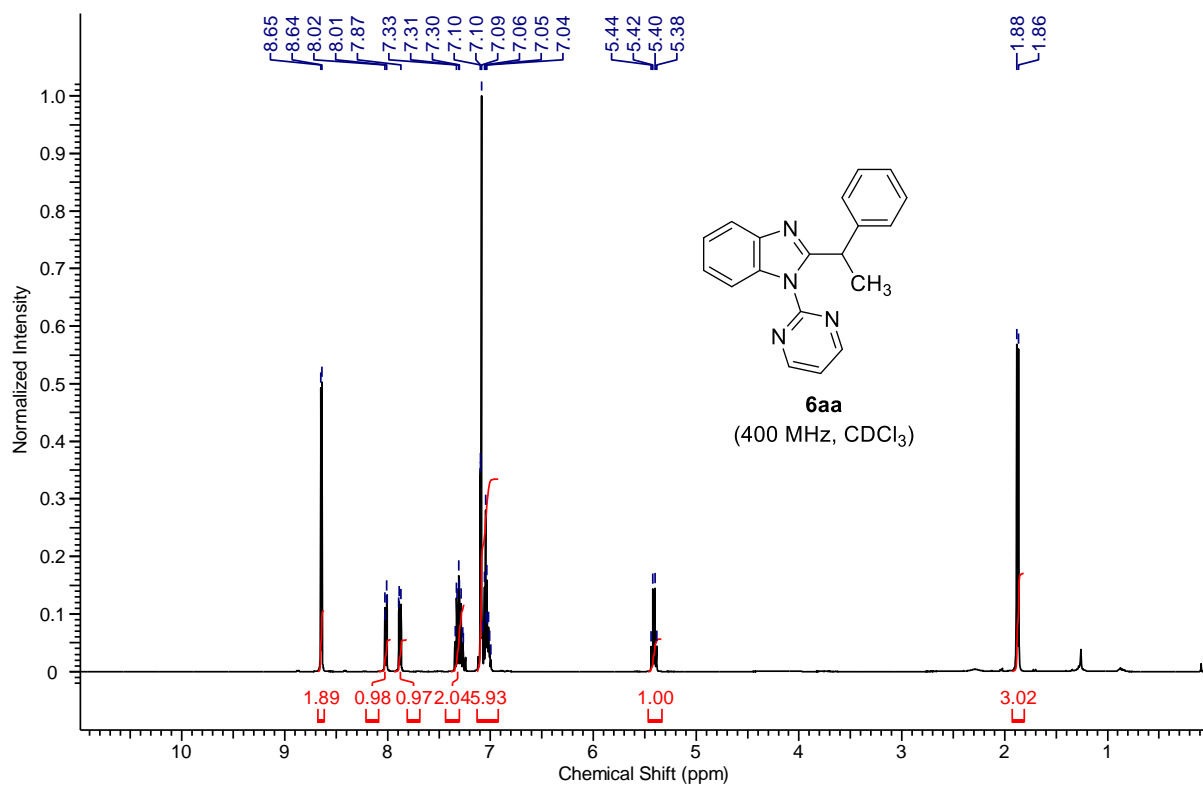


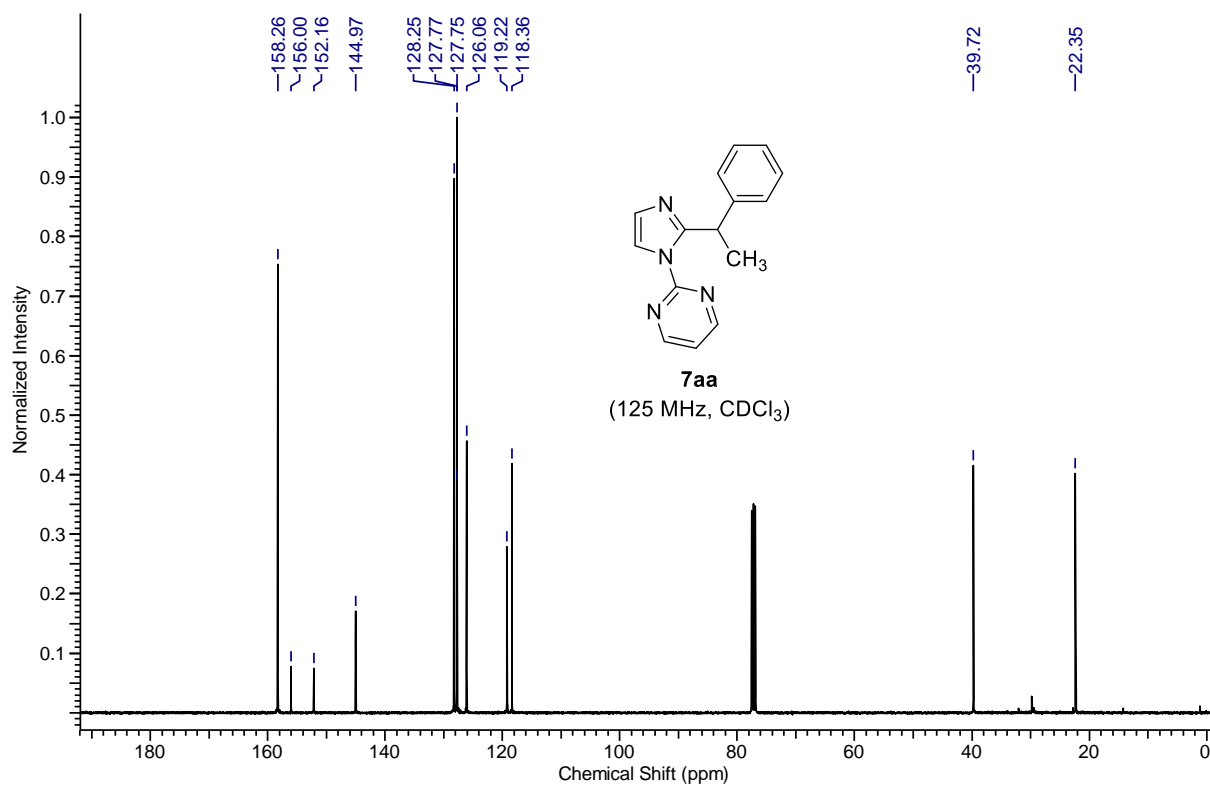
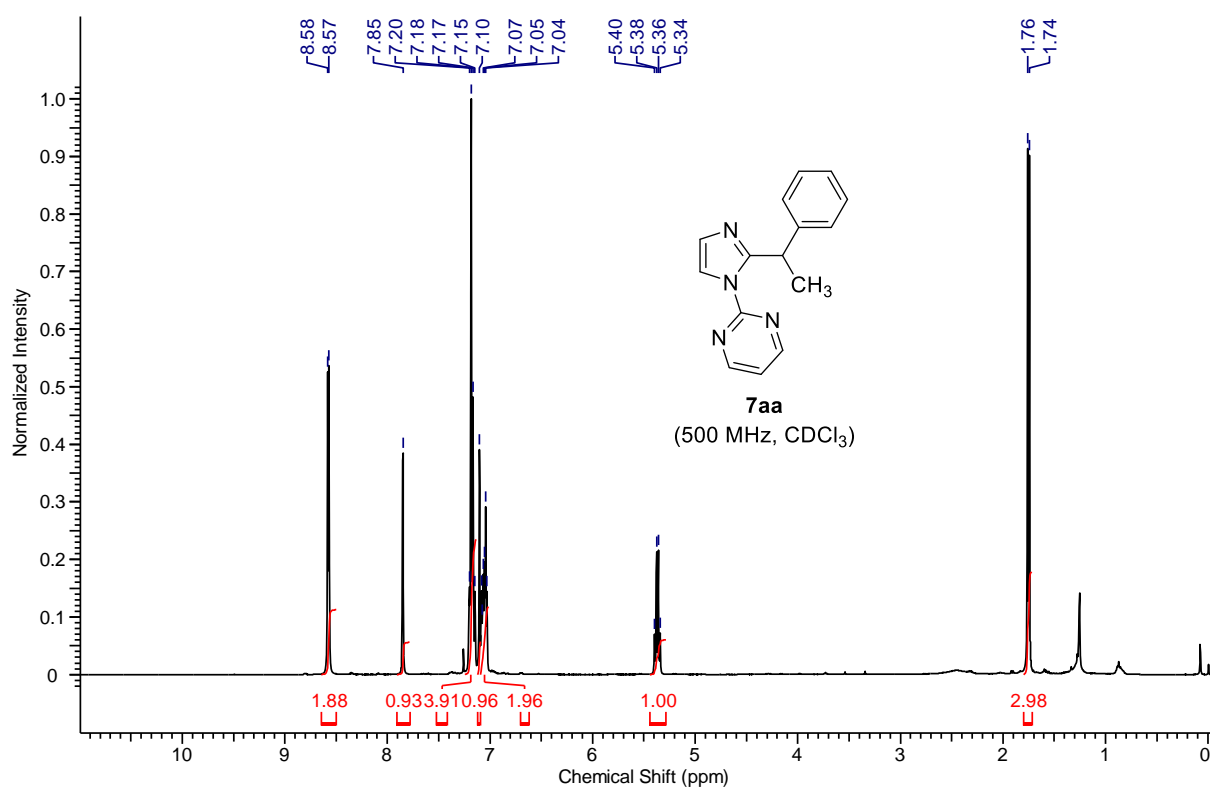












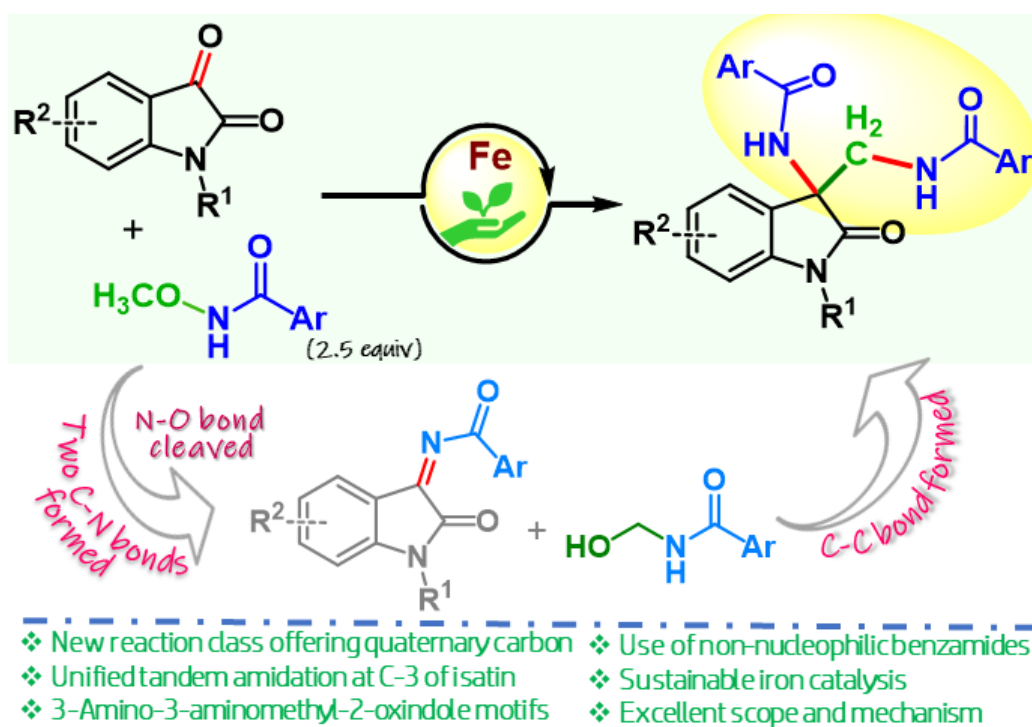
3.5 REFERENCES

- (1) Horton, D. A.; Bourne, G. T.; Smythe, M. L. *Chem. Rev.* **2003**, *103*, 893-930.
- (2) Balbisi, E. A. *Int. J. Clin. Pract.* **2004**, *58*, 695-705.
- (3) Chen, F.-E.; Huang, J. *Chem. Rev.* **2005**, *105*, 4671-4706.
- (4) Kochanowska-Karamyan, A. J.; Hamann, M. T. *Chem. Rev.* **2010**, *110*, 4489-4497.
- (5) Sharma, V.; Kumar, P.; Pathak, D. *J. Heterocycl. Chem.* **2010**, *47*, 491-502.
- (6) Sanford, M. *CNS Drugs* **2012**, *26*, 791-811.
- (7) Melander, R. J.; Minvielle, M. J.; Melander, C. *Tetrahedron* **2014**, *70*, 6363-6372.
- (8) Sheehan, J. C.; Chacko, E.; Lo, Y. S.; Ponzi, D. R.; Sato, E. *J. Org. Chem.* **1978**, *43*, 4856-4859.
- (9) Cornelis, A.; Laszlo, P. *Synthesis* **1985**, *1985*, 909-918.
- (10) Hashimoto, C.; Husson, H.-P. *Tetrahedron Lett.* **1988**, *29*, 4563-4566.
- (11) Dolusic, E.; Larrieu, P.; Blanc, S.; Sapunovic, F.; Norberg, B.; Moineaux, L.; Colette, D.; Stroobant, V.; Pilotte, L.; Colau, D.; Ferain, T.; Fraser, G.; Galeni, M.; Frère, J.-M.; Masereel, B.; Van den Eynde, B.; Wouters, J.; Frédérick, R. *Bioorg. Med. Chem.* **2011**, *19*, 1550-1561.
- (12) Bandini, M.; Melloni, A.; Umani-Ronchi, A. *Angew. Chem. Int. Ed.* **2004**, *43*, 550-556.
- (13) Cacchi, S.; Fabrizi, G. *Chem. Rev.* **2005**, *105*, 2873-2920.
- (14) Minisci Francesco, E. V., and Francesca Fontana *Heterocycles* **1989**, *28*, 489-519.
- (15) Netherton, M. R.; Fu, G. C. *Adv. Synth. Catal.* **2004**, *346*, 1525-1532.
- (16) Ding, Z.; Yoshikai, N. *Beilstein J. Org. Chem.* **2012**, *8*, 1536-1542.
- (17) Satoh, T.; Miura, M. *Chem. Lett.* **2007**, *36*, 200-205.
- (18) Seregin, I. V.; Gevorgyan, V. *Chem. Soc. Rev.* **2007**, *36*, 1173-1193.
- (19) Hirano, K.; Miura, M. *Synlett* **2011**, *2011*, 294-307.
- (20) Pan, S.; Shibata, T. *ACS Catal.* **2013**, *3*, 704-712.
- (21) Ankade, S. B.; Shabade, A. B.; Soni, V.; Punji, B. *ACS Catal.* **2021**, *11*, 3268-3292.
- (22) Jagtap, R. A.; Samal, P. P.; Vinod, C. P.; Krishnamurthy, S.; Punji, B. *ACS Catal.* **2020**, *10*, 7312-7321.
- (23) Jagtap, R. A.; Verma, S. K.; Punji, B. *Org. Lett.* **2020**, *22*, 4643-4647.

-
- (24) Pandey, D. K.; Ankade, S. B.; Ali, A.; Vinod, C. P.; Punji, B. *Chem. Sci.* **2019**, *10*, 9493-9500.
- (25) Punji, B.; Song, W.; Shevchenko, G. A.; Ackermann, L. *Chem. Eur. J.* **2013**, *19*, 10605-10610.
- (26) Soni, V.; Jagtap, R. A.; Gonnade, R. G.; Punji, B. *ACS Catal.* **2016**, *6*, 5666-5672.
- (27) Pan, S.; Ryu, N.; Shibata, T. *J. Am. Chem. Soc.* **2012**, *134*, 17474-17477.
- (28) Schinkel, M.; Marek, I.; Ackermann, L. *Angew. Chem. Int. Ed.* **2013**, *52*, 3977-3980.
- (29) Lu, P.; Feng, C.; Loh, T.-P. *Org. Lett.* **2015**, *17*, 3210-3213.
- (30) Wong, M. Y.; Yamakawa, T.; Yoshikai, N. *Org. Lett.* **2015**, *17*, 442-445.
- (31) Muniraj, N.; Prabhu, K. R. *ACS Omega* **2017**, *2*, 4470-4479.
- (32) Li, J.; Zhang, Z.; Ma, W.; Tang, M.; Wang, D.; Zou, L.-H. *Adv. Synth. Catal.* **2017**, *359*, 1717-1724.
- (33) Zell, D.; Bursch, M.; Müller, V.; Grimme, S.; Ackermann, L. *Angew. Chem. Int. Ed.* **2017**, *56*, 10378-10382.
- (34) Schramm, Y.; Takeuchi, M.; Semba, K.; Nakao, Y.; Hartwig, J. F. *J. Am. Chem. Soc.* **2015**, *137*, 12215-12218.
- (35) Nakao, Y.; Kashihara, N.; Kanyiva, K. S.; Hiyama, T. *Angew. Chem. Int. Ed.* **2010**, *49*, 4451-4454.
- (36) Cornella, J.; Zarate, C.; Martin, R. *Chem. Soc. Rev.* **2014**, *43*, 8081-8097.
- (37) Tobisu, M.; Chatani, N. *Acc. Chem. Res.* **2015**, *48*, 1717-1726.
- (38) Schaub, T.; Backes, M.; Radius, U. *J. Am. Chem. Soc.* **2006**, *128*, 15964-15965.
- (39) Ho, Y. A.; Leiendecker, M.; Liu, X.; Wang, C.; Alandini, N.; Rueping, M. *Org. Lett.* **2018**, *20*, 5644-5647.
- (40) Yang, X.; Sun, H.; Zhang, S.; Li, X. *J. Organometallic Chem.* **2013**, *723*, 36-42.
- (41) Ma, R.; Hu, H.; Li, X.; Mao, G.; Song, Y.; Xin, S. *Catalysts* **2022**, *12*, 1665.
- (42) Yang, J.; Fan, L.; Chen, C.; Wang, M.; Sun, B.; Wang, S.; Zhong, H.; Zhou, Y. *Org. Biomole. Chem.* **2023**, *21*, 494-498.
- (43) Gao, H.; Hu, L.; Hu, Y.; Lv, X.; Wu, Y.-B.; Lu, G. *Chem. Commun.* **2022**, *58*, 8650-8653.

Chapter-4

Iron-Catalyzed Synthesis of 3,3-disubstituted 3-Amino Oxindoles: An Efficient Route to the Construction of Quaternary Stereocenter

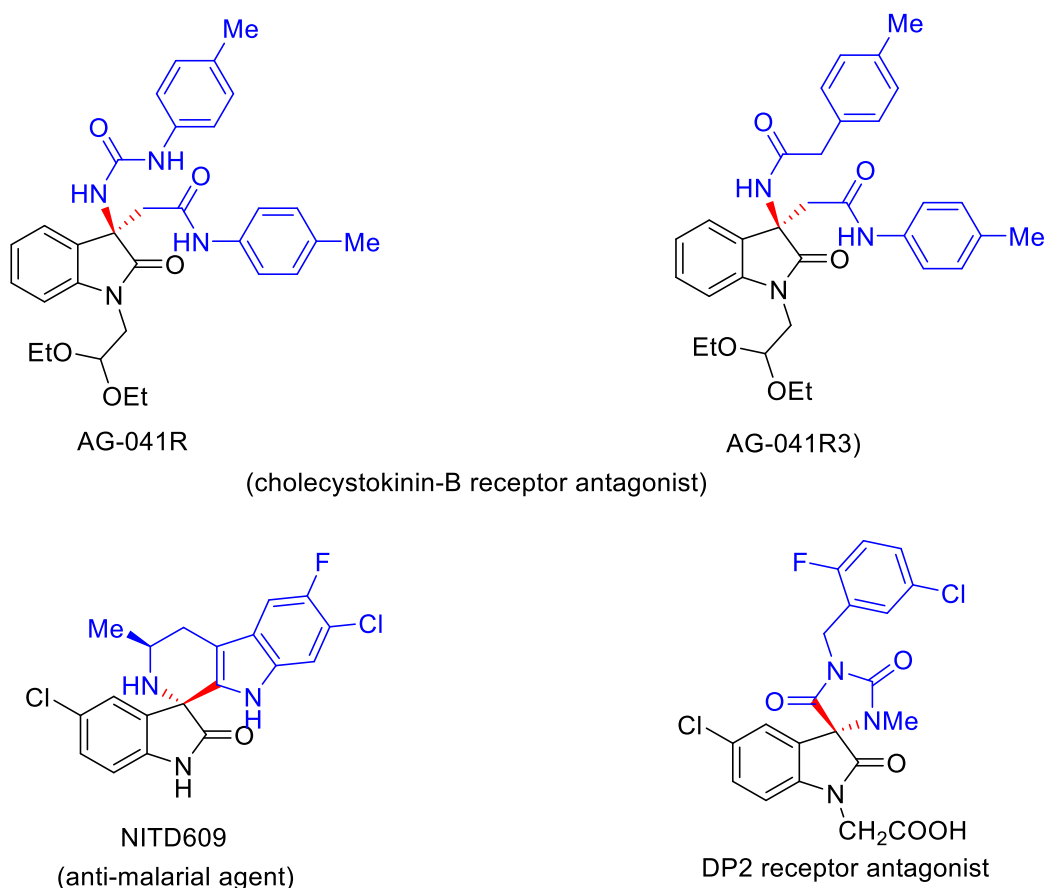


4.1 INTRODUCTION

An oxindole-bearing tetrasubstituted stereogenic quaternary center is present in various biologically active compounds and naturally occurring alkaloids.¹⁻⁶ More particularly, the stereogenic 3,3-disubstituted-3-amino-2-oxindoles are considered as privileged structural motifs and found in a variety of biologically active compounds, such as cholecystokinin-B receptor antagonists AG-041R,⁷ anti-malarial agent NITD609,⁸ or spirohydantoin DP2 receptor antagonist⁹ (Scheme 4.1). Indeed, due to the presence of two nitrogen atoms in spirohydantoin, the stability of the CRTH2 (DP2) receptor enhances in human plasma, and showed good potency and high bioavailability of DP2 receptor antagonists.⁹ Therefore, the development of novel strategy for their sustainable and step-economical synthesis is highly desirable.

Owing to the importance of chiral 3-amino oxindoles in pharmaceuticals, significant attention has been devoted for their synthesis using organocatalysts or chiral transition metal catalysts.¹⁰⁻¹⁴ Generally, for the synthesis of stereogenic 3-amino oxindoles, the nucleophilic addition of different nucleophiles to the isatins or isatin derived ketimines is the most efficient and straightforward synthetic approach.¹⁵⁻³⁶ These nucleophilic addition reaction includes, Mannich reaction, Morita-Baylis-Hillman reaction, Henry reaction, *aza*-Friedel-Craft reaction and Strecker reaction. On the other hand, direct functionalization of oxindoles or 3-substituted oxindoles also provides access for the synthesis of stereogenic 3-substituted 3-amino oxindoles (Chapter 1, Scheme 1.36).³⁷⁻⁴¹ Although, these methodologies provide the synthesis of stereogenic 3-amino oxindoles, they require multi-step process involving the addition of sensitive nucleophiles to isatin-derived ketimines. Thus, there is a need to develop an efficient, straightforward and sustainable method for the construction of stereogenic quaternary centers by replacing sensitive nucleophiles. Given our efforts towards the development of base metal-catalyzed, environmentally benign protocols, we serendipitously discovered a new reaction *via* novel strategy for the synthesis of 3,3-disubstituted 3-amino oxindoles in the presence of an iron catalyst. The reaction of isatins with *N*-methoxy benzamides in the presence of abundant FeCl₃ catalyst led to unexpected reaction and skeletal reorganization to construction the quaternary stereocenter. The product **3aa** having C-3 stereogenic carbon center with four different functionalities, C–Ar, C–C(O)R, C–NH-R and C–CH₂-NHR, has triggered our interest. To the best of our knowledge, the N-O bond cleavage in the presence of iron, followed by MeOH dehydrogenation, and methylene incorporation into the isatin to produce 3-amino oxindole has not been precedented. The advantages of this method are (i) the use of accessible

N-methoxy benzamides and isatins (ii) the generation of stereogenic quaternary centers (iii) the cleavage of N–O bond and the incorporation of the methylene group (iv) the use of an earth-abundant iron catalyst, (v) excellent scope with the tolerance of sensitive and synthetic useful functionalities, and (vi) detailed mechanistic investigation.



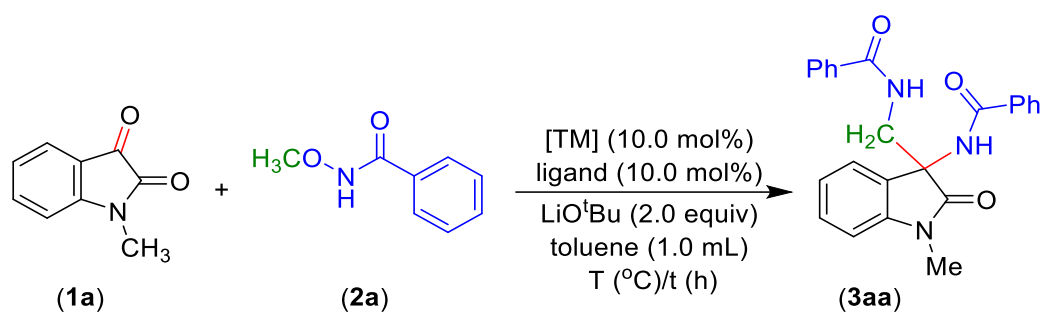
Scheme 4.1. Biologically active 3-amino-2-oxindoles

4.2 RESULTS AND DISCUSSION

4.2.1 Optimization of Reaction Conditions for Synthesis of 3,3-Disubstituted 3-Amino Oxindoles

During our initial investigation towards the reactivity of isatin (**1a**) with *N*-methoxybenzamide (**2a**) under iron catalysis, we found that the reaction was efficiently proceeded in toluene at 120 °C, and **3aa** was obtained in 74% yield (Table 4.1, entry 1). Screening of various Fe(II) and Fe(III) salts as catalysts in the presence of LiO^tBu provided a good yield of **3aa** (Table 4.1, entries 1-5). Notably, the use of FeCl₃ salt as a catalyst for the reaction in toluene at 120 °C afforded 84% yield of **3aa** (entry 5). The molecular structure of

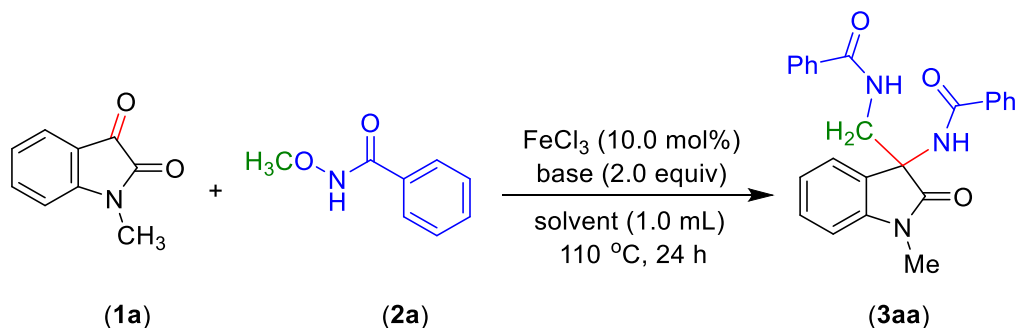
3aa was established by a single-crystal X-ray diffraction. The use of FeCl₃ catalyst along with various ancillary phosphine-based or nitrogen-based ligands such as dppf, xantphos, dppbz, bpy, phen or neocuproine led to slight decreases in the yield of **3aa**, which could be due to the restriction in approach of isatin to FeCl₃ catalyst in presence of other ligands (entries 6-12). The reaction was examined with various mild and strong inorganic bases (LiOAc, NaOAc, KOAc, CsOAc, Li₂CO₃, Na₂CO₃, K₂CO₃, Cs₂CO₃, NaO^tBu and KO^tBu), wherein only LiO^tBu and Cs₂CO₃ bases were found to be effective (Table 4.2). The reaction proceeded smoothly in many other solvents like 1,4-dioxane, *tert*-butyl benzene, mesitylene, and chlorobenzene, whereas the reaction in CH₃CN gave a poor yield of **3aa** (Table 4.2). Notably, the reaction could deliver **3aa** in quantitative yield of 85% even at 110 °C for 24 h (entry 13). Further decrease in the reaction temperature or lowering the catalyst loading (< 10 mol%) resulted in a slightly low yield. A reaction using a 99.99% pure FeCl₃ catalyst also provided the product **3aa** in quantitative yield (entry 14), indicating the trace impurity in FeCl₃ was not responsible for the reaction. We attempted the reaction in the presence of catalytic or stoichiometric amounts of Lewis acids, such as BF₃.Et₂O, BCl₃, and AlCl₃ in the absence of FeCl₃ (entry 15), wherein the reaction failed to deliver the product **3aa**. This indicates that the use of FeCl₃ catalyst is crucial, and is less likely acts as a simple Lewis acid in the reaction. Moreover, the attempted reaction using other transition metal catalysts, such as MnCl₂, NiCl₂, Ni(OTf)₂, CoCl₂, CuCl₂, and PdCl₂ failed to provide **3aa**, whereas the [(*p*-cymene)RuCl₂]₂ as catalyst afforded **3aa** in 56% yield (entries 16-21). These findings highlight the unified role of iron in the present reaction. The use of an iron catalyst and LiO^tBu was essential for this reaction, without which the formation of **3aa** was not observed. Thus, after a careful screening of all reaction parameters, we found that the reaction of **1a** with **2a** (2.5 equiv) employing 10 mol% of FeCl₃ in the presence of LiO^tBu (2.0 equiv) at 110 °C produced **3aa** in 85% yield.

Table 4.1 Optimization of reaction conditions.

Entry	[TM]	Ligand	T (°C)/ t (h)	3aa (%) ^a
1	FeCl ₂	--	120/24	74%
2	FeBr ₂	--	120/24	70%
3	Fe(OTf) ₂	--	120/24	76%
4	Fe(acac) ₃	--	120/24	78%
5	FeCl ₃	--	120/24	84%
6	FeCl ₃	dppf	120/24	64%
7	FeCl ₃	xantphos	120/24	69%
8	FeCl ₃	dppbz	120/24	67%
9	FeCl ₃	bpy	120/24	70%
10	FeCl ₃	^t Bu-bpy	120/24	65%
11	FeCl ₃	phen	120/24	63%
12	FeCl ₃	neocuproine	120/24	58%
13	FeCl₃	--	110/24	85%
14^b	FeCl₃	--	110/24	83%
15 ^c	LA	--	110/24	NR
16	MnCl ₂	--	110/24	NR
17	[Ni]	--	110/24	NR
18	CoCl ₂	--	110/24	NR
19	CuCl ₂	--	110/24	NR
20	PdCl ₂	--	110/24	trace
21	[(p-cym)RuCl ₂] ₂	--	110/24	56%

Reaction Conditions: **1a** (0.032 g, 0.20 mmol), **2a** (0.076 g, 0.503 mmol), [Fe] (0.02 mmol), base (0.40 mmol), solvent (1.0 mL). ^a Isolated yield. ^b A 99.99% pure FeCl₃ was used. ^c Employing 10 mol% of Lewis acids.

Table 4.2 Screening of different bases and solvents.



Entry	Base	Solvent	3aa (%) ^a
1	LiO ^t Bu	toluene	85%
2	NaO ^t Bu	toluene	trace
3	KO ^t Bu	toluene	trace
4	LiOAc	toluene	NR
5	NaOAc	toluene	NR
6	KOAc	toluene	NR
7	CsOAc	toluene	NR
8	Li ₂ CO ₃	toluene	trace
9	Na ₂ CO ₃	toluene	NR
10	K ₂ CO ₃	toluene	NR
11	Cs ₂ CO ₃	toluene	75%
12	LiO ^t Bu	<i>tert</i> -butyl benzene	72%
13	LiO ^t Bu	mesitylene	77%
14	LiO ^t Bu	1,4-dioxane	79%
15	LiO ^t Bu	chlorobenzene	78%
16	LiO ^t Bu	CH ₃ CN	20%

Reaction Conditions: **1a** (0.032 g, 0.20 mmol), **2a** (0.076 g, 0.503 mmol), FeCl₃ (0.02 mmol), base (0.40 mmol), solvent (1.0 mL). ^a Isolated yield.

4.2.2 Substrate Scope for Synthesis of 3,3-Substituted 3-Amino-2-Oxindoles

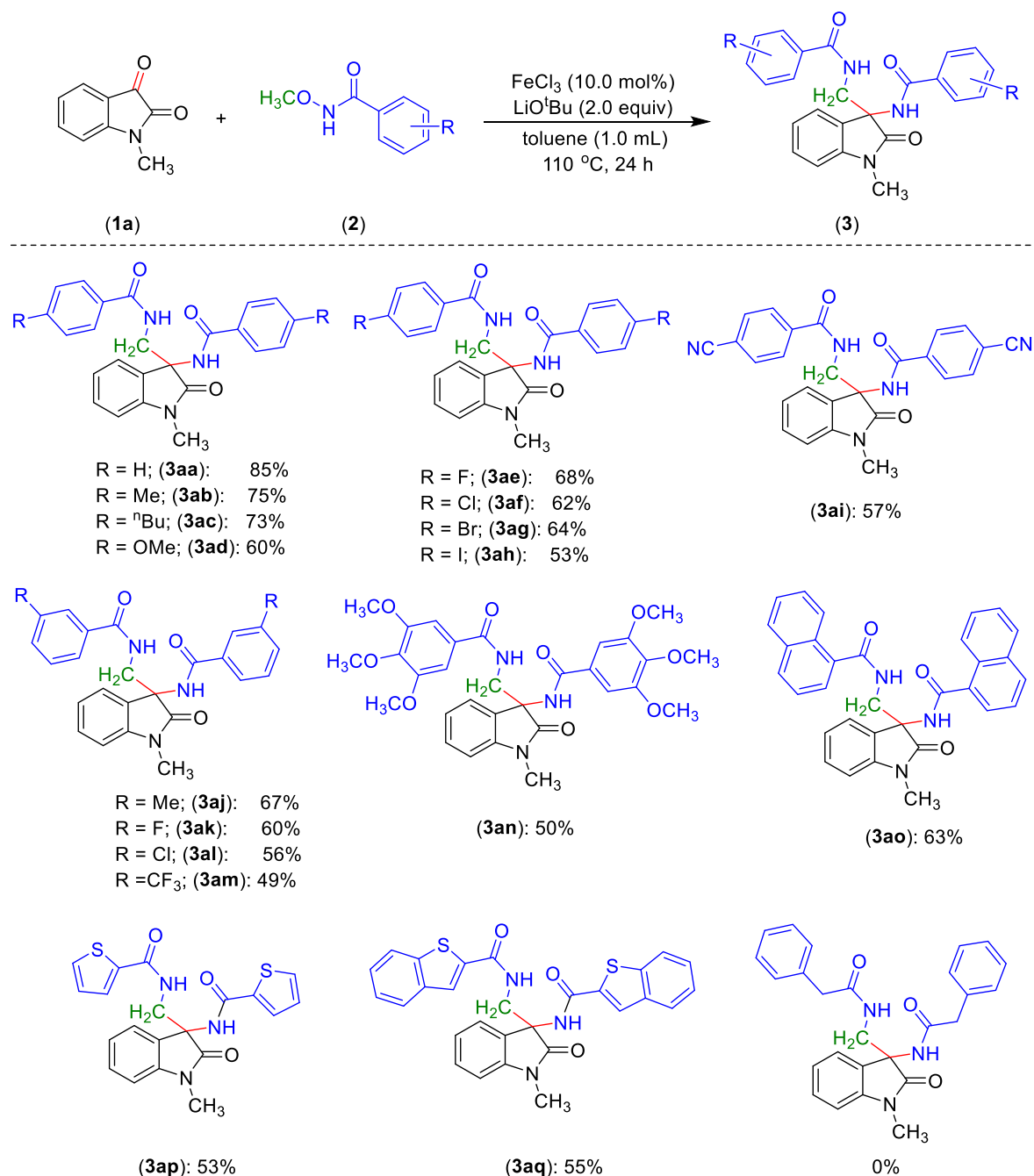
4.2.2.1 Substrate Scope with Benzamides

The scope and limitation for the synthesis of diverse 3,3-substituted 3-amino-2-oxindole derivatives is explored under the optimized reaction conditions using an earth-abundant iron catalyst. Initially, the reaction of various benzamides with 1-methylindoline-2,3-dione was carried out in toluene at 110 °C for 24 h (Scheme 4.2). A range of functional groups at different positions of *N*-methoxybenzamide were well tolerated under the optimized reaction conditions. The *N*-methoxybenzamides bearing alkyl and alkoxy substituents at the para position provided moderate to good yield of desired products (**3ab-3ad**). The *N*-methoxybenzamides containing sensitive functional groups such as –F, –Cl, and –Br, –I, and –CN at the C-4 position smoothly reacted to afford **3ae-3ai** in quantitative yields. The compatibility of such functionalities is important for the post-functionalization and diversification of 3,3-substituted 3-amino-2-oxindole derivatives. The reaction of *meta*-substituted *N*-methoxybenzamides also delivered the desired 3-amino-2-oxindoles in moderate to good yields (**3aj-3am**). The tri-methoxy-substituted *N*-methoxybenzamide and *N*-methoxy-1-naphthamide produced **3an** and **3ao** in 50% and 63% yields, respectively. Importantly, heteroaryl amides such as *N*-methoxythiophene-2-carboxamide and *N*-methoxybenzothiophene-2-carboxamide were participated under the optimal reaction conditions to provide **3ap** and **3aq** in moderate yields. Unfortunately, the aliphatic amide, *N*-methoxy-2-phenylacetamide failed to give desired product under the reaction conditions. Moreover, the *N*-ethoxybenzamide and *N*-benzyloxybenzamide failed to participate in the reaction. It is noted that N–O bond cleavage was observed in the case of *N*-ethoxybenzamide and *N*-(benzyloxy)benzamide substrates.

4.2.2.2 Substrate Scope with Isatins

The protocol was extended to the scope of isatin derivatives. The C-5 substituted isatins bearing electronically distinct functionalities reacted smoothly with *N*-methoxybenzamide and provided the products **3ba-3fa** in moderate to good yields (Scheme 4.3). Isatins containing *N*-alkyl substituents with different chain lengths were efficiently reacted with *N*-methoxybenzamide to deliver the products **3ga-3la** in good yields. An *N*-isobutyl isatin upon reaction with *N*-methoxybenzamide delivered the desired compound **3ma** in 79% yield. The

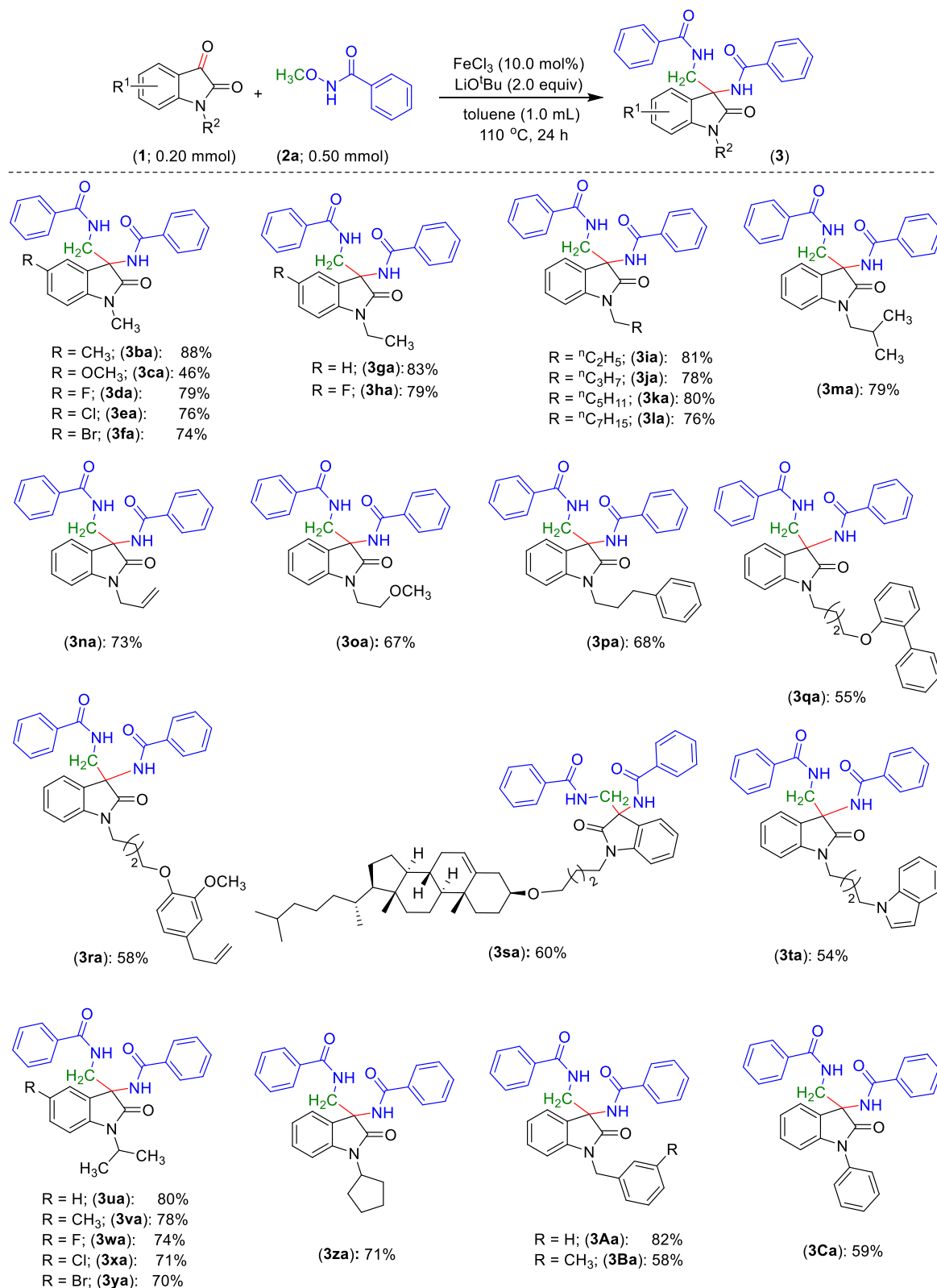
isatins with diverse functional groups such as alkenyl, methyl ether, alkyl-phenyl, and phenyl ether were compatible with the optimal reaction conditions to produce **3na-3qa** in good yields.



Scheme 4.2. Scope with diverse *N*-methoxybenzamide substrates. (Reaction Conditions: **1a** (0.032 g, 0.20 mmol), **2** (0.076 g, 0.503 mmol), FeCl₃ (0.02 mmol), LiO^tBu (0.40 mmol), toluene (1.0 mL))

The biologically relevant compounds such as eugenol and polycyclic cholesterol-derived isatin could participate in the reaction to afford **3ra** and **3sa** in 58% and 60% yields, respectively. Notably, the heteroarene such as indole-containing isatin was also tolerated under the reaction conditions to afford the product **3ta** in 54% yield. Additionally, the isatins bearing

secondary acyclic and cyclic alkyl functionalities at the *N*-position underwent efficient coupling with *N*-methoxybenzamide to give the 3-amino-2-oxindoles **3ua-3za** in good yields. The tolerability of -F, -Cl, and -Br functionality is crucial for the synthetic perspective.

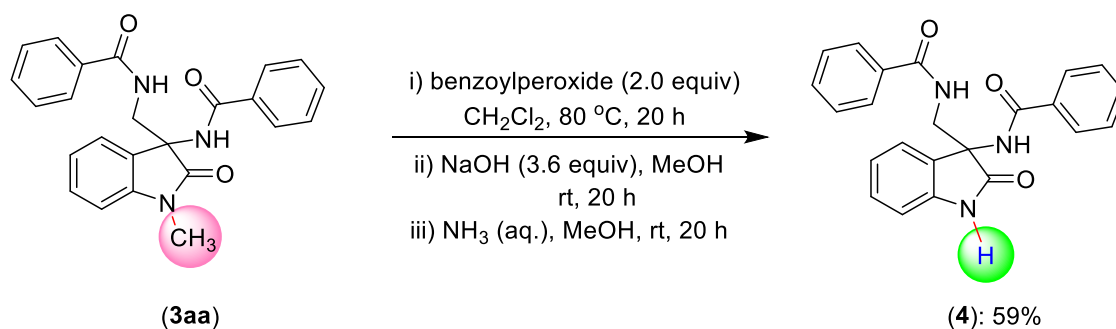


Scheme 4.3. Substrate scope with isatin substrates. (Reaction Conditions: **1** (0.032 g, 0.20 mmol), **2a** (0.076 g, 0.503 mmol), FeCl₃ (0.02 mmol), LiO^tBu (0.40 mmol), toluene (1.0 mL))

Additionally, the *N*-benzyl and *N*-phenyl substituted isatins were effectively reacted with *N*-methoxybenzamide to afford products **3Aa**, **3Ba**, and **3Ca** in 82%, 58%, and 59% yields, respectively. A synthetically important and sensitive functional group, –COOMe, remains unaffected under the reaction condition (**3Ba**).

4.2.3 Gram Scale Synthesis and Derivatization of 3,3-Disubstituted 3-Amino Oxindoles

In order to demonstrate the synthetic and practical importance of stereogenic 3,3-disubstituted 3-amino oxindoles, we have performed a 3.1 mmol scale reaction, wherein 63% yield of **3aa** was obtained under the optimized condition. Considering the usefulness of free *NH* stereogenic 3,3-disubstituted 3-amino oxindole, the *N*-Me group in **3aa** was smoothly converted to *NH* resulting in compound **4** with 59% yield (Scheme 4.4).

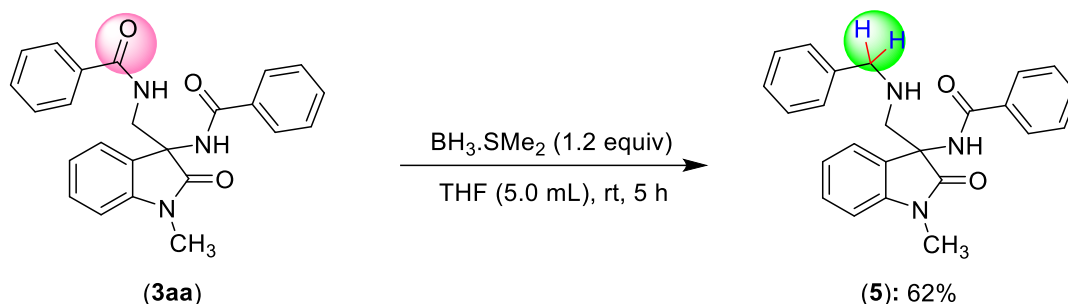


Scheme 4.4. Removal of *N*-Me group of **3aa**.

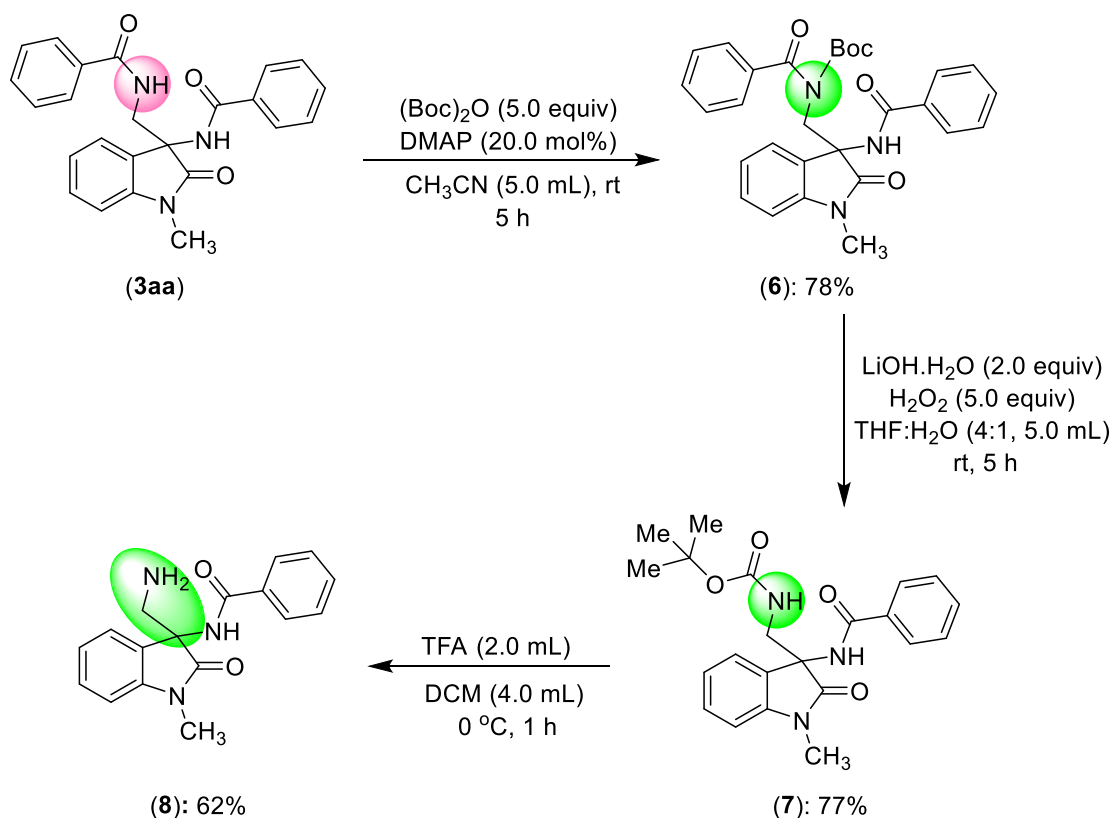
The 3,3-disubstituted-3-amino-2-oxindoles bearing a stereogenic quaternary center present in a variety of biologically active compounds with enormous pharmaceutical properties. Given the importance of this structural motif, one of the carbonyl functionality in compound **3aa** was selectively reduced. Thus, the reaction of **3aa** with BH₃.SMe₂ in THF at room temperature afforded 62% yield of partially reduced product *N*-(3-((benzylamino)methyl)-1-methyl-2-oxindolin-3-yl)benzamide (**5**) (Scheme 4.5). Unfortunately, we failed to reduce all the carbonyl motifs in compound **3aa**.

Furthermore, we attempted the deprotection of the amide functionality of compound **3aa** in three steps (Scheme 4.6). Initially, the free *NH* in compound **3aa** was protected using di-*tert*-butyl dicarbonate (Boc anhydride) and DMAP in acetonitrile at room temperature to deliver compound **6** in 78% yield. The compound **6** was subjected to base-mediated hydrolysis

using LiOH.H₂O and H₂O₂ in a mixture of THF:H₂O at room temperature to yield compound **7** in 77% yield. Next, compound **7** was treated with trifluoroacetic acid (TFA) in dichloromethane at 0 °C to afford compound **8** in 62% yield.



Scheme 4.5. Selective partial reduction of **3aa**.



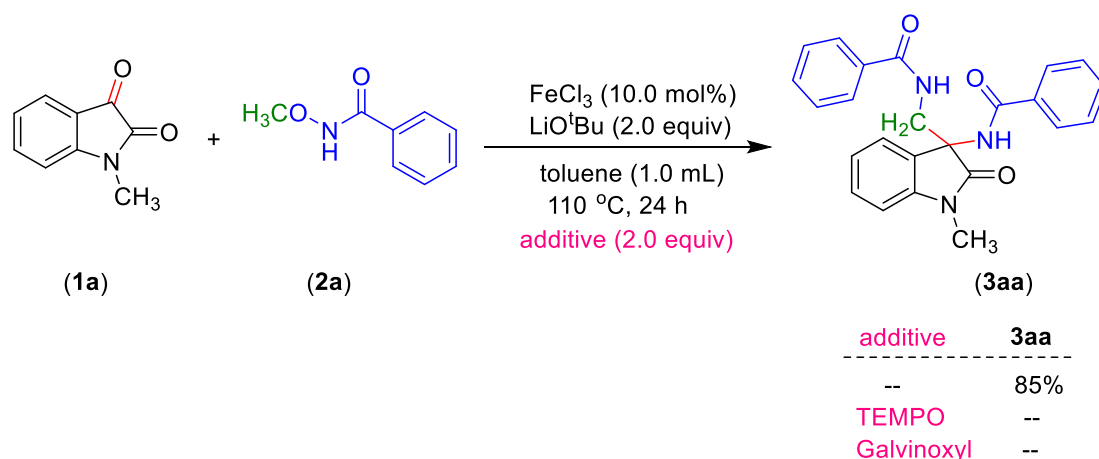
Scheme 4.6. Synthesis of *N*-(3-(aminomethyl)-1-methyl-2-oxindolin-3-yl)benzamide.

4.2.4 Mechanistic Aspects

4.2.4.1 External Additive Experiments

To understand the reaction mechanism, detailed mechanistic studies have been carried out for the synthesis of 3-substituted 3-amino oxindoles in the presence of a FeCl₃ catalyst. The

reaction was completely quenched in the presence of 2 equiv of radical scavengers, TEMPO, and galvinoxyl highlighting the involvement of radical species in this catalytic system (Scheme 4.7). When, both the starting compounds **1a** and **2a** were recovered in quantitative amounts. Notably, the reaction was performed using 0.5 equiv of TEMPO, the product **3aa** obtained in low yield (48%). These results ruled out the participation of odd-electron iron species and also tentatively suggest the involvement of carbon-centric organic radical species. However, we did not observe any TEMPO-bound alkyl species in the attempted controlled experiments.



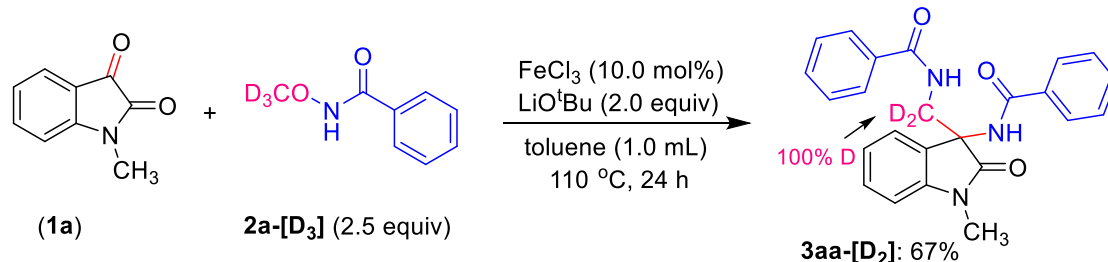
Scheme 4.7. External additive experiments.

4.2.4.2 Deuterium Labeling and Controlled Experiments

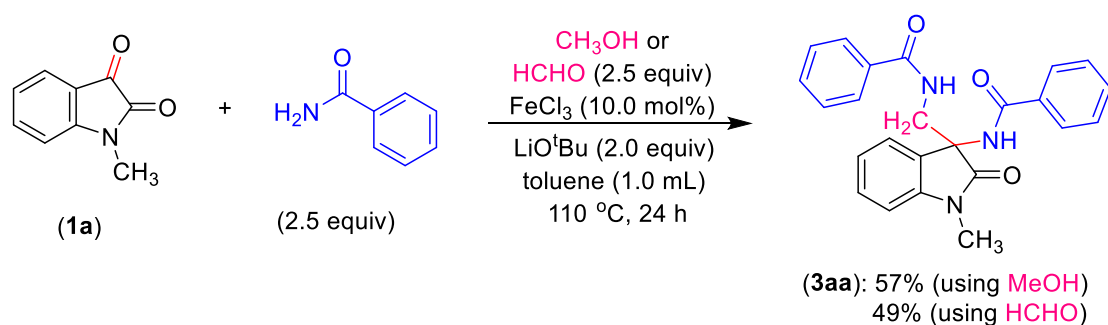
To gain insight into the reaction mechanism, initially we investigated the origin and mode of methylene ($-\text{CH}_2-$) incorporation in the product **3aa**. The reaction of 1-methylindoline-2,3-dione (**1a**) with *N*-(methoxy- d_3)benzamide (**2a**-[D_3]) under the standard catalytic conditions delivered **3aa**-[D_2] in 67% yield with 100% incorporation of deuterium at methylene carbon (Scheme 4.8a). This suggests that the *N*-methoxy group present in substrate **2a** is the sole source of methylene present in **3aa**. Moreover, the independent reaction of **1a** with benzamide (2.5 equiv) in the presence of CH_3OH or HCHO (2.5 equiv) and CD_3OD (2.5 equiv) under the catalytic conditions produced **3aa** and **3aa**-[D_2], respectively (Schemes 4.8b and 4.8c). These findings highlighted the probable dissociation of methoxy ($-\text{OMe}$) group from *N*-methoxybenzamide as CH_3OH , followed by the dehydrogenation to HCHO , prior to the methylene insertion into **3aa**. A reaction of 1-methylindoline-2,3-dione (**1a**) with *N*-methoxybenzamide (**2a**) in the presence of CD_3OD (2.5 equiv) under optimal conditions provided the product **3aa**-[H/D] with 32% deuterium incorporation at methylene (Scheme 4.9a). Similarly, the reaction of **1a** with *N*-(methoxy- d_3)benzamide (**2a**-[D_3]) in the presence

of CH₃OH (2.5 equiv) afforded **3aa**-[H/D] with a 48% deuterium incorporation at methylene center (Scheme 4.9b). These findings suggest that the methoxy (-OCH₃) dissociation from **2a** and methylene (CH₂) transfer to product **3aa**, involving Fe-catalyst and isatin **1a**, does not occur via an intramolecular process; however, it proceeds *via* an intermolecular pathway.

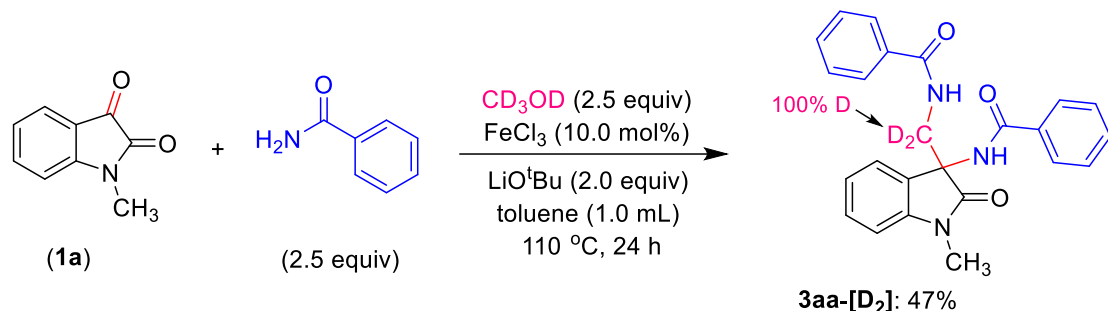
(a) Reaction of **1a** with **2a**-[D₃]



(b) Reaction of **1a** with benzamide in presence of CH₃OH (or HCHO)



(c) Reaction of **1a** with benzamide in presence of CD₃OD

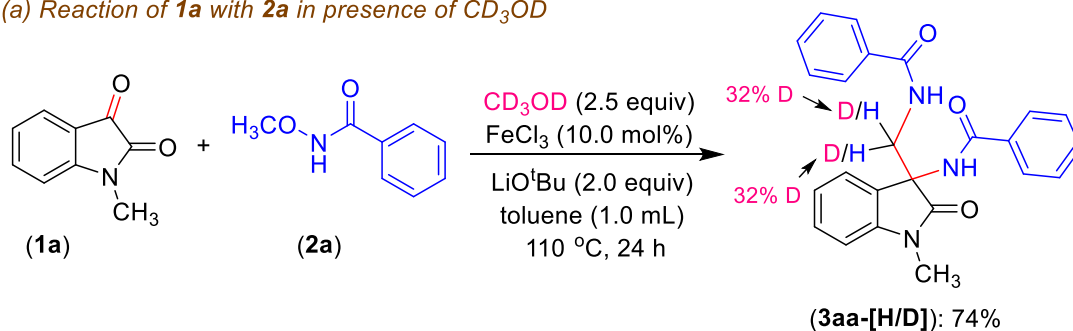


Scheme 4.8. Controlled experiments for the origin of methylene (-CH₂-) group.

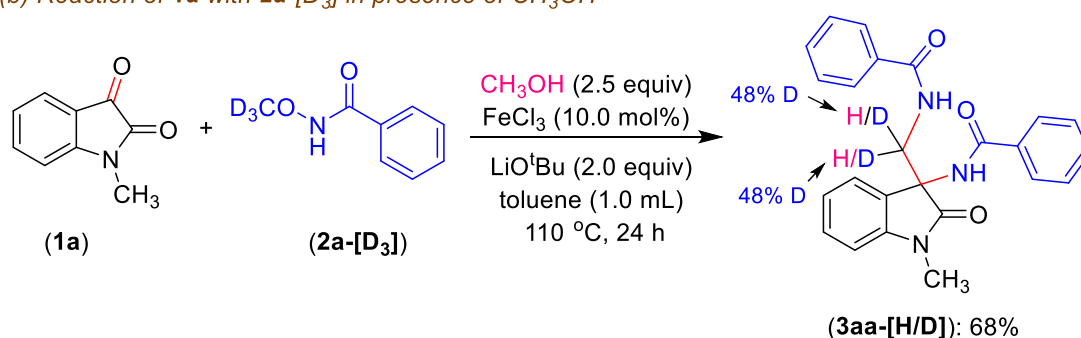
A series of experiments were aimed to investigate the cleavage of N–O bond of *N*-methoxybenzamide. The *N*-methoxybenzamide (**2a**) in the absence of isatin **1a** under standard reaction conditions did not produce benzamide. However, the same reaction in the presence of catalytic amount **1a** led to the generation of benzamide, albeit in 8% yield. This indicates that the presence of isatin **1a** might act as a ligand to form the isatin-chelate FeCl₃ complex, which facilitate the cleavage of N–O bond in *N*-methoxybenzamide to generate benzamide. This

finding is also supported by the low observed yield of **3aa** in the presence of other external ligands under the standard condition (Table 4.1, entries 6-12).

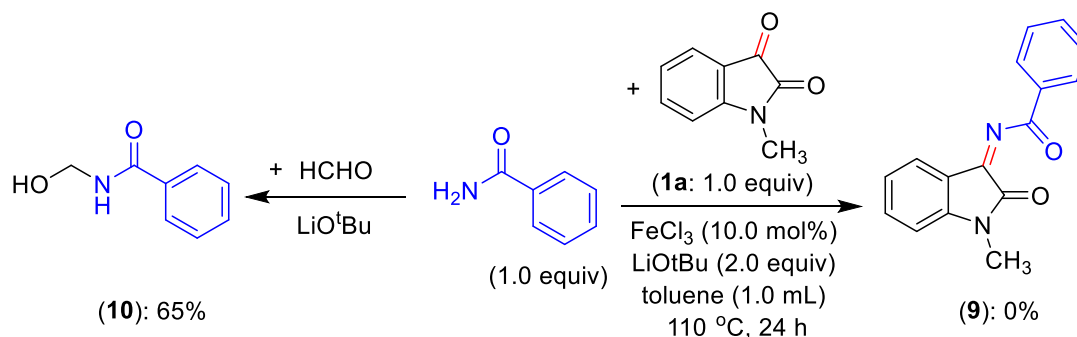
(a) Reaction of **1a** with **2a** in presence of CD_3OD



(b) Reaction of **1a** with **2a-[D₃]** in presence of CH_3OH



(c) Independent reaction of benzamide with **1a** and $HCHO$ (in absence of CH_3OH)



Scheme 4.9. (a & b) Deuterium labeling experiments for the mode of methylene ($-CH_2-$) group. (c) Controlled experiments for the formation of possible intermediates.

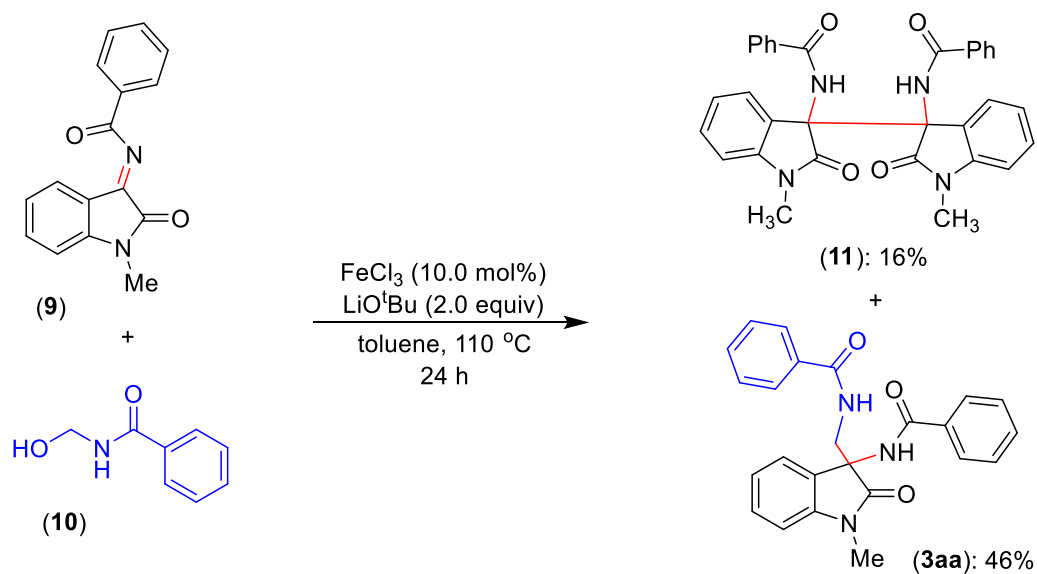
Next, we examined the possible formation of different intermediates originating from benzamide, isatin, and $CH_3OH/HCHO$. As the benzamide and $CH_3OH/HCHO$ involve in the reaction along with isatin **1a** for the formation of product **3aa**, we proposed two tentative intermediates **9** and **10** from the reaction of benzamide with **1a** and benzamide with $HCHO$, respectively (Scheme 4.9c). We hypothesized that the isatin **1a** might directly react with benzamide to form an imine intermediate **9** (Scheme 4.9c). However, the reaction of **1a** with

benzamide in the presence of catalytic FeCl₃ and LiO^tBu, failed to deliver the expected compound **9**, indicating an alternate route for the formation of probable intermediate **9**. The formation of **10** was observed upon the reaction of benzamide with HCHO in presence LiO^tBu in 65% yield.

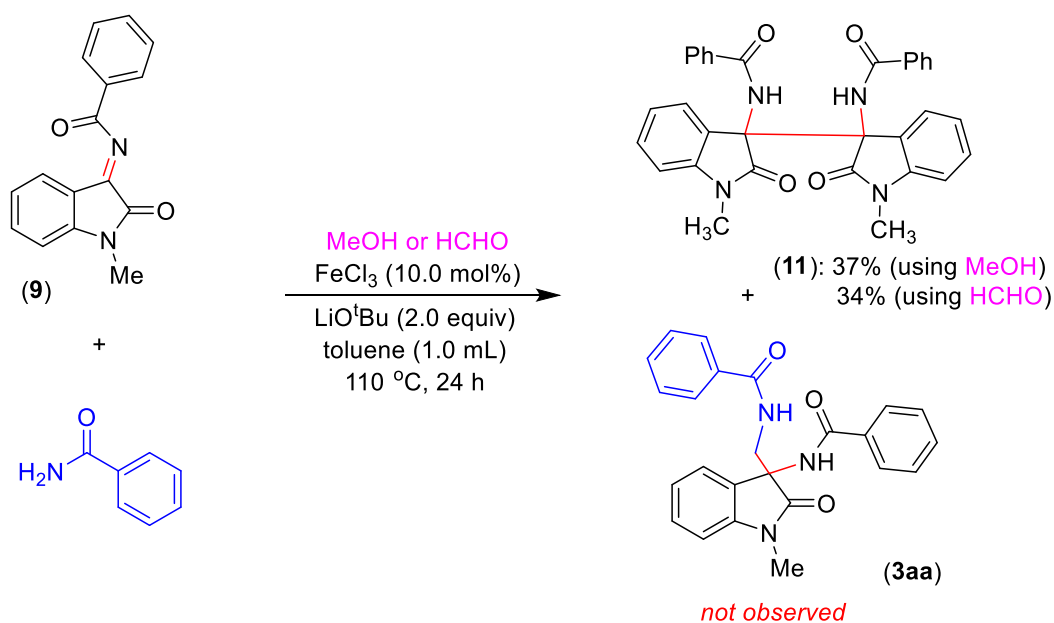
To validate the involvement of intermediates **9** and **10**, they were independently synthesized and characterized by NMR spectroscopy (see section 4.5.6.4). The reaction of compound **9** with compound **10** in the presence of 10 mol% of FeCl₃ and LiO^tBu at 110 °C afforded the desired product *N*-((3-benzamido-1-methyl-2-oxoindolin-3-yl)methyl)benzamide (**3aa**) in 46% yield along with the *N,N'*-(1,1'-dimethyl-2,2'-dioxo-[3,3'-biindoline]-3,3'-diyl)dibenzamide (**11**) in 16% (Scheme 4.10a). Further, to understand the reactivity of intermediate **9**, an attempted reaction of compound **9** with benzamide in the presence of CH₃OH or HCHO (2.5 equiv) under the Fe-catalytic conditions did not produce the desired product **3aa**. However, the formation of self-coupled dimer **11** was obtained in 37% (using CH₃OH) or 34% (using HCHO) yield (Scheme 4.10b). This indicates that the reaction of benzamide with HCHO to form intermediate **10** could be slower than the self-coupling reaction of **9** to form **11**. The molecular structure of **11** was also confirmed by X-ray structural analysis. The formation of dimer **11** could support an involvement of carbon-centric organic radical species in the catalytic reaction, which was further verified by external additive experiments (TEMPO and galvinoxyl) wherein the reaction was completely quenched.

Notably, the reaction of **9** and **10** also occurred even in the absence of FeCl₃ catalyst to provide the product **3aa** in 39% yield and compound **11** in 20% yield. However, in the standard catalytic reaction, the formation of dimeric compound **11** was rarely observed. In addition, the standard reaction was performed for an early time to check the formation of possible intermediates, wherein compound **12** (a probable precursor for intermediate **9**) and product **3aa** was isolated in 48% and 44% yield, respectively (Scheme 4.11). It should be noted that the intermediate **9** does not form directly from benzamide and isatin **1a**, whereas intermediate **10** obtained directly from benzamide and HCHO. Therefore, we assume that intermediate **9** might follow an intramolecular path involving isatin and benzamide, whereas the intermediate **10** formed *via* intermolecular reaction of benzamide with the released HCHO. We proposed two different routes for the formation of **9** and **10** before their recombination to form **3aa**.

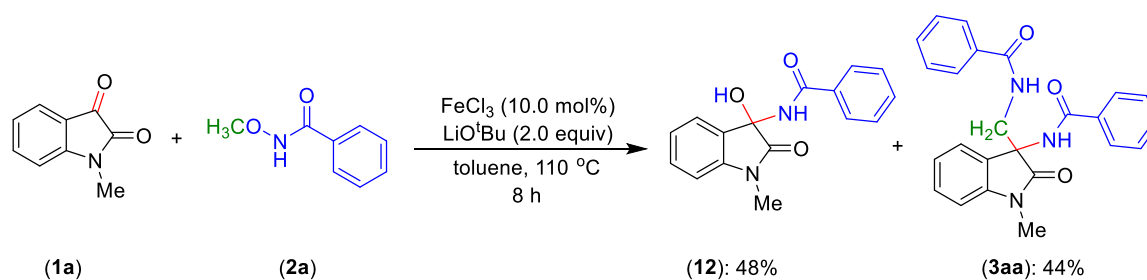
(a) Reaction of probable intermediates **9** and **10**



(b) Reaction of intermediate **10** with benzamide in presence of CH_3OH or HCHO



Scheme 4.10. Controlled experiments of probable intermediates.



Scheme 4.11. Synthesis of intermediate **12** from an early reaction of **1a** with **2a**.

4.2.4.3 DFT Based Calculations

We have performed Density Functional Theory (DFT) based calculations to understand the probable formation and reactivity of catalytic intermediates and the overall reaction pathway. To start with, the active catalyst FeCl_3 involved in the reaction exists in three different spin states namely, doublet, quartet, and sextet. Investigation of absolute electronic energies of these spin state indicates doublet having the maximum stability. So, further calculations are done considering the doublet state of FeCl_3 . The reaction initiates with the coordination of FeCl_3 to isatin **1a** in a bidentate fashion to form complex **A** which is exergonic by 25.3 kcal/mol. Complex **A** formed reacts with *N*-methoxybenzamide (**2a**) in the presence of LiO^tBu resulted in the formation of intermediate **B** through **TS-1** or the benzamide attacks the electrophilic C-3 carbon center in complex **A** leading to species **E** via **TS-4**. The energy barrier obtained for **B** is 20.4 kcal/mol and **E** is 16.8 kcal/mol respectively. Further, both complex **B** and **E** forms complex **C** through **TS-2** (exergonic by 32.7 kcal/mol) and **F** through **TS-5** (exergonic by 34.3 kcal/mol) along with CH_3OH or HCHO as side products, respectively. Complex **C** generates complex **D** and similarly, complex **F** generates **G** and both steps are energetically favorable. Upon protonation, complex **D** leads to benzamide and regenerates the catalytic active complex **A** through **TS-3**. The energy barrier for this step is 23.1 kcal/mol. The benzamide formed reacts with HCHO in the presence of base to form intermediate **10** which is endergonic by 2.8 kcal/mol. Parallellly, complex **G** after protonation followed by dissociation reaction with **1a** leads to intermediate **12** via **TS-6**. The energy barrier for this process is 28.0 kcal/mol. Intermediate **12** undergoes dehydration resulting in imine intermediate **9** which is exergonic by 38.7 kcal/mol. The intermediate **10** forms radical intermediate **J** through **I**. The generation of radical intermediate **J** is endergonic by 6.8 kcal/mol. Additionally, imine intermediate **9** leads to the formation of radical **H** which is endergonic by 5.7 kcal/mol (Figure 4.1). Finally, the reaction between the two radical intermediates, **H** and **J** leads to the final product **3aa** which is exergonic by 30.7 kcal/mol (Figure 4.2). On the other hand, the mechanism can proceed in the presence of $^-\text{O}^t\text{Bu}$ anion. The energetics for that is shown in figure 4.5 for comparison to that of Cl^- anion. The energies suggest that the reaction is more feasible in the presence of Cl^- .

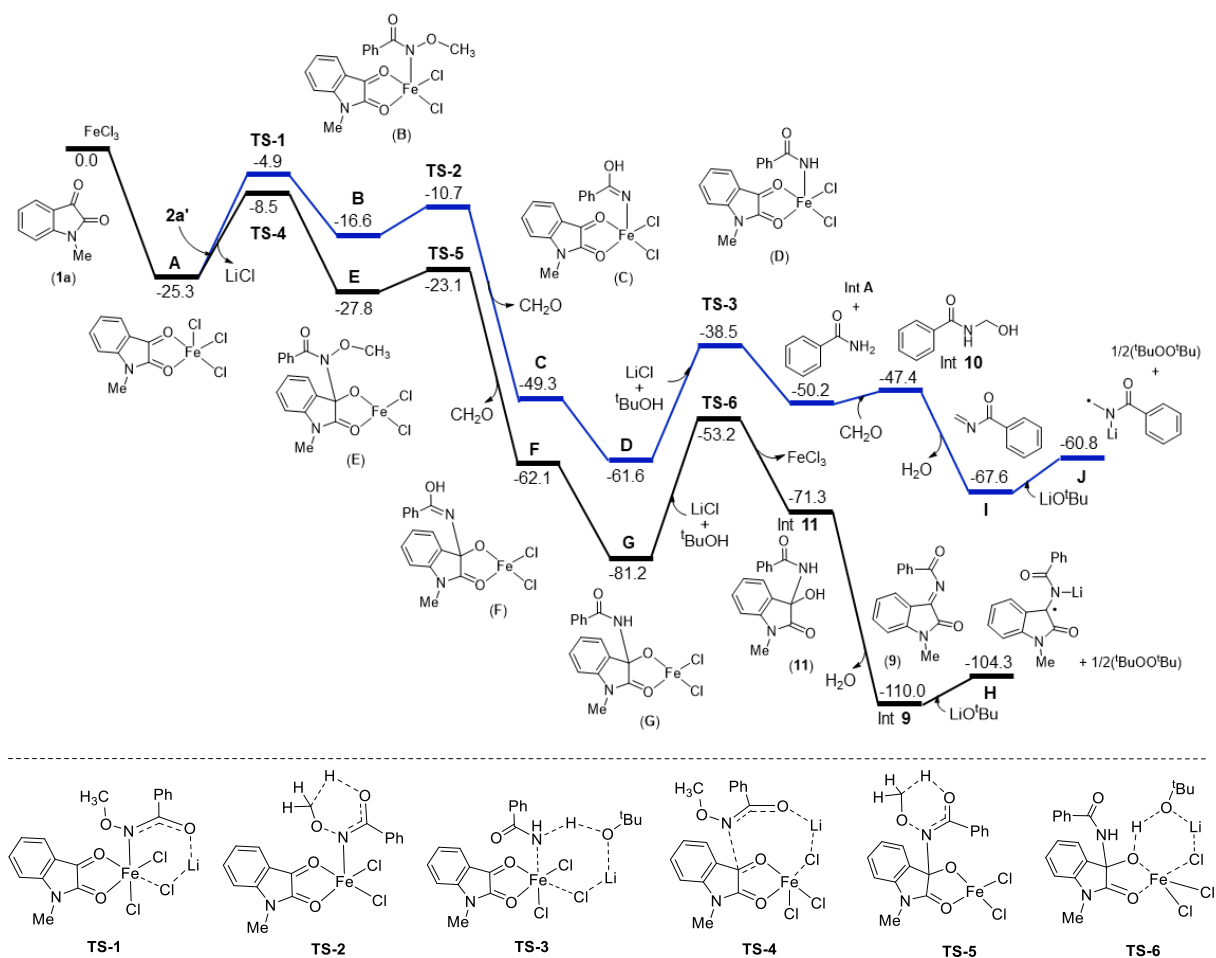


Figure 4.1. Free energy profile for the Fe-catalysed synthesis of 3,3-disubstituted 3-amino oxindole for Cl⁻ anion. The free energy values are given in kcal/mol.

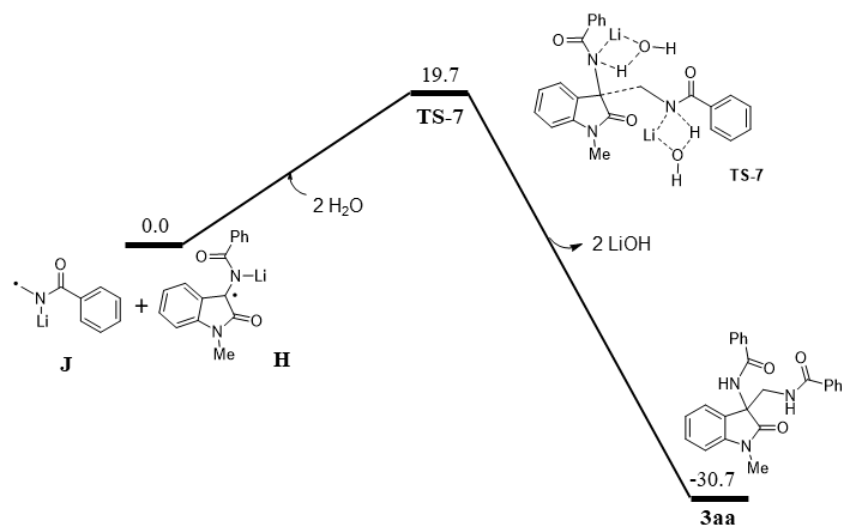


Figure 4.2. Free energy profile for the reaction of two radical species to synthesize **3aa**. The free energy values are given in kcal/mol.

4.2.5 Probable Catalytic Cycle

On the basis of preliminary mechanistic investigation, we have proposed tentative catalytic cycles for the formation of intermediate **9**, **10** and the final product 3,3-disubstituted 3-amino oxindole, **3aa** (Figure 4.3). Initially, the isatin **1a** coordinates to FeCl₃ in a bidentate fashion to form complex **A**. A controlled study indicated the importance of isatin coordination with iron before it involves in further reaction. The reaction of complex **A** with *N*-methoxybenzamide (**2a**) in the presence of LiO^tBu resulted in the formation of intermediate **B**. The complex **B** would deliver the complex **C** and CH₃OH (or HCHO) via N–O bond cleavage. Though, we do not have strong evidence to support the probable path for N–O bond cleavage in complex **B**; the involvement of a nitrene intermediate resulting from species **B** cannot be ruled out. The complex **C** will lead to the formation of intermediate **D** in the presence of ^tBuOH. Upon protonation, the complex **D** will deliver benzamide and regenerate the catalytic active complex **A**. The benzamide would react with formed HCHO in the presence of base to form intermediate **10**. The formation intermediate **9** is proposed to follow a different path. Thus, the benzamide attacks the electrophilic C-3 carbon center in complex **A** leading to species **E**. The reaction of complex **E** in the presence of base would deliver complex **F** and HCHO. The complex **G** after protonation followed by dissociation reaction with **1a** will deliver intermediate **12**. Complex **12** upon dehydration reaction will lead to imine intermediate **9**. Both intermediate **9** and **12** were identified and characterized by various techniques. The reaction of intermediates **9** and **10** in the presence of base will lead to final product **3aa**, which is proposed to occur *via* radical intermediates **H** and **J**.

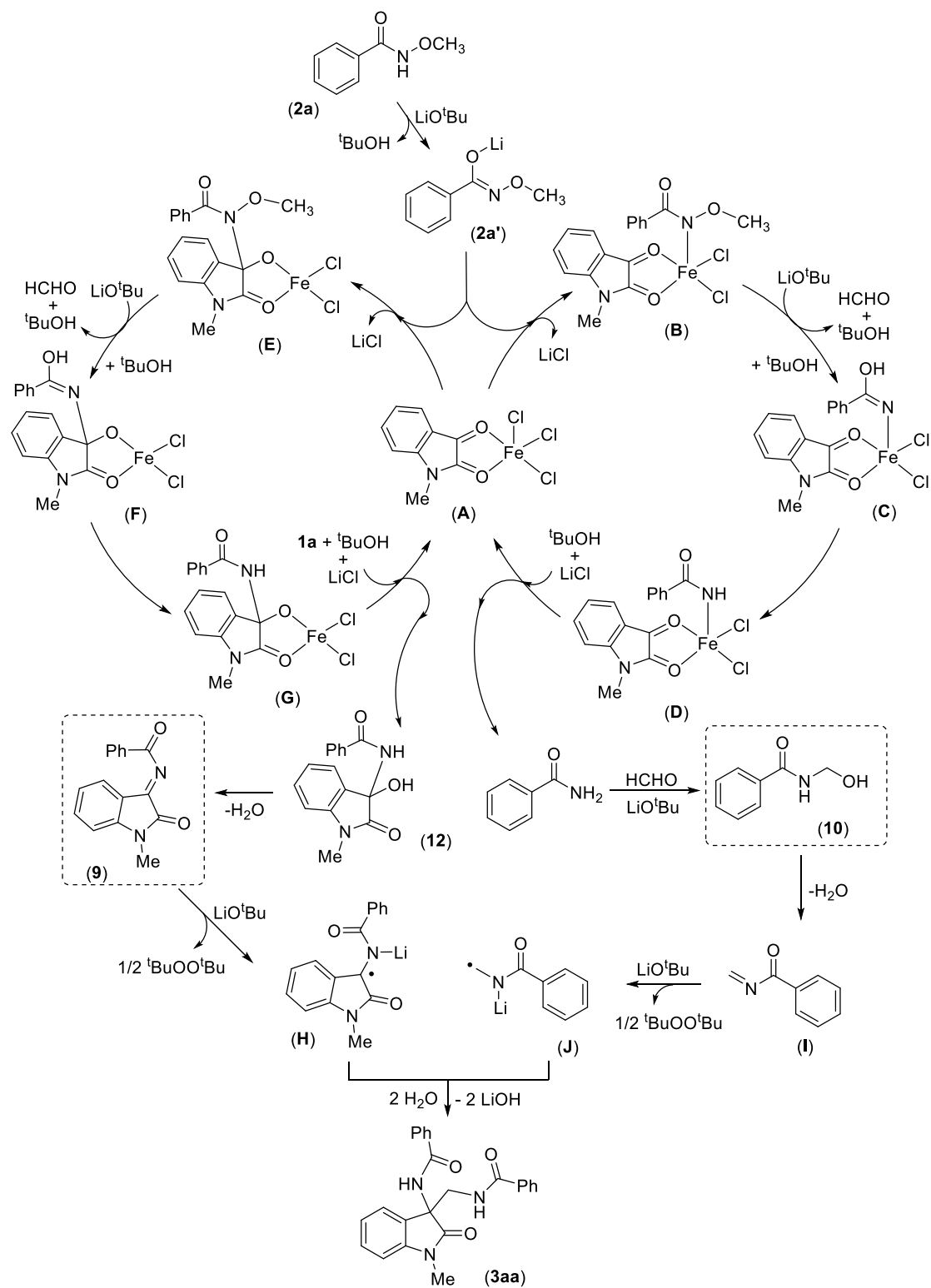


Figure 4.3. Plausible catalytic cycle.

4.3 CONCLUSION

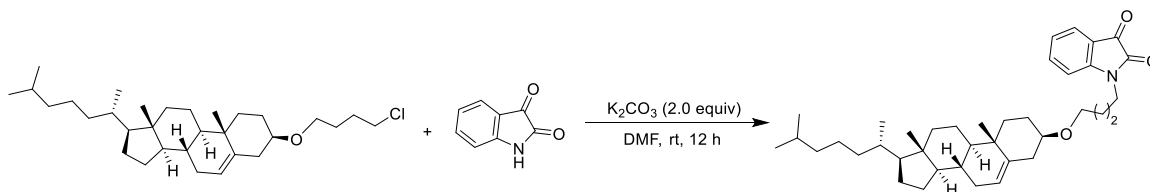
In summary, we have serendipitously discovered a new reaction for the straightforward synthesis of 3,3-disubstituted-3-amino-2-oxindoles with the generation of a stereogenic quaternary center in the presence of a highly abundant and inexpensive iron(III) catalyst. The coupling of *N*-methoxy benzamides with isatin derivatives provided the various biologically relevant 3-substituted-3-amino oxindoles in the presence of a simple iron(III) salt. This protocol is readily applicable for the construction of tetrasubstituted carbon centers using diversely substituted *N*-methoxy benzamides and isatins to deliver desired products in moderate to good yields. Detailed mechanistic studies revealed that the reaction proceeds through the formation of isatin ketimine and *N*-(hydroxymethyl)benzamide intermediates. Controlled experiments including deuterium labeling studies suggested an *N*-methoxy group of benzamide is a source of methylene group in the products. Further functionalization was shown to synthesize *N*-((3-benzamido-2-oxoindolin-3-yl)methyl)benzamide, *N*-(3-((benzylamino)methyl)-1-methyl-2-oxoindolin-3-yl)benzamide, and *N*-(3-(aminomethyl)-1-methyl-2-oxoindolin-3-yl)benzamide. The scalability of this protocol was demonstrated with a gram-scale reaction. Preliminary mechanistic studies suggested the amination reaction proceeds through a single-electron transfer (SET) pathway.

4.4 EXPERIMENTAL SECTION

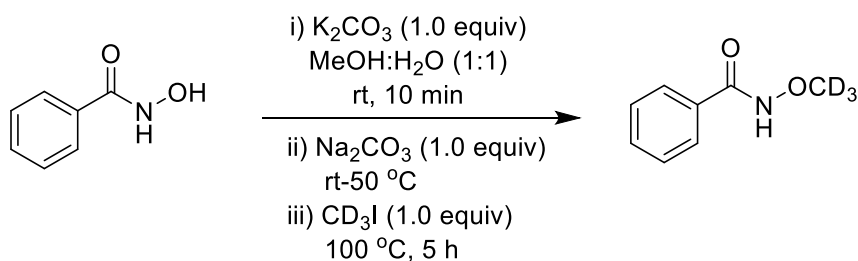
All the manipulations were conducted under an argon atmosphere either in a glove box or using standard Schlenk techniques in pre-dried glasswares. The catalytic reactions were performed in oven-dried reaction vessels with a Teflon screw cap. Solvents were dried over Na/benzophenone or CaH₂ and distilled prior to use. Liquid reagents were flushed with argon prior to use. All other chemicals were obtained from commercial sources and were used without further purification. High-resolution mass spectrometry (HRMS) mass spectra were recorded on a Thermo Scientific Q-Exactive, Accela 1250 pump. NMR: (¹H and ¹³C{¹H}) spectra were recorded at 400 or 500 MHz (¹H), 100 or 125 MHz {¹³C{¹H}}, DEPT (distortionless enhancement by polarization transfer)}, 377 MHz (¹⁹F), respectively in CDCl₃ solutions, if not otherwise specified; chemical shifts (δ) are given in ppm. The ¹H and ¹³C{¹H} NMR spectra are referenced to residual solvent signals (CDCl₃: δ H = 7.26 ppm, δ C = 77.2 ppm). The abbreviations used in NMR data are as follows: s = singlet, br s = broad singlet, d = doublet, t = triplet, dd = double doublet, vt = virtual triplet, dt = double triplet, td = triple doublet, tt = triple triplet.

4.4.1 Synthesis and Characterization of Starting Compounds

4.4.1.1 Synthesis and Characterization of 1-(((3S,8S,9S,10R,13R,14S,17R)-10,13-Dimethyl-17-((R)-6-methylheptan-2-yl)-2,3,4,7,8,9,10,11,12,13,14,15,16,17-tetradecahydro-1H-cyclopenta[a]phenanthren-3-yl)oxy)methyl)indoline-2,3-dione



Representative Procedure for Synthesis of 1q: In an oven-dried round bottom flask indoline-2,3-dione (0.5 g, 3.40 mmol) was dissolved in DMF (30 mL) and K_2CO_3 (0.94 g, 6.80 mmol) was added at room temperature. The resulting reaction mixture was stirred for 20 min and (3R,8R,9R,10S,13S,14R,17S)-3-(4-chlorobutoxy)-10,13-dimethyl-17-((S)-6-methylheptan-2-yl)-2,3,4,7,8,9,10,11,12,13,14,15,16,17-tetradecahydro-1H-cyclopenta[a]phenanthrene (3.50 g, 13.60 mmol) was added and the resultant reaction mixture was stirred at room temperature for 12 h. The reaction was quenched with water (15 mL) and extracted with ethyl acetate (20 mL x 3). The combined organic extract was dried over Na_2SO_4 and the volatiles were evaporated in *vacuo*. The remaining residue was purified by column chromatography on silica gel (petroleum ether/EtOAc: 5/1) yielded **1q** (1.20 g, 60%) as an orange solid. 1H -NMR (400 MHz, $CDCl_3$): δ = 7.59-7.55 (m, 2H, Ar-H), 7.09 (t, J = 7.6 Hz, 1H, Ar-H), 6.93 (d, J = 7.7 Hz, 1H, Ar-H), 5.32-5.31 (m, 1H, CH), 3.75 (t, J = 7.2 Hz, 2H), 3.50 (t, J = 6.1 Hz, 2H), 3.11 (septet, 1H, CH), 2.34-2.30 (m, 1H, CH), 2.19-2.12 (m, 1H, CH), 2.03-1.93 (m, 2H, CH_2), 1.88-1.76 (m, 5H), 1.68-1.60 (m, 2H, CH_2), 1.59-1.23 (m, 11H), 1.18-1.00 (m, 7H), 0.98 (s, 3H, CH_3), 0.90 (d, J = 6.4 Hz, 3H, CH_3), 0.865 (d, J = 6.6 Hz, 6H, CH_3), 0.66 (s, 3H, CH_3). $^{13}C\{^1H\}$ -NMR (100 MHz, $CDCl_3$): δ = 183.8 (C_q), 158.3 (C_q), 151.2 (C_q), 141.0 (C_q), 138.4 (CH), 125.6 (CH), 123.7 (CH), 121.8 (CH), 117.7 (C_q), 110.4 (CH), 79.3 (CH), 67.2 (2C, CH_2), 56.9 (CH), 56.3 (CH), 50.3 (CH), 42.5 (C_q), 40.2 (CH_2), 39.9 (CH_2), 39.7 (CH_2), 39.3 (CH_2), 37.4 (CH_2), 37.0 (CH_2), 36.3 (C_q), 35.9 (CH_2), 32.1 (CH_2), 32.0 (CH_2), 28.6 (CH_2), 28.4 (CH_2), 28.2 (CH_2), 27.5 (CH_2), 24.4 (CH_2), 23.9 (CH_2), 22.9 (CH_3), 22.7 (CH_3), 21.2 (CH_2), 19.5 (CH_3), 18.9 (CH_3), 12.0 (CH_3).

4.4.1.2 Synthesis and Characterization of *N*-(Methoxy-d₃)Benzamide (**2a**-[D₃])

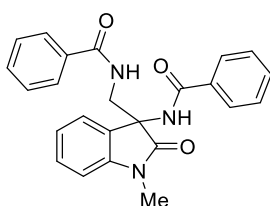
Representative Procedure for Synthesis of (2a-[D₃]): To a solution of *N*-hydroxybenzamide (0.50 g, 3.65 mmol) in MeOH:H₂O (1:1, 15 mL), K_2CO_3 (0.51 g, 3.69 mmol) was added and the reaction mixture was stirred at room temperature for 10 min. Further, Na_2CO_3 (0.39 g, 3.68 mmol) was added and the reaction mixture was heated at 50 °C. The iodomethane-d₃ (0.53 g, 3.64 mmol) was added to the resultant reaction mixture and stirred at 100 °C for 5 h. At ambient temperature, the solvent was concentrated and then acidified with 2M HCl to pH 3. The crude product was extracted with dichloromethane (15 mL x 3). The combined organic extract was dried over Na_2SO_4 and the volatiles were evaporated *in vacuo*. The remaining residue was purified by column chromatography on silica gel (petroleum ether/EtOAc: 3/1) to yield *N*-(methoxy-d₃)benzamide (**2a**-[D₃]) (0.38 g, 68%) as a white solid. ¹H-NMR (400 MHz, CDCl_3): δ = 10.30 (s, 1H, *NH*), 7.75 (d, *J* = 7.3 Hz, 2H, Ar-H), 7.46-7.43 (m, 1H, Ar-H), 7.34 (t, *J* = 7.3 Hz, 2H, Ar-H). ²H-NMR (400 MHz, CHCl_3): δ = 3.58 (s, 3D, OCD_3). ¹³C{¹H}-NMR (100 MHz, CDCl_3): δ = 166.5 (CO), 132.0 (CH), 131.9 (C_q), 128.6 (2C, CH), 127.3 (2C, CH), 63.4 (sept, *J* = 21.3 Hz, 1C, CD_3). HRMS (ESI): *m/z* Calcd for $\text{C}_8\text{H}_7\text{D}_3\text{NO}_2 + \text{H}^+$ [M + H]⁺ 155.0894; Found 155.0893.

4.4.2 Representative Procedure for Synthesis of 3,3-Disubstituted 3-Amino Oxindole and Characterization Data

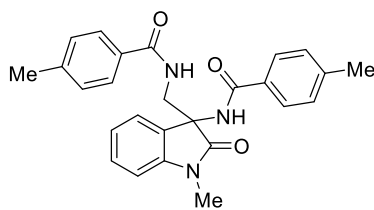
Representative Procedure. *N*-((3-benzamido-1-methyl-2-oxindolin-3-yl)methyl)benzamide (**3aa**): To an oven-dried screw-cap tube equipped with a magnetic stir bar was added 1-methylindoline-2,3-dione (**1a**; 0.032 g, 0.20 mmol), *N*-methoxybenzamide (**2a**; 0.076 g, 0.503 mmol), FeCl_3 (0.0032 g, 0.02 mmol, 10.0 mol%) and LiO^tBu (0.032 g, 0.40 mmol) inside the glove box. To the above reaction mixture in the tube was added toluene (1.0 mL). The resultant reaction mixture in the tube was immersed in a preheated oil bath at 110 °C and stirred for 24 h. At ambient temperature, the reaction mixture was quenched with distilled

H₂O (10.0 mL) and the crude product was extracted with EtOAc (15 mL x 3). The combined organic extract was dried over Na₂SO₄ and the volatiles were evaporated *in vacuo*. The remaining residue was purified by column chromatography on silica gel (petroleum ether/EtOAc: 1/2) to yield **3aa** (0.068 g, 85%) as a light brown solid.

Procedure for a 3.0 mmol Scale Synthesis: To an oven-dried Schlenk flask equipped with a magnetic stir bar was added 1-methylindoline-2,3-dione (**1a**; 0.50 g, 3.103 mmol), *N*-methoxybenzamide (**2a**; 1.172 g, 7.753 mmol), FeCl₃ (0.0503 g, 0.310 mmol, 10.0 mol%) and LiO^tBu (0.496 g, 6.195 mmol) inside the glove box. To the above reaction mixture in the tube was added toluene (12.0 mL). The resultant reaction mixture was heated at 110 °C for 24 h. At ambient temperature, the reaction mixture was quenched with distilled H₂O (15.0 mL) and the crude product was extracted with EtOAc (30 mL x 3). The combined organic extract was dried over Na₂SO₄ and the volatiles were evaporated *in vacuo*. The remaining residue was purified by column chromatography on silica gel (petroleum ether/EtOAc: 1/2) to yield **3aa** (0.782 g, 63%) as a light brown solid.

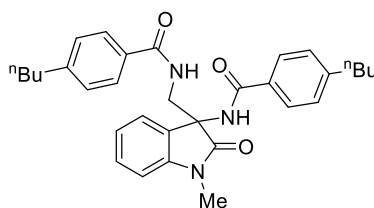


Characterization Data of 3aa. ¹H-NMR (500 MHz, CDCl₃): δ = 9.25 (br s, 1H, *NH*), 7.86 (d, *J* = 7.1 Hz, 2H, Ar-H), 7.79 (d, *J* = 7.1 Hz, 2H, Ar-H), 7.68 (br s, 1H, *NH*), 7.50-7.47 (m, 1H, Ar-H), 7.42 (t, *J* = 7.7 Hz, 3H, Ar-H), 7.38-7.32 (m, 1H, Ar-H), 7.28-7.20 (m, 3H, Ar-H), 7.04 (t, *J* = 7.3 Hz, 1H, Ar-H), 6.90 (d, *J* = 7.7 Hz, 1H, Ar-H), 4.23 (dd, *J* = 14.5, 7.8 Hz, 1H, CH₂), 3.41 (dd, *J* = 14.5, 5.0 Hz, 1H, CH₂), 3.25 (s, 3H, CH₃). ¹³C{¹H}-NMR (125 MHz, CDCl₃): δ = 175.4 (CO), 170.9 (CO), 166.3 (CO), 143.3 (C_q), 132.9 (C_q), 132.5 (C_q), 132.3 (CH), 132.0 (CH), 129.6 (CH), 128.7 (2C, CH), 128.6 (2C, CH), 128.3 (C_q), 127.7 (2C, CH), 127.5 (2C, CH), 123.2 (CH), 122.8 (CH), 108.7 (CH), 63.4 (C_q), 45.7 (CH₂), 26.7 (CH₃). HRMS (ESI): *m/z* Calcd for C₂₄H₂₁N₃O₃ + H⁺ [M + H]⁺ 400.1656; Found 400.1652.



4-Methyl-N-(1-methyl-3-((4-methylbenzamido)methyl)-2-oxindolin-3-yl)benzamide (3ab):

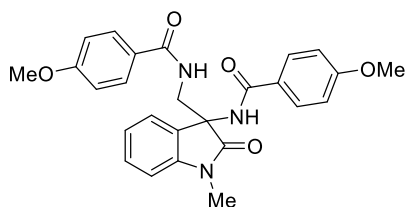
The representative procedure was followed, using 1-methylindoline-2,3-dione (**1a**; 0.032 g, 0.20 mmol) and *N*-methoxy-4-methylbenzamide (**2b**; 0.082 g, 0.50 mmol). Purification by column chromatography on silica gel (petroleum ether/EtOAc: 1/1) yielded **3ab** (0.064 g, 75%) as a brown solid. $^1\text{H-NMR}$ (500 MHz, CDCl_3): δ = 9.12 (br s, 1H, *NH*), 7.77 (d, J = 8.2 Hz, 2H, Ar-H), 7.68 (d, J = 7.7 Hz, 2H, Ar-H), 7.48 (br s, 1H, *NH*), 7.36-7.32 (m, 1H, Ar-H), 7.29 (d, J = 7.2 Hz, 1H, Ar-H), 7.22 (d, J = 8.0 Hz, 2H, Ar-H), 7.08-7.01 (m, 3H, Ar-H), 6.90 (J = 7.7 Hz, 1H, Ar-H), 4.23 (dd, J = 14.5, 7.9 Hz, 1H, CH_2), 3.43 (dd, J = 14.5, 5.0 Hz, 1H, CH_2), 3.29 (s, 3H, CH_3), 2.38 (s, 3H, CH_3), 2.31 (s, 3H, CH_3). $^{13}\text{C}\{^1\text{H}\}$ -NMR (125 MHz, CDCl_3): δ = 175.5 (CO), 170.8 (CO), 166.3 (CO), 143.4 (C_q), 142.8 (C_q), 142.4 (C_q), 130.2 (C_q), 129.8 (C_q), 129.6 (CH), 129.4 (2C, CH), 129.3 (2C, CH), 128.5 (C_q), 127.8 (2C, CH), 127.5 (2C, CH), 123.2 (CH), 122.8 (CH), 108.6 (CH), 63.4 (C_q), 45.6 (CH_2), 26.7 (CH_3), 21.6 (CH_3), 21.5 (CH_3). HRMS (ESI): m/z Calcd for $\text{C}_{26}\text{H}_{25}\text{N}_3\text{O}_3 + \text{H}^+$ [M + H] $^+$ 428.1969; Found 428.1966.



4-Butyl-N-((3-(4-butylbenzamido)-1-methyl-2-oxindolin-3-yl)methyl)benzamide (3ac):

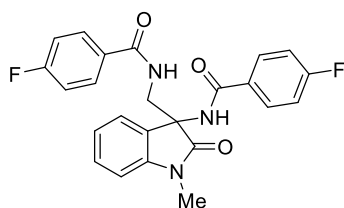
The representative procedure was followed, using 1-methylindoline-2,3-dione (**1a**; 0.032 g, 0.20 mmol) and 4-butyl-*N*-methoxybenzamide (**2c**; 0.103 g, 0.50 mmol). Purification by column chromatography on silica gel (petroleum ether/EtOAc: 1/1) yielded **3ac** (0.075 g, 73%) as a brown solid. $^1\text{H-NMR}$ (400 MHz, CDCl_3): δ = 9.22 (br s, 1H, *NH*), 7.81 (d, J = 7.6 Hz, 2H, Ar-H), 7.71-7.66 (m, 1H, *NH*; 2H, Ar-H), 7.34 (t, J = 7.7 Hz, 1H, Ar-H), 7.29 (d, J = 7.2 Hz, 1H, Ar-H), 7.23 (d, J = 7.6 Hz, 2H, Ar-H), 7.05 (t, J = 7.5 Hz, 1H, Ar-H), 6.98 (d, J = 7.6 Hz, 2H, Ar-H), 6.91 (d, J = 7.7 Hz, 1H, Ar-H), 4.25 (dd, J = 14.3, 7.6 Hz, 1H, CH_2), 3.40 (dd, J = 14.3, 4.3 Hz, 1H, CH_2), 3.27 (s, 3H, CH_3), 2.63 (t, J = 7.6 Hz, 2H, CH_2), 2.53 (t, J = 7.6 Hz, 2H, CH_2), 1.61-1.50 (m, 4H, CH_2), 1.37-1.30 (m, 4H, CH_2), 0.95-0.90 (m, 6H, CH_3). $^{13}\text{C}\{^1\text{H}\}$ -NMR (100 MHz, CDCl_3): δ = 175.6 (CO), 170.8 (CO), 166.3 (CO), 147.5 (C_q), 147.4 (C_q),

143.3 (C_q), 130.1 (C_q), 130.0 (2C, C_q), 129.6 (CH), 128.7 (3C, CH), 128.6 (CH), 127.8 (2C, CH), 127.5 (2C, CH), 123.2 (CH), 122.8 (CH), 108.6 (CH), 63.5 (C_q), 45.8 (CH₂), 35.7 (2C, CH₂), 33.5 (2C, CH₂), 26.7 (CH₃), 22.5 (2C, CH₂), 14.1 (2C, CH₃). HRMS (ESI): m/z Calcd for C₃₂H₃₇N₃O₃ + H⁺ [M + H]⁺ 512.2916; Found 512.2914.



4-Methoxy-N-((3-(4-methoxybenzamido)-1-methyl-2-oxoindolin-3-yl)methyl)benzamide

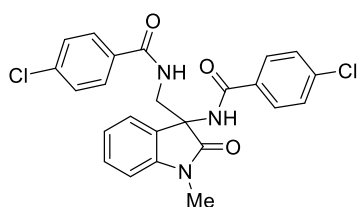
(3ad): The representative procedure **C** was followed, using 1-methylindoline-2,3-dione (**1a**; 0.032 g, 0.20 mmol) and *N*,4-dimethoxybenzamide (**2d**; 0.090 g, 0.50 mmol). Purification by column chromatography on silica gel (petroleum ether/EtOAc: 1/3) yielded **3ad** (0.055 g, 60%) as a brown solid. ¹H-NMR (500 MHz, CDCl₃): δ = 9.14 (br s, 1H, *NH*), 7.84 (d, J = 8.7 Hz, 2H, Ar-H), 7.79 (d, J = 8.7 Hz, 2H, Ar-H), 7.36-7.29 (m, 1H, *NH*; 2H, Ar-H), 7.06 (t, J = 7.5 Hz, 1H, Ar-H), 6.91 (t, J = 8.0 Hz, 3H, Ar-H), 7.78 (d, J = 8.7 Hz, 2H, Ar-H), 4.23-4.17 (m, 1H, CH₂), 3.83 (s, 3H, OCH₃), 3.79 (s, 3H, OCH₃), 3.45 (dd, J = 14.6, 4.9 Hz, 1H, CH₂), 3.30 (s, 3H, CH₃). ¹³C{¹H}-NMR (125 MHz, CDCl₃): δ = 175.5 (CO), 170.4 (CO), 165.9 (CO), 162.8 (C_q), 162.5 (C_q), 143.3 (C_q), 129.6 (2C, CH), 129.4 (2C, CH), 128.5 (C_q), 125.3 (C_q), 125.1 (C_q), 123.1 (CH), 122.8 (CH), 113.9 (2C, CH), 113.8 (2C, CH), 108.7 (2C, CH), 63.4 (C_q), 55.6 (OCH₃), 55.5 (OCH₃), 45.6 (CH₂), 26.7 (CH₃). HRMS (ESI): m/z Calcd for C₂₆H₂₅N₃O₅ + H⁺ [M + H]⁺ 460.1867; Found 460.1867.



4-Fluoro-N-((3-(4-fluorobenzamido)-1-methyl-2-oxoindolin-3-yl)methyl)benzamide (3ae):

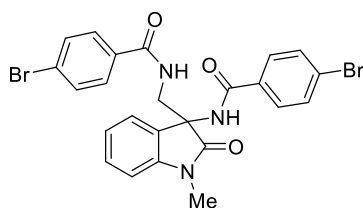
The representative procedure was followed, using 1-methylindoline-2,3-dione (**1a**; 0.032 g, 0.20 mmol) and 4-fluoro-*N*-methoxybenzamide (**2e**; 0.084 g, 0.50 mmol). Purification by column chromatography on silica gel (petroleum ether/EtOAc: 1/2) yielded **3ae** (0.059 g, 68%) as a brown solid. ¹H-NMR (500 MHz, CDCl₃): δ = 9.35 (br s, 1H, *NH*), 7.92-7.88 (m, 3H, Ar-H), 7.81-7.78 (m, 2H, Ar-H), 7.38-7.34 (m, 1H, Ar-H), 7.30 (d, J = 7.3 Hz, 1H, Ar-H), 7.14-

7.06 (m, 1H, *NH*; 2H, Ar-H), 6.93 (d, $J = 7.7$ Hz, 1H, Ar-H), 6.79 (t, $J = 8.5$ Hz, 2H, Ar-H), 4.34 (dd, $J = 14.6, 7.7$ Hz, 1H, CH₂), 3.32 (dd, $J = 14.6, 5.1$ Hz, 1H, CH₂), 3.25 (s, 3H, CH₃). ¹³C{¹H}-NMR (125 MHz, CDCl₃): $\delta = 175.5$ (CO), 169.9 (CO), 165.3 (d, $^1J_{C-F} = 252.5$ Hz, C_q), 165.2 (d, $^1J_{C-F} = 253.3$ Hz, C_q), 165.1 (CO), 143.2 (C_q), 130.1 (d, $^3J_{C-F} = 16.7$ Hz, 2C, CH), 130.0 (d, $^3J_{C-F} = 16.7$ Hz, 2C, CH), 129.8 (CH), 128.9 (d, $^4J_{C-F} = 3.0$ Hz, C_q), 128.7 (d, $^4J_{C-F} = 3.0$ Hz, C_q), 128.2 (C_q), 123.4 (CH), 122.7 (CH), 115.8 (d, $^2J_{C-F} = 21.3$ Hz, 2C, CH), 115.7 (d, $^2J_{C-F} = 22.1$ Hz, 2C, CH), 108.8 (CH), 63.6 (C_q), 45.9 (CH₂), 26.7 (CH₃). ¹⁹F-NMR (376 MHz, CDCl₃): $\delta = -106.9$ (s), -107.3 (s). HRMS (ESI): m/z Calcd for C₂₄H₁₉F₂N₃O₃ + H⁺ [M + H]⁺ 436.1467; Found 436.1464.



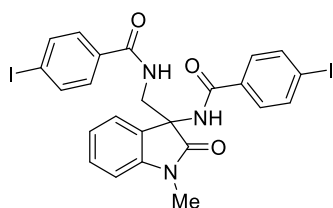
4-Chloro-N-((3-(4-chlorobenzamido)-1-methyl-2-oxindolin-3-yl)methyl)benzamide (3af):

The representative procedure was followed, using 1-methylindoline-2,3-dione (**1a**; 0.032 g, 0.20 mmol) and 4-chloro-*N*-methoxybenzamide (**2f**; 0.093 g, 0.50 mmol). Purification by column chromatography on silica gel (petroleum ether/EtOAc: 1/1) yielded **3af** (0.058 g, 62%) as a brown solid. ¹H-NMR (500 MHz, CDCl₃): $\delta = 9.41$ (br s, 1H, *NH*), 8.04 (br s, 1H, *NH*), 7.85 (d, $J = 8.5$ Hz, 2H, Ar-H), 7.67 (d, $J = 8.6$ Hz, 2H, Ar-H), 7.45 (d, $J = 8.5$ Hz, 2H, Ar-H), 7.38 (t, $J = 7.3$ Hz, 1H, Ar-H), 7.32 (d, $J = 7.0$ Hz, 1H, Ar-H), 7.11 (t, $J = 7.5$ Hz, 1H, Ar-H), 6.98-6.93 (m, 3H, Ar-H), 4.38 (dd, $J = 14.6, 7.7$ Hz, 1H, CH₂), 3.31-3.26 (m, 1H, CH₂; 3H, CH₃). ¹³C{¹H}-NMR (125 MHz, CDCl₃): $\delta = 175.5$ (CO), 170.0 (CO), 165.2 (CO), 143.1 (C_q), 138.7 (C_q), 138.6 (C_q), 130.8 (C_q), 130.7 (C_q), 129.9 (CH), 129.2 (2C, CH), 129.1 (2C, CH), 128.9 (2C, CH), 128.8 (2C, CH), 128.1 (C_q), 123.5 (CH), 122.8 (CH), 108.8 (CH), 63.7 (C_q), 45.9 (CH₂), 26.7 (CH₃). HRMS (ESI): m/z Calcd for C₂₄H₁₉Cl₂N₃O₃ + H⁺ [M + H]⁺ 468.0884; Found 468.0882.

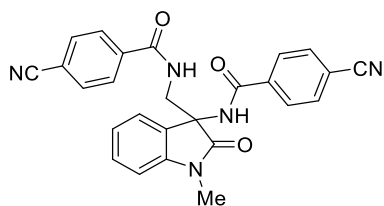


4-Bromo-*N*-((3-(4-bromobenzamido)-1-methyl-2-oxoindolin-3-yl)methyl)benzamide (3ag):

The representative procedure was followed, using 1-methylindoline-2,3-dione (**1a**; 0.032 g, 0.20 mmol) and 4-bromo-*N*-methoxybenzamide (**2g**; 0.115 g, 0.50 mmol). Purification by column chromatography on silica gel (petroleum ether/EtOAc: 1/2) yielded **3ag** (0.071 g, 64%) as a brown solid. $^1\text{H-NMR}$ (400 MHz, CDCl_3): δ = 9.49 (br s, 1H, *NH*), 8.20 (br s, 1H, *NH*), 7.79 (d, J = 7.1 Hz, 2H, Ar-H), 7.63 (d, J = 7.2 Hz, 2H, Ar-H), 7.56 (d, J = 7.2 Hz, 2H, Ar-H), 7.40-7.33 (m, 2H, Ar-H), 7.12 (t, J = 7.3 Hz, 1H, Ar-H), 7.02 (d, J = 7.5 Hz, 2H, Ar-H), 6.94 (d, J = 7.7 Hz, 1H, Ar-H), 4.41 (dd, J = 14.4, 7.2 Hz, 1H, CH_2), 3.28-3.24 (m, 1H, CH_2 ; 3H, CH_3). $^{13}\text{C}\{^1\text{H}\}$ -NMR (100 MHz, CDCl_3): δ = 175.7 (CO), 170.0 (CO), 165.3 (CO), 142.9 (C_q), 132.3 (2C, CH), 131.7 (2C, CH), 131.2 (C_q), 131.0 (C_q), 129.9 (CH), 129.3 (2C, CH), 129.0 (2C, CH), 128.1 (C_q), 127.4 (C_q), 127.2 (C_q), 123.6 (CH), 122.8 (CH), 108.8 (CH), 63.8 (C_q), 46.1 (CH_2), 26.7 (CH_3). HRMS (ESI): m/z Calcd for $\text{C}_{24}\text{H}_{19}\text{Br}_2\text{N}_3\text{O}_3 + \text{H}^+$ [$\text{M} + \text{H}$] $^+$ 557.9851; Found 557.9852.

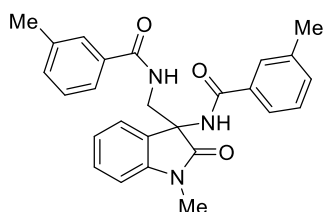
**4-Iodo-*N*-((3-(4-iodobenzamido)-1-methyl-2-oxoindolin-3-yl)methyl)benzamide (3ah):**

The representative procedure was followed, using 1-methylindoline-2,3-dione (**1a**; 0.032 g, 0.20 mmol) and 4-iodo-*N*-methoxybenzamide (**3h**; 0.138 g, 0.50 mmol). Purification by column chromatography on silica gel (petroleum ether/EtOAc: 1/2) yielded **3ah** (0.069 g, 53%) as a brown solid. $^1\text{H-NMR}$ (400 MHz, CDCl_3): δ = 9.57 (br s, 1H, *NH*), 8.38 (br s, 1H, *NH*), 7.86 (d, J = 7.9 Hz, 2H, Ar-H), 7.66 (d, J = 7.7 Hz, 2H, Ar-H), 7.40-7.34 (m, 4H, Ar-H), 7.19-7.10 (m, 3H, Ar-H), 6.95 (d, J = 7.7 Hz, 1H, Ar-H), 4.44 (dd, J = 14.3, 7.2 Hz, 1H, CH_2), 3.23-3.31 (m, 1H, CH_2 ; 3H, CH_3). $^{13}\text{C}\{^1\text{H}\}$ -NMR (100 MHz, CDCl_3): δ = 175.6 (CO), 170.2 (CO), 165.5 (CO), 142.9 (C_q), 138.3 (2C, CH), 137.7 (2C, CH), 131.7 (C_q), 131.5 (C_q), 129.9 (CH), 129.2 (2C, CH), 128.9 (2C, CH), 128.1 (C_q), 123.7 (CH), 122.8 (CH), 108.8 (CH), 100.1 (C_q), 99.9 (C_q), 63.9 (C_q), 46.1 (CH_2), 26.7 (CH_3). HRMS (ESI): m/z Calcd for $\text{C}_{24}\text{H}_{19}\text{I}_2\text{N}_3\text{O}_3 + \text{H}^+$ [$\text{M} + \text{H}$] $^+$ 651.9606; Found 651.9604.



4-Cyano-N-((3-(4-cyanobenzamido)-1-methyl-2-oxoindolin-3-yl)methyl)benzamide (3ai):

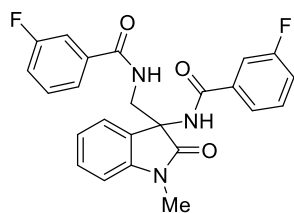
The representative procedure was followed, using 1-methylindoline-2,3-dione (**1a**; 0.032 g, 0.20 mmol) and 4-cyano-*N*-methoxybenzamide (**3i**; 0.088 g, 0.50 mmol). Purification by column chromatography on silica gel (petroleum ether/EtOAc: 1/2) yielded **3ai** (0.051 g, 57%) as a brown solid. $^1\text{H-NMR}$ (500 MHz, CDCl_3): δ = 9.13 (br s, 1H, *NH*), 7.89-7.86 (m, 4H, Ar-H), 7.66 (d, J = 7.7 Hz, 2H, Ar-H), 7.58 (d, J = 7.6 Hz, 2H, Ar-H), 7.46 (br s, 1H, *NH*), 7.32 (t, J = 7.7 Hz, 1H, Ar-H), 7.22-7.19 (m, 1H, Ar-H), 7.03 (vt, J = 7.4 Hz, 1H, Ar-H), 6.89 (d, J = 7.7 Hz, 1H, Ar-H), 4.26 (dd, J = 14.6, 8.1 Hz, 1H, CH_2), 3.34-3.30 (m, 1H, CH_2), 3.23 (s, 3H, CH_3). $^{13}\text{C}\{^1\text{H}\}$ -NMR (125 MHz, CDCl_3): δ = 174.7 (CO), 169.4 (CO), 164.4 (CO), 143.3 (C_q), 136.7 (CN), 136.2 (CN), 132.7 (2C, CH), 132.6 (2C, CH), 130.2 (CH), 128.3 (2C, CH), 128.2 (2C, CH), 127.4 (C_q), 123.5 (CH), 122.7 (CH), 118.1 (C_q), 117.8 (C_q), 116.2 (C_q), 115.8 (C_q), 109.1 (CH), 63.5 (C_q), 45.7 (CH_2), 26.9 (CH_3). HRMS (ESI): m/z Calcd for $\text{C}_{26}\text{H}_{19}\text{N}_5\text{O}_3 + \text{H}^+$ [M + H] $^+$ 450.1561; Found 450.1553.



3-Methyl-N-(1-methyl-3-((3-methylbenzamido)methyl)-2-oxoindolin-3-yl)benzamide (3aj):

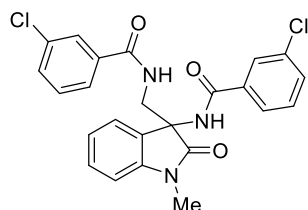
The representative procedure was followed, using 1-methylindoline-2,3-dione (**1a**; 0.032 g, 0.20 mmol) and *N*-methoxy-3-methylbenzamide (**2j**; 0.082 g, 0.50 mmol). Purification by column chromatography on silica gel (petroleum ether/EtOAc: 1/2) yielded **3aj** (0.057 g, 67%) as a brown solid. $^1\text{H-NMR}$ (500 MHz, CDCl_3): δ = 9.00 (br s, 1H, *NH*), 7.67-7.65 (m, 3H, Ar-H), 7.64 (br s, 1H, *NH*), 7.36-7.31 (m, 1H, Ar-H), 7.30-7.23 (m, 6H, Ar-H), 7.05 (t, J = 7.6 Hz, 1H, Ar-H), 6.90 (d, J = 7.7 Hz, 1H, Ar-H), 4.22 (dd, J = 14.6, 8.2 Hz, 1H, CH_2), 3.45 (dd, J = 14.5, 4.9 Hz, 1H, CH_2), 3.30 (s, 3H, CH_3), 2.36 (s, 6H, CH_3). $^{13}\text{C}\{^1\text{H}\}$ -NMR (125 MHz, CDCl_3): δ = 175.3 (CO), 171.0 (CO), 166.5 (CO), 143.5 (C_q), 138.8 (C_q), 138.4 (C_q), 133.2 (CH), 133.1 (C_q), 132.7 (CH), 132.5 (C_q), 129.7 (CH), 128.8 (CH), 128.6 (CH), 128.5 (CH), 128.3 (C_q), 128.2 (CH), 124.6 (CH), 124.5 (CH), 123.1 (CH), 122.8 (CH), 108.7 (CH), 63.2

(C_q), 45.4 (CH₂), 26.8 (CH₃), 21.5 (CH₃), 21.4 (CH₃). HRMS (ESI): m/z Calcd for C₂₆H₂₅N₃O₃ + H⁺ [M + H]⁺ 428.1969; Found 428.1967.



3-Fluoro-N-((3-(3-fluorobenzamido)-1-methyl-2-oxoindolin-3-yl)methyl)benzamide (3ak):

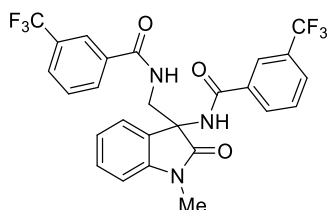
The representative procedure was followed, using 1-methylindoline-2,3-dione (**1a**; 0.032 g, 0.20 mmol) and 3-fluoro-*N*-methoxybenzamide (**2k**; 0.084 g, 0.50 mmol). Purification by column chromatography on silica gel (petroleum ether/EtOAc: 1/2) yielded **3ak** (0.052 g, 60%) as a brown solid. ¹H-NMR (400 MHz, CDCl₃): δ = 9.25 (br s, 1H, *NH*), 7.22 (br s, 1H, *NH*), 7.65 (d, *J* = 7.7 Hz, 1H, Ar-H), 7.59-7.51 (m, 3H, Ar-H), 7.45-7.34 (m, 2H, Ar-H), 7.29 (d, *J* = 7.2 Hz, 1H, Ar-H), 7.22-7.18 (m, 1H, Ar-H), 7.14-7.06 (m, 3H, Ar-H), 6.93 (d, *J* = 7.7 Hz, 1H, Ar-H), 4.30 (dd, *J* = 14.6, 7.8 Hz, 1H, CH₂), 3.36 (dd, *J* = 14.6, 5.0 Hz, 1H, CH₂), 3.26 (s, 3H, CH₃). ¹³C{¹H}-NMR (100 MHz, CDCl₃): δ = 175.2 (CO), 169.7 (d, ⁴*J*_{C-F} = 2.3 Hz, CO), 165.1 (d, ⁴*J*_{C-F} = 2.3 Hz, CO), 162.9 (d, ¹*J*_{C-F} = 247.2 Hz, C_q), 162.8 (d, ¹*J*_{C-F} = 248.7 Hz, C_q), 143.2 (C_q), 135.0 (d, ³*J*_{C-F} = 6.9 Hz, C_q), 134.8 (d, ³*J*_{C-F} = 7.6 Hz, C_q), 130.4 (d, ³*J*_{C-F} = 7.6 Hz, 2C, CH), 129.9 (CH), 127.9 (C_q), 123.4 (CH), 123.1 (d, ⁴*J*_{C-F} = 2.3 Hz, CH), 122.8 (d, ⁴*J*_{C-F} = 3.0 Hz, CH), 122.7 (CH), 119.5 (d, ²*J*_{C-F} = 21.4 Hz, CH), 119.1 (d, ²*J*_{C-F} = 21.4 Hz, CH), 115.1 (d, ²*J*_{C-F} = 23.6 Hz, CH), 115.0 (d, ²*J*_{C-F} = 22.8 Hz, CH), 108.8 (CH), 63.5 (C_q), 45.8 (CH₂), 26.8 (CH₃). ¹⁹F-NMR (376 MHz, CDCl₃): δ = -111.3 (s), -111.8 (s). HRMS (ESI): m/z Calcd for C₂₄H₁₉F₂N₃O₃ + H⁺ [M + H]⁺ 436.1467; Found 436.1454.



3-Chloro-N-((3-(3-chlorobenzamido)-1-methyl-2-oxoindolin-3-yl)methyl)benzamide (3al):

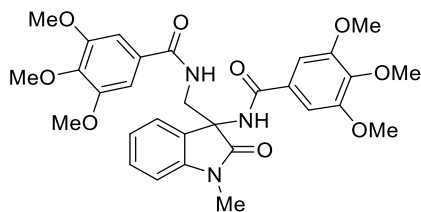
The representative procedure was followed, using 1-methylindoline-2,3-dione (**1a**; 0.032 g, 0.20 mmol) and 3-chloro-*N*-methoxybenzamide (**2l**; 0.093 g, 0.50 mmol). Purification by column chromatography on silica gel (petroleum ether/EtOAc: 1/2) yielded **3al** (0.053 g, 57%) as a brown solid. ¹H-NMR (500 MHz, CDCl₃): δ = 9.33 (br s, 1H, *NH*), 7.87-7.82 (m, 1H, *NH*);

2H, Ar-H), 7.74 (d, $J = 7.7$ Hz, 1H, Ar-H), 7.70 (d, $J = 7.8$ Hz, 1H, Ar-H), 7.48 (d, $J = 8.0$ Hz, 1H, Ar-H), 7.41-7.35 (m, 3H, Ar-H), 7.30 (d, $J = 7.2$ Hz, 1H, Ar-H), 7.09 (t, $J = 7.3$ Hz, 2H, Ar-H), 6.93 (d, $J = 7.7$ Hz, 1H, Ar-H), 4.34 (dd, $J = 14.6, 7.7$ Hz, 1H, CH₂), 3.34 (dd, $J = 14.6, 5.0$ Hz, 1H, CH₂), 3.25 (CH₃). ¹³C{¹H}-NMR (125 MHz, CDCl₃): $\delta = 175.2$ (CO), 169.6 (CO), 165.1 (CO), 143.2 (C_q), 135.1 (C_q), 134.9 (C_q), 134.3 (C_q), 134.2 (C_q), 130.0 (CH), 129.9 (2C, CH), 128.3 (CH), 128.1 (2C, CH), 127.9 (C_q), 125.6 (2C, CH), 125.4 (CH), 123.5 (CH), 122.8 (CH), 108.8 (CH), 63.5 (C_q), 45.7 (CH₂), 26.8 (CH₃). HRMS (ESI): m/z Calcd for C₂₄H₁₉Cl₂N₃O₃ + H⁺ [M + H]⁺ 469.1288; Found 469.1285.

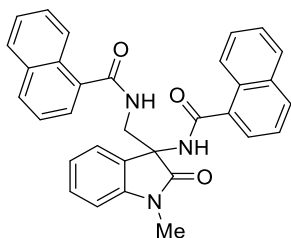


***N*-(1-Methyl-2-oxo-3-((3-(trifluoromethyl)benzamido)methyl)indolin-3-yl)-3-**

(trifluoromethyl)benzamide (3am): The representative procedure was followed, using 1-methylindoline-2,3-dione (**1a**; 0.032 g, 0.20 mmol) and *N*-methoxy-3-(trifluoromethyl)benzamide (**2m**; 0.109 g, 0.50 mmol). Purification by column chromatography on silica gel (petroleum ether/EtOAc: 1/2) yielded **3am** (0.052 g, 49%) as a light brown solid. ¹H-NMR (400 MHz, DMSO-*d*₆): $\delta = 9.68$ (br s, 1H, *NH*), 9.18 (br s, 1H, *NH*), 8.18 (s, 1H, Ar-H), 8.12 (d, $J = 7.8$ Hz, 1H, Ar-H), 8.06 (s, 2H, Ar-H), 7.97-7.92 (m, 2H, Ar-H), 7.79-7.72 (m, 2H, Ar-H), 7.30-7.27 (m, 2H, Ar-H), 7.03 (d, $J = 7.8$ Hz, 1H, Ar-H), 6.96 (t, $J = 7.5$ Hz, 1H, Ar-H), 3.99 (dd, $J = 13.8, 6.7$ Hz, 1H, CH₂), 3.67 (dd, $J = 13.8, 5.8$ Hz, 1H, CH₂), 3.21 (s, 3H, CH₃). ¹³C{¹H}-NMR (100 MHz, DMSO-*d*₆): $\delta = 174.0$ (CO), 167.3 (CO), 163.8 (CO), 143.7 (C_q), 134.7 (C_q), 133.8 (C_q), 131.5 (2C, CH), 130.1 (CH), 129.9 (CH), 129.4 (q, ² $J_{C-F} = 32.0$ Hz, C_q), 129.2 (q, ² $J_{C-F} = 32.0$ Hz, C_q), 128.9 (CH), 128.5 (q, ³ $J_{C-F} = 3.0$ Hz, CH), 128.3 (q, ³ $J_{C-F} = 3.0$ Hz, CH), 128.3 (C_q), 124.2 (q, ³ $J_{C-F} = 3.8$ Hz, CH), 123.7 (q, ³ $J_{C-F} = 3.8$ Hz, CH), 123.9 (q, ¹ $J_{C-F} = 272.2$ Hz, 2C, CF₃), 123.0 (CH), 122.1 (CH), 108.2 (CH), 62.9 (C_q), 44.7 (CH₂), 26.5 (CH₃). ¹⁹F-NMR (376 MHz, DMSO-*d*₆): $\delta = -56.5$ (s), -56.6 (s). HRMS (ESI): m/z Calcd for C₂₆H₁₉F₆N₃O₃ + H⁺ [M + H]⁺ 536.1403; Found 536.1404.

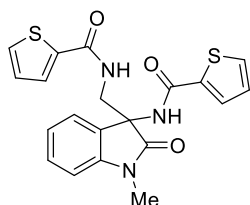


3,4,5-Trimethoxy-N-(1-methyl-2-oxo-3-((3,4,5-trimethoxybenzamido)methyl)indolin-3-yl)benzamide (3an): The representative procedure was followed, using 1-methylindoline-2,3-dione (**1a**; 0.032 g, 0.20 mmol) and *N*,3,4,5-tetramethoxybenzamide (**2n**; 0.120 g, 0.50 mmol). Purification by column chromatography on silica gel (petroleum ether/EtOAc: 1/4) yielded **3an** (0.058 g, 50%) as a brown solid. $^1\text{H-NMR}$ (400 MHz, CDCl_3): δ = 9.17 (br s, 1H, *NH*), 7.35 (t, J = 7.7 Hz, 1H, Ar-H), 7.31 (d, J = 7.2 Hz, 1H, Ar-H), 7.20 (br s, 1H, *NH*), 7.15 (s, 2H, Ar-H), 7.11 (s, 2H, Ar-H), 7.09-7.04 (m, 1H, Ar-H), 6.92 (d, J = 7.7 Hz, 1H, Ar-H), 4.19 (dd, J = 14.5, 8.0 Hz, 1H, CH_2), 3.88 (s, 9H, OCH_3), 3.86 (s, 3H, OCH_3), 3.85 (s, 6H, OCH_3), 3.47 (dd, J = 14.5, 5.0 Hz, 1H, CH_2), 3.30 (s, 3H, CH_3). $^{13}\text{C}\{^1\text{H}\}$ -NMR (100 MHz, CDCl_3): δ = 175.1 (CO), 170.8 (CO), 165.7 (CO), 153.4 (2C, C_q), 153.1 (2C, C_q), 143.5 (C_q), 141.9 (C_q), 141.2 (C_q), 129.8 (CH), 128.3 (C_q), 128.1 (C_q), 127.7 (C_q), 123.2 (CH), 122.8 (CH), 108.7 (CH), 104.9 (2C, CH), 104.8 (2C, CH), 63.5 (C_q), 61.1 (2C, OCH_3), 56.4 (2C, OCH_3), 56.3 (2C, OCH_3), 45.7 (CH_2), 26.9 (CH_3). HRMS (ESI): m/z Calcd for $\text{C}_{30}\text{H}_{33}\text{N}_3\text{O}_9 + \text{H}^+$ [$\text{M} + \text{H}$] $^+$ 580.2290; Found 580.2283.



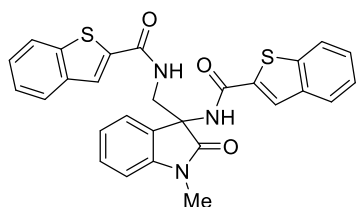
N-((3-(1-Naphthamido)-1-methyl-2-oxoindolin-3-yl)methyl)-1-naphthamide (3ao): The representative procedure was followed, using 1-methylindoline-2,3-dione (**1a**; 0.032 g, 0.20 mmol) and *N*-methoxy-1-naphthamide (**2o**; 0.100 g, 0.50 mmol). Purification by column chromatography on silica gel (petroleum ether/EtOAc: 1/2) yielded **3ao** (0.063 g, 63%) as a brown solid. $^1\text{H-NMR}$ (400 MHz, CDCl_3): δ = 8.50 (br s, 1H, *NH*), 8.24 (t, J = 9.8 Hz, 2H, Ar-H), 7.93 (d, J = 8.1 Hz, 1H, Ar-H), 7.87 (d, J = 9.3 Hz, 2H, Ar-H), 7.80 (d, J = 8.0 Hz, 1H, Ar-H), 7.76 (d, J = 7.0 Hz, 1H, Ar-H), 7.71 (d, J = 7.0 Hz, 1H, Ar-H), 7.50-7.33 (m, 1H, *NH*; 7H, Ar-H), 7.12-7.06 (m, 2H, Ar-H), 6.95 (d, J = 7.7 Hz, 1H, Ar-H), 4.43 (dd, J = 14.3, 8.6 Hz, 1H, CH_2), 3.39 (dd, J = 14.5, 3.6 Hz, 1H, CH_2), 3.34 (s, 3H, CH_3). $^{13}\text{C}\{^1\text{H}\}$ -NMR (100 MHz, CDCl_3): δ = 175.2 (CO), 172.4 (CO), 169.1 (CO), 143.7 (C_q), 133.9 (C_q), 133.8 (C_q),

132.9 (C_q), 132.7 (C_q), 131.7 (2C, CH), 131.1 (CH), 130.5 (C_q), 130.2 (C_q), 129.7 (CH), 128.5 (CH), 128.3 (CH), 128.2 (C_q), 127.5 (CH), 127.3 (CH), 126.7 (CH), 126.3 (CH), 125.8 (CH), 125.7 (CH), 125.6 (CH), 125.3 (CH), 124.9 (CH), 123.2 (CH), 122.7 (CH), 108.9 (CH), 63.0 (C_q), 45.0 (CH₂), 26.9 (CH₃). HRMS (ESI): m/z Calcd for C₃₂H₂₅N₃O₃ + H⁺ [M + H]⁺ 500.1969; Found 500.1916.



***N*-(1-Methyl-2-oxo-3-((thiophene-2-carboxamido)methyl)indolin-3-yl)thiophene-2-**

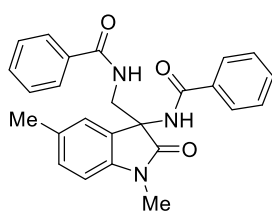
carboxamide (3ap): The representative procedure was followed, using 1-methylindoline-2,3-dione (**1a**; 0.032 g, 0.20 mmol) and *N*-methoxythiophene-2-carboxamide (**2p**; 0.079 g, 0.503 mmol). Purification by column chromatography on silica gel (petroleum ether/EtOAc: 1/2) yielded **3ap** (0.044 g, 53%) as an orange solid. ¹H-NMR (500 MHz, DMSO-*d*₆): δ = 9.47 (br s, 1H, NH), 8.99 (br s, 1H, NH), 7.83-7.80 (m, 2H, Ar-H), 7.78-7.77 (m, 1H, Ar-H), 7.74-7.73 (m, 1H, Ar-H), 7.29 (t, J = 7.6 Hz, 1H, Ar-H), 7.23-7.16 (m, 3H, Ar-H), 7.03 (t, J = 7.9 Hz, 1H, Ar-H), 6.98 (vt, J = 7.4 Hz, 1H, Ar-H), 3.84 (dd, J = 14.0, 6.1 Hz, 1H, CH₂), 3.52 (dd, J = 14.0, 6.1 Hz, 1H, CH₂), 3.18 (s, 3H, CH₃). ¹³C{¹H}-NMR (125 MHz, DMSO-*d*₆): δ = 173.9 (CO), 163.5 (CO), 159.9 (CO), 143.5 (C_q), 138.4 (C_q), 138.2 (C_q), 131.8 (CH), 131.7 (CH), 129.2 (CH), 128.8 (CH), 128.7 (CH), 128.3 (C_q), 128.2 (2C, CH), 128.8 (CH), 122.1 (CH), 108.3 (CH), 63.7 (C_q), 45.7 (CH₂), 26.4 (CH₃). HRMS (ESI): m/z Calcd for C₂₀H₁₇N₃O₃S₂ + H⁺ [M + H]⁺ 412.0784; Found 412.0778.



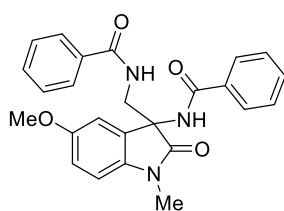
***N*-((3-(benzo[b]thiophene-2-carboxamido)-1-methyl-2-oxoindolin-3-**

yl)methyl)benzo[b]thiophene-2-carboxamide (3aq): The representative procedure was followed, using 1-methylindoline-2,3-dione (**1a**; 0.032 g, 0.20 mmol) and *N*-methoxybenzo[b]thiophene-2-carboxamide (**2q**; 0.104 g, 0.502 mmol). Purification by column chromatography on silica gel (petroleum ether/EtOAc: 1/2) yielded **3aq** (0.056 g, 55%) as a

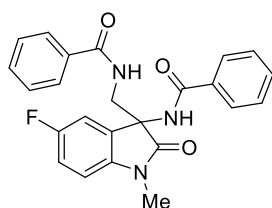
dark brown solid. $^1\text{H-NMR}$ (400 MHz, CDCl_3): δ = 9.68 (br s, 1H, *NH*), 8.34 (br s, 1H, *NH*), 8.02 (s, 1H, Ar-H), 8.01-7.99 (m, 1H, Ar-H), 7.87-7.85 (m, 1H, Ar-H), 7.70 (s, 1H, Ar-H), 7.48-7.43 (m, 2H, Ar-H), 7.39-7.35 (m, 3H, Ar-H), 7.20-7.15 (m, 2H, Ar-H), 7.10 (vt, J = 7.4 Hz, 1H, Ar-H), 6.92-6.85 (m, 2H, Ar-H), 4.45 (dd, J = 14.6, 7.5 Hz, 1H, CH_2), 3.37 (dd, J = 14.6, 5.1 Hz, 1H, CH_2), 3.21 (s, 3H, CH_3). $^{13}\text{C}\{^1\text{H}\}$ -NMR (100 MHz, CDCl_3): δ = 175.3 (CO), 166.2 (CO), 162.0 (CO), 142.9 (C_q), 141.7 (C_q), 141.5 (C_q), 139.5 (C_q), 139.1 (C_q), 137.9 (C_q), 136.8 (C_q), 129.9 (CH), 128.0 (C_q), 126.9 (CH), 126.6 (CH), 126.5 (CH), 126.4 (CH), 125.7 (CH), 125.4 (CH), 125.0 (CH), 124.7 (CH), 123.6 (CH), 122.9 (2C, CH), 122.4 (CH), 108.8 (CH), 63.7 (C_q), 46.2 (CH_2), 26.7 (CH_3).



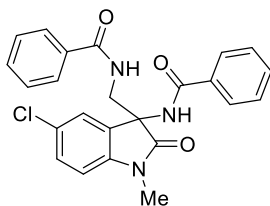
***N*-((3-Benzamido-1,5-dimethyl-2-oxindolin-3-yl)methyl)benzamide (3ba):** The representative procedure was followed, using 1,5-dimethylindoline-2,3-dione (**1b**; 0.035 g, 0.20 mmol) and *N*-methoxybenzamide (**2a**; 0.076 g, 0.503 mmol). Purification by column chromatography on silica gel (petroleum ether/EtOAc: 1/2) yielded **3ba** (0.073 g, 88%) as a brown solid. $^1\text{H-NMR}$ (500 MHz, CDCl_3): δ = 9.07 (br s, 1H, *NH*), 7.88 (d, J = 7.2 Hz, 2H, Ar-H), 7.83 (d, J = 7.3 Hz, 2H, Ar-H), 7.51-7.48 (m, 1H, *NH*; 1H, Ar-H), 7.46-7.40 (m, 3H, Ar-H), 7.30 (t, J = 7.7 Hz, 2H, Ar-H), 7.14 (d, J = 7.8 Hz, 1H, Ar-H), 7.11 (s, 1H, Ar-H), 6.81 (d, J = 7.8 Hz, 1H, Ar-H), 4.29 (dd, J = 14.6, 8.1 Hz, 1H, CH_2), 3.38 (dd, J = 14.5, 4.8 Hz, 1H, CH_2), 3.27 (s, 3H, CH_3), 2.30 (s, 3H, CH_3). $^{13}\text{C}\{^1\text{H}\}$ -NMR (125 MHz, CDCl_3): δ = 175.3 (CO), 170.9 (CO), 166.3 (CO), 141.0 (C_q), 133.2 (C_q), 132.8 (C_q), 132.6 (C_q), 132.3 (CH), 132.0 (CH), 129.9 (CH), 128.8 (2C, CH), 128.7 (2C, CH), 128.3 (C_q), 127.7 (2C, CH), 127.5 (2C, CH), 123.6 (CH), 108.5 (CH), 63.4 (C_q), 45.6 (CH_2), 26.8 (CH_3), 21.3 (CH_3). HRMS (ESI): m/z Calcd for $\text{C}_{25}\text{H}_{23}\text{N}_3\text{O}_3 + \text{H}^+$ [M + H] $^+$ 414.1812; Found 414.1810.



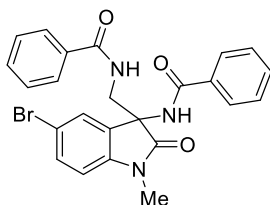
***N*-((3-Benzamido-5-methoxy-1-methyl-2-oxoindolin-3-yl)methyl)benzamide (3ca):** The representative procedure was followed, using 5-methoxy-1-methylindoline-2,3-dione (**1c**; 0.038 g, 0.20 mmol) and *N*-methoxybenzamide (**2a**; 0.076 g, 0.503 mmol). Purification by column chromatography on silica gel (petroleum ether/EtOAc: 1/3) yielded **3ca** (0.040 g, 47%) as a brown solid. ¹H-NMR (500 MHz, CDCl₃): δ = 9.18 (br s, 1H, *NH*), 7.88 (d, *J* = 7.6 Hz, 2H, Ar-H), 7.80 (d, *J* = 7.7 Hz, 2H, Ar-H), 7.66 (br s, 1H, *NH*), 7.48 (d, *J* = 7.0 Hz, 1H, Ar-H), 7.44-7.40 (m, 3H, Ar-H), 7.25-7.21 (m 2H, Ar-H), 6.90 (s, 1H, Ar-H), 6.87-6.81 (m, 2H, Ar-H), 4.26 (dd, *J* = 14.5, 7.8 Hz, 1H, CH₂), 3.73 (s, 3H, OCH₃), 3.39 (dd, *J* = 14.5, 4.5 Hz, 1H, CH₂), 3.25 (s, 3H, CH₃). ¹³C{¹H}-NMR (125 MHz, CDCl₃): δ = 175.1 (CO), 170.9 (CO), 166.3 (CO), 156.5 (C_q), 136.7 (C_q), 133.0 (C_q), 132.5 (C_q), 132.3 (CH), 132.0 (CH), 129.6 (C_q), 128.7 (2C, CH), 128.6 (2C, CH), 127.7 (2C, CH), 127.5 (2C, CH), 113.9 (CH), 110.2 (CH), 109.1 (CH), 63.7 (C_q), 55.9 (OCH₃), 45.7 (CH₂), 26.8 (CH₃). HRMS (ESI): *m/z* Calcd for C₂₅H₂₃N₃O₄ + H⁺ [M + H]⁺ 430.1761; Found 430.1764.



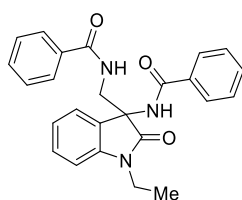
***N*-((3-Benzamido-5-fluoro-1-methyl-2-oxoindolin-3-yl)methyl)benzamide (3da):** The representative procedure was followed, using 5-fluoro-1-methylindoline-2,3-dione (**1d**; 0.036 g, 0.20 mmol) and *N*-methoxybenzamide (**2a**; 0.076 g, 0.503 mmol). Purification by column chromatography on silica gel (petroleum ether/EtOAc: 1/2) yielded **3da** (0.066 g, 79%) as a brown solid. ¹H-NMR (500 MHz, CDCl₃): δ = 9.38 (br s, 1H, *NH*), 7.87 (d, *J* = 8.1 Hz, 2H, Ar-H), 7.84-7.77 (m, 3H, Ar-H), 7.49 (d, *J* = 7.1 Hz, 1H, Ar-H), 7.44-7.37 (m, 1H, *NH*; 2H, Ar-H), 7.24-7.20 (m, 2H, Ar-H), 7.03-6.98 (m, 2H, Ar-H), 6.81-6.78 (m, 1H, Ar-H), 4.15- (dd, *J* = 14.3, 7.5 Hz, 1H, CH₂), 3.40 (dd, *J* = 14.5, 4.7 Hz, 1H, CH₂), 3.20 (s, 3H, CH₃). ¹³C{¹H}-NMR (125 MHz, CDCl₃): δ = 175.2 (CO), 170.9 (CO), 165.5 (CO), 159.5 (d, ¹*J*_{C-F} = 241.8 Hz, C_q), 139.2 (C_q), 132.8 (C_q), 132.4 (C_q), 132.3 (CH), 132.2 (CH), 129.9 (d, ³*J*_{C-F} = 7.6 Hz, C_q), 128.7 (2C, CH), 128.6 (2C, CH), 127.7 (2C, CH), 127.5 (2C, CH), 115.7 (d, ²*J*_{C-F} = 23.6 Hz, CH), 111.1 (d, ²*J*_{C-F} = 25.2 Hz, CH), 109.2 (d, ³*J*_{C-F} = 7.6 Hz, CH), 63.6 (C_q), 45.6 (CH₂), 26.8 (CH₃). ¹⁹F-NMR (376 MHz, CDCl₃): δ = -119.4 (s). HRMS (ESI): *m/z* Calcd for C₂₄H₂₀FN₃O₃ + Na⁺ [M + Na]⁺ 440.1381; Found 440.1376.



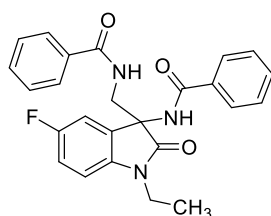
N-((3-Benzamido-5-chloro-1-methyl-2-oxoindolin-3-yl)methyl)benzamide (3ea): The representative procedure was followed, using 5-chloro-1-methylindoline-2,3-dione (**1e**; 0.039 g, 0.20 mmol) and *N*-methoxybenzamide (**2a**; 0.076 g, 0.503 mmol). Purification by column chromatography on silica gel (petroleum ether/EtOAc: 1/2) yielded **3ea** (0.066 g, 76%) as a brown solid. $^1\text{H-NMR}$ (400 MHz, CDCl_3): δ = 9.17 (br s, 1H, *NH*), 7.86-7.83 (m, 4H, Ar-H), 7.51-7.48 (m, 1H, *NH*; 1H, Ar-H), 7.44-7.35 (m, 4H, Ar-H), 7.33-7.30 (m, 2H, Ar-H), 7.25-7.24 (m, 1H, Ar-H), 6.84 (d, J = 8.2 Hz, 1H, Ar-H), 4.18 (dd, J = 14.6, 8.0 Hz, 1H, CH_2), 3.46 (dd, J = 14.6, 5.0 Hz, 1H, CH_2), 3.28 (s, 3H, CH_3). $^{13}\text{C}\{^1\text{H}\}$ -NMR (100 MHz, CDCl_3): δ = 174.9 (CO), 171.0 (CO), 165.5 (CO), 141.9 (C_q), 132.9 (C_q), 132.5 (CH), 132.2 (C_q), 132.1 (CH), 129.9 (C_q), 129.6 (CH), 128.9 (2C, CH), 128.7 (2C, CH), 128.6 (C_q), 127.7 (2C, CH), 127.5 (2C, CH), 123.3 (CH), 109.7 (CH), 63.4 (C_q), 45.4 (CH_2), 26.9 (CH_3). HRMS (ESI): m/z Calcd for $\text{C}_{24}\text{H}_{20}\text{ClN}_3\text{O}_3 + \text{Na}^+$ [$\text{M} + \text{Na}$] $^+$ 456.1085; Found 456.1083.



N-((3-Benzamido-5-bromo-1-methyl-2-oxoindolin-3-yl)methyl)benzamide (3fa): The representative procedure was followed, using 5-bromo-1-methylindoline-2,3-dione (**1f**; 0.048 g, 0.20 mmol) and *N*-methoxybenzamide (**2a**; 0.076 g, 0.503 mmol). Purification by column chromatography on silica gel (petroleum ether/EtOAc: 1/2) yielded **3fa** (0.071 g, 74%) as a brown solid. $^1\text{H-NMR}$ (500 MHz, CDCl_3): δ = 9.05 (br s, 1H, *NH*), 7.85-7.80 (m, 4H, Ar-H), 7.51-7.46 (m, 2H, Ar-H), 7.43-7.35 (m, 1H, *NH*; 3H, Ar-H), 7.30-7.28 (m, 2H, Ar-H), 7.06 (vt, J = 7.4 Hz, 1H, Ar-H), 6.92 (d, J = 7.6 Hz, 1H, Ar-H), 4.22 (dd, J = 14.2, 8.5 Hz, 1H, CH_2), 3.48 (d, J = 14.5 Hz, 1H, CH_2), 3.31 (s, 3H, CH_3). $^{13}\text{C}\{^1\text{H}\}$ -NMR (125 MHz, CDCl_3): δ = 174.8 (CO), 171.0 (CO), 166.5 (CO), 142.3 (C_q), 132.8 (C_q), 132.4 (2C, CH), 132.2 (CH), 132.1 (C_q), 130.3 (C_q), 128.8 (2C, CH), 128.7 (2C, CH), 127.7 (2C, CH), 127.5 (2C, CH), 126.0 (CH), 115.8 (C_q), 110.1 (CH), 63.4 (C_q), 45.5 (CH_2), 26.8 (CH_3). HRMS (ESI): m/z Calcd for $\text{C}_{24}\text{H}_{20}\text{BrN}_3\text{O}_3 + \text{H}^+$ [$\text{M} + \text{H}$] $^+$ 478.0761, 480.0746; Found 478.0764, 480.0744.

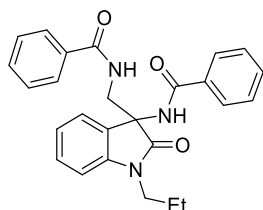


***N*-((3-Benzamido-1-ethyl-2-oxoindolin-3-yl)methyl)benzamide (3ga):** The representative procedure was followed, using 1-ethylindoline-2,3-dione (**1g**; 0.035 g, 0.20 mmol) and *N*-methoxybenzamide (**2a**; 0.076 g, 0.503 mmol). Purification by column chromatography on silica gel (petroleum ether/EtOAc: 1/2) yielded **3ga** (0.069 g, 83%) as a brown solid. $^1\text{H-NMR}$ (400 MHz, CDCl_3): δ = 9.15 (br s, 1H, *NH*), 7.86 (d, J = 7.2 Hz, 2H, Ar-H), 7.80 (d, J = 7.5 Hz, 2H, Ar-H), 7.64 (br s, 1H, *NH*), 7.49-7.24 (m, 8H, Ar-H), 7.02 (vt, J = 7.3 Hz, 1H, Ar-H), 6.92 (d, J = 7.7 Hz, 1H, Ar-H), 4.21 (dd, J = 14.4, 7.7 Hz, 1H, CH_2), 3.85-3.75 (m, 2H, CH_2), 3.41 (dd, J = 14.4, 4.4 Hz, 1H, CH_2), 1.32 (t, J = 6.9 Hz, 3H, CH_3). $^{13}\text{C}\{^1\text{H}\}$ -NMR (100 MHz, CDCl_3): δ = 174.9 (CO), 170.9 (CO), 166.3 (CO), 142.4 (C_q), 133.1 (C_q), 132.7 (C_q), 132.2 (CH), 131.9 (CH), 129.5 (CH), 128.7 (2C, CH), 128.6 (2C, CH), 127.7 (2C, CH), 127.5 (2C, CH), 127.3 (C_q), 122.9 (2C, CH), 108.8 (CH), 63.3 (C_q), 45.7 (CH_2), 35.2 (CH_2), 12.5 (CH_3). HRMS (ESI): m/z Calcd for $\text{C}_{25}\text{H}_{23}\text{N}_3\text{O}_3 + \text{H}^+$ [M + H] $^+$ 414.1812; Found 414.1813.

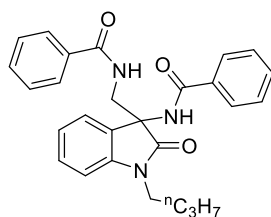


***N*-((3-Benzamido-1-ethyl-5-fluoro-2-oxoindolin-3-yl)methyl)benzamide (3ha):** The representative procedure was followed, using 1-ethyl-5-fluoroindoline-2,3-dione (**1h**; 0.039 g, 0.202 mmol) and *N*-methoxybenzamide (**2a**; 0.076 g, 0.503 mmol). Purification by column chromatography on silica gel (petroleum ether/EtOAc: 1/2) yielded **3ha** (0.069 g, 80%) as a brown solid. $^1\text{H-NMR}$ (400 MHz, CDCl_3): δ = 9.23 (br s, 1H, *NH*), 7.87-7.81 (m, 4H, Ar-H), 7.66 (br s, 1H, *NH*), 7.51-7.39 (m, 4H, Ar-H), 7.31-7.27 (m, 2H, Ar-H), 7.03-6.98 (m, 2H, Ar-H), 6.84-6.81 (m, 1H, Ar-H), 4.14 (dd, J = 14.5, 7.7 Hz, 1H, CH_2), 3.83-3.71 (m, 2H, CH_2), 3.44 (dd, J = 14.5, 4.9 Hz, 1H, CH_2), 1.30 (t, J = 7.1 Hz, 3H, CH_3). $^{13}\text{C}\{^1\text{H}\}$ -NMR (100 MHz, CDCl_3): δ = 174.8 (CO), 170.9 (CO), 165.5 (CO), 159.4 (d, $^1J_{\text{C-F}}$ = 241.8 Hz, C_q), 138.3 (C_q), 132.9 (C_q), 132.4 (C_q), 132.3 (CH), 132.1 (CH), 130.2 (d, $^3J_{\text{C-F}}$ = 7.6 Hz, C_q), 128.8 (2C, CH), 128.7 (2C, CH), 127.7 (2C, CH), 127.5 (2C, CH), 115.7 (d, $^2J_{\text{C-F}}$ = 23.6 Hz, CH), 111.2 (d,

$^2J_{C-F} = 25.2$ Hz, CH), 109.4 (d, $^3J_{C-F} = 7.6$ Hz, CH), 63.5 (C_q), 45.6 (CH₂), 35.4 (CH₂), 12.4 (CH₃). ^{19}F -NMR (376 MHz, CDCl₃): $\delta = -119.9$ (s). HRMS (ESI): m/z Calcd for C₂₅H₂₃FN₃O₃ + Na⁺ [M + Na]⁺ 432.1718; Found 432.1723.

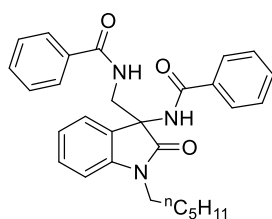


N-((3-Benzamido-2-oxo-1-propylindolin-3-yl)methyl)benzamide (3ia): The representative procedure was followed, using 1-propylindoline-2,3-dione (**1i**; 0.038 g, 0.20 mmol) and *N*-methoxybenzamide (**2a**; 0.076 g, 0.503 mmol). Purification by column chromatography on silica gel (petroleum ether/EtOAc: 1/2) yielded **3ia** (0.069 g, 81%) as a brown solid. 1H -NMR (500 MHz, CDCl₃): $\delta = 9.02$ (br s, 1H, *NH*), 7.85 (d, $J = 8.0$ Hz, 4H, Ar-H), 7.49-7.45 (m, 1H, *NH*; 2H, Ar-H), 7.48-7.28 (m, 6H, Ar-H), 7.02 (t, $J = 7.5$ Hz, 1H, Ar-H), 6.92 (d, $J = 7.8$ Hz, 1H, Ar-H), 4.19 (dd, $J = 14.5, 8.0$ Hz, 1H, CH₂), 3.73 (t, $J = 7.2$ Hz, 2H, CH₂), 3.43 (dd, $J = 14.5, 4.7$ Hz, 1H, CH₂), 1.84-1.74 (m, 2H, CH₂), 1.00 (t, $J = 7.3$ Hz, 3H, CH₃). $^{13}C\{^1H\}$ -NMR (125 MHz, CDCl₃): $\delta = 175.2$ (CO), 170.9 (CO), 166.3 (CO), 142.9 (C_q), 133.3 (C_q), 132.7 (C_q), 132.4 (CH), 131.9 (CH), 129.5 (CH), 128.8 (2C, CH), 128.6 (2C, CH), 128.4 (C_q), 127.7 (2C, CH), 127.5 (2C, CH), 122.9 (CH), 122.8 (CH), 109.0 (CH), 63.2 (C_q), 45.7 (CH₂), 42.2 (CH₂), 20.9 (CH₂), 11.6 (CH₃). HRMS (ESI): m/z Calcd for C₂₆H₂₅N₃O₃ + H⁺ [M + H]⁺ 428.1974; Found 428.1976.

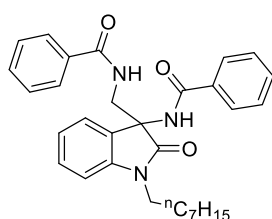


N-((3-Benzamido-1-butyl-2-oxoindolin-3-yl)methyl)benzamide (3ja): The representative procedure was followed, using 1-butyldiolindoline-2,3-dione (**1j**; 0.041 g, 0.202 mmol) and *N*-methoxybenzamide (**2a**; 0.076 g, 0.503 mmol). Purification by column chromatography on silica gel (petroleum ether/EtOAc: 1/1) yielded **3ja** (0.069 g, 78%) as a brown solid. 1H -NMR (400 MHz, CDCl₃): $\delta = 9.12$ (br s, 1H, *NH*), 7.87-7.82 (m, 4H, Ar-H), 7.60 (br s, 1H, *NH*), 7.49-7.38 (m, 4H, Ar-H), 7.31 (vt, $J = 7.7$ Hz, 3H, Ar-H), 7.25 (d, $J = 8.2$ Hz, 1H, Ar-H), 7.00 (t, $J = 7.3$ Hz, 1H, Ar-H), 6.91 (d, $J = 7.7$ Hz, 1H, Ar-H), 4.17 (dd, $J = 14.5, 7.8$ Hz, 1H, CH₂),

3.72 (t, $J = 7.3$ Hz, 2H, CH₂), 3.40 (dd, $J = 14.5, 4.8$ Hz, 1H, CH₂), 1.76-1.67 (m, 2H, CH₂), 1.46-1.36 (m, 2H, CH₂), 0.93 (t, $J = 7.3$ Hz, 3H, CH₃). ¹³C{¹H}-NMR (100 MHz, CDCl₃): $\delta = 175.1$ (CO), 170.8 (CO), 166.2 (CO), 142.8 (C_q), 133.2 (C_q), 132.7 (C_q), 132.3 (CH), 131.9 (CH), 129.5 (CH), 128.8 (2C, CH), 128.6 (2C, CH), 128.4 (C_q), 127.7 (2C, CH), 127.5 (2C, CH), 122.9 (CH), 122.8 (CH), 108.9 (CH), 63.1 (C_q), 45.7 (CH₂), 40.3 (CH₂), 29.4 (CH₂), 20.4 (CH₂), 13.9 (CH₃). HRMS (ESI): m/z Calcd for C₂₇H₂₇N₃O₃ + H⁺ [M + H]⁺ 442.2125; Found 442.2125.

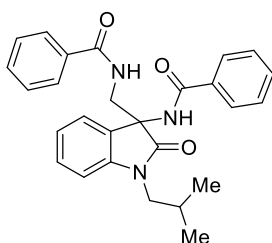


***N*-((3-Benzamido-1-hexyl-2-oxoindolin-3-yl)methyl)benzamide (3ka)**: The representative procedure was followed, using 1-hexylindoline-2,3-dione (**1k**; 0.047 g, 0.203 mmol) and *N*-methoxybenzamide (**2a**; 0.076 g, 0.503 mmol). Purification by column chromatography on silica gel (petroleum ether/EtOAc: 1/2) yielded **3ka** (0.076 g, 80%) as a light brown solid. ¹H-NMR (400 MHz, CDCl₃): $\delta = 9.02$ (br s, 1H, *NH*), 7.85 (vt, $J = 6.3$ Hz, 4H, Ar-H), 7.48-7.45 (m, 1H, *NH*; 2H, Ar-H), 7.42-7.28 (m, 6H, Ar-H), 7.02 (vt, $J = 7.4$ Hz, 1H, Ar-H), 6.91 (d, $J = 7.7$ Hz, 1H, Ar-H), 4.19 (dd, $J = 14.5, 8.0$ Hz, 1H, CH₂), 3.78-3.70 (m, 2H, CH₂), 3.42 (dd, $J = 14.5, 4.7$ Hz, 1H, CH₂), 1.79-1.72 (m, 2H, CH₂), 1.42-1.24 (m, 6H, CH₂), 0.90-0.86 (m, 3H, CH₃). ¹³C{¹H}-NMR (100 MHz, CDCl₃): $\delta = 175.1$ (CO), 170.9 (CO), 166.2 (CO), 142.9 (C_q), 133.3 (C_q), 132.7 (C_q), 132.3 (CH), 131.9 (CH), 129.5 (CH), 128.8 (2C, CH), 128.6 (2C, CH), 128.4 (C_q), 127.7 (2C, CH), 127.5 (2C, CH), 122.9 (CH), 122.8 (CH), 108.9 (CH), 63.1 (C_q), 45.6 (CH₂), 40.6 (CH₂), 31.6 (CH₂), 27.3 (CH₂), 26.8 (CH₂), 22.8 (CH₂), 14.2 (CH₃). HRMS (ESI): m/z Calcd for C₂₉H₃₁N₃O₃ + H⁺ [M + H]⁺ 470.2438; Found 470.2440.

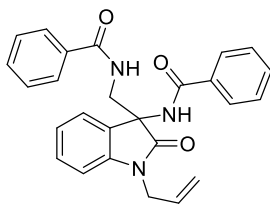


***N*-((3-Benzamido-1-octyl-2-oxoindolin-3-yl)methyl)benzamide (3la)**: The representative procedure was followed, using 1-octylindoline-2,3-dione (**1l**; 0.052 g, 0.201 mmol) and *N*-methoxybenzamide (**2a**; 0.076 g, 0.503 mmol). Purification by column chromatography on

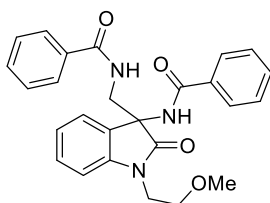
silica gel (petroleum ether/EtOAc: 1/2) yielded **3la** (0.076 g, 76%) as a light brown solid. $^1\text{H-NMR}$ (400 MHz, CDCl_3): δ = 9.16 (br s, 1H, *NH*), 7.87 (d, J = 7.7 Hz, 2H, Ar-H), 7.82 (d, J = 7.8 Hz, 2H, Ar-H), 7.65 (br s, 1H, *NH*), 7.49-7.39 (m, 4H, Ar-H), 7.33-7.25 (m, 4H, Ar-H), 7.01 (t, J = 7.5 Hz, 1H, Ar-H), 6.90 (d, J = 7.7 Hz, 1H, Ar-H), 4.19 (dd, J = 14.5, 7.7 Hz, 1H, CH_2), 3.70 (t, J = 7.3 Hz, 2H, CH_2), 3.38 (dd, J = 14.3, 4.5 Hz, 1H, CH_2), 1.79-1.68 (m, 2H, CH_2), 1.40-1.26 (m, 10H, CH_2), 0.87 (t, J = 6.5 Hz, 3H, CH_3). $^{13}\text{C}\{^1\text{H}\}$ -NMR (100 MHz, CDCl_3): δ = 175.1 (CO), 170.9 (CO), 166.2 (CO), 142.7 (C_q), 133.1 (C_q), 132.6 (C_q), 132.3 (CH), 131.9 (CH), 129.5 (CH), 128.7 (2C, CH), 128.6 (2C, CH), 128.4 (C_q), 127.7 (2C, CH), 127.5 (2C, CH), 122.9 (2C, CH), 108.9 (CH), 63.2 (C_q), 45.7 (CH_2), 40.6 (CH_2), 31.9 (CH_2), 29.4 (CH_2), 29.3 (CH_2), 27.3 (CH_2), 27.1 (CH_2), 22.8 (CH_2), 14.3 (CH_3). HRMS (ESI): m/z Calcd for $\text{C}_{31}\text{H}_{35}\text{N}_3\text{O}_3 + \text{H}^+$ $[\text{M} + \text{H}]^+$ 498.2751; Found 498.2744.



***N*-((3-Benzamido-1-isobutyl-2-oxoindolin-3-yl)methyl)benzamide (3ma)**: The representative procedure was followed, using 1-isobutylindoline-2,3-dione (**1m**; 0.041 g, 0.201 mmol) and *N*-methoxybenzamide (**2a**; 0.076 g, 0.503 mmol). Purification by column chromatography on silica gel (petroleum ether/EtOAc: 1/1) yielded **3ma** (0.070 g, 79%) as a brown solid. $^1\text{H-NMR}$ (400 MHz, CDCl_3): δ = 8.92 (br s, 1H, *NH*), 7.76 (d, J = 7.6 Hz, 4H, Ar-H), 7.41-7.35 (m, 1H, *NH*; 2H, Ar-H), 7.32-7.28 (m, 4H, Ar-H), 7.21 (t, J = 7.7 Hz, 1H, Ar-H), 7.15 (d, J = 7.3 Hz, 1H, Ar-H), 6.91 (t, J = 7.5 Hz, 1H, Ar-H), 6.82 (d, J = 7.8 Hz, 1H, Ar-H), 4.06 (dd, J = 14.5, 8.0 Hz, 1H, CH_2), 3.54-3.48 (m, 1H, CH_2), 3.45-3.40 (m, 1H, CH_2), 3.32 (dd, J = 14.5, 4.6 Hz, 1H, CH_2), 2.15-2.08 (m, 1H, CH), 0.94 (d, J = 6.6 Hz, 3H, CH_3), 0.88 (d, J = 6.6 Hz, 3H, CH_3). $^{13}\text{C}\{^1\text{H}\}$ -NMR (100 MHz, CDCl_3): δ = 175.3 (CO), 170.7 (CO), 166.2 (CO), 143.2 (C_q), 133.3 (C_q), 132.8 (C_q), 132.3 (CH), 131.9 (CH), 129.4 (CH), 128.8 (2C, CH), 128.6 (2C, CH), 128.3 (C_q), 127.7 (2C, CH), 127.5 (2C, CH), 122.8 (2C, CH), 109.1 (CH), 63.0 (C_q), 48.1 (CH_2), 45.8 (CH_2), 27.4 (CH), 20.5 (2C, CH_3). HRMS (ESI): m/z Calcd for $\text{C}_{27}\text{H}_{27}\text{N}_3\text{O}_3 + \text{H}^+$ $[\text{M} + \text{H}]^+$ 442.2125; Found 442.2127.

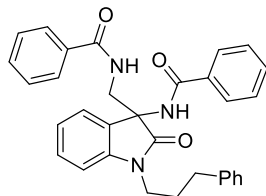


***N*-(1-Allyl-3-(benzamidomethyl)-2-oxoindolin-3-yl)benzamide (3na)**: The representative procedure was followed, using 1-allylindoline-2,3-dione (**1n**; 0.038 g, 0.202 mmol) and *N*-methoxybenzamide (**2a**; 0.076 g, 0.503 mmol). Purification by column chromatography on silica gel (petroleum ether/EtOAc: 1/2) yielded **3na** (0.063 g, 73%) as a brown solid. ¹H-NMR (400 MHz, CDCl₃): δ = 9.21 (br s, 1H, *NH*), 7.86 (d, *J* = 7.1 Hz, 2H, Ar-H), 7.81 (d, *J* = 7.2 Hz, 2H, Ar-H), 7.60 (br s, 1H, *NH*), 7.49-7.45 (m, 1H, Ar-H), 7.43-7.38 (m, 3H, Ar-H), 7.30-7.25 (m, 4H, Ar-H), 7.01 (t, *J* = 7.5 Hz, 1H, Ar-H), 6.88 (d, *J* = 7.7 Hz, 1H, Ar-H), 5.92-5.82 (m, 1H, CH), 5.39 (d, *J* = 17.2 Hz, 1H, CH₂), 5.22 (d, *J* = 10.4 Hz, 1H, CH₂), 4.37 (d, *J* = 5.0 Hz, 2H, CH₂), 4.19 (dd, *J* = 14.5, 7.7 Hz, 1H, CH₂), 3.42 (dd, *J* = 14.5, 5.0 Hz, 1H, CH₂). ¹³C{¹H}-NMR (100 MHz, CDCl₃): δ = 175.1 (CO), 170.9 (CO), 166.3 (CO), 142.4 (C_q), 132.9 (C_q), 132.6 (C_q), 132.2 (CH), 131.9 (CH), 131.2 (CH), 129.4 (CH), 128.6 (2C, CH), 128.5 (2C, CH), 128.3 (C_q), 127.7 (2C, CH), 127.5 (2C, CH), 123.1 (CH), 122.7 (CH), 117.9 (CH₂), 109.6 (CH), 63.3 (C_q), 45.7 (CH₂), 42.8 (CH₂). HRMS (ESI): *m/z* Calcd for C₂₆H₂₃N₃O₃⁺ [M]⁺ 425.1734; Found 425.1721.

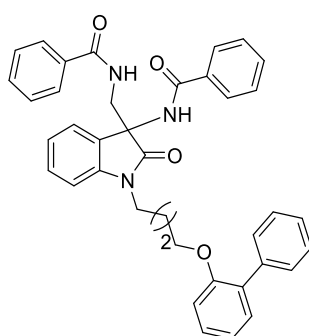


***N*-(3-Benzamido-1-(2-methoxyethyl)-2-oxoindolin-3-yl)methylbenzamide (3oa)**: The representative procedure was followed, using 1-(2-methoxyethyl)indoline-2,3-dione (**1o**; 0.041 g, 0.20 mmol) and *N*-methoxybenzamide (**2a**; 0.076 g, 0.503 mmol). Purification by column chromatography on silica gel (petroleum ether/EtOAc: 1/2) yielded **3oa** (0.059 g, 67%) as a brown solid. ¹H-NMR (500 MHz, CDCl₃): δ = 9.11 (br s, 1H, *NH*), 7.84 (t, *J* = 7.2 Hz, 4H, Ar-H), 7.48-7.39 (m, 1H, *NH*; 4H, Ar-H), 7.38-7.28 (m, 3H, Ar-H), 7.24 (d, *J* = 7.5 Hz, 1H, Ar-H), 7.02 (d, *J* = 7.2 Hz, 2H, Ar-H), 4.16-4.03 (m, 2H, CH₂), 3.88-3.82 (m, 1H, CH₂), 3.72-3.61 (m, 2H, CH₂), 3.49 (dd, *J* = 14.5, 4.8 Hz, 1H, CH₂), 3.34 (s, 3H, OCH₃). ¹³C{¹H}-NMR (125 MHz, CDCl₃): δ = 175.4 (CO), 170.9 (CO), 166.3 (CO), 142.9 (C_q), 133.2 (C_q), 132.6 (C_q), 132.3 (CH), 131.9 (CH), 129.5 (CH), 128.8 (2C, CH), 128.6 (2C, CH), 128.2 (C_q), 127.7 (2C,

CH), 127.5 (2C, CH), 122.9 (CH), 122.8 (CH), 109.4 (CH), 69.6 (CH₂), 63.2 (C_q), 59.1 (OCH₃), 45.6 (CH₂), 40.3 (CH₂). HRMS (ESI): m/z Calcd for C₂₆H₂₅N₃O₄ + H⁺ [M + H]⁺ 444.1918; Found 444.1916.

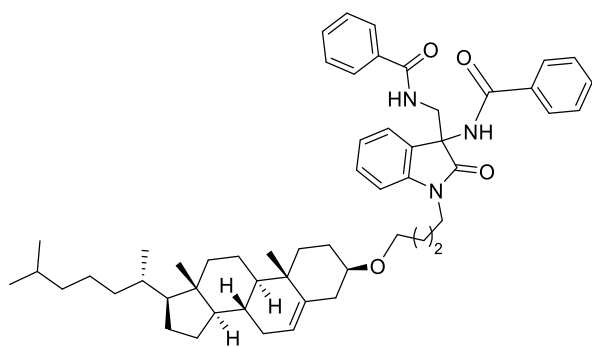


N-((3-benzamido-2-oxo-1-(3-phenylpropyl)indolin-3-yl)methyl)benzamide (3pa): The representative procedure was followed, using 1-(3-phenylpropyl)indoline-2,3-dione (**1p**; 0.053 g, 0.20 mmol) and *N*-methoxybenzamide (**2a**; 0.076 g, 0.503 mmol). Purification by column chromatography on silica gel (petroleum ether/EtOAc: 1/2) yielded **3pa** (0.068 g, 68%) as a brown solid. ¹H-NMR (400 MHz, CDCl₃): δ = 9.04 (br s, 1H, *NH*), 7.86 (d, J = 7.2 Hz, 2H, Ar-H), 7.81 (d, J = 7.5 Hz, 2H, Ar-H), 7.49-7.38 (m, 1H, *NH*; 4H, Ar-H), 7.32-7.23 (m, 6H, Ar-H), 7.20-7.15 (m, 3H, Ar-H), 7.03 (t, J = 7.5 Hz, 1H, Ar-H), 6.80 (d, J = 7.8 Hz, 1H, Ar-H), 4.16 (dd, J = 14.5, 8.0 Hz, 1H, CH₂), 3.83-3.69 (m, 2H, CH₂), 3.32 (dd, J = 14.5, 4.8 Hz, 1H, CH₂), 2.82-2.68 (m, 2H, CH₂), 2.15-2.03 (m, 2H, CH₂). ¹³C{¹H}-NMR (100 MHz, CDCl₃): δ = 175.2 (CO), 170.9 (CO), 166.2 (CO), 142.7 (C_q), 141.3 (C_q), 133.1 (C_q), 132.7 (C_q), 132.3 (CH), 131.9 (CH), 129.5 (CH), 128.7 (2C, CH), 128.6 (4C, CH), 128.5 (2C, CH), 128.5 (C_q), 127.7 (2C, CH), 127.5 (2C, CH), 126.2 (CH), 122.9 (2C, CH), 108.8 (CH), 63.2 (C_q), 45.6 (CH₂), 40.1 (CH₂), 33.3 (CH₂), 28.7 (CH₂). HRMS (ESI): m/z Calcd for C₃₂H₂₉N₃O₃ + H⁺ [M + H]⁺ 504.2282; Found 504.2282.



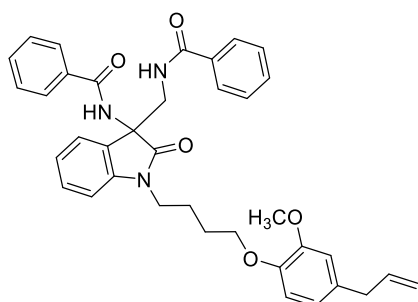
N-(1-(4-([1,1'-Biphenyl]-2-yloxy)butyl)-3-(benzamidomethyl)-2-oxoindolin-3-yl)benzamide (3qa): The representative procedure was followed, using 1-(4-([1,1'-biphenyl]-2-yloxy)butyl)indoline-2,3-dione (**1q**; 0.072 g, 0.201 mmol) and *N*-methoxybenzamide (**2a**; 0.076 g, 0.503 mmol). Purification by column chromatography on silica gel (petroleum

ether/EtOAc: 1/2) yielded **3qa** (0.066 g, 55%) as a light orange solid. $^1\text{H-NMR}$ (500 MHz, CDCl_3): δ = 9.04 (br s, 1H, *NH*), 7.85 (t, J = 7.6 Hz, 4H, Ar-H), 7.52 (d, J = 7.0 Hz, 2H, Ar-H), 7.50 (q, J = 7.6 Hz, 2H, Ar-H), 7.42-7.32 (m, 1H, *NH*; 7H, Ar-H), 7.30-7.27 (m, 4H, Ar-H), 7.03 (q, J = 7.0 Hz, 2H, Ar-H), 6.96 (d, J = 8.2 Hz, 1H, Ar-H), 6.80 (d, J = 7.9 Hz, 1H, Ar-H), 4.09 (dd, J = 14.6, 7.9 Hz, 1H, CH_2), 4.06-3.97 (m, 2H, CH_2), 3.79-3.72 (m, 2H, CH_2), 3.40 (dd, J = 14.6, 4.8 Hz, 1H, CH_2), 1.91-1.82 (m, 4H, CH_2). $^{13}\text{C}\{^1\text{H}\}$ -NMR (125 MHz, CDCl_3): δ = 175.1 (CO), 170.9 (CO), 166.2 (CO), 155.9 (C_q), 142.7 (C_q), 138.8 (C_q), 133.3 (C_q), 132.7 (C_q), 132.4 (CH), 131.9 (CH), 131.0 (CH), 129.7 (2C, CH), 129.6 (CH), 128.9 (2C, CH), 128.8 (CH), 128.6 (2C, CH), 128.4 (2C, C_q), 127.9 (3C, CH), 127.7 (2C, CH), 127.4 (2C, CH), 126.7 (CH), 122.9 (CH), 121.1 (CH), 112.7 (CH), 108.9 (CH), 67.8 (CH_2), 63.2 (C_q), 45.6 (CH_2), 40.1 (CH_2), 26.7 (CH_2), 24.2 (CH_2). HRMS (ESI): m/z Calcd for $\text{C}_{38}\text{H}_{33}\text{N}_3\text{O}_4 + \text{H}^+ [\text{M} + \text{H}]^+$ 596.2549; Found 596.2551.



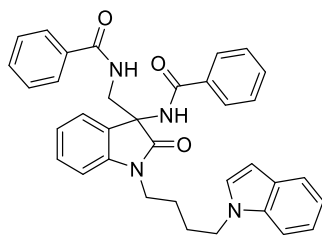
***N*-((3-Benzamido-1-(4-(((3*R*,8*R*,9*R*,10*S*,13*S*,14*R*,17*S*)-10,13-dimethyl-17-((*S*)-6-methylheptan-2-yl)-2,3,4,7,8,9,10,11,12,13,14,15,16,17-tetradecahydro-1*H*-cyclopenta[*a*]phenanthren-3-yl)oxy)butyl)-2-oxoindolin-3-yl)methyl)benzamide (3ra)**: The representative procedure was followed, using 1-(4-(((3*R*,8*R*,9*R*,10*S*,13*S*,14*R*,17*S*)-10,13-dimethyl-17-((*S*)-6-methylheptan-2-yl)-2,3,4,7,8,9,10,11,12,13,14,15,16,17-tetradecahydro-1*H*-cyclopenta[*a*]phenanthren-3-yl)oxy)butyl)indoline-2,3-dione (**1r**; 0.115 g, 0.20 mmol) and *N*-methoxybenzamide (**2a**; 0.076 g, 0.503 mmol). Purification by column chromatography on silica gel (petroleum ether/EtOAc: 1/2) yielded **3ra** (0.099 g, 60%) as a orange solid. $^1\text{H-NMR}$ (400 MHz, CDCl_3): δ = 9.09 (br s, 1H, *NH*), 7.79-7.74 (m, 4H, Ar-H), 7.54 (br s, 1H, *NH*), 7.41-7.36 (m, 2H, Ar-H), 7.33 (d, J = 7.6 Hz, 2H, Ar-H), 7.24-7.20 (m, 3H, Ar-H), 7.17 (d, J = 8.2 Hz, 1H, Ar-H), 6.93 (t, J = 7.5 Hz, 1H, Ar-H), 6.86 (d, J = 7.8 Hz, 1H, Ar-H), 5.26 (s, 1H, CH), 4.09 (dd, J = 14.5, 7.8 Hz, 1H, CH_2), 3.70-3.66 (m, 2H, CH_2), 3.44-3.36 (m, 2H, CH_2), 3.32 (dd, J = 14.5, 4.8 Hz, 1H, CH_2), 3.08-3.01 (m, 1H, CH_2), 2.28-2.25 (m, 1H, CH_2), 2.13-2.06 (m, 1H, CH), 1.96-1.71 (m, 7H), 1.60-1.17 (m, 17H), 1.11-0.97 (m, 6H), 0.91 (s, 3H,

CH₃), 0.84 (d, $J = 6.5$ Hz, 3H, CH₃), 0.79 (d, $J = 1.7$ Hz, 3H, CH₃), 0.78 (d, $J = 1.7$ Hz, 3H, CH₃) 0.60 (s, 3H, CH₃). ¹³C{¹H}-NMR (100 MHz, CDCl₃): $\delta = 175.1$ (CO), 170.8 (CO), 166.2 (CO), 142.7 (C_q), 141.0 (C_q), 133.1 (C_q), 132.6 (C_q), 132.3 (CH), 131.9 (CH), 129.5 (CH), 128.7 (2C, CH), 128.6 (2C, CH), 128.4 (C_q), 127.7 (2C, CH), 127.5 (2C, CH), 122.9 (CH), 121.7 (CH), 109.0 (CH), 79.1 (CH), 67.4 (CH₂), 63.2 (C_q), 56.9 (CH), 56.3 (CH), 50.3 (CH), 45.7 (CH₂), 42.4 (C_q), 40.3 (CH₂), 39.9 (CH₂), 39.6 (CH₂), 39.3 (CH₂), 37.4 (C_q), 37.0 (CH₂), 36.3 (CH₂), 35.9 (CH), 32.1 (CH₂), 32.0 (CH₃), 28.6 (CH₂), 28.4 (CH₂), 28.1 (CH), 27.5 (CH₂), 24.4 (CH₂), 24.2 (CH₂), 23.9 (CH₂), 22.9 (CH₃), 22.7 (2C, CH), 21.2 (CH₂), 19.5 (CH₃), 18.9 (CH₃), 11.9 (CH₃). HRMS (ESI): m/z Calcd for C₅₄H₇₁N₃O₄ + K⁺ [M + K]⁺ 864.5181; Found 864.5181.



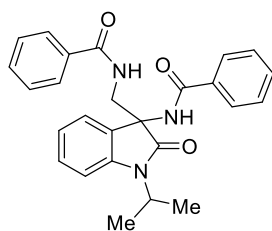
***N*-(1-(4-(4-Allyl-2-methoxyphenoxy)butyl)-3-(benzamidomethyl)-2-oxindolin-3-**

yl)benzamide (3sa): The representative procedure was followed, using 1-(4-(4-allyl-2-methoxyphenoxy)butyl)indoline-2,3-dione (**1s**; 0.073 g, 0.20 mmol) and *N*-methoxybenzamide (**2a**; 0.076 g, 0.503 mmol). Purification by column chromatography on silica gel (petroleum ether/EtOAc: 1/2) yielded **3sa** (0.070 g, 58%) as a light orange sticky liquid. ¹H-NMR (400 MHz, CDCl₃): $\delta = 9.02$ (br s, 1H, *NH*), 7.85-7.83 (m, 4H, Ar-H), 7.51-7.44 (m, 1H, *NH*; 1H, Ar-H), 7.41-7.35 (m, 4H, Ar-H), 7.32-7.25 (m, 3H, Ar-H), 7.02 (t, $J = 7.5$ Hz, 1H, Ar-H), 6.96 (d, $J = 7.7$ Hz, 1H, Ar-H), 6.80 (d, $J = 8.1$ Hz, 1H, Ar-H), 6.70-6.68 (m, 2H, Ar-H), 6.00-5.90 (m, 1H, CH), 5.09-5.04 (m, 2H, CH₂), 4.16 (dd, $J = 14.5, 8.0$ Hz, 1H, CH₂), 4.09-4.00 (m, 2H, CH₂), 3.89-3.84 (m, 2H, CH₂), 3.81 (s, 3H, OCH₃), 3.44 (dd, $J = 14.5, 4.9$ Hz, 1H, CH₂), 3.31 (d, $J = 6.6$ Hz, 2H, CH₂), 1.96-1.95 (m, 4H, CH₂). ¹³C{¹H}-NMR (100 MHz, CDCl₃): $\delta = 175.2$ (CO), 170.9 (CO), 166.2 (CO), 149.5 (C_q), 146.8 (C_q), 142.7 (C_q), 137.8 (CH), 133.2 (C_q), 133.1 (C_q), 132.7 (C_q), 132.3 (CH), 131.9 (CH), 129.5 (CH), 128.8 (2C, CH), 128.6 (2C, CH), 128.4 (C_q), 127.7 (2C, CH), 127.5 (2C, CH), 127.3 (CH), 122.9 (CH), 120.7 (CH), 115.8 (CH₂), 113.7 (CH), 112.6 (CH), 109.0 (CH), 68.7 (CH₂), 63.2 (C_q), 56.0 (OCH₃), 45.7 (CH₂), 40.1 (CH₂), 39.9 (CH₂), 26.7 (CH₂), 24.1 (CH₂). HRMS (ESI): m/z Calcd for C₃₇H₃₇N₃O₅ + H⁺ [M + H]⁺ 604.2806; Found 604.2833.



***N*-(1-(4-(1*H*-Indol-1-yl)butyl)-3-(benzamidomethyl)-2-oxoindolin-3-yl)benzamide (3ta):**

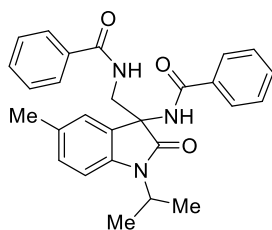
The representative procedure was followed, using 1-(4-(1*H*-indol-1-yl)butyl)indoline-2,3-dione (**1t**; 0.064 g, 0.201 mmol) and *N*-methoxybenzamide (**2a**; 0.076 g, 0.503 mmol). Purification by column chromatography on silica gel (petroleum ether/EtOAc: 1/2) yielded **3ta** (0.060 g, 54%) as a brown solid. ¹H-NMR (400 MHz, CDCl₃): δ = 9.06 (br s, 1H, *NH*), 7.86-7.81 (m, 4H, Ar-H), 7.60 (d, *J* = 7.9 Hz, 1H, Ar-H), 7.51-7.45 (m, 2H, Ar-H), 7.41-7.33 (m, 1H, *NH*; 4H, Ar-H), 7.29-7.23 (m, 3H, Ar-H), 7.17-7.05 (m, 3H, Ar-H), 7.00 (t, *J* = 7.4 Hz, 1H, Ar-H), 6.77 (d, *J* = 7.7 Hz, 1H, Ar-H), 6.48-6.45 (m, 1H, Ar-H), 4.22-4.11 (m, 2H, CH₂), 4.06 (dd, *J* = 14.4, 7.9 Hz, 1H, CH₂), 3.84-3.77 (m, 1H, CH₂), 3.70-3.62 (m, 1H, CH₂), 3.38 (dd, *J* = 14.4, 4.6 Hz, 1H, CH₂), 2.06-1.92 (m, 2H, CH₂), 1.84-1.67 (m, 2H, CH₂). ¹³C{¹H}-NMR (100 MHz, CDCl₃): δ = 175.2 (CO), 170.9 (CO), 166.2 (CO), 142.5 (C_q), 136.1 (C_q), 133.2 (C_q), 132.6 (C_q), 132.4 (CH), 131.9 (CH), 129.6 (CH), 128.9 (2C, CH), 128.8 (C_q), 128.7 (CH), 128.6 (2C, CH), 128.3 (C_q), 128.0 (CH), 127.7 (2C, CH), 127.5 (2C, CH), 122.9 (CH), 121.5 (CH), 121.1 (CH), 119.3 (CH), 109.6 (CH), 108.7 (CH), 101.2 (CH), 63.2 (C_q), 45.9 (CH₂), 45.6 (CH₂), 39.8 (CH₂), 27.8 (CH₂), 24.8 (CH₂). HRMS (ESI): *m/z*. Calcd for C₃₅H₃₂N₄O₃ + H⁺ [M + H]⁺ 557.2547; Found 557.2548.



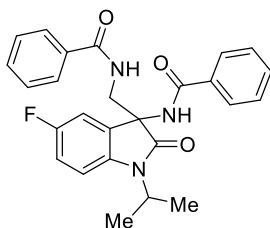
***N*-(3-Benzamido-1-isopropyl-2-oxoindolin-3-yl)methyl)benzamide (3ua):**

The representative procedure was followed, using 1-isopropylindoline-2,3-dione (**1u**; 0.038 g, 0.20 mmol) and *N*-methoxybenzamide (**2a**; 0.076 g, 0.503 mmol). Purification by column chromatography on silica gel (petroleum ether/EtOAc: 1/1) yielded **3ua** (0.068 g, 80%) as a brown solid. ¹H-NMR (400 MHz, CDCl₃): δ = 8.93 (br s, 1H, *NH*), 7.86-7.82 (m, 4H, Ar-H), 7.51-7.36 (m, 1H, *NH*, 5H, Ar-H), 7.30-7.24 (m, 3H, Ar-H), 7.07 (t, *J* = 7.8 Hz, 1H, Ar-H),

6.99 (t, $J = 7.3$ Hz, 1H, Ar-H), 4.72-4.65 (m, 1H, CH), 4.13 (dd, $J = 14.3, 8.1$ Hz, 1H, CH₂), 3.43 (dd, $J = 14.6, 4.6$ Hz, 1H, CH₂), 1.56 (d, $J = 6.8$ Hz, 3H, CH₃), 1.52 (d, $J = 7.0$ Hz, 3H, CH₃). ¹³C{¹H}-NMR (100 MHz, CDCl₃): $\delta = 174.9$ (CO), 170.9 (CO), 162.3 (CO), 142.2 (C_q), 133.7 (C_q), 132.8 (C_q), 132.4 (CH), 131.8 (CH), 129.3 (CH), 128.9 (2C, CH), 128.7 (C_q), 128.6 (2C, CH), 127.7 (2C, CH), 127.5 (2C, CH), 123.1 (CH), 122.5 (CH), 110.5 (CH), 62.8 (C_q), 45.5 (CH₂), 44.4 (CH), 19.7 (CH₃), 19.3 (CH₃). HRMS (ESI): m/z Calcd for C₂₆H₂₅N₃O₃ + H⁺ [M + H]⁺ 428.1969; Found 428.1969.

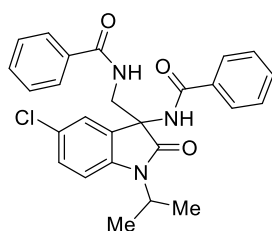


N-((3-Benzamido-1-isopropyl-5-methyl-2-oxindolin-3-yl)methyl)benzamide (3va): The representative procedure was followed, using 1-isopropyl-5-methylindoline-2,3-dione (**1u**; 0.041 g, 0.201 mmol) and *N*-methoxybenzamide (**2a**; 0.076 g, 0.503 mmol). Purification by column chromatography on silica gel (petroleum ether/EtOAc: 1/1) yielded **3va** (0.069 g, 78%) as a brown solid. ¹H-NMR (400 MHz, CDCl₃): $\delta = 8.97$ (br s, 1H, *NH*), 7.87 (d, $J = 8.0$ Hz, 4H, Ar-H), 7.58-7.52 (m, 1H, Ar-H), 7.49-7.44 (m, 2H, Ar-H), 7.41 (br s, 1H, *NH*), 7.40-7.35 (m, 3H, Ar-H), 7.10-7.08 (m, 2H, Ar-H), 6.99-6.97 (m, 1H, Ar-H), 4.73-4.63 (m, 1H, CH), 4.26 (dd, $J = 14.3, 8.1$ Hz, 1H, CH₂), 3.34 (dd, $J = 14.5, 4.6$ Hz, 1H, CH₂), 2.27 (s, 3H, CH₃), 1.55 (d, $J = 7.0$ Hz, 3H, CH₃), 1.51 (d, $J = 7.0$ Hz, 3H, CH₃). ¹³C{¹H}-NMR (100 MHz, CDCl₃): $\delta = 175.0$ (CO), 170.9 (CO), 166.3 (CO), 139.5 (C_q), 133.3 (C_q), 132.8 (C_q), 132.2 (C_q), 131.8 (CH), 129.6 (CH), 128.8 (2C, CH), 128.7 (C_q), 128.6 (2C, CH), 127.7 (2C, CH), 127.5 (2C, CH), 130.2 (CH), 123.9 (CH), 110.3 (CH), 62.8 (C_q), 45.5 (CH₂), 44.4 (CH), 21.1 (CH₃), 19.7 (CH₃), 19.3 (CH₃). HRMS (ESI): m/z Calcd for C₂₇H₂₇N₃O₃ + H⁺ [M + H]⁺ 442.2125; Found 442.2127.

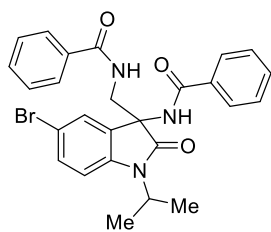


N-((3-Benzamido-5-fluoro-1-isopropyl-2-oxindolin-3-yl)methyl)benzamide (3wa): The representative procedure was followed, using 5-fluoro-1-isopropylindoline-2,3-dione (**1w**;

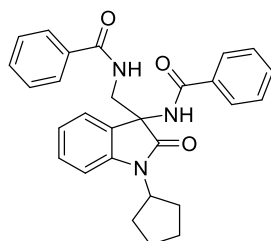
0.042 g, 0.203 mmol) and *N*-methoxybenzamide (**2a**; 0.076 g, 0.503 mmol). Purification by column chromatography on silica gel (petroleum ether/EtOAc: 1/1) yielded **3wa** (0.067 g, 74%) as a brown solid. $^1\text{H-NMR}$ (400 MHz, CDCl_3): δ = 8.97 (br s, 1H, *NH*), 7.87-7.81 (m, 4H, Ar-H), 7.55-7.51 (m, 1H, Ar-H), 7.50-7.38 (m, 5H, Ar-H), 7.21 (br s, 1H, *NH*), 7.03-6.94 (m, 3H, Ar-H), 4.68 (septet, J = 7.0 Hz, 1H, CH), 4.10 (dd, J = 14.5, 8.0 Hz, 1H, CH_2), 3.49 (dd, J = 14.5, 4.9 Hz, 1H, CH_2), 1.56 (d, J = 7.0 Hz, 3H, CH_3), 1.53 (d, J = 7.0 Hz, 3H, CH_3). $^{13}\text{C}\{^1\text{H}\}$ -NMR (100 MHz, CDCl_3): δ = 174.8 (CO), 171.0 (CO), 166.5 (CO), 159.1 (d, $^1J_{\text{C-F}}$ = 241.8 Hz, C_q), 138.0 (d, $^4J_{\text{C-F}}$ = 2.29 Hz, C_q), 132.8 (d, $^3J_{\text{C-F}}$ = 70.2 Hz, C_q), 132.5 (CH), 132.0 (CH), 130.6 (C_q), 130.5 (C_q), 128.9 (2C, CH), 128.7 (2C, CH), 127.7 (2C, CH), 127.5 (2C, CH), 115.5 (d, $^2J_{\text{C-F}}$ = 23.6 Hz, CH), 111.2 (d, $^2J_{\text{C-F}}$ = 32.8 Hz, CH), 111.1 (CH), 63.0 (C_q), 45.4 (CH_2), 44.6 (CH), 19.7 (CH_3), 19.3 (CH_3). $^{19}\text{F-NMR}$ (376 MHz, CDCl_3): δ = -120.6 (s). HRMS (ESI): m/z Calcd for $\text{C}_{26}\text{H}_{24}\text{FN}_3\text{O}_3 + \text{H}^+$ [M + H] $^+$ 446.1874; Found 446.1873.



***N*-((3-Benzamido-5-chloro-1-isopropyl-2-oxoindolin-3-yl)methyl)benzamide (3xa)**: The representative procedure was followed, using 5-chloro-1-isopropylindoline-2,3-dione (**1x**; 0.045 g, 0.201 mmol) and *N*-methoxybenzamide (**2a**; 0.076 g, 0.503 mmol). Purification by column chromatography on silica gel (petroleum ether/EtOAc: 1/1) yielded **3xa** (0.066 g, 71%) as a brown solid. $^1\text{H-NMR}$ (500 MHz, CDCl_3): δ = 8.92 (br s, 1H, *NH*), 7.88 (d, J = 7.2 Hz, 2H, Ar-H), 7.83 (d, J = 7.2 Hz, 2H, Ar-H), 7.57-7.54 (m, 1H, Ar-H), 7.49-7.45 (m, 1H, *NH*; 2H, Ar-H), 7.42-7.38 (m, 2H, Ar-H), 7.29-7.28 (m, 2H, Ar-H), 7.07-7.01 (m, 2H, Ar-H), 4.69 (septet, J = 7.0 Hz, 1H, CH), 4.11 (dd, J = 14.6, 8.2 Hz, 1H, CH_2), 3.50 (dd, J = 14.6, 4.9 Hz, 1H, CH_2), 1.57 (d, J = 7.0 Hz, 3H, CH_3), 1.54 (d, J = 7.0 Hz, 3H, CH_3). $^{13}\text{C}\{^1\text{H}\}$ -NMR (125 MHz, CDCl_3): δ = 174.6 (CO), 171.0 (CO), 166.5 (CO), 140.6 (C_q), 133.1 (C_q), 132.5 (C_q), 132.4 (CH), 132.0 (CH), 130.5 (C_q), 129.2 (CH), 128.9 (2C, CH), 128.6 (2C, CH), 128.0 (C_q), 127.7 (2C, CH), 127.5 (2C, CH), 123.7 (CH), 111.4 (CH), 62.9 (C_q), 45.4 (CH_2), 44.6 (CH), 19.7 (CH_3), 19.2 (CH_3). HRMS (ESI): m/z Calcd for $\text{C}_{26}\text{H}_{24}\text{ClN}_3\text{O}_3 + \text{H}^+$ [M + H] $^+$ 462.1579; Found 462.1579.

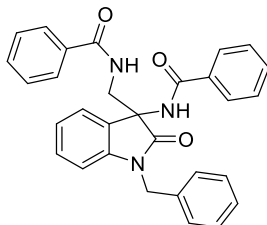


***N*-((3-Benzamido-5-bromo-1-isopropyl-2-oxoindolin-3-yl)methyl)benzamide (3ya):** The representative procedure was followed, using 5-bromo-1-isopropylindoline-2,3-dione (**1y**; 0.054 g, 0.201 mmol) and *N*-methoxybenzamide (**2a**; 0.076 g, 0.503 mmol). Purification by column chromatography on silica gel (petroleum ether/EtOAc: 1/1) yielded **3ya** (0.071 g, 70%) as a brown solid. $^1\text{H-NMR}$ (400 MHz, CDCl_3): δ = 9.03 (br s, 1H, *NH*), 7.87-7.83 (m, 4H, Ar-H), 7.53-7.45 (m, 1H, *NH*; 1H, Ar-H), 7.42-7.36 (m, 6H, Ar-H), 7.28-7.27 (m, 1H, Ar-H), 6.95 (d, J = 8.4 Hz, 1H, Ar-H), 4.65 (septet, J = 7.0 Hz, 1H, CH), 4.11 (dd, J = 14.5, 8.0 Hz, 1H, CH_2), 3.46-3.43 (m, 1H, CH_2), 1.54 (d, J = 6.9 Hz, 3H, CH_3), 1.50 (d, J = 7.0 Hz, 3H, CH_3). $^{13}\text{C}\{^1\text{H}\}$ -NMR (100 MHz, CDCl_3): δ = 174.5 (CO), 171.0 (CO), 166.4 (CO), 141.2 (C_q), 133.2 (C_q), 132.5 (CH), 132.4 (C_q), 132.1 (CH), 132.0 (CH), 130.9 (C_q), 128.9 (2C, CH), 128.7 (2C, CH), 127.7 (2C, CH), 127.5 (2C, CH), 126.3 (CH), 115.3 (C_q), 111.9 (CH), 62.8 (C_q), 45.4 (CH_2), 44.6 (CH), 19.6 (CH_3), 19.2 (CH_3). HRMS (ESI): m/z Calcd for $\text{C}_{26}\text{H}_{24}\text{BrN}_3\text{O}_3 + \text{H}^+$ [M + H] $^+$ 506.1074, 508.1073; Found 506.1077, 508.1075.

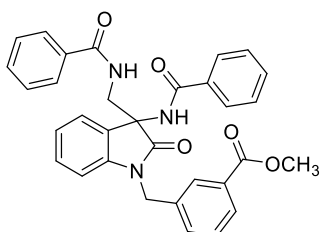


***N*-((3-Benzamido-1-cyclopentyl-2-oxoindolin-3-yl)methyl)benzamide (3za):** The representative procedure was followed, using 1-cyclopentylindoline-2,3-dione (**1z**; 0.043 g, 0.20 mmol) and *N*-methoxybenzamide (**2a**; 0.076 g, 0.503 mmol). Purification by column chromatography on silica gel (petroleum ether/EtOAc: 1/2) yielded **3za** (0.064 g, 71%) as a brown solid. $^1\text{H-NMR}$ (500 MHz, CDCl_3): δ = 9.02 (br s, 1H, *NH*), 7.75-7.69 (m, 4H, Ar-H), 7.52 (br s, 1H, *NH*), 7.36-7.28 (m, 4H, Ar-H), 7.20-7.11 (m, 4H, Ar-H), 7.86 (d, J = 8.1 Hz, 2H, Ar-H), 4.63 (septet, J = 8.4 Hz, 1H, CH), 4.05-3.98 (m, 1H, CH_2), 3.25-3.21 (m, 1H, CH_2), 2.09-1.98 (m, 2H, CH_2), 1.79 (s, 4H, CH_2), 1.54 (s, 2H, CH_2). $^{13}\text{C}\{^1\text{H}\}$ -NMR (125 MHz, CDCl_3): δ = 175.3 (CO), 170.9 (CO), 166.3 (CO), 142.1 (C_q), 133.2 (C_q), 132.7 (C_q), 132.2 (CH), 131.8 (CH), 129.2 (CH), 128.7 (2C, CH), 128.6 (1C, C_q ; 2C, CH), 127.7 (2C, CH), 127.5

(2C, CH), 122.9 (CH), 122.6 (CH), 110.1 (CH), 62.9 (C_q), 53.0 (CH), 45.6 (CH₂), 28.1 (CH₂), 27.6 (CH₂), 25.4 (2C, CH₂). HRMS (ESI): m/z Calcd for C₂₈H₂₇N₃O₃ + H⁺ [M + H]⁺ 454.2125; Found 454.2147.

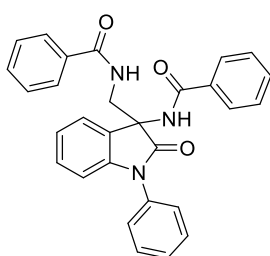


***N*-((3-Benzamido-1-benzyl-2-oxoindolin-3-yl)methyl)benzamide (3Aa):** The representative procedure was followed, using 1-benzylindoline-2,3-dione (**1A**; 0.048 g, 0.202 mmol) and *N*-methoxybenzamide (**2a**; 0.076 g, 0.503 mmol). Purification by column chromatography on silica gel (petroleum ether/EtOAc: 1/2) yielded **3Aa** (0.079 g, 82%) as an orange solid. ¹H-NMR (500 MHz, CDCl₃): δ = 9.09 (br s, 1H, *NH*), 7.90-7.87 (m, 3H, Ar-H), 7.56-7.50 (m, 1H, Ar-H), 7.48-7.40 (m, 7H, *NH*, Ar-H), 7.36 (t, J = 7.5 Hz, 2H, Ar-H), 7.27 (d, J = 7.3 Hz, 2H, Ar-H), 7.22-7.18 (m, 3H, Ar-H), 7.01 (t, J = 7.5 Hz, 1H, Ar-H), 6.74 (d, J = 7.8 Hz, 1H, Ar-H), 5.09-4.98 (m, 2H, CH₂), 4.16 (dd, J = 14.6, 8.0 Hz, 1H, CH₂), 3.63 (dd, J = 14.6, 5.1 Hz, 1H, CH₂). ¹³C{¹H}-NMR (125 MHz, CDCl₃): δ = 175.2 (CO), 171.1 (CO), 166.3 (CO), 142.5 (C_q), 135.8 (C_q), 133.3 (C_q), 132.6 (CH), 131.9 (CH), 129.5 (CH), 129.0 (2C, CH), 128.9 (2C, CH), 128.8 (C_q), 128.6 (2C, CH), 128.1 (C_q), 127.8 (CH), 127.7 (2C, CH), 127.5 (2C, CH), 127.3 (2C, CH), 123.1 (CH), 122.9 (CH), 109.9 (CH), 63.4 (C_q), 45.7 (CH₂), 44.3 (CH₂). HRMS (ESI): m/z Calcd for C₃₀H₂₅N₃O₃ + H⁺ [M + H]⁺ 476.1969; Found 476.1969.



Methyl 3-((3-benzamido-3-(benzamidomethyl)-2-oxoindolin-1-yl)methyl)benzoate (3Ba): The representative procedure was followed, using methyl 3-((2,3-dioxindolin-1-yl)methyl)benzoate (**1B**; 0.059 g, 0.20 mmol) and *N*-methoxybenzamide (**2a**; 0.076 g, 0.503 mmol). Purification by column chromatography on silica gel (petroleum ether/EtOAc: 1/2) yielded **3Ba** (0.062 g, 58%) as an orange solid. ¹H-NMR (500 MHz, CDCl₃): δ = 9.17 (br s, 1H, *NH*), 8.06 (br s, 1H, *NH*), 7.94 (d, J = 7.7 Hz, 1H, Ar-H), 7.89-7.88 (m, 4H, Ar-H), 7.71

(d, $J = 7.6$ Hz, 1H, Ar-H), 7.53-7.50 (m, 1H, Ar-H), 7.48-7.39 (m, 6H, Ar-H), 7.27 (vt, $J = 6.8$ Hz, 2H, Ar-H), 7.19 (t, $J = 7.7$ Hz, 1H, Ar-H), 7.00 (t, $J = 6.9$ Hz, 1H, Ar-H), 6.69 (d, $J = 7.5$ Hz, 1H, Ar-H), 5.05 (s, 2H, CH₂), 4.16 (dd, $J = 14.5, 7.9$ Hz, 1H, CH₂), 3.91 (s, 3H, OCH₃), 3.64-3.60 (m, 1H, CH₂). ¹³C{¹H}-NMR (125 MHz, CDCl₃): $\delta = 175.2$ (CO), 171.1 (CO), 167.1 (CO), 166.3 (CO), 142.2 (C_q), 136.4 (C_q), 133.2 (C_q), 132.6 (C_q), 132.5 (CH), 132.0 (CH), 131.9 (CH), 130.7 (C_q), 129.5 (CH), 129.4 (CH), 128.2 (CH), 128.9 (2C, CH), 128.6 (2C, CH), 128.4 (CH), 128.2 (C_q), 127.7 (2C, CH), 127.5 (2C, CH), 123.3 (CH), 122.9 (CH), 109.7 (CH), 63.5 (C_q), 52.4 (OCH₃), 45.6 (CH₂), 43.9 (CH₂). HRMS (ESI): m/z Calcd for C₃₂H₂₇N₃O₅ + H⁺ [M + H]⁺ 534.2023; Found 534.2020.



N-((3-Benzamido-2-oxo-1-phenylindolin-3-yl)methyl)benzamide (3Ca): The representative procedure was followed, using 1-phenylindoline-2,3-dione (**1C**; 0.045 g, 0.201 mmol) and *N*-methoxybenzamide (**2a**; 0.076 g, 0.503 mmol). Purification by column chromatography on silica gel (petroleum ether/EtOAc: 1/2) yielded **3Ca** (0.055 g, 59%) as an orange sticky liquid. ¹H-NMR (400 MHz, CDCl₃): $\delta = 9.27$ (br s, 1H, *NH*), 7.89 (d, $J = 7.9$ Hz, 2H, Ar-H), 7.81 (d, $J = 7.8$ Hz, 2H, Ar-H), 7.67 (br s, 1H, *NH*), 7.55-7.51 (m, Ar-H), 7.48 (d, $J = 7.1$ Hz, 1H, Ar-H), 7.44-7.34 (m, 7H, Ar-H), 7.30-7.28 (m, 1H, Ar-H), 7.21 (t, $J = 7.5$ Hz, 2H, Ar-H), 7.09 (t, $J = 7.5$ Hz, 1H, Ar-H), 6.88 (d, $J = 7.9$ Hz, 1H, Ar-H), 4.38 (dd, $J = 14.5, 7.9$ Hz, 1H, CH₂), 3.26 (dd, $J = 14.4, 4.1$ Hz, 1H, CH₂). ¹³C{¹H}-NMR (100 MHz, CDCl₃): $\delta = 175.0$ (CO), 171.0 (CO), 166.6 (CO), 143.6 (C_q), 134.7 (C_q), 132.9 (C_q), 132.6 (C_q), 132.2 (CH), 132.0 (CH), 129.8 (2C, CH), 129.6 (CH), 128.7 (4C, CH), 128.5 (CH), 128.0 (C_q), 127.7 (2C, CH), 127.5 (2C, CH), 127.0 (2C, CH), 123.6 (CH), 123.1 (CH), 109.9 (CH), 63.4 (C_q), 45.1 (CH₂). HRMS (ESI): m/z Calcd for C₂₉H₂₃N₃O₃ + H⁺ [M + H]⁺ 462.1812; Found 462.1807.

4.4.3 Procedure for Removal of *N*-Me Group

To an oven-dried screw-cap tube, *N-((3-benzamido-1-methyl-2-oxoindolin-3-yl)methyl)benzamide (3aa*; 0.100 g, 0.25 mmol) and benzoyl peroxide (0.121 g, 0.50 mmol) were introduced and dissolved in dry CH₂Cl₂ (5.0 mL). The resultant reaction mixture was stirred at 80 °C for 20 h. At ambient temperature, the solvent was evaporated *in vacuo* and

remaining residue was dissolved in MeOH (5 mL). The NaOH (0.036 g, 0.90 mmol) was added to the reaction mixture and stirred at room temperature for 20 h. The reaction mixture was quenched with saturated aqueous NH₄Cl (6.0 mL) and the crude product was extracted with dichloromethane (10 mL x 3). The combined organic extract was dried over Na₂SO₄ and the volatiles were evaporated *in vacuo*. The remaining residue was redissolved in methanolic ammonia solution (6 mL, 7M) and the reaction mixture was stirred at room temperature for 20 h. The solvent was evaporated and the residue was extracted with EtOAc (10 mL x 3). The combined organic extract was dried over Na₂SO₄ and the volatiles were evaporated *in vacuo*. The crude product purified by column chromatography on silica gel (petroleum ether/EtOAc: 1/2) to yield **4** (0.057 g, 59%) as a brown solid. ¹H-NMR (400 MHz, DMSO-d₆): δ = 10.54 (br s, 1H, NH), 9.54 (br s, 1H, NH), 9.01 (br s, 1H, NH), 7.88 (d, *J* = 7.9 Hz, 2H, Ar-H), 7.83 (d, *J* = 7.9 Hz, 2H, Ar-H), 7.59-7.56 (m, 2H, Ar-H), 7.53-7.49 (m, 4H, Ar-H), 7.20 (t, *J* = 7.7 Hz, 1H, Ar-H), 7.14 (d, *J* = 7.4 Hz, 1H, Ar-H), 6.91-6.87 (m, 2H, Ar-H), 3.78 (dd, *J* = 14.0, 5.7 Hz, 1H, CH₂), 3.58 (dd, *J* = 14.1, 6.5 Hz, 1H, CH₂). ¹³C{¹H}-NMR (100 MHz, DMSO-d₆): δ = 176.7 (CO), 171.1 (CO), 166.4 (CO), 140.7 (C_q), 133.3 (C_q), 132.5 (1C, C_q; 1C, CH), 132.0 (CH), 129.6 (CH), 128.9 (2C, CH), 128.7 (2C, CH), 128.5 (C_q), 127.7 (2C, CH), 127.5 (2C, CH), 123.1 (CH), 122.9 (CH), 110.7 (CH), 63.8 (C_q), 45.5 (CH₂). HRMS (ESI): *m/z* Calcd for C₂₃H₁₉N₃O₃ + H⁺ [M + H]⁺ 386.1499; Found 386.1493.

4.4.4 Procedure for Partial Reduction of **3aa**

To a solution of *N*-((3-benzamido-1-methyl-2-oxoindolin-3-yl)methyl)benzamide (**3aa**; 0.080 g, 0.20 mmol) in THF (5.0 mL) was added BH₃.SMe₂ (0.24 mL, 1.0 M, 1.2 equiv). The resultant reaction mixture was stirred at room temperature for 5 h. The reaction was quenched with MeOH and solvent was evaporated *in vacuo*. The crude product was extracted with EtOAc (10 mL x 3). The combined organic extract was dried over Na₂SO₄ and the volatiles were evaporated *in vacuo* and purified by column chromatography on silica gel (petroleum ether/EtOAc: 3/1) to yield **5** (0.048 g, 62%) as an orange solid. ¹H-NMR (400 MHz, CDCl₃): δ = 8.05 (br s, 1H, NH), 7.79 (d, *J* = 7.3 Hz, 2H, Ar-H), 7.49 (d, *J* = 7.1 Hz, 1H, Ar-H), 7.43-7.38 (m, 1H, NH; 2H, Ar-H), 7.36-7.28 (m, 6H, Ar-H), 7.17 (d, *J* = 7.3 Hz, 1H, Ar-H), 7.01 (t, *J* = 7.5 Hz, 1H, Ar-H), 6.89 (d, *J* = 7.7 Hz, 1H, Ar-H), 3.86 (s, 2H, CH₂), 3.29 (s, 3H, CH₃), 2.98-2.90 (m, 2H, CH₂). ¹³C{¹H}-NMR (100 MHz, CDCl₃): δ = 176.3 (CO), 165.5 (CO), 143.8 (C_q), 139.6 (C_q), 133.3 (C_q), 131.9 (CH), 129.3 (CH), 128.8 (2C, CH), 128.7 (C_q), 128.6 (2C, CH), 128.3 (2C, CH), 127.6 (CH), 127.5 (2C, CH), 122.8 (CH), 122.3 (CH), 108.6

(CH), 60.8 (C_q), 54.0 (CH₂), 53.8 (CH₂), 26.7 (CH₃). HRMS (ESI): m/z Calcd for C₂₄H₂₃N₃O₂ + H⁺ [M + H]⁺ 386.1863; Found 386.1861.

4.4.5 Procedure for Synthesis of *N*-(3-(aminomethyl)-1-methyl-2-oxoindolin-3-yl)benzamide

Procedure for synthesis of compound 6: To a solution of *N*-((3-benzamido-1-methyl-2-oxoindolin-3-yl)methyl)benzamide (**3aa**; 0.100 g, 0.25 mmol) and DMAP (0.006 g, 0.05 mmol) in acetonitrile (5 mL), (Boc)₂O (0.272 g, 1.25 mmol) was added and the reaction mixture was stirred at room temperature for 5 h. The volatiles were evaporated *in vacuo*. The crude product purified by column chromatography on silica gel (petroleum ether/EtOAc: 3/1) to yield **6** (0.097 g, 78%) as a light brown solid. ¹H-NMR (500 MHz, CDCl₃): δ = 9.59 (br s, 1H, *NH*), 7.96 (d, *J* = 7.1 Hz, 2H, Ar-H), 7.67 (d, *J* = 7.3 Hz, 2H, Ar-H), 7.52-7.49 (m, 2H, Ar-H), 7.46-7.40 (m, 4H, Ar-H), 7.34-7.29 (m, 1H, Ar-H), 7.22 (d, *J* = 7.2 Hz, 1H, Ar-H), 7.02-6.98 (m, 1H, Ar-H), 6.91 (d, *J* = 7.7 Hz, 1H, Ar-H), 4.28 (s, 2H, CH₂), 3.28 (s, 3H, CH₃), 1.10 (s, 9H, CH₃). ¹³C{¹H}-NMR (125 MHz, CDCl₃): δ = 174.4 (2C, CO), 165.8 (CO), 143.8 (2C, C_q), 137.1 (CO), 132.9 (C_q), 131.8 (CH), 131.6 (CH), 129.4 (CH), 128.5 (3C, CH), 128.3 (C_q), 128.2 (2C, CH), 128.1 (CH), 127.6 (2C, CH), 122.6 (CH), 122.2 (CH), 108.6 (CH), 84.9 (C_q), 61.6 (C_q), 49.9 (CH₂), 27.2 (3C, CH₃), 26.7 (CH₃). HRMS (ESI): m/z Calcd for C₂₉H₂₉N₃O₅ + H⁺ [M + H]⁺ 500.2180; Found 500.2128.

Procedure for synthesis of compound 7: To a solution of *tert*-butyl ((3-benzamido-1-methyl-2-oxoindolin-3-yl)methyl)(benzoyl)carbamate (**6**; 0.090 g, 0.18 mmol) and LiOH.H₂O (0.015 g, 0.36 mmol) in mixture of THF:H₂O (4:1, 5 mL), 30% H₂O₂ (0.028 mL, 0.90 mmol) was added. The resultant reaction mixture was stirred at room temperature for 5 h. The reaction mixture was acidified to pH 2 using 0.5 M HCl and the crude product was extracted with CH₂Cl₂ (10 mL x 3). The combined organic extract was dried over Na₂SO₄ and the volatiles were evaporated *in vacuo*. The crude product was purified by column chromatography on silica gel (petroleum ether/EtOAc: 5/1) to yield **7** (0.055 g, 77%) as a white solid. ¹H-NMR (500 MHz, CDCl₃): δ = 8.86 (br s, 1H, *NH*), 7.85 (d, *J* = 7.5 Hz, 2H, Ar-H), 7.48-7.44 (m, 1H, Ar-H), 7.37 (t, *J* = 7.6 Hz, 2H, Ar-H), 7.31 (t, *J* = 7.7 Hz, 1H, Ar-H), 7.23 (d, *J* = 7.2 Hz, 1H, Ar-H), 7.02 (t, *J* = 7.5 Hz, 1H, Ar-H), 6.89 (d, *J* = 7.7 Hz, 1H, Ar-H), 5.41 (br s, 1H, *NH*), 3.58 (dd, *J* = 14.8, 8.0 Hz, 1H, CH₂), 3.39 (dd, *J* = 14.8, 5.3 Hz, 1H, CH₂), 3.29 (s, 3H, CH₃), 1.51 (s, 9H, CH₃). ¹³C{¹H}-NMR (125 MHz, CDCl₃): δ = 174.9 (CO), 166.1 (CO), 158.8 (CO), 143.5 (C_q), 132.6 (C_q), 131.9 (CH), 129.4 (CH), 128.5 (2C, CH), 128.3 (C_q), 127.5 (2C, CH),

122.8 (CH), 122.7 (CH), 108.6 (CH), 81.2 (C_q), 63.2 (C_q), 46.1 (CH₂), 28.4 (3C, CH₃), 26.7 (CH₃). HRMS (ESI): *m/z* Calcd for C₂₂H₂₅N₃O₄ + H⁺ [M + H]⁺ 396.1923; Found 396.1925.

Procedure for synthesis of compound 8: In a 50 mL round bottom flask, tert-butyl ((3-benzamido-1-methyl-2-oxoindolin-3-yl)methyl)carbamate (**7**; 0.050 g, 0.126 mmol) was added and dissolved in CH₂Cl₂ (4 mL) at 0 °C. To the stirring reaction mixture, trifluoroacetic acid (2 mL) was added and stirred at 0 °C for 1 h. The crude product was extracted with EtOAc (10 mL x 3). The combined organic extract was dried over Na₂SO₄ and the volatiles were evaporated *in vacuo*. The crude product was purified by column chromatography on silica gel (EtOAc) to yield **8** (0.022 g, 59%) as an oily liquid. ¹H-NMR (400 MHz, CDCl₃): δ = 7.81 (d, *J* = 7.1 Hz, 2H, Ar-H), 7.52-7.48 (m, 1H, Ar-H), 7.45-7.39 (m, 3H, Ar-H), 7.35-7.31 (m, 1H, Ar-H), 7.28 (br s, 1H, NH), 7.08 (vt, *J* = 7.5 Hz, 1H, Ar-H), 6.87 (d, *J* = 7.7 Hz, 1H, Ar-H), 4.15 (dd, *J* = 13.7, 8.6 Hz, 1H, CH₂), 3.30 (dd, *J* = 13.6, 2.7 Hz, 1H, CH₂), 3.21 (s, 3H, CH₃), 2.08 (br s, 2H, NH₂),. ¹³C{¹H}-NMR (100 MHz, CDCl₃): δ = 179.3 (CO), 167.8 (CO), 143.0 (C_q), 134.3 (C_q), 131.7 (CH), 130.1 (C_q), 129.8 (CH), 128.7 (2C, CH), 127.2 (2C, CH), 123.9 (CH), 123.5 (CH), 108.8 (CH), 59.9 (C_q), 46.2 (CH₂), 26.1 (CH₃). HRMS (ESI): *m/z* Calcd for C₁₇H₁₇N₃O₂ + H⁺ [M + H]⁺ 296.1394; Found 296.1392.

4.4.6 Mechanistic Experiments

4.4.6.1 External Addition Experiment

Procedure for TEMPO/galvinoxyl added experiment: To an oven-dried screw-cap tube equipped with a magnetic stir bar was added 1-methylindoline-2,3-dione (**1a**; 0.032 g, 0.20 mmol), *N*-methoxybenzamide (**2a**; 0.076 g, 0.503 mmol), FeCl₃ (0.0032 g, 0.02 mmol), LiO^tBu (0.032 g, 0.40 mmol) and TEMPO (0.063 g, 0.403 mmol) [or galvinoxyl (0.169 g, 0.40 mmol) inside the glove box. Toluene (1.0 mL) was added to the reaction mixture. The resultant reaction mixture was immersed in a preheated oil bath at 110 °C and stirred for 24 h. At ambient temperature, the reaction mixture was quenched with distilled H₂O (10.0 mL) and the crude mixture was extracted with EtOAc (15 mL x 3). The combined organic extract was dried over Na₂SO₄ and the volatiles were evaporated *in vacuo*. The ¹H NMR analysis of crude mixture indicated the absence of expected compound **3aa**. The starting compounds **1a** and **2a** were present in quantitative amount.

4.4.6.2 Deuterium Labeling Experiments

Synthesis of *N*-((3-Benzamido-1-methyl-2-oxindolin-3-yl)methyl-d₂)benzamide (3aa**-[D₂]):** The representative procedure was followed, using 1-methylindoline-2,3-dione (**1a**; 0.032 g, 0.20 mmol) and *N*-(methoxy-d₃)benzamide (**2b**-[D₃]; 0.077 g, 0.50 mmol). Purification by column chromatography on silica gel (petroleum ether/EtOAc: 1/2) yielded **3aa**-[D₂] (0.054 g, 67%) as a brown solid. ¹H-NMR (400 MHz, CDCl₃): δ = 9.21 (br s, 1H, NH), 7.87 (d, *J* = 7.2 Hz, 2H, Ar-H), 7.80 (d, *J* = 7.3 Hz, 2H, Ar-H), 7.58 (br s, 1H, NH), 7.47 (d, *J* = 7.2 Hz, 1H, Ar-H), 7.43-7.40 (m, 3H, Ar-H), 7.34 (t, *J* = 7.7 Hz, 1H, Ar-H), 7.27-7.23 (m, 3H, Ar-H), 7.05 (t, *J* = 7.3 Hz, 1H, Ar-H), 6.90 (d, *J* = 7.6 Hz, 1H, Ar-H), 3.27 (s, 3H, CH₃). ¹³C{¹H}-NMR (100 MHz, CDCl₃): δ = 175.4 (CO), 170.9 (CO), 166.3 (CO), 143.4 (C_q), 133.1 (C_q), 132.5 (C_q), 132.3 (CH), 132.0 (CH), 129.7 (CH), 128.8 (2C, CH), 128.7 (2C, CH), 128.3 (C_q), 127.7 (2C, CH), 127.5 (2C, CH), 123.2 (CH), 122.8 (CH), 108.7 (CH), 63.3 (C_q), 26.7 (CH₃). ²H-NMR (400 MHz, CHCl₃): δ = 4.19 (s, 1D, CD), 3.45 (s, 1D, CD). HRMS (ESI): *m/z* Calcd for C₂₄H₁₉D₂N₃O₃ + H⁺ [M + H]⁺ 402.1781; Found 402.1775.

Procedure for deuterium labeling experiment: To an oven-dried screw-cap tube equipped with a magnetic stir bar was added 1-methylindoline-2,3-dione (**1a**; 0.032 g, 0.20 mmol), *N*-methoxybenzamide (**2a**; 0.076 g, 0.503 mmol) [or *N*-(methoxy-d₃)benzamide (**2a**-[D₃]; 0.077 g, 0.50 mmol)], FeCl₃ (0.0032 g, 0.02 mmol, 10.0 mol%), LiO^tBu (0.032 g, 0.40 mmol) and CH₃OH (0.016 g, 0.50 mmol) [or CD₃OD (0.018 g, 0.50 mmol)] inside the glove box. Toluene (1.0 mL) was added to the reaction mixture. The resultant reaction mixture was stirred at 110 °C for 24 h. At ambient temperature, the reaction mixture was quenched with distilled H₂O (10.0 mL) and the crude mixture was extracted with EtOAc (15 mL x 3). The combined organic extract was dried over Na₂SO₄ and the volatiles were evaporated *in vacuo*. The remaining residue was purified by column chromatography on silica gel (petroleum ether/EtOAc: 1/2) to yield deuterated **3aa**-[H/D] in (0.059 g) 74% and (0.054 g) 68%, respectively using in CD₃OD and CH₃OH.

4.4.6.3 Procedure for Controlled Experiments

To an oven-dried screw-cap tube equipped with a magnetic stir bar was introduced 1-methylindoline-2,3-dione (**1a**; 0.032 g, 0.20 mmol), benzamide (0.060 g, 0.50 mmol), FeCl₃ (0.0032 g, 0.02 mmol, 10.0 mol%), LiO^tBu (0.032 g, 0.40 mmol) and CH₃OH (0.016 g, 0.50 mmol) [or CD₃OD (0.018 g, 0.50 mmol) or HCHO (0.015 g, 0.50 mmol)]. Toluene (1.0 mL) was added to the reaction mixture. The resultant reaction mixture was heated at 110 °C for 24

h. At ambient temperature, the reaction mixture was quenched with distilled H₂O (10.0 mL) and the crude mixture was extracted with EtOAc (15 mL x 3). The combined organic extract was dried over Na₂SO₄ and the volatiles were evaporated *in vacuo*. The crude product was purified by column chromatography on silica gel (petroleum ether/EtOAc: 1/2) to yield **3aa**, or **3aa**-[D₂], or **3aa** in 57%, 47% and 49%, respectively

4.4.6.4 Synthesis and Characterization of Intermediates

Procedure for synthesis of N-(1-methyl-2-oxoindolin-3-ylidene)benzamide (9): To an oven-dried Schlenk flask, 1-methylindoline-2,3-dione (1.00 g, 6.20 mmol) and benzamide (0.90 g, 7.43 mmol) were added and dissolved in dichloromethane (15 mL). The Ti(OⁱPr)₄ (1.76 g, 6.19 mmol) was added to the stirring solution at room temperature. The resultant mixture was stirred at room temperature for 12 h. The volatiles were evaporated under reduced pressure and the crude product was purified by column chromatography on silica gel (petroleum ether/EtOAc: 5/1) to yield **9** (0.86 g, 52%) as an orange solid. ¹H-NMR (400 MHz, CDCl₃): δ = 7.76 (d, *J* = 7.3 Hz, 2H, Ar-H), 7.53-7.46 (m, 2H, Ar-H), 7.38 (t, *J* = 7.7 Hz, 2H, Ar-H), 7.08 (t, *J* = 7.5 Hz, 1H, Ar-H), 6.98 (s, 1H, Ar-H), 6.89 (d, *J* = 7.7 Hz, 1H, Ar-H), 3.30 (s, 3H, CH₃). ¹³C{¹H}-NMR (100 MHz, CDCl₃): δ = 172.8 (CO), 165.7 (CO), 144.6 (C_q), 133.3 (C_q), 132.1 (CH), 130.9 (CH), 128.6 (2C, CH), 127.4 (2C, CH), 126.0 (C_q), 124.9 (CH), 123.2 (CH), 108.7 (CH), 85.3 (C_q), 26.7 (CH₃). HRMS (ESI): *m/z* Calcd for C₁₆H₁₂N₂O₂ + H⁺ [M + H]⁺ 265.0972; Found 265.0971.

Procedure for synthesis of N-(3-hydroxy-1-methyl-2-oxoindolin-3-yl)benzamide (11): To an oven-dried screw-cap tube equipped with a magnetic stir bar was added 1-methylindoline-2,3-dione (**1a**; 0.032 g, 0.20 mmol), *N*-methoxybenzamide (**2a**; 0.076 g, 0.503 mmol), FeCl₃ (0.0032 g, 0.02 mmol, 10.0 mol%) and LiO^tBu (0.032 g, 0.40 mmol) inside the glove box. To the above reaction mixture in the tube was added toluene (1.0 mL). The resultant reaction mixture in the tube was immersed in a preheated oil bath at 110 °C and stirred for 8 h. At ambient temperature, the reaction mixture was quenched with distilled H₂O (10.0 mL) and the crude product was extracted with EtOAc (15 mL x 3). The combined organic extract was dried over Na₂SO₄ and the volatiles were evaporated *in vacuo*. The remaining residue was purified by column chromatography on silica gel to yield intermediate **11** (0.027 g, 48%) and **3aa** (0.035 g, 44%) as a white solid and light brown solid respectively. ¹H-NMR (400 MHz, DMSO-*d*₆): δ = 9.25 (br s, 1H, *NH*), 7.76 (d, *J* = 7.1 Hz, 2H, Ar-H), 7.63-7.59 (m, 1H, Ar-H),

7.55-7.52 (m, 2H, Ar-H), 7.15-7.11 (m, 1H, Ar-H), 6.92 (d, $J = 6.6$ Hz, 1H, Ar-H), 6.88-6.84 (m, 1H, Ar-H), 6.80 (d, $J = 7.7$ Hz, 1H, Ar-H), 3.25 (s, 3H, CH₃). ¹³C{¹H}-NMR (125 MHz, DMSO-*d*₆): $\delta = 173.1$ (CO), 164.9 (CO), 143.6 (C_q), 132.4 (C_q), 132.3 (CH), 129.9 (CH), 128.9 (2C, CH), 126.9 (2C, CH), 123.9 (C_q), 122.5 (CH), 121.4 (CH), 108.5 (CH), 61.7 (C_q), 26.3 (CH₃). HRMS (ESI): m/z Calcd for C₁₆H₁₄N₂O₃ + Na⁺ [M - 2H]⁺ 303.0740; Found 303.0755.

Procedure for synthesis of *N,N'*-(1,1'-dimethyl-2,2'-dioxo-[3,3'-biindoline]-3,3'-diyl)dibenzamide (12): To an oven-dried screw-cap tube equipped with a magnetic stir bar was added *N*-(1-methyl-2-oxoindolin-3-ylidene)benzamide (**1a**; 0.080 g, 0.302 mmol), benzamide (0.037 g, 0.305 mmol), FeCl₃ (0.0049 g, 0.03 mmol, 10.0 mol%), LiO^tBu (0.049 g, 0.612 mmol) and MeOH (12 μ L, 0.312 mmol) [or HCHO (0.010 g, 0.333 mmol)] inside the glove box. Toluene (1.5 mL) was added to the above reaction mixture. The resultant reaction mixture was stirred at 110 °C for 24 h. At ambient temperature, the reaction mixture was quenched with distilled H₂O (10.0 mL) and the crude product was extracted with EtOAc (15 mL x 3). The combined organic extract was dried over Na₂SO₄ and the volatiles were evaporated *in vacuo*. The ¹H NMR analysis of crude mixture indicated the absence of expected compound **3aa**. The crude mixture was purified by column chromatography on silica gel to yield brown coloured compound **12** (0.030 g, 37%) or (0.027 g, 34%), respectively. ¹H-NMR (400 MHz, CDCl₃): $\delta = 9.33$ (br s, 2H, NH), 7.90 (d, $J = 7.7$ Hz, 4H, Ar-H), 7.52-7.49 (m, 2H, Ar-H), 7.44-7.40 (m, 4H, Ar-H), 7.10 (d, $J = 7.6$ Hz, 2H, Ar-H), 7.01 (d, $J = 7.3$ Hz, 2H, Ar-H), 6.84 (t, $J = 7.6$ Hz, 2H, Ar-H), 6.58 (d, $J = 7.8$ Hz, 2H, Ar-H), 3.34 (s, 6H, CH₃). ¹³C{¹H}-NMR (125 MHz, CDCl₃): $\delta = 174.1$ (2C, CO), 166.2 (2C, CO), 143.9 (2C, C_q), 132.6 (2C, C_q), 132.3 (2C, CH), 130.3 (2C, CH), 128.8 (4C, CH), 127.6 (4C, CH), 124.3 (2C, C_q), 122.8 (2C, CH), 122.1 (2C, CH), 108.4 (2C, CH), 62.4 (2C, C_q), 26.6 (2C, CH₃). HRMS (ESI): m/z Calcd for C₃₂H₂₆N₄O₄ + H⁺ [M + H]⁺ 531.2027; Found 531.1971. The molecular structure of **12** was further confirmed by X-ray structural analysis.

4.4.6.5 Procedure for Synthesis of 3aa from the Intermediates 9 and 10

To an oven-dried screw-cap tube equipped with a magnetic stir bar was introduced *N*-(1-methyl-2-oxoindolin-3-ylidene)benzamide (**9**; 0.053 g, 0.20 mmol), *N*-(hydroxymethyl)benzamide (**10**; 0.031 g, 0.205 mmol), FeCl₃ (0.0032 g, 0.02 mmol, 10.0 mol%), LiO^tBu (0.032 g, 0.40 mmol). Toluene (1.0 mL) was added to the reaction mixture. The resultant reaction mixture was stirred at 110 °C for 24 h. At ambient temperature, the reaction mixture was quenched with distilled H₂O (10.0 mL) and the crude mixture was

extracted with EtOAc (15 mL x 3). The combined organic extract was dried over Na₂SO₄ and the volatiles were evaporated *in vacuo*. The crude product was purified by column chromatography on silica gel (petroleum ether/EtOAc: 1/2) to afford **3aa** and **12** in (0.037 g) 46% and (0.009 g) 16% yield, respectively.

4.4.6.6 DFT Energy Calculations

All molecular structures were generated and optimized using Density Functional Theory (DFT) based methodology as implemented in the Gaussian 09 package.¹ All calculations were carried out explicitly in presence of ligand. The structures were optimized using B3LYP level of theory with a def2-SVP using def2-TZVP basis set for C, H, O, Cl and N atoms and LANL2DZ for Fe and Li. Additionally, Grimme's DFT empirical dispersion correction with the Becke-Jonson (D3BJ) damping function are also included. Optimized minima for geometries and transition states (TSs) were verified by performing harmonic vibrational analysis to confirm no and one imaginary frequency, respectively. Solvent effects were included in the calculations as implemented in PCM model for toluene. The energies reported in the free energy profile are ΔG values incorporated with zero-point energy corrections for the optimized minima at 298.15 K.

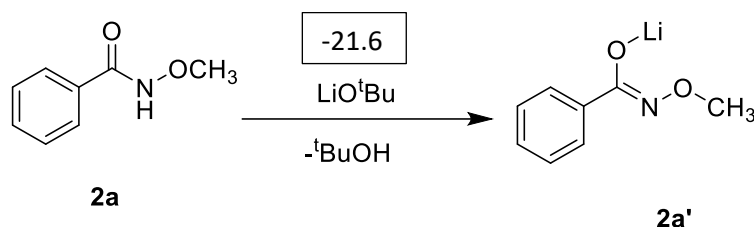


Figure 4.4. Free energy profile for formation enolate (**2a'**). The free energy values are given in kcal/mol.

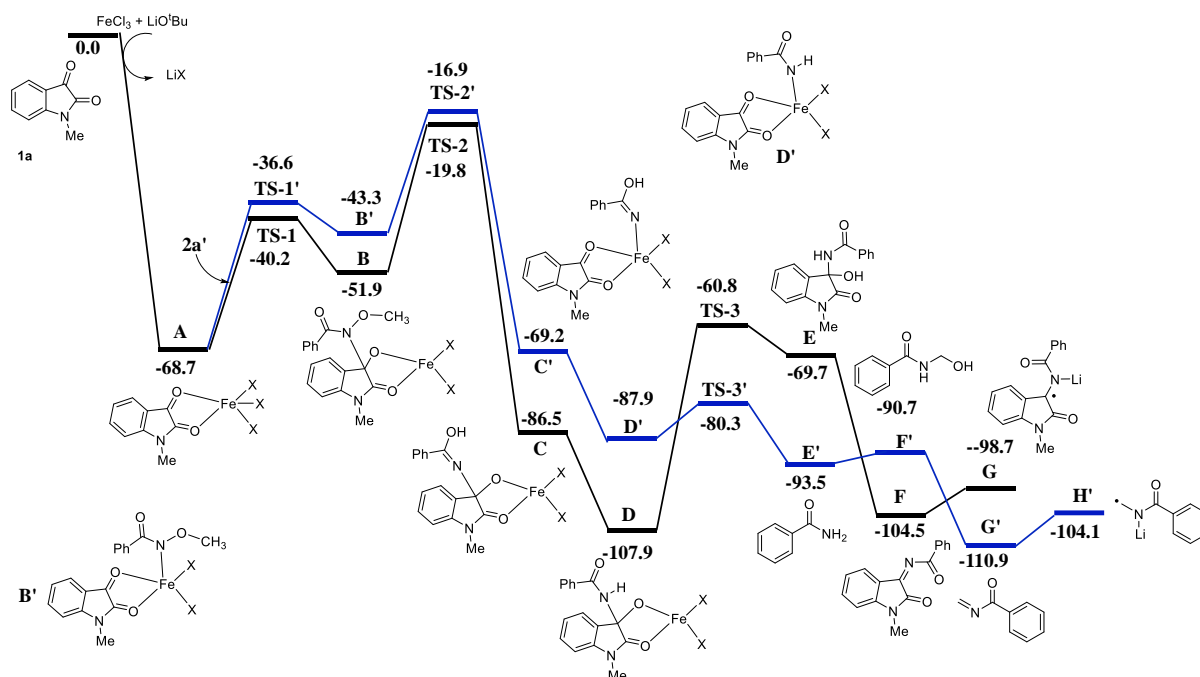


Figure 4.5. Free energy profile for the Fe-catalysed synthesis of 3,3-disubstituted 3-amino oxindole for X= O^tBu. The free energy values are given in kcal/mol.

4.4.7 X-ray Structure Analysis

X-ray intensity data measurements of compounds **3aa**, **3ma**, and **11** (Figures 4.6-4.8) was carried out on a Bruker D8 VENTURE Kappa Duo PHOTON II CPAD diffractometer equipped with Incoatech multilayer mirrors optics. The intensity measurements were carried out with Mo and Cu micro-focus sealed tube diffraction sources (MoK_α= 0.71073 Å, Cu K_α= 1.54178 Å). The X-ray generator was operated at 50 kV and 1.4 mA and 50 kV and 1.1 mA for Mo and Cu radiations, respectively. A preliminary set of cell constants and an orientation matrix were calculated from three matrix sets of 36 frames and 40 frames for Mo and Cu radiations, respectively. Data were collected with ω scan width of 0.5° at different settings of φ and 2θ with a frame time of 10-20 sec depending on the diffraction power of the crystals keeping the sample-to-detector distance fixed at 5.00 cm. The X-ray data collection was monitored by APEX3 program (Bruker, 2016).⁴² All the data were corrected for Lorentzian, polarization and absorption effects using SAINT and SADABS programs (Bruker, 2016). Using the APEX3 (Bruker) program suite, the structure was solved with the ShelXS-97 (Sheldrick, 2008)⁴³ structure solution program, using direct methods. The model was refined with a version of ShelXL-2018/3 (Sheldrick, 2015)⁴⁴ using Least Squares minimization. All the hydrogen atoms were placed in a geometrically idealized position and constrained to ride

on its parent atoms. An *ORTEP* III⁴⁵ view of the compounds was drawn with 50% probability displacement ellipsoids, and H atoms are shown as small spheres of arbitrary radii.

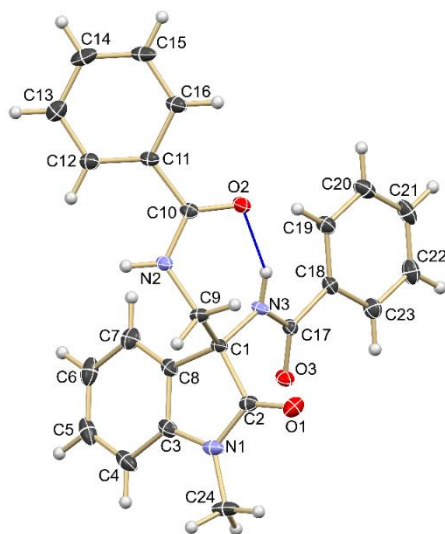


Figure 4.6. ORTEP of compound **3aa** showing the atom-numbering scheme. The displacement ellipsoids are drawn at the 30% probability level and H atoms are shown as small spheres with arbitrary radii.

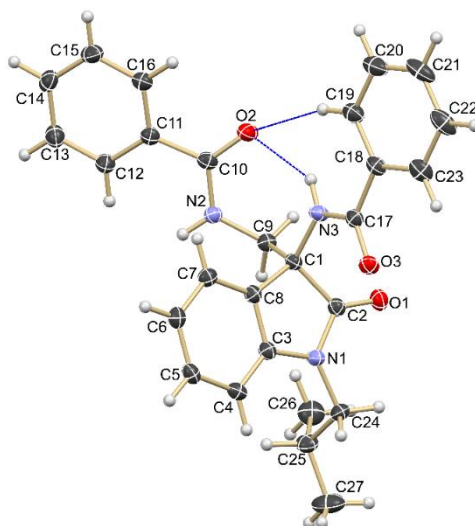


Figure 4.7. ORTEP of compound **3ma** showing the atom-numbering scheme. The displacement ellipsoids are drawn at the 30% probability level and H atoms are shown as small spheres with arbitrary radii.

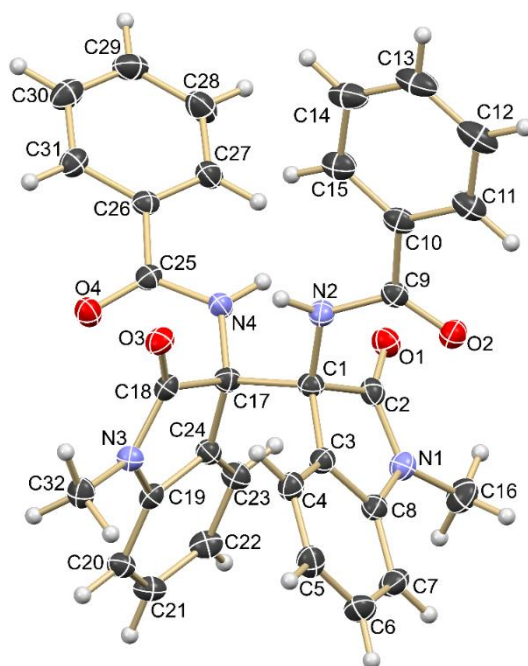
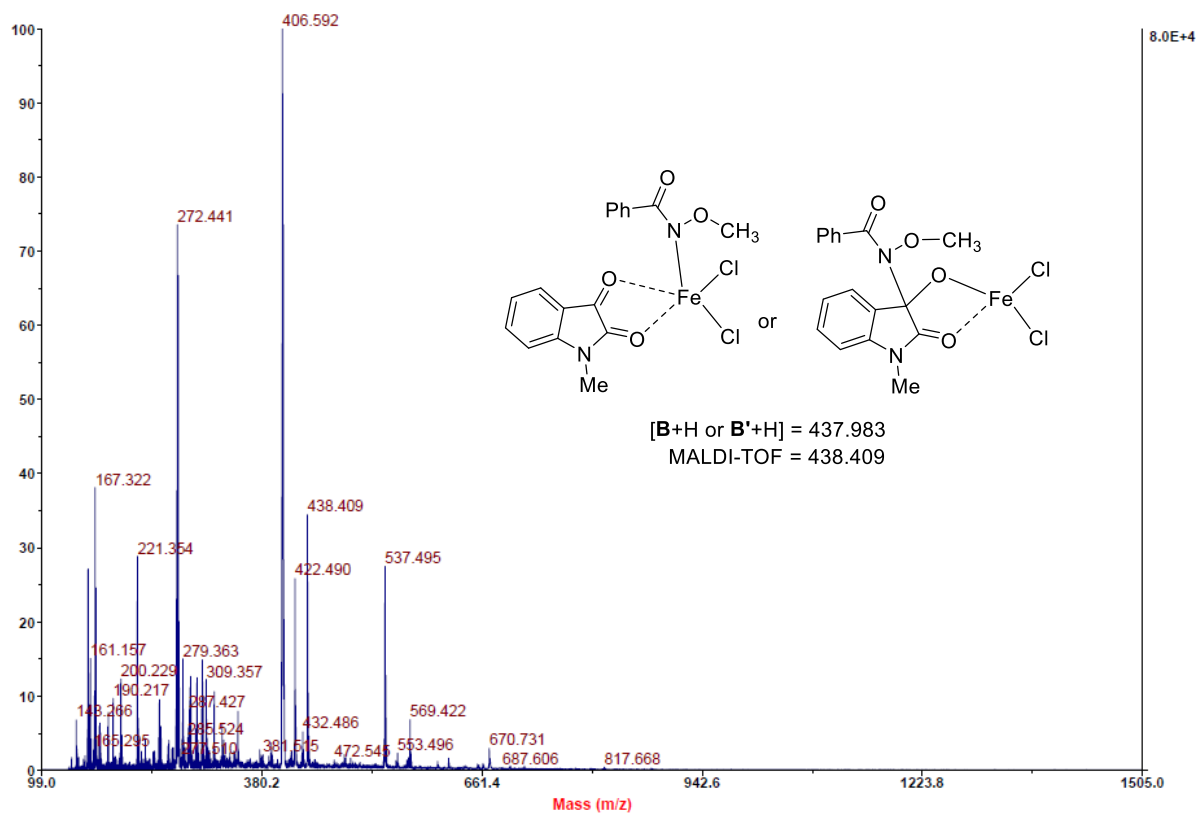
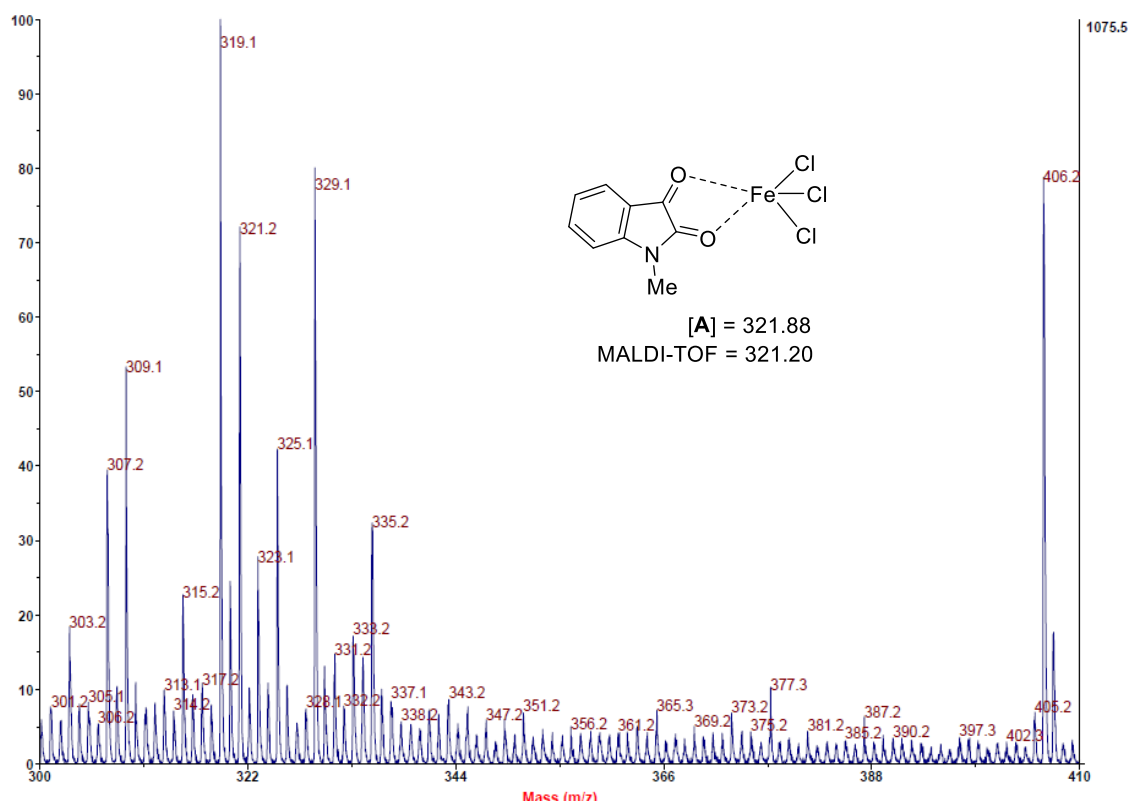
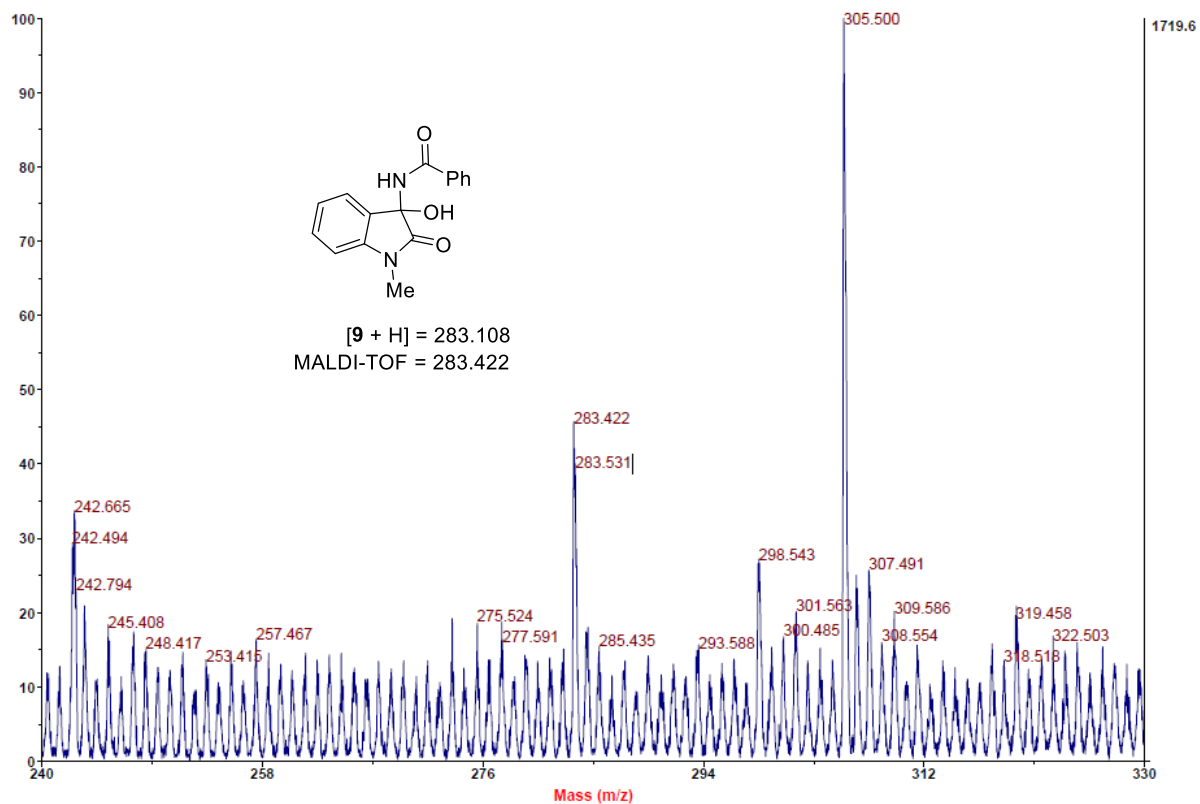
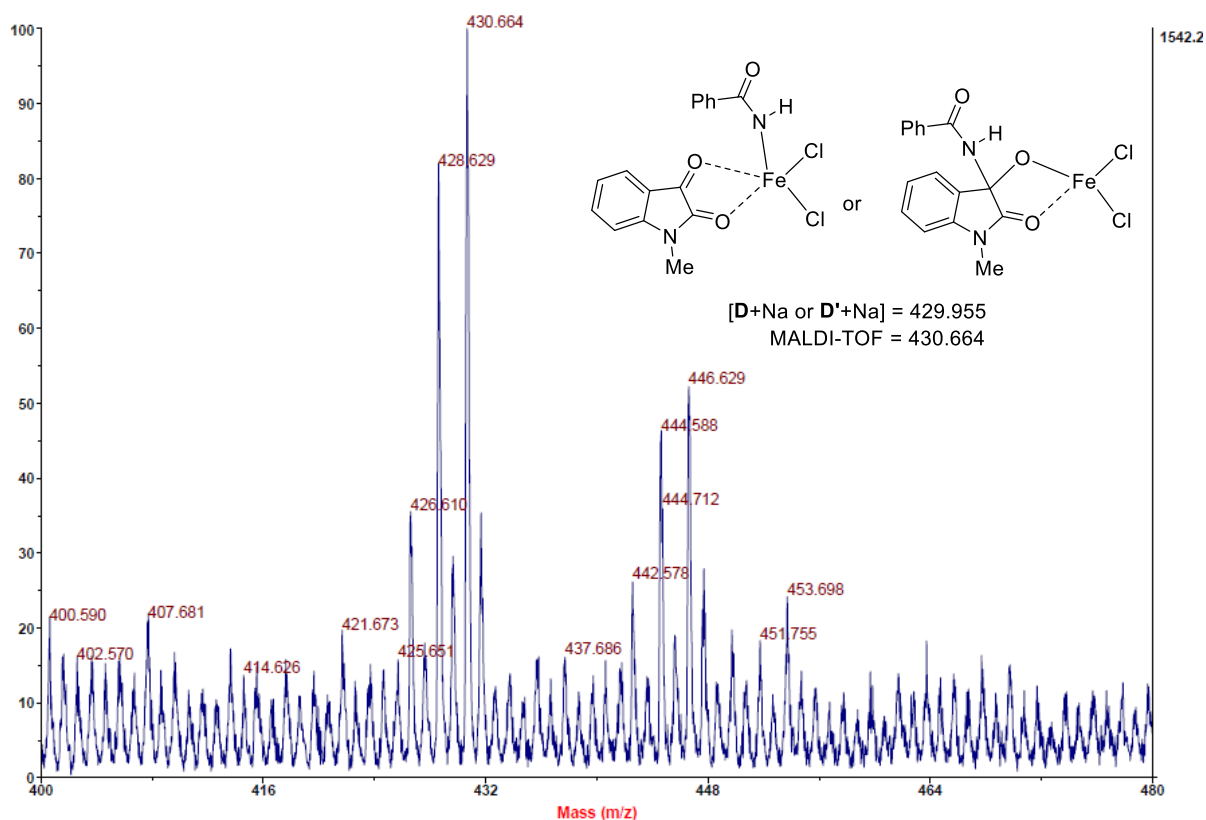
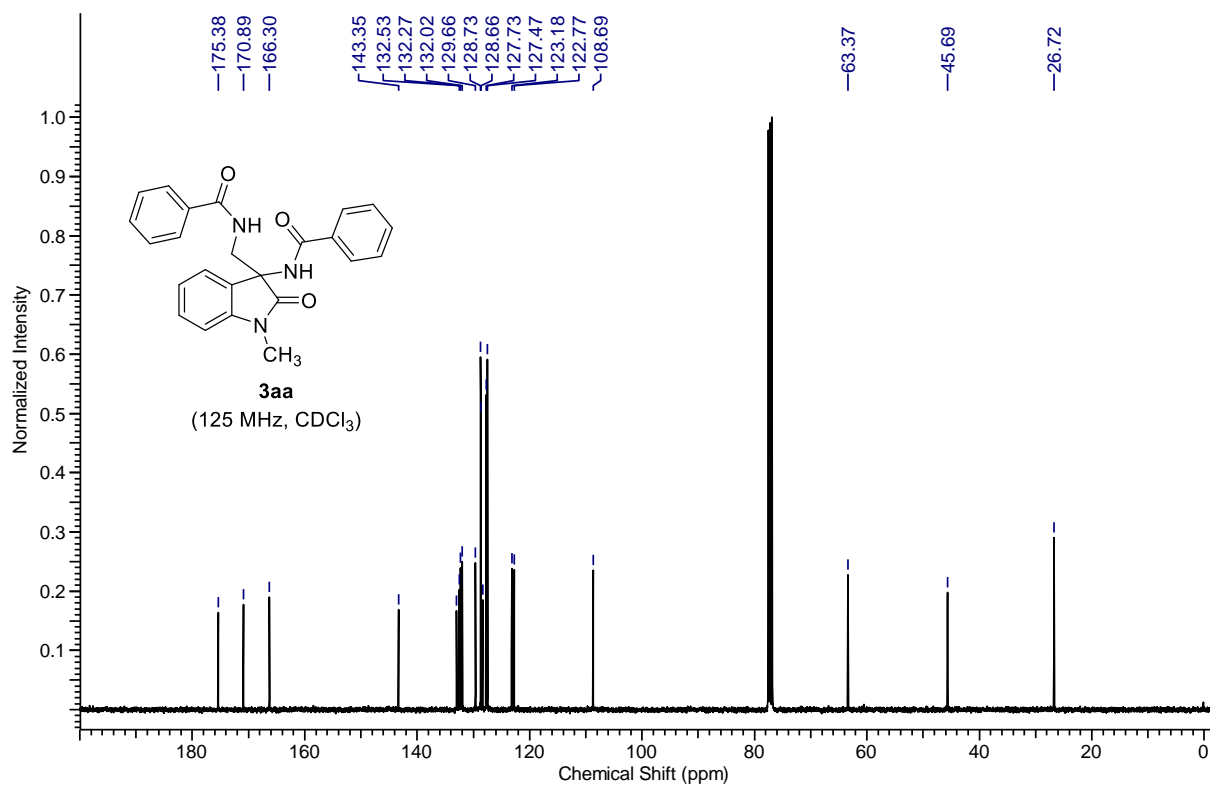
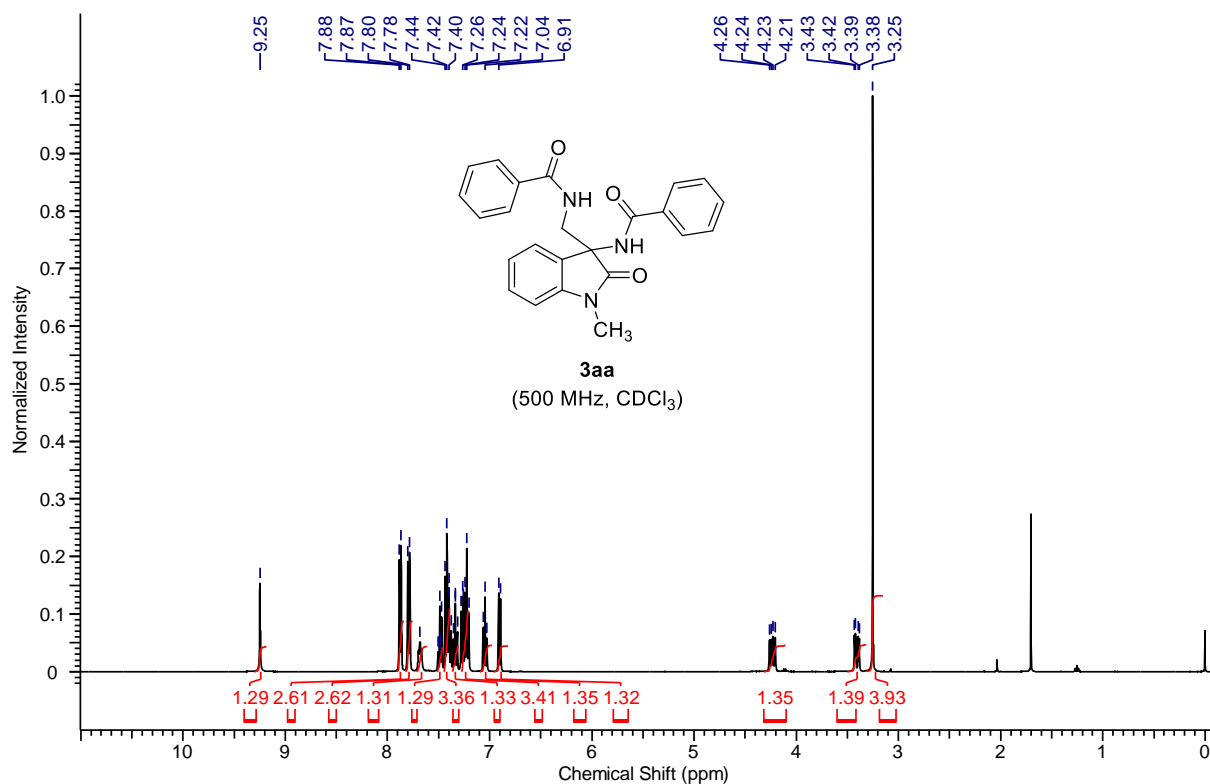


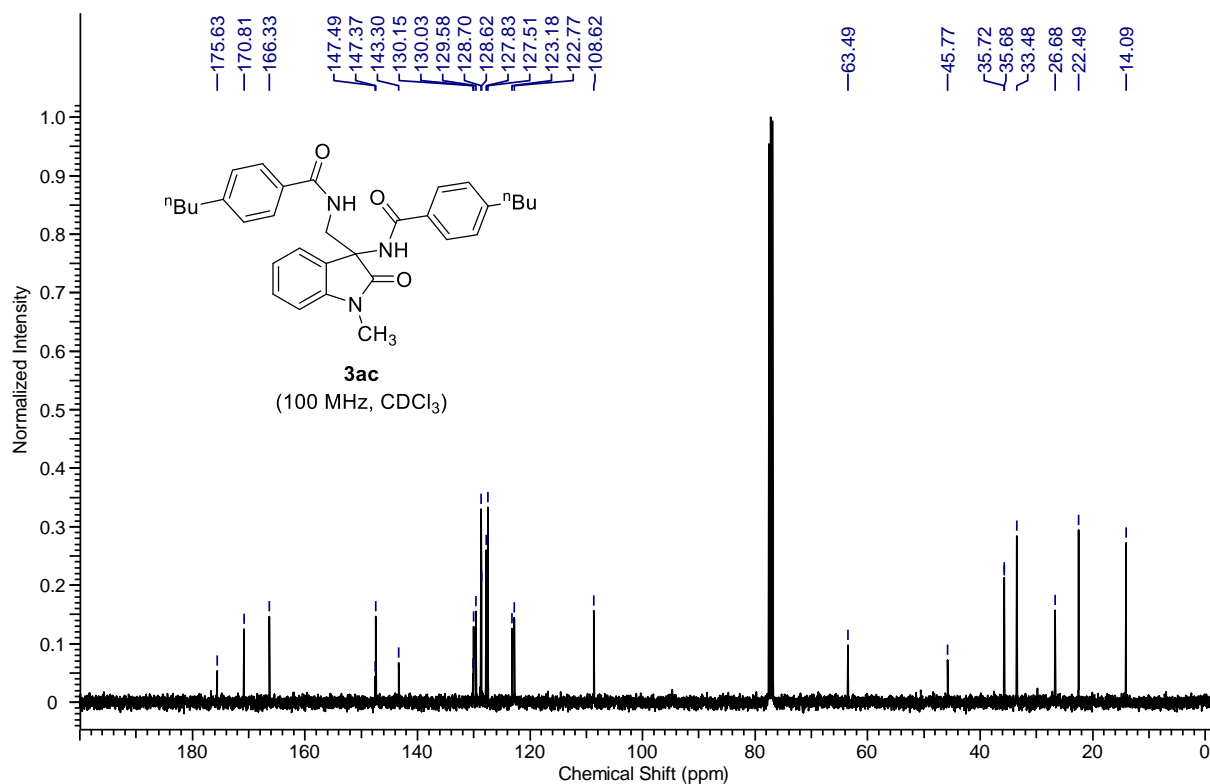
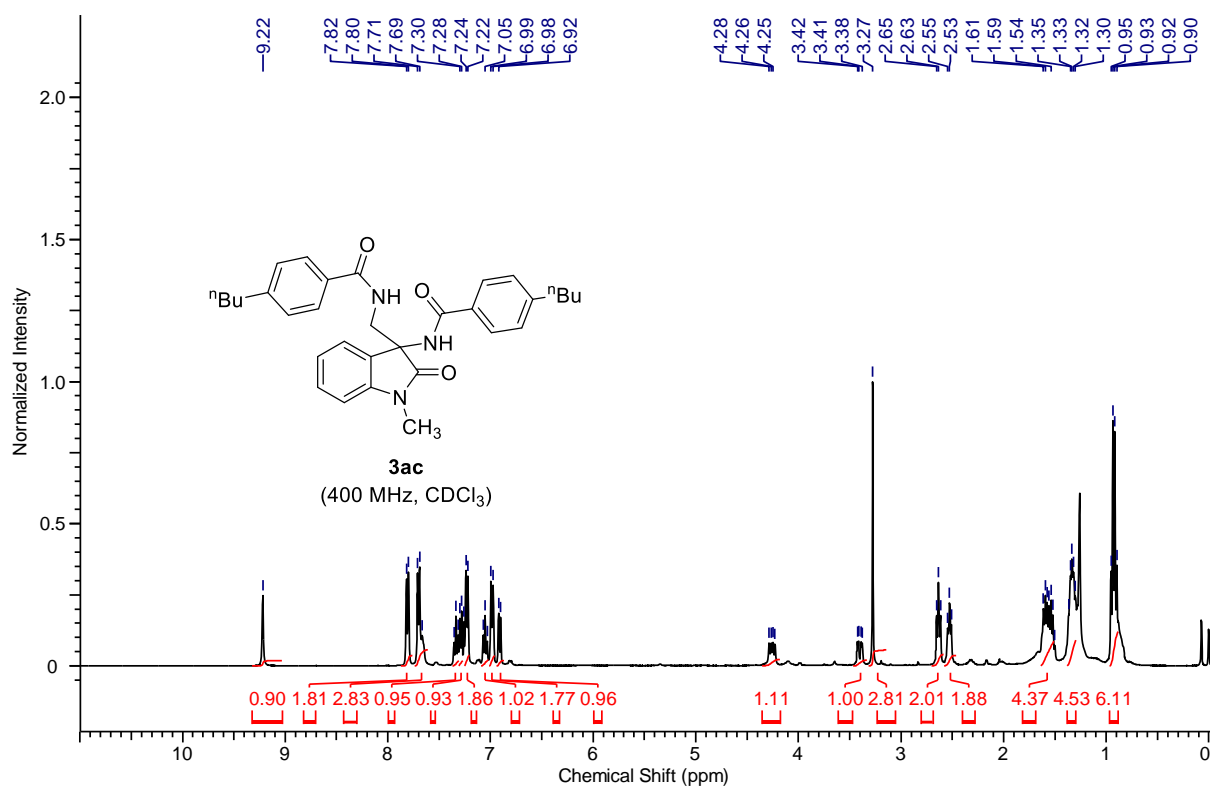
Figure 4.8. ORTEP of compound **11** showing the atom-numbering scheme. The displacement ellipsoids are drawn at the 30% probability level and H atoms are shown as small spheres with arbitrary radii.

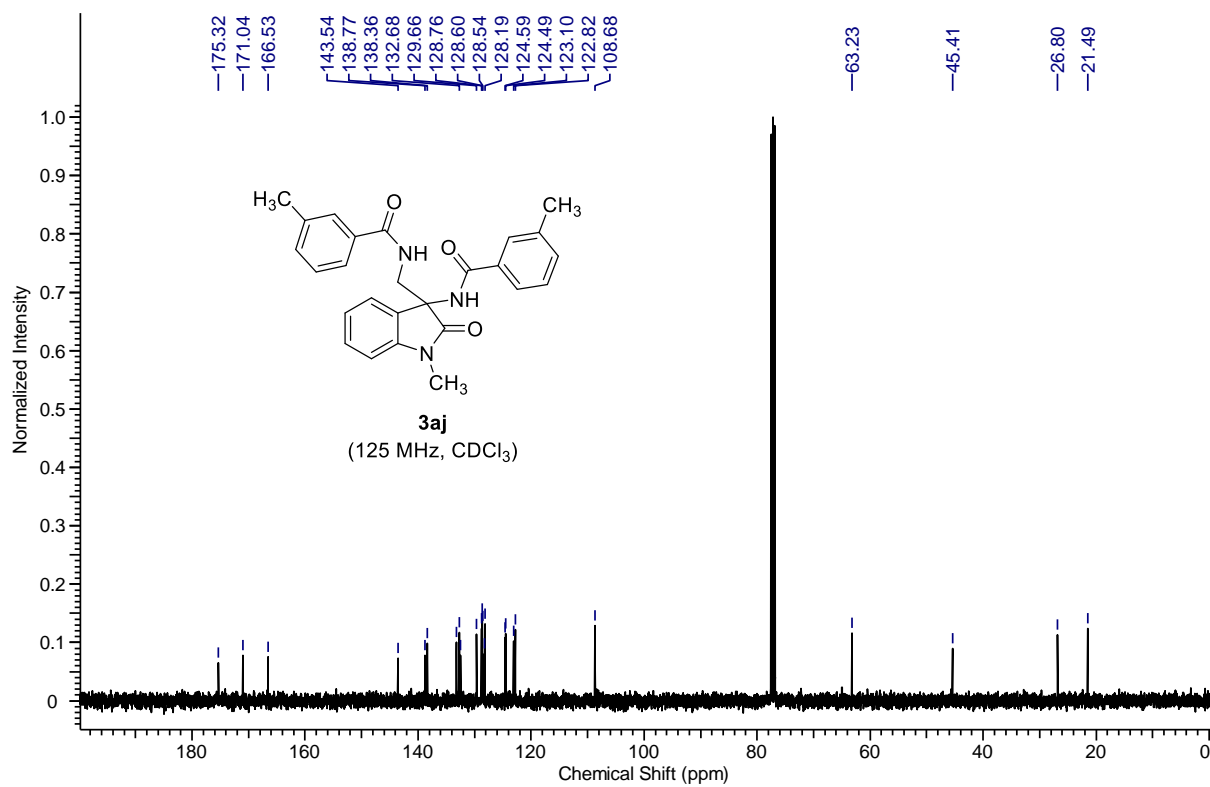
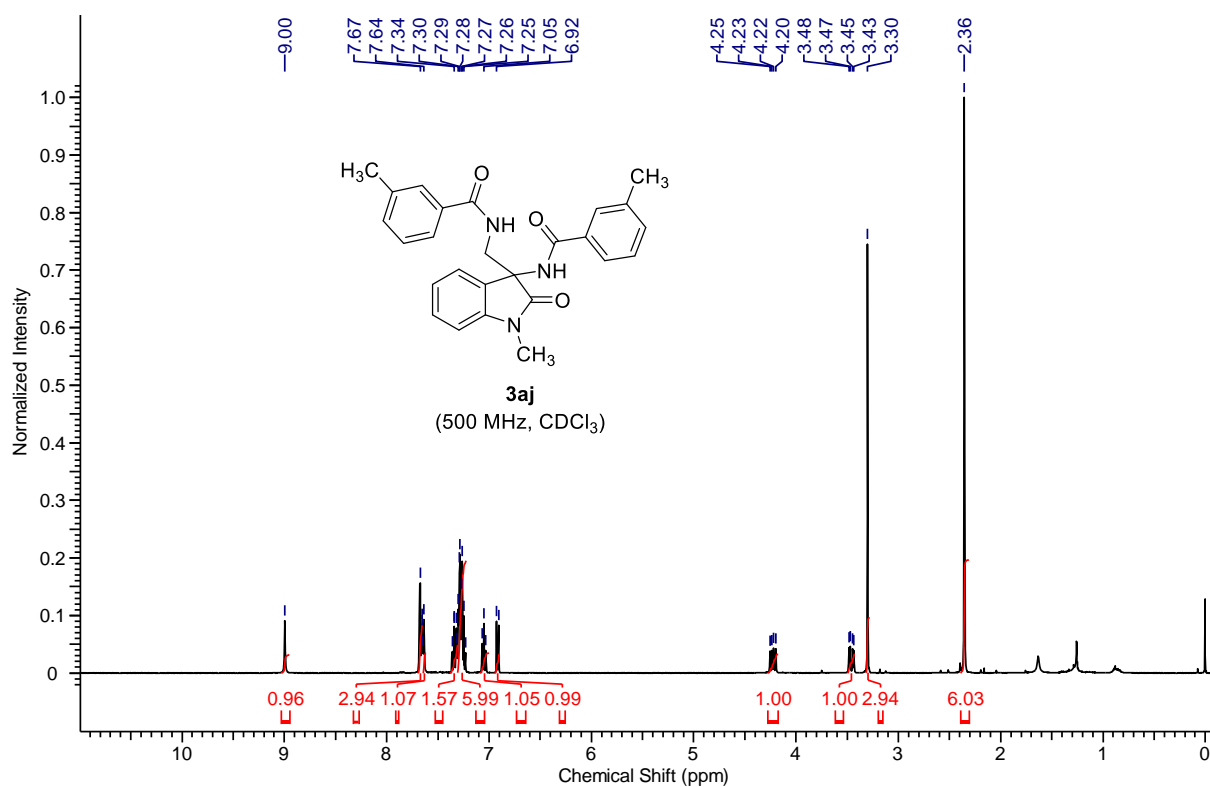
4.4.8 MALDI-TOF Spectra of Intermediates

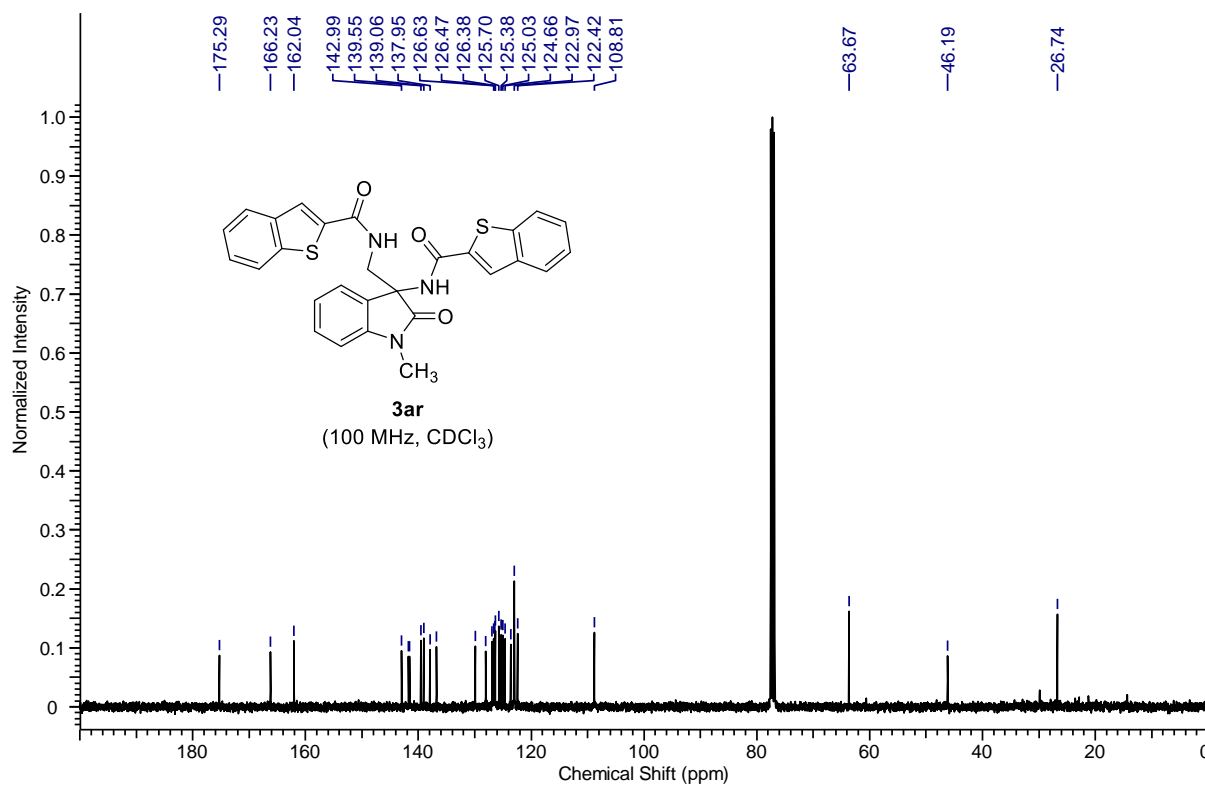
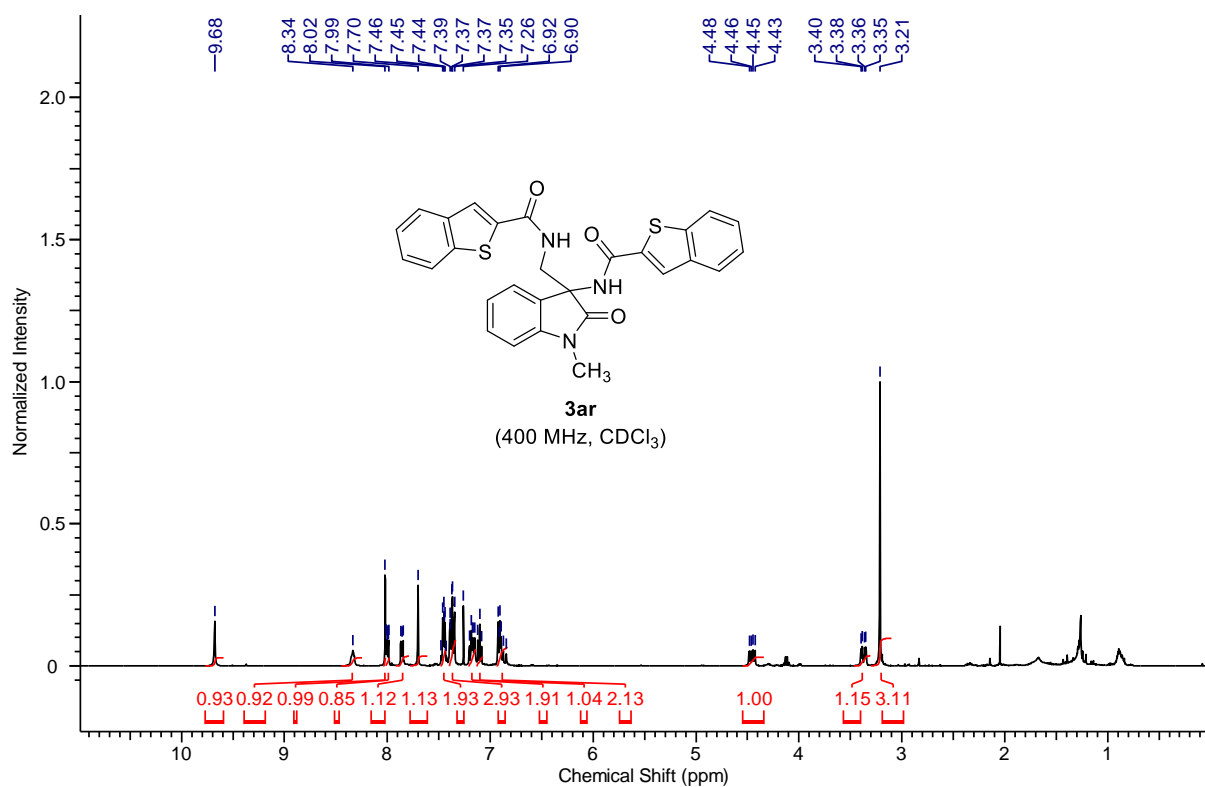


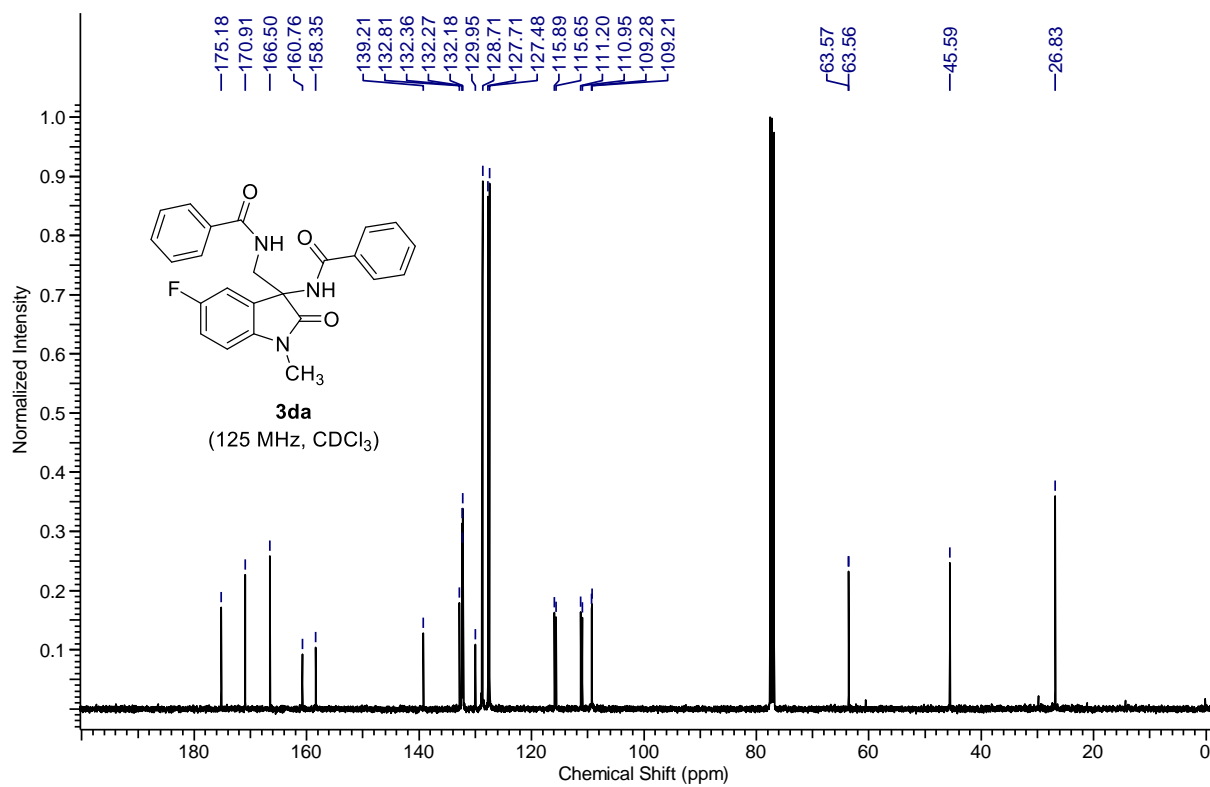
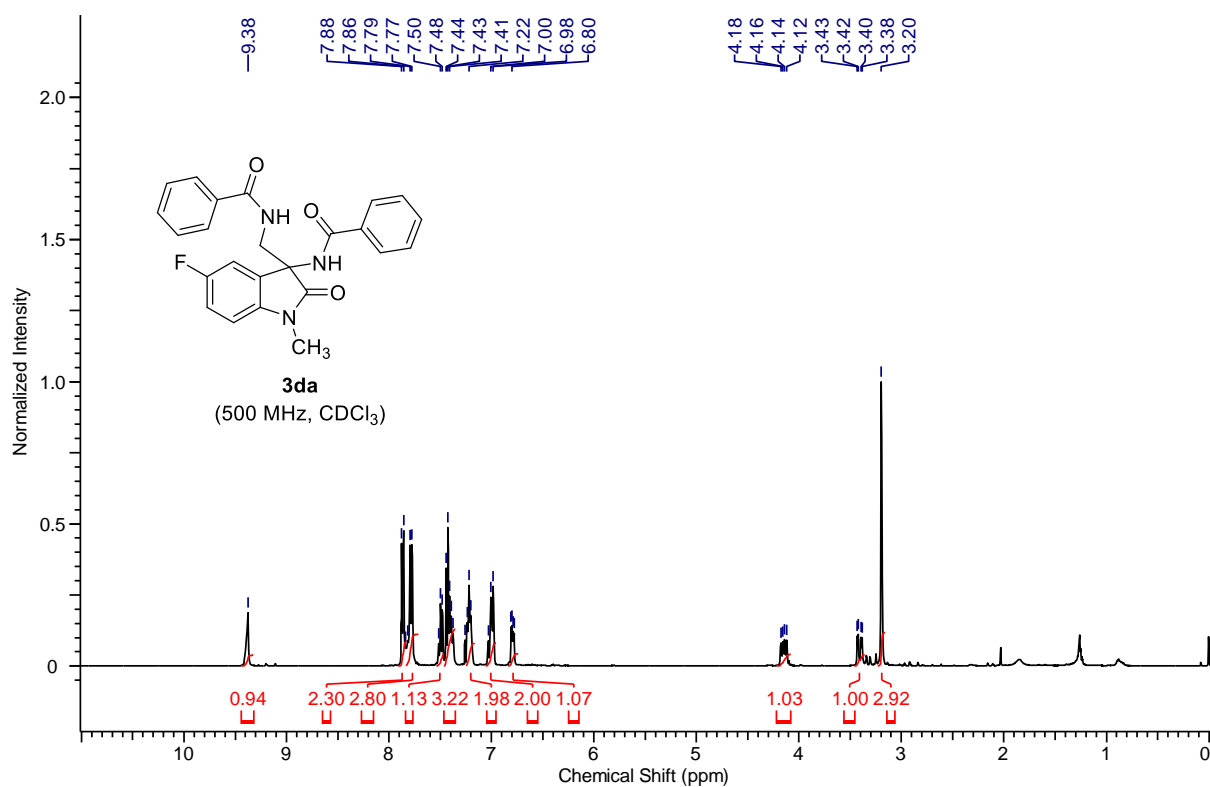


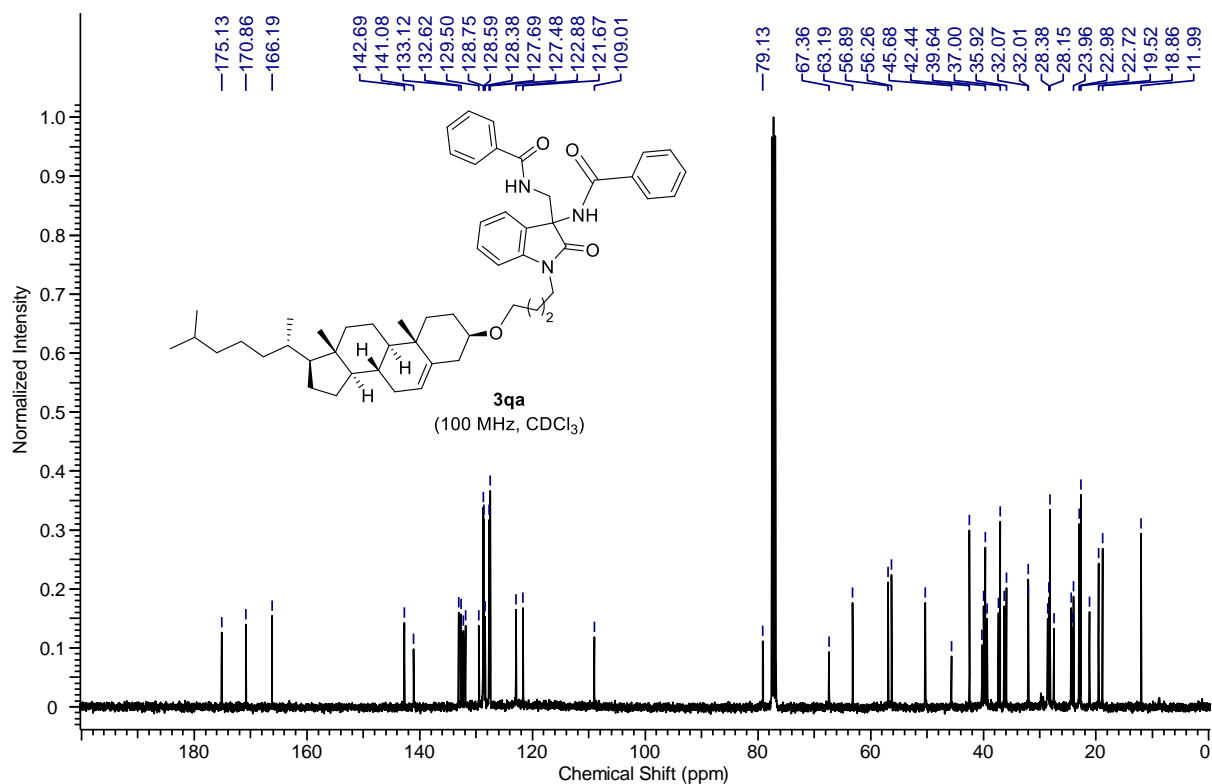
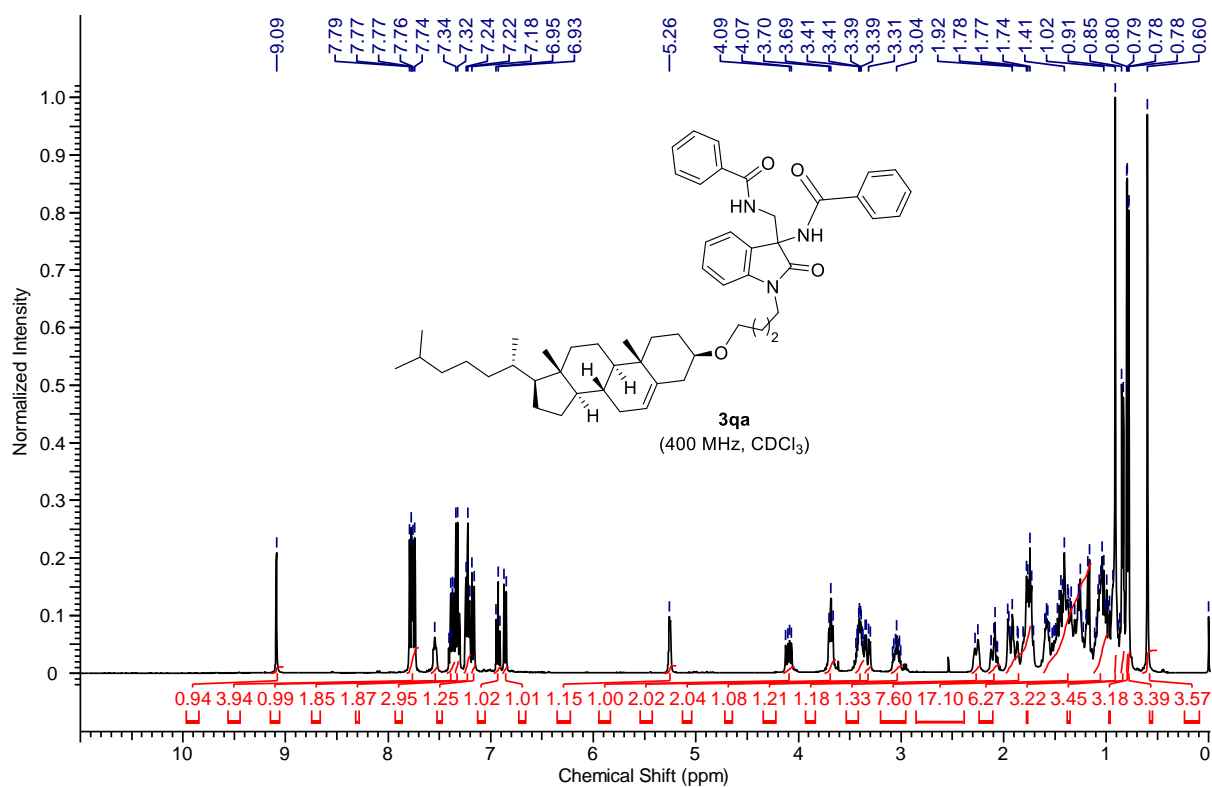
4.4.9 ^1H and ^{13}C NMR Spectra of Aminated Compounds

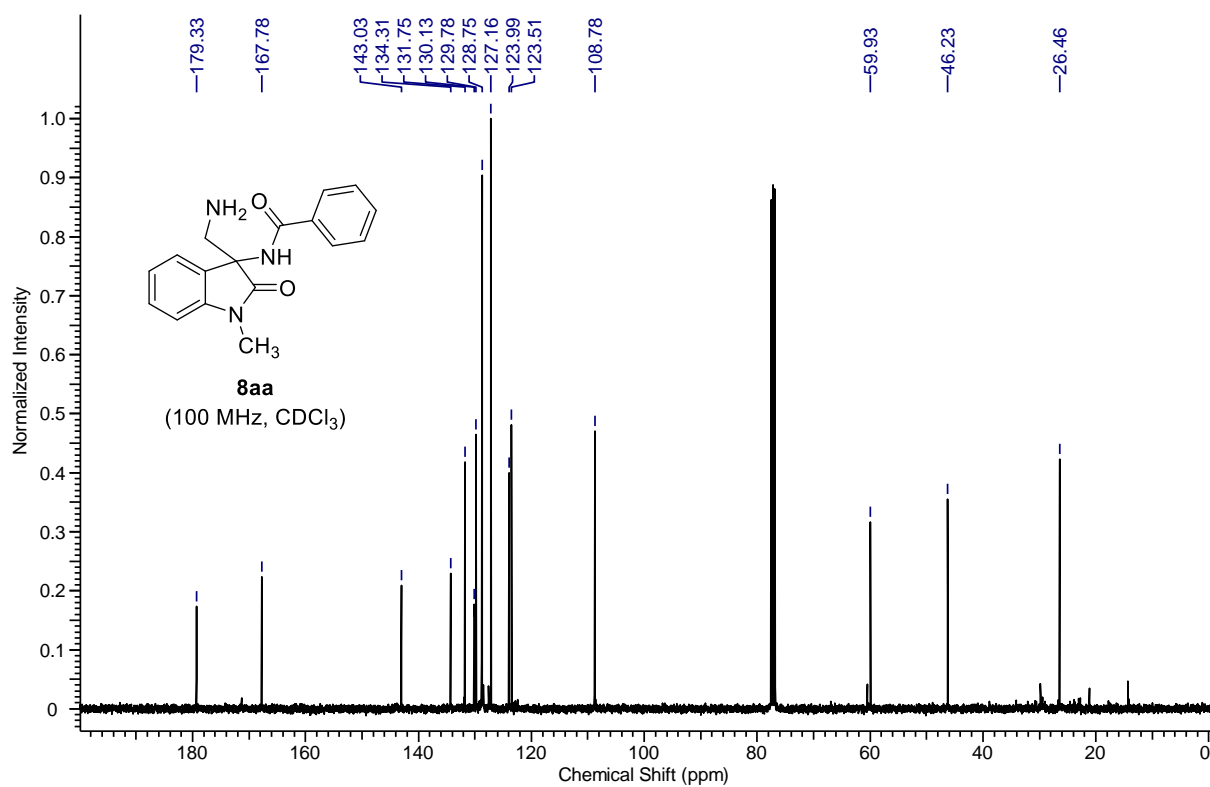
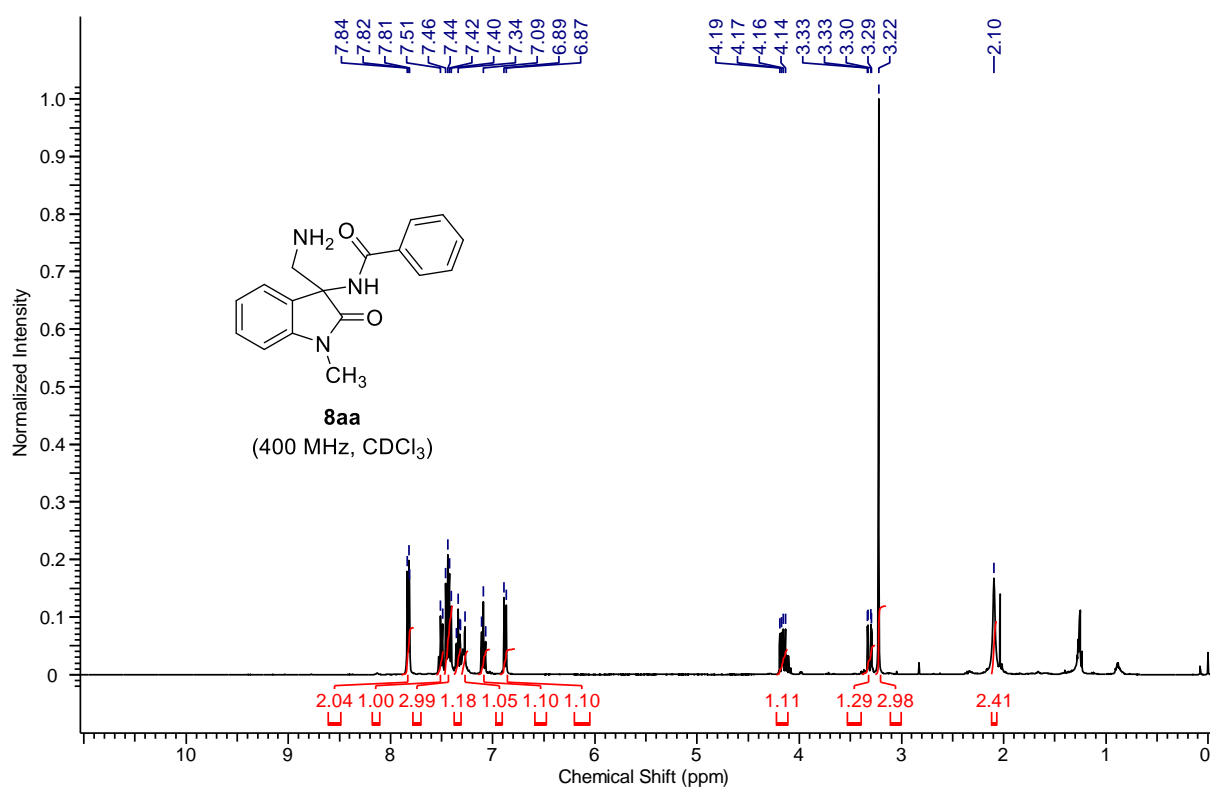












4.5 REFERENCES

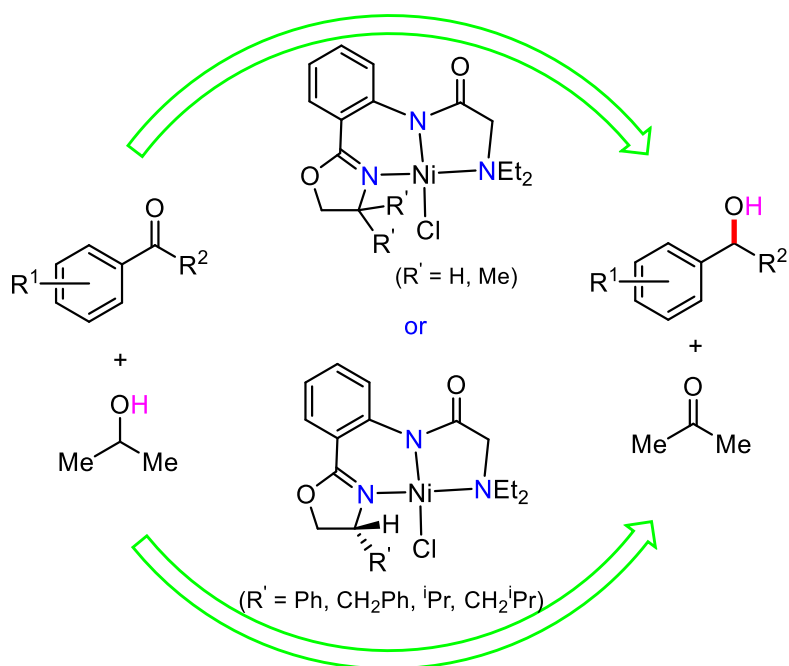
- (1) Galliford, C. V.; Prof Scheidt, K. A. *Angew. Chem. Int. Ed.* **2007**, *46*, 8748-8758.
- (2) Klein, J. E. M. N.; Taylor, R. J. K. *Eur. J. Org. Chem.* **2011**, *2011*, 6821-6841.
- (3) Liu, Y.-L.; Wang, B.-L.; Cao, J.-J.; Chen, L.; Zhang, Y.-X.; Wang, C.; Zhou, J. *J. Am. Chem. Soc.* **2010**, *132*, 15176-15178.
- (4) Paniagua-Vega, D.; Cerda-Garcia-Rojas, C. M.; Ponce-Noyola, T.; Ramos-Valdivia, A. C. *Nat. prod. commun.* **2012**, *7*, 1441-1444.
- (5) Kaur, J.; Chimni, S. S.; Mahajan, S.; Kumar, A. *RSC Adv.* **2015**, *5*, 52481-52496.
- (6) Aslam, N. A.; Babu, S. A.; Rani, S.; Mahajan, S.; Solanki, J.; Yasuda, M.; Baba, A. *Eur. J. Org. Chem.* **2015**, *2015*, 4168-4189.
- (7) Ochi, M.; Kawasaki, K.; Kataoka, H.; Uchio, Y.; Nishi, H. *Biochem. Biophys. Res. Commun.* **2001**, *283*, 1118-1123.
- (8) Rottmann, M.; McNamara, C.; Yeung, B. K. S.; Lee, M. C. S.; Zou, B.; Russell, B.; Seitz, P.; Plouffe, D. M.; Dharia, N. V.; Tan, J.; Cohen, S. B.; Spencer, K. R.; González-Pérez, G. E.; Lakshminarayana, S. B.; Goh, A.; Suwanarusk, R.; Jegla, T.; Schmitt, E. K.; Beck, H.-P.; Brun, R.; Nosten, F.; Renia, L.; Dartois, V.; Keller, T. H.; Fidock, D. A.; Winzeler, E. A.; Diagana, T. T. *Science* **2010**, *329*, 1175-1180.
- (9) Crosignani, S.; Jorand-Lebrun, C.; Page, P.; Campbell, G.; Colovray, V. r.; Missotten, M.; Humbert, Y.; Cleva, C.; Arrighi, J.-F. o.; Gaudet, M. n.; Johnson, Z.; Ferro, P.; Chollet, A. *ACS Med. Chem. Lett.* **2011**, *2*, 644-649.
- (10) Zhou, F.; Liu, Y.-L.; Zhou, J. *Adv. Synth. Catal.* **2010**, *352*, 1381-1407.
- (11) Shen, K.; Liu, X.; Lin, L.; Feng, X. *Chem. Sci.* **2012**, *3*, 327-334.
- (12) Dalpozzo, R.; Bartoli, G.; Bencivenni, G. *Chem. Soc. Rev.* **2012**, *41*, 7247-7290.
- (13) Kaur, J.; Chimni, S. S. *Org. Biomol. Chem.* **2018**, *16*, 3328-3347.
- (14) Kaur, J.; Kaur, B. P.; Chimni, S. S. *Org. Biomol. Chem.* **2020**, *18*, 4692-4708.
- (15) Wang, D.; Liang, J.; Feng, J.; Wang, K.; Sun, Q.; Zhao, L.; Li, D.; Yan, W.; Wang, R. *Adv. Synth. Catal.* **2012**, *355*, 548-558.
- (16) Zhao, J.; Fang, B.; Luo, W.; Hao, X.; Liu, X.; Lin, L.; Feng, X. *Angew. Chem. Int. Ed.* **2014**, *54*, 241-244.
- (17) Kumar, A.; Kaur, J.; Chimni, S. S.; Jassal, A. K. *RSC Adv.* **2014**, *4*, 24816-24819.

-
- (18) Holmquist, M.; Blay, G.; Pedro, J. R. *Chem. Commun.* **2014**, *50*, 9309-9312.
- (19) Lesma, G.; Meneghetti, F.; Sacchetti, A.; Stucchi, M.; Silvani, A. *Beilstein J. Org. Chem.* **2014**, *10*, 1383-1389.
- (20) Engl, O. D.; Fritz, S. P.; Wennemers, H. *Angew. Chem. Int. Ed.* **2015**, *54*, 8193-8197.
- (21) Fang, B.; Liu, X.; Zhao, J.; Tang, Y.; Lin, L.; Feng, X. *J. Org. Chem.* **2015**, *80*, 3332-3338.
- (22) He, Q.; Wu, L.; Kou, X.; Butt, N.; Yang, G.; Zhang, W. *Org. Lett.* **2016**, *18*, 288-291.
- (23) Menapara, T.; Choudhary, M. K.; Tak, R.; Kureshy, R. I.; Khan, N.-u. H.; Abdi, S. H. R. *J. Mole. Catal. A: Chemical* **2016**, *421*, 161-166.
- (24) Dai, J.; Xiong, D.; Yuan, T.; Liu, J.; Chen, T.; Shao, Z. *Angew. Chem. Int. Ed.* **2017**, *56*, 12697-12701.
- (25) Hajra, S.; Bhosale, S. S.; Hazra, A. *Org. Biomol. Chem.* **2017**, *15*, 9217-9225.
- (26) Cheng, C.; Lu, X.; Ge, L.; Chen, J.; Cao, W.; Wu, X.; Zhao, G. *Org. Chem. Front.* **2017**, *4*, 101-114.
- (27) Chen, Q.; Xie, L.; Li, Z.; Tang, Y.; Zhao, P.; Lin, L.; Feng, X.; Liu, X. *Chem. Commun.* **2018**, *54*, 678-681.
- (28) Sawa, M.; Miyazaki, S.; Yonesaki, R.; Morimoto, H.; Ohshima, T. *Org. Lett.* **2018**, *20*, 5393-5397.
- (29) Huang, Q.; Cheng, Y.; Yuan, H.; Chang, X.; Li, P.; Li, W. *Org. Chem. Front.* **2018**, *5*, 3226-3230.
- (30) Wang, J.-Y.; Li, M.-W.; Li, M.-F.; Hao, W.-J.; Li, G.; Tu, S.-J.; Jiang, B. *Org. Lett.* **2018**, *20*, 6616-6621.
- (31) Kang, T.; Cao, W.; Hou, L.; Tang, Q.; Zou, S.; Liu, X.; Feng, X. *Angew. Chem. Int. Ed.* **2019**, *58*, 2464-2468.
- (32) Arai, T.; Araseki, K.; Kakino, J. *Org. Lett.* **2019**, *21*, 8572-8576.
- (33) Hajra, S.; Laskar, S.; Jana, B. *Chem. Eur. J.* **2019**, *25*, 14688-14693.
- (34) Li, G.; Liu, M.; Zou, S.; Feng, X.; Lin, L. *Org. Lett.* **2020**, *22*, 8708-8713.
- (35) Yonesaki, R.; Kusagawa, I.; Morimoto, H.; Hayashi, T.; Ohshima, T. *Chem. Asian. J.* **2020**, *15*, 499-502.
- (36) Yang, W.; Dong, P.; Xu, J.; Yang, J.; Liu, X.; Feng, X. *Chem. Eur. J.* **2021**, *27*, 9272-9275.
- (37) Bui, T.; Borregan, M.; Barbas, C. F., III *J. Org. Chem.* **2009**, *74*, 8935-8938.
-

- (38) Qian, Z.-Q.; Zhou, F.; Du, T.-P.; Wang, B.-L.; Ding, M.; Zhao, X.-L.; Zhou, J. *Chem. Commun.* **2009**, 6753-6755.
- (39) Cheng, L.; Liu, L.; Wang, D.; Chen, Y.-J. *Org. Lett.* **2009**, *11*, 3874-3877.
- (40) Mouri, S.; Chen, Z.; Mitsunuma, H.; Furutachi, M.; Matsunaga, S.; Shibasaki, M. *J. Am. Chem. Soc.* **2010**, *132*, 1255-1257.
- (41) Lai, Y.-H.; Wu, R.-S.; Huang, J.; Huang, J.-Y.; Xu, D.-Z. *Org. Lett.* **2020**, *22*, 3825-3829.
- (42) Bruker, *APEX3, SAINT and SADABS*. Bruker AXS Inc., Madison, Wisconsin, USA. **2016**.
- (43) Sheldrick, G. M., *Acta Crystallogr.* **2008**, *A64*, 112-122.
- (44) Sheldrick, G. M., *Acta Crystallogr.* **2015**, *C71*, 3-8.
- (45) Farrugia, L. J., *J. Appl. Cryst.* **2012**, *45*, 849-854.

Chapter-5

Oxazoline Based Pincer Nickel Complexes: Implication towards Transfer Hydrogenation of Ketones



This chapter has been adapted from the publication “Achiral and chiral NNN-pincer nickel complexes with oxazolinyl backbones: application in transfer hydrogenation of ketones” Jagtap, R. A.; Ankade, S. B.; Gonnade, R. G.; and Punji, B. *New J. Chem.*, **2021**, *45*, 11927–11936.

5.1 INTRODUCTION

Tridentate pincer-ligated transition metal complexes are extensively used as catalysts in various organic transformations due to their high thermal stability and unique chemical reactivity.¹⁻⁴ In particular, several pincer complexes containing group 10 transition metals, like Pd and Pt, have largely been studied in the area of organometallic chemistry and catalysis.⁵⁻⁷ Contrastingly, the pincer nickel complexes have given recent attention in view of their economic viability, sustainability, and environmental benign.⁸⁻¹² The nickel complexes based on PCP,¹³⁻²⁰ POCOP,²¹⁻³⁴ NCN,³⁵⁻⁴¹ PCN,⁴²⁻⁴⁸ PNP,⁴⁹⁻⁵⁶ CNC,⁵⁷⁻⁵⁹ and CCC^{60,61} ligand systems are considerably developed and exploited in the catalytic traditional coupling reactions, hydrosilylation, hydroboration, C–H functionalization and many other reactions. Many of these nickel catalysts are associated with high activity and excellent scope for the desired transformations. In their interesting contribution, Sun and Khalimon independently demonstrated the synthesis of CNN- and POCN-ligated nickel complexes, respectively, for the transfer hydrogenation of ketones.^{62,63}

The phosphine-free, nitrogen-ligated NNN-pincer nickel complexes would be more economical and can be handled smoothly without any special inert atmosphere techniques. Moreover, the strong σ -donor nitrogen atoms on the ligand would make the nickel complex electron-rich. This can lead to the stabilization of nickel complexes in a high oxidation state and would facilitate oxidative addition, an important elementary step in the various catalytic reaction. Previously, a variety of NNN-nickel complexes were developed and used in diverse catalytic applications. Hu has developed *NNN*-nickamine and is extensively employed in traditional C–C couplings and C–H functionalization reactions (Figure 5.1).⁶⁴⁻⁷² Recently, our group demonstrated the synthesis and catalytic activity of many robust NNN pincer nickel complexes (Figure 5.1).⁷³⁻⁷⁷ All these NNN-ligated complexes were exceptional in the desired organic transformations. Therefore, further development on the NNN-Ni pincer system, particularly the chiral analog, is essential to understand their potential in chiral transformations. In that context, in this chapter we demonstrate the synthesis and characterization of a series of achiral and chiral oxazolinyl-based NNN-pincer nickel complexes. These complexes are utilized for the transfer hydrogenation of ketones to alcohols using isopropanol as a sacrificial hydrogen source.

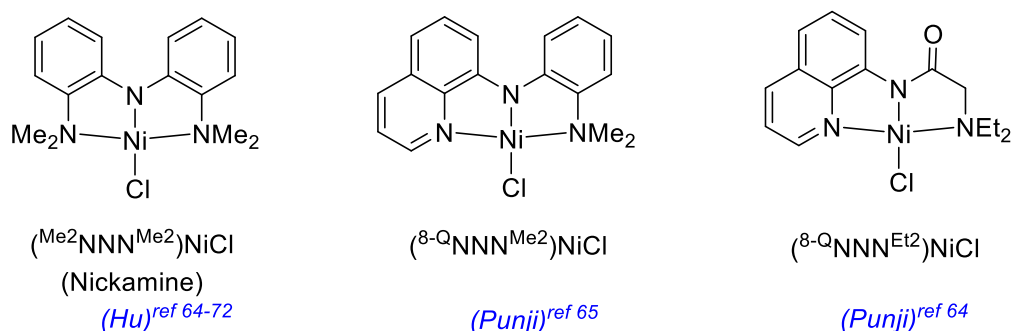
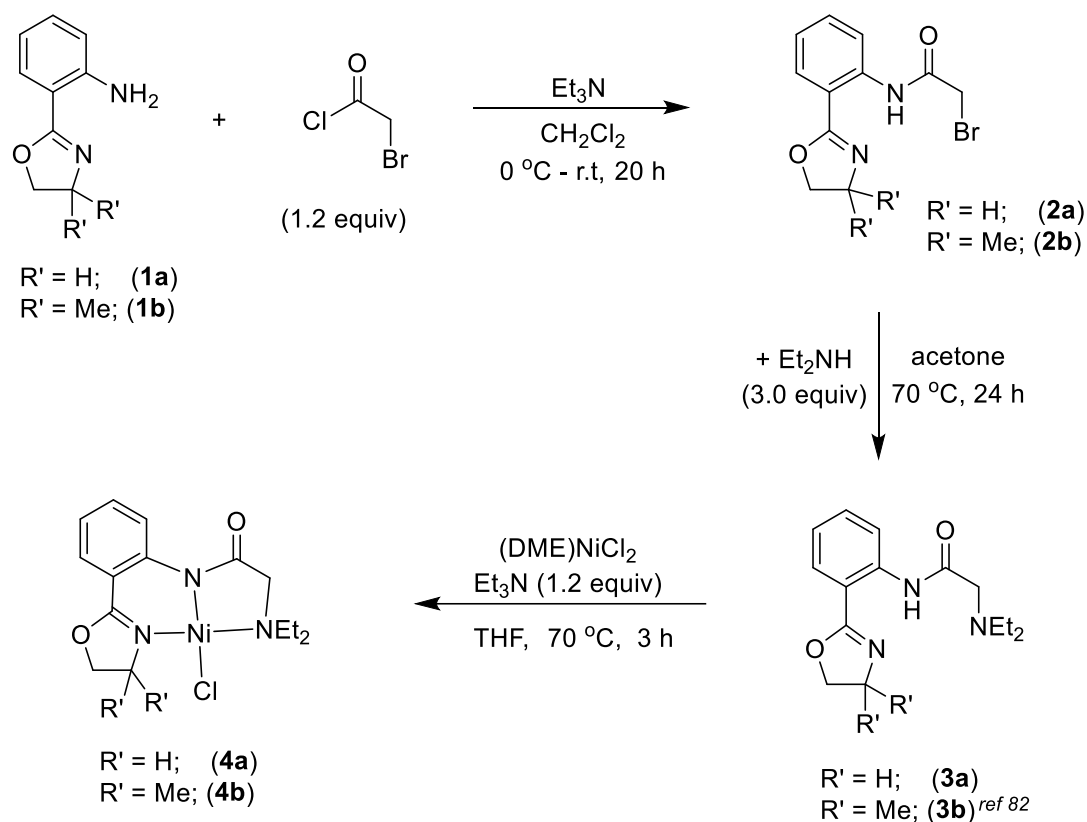


Figure 5.1. Representative amido-(NNN)Ni pincer systems.

5.2 RESULTS AND DISCUSSION

5.2.1 Synthesis and Characterization of ($\text{R}^1\text{-OxNNN}^{\text{Et}_2}$)–H Ligands and Nickel Complexes

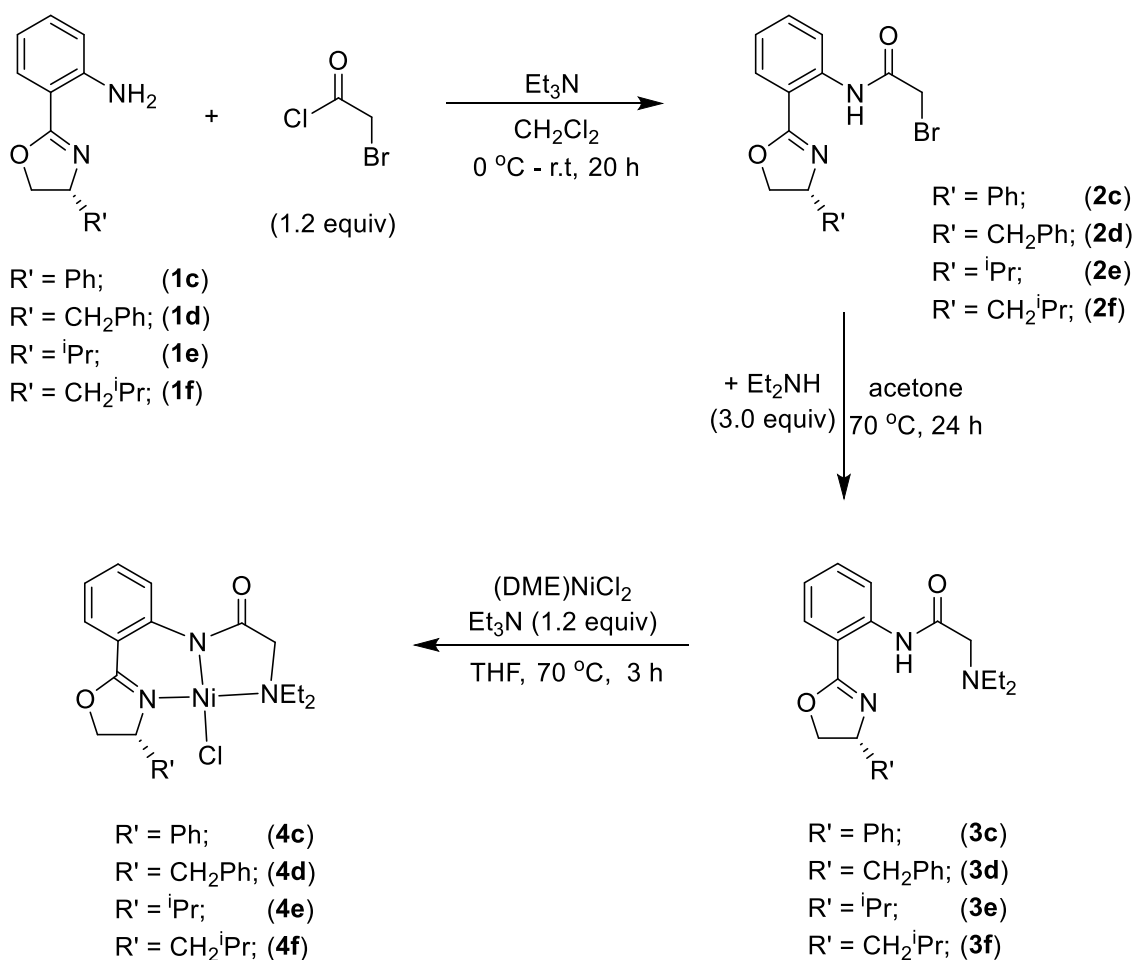
Recently our group synthesized 2-diethylamino-*N*-(quinolinyl)acetamide ligand, $\text{Et}_2\text{N-CH}_2\text{C(O)N(H)C}_9\text{H}_6\text{N}$, ($\text{Et}_2\text{NNN}^{8\text{Q}}\text{-H}$) by introducing 8-aminoquinoline into the pincer system. The developed (quinolinyl)amido pincer nickel complex containing this ligand, ($\text{Et}_2\text{NNN}^{8\text{Q}}\text{-Q}$)NiCl, was found as an efficient catalyst for the regioselective C–H bond alkylation, benzylation, and arylation of indoles.^{73,75,76} Similarly, the developed palladium complexes, ($\text{Et}_2\text{NNN}^{8\text{Q}}\text{-Q}$)PdX (X = Cl, OAc), were efficient and robust catalysts for the arylation of diverse azoles.⁷⁸ Encouraged by these developments, we were eager to develop a chiral catalyst of a similar system. To synthesize the oxazolinyll analog, initially, we prepared 2-amino-oxazolinyll compounds, **1a-1f**, using different achiral and chiral amino acid derivatives.⁷⁹⁻⁸¹ The treatment of (oxazolinyll)anilines, **1a** and **1b** with 2-bromoacetyl chloride in the presence of triethylamine afforded the bromo-(oxazolinyll)acetamides, **2a** and **2b**,⁸² respectively, in good yields (Scheme 5.1). Similarly, the chiral derivatives **2c-2f** were synthesized from the corresponding (oxazolinyll)anilines, **1c-1f**, in moderate to good yields (Scheme 5.2). Notably, the isopropyl and isobutyl derivatives, **2e** and **2f**, resulted in moderate yields, which could be accounted for partial decomposition. All the bromo-derivatives, **2a-2f**, were easily purified by column chromatography and thoroughly characterized by ^1H and ^{13}C NMR spectroscopy as well as by the HRMS analysis. Though the methylene ($-\text{OCH}_2-$) protons of oxazolinyll-moiety in **2a** shows a single set of the peak, the same protons in the compounds **2c-2f** displayed two sets of the peak due to the neighboring chiral center.



Scheme 5.1. Synthesis of achiral *NNN*-oxazolinyl ligands and nickel complexes.

The reaction of compounds **2a-2f** with an excess of diethylamine in acetone under reflux conditions afforded the corresponding ligands, $(\text{R}'\text{-OxNNN}^{\text{Et}_2})\text{-H}$ (**3a-3f**), in quantitative yields (Schemes 5.1 and 5.2). These ligands were purified by column chromatography and obtained either as a liquid or a solid. Systematic characterization by ^1H and ^{13}C NMR spectroscopy and by the HRMS analysis confirmed the ligands' molecular architecture. As expected, the methylene protons ($-\text{OCH}_2$) on oxazolinyl-moiety of **3c-3f**, close to the chiral center, displayed separate sets of signals.

The nickelation reaction of ligand $(\text{R}'\text{-OxNNN}^{\text{Et}_2})\text{-H}$ (**3a** and **3b**) with $(\text{DME})\text{NiCl}_2$ in the presence of triethylamine in THF under reflux condition gave $(\text{OxNNN}^{\text{Et}_2})\text{NiCl}$ (**4a**) and $(\text{Me}_2\text{-OxNNN}^{\text{Et}_2})\text{NiCl}$ (**4b**), respectively, in very good yields (Scheme 5.1). Both complexes were obtained as a dark purple crystalline solid.



Scheme 5.2. Synthesis of chiral *NNN*-oxazolinyl ligands and nickel complexes.

The ^1H NMR analysis of complexes **4a** and **4b** indicated the formation of an amido-nickel covalent bond, as the signal corresponding to $-\text{NH}$ proton on the ligand backbone was disappeared. Moreover, the methylene protons on the $-\text{NEt}_2$ group showed two sets of multiplet against a single set in corresponding ligands **3a** and **3b**. This finding highlighted the coordination of the $-\text{NEt}_2$ arm to the nickel center. Among two multiplets for the methylene protons, one appeared in the up-field region and the other in the down-field region compared to that observed in free-ligand. Notably, the ^1H NMR signals of the protons on oxazolinyl-moiety are observed in the down-field region compared to the free-ligand, which suggests the coordination of oxazolinyl-backbone to the nickel center. Both complexes **4a** and **4b** were further characterized by ^{13}C NMR and elemental analysis. The molecular structure of complex **4a** was elucidated by a single-crystal X-ray diffraction study (Figure 5.2).

The chiral pincer nickel complexes, $[(R)-(R'-O_xNNN^{Et_2})NiCl]$; $R' = Ph$ (**4c**); $R' = CH_2Ph$ (**4d**); $R' = ^iPr$ (**4e**); $R' = CH_2^iPr$ (**4f**), were synthesized in good to excellent yields by the reaction of $(R'-O_xNNN^{Et_2})-H$ (**3c-3f**) with $(DME)NiCl_2$ in the presence of triethylamine (Scheme 5.2). A careful analysis of 1H NMR signals of the complexes **4c-4f** suggested the coordination of $-NEt_2$ and oxazolinyl-arm to the nickel center in each complex. Moreover, the disappearance of the signal corresponding to the $-NH$ proton highlighted the covalent coordination of the central N -atom. The ^{13}C NMR and elemental analysis further validated the molecular architecture of these complexes. The molecular structures of complexes **4d** and **4f** were determined by the single-crystal X-ray diffraction study (Figure 5.3 and 5.4).

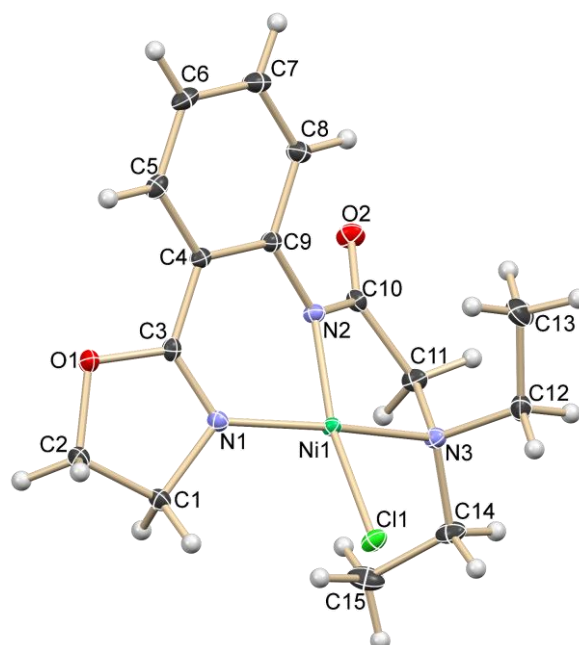


Figure 5.2. ORTEP of compound $(O_xNNN^{Et_2})NiCl$ (**4a**). Displacement ellipsoids are drawn at the 50% probability level.

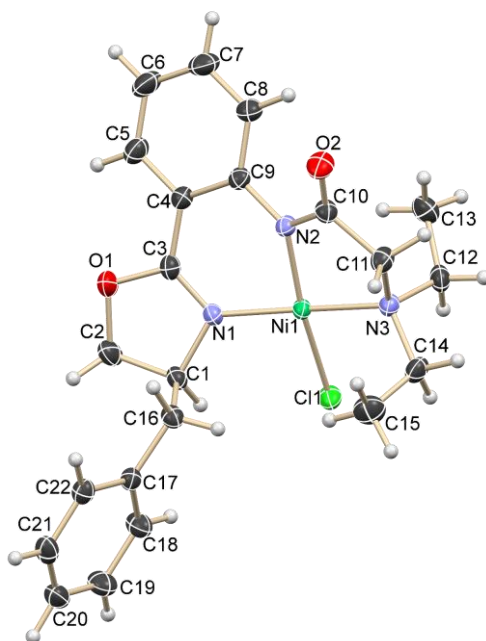


Figure 5.3. ORTEP of compound ($\text{PhCH}_2\text{-OxNNN}^{\text{Et}_2}$)NiCl (**4d**). Displacement ellipsoids are drawn at the 50% probability level.

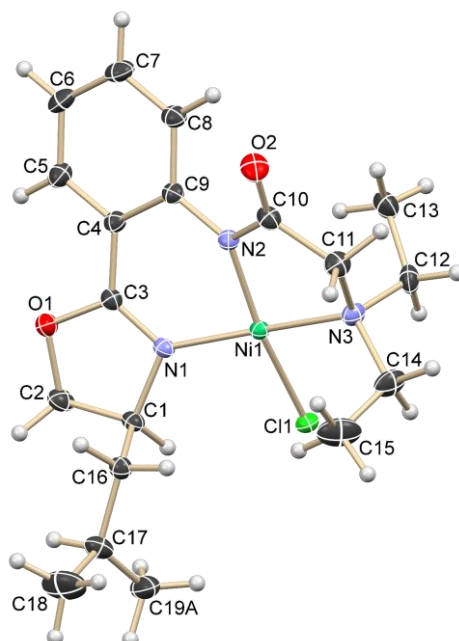


Figure 5.4. ORTEP of compound ($\text{iPrCH}_2\text{-OxNNN}^{\text{Et}_2}$)NiCl (**4f**). Displacement ellipsoids are drawn at the 50% probability level. One of the terminal C-atom (C19) of the isopropyl group showed thermal disorder over two positions. Only one position of the C19 atom (C19A) is shown for clarity.

Table 5.1 Selected bond length [Å] and angles [deg] for **4a**, **4d** and **4f**.

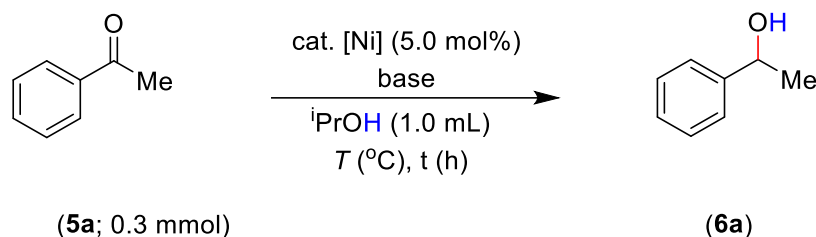
	4a	4d	4f
Ni(1)–N(1)	1.8780(10)	1.8904(12)	1.8887(12)
Ni(1)–N(2)	1.8806(10)	1.8826(12)	1.8860(12)
Ni(1)–N(3)	1.9514(10)	1.9611(12)	1.9569(13)
Ni(1)–Cl(1)	2.2025(4)	2.1896(4)	2.1952(4)
N(1)–Ni(1)–N(2)	91.05(4)	91.69(5)	92.04(5)
N(2)–Ni(1)–N(3)	85.93(4)	85.96(5)	85.95(5)
N(1)–Ni(1)–N(3)	167.95(4)	172.85(6)	173.47(6)
N(1)–Ni(1)–Cl(1)	92.46(3)	91.73(4)	91.43(4)
N(3)–Ni(1)–Cl(1)	93.28(3)	91.55(4)	91.60(4)
N(2)–Ni(1)–Cl(1)	165.90(3)	171.32(4)	169.78(4)

The ORTEP diagrams of complexes **4a**, **4d** and **4f** are shown in Figure 5.2, 5.3, and 5.4, respectively. Selected bond lengths and bond angles are given in Table 5.1. In all three complexes, the oxazoliny-amine ligands furnished tridentate coordination to the nickel through oxazoliny-*N1*, amido-*N2*, and amine-*N3*, and the fourth side is occupied by anionic ligand, –Cl. A distorted square-planar coordination geometry is observed around the nickel in all three complexes. Various bond lengths among these three complexes are comparable to each other. The Ni(1)–N(1) bond lengths are in the range of 1.879(0)-1.891(6) Å, which are slightly shorter than the Ni–N bond length (1.9107(10) Å) in a similar complex, (^{Et}2NNN^{8-Q})NiCl.⁷³ However, the Ni(1)–N(2) and Ni(1)–N(3) bond lengths, 1.8806(10)-1.8860(12) Å and 1.9514(10)-1.9611(12) Å, respectively, are comparable with the corresponding bond lengths in (^{Et}2NNN^{8-Q})NiCl.⁷³ Notably, the N(1)–Ni(1)–N(3) bond angle (167.95(4)°) in complex **4a** is significantly smaller than that in chiral complexes, **4d** and **4f** (172.85(6)° and 173.47(6)°). Similarly, the N(2)–Ni(1)–Cl(1) bond angle (165.90(3)°) in complex **4a** is smaller than that observed in the chiral complexes, **4d** and **4f** (171.32(4)° and 169.78(4)°). This finding indicates that the geometry around nickel in complex **4a** is highly distorted compared to

that in complexes **4d** and **4f**. Notably, the bond angles around the nickel complexes **4d** and **4f** are comparable with that observed in complex $(\text{Et}^2\text{NNN}^{8\text{-Q}})\text{NiCl}$.⁷³

5.2.2 Transfer Hydrogenation of Ketones

The hydrogenation of ketones to achieve chiral alcohols has given significant recent attention, particularly employing the earth-abundant and inexpensive 3d transition metal catalysts.^{8,83} Among 3d metals, cobalt and iron complexes are substantially explored in the hydrogenation of ketones. However, the nickel complexes for such reactions are elusive. Mostly, the nickel precursors in combination with an expensive bisphosphine ligand are explored for the hydrogenation of alkene derivatives.⁸⁴⁻⁸⁸ After synthesizing and characterizing the phosphine-free achiral and chiral pincer nickel complexes, we intended to employ them for the asymmetric hydrogenation of prochiral ketones. At the outset, we chose acetophenone (**5a**) for the transfer hydrogenation in the presence of ⁱPrOH as a hydrogen source using a nickel catalyst, a condition reported for ruthenium catalysis (Table 5.2).⁸⁹⁻⁹¹ The reaction was performed with 0.3 mmol of acetophenone, 5 mol% of nickel catalyst **4a** and varied amount of KOH in isopropanol. As can be seen from the initial results in Table 5.2 (entries 1-4) that complex **4a** gave the best result with 2.0 equiv of KOH. The employment of an excess of KOH led to an undesired side product (entry 2), whereas with a lower amount of KOH, the reaction remained incomplete. In addition to KOH, the NaOH base was also competent. The reaction proceeded smoothly at 100 °C, whereas incomplete conversion was observed at low reaction temperature (entries 3 and 6). Notably, the use of nickel complex **4b** provided only 35% of hydrogenated product **6a**, whereas other nickel complexes **4c-4f** produced a very good yield (entries 7-11). Unfortunately, we did not observe enantiomeric excess (ee) for the alcohol product (**6a**) using chiral catalysts, **4c-4f**. We assume that the lack of stereocontrol is due to the low steric crowding around the nickel complexes, which could be partially because of the involvement of the six-membered nickelacycle with the oxazolinyl ring. The employment of (DME)NiCl₂ as a catalyst gave only 33% of hydrogenated product **6a** (entry 12). Notably, the reaction in the absence of KOH failed to provide the hydrogenation, whereas the use of EtOH as a hydrogenation source was ineffective (entries 13, 14).

Table 5.2 Optimization of reaction conditions for transfer hydrogenation of ketones.

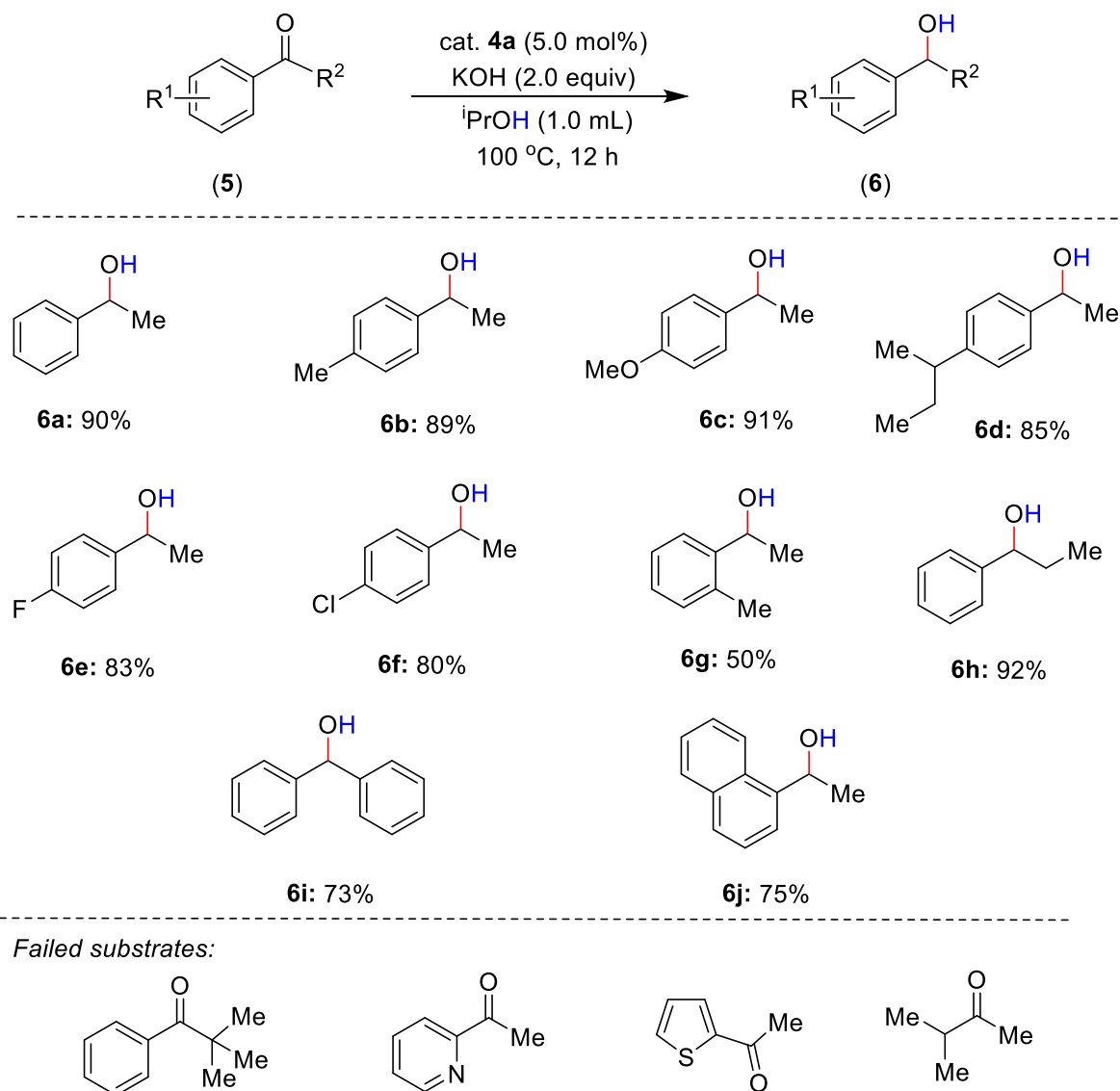
Entry	Cat. [Ni]	Base (equiv)	T (°C)/ t (h)	6a (%) ^a
1	4a	KOH (0.2)	100 / 12	20
2	4a	KOH (6)	100 / 12	60
3	4a	KOH (2)	100 / 12	98 (90)
4	4a	KOH (1)	100 / 12	68
5	4a	NaOH (1)	100 / 12	70
6	4a	KOH (2)	80 / 12	62
7	4b	KOH (2)	100 / 12	35
8	4c	KOH (2)	100 / 12	80
9	4d	KOH (2)	100 / 12	83
10	4e	KOH (2)	100 / 12	85
11	4f	KOH (2)	100 / 12	92
12	(DME)NiCl ₂	KOH (2)	100 / 12	33
13	4a	--	100 / 12	0
14	4a ^b	KOH (2)	100 / 12	trace

Reaction conditions: Compound **5a** (0.036 g, 0.3 mmol), base (0.6 mmol), ⁱPrOH (1.0 mL), [Ni] (0.015 mmol). ^a GC yield, isolated yield is in parenthesis. ^bEtOH as a solvent.

5.2.3 Substrate Scope for the Transfer Hydrogenation of Ketones

We have investigated the scope and limitations of this hydrogenation protocol (Scheme 5.3). Thus, the acetophenone having -Me, -OMe, alkyl, -F, and -Cl substituents reacted smoothly and provided the corresponding hydrogenated products (**6a-6f**) in good yields. The *ortho*-substituted compound **5g** afforded the hydrogenated product **6g** in low yield (50%), which could account for the steric influence. A propiophenone derivative can be smoothly

hydrogenated under optimized conditions (**6h**). Similarly, the challenging benzophenone was easily hydrogenated to diphenylmethanol, **6i**, in 73% yield. A naphthalenyl ethanone compound was also tolerated under the reaction conditions.



Scheme 5.3. Scope and limitation of transfer hydrogenation catalyzed by **4a**.

Unfortunately, highly bulky ketones (2-butanone), heteroarene-substituted ketones (3-methylbutan-2-one), and aliphatic ketones (cyclohexanone) were unreactive under the reaction conditions. Though our objective of achieving asymmetric hydrogenation was unsuccessful, we could demonstrate the simple phosphine-free nickel complexes for the transfer hydrogenation of various ketone derivatives. Notably, the CNN- and POCN-ligated pincer

nickel complexes were previously reported for the transfer hydrogenation of ketones showing similar activity as **4a**; however, relatively strong bases (NaO^tBu, KO^tBu) were employed.^{62,63}

5.2.4 Probable Catalytic Cycle

On the basis of previous literature on the transfer hydrogenation of ketones,^{62,63} we have proposed a plausible catalytic cycle (Figure 5.5). The reaction of complex **4a** with isopropanol in the presence of a base produced alkoxide complex **A**. The β -hydride elimination would result in Ni-hydride complex **B**. The coordination of substrate ketones followed by insertion resulted in complex **D**. The intermediate **D** gave the desired alcohol product **6** upon reaction with isopropanol, and completed the catalytic cycle.

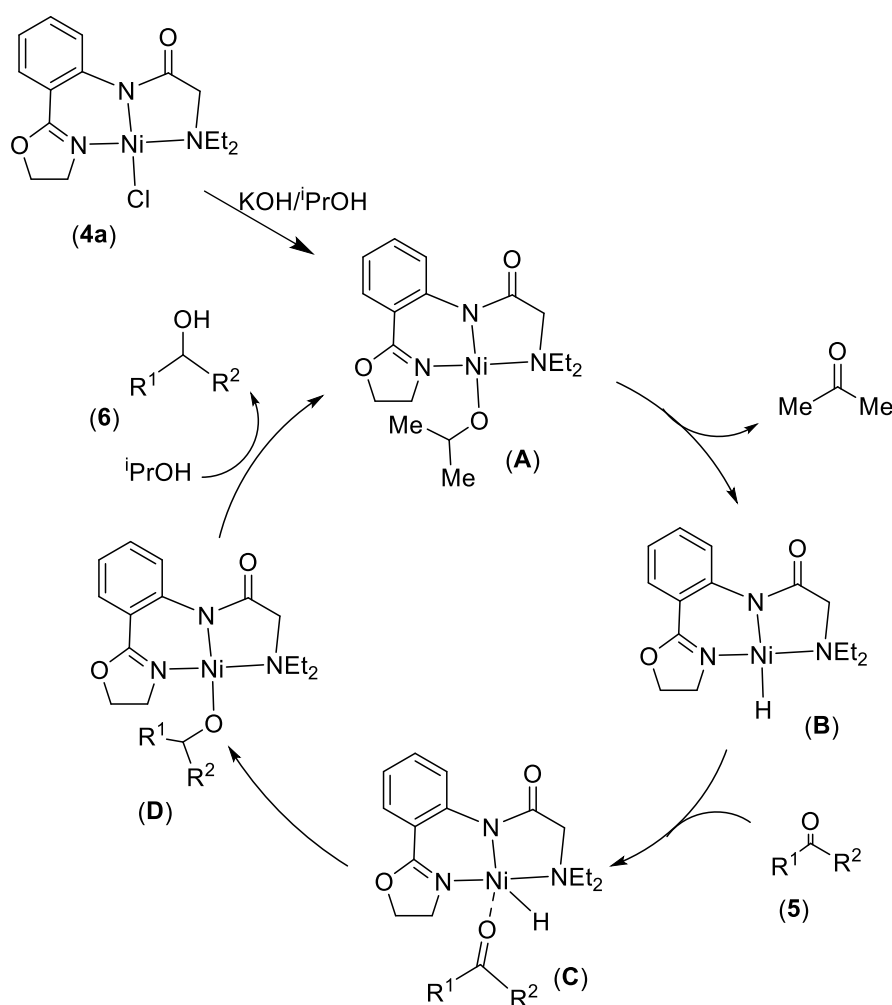


Figure 5.5. Proposed catalytic cycle.

5.3 CONCLUSIONS

In summary, we have described the synthesis of a series of new *NNN*-ligands containing oxazolanyl-backbone and their pincer nickel complexes. Both the achiral [(^{R'}2-O_xNNN^{Et}2)-H (**3a,b**) and chiral [(*R*)-(^{R'}2-O_xNNN^{Et}2)-H (**3c-f**) ligands were synthesized in good yields. These ligands were used to develop pincer nickel complexes, (^{R'}2-O_xNNN^{Et}2)NiCl (**4a,b**) and [(*R*)-(^{R'}2-O_xNNN^{Et}2)NiCl] (**4c-f**) under mild conditions. All the ligand precursors and nickel complexes were thoroughly characterized by NMR spectroscopy, HRMS, or elemental analysis. The single-crystal X-ray diffraction study elucidated the molecular structures of complexes (^O_xNNN^{Et}2)NiCl (**4a**), (*R*)-(PhCH₂-^O_xNNN^{Et}2)NiCl (**4d**) and (*R*)-(iPrCH₂-^O_xNNN^{Et}2)NiCl (**4f**). The nickel complex **4a** efficiently catalyzes the transfer hydrogenation of ketones using isopropanol as a hydrogen source. Despite many attempts, we could not achieve enantioselective hydrogenation of ketones, and which need further investigation.

5.4 EXPERIMENTAL SECTION

All manipulations were conducted under an argon atmosphere either in a glove box or using standard Schlenk techniques in pre-dried glasswares. The catalytic reactions were performed in flame-dried reaction vessels with a Teflon screw cap. Solvents were dried over Na/benzophenone or CaH₂ or Mg-cake (iPrOH) and distilled before use. Liquid reagents were flushed with argon before use. The 2-(oxazol-2-yl)aniline derivatives (**1a-1f**)⁷⁹⁻⁸¹ and compounds **2b**⁸² and **3b**⁸² were synthesized according to the previously described procedures. All other chemicals were obtained from commercial sources and were used without further purification. Yields refer to isolated compounds, estimated to be >95% pure as determined by ¹H-NMR spectroscopy. HRMS spectra were recorded using a Thermo Scientific Q-Exactive, Accela 1250 pump. NMR (¹H and ¹³C) spectra were recorded at 400 or 500 MHz (¹H) and 100 or 125 MHz (¹³C) [DEPT (distortionless enhancement by polarization transfer)] using Bruker AV 400 and AV 500 spectrometers, respectively, in CDCl₃ solutions, if not then specified; chemical shifts (δ) are given in ppm. The ¹H and ¹³C NMR spectra are referenced to residual solvent signals (CDCl₃: δ H = 7.26 ppm, δ C = 77.2 ppm).

5.4.1 Procedure for Synthesis of Ligand Precursor

Representative procedure A: Synthesis of 2-Bromo-N-(2-(4,5-dihydrooxazol-2-yl)phenyl)acetamide (2a). To a solution of 2-(4,5-dihydrooxazol-2-yl)aniline (**1a**; 1.0 g, 6.165 mmol) in dichloromethane (20 mL), Et₃N (0.75 g, 7.41 mmol) was added and the reaction mixture was stirred at room temperature for 20 min. 2-Bromoacetyl chloride (1.16 g, 7.37 mmol) was added dropwise at 0 °C and the resultant mixture was continued stirring for 20 h at room temperature. At ambient temperature, the reaction mixture was quenched with water (15 mL) and extracted with CH₂Cl₂ (15 mL x 3). The combined organic phase was washed with H₂O (15 mL x 3) and dried over Na₂SO₄. After filtration and evaporation of the solvents in *vacuo*, the crude product was purified by column chromatography on silica gel (petroleum ether /EtOAc: 3/1) to yield **2a** (1.30 g, 74%) as a white solid. ¹H-NMR (400 MHz, CDCl₃): δ = 11.76 (br s, 1H, NH), 8.57 (d, *J* = 8.3 Hz, 1H, Ar-H), 7.56-7.49 (m, 2H, Ar-H), 7.15 (t, *J* = 7.4 Hz, 1H, Ar-H), 4.17 (s, 2H, CH₂), 3.90-3.79 (m, 2H, CH₂), 3.76-3.58 (m, 2H, CH₂). ¹³C{¹H}-NMR (100 MHz, CDCl₃): δ = 168.9 (C_q, CO), 165.3 (C_q), 138.6 (C_q), 133.0 (CH), 126.9 (CH), 124.0 (CH), 121.7 (CH), 120.9 (C_q), 43.9 (CH₂), 43.3 (CH₂), 41.7 (CH₂). HRMS (ESI): *m/z* Calcd for C₁₁H₁₁N₂O₂Br + H⁺ [M + H]⁺ 283.0083, 285.0062; Found 283.0077, 285.1216.

Synthesis of 2-Bromo-N-(2-(4-phenyl-4,5-dihydrooxazol-2-yl)phenyl)acetamide (2c). The representative procedure **A** was followed using 2-(4-phenyl-4,5-dihydrooxazol-2-yl)aniline (**1c**; 1.5 g, 6.295 mmol), Et₃N (0.7 g, 6.918 mmol), 2-bromoacetyl chloride (1.09 g, 6.925 mmol). Purification by column chromatography on silica gel (petroleum ether/EtOAc: 3/1) yielded **2c** (1.41 g, 62%) as a light-yellow solid. ¹H-NMR (500 MHz, CDCl₃): δ = 12.96 (br s, 1H, NH), 8.77 (d, *J* = 8.3 Hz, 1H, Ar-H), 7.96-7.94 (m, 1H, Ar-H), 7.55-7.50 (m, 1H, Ar-H), 7.40-7.30 (m, 5H, Ar-H), 7.18 (t, *J* = 7.6 Hz, 1H, Ar-H), 5.53 (t, *J* = 8.3 Hz, 1H, CH₂), 4.80-4.76 (m, 1H, CH₂), 4.25 (t, *J* = 8.3 Hz, 1H, CH), 4.12 (s, 2H, CH₂). ¹³C{¹H}-NMR (125 MHz, CDCl₃): δ = 165.9 (C_q, CO), 164.4 (C_q), 141.7 (C_q), 139.3 (C_q), 132.9 (CH), 129.5 (CH), 128.9 (2C, CH), 127.9 (CH), 126.6 (2C, CH), 123.4 (CH), 120.1 (CH), 113.9 (C_q), 73.5 (CH₂), 70.0 (CH), 43.6 (CH₂). HRMS (ESI): *m/z* Calcd for C₁₇H₁₅N₂O₂Br + H⁺ [M + H]⁺ 359.0395, 361.0375; Found 359.0398, 361.0396.

Synthesis of *N*-(2-(4-Benzyl-4,5-dihydrooxazol-2-yl)phenyl)-2-bromoacetamide (2d). The representative procedure **A** was followed using 2-(4-benzyl-4,5-dihydrooxazol-2-yl)aniline (**1d**; 0.4 g, 1.585 mmol), Et₃N (0.18 g, 1.778 mmol), 2-bromoacetyl chloride (0.27 g, 1.715 mmol). Purification by column chromatography on silica gel (petroleum ether/EtOAc: 3/1) yielded **2d** (0.42 g, 71%) as a light yellow solid. ¹H-NMR (400 MHz, CDCl₃): δ = 12.47 (br s, 1H, NH), 9.38 (d, *J* = 8.3 Hz, 1H, Ar-H), 8.31 (t, *J* = 8.3 Hz, 1H, Ar-H), 8.25 (d, *J* = 7.6 Hz, 1H, Ar-H), 8.17-8.14 (m, 2H, Ar-H), 8.11-8.07 (m, 3H, Ar-H), 7.97-7.94 (m, 1H, Ar-H), 5.53-5.48 (m, 1H, CH), 4.98 (m, 2H, CH₂), 4.60-4.57 (m, 1H, CH₂), 4.46-4.42 (m, 1H, CH₂), 3.90-3.82 (m, 2H, CH₂). ¹³C{¹H}-NMR (100 MHz, CDCl₃): δ = 168.2 (C_q, CO), 165.3 (C_q), 138.6 (C_q), 136.6 (C_q), 133.0 (CH), 129.4 (2C, CH), 129.0 (2C, CH), 127.3 (CH), 126.7 (CH), 124.0 (CH), 121.8 (CH), 121.2 (C_q), 51.0 (CH), 46.7 (CH₂), 43.3 (CH₂), 37.6 (CH₂). HRMS (ESI): *m/z* Calcd for C₁₈H₁₇N₂O₂Br + H⁺ [M + H]⁺ 373.0555, 375.0531; Found 373.0546, 375.0533.

Synthesis of 2-Bromo-*N*-(2-(4-isopropyl-4,5-dihydrooxazol-2-yl)phenyl)acetamide (2e). The representative procedure **A** was followed using 2-(4-isopropyl-4,5-dihydrooxazol-2-yl)aniline (**1e**; 1.0 g, 4.895 mmol), Et₃N (0.545 g, 5.385 mmol), 2-bromoacetyl chloride (0.847 g, 5.385 mmol). Purification by column chromatography on silica gel (petroleum ether/EtOAc: 3/1) yielded **2e** (0.82 g, 52%) as a light-yellow liquid. ¹H-NMR (400 MHz, CDCl₃): δ = 12.90 (br s, 1H, NH), 8.72 (d, *J* = 8.4 Hz, 1H, Ar-H), 7.87-7.84 (m, 1H, Ar-H), 7.49-7.45 (m, 1H, Ar-H), 7.12 (t, *J* = 7.4 Hz, 1H, Ar-H), 4.40-4.36 (m, 1H, CH₂), 4.23-4.17 (m, 3H, CH, CH₂), 4.09-4.05 (m, 1H, CH₂), 1.89-1.81 (m, 1H, CH), 1.02 (d, *J* = 6.8 Hz, 3H, CH₃), 0.96 (d, *J* = 6.7 Hz, 3H, CH₃). ¹³C{¹H}-NMR (100 MHz, CDCl₃): δ = 165.7 (C_q, CO), 163.1 (C_q), 139.1 (C_q), 132.5 (CH), 129.3 (CH), 123.2 (CH), 120.0 (CH), 114.2 (C_q), 72.8 (CH), 69.3 (CH₂), 43.6 (CH₂), 33.0 (CH), 18.9 (CH₃), 18.6 (CH₃). HRMS (ESI): *m/z* Calcd for C₁₄H₁₇N₂O₂Br + H⁺ [M + H]⁺ 325.0552, 327.0531; Found 325.0573, 327.0548.

Synthesis of 2-Bromo-*N*-(2-(4-isobutyl-4,5-dihydrooxazol-2-yl)phenyl)acetamide (2f). The representative procedure **A** was followed using 2-(4-isobutyl-4,5-dihydrooxazol-2-yl)aniline (**1f**; 1.0 g, 4.581 mmol), Et₃N (0.51 g, 5.04

mmol), 2-bromoacetyl chloride (0.79 g, 5.02 mmol). Purification by column chromatography on silica gel (petroleum ether/EtOAc: 3/1) yielded **2f** (0.89 g, 57%) as a white solid. $^1\text{H-NMR}$ (500 MHz, CDCl_3): δ = 12.89 (br s, 1H, *NH*), 8.72 (d, J = 8.3 Hz, 1H, Ar–H), 7.85 (d, J = 7.6 Hz, 1H, Ar–H), 7.46 (t, J = 8.3 Hz, 1H, Ar–H), 7.12 (t, J = 7.2 Hz, 1H, Ar–H), 4.48-4.42 (m, 2H, CH_2), 4.18 (s, 2H, CH_2), 3.97-3.91 (m, 1H, CH), 1.95-1.87 (m, 1H, CH_2), 1.71-1.65 (m, 1H, CH_2), 1.42-1.37 (m, 1H, CH), 1.00-0.96 (m, 6H, CH_3). $^{13}\text{C}\{^1\text{H}\}$ -NMR (125 MHz, CDCl_3): δ = 165.7 (C_q , CO), 163.0 (C_q), 139.1 (C_q), 132.4 (CH), 129.2 (CH), 123.2 (CH), 120.0 (CH), 114.2 (C_q), 72.0 (CH_2), 65.0 (CH), 45.7 (CH_2), 43.6 (CH_2), 25.5 (CH_3), 23.1 (CH_3), 22.4 (CH). HRMS (ESI): m/z Calcd for $\text{C}_{15}\text{H}_{19}\text{N}_2\text{O}_2\text{Br} + \text{H}^+$ [$\text{M} + \text{H}$] $^+$ 339.0708, 341.0688; Found 339.0729, 341.0697.

5.4.2 Synthesis of ($\text{R-OxNNN}^{\text{Et}_2}$)–H ligands

Representative procedure B: Synthesis of 2-(diethylamino)-N-(2-(4,5-dihydrooxazol-2-yl)phenyl)acetamide, ($\text{OxNNN}^{\text{Et}_2}$)–H (3a**).** To a solution of 2-bromo-N-(2-(4,5-dihydrooxazol-2-yl)phenyl)acetamide (**2a**; 0.85 g, 3.0 mmol) in acetone (20 mL), diethyl amine (0.66 g, 9.0 mmol) was added at room temperature. The resultant mixture was heated at 70 °C for 24 h. At ambient temperature, acetone was evaporated *in vacuo*, quenched with water (15 mL) and extracted with dichloromethane (15 mL x 3). The combined organic phase was washed with H_2O (15 mL x 3) and dried over Na_2SO_4 . After filtration and evaporation of the solvents *in vacuo*, the crude product was purified by column chromatography on silica gel (petroleum ether /EtOAc: 3/1) to yield **3a** (0.72 g, 87%) as a white solid. $^1\text{H-NMR}$ (400 MHz, CDCl_3): δ = 11.51 (br s, 1H, *NH*), 8.55 (d, J = 8.3 Hz, 1H, Ar–H), 7.48-7.43 (m, 2H, Ar–H), 7.07 (t, J = 7.5 Hz, 1H, Ar–H), 3.79-3.70 (m, 4H, CH_2), 3.16 (s, 2H, CH_2), 2.66 (q, J = 7.0 Hz, 4H, CH_2), 1.09 (t, J = 7.0 Hz, 6H, CH_3). $^{13}\text{C}\{^1\text{H}\}$ -NMR (100 MHz, CDCl_3): δ = 172.1 (C_q , CO), 168.7 (C_q), 138.1 (C_q), 132.3 (CH), 127.0 (CH), 123.2 (CH), 122.8 (C_q), 121.9 (CH), 58.6 (CH_2), 48.8 (2C, CH_2), 43.8 (CH_2), 41.7 (CH_2), 12.3 (2C, CH_3). HRMS (ESI): m/z Calcd for $\text{C}_{15}\text{H}_{21}\text{N}_3\text{O}_2 + \text{H}^+$ [$\text{M} + \text{H}$] $^+$ 276.1712; Found 276.1706.

Synthesis of ($\text{Me}_2\text{-OxNNN}^{\text{Et}_2}$)–H (3b**).**⁸² The representative procedure **B** was followed using 2-chloro-N-(2-(4,4-dimethyl-4,5-dihydrooxazol-2-yl)phenyl)acetamide

(**2b**; 0.5 g, 1.61 mmol), diethyl amine (0.353 g, 4.83 mmol). Purification by column chromatography on silica gel (petroleum ether/EtOAc: 3/1) yielded **3b** (0.40 g, 82%) as a light orange solid. $^1\text{H-NMR}$ (500 MHz, CDCl_3): δ = 12.63 (br s, 1H, *NH*), 8.89 (d, J = 8.3 Hz, 1H, Ar-H), 7.84 (d, J = 8.3 Hz, 1H, Ar-H), 7.43 (t, J = 6.8 Hz, 1H, Ar-H), 7.06 (t, J = 6.8 Hz, 1H, Ar-H), 4.03 (s, 2H, CH_2), 3.22 (s, 2H, CH_2), 2.67 (q, J = 7.6 Hz, 4H, CH_2), 1.39 (s, 6H, CH_3), 1.08 (t, J = 7.6 Hz, 6H, CH_3). $^{13}\text{C}\{^1\text{H}\}$ -NMR (125 MHz, CDCl_3): δ = 172.6 (C_q , CO), 160.7 (C_q), 139.3 (C_q), 131.9 (CH), 128.9 (CH), 122.0 (CH), 119.7 (CH), 114.0 (C_q), 76.5 (CH_2), 68.0 (C_q), 58.0 (CH_2), 49.0 (2C, CH_2), 28.3 (2C, CH_3), 11.8 (2C, CH_3). HRMS (ESI): m/z Calcd for $\text{C}_{17}\text{H}_{25}\text{N}_3\text{O}_2 + \text{H}^+$ [$\text{M} + \text{H}$] $^+$ 304.2030; Found 304.2022.

Synthesis of (R)-(Ph-OxNNN^{Et2})-H (3c). The representative procedure **B** was followed using (R)-2-bromo-N-(2-(4-phenyl-4,5-dihydrooxazol-2-yl)phenyl)acetamide (**2c**; 0.88 g, 2.45 mmol), diethyl amine (0.54 g, 7.38 mmol). Purification by column chromatography on silica gel (petroleum ether/EtOAc: 3/1) yielded **3c** (0.84 g, 98%) as a light brown liquid. $^1\text{H-NMR}$ (500 MHz, CDCl_3): δ = 12.81 (br s, 1H, *NH*), 8.91 (d, J = 9.1 Hz, 1H, Ar-H), 7.96-7.94 (m, 1H, Ar-H), 7.51-7.47 (m, 1H, Ar-H), 7.36-7.29 (m, 5H, Ar-H), 7.11 (t, J = 6.8 Hz, 1H, Ar-H), 5.47-5.43 (m, 1H, CH_2), 4.77-4.72 (m, 1H, CH_2), 4.22 (t, J = 9.1 Hz, 1H, CH), 3.14 (s, 2H, CH_2), 2.35 (q, J = 7.6 Hz, 4H, CH_2), 0.83 (t, J = 6.8 Hz, 6H, CH_3). $^{13}\text{C}\{^1\text{H}\}$ -NMR (125 MHz, CDCl_3): δ = 173.1 (C_q , CO), 163.8 (C_q), 142.3 (C_q), 140.0 (C_q), 132.7 (CH), 129.6 (CH), 128.7 (2C, CH), 127.8 (CH), 127.0 (2C, CH), 122.4 (CH), 120.2 (CH), 113.8 (C_q), 73.5 (CH_2), 70.8 (CH), 58.5 (CH_2), 48.6 (2C, CH_2), 11.7 (2C, CH_3). HRMS (ESI): m/z Calcd for $\text{C}_{21}\text{H}_{25}\text{N}_3\text{O}_2 + \text{H}^+$ [$\text{M} + \text{H}$] $^+$ 352.2033; Found 352.2020.

Synthesis of (R)-(PhCH₂-OxNNN^{Et2})-H (3d). The representative procedure **B** was followed using (R)-N-(2-(4-benzyl-4,5-dihydrooxazol-2-yl)phenyl)-2-bromoacetamide (**2d**; 0.40 g, 1.07 mmol), diethyl amine (0.24 g, 3.28 mmol). Purification by column chromatography on silica gel (petroleum ether/EtOAc: 3/1) yielded **3d** (0.35 g, 90%) as a light brown liquid. $^1\text{H-NMR}$ (500 MHz, CDCl_3): δ = 12.71 (br s, 1H, *NH*), 8.90 (d, J = 8.3 Hz, 1H, Ar-H), 7.87 (d, J = 8.0 Hz, 1H, Ar-H), 7.50 (t, J = 8.3 Hz, 1H, Ar-H), 7.36 (t, J = 7.2 Hz, 2H, Ar-H), 7.30-7.27 (m, 3H, Ar-H), 7.11 (t, J = 7.2 Hz, 1H, Ar-

H), 4.75-4.69 (m, 1H, CH), 4.31 (t, $J = 8.3$ Hz, 1H, CH₂), 4.12 (t, $J = 7.6$ Hz, 1H, CH₂), 3.34-3.28 (m, 3H, CH₂), 2.82-2.77 (m, 1H, CH₂), 2.71 (q, $J = 7.2$ Hz, 4H, CH₂), 1.15 (t, $J = 7.2$ Hz, 6H, CH₃). ¹³C{¹H}-NMR (125 MHz, CDCl₃): $\delta = 172.7$ (C_q, CO), 163.2 (C_q), 139.7 (C_q), 137.8 (C_q), 132.4 (CH), 129.4 (CH), 129.2 (2C, CH), 128.8 (2C, CH), 126.8 (CH), 122.4 (CH), 120.2 (CH), 114.0 (C_q), 70.5 (CH₂), 68.3 (CH), 58.9 (CH₂), 48.7 (2C, CH₂), 41.9 (CH₂), 12.1 (2C, CH₃). HRMS (ESI): m/z Calcd for C₂₂H₂₇N₃O₂ + H⁺ [M + H]⁺ 366.2182; Found 366.2092.

Synthesis of (R)-(iPr-OxNNN^{Et2})-H (3e). The representative procedure **B** was followed using (R)-2-bromo-N-(2-(4-isopropyl-4,5-dihydrooxazol-2-yl)phenyl)acetamide (**2e**; 0.48 g, 1.48 mmol), diethyl amine (0.33 g, 4.51 mmol). Purification by column chromatography on silica gel (petroleum ether/EtOAc: 3/1) yielded **3e** (0.30 g, 64%) as a colorless liquid. ¹H-NMR (400 MHz, CDCl₃): $\delta = 12.49$ (br s, 1H, NH), 8.86-8.83 (m, 1H, Ar-H), 7.83 (dd, $J = 7.9, 1.5$ Hz, 1H, Ar-H), 7.44-7.40 (m, 1H, Ar-H), 7.04 (t, $J = 7.3$ Hz, 1H, Ar-H), 4.32-4.28 (m, 1H, CH₂), 4.21-4.15 (m, 1H, CH), 4.05 (t, $J = 7.8$ Hz, 1H, CH₂), 3.27-3.18 (m, 2H, CH₂), 2.63 (q, $J = 7.0$ Hz, 4H, CH₂), 1.91-1.82 (m, 1H, CH), 1.06-1.01 (m, 9H, CH₃), 0.91 (d, $J = 6.7$ Hz, 3H, CH₃). ¹³C{¹H}-NMR (100 MHz, CDCl₃): $\delta = 172.4$ (C_q, CO), 162.4 (C_q), 139.5 (C_q), 132.1 (CH), 129.3 (CH), 122.3 (CH), 120.2 (CH), 114.1 (C_q), 73.0 (CH₂), 68.4 (CH), 58.6 (CH₂), 48.8 (2C, CH₂), 32.7 (CH), 19.0 (CH₃), 17.9 (CH₃), 11.8 (2C, CH₃). HRMS (ESI): m/z Calcd for C₁₈H₂₇N₃O₂ + H⁺ [M + H]⁺ 318.2182; Found 318.2194.

Synthesis of (R)-(iPrCH₂-OxNNN^{Et2})-H (3f). The representative procedure **B** was followed using (R)-2-bromo-N-(2-(4-isobutyl-4,5-dihydrooxazol-2-yl)phenyl)acetamide (**2f**; 1.04 g, 3.07 mmol), diethyl amine (0.68 g, 9.29 mmol). Purification by column chromatography on silica gel (petroleum ether/EtOAc: 3/1) yielded **3f** (0.92 g, 91%) as a white solid. ¹H-NMR (500 MHz, CDCl₃): $\delta = 12.55$ (br s, 1H, NH), 8.85 (d, $J = 8.6$ Hz, 1H, Ar-H), 7.84 (dd, $J = 7.6, 1.2$ Hz, 1H, Ar-H), 7.43 (t, $J = 7.3$ Hz, 1H, Ar-H), 7.06 (t, $J = 7.3$ Hz, 1H, Ar-H), 4.44-4.36 (m, 2H, CH₂), 3.94-3.91 (m, 1H, CH), 3.27-3.19 (m, 2H, CH₂), 2.63 (q, $J = 7.1$ Hz, 4H, CH₂), 1.88-1.80 (m, 1H, CH₂), 1.76-1.70 (m, 1H, CH₂), 1.43-1.37 (m, 1H, CH), 1.07 (t, $J = 7.0$ Hz, 6H, CH₃), 0.99-0.96 (m, 6H, CH₃). ¹³C{¹H}-NMR (125 MHz, CDCl₃): $\delta = 172.6$ (C_q, CO), 162.4

(C_q), 139.5 (C_q), 132.2 (CH), 129.3 (CH), 122.4 (CH), 120.2 (CH), 114.3 (C_q), 71.7 (CH₂), 65.6 (CH), 58.8 (CH₂), 48.9 (2C, CH₂), 45.9 (CH₂), 25.4 (CH), 23.0 (CH₃), 22.8 (CH₃), 12.1 (2C, CH₃). HRMS (ESI): *m/z* Calcd for C₁₉H₂₉N₃O₂ + H⁺ [M + H]⁺ 332.2338; Found 332.2352.

5.4.3 Synthesis of nickel complexes (R¹-OxNNN^{Et2})NiCl

Representative procedure C: Synthesis of (OxNNN^{Et2})NiCl (4a). The nickel complexes of the oxazoline-based ligands were synthesized following the precedented literature developed by our group.^{13a} In a standard procedure, to the mixture of 2-(diethylamino)-*N*-(2-(4,5-dihydrooxazol-2-yl)phenyl)acetamide (**3a**; 0.88 g, 3.195 mmol) and (DME)NiCl₂ (0.70 g, 3.19 mmol) in THF (10 mL), Et₃N (0.39 g, 3.85 mmol) was added and the resultant mixture was refluxed for 3 h. At ambient temperature, the reaction mixture was filtered and concentrated under vacuum. To the concentrated solution, *n*-hexane was added to precipitate the product, which was then cannula filtered and dried under vacuum to obtain nickel complex **4a** (0.92 g, 78%) as a dark purple solid. ¹H-NMR (400 MHz, CDCl₃): δ = 8.29 (d, *J* = 9.3 Hz, 1H, Ar-H), 7.56 (dd, *J* = 7.8, 1.5 Hz, 1H, Ar-H), 7.36-7.32 (m, 1H, Ar-H), 6.96-6.92 (m, 1H, Ar-H), 4.39 (t, *J* = 9.7 Hz, 2H, CH₂), 3.95 (t, *J* = 9.7 Hz, 2H, CH₂), 3.24 (s, 2H, CH₂), 2.92-2.83 (m, 2H, CH₂), 2.16 (t, *J* = 7.1 Hz, 6H, CH₃), 2.05-1.96 (m, 2H, CH₂). ¹³C{¹H}-NMR (100 MHz, CDCl₃): δ = 177.6 (C_q, CO), 163.1 (C_q), 145.0 (C_q), 132.7 (CH), 128.3 (CH), 125.1 (CH), 121.7 (CH), 114.5 (C_q), 67.9 (CH₂), 60.8 (CH₂), 55.6 (2C, CH₂), 53.7 (CH₂), 12.9 (2C, CH₃). Anal. Calcd. for C₁₅H₂₀ClN₃O₂Ni: C, 48.89; H, 5.47; N, 11.40. Found: C, 49.15; H, 5.20; N, 11.43.

Synthesis of (Me₂-OxNNN^{Et2})NiCl (4b). The representative procedure C was followed using 2-(diethylamino)-*N*-(2-(4,4-dimethyl-4,5-dihydrooxazol-2-yl)phenyl)acetamide (**3b**; 0.20 g, 0.659 mmol), (DME)NiCl₂ (0.145 g, 0.659 mmol) and Et₃N (0.08 g, 0.80 mmol) to yield **4b** (0.195 g, 75%) as a dark purple solid. ¹H-NMR (400 MHz, CDCl₃): δ = 8.20 (s, 1H, Ar-H), 7.63-7.51 (m, 2H, Ar-H), 6.91 (s, 1H, Ar-H), 4.10 (s, 6H, CH₃), 2.68-2.31 (m, 8H, CH₂), 1.83 (s, 6H, CH₃). ¹³C{¹H}-NMR (100 MHz, CDCl₃): δ = 179.0 (C_q, CO), 165.9 (C_q), 144.1 (C_q), 133.0 (CH), 127.1 (CH), 122.0 (2C, CH), 118.8 (C_q), 83.8 (CH₂), 74.6 (C_q), 57.3 (CH₂), 52.5 (2C, CH₂), 28.2

(2C, CH₃), 14.6 (2C, CH₃). Anal. Calcd. for C₁₇H₂₄ClN₃O₂Ni: C, 51.49; H, 6.10; N, 10.60. Found: C, 51.68; H, 5.93; N, 9.98.

Synthesis of (R)-(Ph-OxNNN^{Et2})NiCl (4c). The representative procedure **C** was followed using (R)-2-(diethylamino)-N-(2-(4-phenyl-4,5-dihydrooxazol-2-yl)phenyl)acetamide (**3c**; 0.20 g, 0.569 mmol), (DME)NiCl₂ (0.125 g, 0.569 mmol) and Et₃N (0.068 g, 0.672 mmol) to yield **4c** (0.189 g, 75%) as a dark purple solid. ¹H-NMR (500 MHz, CDCl₃): δ = 8.35 (s, 1H, Ar-H), 7.61-7.37 (m, 7H, Ar-H), 6.98 (s, 1H, Ar-H), 5.35 (br s, 1H, CH₂), 4.63 (br s, 1H, CH₂), 4.33 (1H, CH), 3.62-3.59 (m, 1H, CH₂), 2.82 (s, 1H, CH₂), 2.47 (s, 2H, CH₂), 1.95-1.44 (m, 8H, CH₂, CH₃). ¹³C{¹H}-NMR (125 MHz, CDCl₃): δ = 177.8 (C_q, CO), 162.6 (C_q), 145.6 (C_q), 142.0 (C_q), 133.1 (CH), 129.3 (2C, CH), 128.8 (2C, CH), 128.0 (2C, CH), 125.0 (CH), 121.7 (CH), 114.3 (C_q), 75.1 (CH₂), 67.1 (CH), 60.1 (CH₂), 57.1 (CH₂), 54.3 (CH₂), 12.5 (CH₃), 11.6 (CH₃). Anal. Calcd. for C₂₁H₂₄ClN₃O₂Ni: C, 56.73; H, 5.44; N, 9.45. Found: C, 57.02; H, 5.69; N, 9.36.

Synthesis of (R)-(PhCH₂-OxNNN^{Et2})NiCl (4d). The representative procedure **C** was followed using (R)-N-(2-(4-benzyl-4,5-dihydrooxazol-2-yl)phenyl)-2-(diethylamino)acetamide (**3d**; 0.11 g, 0.30 mmol), (DME)NiCl₂ (0.066 g, 0.30 mmol) and Et₃N (0.037 g, 0.365 mmol) to yield **4d** (0.135 g, 98%) as a dark purple solid. ¹H-NMR (400 MHz, CDCl₃): δ = 8.31 (s, 1H, Ar-H), 7.53-7.26 (m, 7H, Ar-H), 6.93 (s, 1H, Ar-H), 4.59-4.12 (m, 4H, CH₂), 3.88-3.74 (m, 1H, CH), 3.06-2.70 (m, 4H, CH₂), 2.33 (s, 4H, CH₂, CH₃), 1.89 (s, 4H, CH₂, CH₃). ¹³C{¹H}-NMR (100 MHz, CDCl₃): δ = 177.4 (C_q, CO), 162.4 (C_q), 145.3 (C_q), 136.7 (C_q), 133.0 (CH), 129.6 (2C, CH), 129.0 (2C, CH), 128.7 (CH), 127.2 (CH), 124.9 (CH), 121.6 (CH), 114.2 (C_q), 71.1 (CH₂), 64.9 (CH), 60.5 (CH₂), 56.8 (CH₂), 54.0 (CH₂), 42.3 (CH₂), 12.7 (2C, CH₃). Anal. Calcd. for C₂₂H₂₆ClN₃O₂Ni: C, 57.62; H, 5.71; N, 9.16. Found: C, 57.98; H, 5.73; N, 9.36.

Synthesis of (R)-(iPr-OxNNN^{Et2})NiCl (4e). The representative procedure **C** was followed using (R)-2-(diethylamino)-N-(2-(4-isopropyl-4,5-dihydrooxazol-2-yl)phenyl)acetamide (**3e**; 0.11 g, 0.346 mmol), (DME)NiCl₂ (0.076 g, 0.346 mmol) and Et₃N (0.042 g, 0.415 mmol) to yield **4e** (0.093 g, 66%) as a dark purple solid. ¹H-NMR

(400 MHz, CDCl₃): δ = 8.34 (s, 1H, Ar-H), 7.55-7.34 (m, 2H, Ar-H), 6.93 (s, 1H, Ar-H), 4.23-3.85 (m, 4H, CH₂), 3.32-2.64 (m, 5H, CH, CH₂), 2.30-1.85 (m, 7H, CH, CH₃), 1.40-1.05 (m, 6H, CH₃). ¹³C{¹H}-NMR (100 MHz, CDCl₃): δ = 177.2 (C_q, CO), 161.6 (C_q), 145.2 (C_q), 132.8 (CH), 128.7 (CH), 124.5 (CH), 121.5 (CH), 114.3 (C_q), 68.1 (CH₂), 67.7 (CH), 60.4 (CH₂), 56.6 (CH₂), 53.8 (CH₂), 31.2 (CH), 19.0 (CH₃), 14.7 (CH₃), 12.6 (CH₃), 12.3 (CH₃). Anal. Calcd. for C₁₈H₂₆ClN₃O₂Ni: C, 52.66; H, 6.38; N, 10.23. Found: C, 52.21; H, 6.08; N, 9.91.

Synthesis of (R)-(*i*PrCH₂-OxNNN^{Et}₂)NiCl (4f). The representative procedure **C** was followed using (R)-2-(diethylamino)-N-(2-(4-isobutyl-4,5-dihydrooxazol-2-yl)phenyl)acetamide (**3f**; 0.090 g, 0.272 mmol), (DME)NiCl₂ (0.060 g, 0.272 mmol) and Et₃N (0.031 g, 0.306 mmol) to yield **4f** (0.096 g, 83%) as a dark purple solid. ¹H-NMR (500 MHz, CDCl₃): δ = 8.31 (d, *J* = 8.6 Hz, 1H, Ar-H), 7.55 (d, *J* = 7.9 Hz, 1H, Ar-H), 7.33 (t, *J* = 7.3 Hz, 1H, Ar-H), 6.93 (t, *J* = 7.6 Hz, 1H, Ar-H), 4.33-4.28 (m, 2H, CH₂), 4.21-4.14 (m, 1H, CH), 3.89-3.86 (m, 1H, CH₂), 2.97-2.93 (m, 1H, CH₂), 2.90-2.84 (m, 2H, CH₂), 2.68-2.65 (m, 1H, CH), 2.33 (t, *J* = 7.0 Hz, 3H, CH₂), 2.27-2.20 (m, 1H, CH₂), 1.83 (t, *J* = 7.3 Hz, 3H, CH₃), 1.79-1.74 (m, 3H, CH₃), 1.10 (d, *J* = 6.1 Hz, 3H, CH₃), 1.02 (d, *J* = 6.7 Hz, 3H, CH₃). ¹³C{¹H}-NMR (125 MHz, CDCl₃): δ = 177.2 (C_q, CO), 161.7 (C_q), 145.2 (C_q), 132.8 (CH), 128.7 (CH), 124.8 (CH), 121.6 (CH), 114.6 (C_q), 72.2 (CH₂), 62.7 (CH), 60.5 (CH₂), 56.8 (CH₂), 53.9 (CH₂), 45.9 (CH₂), 25.8 (CH), 24.1 (CH₃), 22.0 (CH₃), 12.7 (CH₃), 12.6 (CH₃). Anal. Calcd. for C₁₉H₂₈ClN₃O₂Ni: C, 53.75; H, 6.65; N, 9.90. Found: C, 53.96; H, 6.50; N, 9.89.

5.4.4 Representative procedure for transfer hydrogenation of ketones

Synthesis of 1-phenylethan-1-ol (6a). To a flame-dried screw-cap tube equipped with magnetic stir bar were introduced acetophenone (0.036 g, 0.30 mmol), catalyst **4a** (0.0055 g, 0.015 mmol, 5.0 mol %) and KOH (0.034 g, 0.60 mmol) inside the glove box. To the above mixture in the tube was added isopropanol (1.5 mL). The resultant reaction mixture in the tube was immersed in a preheated oil bath at 100 °C and stirred for 12 h. At ambient temperature, the reaction mixture was diluted with EtOAc (5.0 mL) and the volatiles were evaporated *in vacuo*. The remaining residue was purified by column chromatography on silica gel (petroleum ether/EtOAc: 5/1) to yield **6a** (0.033

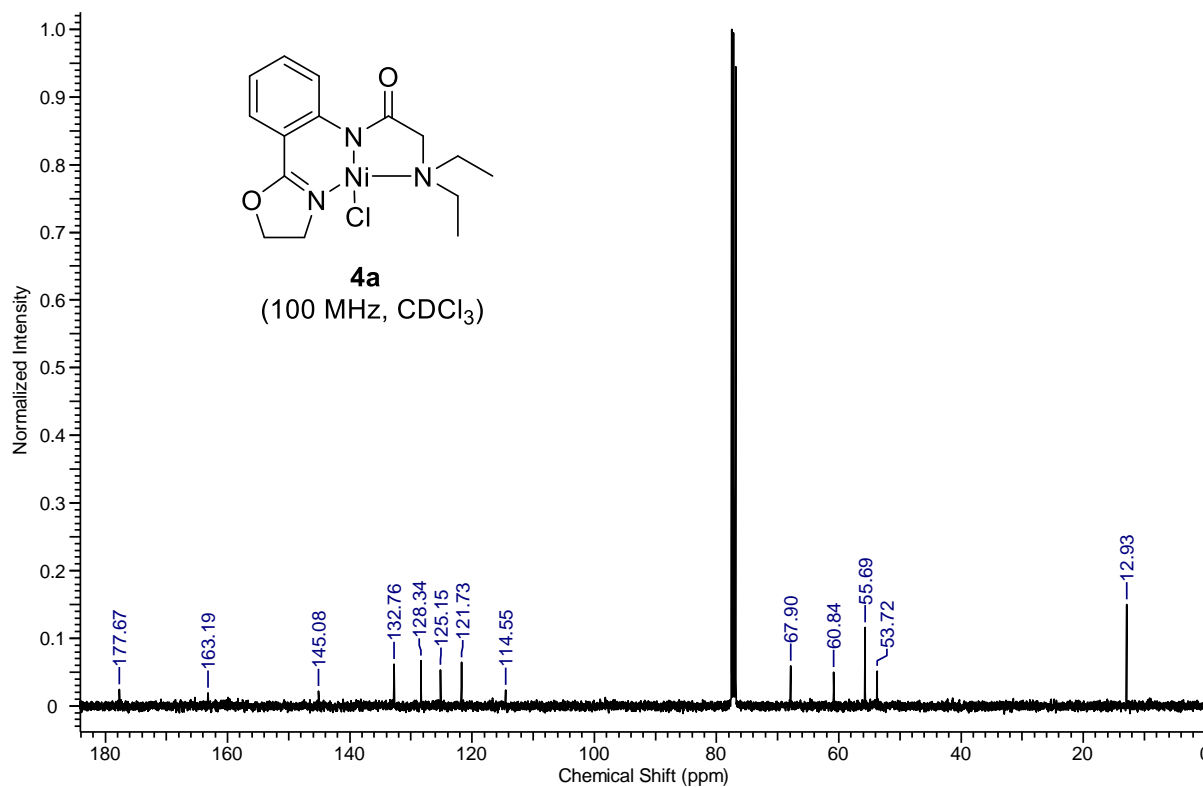
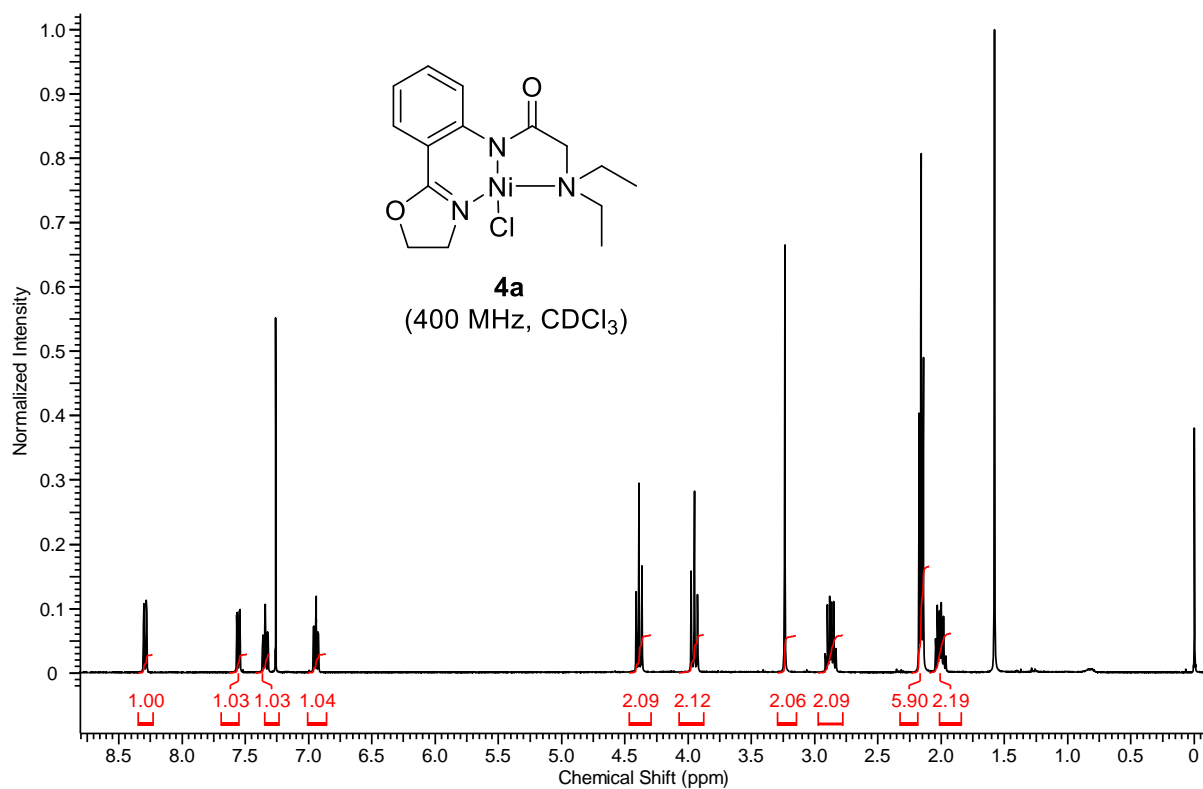
g, 90%) as a colourless liquid. $^1\text{H-NMR}$ (400 MHz, CDCl_3): $\delta = 7.37\text{--}7.32$ (m, 4H, Ar-H), 7.28–7.24 (m, 1H, Ar-H), 4.88 (q, $J = 6.8$ Hz, 1H, CH), 2.09 (br s, 1H, OH), 1.46 (d, $J = 6.8$ Hz, 3H, CH_3). $^{13}\text{C}\{^1\text{H}\}\text{-NMR}$ (100 MHz, CDCl_3): $\delta = 145.9$ (C_q), 128.6 (CH), 127.5 (CH), 125.5 (3C, CH), 70.5 (CH), 25.2 (CH_3).

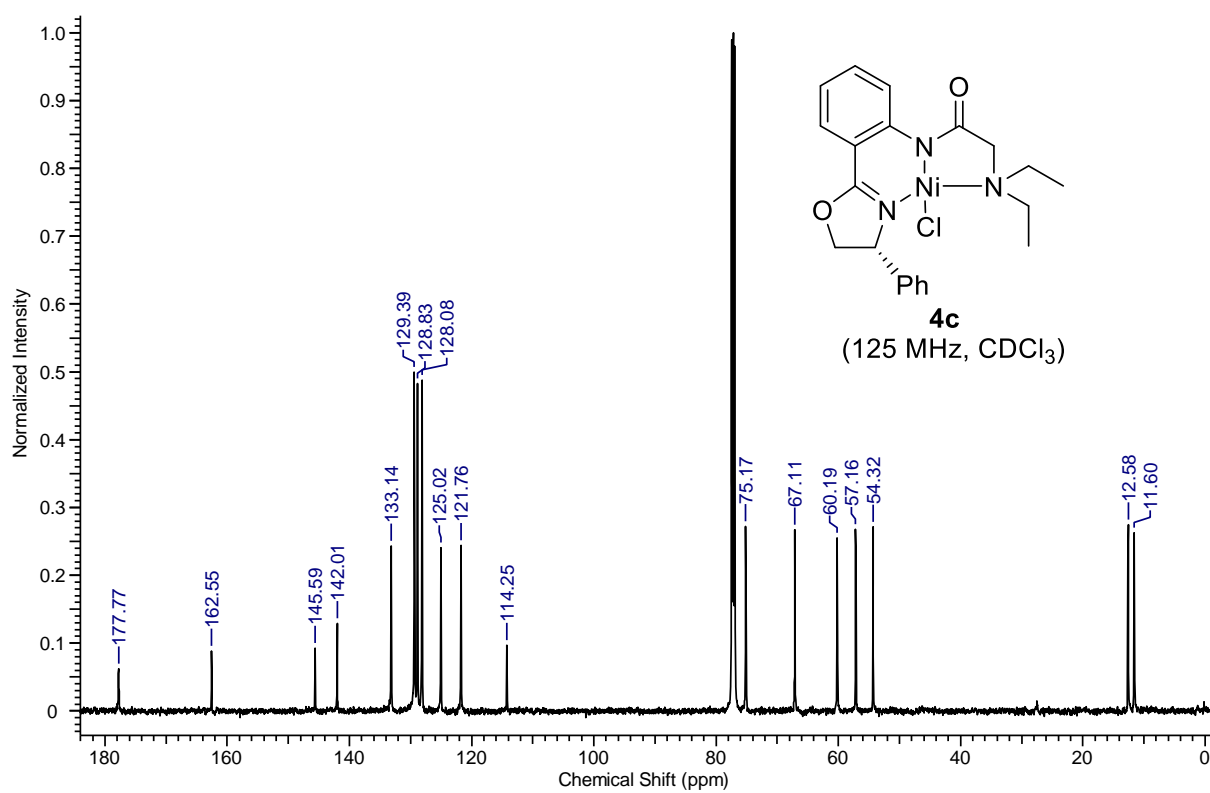
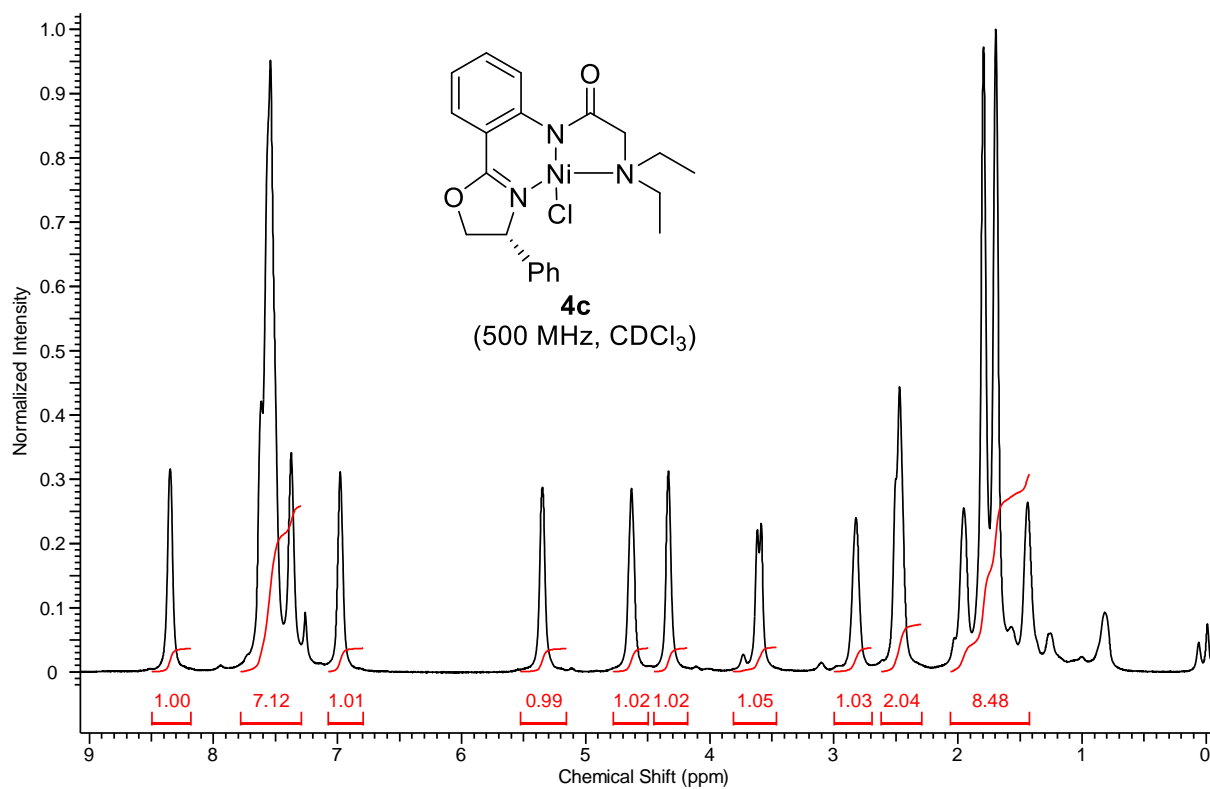
5.4.5 X-ray Structure Analysis

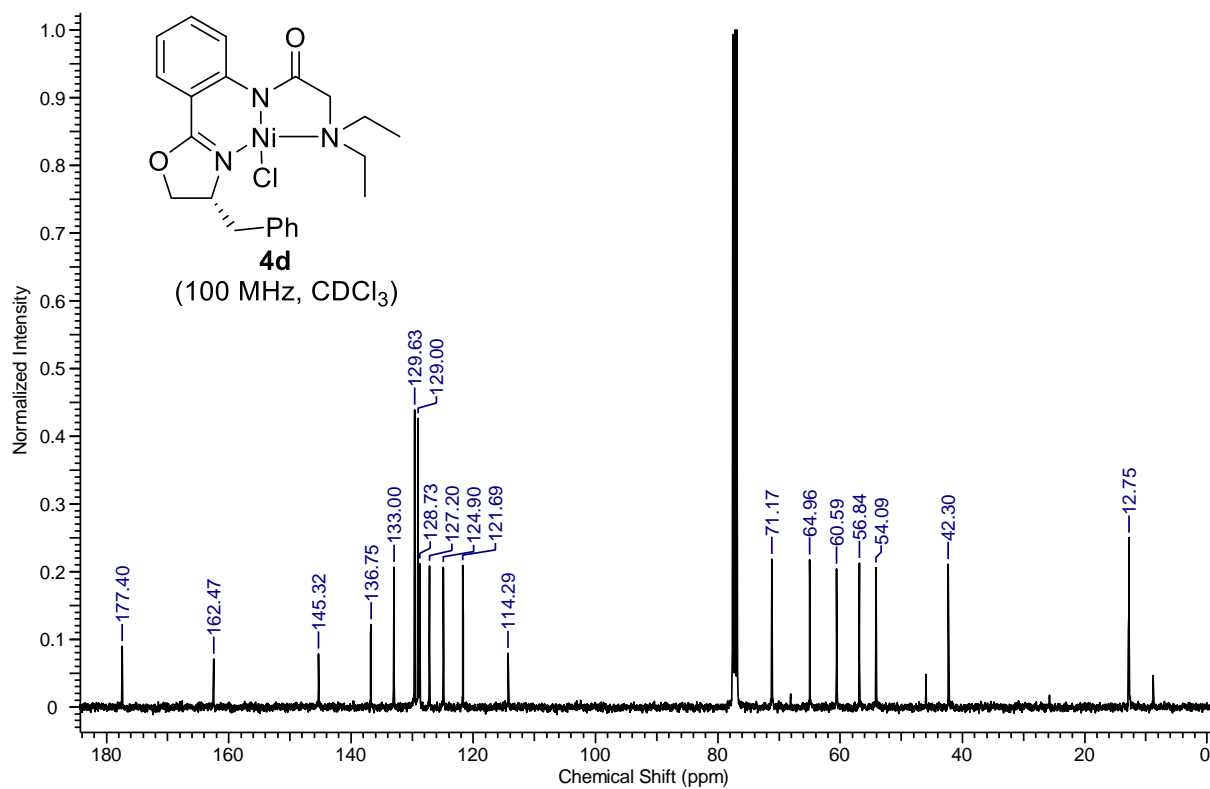
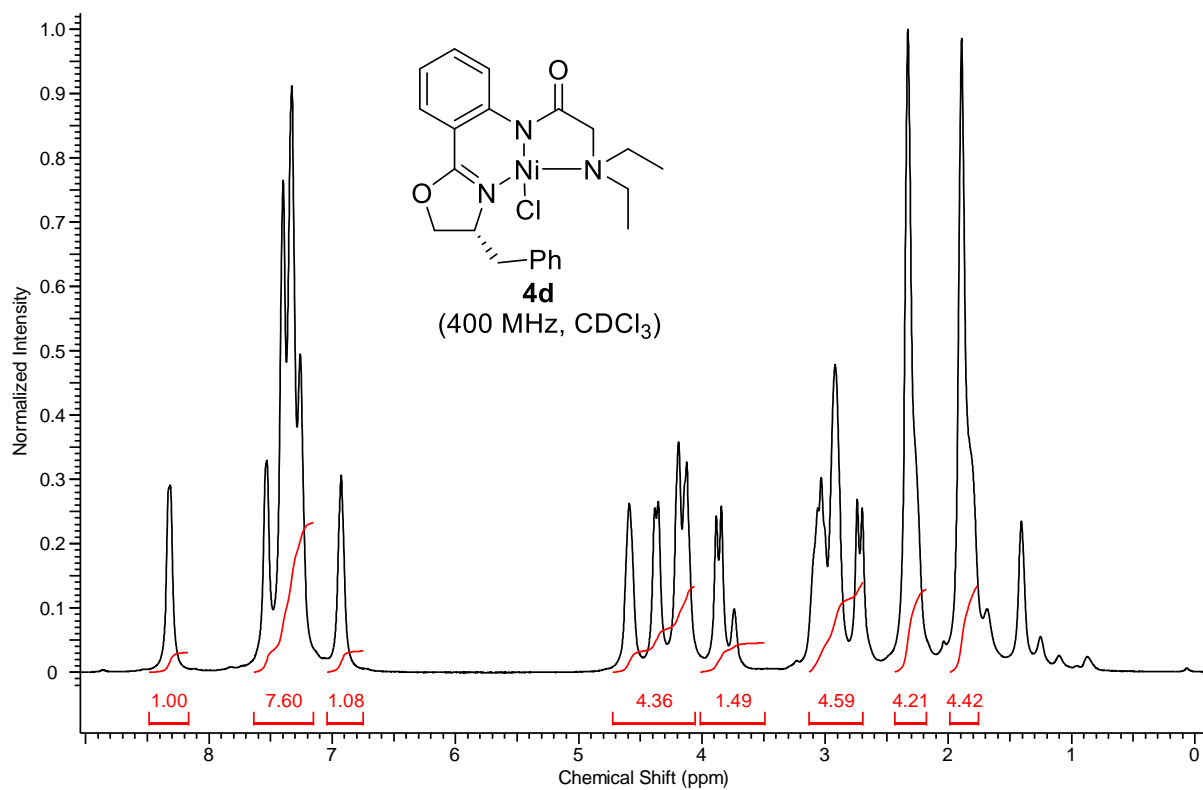
X-ray intensity data measurement of compounds **4a**, **4d** and **4f** was carried out on a Bruker D8 VENTURE Kappa Duo PHOTON II CPAD diffractometer equipped with Incoatech multilayer mirrors optics. The intensity measurements were carried out with Mo micro-focus sealed tube diffraction source ($\text{MoK}\alpha = 0.71073 \text{ \AA}$) at 100(2) K temperature. The X-ray generator was operated at 50 kV and 1.4 mA. A preliminary set of cell constants and an orientation matrix were calculated from three matrix sets of 36 frames (each matrix run consists of 12 frames). Data were collected with ω scan width of 0.5° at different settings of φ and 2θ with a frame time of 10-20 sec depending on the diffraction power of the crystals keeping the sample-to-detector distance fixed at 5.00 cm. The X-ray data collection was monitored by APEX3 program (Bruker, 2016).⁹² All the data were corrected for Lorentzian, polarization and absorption effects using SAINT and SADABS programs (Bruker, 2016). Using the APEX3 (Bruker) program suite, the structure was solved with the ShelXS-97 (Sheldrick, 2008)⁹³ structure solution program, using direct methods. The model was refined with a version of ShelXL-2018/3 (Sheldrick, 2015)⁹⁴ using Least Squares minimization. All the hydrogen atoms were placed in a geometrically idealized position and constrained to ride on its parent atoms. An ORTEP III⁹⁵ view of the compounds was drawn with 50% probability displacement ellipsoids, and H atoms are shown as small spheres of arbitrary radii. Crystal data for the structures have been deposited in the Cambridge Crystallographic Data Center with numbers (compound numbers) CCDC-2074093 (**4a**), CCDC-2074094 (**4d**) and CCDC-2074095 (**4f**).

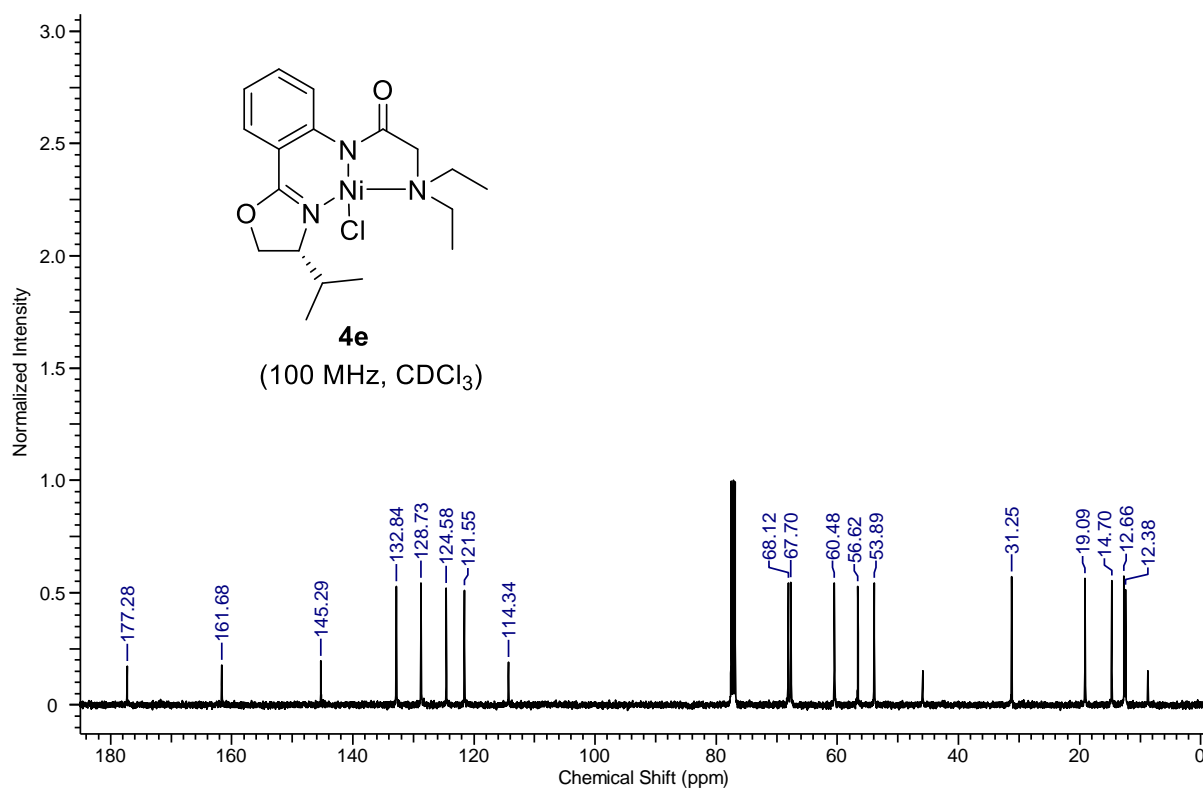
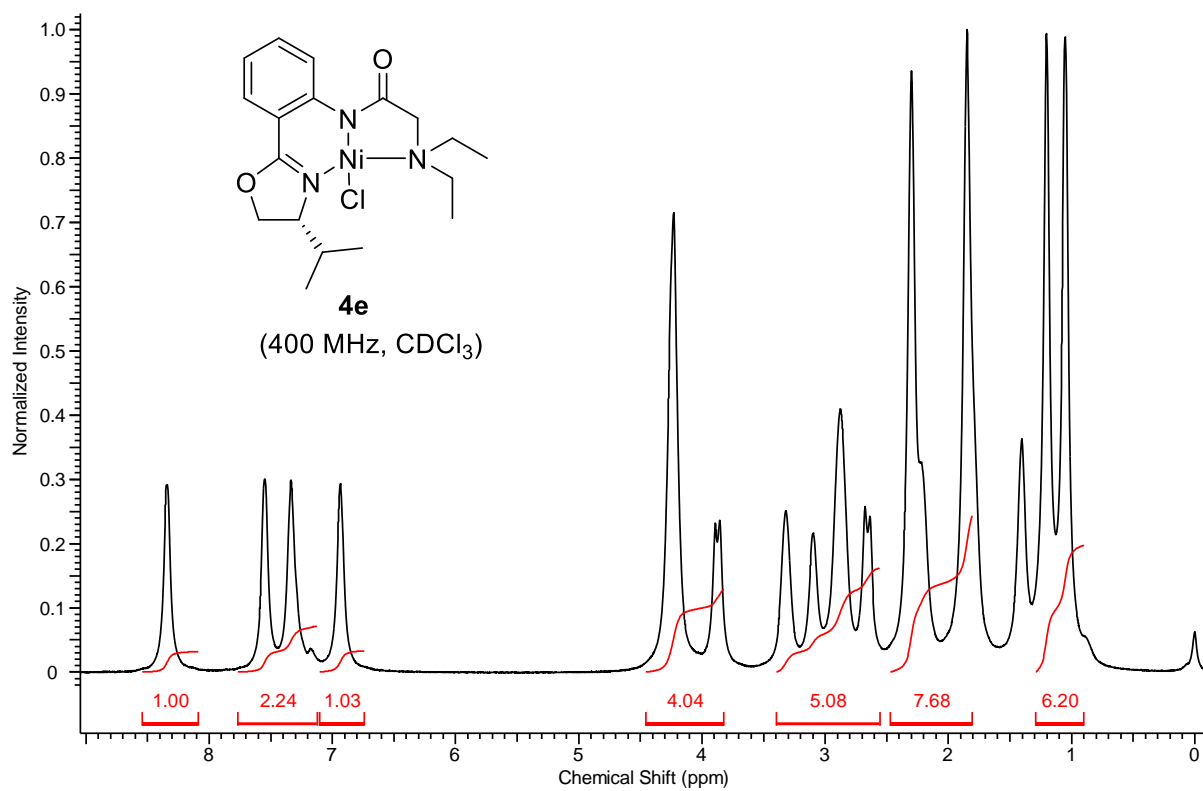
Table 5.3. Crystal data of complexes **4a**, **4d** and **4f**.

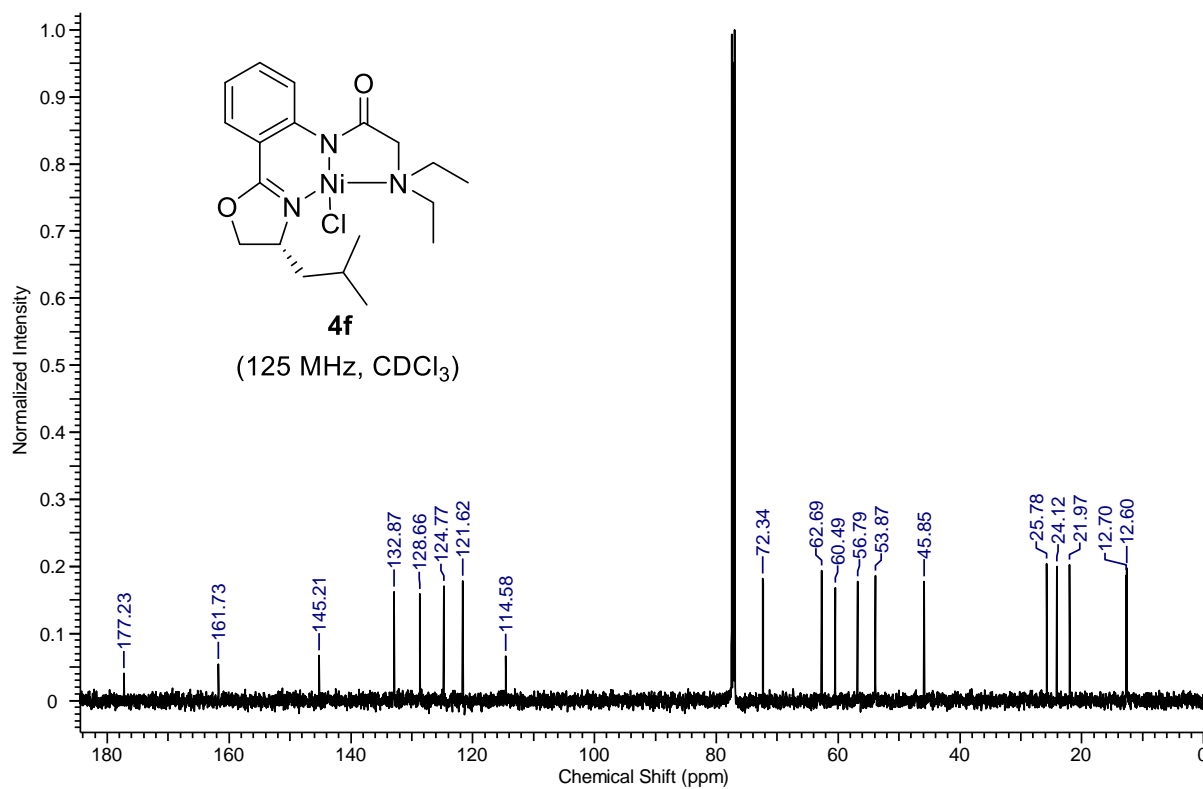
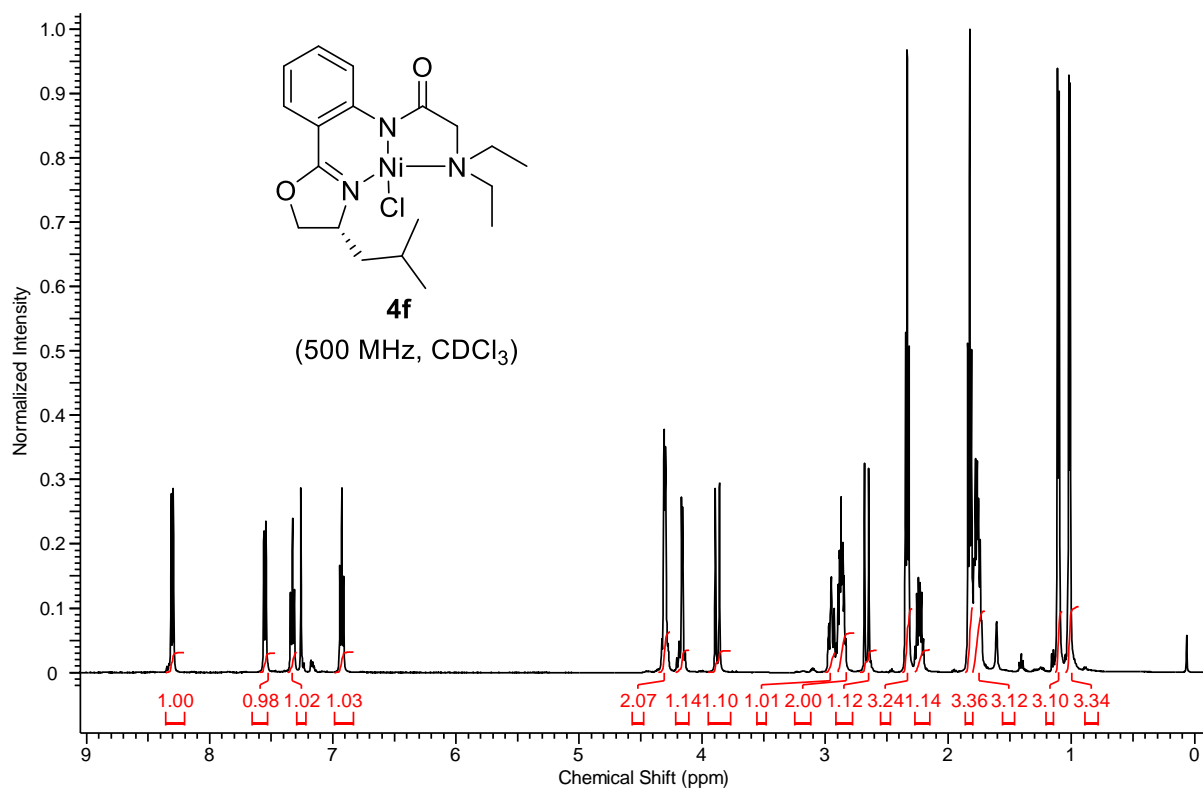
Crystal Data	4a	4d	4f
Formula	C ₁₅ H ₂₀ ClN ₃ NiO ₂	C ₂₂ H ₂₆ ClN ₃ NiO ₂	C ₁₉ H ₂₈ ClN ₃ NiO ₂
Molecular weight	368.50	458.62	424.60
Crystal Size, mm	0.158 × 0.138 × 0.041	0.21 × 0.15 × 0.03	0.20 × 0.17 × 0.05
Temp. (K)	100(2)	100(2)	100(2)
Wavelength (Å)	0.71073	0.71073	0.71073
Crystal Syst.	orthorhombic	orthorhombic	orthorhombic
Space Group	<i>Pbca</i>	<i>P2₁2₁2₁</i>	<i>P2₁2₁2₁</i>
<i>a</i> (Å)	16.793(3)	9.9695(4)	9.7315(3)
<i>b</i> (Å)	9.9261(18)	10.0137(3)	9.8437(3)
<i>c</i> (Å)	19.198(4)	21.4431(7)	21.1840(7)
<i>V</i> /Å ³	3200.2(10)	2140.70(13)	2029.30(11)
<i>Z</i>	8	4	4
<i>D</i> _{calc} /g cm ⁻³	1.530	1.423	1.390
<i>μ</i> /mm ⁻¹	1.389	1.054	1.105
<i>F</i> (000)	1536	960	896
<i>Ab. Correct.</i>	multi-scan	multi-scan	multi-scan
<i>T</i> _{min} / <i>T</i> _{max}	0.819/0.945	0.809/0.969	0.809/0.947
2 θ _{max}	60	69.26	62
Total reflns.	41734	44424	36549
Unique reflns.	4658	8381	6183
Obs. reflns.	4192	7601	6036
<i>h, k, l</i> (min, max)	(-23, 23), (-12, 13), (-25, 27)	(-14, 15), (-15, 15), (-34, 33)	(-13, 13), (-14, 14), (-30, 30)
<i>R</i> _{int} / <i>R</i> _{sig}	0.0329/0.0165	0.0362/0.0349	0.0240/0.0249
No. of para.	201	264	245
<i>RI</i> [<i>I</i> > 2 σ (<i>I</i>)]	0.0231	0.0264	0.0187
<i>wR2</i> [<i>I</i> > 2 σ (<i>I</i>)]	0.0552	0.0557	0.0481
<i>RI</i> [all data]	0.0272	0.0338	0.0193
<i>wR2</i> [all data]	0.0575	0.0585	0.0483
goodness-of-fit	1.028	1.036	1.030
$\Delta\rho$ _{max} , $\Delta\rho$ _{min} (eÅ ⁻³)	+0.456, -0.461	+0.254, -0.369	+0.305, -0.295
CCDC No.	2074093	2074094	2074095

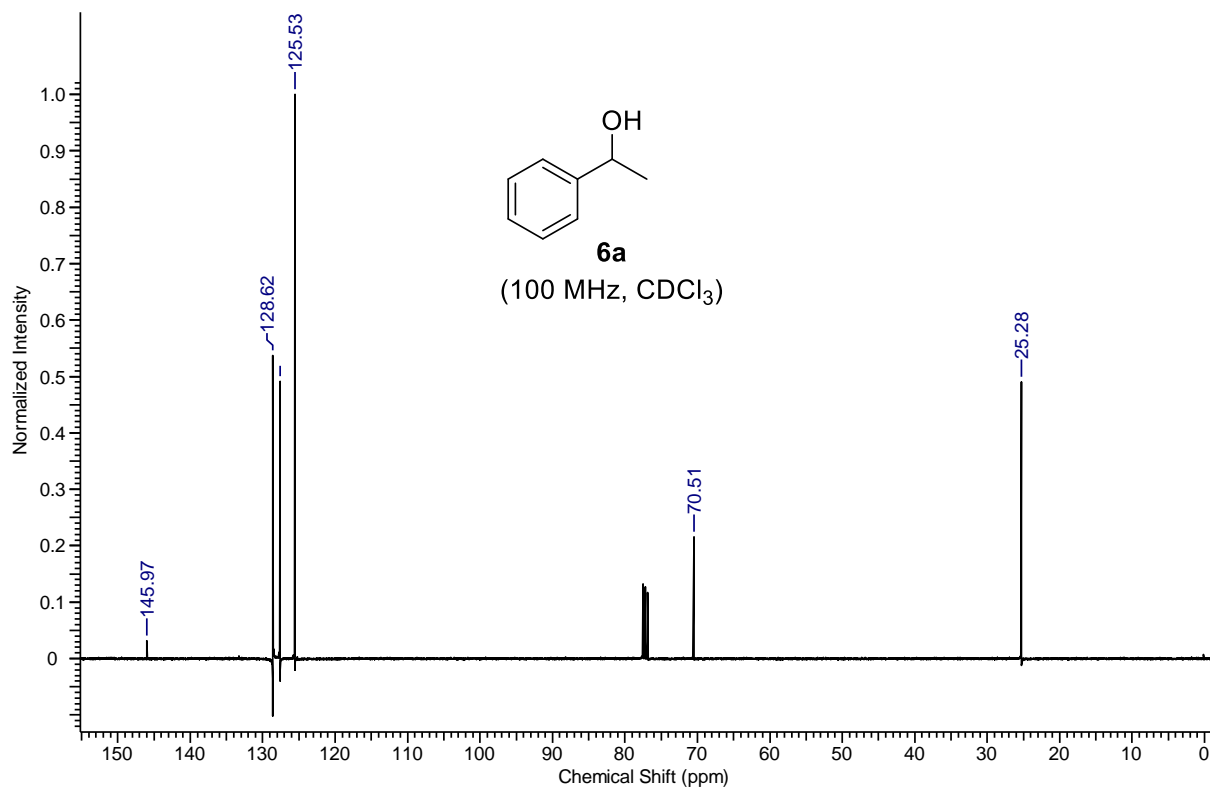
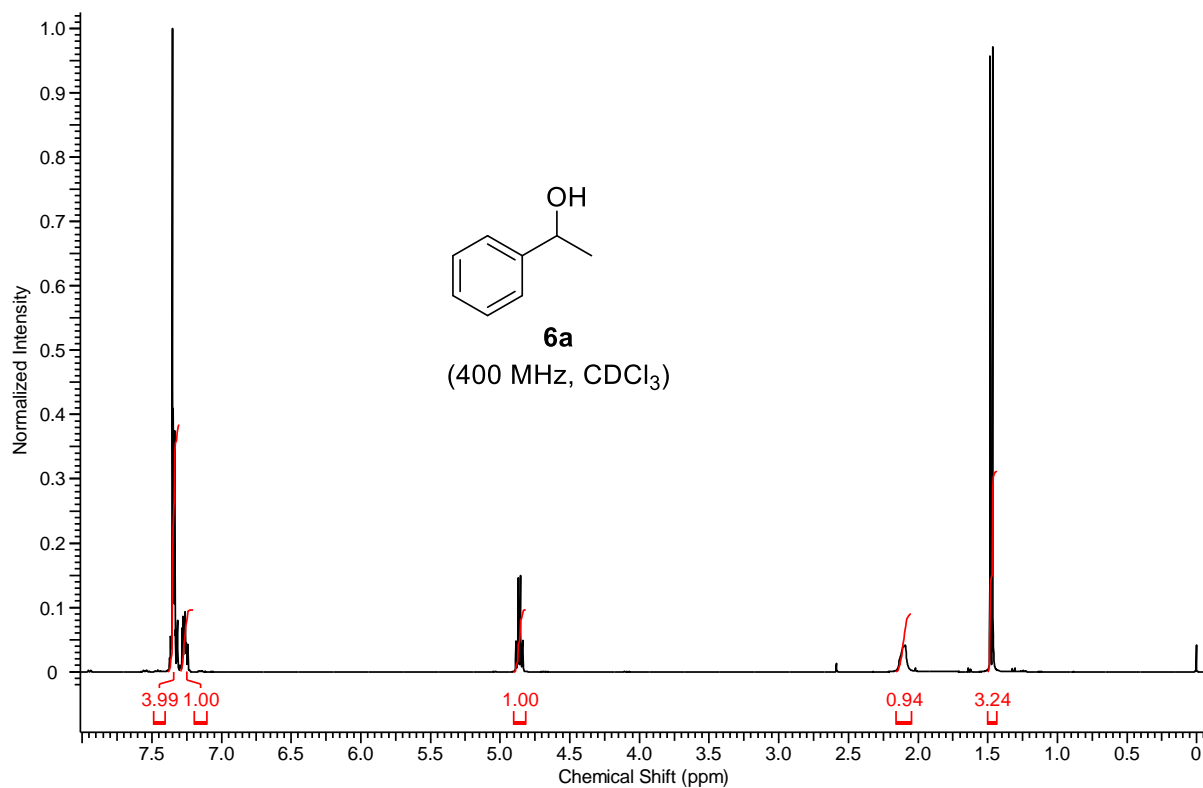
5.4.6 ^1H and ^{13}C NMR Spectra of Nickel Complexes









5.4.7 ^1H and ^{13}C NMR Spectra of 6a.

5.5 REFERENCES

- (1) van der Boom, M. E.; Milstein, D. *Chem. Rev.* **2003**, *103*, 1759-1792.
- (2) D. Morales-Morales and C. M. Jensen, *The Chemistry of Pincer Compounds*, Elsevier, Amsterdam, **2007**.
- (3) M O'Reilly, M. E.; Veige, A. S. *Chem. Soc. Rev.* **2014**, *43*, 6325-6369.
- (4) Asay, M.; Morales-Morales, D. *Dalton Trans.* **2015**, *44*, 17432-17447.
- (5) Albrecht, M.; van Koten, G. *Angew. Chem. Int. Ed.* **2001**, *40*, 3750-3781.
- (6) Selander, N.; Szabó, K. J. *Chem. Rev.* **2011**, *111*, 2048-2076.
- (7) Niu, J.-L.; Hao, X.-Q.; Gong, J.-F.; Song, M.-P. *Dalton Trans.* **2011**, *40*, 5135-5150.
- (8) Wang, Z.-X.; Liu, N. *Eur. J. Inorg. Chem.* **2012**, *2012*, 901-911.
- (9) D. Zargarian, A. Castonguay and D. M. Spasyuk, *Top. Organomet. Chem.*, **2013**, *40*, 131-174.
- (10) Chakraborty, S.; Bhattacharya, P.; Dai, H.; Guan, H. *Acc. Chem. Res.* **2015**, *48*, 1995-2003.
- (11) Shi, R.; Zhang, Z.; Hu, X. *Acc. Chem. Res.* **2019**, *52*, 1471-1483.
- (12) Arora, V.; Narjinari, H.; Nandi, P. G.; Kumar, A. *Dalton Trans.* **2021**, *50*, 3394-3428.
- (13) Moulton, C. J.; Shaw, B. L. *J. Chem. Soc. Dalton Trans.* **1976**, 1020-1024
- (14) van der Boom, M. E.; Liou, S.-Y.; Shimon, L. J. W.; Ben-David, Y.; Milstein, D. *Inorg. Chim. Acta* **2004**, *357*, 4015-4023.
- (15) Benito-Garagorri, D.; Becker, E.; Wiedermann, J.; Lackner, W.; Pollak, M.; Mereiter, K.; Kisala, J.; Kirchner, K. *Organometallics* **2006**, *25*, 1900-1913.
- (16) Castonguay, A.; Beauchamp, A. L.; Zargarian, D. *Organometallics* **2008**, *27*, 5723-5732.
- (17) Castonguay, A.; Beauchamp, A. L.; Zargarian, D. *Inorg. Chem.* **2009**, *48*, 3177-3184.
- (18) Castonguay, A.; Spasyuk, D. M.; Madern, N.; Beauchamp, A. L.; Zargarian, D. *Organometallics* **2009**, *28*, 2134-2141.
- (19) Schmeier, T. J.; Hazari, N.; Incarvito, C. D.; Raskatov, J. A. *Chem. Commun.* **2011**, *47*, 1824-1826.

-
- (20) Schmeier, T. J.; Nova, A.; Hazari, N.; Maseras, F. *Chem. Eur. J.* **2012**, *18*, 6915-6927.
- (21) Gómez-Benítez, V.; Baldovino-Pantaleón, O.; Herrera-Álvarez, C.; Toscano, R.; Morales-Morales, D. *Tetrahedron Letters* **2006**, *47*, 5059-5062.
- (22) Pandarus, V.; Zargarian, D. *Organometallics* **2007**, *26*, 4321-4334.
- (23) Pandarus, V.; Zargarian, D. *Chem. Commun.* **2007**, 978-980.
- (24) Chakraborty, S.; Krause, J. A.; Guan, H. *Organometallics* **2009**, *28*, 582-586.
- (25) Chakraborty, S.; Zhang, J.; Krause, J. A.; Guan, H. *J. Am. Chem. Soc.* **2010**, *132*, 8872-8873.
- (26) Zhang, J.; Medley, C. M.; Krause, J. A.; Guan, H. *Organometallics* **2010**, *29*, 6393-6401.
- (27) Lefèvre, X.; Durieux, G.; Lesturgez, S.; Zargarian, D. *J. Mol. Catal. A: Chem.* **2011**, *335*, 1-7.
- (28) Salah, A. B.; Offenstein, C.; Zargarian, D. *Organometallics* **2011**, *30*, 5352-5364.
- (29) Salah, A. B.; Zargarian, D. *Dalton Trans.* **2011**, *40*, 8977-8985.
- (30) Chakraborty, S.; Patel, Y. J.; Krause, J. A.; Guan, H. *Angew. Chem. Int. Ed.* **2013**, *52*, 7523-7526.
- (31) Chakraborty, S.; Zhang, J.; Patel, Y. J.; Krause, J. A.; Guan, H. *Inorg. Chem.* **2013**, *52*, 37-47.
- (32) J. Hao, B. Vabre, B. Mougang-Soume' and D. Zargarian, *Chem. Eur. J.*, **2014**, *20*, 12544-12552.
- (33) Vabre, B.; Petiot, P.; Declercq, R.; Zargarian, D. *Organometallics* **2014**, *33*, 5173-5184.
- (34) Liu, T.; Meng, W.; Ma, Q.-Q.; Zhang, J.; Li, H.; Li, S.; Zhao, Q.; Chen, X. *Dalton Trans.* **2017**, *46*, 4504-4509.
- (35) Grove, D. M.; Van Koten, G.; Zoet, R.; Murrall, N. W.; Welch, A. J. *J. Am. Chem. Soc.* **1983**, *105*, 1379-1380.
- (36) Grove, D. M.; Van Koten, G.; Ubbels, H. J. C.; Zoet, R.; Spek, A. L. *Organometallics* **1984**, *3*, 1003-1009.
- (37) Gossage, R. A.; van de Kuil, L. A.; van Koten, G. *Acc. Chem. Res.* **1998**, *31*, 423-431.

- (38) Torresan, I.; Michelin, R. A.; Marsella, A.; Zanardo, A.; Pinna, F.; Strukul, G. *Organometallics* **1991**, *10*, 623-631.
- (39) Shao, D.-D.; Niu, J.-L.; Hao, X.-Q.; Gong, J.-F.; Song, M.-P. *Dalton Trans.* **2011**, *40*, 9012-9019.
- (40) Zhang, J.; Gao, W.; Lang, X.; Wu, Q.; Zhang, L.; Mu, Y. *Dalton Trans.* **2012**, *41*, 9639-9645.
- (41) Cloutier J. P.; Vabre B.; Mougang-Soume' B; and Zargarian D., *Organometallics*, **2015**, *34*, 133–145.
- (42) Spasyuk, D. M.; Zargarian, D.; van der Est, A. *Organometallics* **2009**, *28*, 6531-6540.
- (43) Spasyuk D. M.; and Zargarian D. *Inorg. Chem.*, **2010**, *49*, 6203–6213.
- (44) Zhang, B.-S.; Wang, W.; Shao, D.-D.; Hao, X.-Q.; Gong, J.-F.; Song, M.-P. *Organometallics* **2010**, *29*, 2579-2587.
- (45) Niu, J.-L.; Chen, Q.-T.; Hao, X.-Q.; Zhao, Q.-X.; Gong, J.-F.; Song, M.-P. *Organometallics* **2010**, *29*, 2148-2156.
- (46) Yang, M.-J.; Liu, Y.-J.; Gong, J.-F.; Song, M.-P. *Organometallics* **2011**, *30*, 3793-3803.
- (47) Mougang-Soumé, B.; Belanger-Gariépy, F.; Zargarian, D. *Organometallics* **2014**, *33*, 5990-6002.
- (48) Smith, J. B.; Miller, A. J. M. *Organometallics* **2015**, *34*, 4669-4677.
- (49) Suh, H.-W.; Schmeier, T. J.; Hazari, N.; Kemp, R. A.; Takase, M. K. *Organometallics* **2012**, *31*, 8225-8236.
- (50) Vasudevan, K. V.; Scott, B. L.; Hanson, S. K. *Eur. J. Inorg. Chem.* **2012**, *2012*, 4898-4906.
- (51) Grüger, N.; Rodríguez, L.-I.; Wadepohl, H.; Gade, L. H. *Inorg. Chem.* **2015**, *52*, 2050-2059.
- (52) Vogt, M.; Rivada-Wheelaghan, O.; Iron, M. A.; Leitus, G.; Diskin-Posner, Y.; Shimon, L. J. W.; Ben-David, Y.; Milstein, D. *Organometallics* **2013**, *32*, 300-308.
- (53) Venkanna, G. T.; Tammineni, S.; Arman, H. D.; Tonzetich, Z. J. *Organometallics* **2013**, *32*, 4656-4663.

- (54) Tu, T.; Mao, H.; Herbert, C.; Xu, M.; Dötz, K. H. *Chem. Commun.* **2010**, *46*, 7796-7798.
- (55) Yang, Z.; Liu, D.; Liu, Y.; Sugiya, M.; Imamoto, T.; Zhang, W. *Organometallics*, **2015**, *34*, 1228-1237.
- (56) Schneck, F.; Finger, M.; Tromp, M.; Schneider, S. *Chem. Eur. J.* **2016**, *23*, 33-37.
- (57) Inamoto K.; Kuroda J.i.; Hiroya K.; Noda Y.; Watanabe M.; and Sakamoto T. *Organometallics*, **2006**, *25*, 3095–3098.
- (58) Inamoto K.; Kuroda J.-I.; Kwon E.; Hiroya K.; and Doi T. *J. Organomet. Chem.*, **2009**, *694*, 389–396.
- (59) Kuroda J.-I.; Inamoto K.; Hiroya K.; and Doi T. *Eur. J. Org. Chem.*, **2009**, 2251–2261.
- (60) Peris E.; and Crabtree R. H. *Coord. Chem. Rev.*, **2004**, *248*, 2239–2246.
- (61) Liu A.; Zhang X.; and Chen W. *Organometallics*, **2009**, *28*, 4868–4871.
- (62) Wang, Z.; Li, X.; Xie, S.; Zheng, T.; Sun, H. *Appl. Organometal. Chem.* **2019**, *33*, e4932
- (63) Segizbayev, M.; Öztopçu, Ö.; Hayrapetyan, D.; Shakhman, D.; Lyssenko, K. A.; Khalimon, A. Y. *Dalton Trans.* **2020**, *49*, 11950-11957.
- (64) Csok, Z.; Vechorkin, O.; Harkins, S. B.; Scopelliti, R.; Hu, X. *J. Am. Chem. Soc.* **2008**, *130*, 8156-8157.
- (65) Vechorkin, O.; Barmaz, D.; Proust, V.; Hu, X. *J. Am. Chem. Soc.* **2009**, *131*, 12078-12079.
- (66) Vechorkin, O.; Proust, V.; Hu, X. *J. Am. Chem. Soc.* **2009**, *131*, 9756-9766.
- (67) Vechorkin, O.; Hu, X. *Angew. Chem. Int. Ed.* **2009**, *48*, 2937-2940.
- (68) Vechorkin O.; Proust V.; and Hu X., *Angew. Chem., Int. Ed.*, **2010**, *49*, 3061–3064.
- (69) Vechorkin O., Godinat A.; Scopelliti R.; and Hu X. *Angew. Chem., Int. Ed.*, **2011**, *50*, 11777–11781.
- (70) Buslov, I.; Becouse, J.; Mazza, S.; Montandon-Clerc, M.; Hu, X. *Angew. Chem. Int. Ed.* **2015**, *54*, 14523-14526.
- (71) Pérez García, P. M.; Ren, P.; Scopelliti, R.; Hu, X. *ACS Catal.* **2015**, *5*, 1164-1171.

- (72) Perez Garcia, P. M.; Di Franco, T.; Epenoy, A.; Scopelliti, R.; Hu, X. *ACS Catal.* **2016**, *6*, 258-261.
- (73) Soni, V.; Jagtap, R. A.; Gonnade, R. G.; Punji, B. *ACS Catal.* **2016**, *6*, 5666-5672.
- (74) Patel, U. N.; Pandey, D. K.; Gonnade, R. G.; Punji, B. *Organometallics* **2016**, *35*, 1785-1793.
- (75) Soni, V.; Khake, S. M.; Punji, B. *ACS Catal.* **2017**, *7*, 4202-4208.
- (76) Jagtap R. A.; Soni V.; and Punji B. *ChemSusChem*, **2017**, *10*, 2242–2248.
- (77) Patel U. N.; Jain S.; Pandey D. K.; Gonnade R. G.; Vanka K.; and Punji B. *Organometallics*, **2018**, *37*, 1017–1025.
- (78) Pandiri H.; Soni V.; Gonnade R. G.; and Punji B. *New J. Chem.*, **2017**, *41*, 3543–3554.
- (79) Shang, M.; Sun, S.-Z.; Dai, H.-X.; Yu, J.-Q. *J. Am. Chem. Soc.* **2014**, *136*, 3354-3357.
- (80) Luo M. *Curr. Org. Synth.*, **2015**, *12*, 660–672.
- (81) Mukhina O. A.; and Kutateladze A. G. *J. Am. Chem. Soc.*, **2016**, *138*, 2110–2113.
- (82) Herasymchuk, K.; Huynh, J.; Lough, A. J.; Roces Fernández, L.; Gossage, R. A. *Synthesis* **2016**, *48*, 2121-2129.
- (83) Li, Y.-Y.; Yu, S.-L.; Shen, W.-Y.; Gao, J.-X. *Acc. Chem. Res.* **2015**, *48*, 2587-2598.
- (84) Yang P.; Xu H.; and Zhou J. *Angew. Chem., Int. Ed.*, **2014**, *53*, 12210–12213.
- (85) Xu H.; Yang P.; Chuanprasit P.; Hirao H.; and Zhou J. *Angew. Chem., Int. Ed.*, **2015**, *54*, 5112–5116.
- (86) Shevlin M.; Friedfeld M. R.; Sheng H.; Pierson N. A.; Hoyt J. M.; Campeau L.-C.; and Chirik P. J. *J. Am. Chem. Soc.*, **2016**, *138*, 3562–3569.
- (87) Long J.; Gao W.; Guan Y.; Lv H.; and Zhang X. *Org. Lett.*, **2018**, *20*, 5914–5917.
- (88) Liu Y.; Yi Z.; Yang X.; Wang H.; Yin C.; Wang M.; Dong X.-Q.; and Zhang X. *ACS Catal.*, **2020**, *10*, 11153–11161.
- (89) Du, W.; Wu, P.; Wang, Q.; Yu, Z. *Organometallics* **2013**, *32*, 3083-3090.
- (90) Du W.; Wang Q.; Wang L.; and Yu Z. *Organometallics*, **2014**, *33*, 974–982.

- (91) Li K.; Niu J.-L.; Yang M.-Z.; Li Z.; Wu L.-Y.; Hao X.-Q.; and Song M.-P. *Organometallics*, **2015**, *34*, 1170–1176.
- (92) Bruker (**2016**). APEX2, SAINT and SADABS. Bruker AXS Inc., Madison, Wisconsin, USA.
- (93) Sheldrick G. M. *Acta Crystallogr.*, **2008**, *A64*, 112.
- (94) Sheldrick G. M. *Acta Crystallogr.*, **2015**, *C71*, 3–8.
- (95) Farrugia L. J. *J. Appl. Crystallogr.* **2012**, *45*, 849–854.

Chapter-6

Summary and Outlook

6.1 SUMMARY

The Thesis described our efforts to the development of novel methodologies for 3d metal-catalyzed functionalization of heteroarenes and hydrogenation of ketones. We could successfully demonstrate the intramolecular C(sp²)-H/C-(sp³)-H oxidative coupling to synthesize cycloindolones, hydrocarbazolones, and indenoindolones for the first time using a nickel catalyst. Similarly, nickel-catalyzed alkylation of indoles and Fe-catalyzed synthesis of 3-substituted 3-amino oxindoles were elaborately discussed. Moreover, pincer-ligated nickel complexes were developed and employed in the transfer hydrogenation reaction. Additionally, detailed mechanistic studies were performed for all the protocols to understand the reaction pathways, which could help in the future development of efficient and novel catalytic systems.

In Chapter 1, we have summarized recent developments in the field of base metal-catalyzed functionalization of heteroarenes and hydrogenation reactions. This chapter mainly highlights the Mn, Fe, Co, Ni, and Cu-catalyzed recent developments in C-H functionalization of heteroarenes. Chapter-2 describes an efficient method for nickel-catalyzed intramolecular C(sp²)-H/C(sp³)-H and C(sp²)-H/C(sp²)-H oxidative coupling in indoles *via* monodentate chelation assistance. This reaction provided a direct approach for the synthesis of diversely functionalized, biologically relevant indolones in high yields and good chemoselectivity. An extensive mechanistic investigation by various controlled experiments, kinetic analysis, deuterium labeling experiments, and DFT calculations revealed a facile indole's C(2)-H nickelation and a rate-limiting reductive elimination process. This intramolecular oxidative cyclization operates via a probable Ni(II)/Ni(III) pathway involving a single-electron transfer (SET) process.

In chapter-3, a straightforward nickel-catalyzed protocol for the regioselective C(2)-H bond alkylation of indoles and other heteroarenes with a wide range of alkenes is discussed. The current protocol showed the coupling of diverse aromatic alkenes with heteroarenes including indole, imidazole, and benzimidazole derivatives and provided moderate to excellent yields of alkylated products. This nickel-catalyzed reaction exclusively provided the Markovnikov selective alkylated products. Preliminary mechanistic studies suggested a single-electron transfer (SET) pathway for the reaction.

To extend our studies for the development of novel methods for the functionalization of heteroarenes, Chapter-4 highlights an efficient method for the straightforward synthesis of 3,3-disubstituted-3-amino-2-oxindoles with the generation of a stereogenic quaternary center in the presence of inexpensive iron(III) catalyst. The reaction conceded the coupling of

diversely substituted *N*-methoxy benzamides with isatin derivatives and provided various biologically relevant 3-substituted-3-amino oxindoles in presence of a simple iron(III) salt. An extensive mechanistic investigation by experiments and theoretical calculations revealed the reaction proceeds *via* the formation of isatin ketimine and *N*-(hydroxymethyl)benzamide intermediates. The scalability of this protocol was demonstrated with a gram-scale reaction. The amination reaction proceeds through a single-electron transfer (SET) process.

Further, we describe the synthesis of new NNN-oxazolinyl-pincer nickel complexes and their application in the transfer hydrogenation of ketones. A range of achiral and chiral NNN-oxazolinyl based ligands and their nickel complexes were synthesized in moderate to good yields. All the synthesized ligand precursors and nickel complexes were thoroughly characterized by NMR spectroscopy, HRMS, and elemental analysis. The single-crystal X-ray diffraction study elucidated the molecular structures of some nickel complexes. The well-defined nickel complexes efficiently catalyzed the transfer hydrogenation of ketones using isopropanol as a hydrogen source.

6.2 OUTLOOK

In the last few decades, significant progress has been achieved to functionalize various heteroarenes employing base metal catalysts. However, many protocols required extreme conditions, such as high temperature, use of a strong base, and the usage of the stoichiometric amount of metal oxidants. Thus, the development of environment-friendly and sustainable methods is essential. Furthermore, the base metal-catalyzed asymmetric functionalization of heteroarenes remains as a challenge in organic synthesis. Hence, there is a need to develop an efficient protocol for the enantioselective C–H alkylation as well as the synthesis of chiral 3-amino oxindoles using base metal catalysts. A design of suitable chiral oxazoline-based amino phosphine ligands or chiral carbene ligands could help in asymmetric transformations. Our studies show that base metal is able to synthesize 3-amino oxindoles, thus, the development of efficient protocols for the synthesis of spirocyclic oxindoles using base metal catalyst would be highly desirable. Moreover, an enantioselective hydrogenation of ketones using chiral nickel complexes is rarely studied. Therefore, the design of a suitable chiral nickel catalyst to achieve chiral synthesis is highly desirable. A rigid NNP- or PNP-pincer ligand system along with nickel precursor could reduce prochiral ketones to achieve chiral alcohols. The outlook of the thesis would help to find a better catalytic system for milder and selective functionalization of heteroarenes and enantioselective hydrogenation reactions.

ABSTRACT

Name of the Student: Shidheshwar Baliram Ankade

Registration No: 10CC18J26001

Faculty of Study: Chemical Science

Year of Submission: 2023

AcSIR academic centre/CSIR Lab: CSIR-NCL

Name of the Supervisor: Dr. Benudhar Punji

Title of the Thesis: “Iron and Nickel-Catalyzed Functionalization of Heteroarenes and Hydrogenation of Ketones”

Chapter 1 deals with the detailed literature survey on recent development for the base metal-catalyzed C–H functionalization of heteroarenes and hydrogenation of ketones. In Chapter 2, the C(sp²)–H/C(sp³)–H and C(sp²)–H/C(sp²)–H intramolecular oxidative couplings in indoles for the synthesis of biologically relevant indolones employing an air-stable and defined nickel catalyst, (bpy)Ni(OAc)₂ have been described. An extensive mechanistic investigation by the controlled study, kinetic analysis, deuterium labeling experiments, and DFT calculations supported a Ni(II)/Ni(III) pathway for the oxidative coupling comprising the rate-limiting reductive elimination process.

An efficient protocol for the C–H alkylation of indoles with alkenes using a nickel catalyst *via* a hydroarylation strategy was achieved under solvent-free conditions (Chapter 3). This method is applicable to both the electron-rich as well as electron-poor indoles providing Markovnikov selective alkylated products. Preliminary mechanistic studies suggested that the alkylation reaction proceeds through a single-electron transfer (SET) pathway.

Chapter 4 deals with the development of an efficient method for the synthesis of 3,3-disubstituted-3-amino-2-oxindoles with the generation of a stereogenic quaternary center in the presence of an iron(III) catalyst. The coupling of *N*-methoxy benzamides with isatin derivatives provided various biologically relevant 3-substituted-3-amino oxindoles. Detailed mechanistic studies revealed that the reaction proceeds *via* the formation of isatin ketimine and *N*-(hydroxymethyl)benzamide intermediates, and the *N*-methoxy group of benzamide is the source of methylene group in products.

Synthesis and characterization of new NNN-oxazolinyl-pincer nickel complexes and their application for the transfer hydrogenation of ketones were described in Chapter 5. A series of achiral and chiral *NNN*-ligands and pincer nickel complexes were synthesized in good yields. All the ligand precursors and nickel complexes were characterized by NMR spectroscopy, HRMS or elemental analysis.

LIST OF PUBLICATIONS

1. **Ankade, S. B.**; Samal, P. P.; Soni, V.; Gonnade, R. G.; Krishnamurty, S.; and Punji, B. “Ni(II)-Catalyzed Intramolecular C–H/C–H Oxidative Coupling: An Efficient Route to Functionalized Cycloindolones and Indenoindolones”, *ACS Catal.* **2021**, *11*, 12384-12393.
2. **Ankade, S. B.**; Shabade, A. B.; Soni, V.; and Punji, B. “Unactivated Alkyl Halides in Transition-Metal-Catalyzed C–H Bond Alkylation”, *ACS Catal.* **2021**, *11*, 3268-3292.
3. Jagtap, R. A.;[‡] **Ankade, S. B.**;[‡] Gonnade, R. G.; and Punji, B. “Achiral and Chiral *NNN*-Pincer Nickel Complexes with Oxazolinyl Backbone: Application in Transfer Hydrogenation of Ketones”, *New J. Chem.* **2021**, *45*, 11927-11936. ([‡]both authors contributed equally)
4. Pandey, D. K.; **Ankade, S. B.**; Ali, A.; Vinod, C. P.; and Punji, B. “Nickel-Catalyzed C–H Alkylation of Indoles with Unactivated Alkyl Chlorides: Evidence of Ni(I)/Ni(III) Pathway”, *Chem. Sci.* **2019**, *10*, 9493-9500.
5. **Ankade, S. B.**; Pradhan, C.; Samal, P. P. R.; Gonnade, G.; Krishnamurty, S.; and Punji, B. “Iron-Catalyzed Synthesis of 3,3-disubstituted 3-Amino Oxindoles: An Efficient Route to the Construction of Quaternary Stereocenter”. *Manuscript Communicated*
6. **Ankade, S. B.**; Banerjee, S.; and Punji, B. “Regioselective C–H Alkylation of Heteroarenes with Alkenes Using Nickel Catalyst”. *Manuscript Communicated*

LIST OF PATENT

1. Punji, B.; **Ankade, S. B.**; and Pradhan, C. “A Stereogenic 3,3-Disubstituted 3-Amino Oxindole Compounds and Process for Preparation Thereof” (*Provisional Patent Filed, 2022*)

LIST OF PUBLICATIONS

AWARDS

1. **2022:** “*Best Research Scholar Award*” in Chemical Science by NCL-Research Foundation for the year 2022.
2. **2022:** “*Best Oral Presentation Award*” at 4th NCL-RF annual student conference held at CSIR-National Chemistry Laboratory, Pune during 29-30 November 2022.
3. **2021:** “*Best Published Research Paper Award*” in organic chemistry by NCL-Research Foundation for the year 2021.
4. **2020:** “*Best poster prize*” for the poster presented in the science day celebration at CSIR- NCL.

LIST OF NATIONAL/INTERNATIONAL CONFERENCES

1. **Ankade, S. B.;** Punji, B. “Iron-Catalyzed Synthesis of 3,3-disubstituted 3-Amino Oxindoles: An Efficient Route to the Construction of Quaternary Stereocenter” *Poster presentation in International Conference on Modern Trends in Inorganic Chemistry (MTIC-XIX) 2022* at department of Chemistry, Banaras Hindu University, Varanasi.
2. **Ankade, S. B.;** Punji, B. “Ni(II)-Catalyzed Intramolecular C–H/C–H Oxidative Coupling: An Efficient Route to Functionalized Cycloindolones and Indenoindolones” *Presentation in 2nd International Workshop on Cutting-Edge Homogeneous Catalysis (CEHC-2) 2022* at Leipzig, Germany. (Online attended)
3. **Ankade, S. B.;** Punji, B. “Ni(II)-Catalyzed Intramolecular C–H/C–H Oxidative Coupling: An Efficient Route to Functionalized Cycloindolones and Indenoindolones” *Presentation in XVII JNOST Conference for Research Scholars 2022* at University of Hyderabad.
4. **Ankade, S. B.;** Punji, B. “Iron-Catalyzed Synthesis of 3,3-disubstituted 3-Amino Oxindoles: An Efficient Route to the Construction of Quaternary Stereocenter” *Presentation in 4th NCL-RF annual student conference 2022* at CSIR-National Chemistry Laboratory, Pune.
5. **Ankade, S. B.;** Punji, B. “Ni(II)-Catalyzed Intramolecular C–H/C–H Oxidative Coupling: An Efficient Route to Functionalized Cycloindolones and Indenoindolones” *Poster presentation in Science Day celebration 2020* at CSIR-National Chemistry Laboratory, Pune.

Ni(II)-Catalyzed Intramolecular C–H/C–H Oxidative Coupling: An Efficient Route to Functionalized Cycloindolones and Indenoindolones

Shidheshwar B. Ankade, Pragnya Paramita Samal, Vineeta Soni, Rajesh G. Gonnade, Sailaja Krishnamurthy, and Benudhar Punji*



Cite This: *ACS Catal.* 2021, 11, 12384–12393



Read Online

ACCESS |



Metrics & More



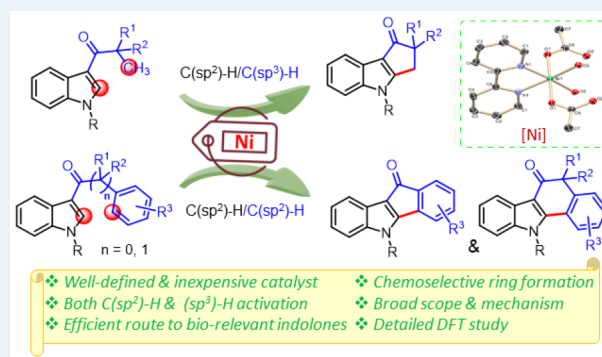
Article Recommendations



Supporting Information

ABSTRACT: Nickel(II)-catalyzed intramolecular C(sp²)-H/C(sp³)-H and C(sp²)-H/C(sp²)-H oxidative couplings in indoles are achieved via chelation assistance. These reactions provide access to biologically relevant five- and six-membered substituted cyclopentaindolones, carbazolones, and indenoindolones in high yields and good chemoselectivity employing an air-stable and defined nickel catalyst, (bpy)Ni(OAc)₂. The oxidative cyclizations proceeded either through a six-membered or an unconventional seven-membered nickelacycle. An extensive mechanistic investigation by experiments and theoretical calculations revealed a facile indole's C(2)-H nickelation and a rate-limiting reductive elimination process. This intramolecular oxidative cyclization operates via a probable Ni(II)/Ni(III) pathway involving single-electron oxidation of nickel without the participation of a carbon-based radical.

KEYWORDS: C–H activation, cycloindolones, indenoindolones, indoles, mechanism, nickel, oxidative coupling



INTRODUCTION

The indole represents a privileged structural motif, embedded in diverse biologically active molecules and natural products, including functional materials.¹ In particular, polycyclic derivatives of indole, possessing five- and six-membered rings, are of great significance due to their enormous pharmacological activities like anticancer,² anti-Alzheimer's disease,³ antihypertensive,⁴ anti-inflammatory⁵ and antimigraine,⁶ inhibitors of protein kinase CK2,⁷ and their direct use in the development of potential therapeutic agents (Scheme 1a).⁸ Therefore, significant effort has been devoted to developing efficient protocols for the site-selective functionalization of indoles.⁹ Most synthetic methods leading to polycyclic indoles rely on sequential multistep process,¹⁰ limiting the creation of substitution-diversity in the final product and/or needed harsh conditions. Recent progress in C–H functionalization led to the synthesis of various chiral and achiral five- and six-membered-ring products via hydrofunctionalization¹¹ or direct intramolecular couplings.¹² Notably, many of these protocols utilize high loading of expensive noble metal catalysts like palladium, rhodium, iridium, and/or acidic reaction conditions.

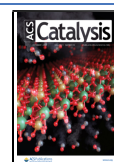
More recently, C–H/C–H oxidative coupling has been established as a powerful tool for building complex molecules from simple precursors,¹³ as it does not necessitate the

prefunctionalization of substrates. Owing to the sustainability and cost advantage,¹⁴ the 3d transition metal catalyst for C(sp²)-H/C(sp²)-H oxidative coupling has been substantially explored.^{13,15} However, the activation and coupling of a more strenuous C(sp³)-H bond continues to remain challenging.¹⁶ Relevant to this work, nickel catalysts have been successfully applied to the C(sp²)-H/C(sp³)-H oxidative couplings in amides.¹⁷ In fact, Chatani reported an oxidative coupling involving a C(sp³)-H bond in toluene derivatives with benzamides in the Ni(II)-catalyzed reaction.¹⁸ Similarly, Cai demonstrated the C(sp³)-H coupling of 1,4-dioxane with C2- and C3-positions of indoles (Scheme 1b).¹⁹ Our group found that a Ni(II) precatalyst can effectively catalyze the C(sp²)-H/C(sp³)-H oxidative coupling of indoles with toluene using 2-iodobutane as a mild oxidant (Scheme 1c).²⁰ Notably, an excess of the C(sp³)-H containing partner is used in these reactions to favor the intermolecular coupling entropically; a privilege that cannot be

Received: July 23, 2021

Revised: September 8, 2021

Published: September 22, 2021




 Cite this: *New J. Chem.*, 2021, 45, 11927

Achiral and chiral NNN-pincer nickel complexes with oxazolinyll backbones: application in transfer hydrogenation of ketones†

 Rahul A. Jagtap,^{‡,ab} Shidheshwar B. Ankade,^{‡,ab} Rajesh G. Gonnade^{id} ^c and Benudhar Punji^{id} ^{*ab}

We describe the synthesis of new NNN-oxazolinyll-pincer nickel complexes and their application in the transfer hydrogenation of ketones. Achiral NNN-ligands, R'_2 -oxazolinyll-2- C_6H_4 -NH-C(O)CH₂NEt₂ [(R'^2 -OxNNN^{Et2})-H; $R' = H$ (**3a**), $R' = Me$ (**3b**)], and chiral ligands, (R)- R' -oxazolinyll-2- C_6H_4 -NH-C(O)CH₂NEt₂ [(R)-(R' -OxNNN^{Et2})-H; $R' = Ph$ (**3c**), $R' = CH_2Ph$ (**3d**), $R' = ^iPr$ (**3e**), $R' = CH_2^iPr$ (**3f**)], were efficiently synthesized. Treatment of these ligands with (DME)NiCl₂ afforded the desired amido-pincer nickel complexes, (R'^2 -OxNNN^{Et2})NiCl [$R' = H$ (**4a**), $R' = Me$ (**4b**)] and (R' -OxNNN^{Et2})NiCl [$R' = Ph$ (**4c**), $R' = CH_2Ph$ (**4d**), $R' = ^iPr$ (**4e**), $R' = CH_2^iPr$ (**4f**)], in good yields. All the ligand precursors and nickel complexes were thoroughly characterized by various analytical techniques. The molecular structures of **4a**, **4d** and **4f** were established by X-ray crystallography. The developed nickel complexes were found to be efficient catalysts for the transfer hydrogenation of ketones using ⁱPrOH as a viable hydrogen source. Enantioselectivity in hydrogenation was not observed with the developed chiral catalysts.

 Received 7th April 2021,
 Accepted 30th May 2021

DOI: 10.1039/d1nj01698a

rsc.li/njc

Introduction

Tridentate pincer-ligated transition metal complexes are extensively used as catalysts in various organic transformations due to their high thermal stability and unique chemical reactivity.¹ In particular, a number of pincer complexes containing group 10 transition metals, like Pd and Pt, have largely been studied in the area of organometallic chemistry and catalysis.² In contrast, recently, pincer nickel complexes have attracted much attention in view of their economic viability, sustainability and environmental benignity.³ Nickel complexes based on PCP,⁴ POCOP,⁵ NCN,⁶ PCN,⁷ PNP,⁸ CNC,⁹ and CCC¹⁰ ligand systems are considerably developed and exploited by traditional catalytic coupling reactions, hydrosilylation, hydroboration, C–H functionalization and many other reactions. Many of these nickel

catalysts are associated with high activity, and there is an excellent scope for their desired transformations. In their interesting contribution, Sun and Khalimon independently demonstrated the synthesis of CNN- and POCN-ligated nickel complexes, respectively, for the transfer hydrogenation of ketones.¹¹

Phosphine-free, nitrogen-ligated NNN-pincer nickel complexes would be more economical and can be handled smoothly without any special inert atmosphere techniques. Moreover, the strong σ -donor nitrogen atoms in the ligands would make the nickel complexes electron-rich. This can lead to the stabilization of nickel complexes under a high oxidation state and would facilitate oxidative addition, an important elementary step in various catalytic reactions. Previously, a variety of NNN-nickel complexes were developed and used in diverse catalytic applications. Hu developed NNN-nickamine and extensively employed it in traditional C–C couplings and C–H functionalization reactions (Fig. 1).¹² Recently, our group demonstrated the synthesis and catalytic activity of many robust NNN-pincer nickel complexes (Fig. 1).¹³ All these NNN-ligated complexes were exceptional in the desired organic transformations. Therefore, further development of NNN-Ni-pincer systems, particularly the chiral analog, is essential to understand their potential in chiral transformations. In this context, herein, we report the synthesis and characterization of a series of achiral and chiral oxazolinyll-based NNN-pincer nickel complexes. These complexes are used for the transfer hydrogenation of ketones to alcohols using isopropanol as a sacrificial hydrogen source.

^a Organometallic Synthesis and Catalysis Lab, Chemical Engineering Division, CSIR–National Chemical Laboratory (CSIR–NCL), Dr Homi Bhabha Road, Pune – 411 008, Maharashtra, India. E-mail: b.punji@ncl.res.in; Fax: +91-20-2590 2621; Tel: +91-20-2590 2733

^b Academy of Scientific and Innovative Research (AcSIR), Ghaziabad-201 002, India

^c Centre for Material Characterization, CSIR–National Chemical Laboratory, Dr Homi Bhabha Road, Pune – 411 008, India

† Electronic supplementary information (ESI) available: ¹H and ¹³C NMR spectra of pincer ligands and nickel complexes. CCDC 2074093 (**4a**), 2074094 (**4d**) and 2074095 (**4f**). For ESI and crystallographic data in CIF or other electronic format see DOI: 10.1039/d1nj01698a

‡ These authors contributed equally.

Unactivated Alkyl Halides in Transition-Metal-Catalyzed C–H Bond Alkylation

Shidheshwar B. Ankade, Anand B. Shabade, Vineeta Soni, and Benudhar Punji*



Cite This: *ACS Catal.* 2021, 11, 3268–3292



Read Online

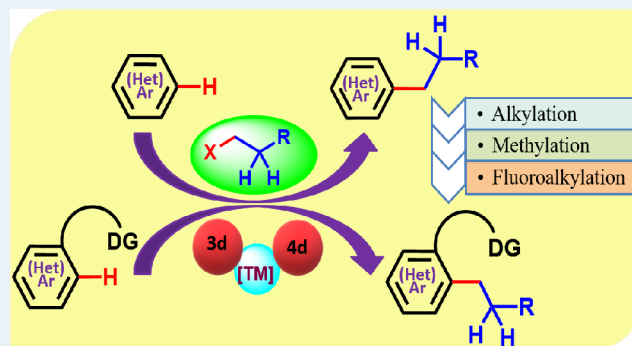
ACCESS |

Metrics & More

Article Recommendations

ABSTRACT: Alkylation represents an important organic transformation in molecular science to develop privileged alkylated arenes and heteroarenes. Especially, the direct C–H bond alkylation using unactivated alkyl halides is a straightforward and attractive approach from both the step-economy and chemoselectivity perspectives. Substantial progress has been made in the direct alkylation using primary, secondary, and tertiary alkyl halides along with the methylation and fluoroalkylation. This Review broadly summarizes the transition-metal-catalyzed alkylations of C–H bonds on various arenes and heteroarenes with unactivated alkyl halides until October 2020. On the basis of the substrates utilized for alkylation, the Review is divided into two major sections: alkylation of arenes and alkylation of heteroarenes.

KEYWORDS: alkylation, unactivated alkyl halides, C–H activation, (hetero)arenes, transition metals



1. INTRODUCTION

Alkyl arenes and heteroarenes are the privileged structural motifs with vast applications in pharmaceutical and perfumery industries as well as in functional materials. They possess intrinsic lipophilic character because of the presence of an alkyl chain; thus, they provide the desired characteristic features for the drugs and agrochemicals. The classical alkylation strategy is mostly based on Friedel–Crafts reaction¹ or radical alkylation,² both of which suffer from several drawbacks, including reaction inefficiency, low selectivity, and limited substrate scope. The development of transition-metal-catalyzed cross-coupling of organometallic substrates with an alkyl electrophile has been envisaged as an alternative protocol for alkylation.³ Various precious metal catalysts and inexpensive 3d metal catalysts are efficiently demonstrated for this process and could address the limitations associated with earlier approaches. Though this traditional cross-coupling has found extensive applications in academia and across industries, the protocol still needs prefunctionalized organometallic substrates. Thus, it involves multistep synthesis leading to the formation of stoichiometric metallic-waste. In recent years, transition-metal-catalyzed direct C–H bond alkylation has emerged as a robust and beneficial alternative to traditional alkylation.⁴ Notably, compared with the installation of aryl, alkenyl, or alkynyl functionalities, the direct C–H bond alkylation is more challenging for various reasons. However, recent advancement in this area led to the development of several environmentally friendly and efficient processes for the direct introduction of an

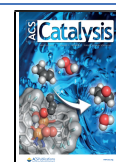
alkyl group onto the organic scaffolds with the assistance of transition metal catalysts.⁵

A variety of alkylating reagents have been employed for the C–H bond alkylation of (hetero)arenes. The alkylating source includes alkyl halides, alkenes, alkyl organometallic reagents, azo-alkyls, carboxylic acid derivatives, alkanes, and alcohols (Scheme 1).⁶ Particularly, the alkyl halides and alkenes are most commonly employed for alkylation, whereas the azo-alkyls are gaining recent attention. The use of alkenes for the alkylation, which proceeds via a hydroarylation protocol, has been extensively studied and recently summarized in reviews.⁷ Though a range of cheap alkenes can be used as coupling partners for the alkylation via hydro-functionalization, the linear versus branched selectivity poses a significant hurdle. On the other hand, direct alkylation of the C–H bond with unactivated alkyl halides provides a specific and targeted product, though it produces halide waste. Moreover, alkyl halides are prevalent chemical building blocks, and they are widely commercially available and easily synthesized from abundant starting compounds. However, the use of unactivated alkyl halides containing β -hydrogens in transition-metal-

Received: December 20, 2020

Revised: February 20, 2021

Published: March 1, 2021







Cite this: DOI: 10.1039/c9sc01446b

 All publication charges for this article have been paid for by the Royal Society of ChemistryReceived 24th March 2019
Accepted 17th August 2019DOI: 10.1039/c9sc01446b
rsc.li/chemical-science

Nickel-catalyzed C–H alkylation of indoles with unactivated alkyl chlorides: evidence of a Ni(I)/Ni(III) pathway†

Dilip K. Pandey,^{ab} Shidheshwar B. Ankade,^{ab} Abad Ali,^a C. P. Vinod ^c and Benudhar Punji ^{*ab}

A mild and efficient nickel-catalyzed method for the coupling of unactivated primary and secondary alkyl chlorides with the C–H bond of indoles and pyrroles is described which demonstrates a high level of chemo and regioselectivity. The reaction tolerates numerous functionalities, such as halide, alkenyl, alkynyl, ether, thioether, furanyl, pyrrolyl, indolyl and carbazolyl groups including acyclic and cyclic alkyls under the reaction conditions. Mechanistic investigation highlights that the alkylation proceeds through a single-electron transfer (SET) process with Ni(I)-species being the active catalyst. Overall, the alkylation follows a Ni(I)/Ni(III) pathway involving the rate-influencing two-step single-electron oxidative addition of alkyl chlorides.

Introduction

Functionalized heterocycles are core structures that are found in many natural products, vital drug candidates, and other compounds with significant biological activity.¹ Therefore, direct and regioselective C–H functionalization of heteroarenes,² including that of privileged indoles,³ by transition-metal catalysis has attracted considerable attention. Particularly, the regioselective alkylation of indoles to synthesize alkylated indoles is an important yet challenging reaction.⁴ The biggest hurdles in the development of an alkylation protocol using unactivated alkyl halides, especially those with β -hydrogen atoms, are the reluctance of these electrophiles to undergo oxidative addition, and their tendency to encounter competitive side reactions (β -hydrogen elimination and hydrodehalogenation).

Although the C-3 alkylation of indoles can be achieved by catalytic Friedel–Crafts alkylation, allylic alkylation, and conjugate addition,⁵ the regioselective direct C(2)–H alkylation of indoles with alkyl halides is extremely limited.⁶ For example, Bach has demonstrated the C-2 alkylation of indoles with alkyl bromides *via* a norbornene-mediated Catellani-type reaction,⁷ using a high loading of the precious Pd-catalyst. In contrast, nickel-catalyzed alkylation of indoles using alkyl iodides was

demonstrated by us,⁸ wherein a high reaction temperature (150 °C) is essential for successful reaction.

Surprisingly, to date, the selective alkylation of indoles and other related arenes has primarily been achieved by employing reactive alkyl iodides or bromides.⁹ However, the attempt to use high-demand and inexpensive alkyl chlorides has been less successful.¹⁰ Therefore, a generalized protocol for the direct C-2 alkylation of privileged indoles and related heteroarenes using readily available, inexpensive and challenging alkyl chlorides under mild conditions is highly desirable. Herein, we report the first general method for the coupling of unactivated alkyl chlorides with the C–H bond of indoles and pyrroles using a naturally abundant and inexpensive Ni(II)-catalyst at 60 °C. Notable aspects of this work include (i) mild and efficient C–H alkylation of indoles and pyrroles, (ii) ample scope with challenging alkyl chlorides with a high degree of tolerance in functionality, (iii) exceptional chemo and regioselectivity for C–halide activation, and (iv) mechanistic insights by detailed experimental study.

Results and discussion

In general, most of the previous nickel-catalyzed C–H functionalizations employ high reaction temperatures (130–160 °C) to achieve the desired coupling products,¹¹ which significantly limit the methodologies. To make the Ni-catalyzed C–H functionalization more general and practical, the major challenge is to perform the reaction under mild conditions employing a wide variety of inexpensive and high-demand unactivated chloro-electrophiles. To achieve this target for alkylation, we screened the coupling of alkyl chlorides with indoles in the presence of lithium bis(trimethylsilyl)amide (LiHMDS) at 60 °C. An optimization study was initiated for the coupling of 1-

^aOrganometallic Synthesis and Catalysis Group, Chemical Engineering Division, CSIR–National Chemical Laboratory (CSIR–NCL), Dr. Homi Bhabha Road, Pune 411 008, Maharashtra, India. E-mail: b.punji@ncl.res.in

^bAcademy of Scientific and Innovative Research (AcSIR), CSIR–NCL, Dr. Homi Bhabha Road, Pune, India

^cCatalysis Division, CSIR–NCL, Dr. Homi Bhabha Road, Pune, India

† Electronic supplementary information (ESI) available: Full experimental procedures and characterization data, including ¹H and ¹³C NMR of all compounds. See DOI: 10.1039/c9sc01446b

